BNL-52663-V.2
Formal Report

Proceedings of the Electron Ion Collider Workshops

February 26 - March 2, 2002
Brookhaven National Laboratory

VOLUME 2

Physics Opportunities and Detector Issues

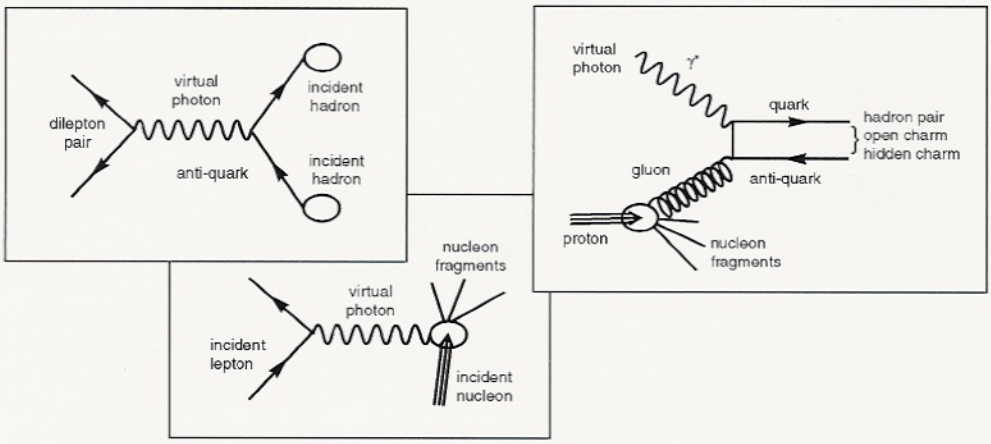

BNL-52663-V.2
Formal Report

Proceedings of the Electron Ion Collider Workshops

February 26 - March 2, 2002
Brookhaven National Laboratory

VOLUME 2

Physics Opportunities and Detector Issues

Edited by:

M.S. Davis
A. Deshpande
S. Ozaki
R. Venugopalan

Disclaimer

This report was prepared as an account of work sponsored by an agency of the United States Government. Neither the United States Government nor any agency thereof, nor any employees, nor any of their contractors, subcontractors or their employees, makes any warranty, express or implied, or assumes any legal liability or responsibility for the accuracy, completeness, or any third party's use or the results of such use of any information, apparatus, product or process disclosed, or represents that its use would not infringe privately owned rights. Reference herein to any specific commercial product, process, or service by trade name, trademark, manufacturer, or otherwise does not necessarily constitute or imply its endorsement, recommendation, or favoring by the United States Government or any agency thereof or it contractors or subcontractors. The views and opinions of authors expressed herein do not necessarily state or reflect those of the United Stated Government or any agency thereof.

Table of Contents

Volume I: Accelerator Concepts

Preface

Agenda

First Plenary Session

Goal of the Workshop (S. Ozaki, BNL)

EIC Status and Considerations (S. Peggs, BNL)

Ring-Ring Collider Scheme (Y. Shatunov, BINP)

Exploration of the Derbenev-Kondratenko Equation in the MIT Bastes South Hall Ring (T. Zwart, MIT Bates)

Advanced Concepts for EIC (Ya. Derbenev, TJNAF)

EIC: An Electron-Light Ion Collider Based at CEBAF (L. Merminga, TJNAF)

RHIC Accelerator Performance and Status (T. Roser, BNL)

Ring-Ring, Linac-Ring Joint Working Group Session

Electron Cooling at RHIC (Y. Shatunov, BNL)

Electron Cooling Facility for RHIC (D. Wang, MIT Bates)

Linac Ring Working Group

Polarized Electron Sources for a Linac-Ring EIC (M. Farkhondeh, MIT-Bates)

Energy Recovering Linac Issues (L. Merminga, TJNAF)

RF Issues in Energy Recovery Linacs (J. Delayen, TJNAF)

Analysis and Simulation of Beam-Beam Effects in a Linac-Ring Collider (L. Merminga, TJNAF)

Ring-Ring Working Group

Electrons are not Protons: (D. Barber, DESY)

Self Polarization Tests at Bates (D. Wang, MIT-Bates)

Interaction Region Working Group

HERA ep Interaction Regions (U. Schneekloth, DESY)

The PEP-II Interaction Region (U. Wienands, SLAC-PEP II)

Luminosity Scaling with IR Parameters (S. Peggs, BNL)

Spin Rotators with the Energy Range from 2 GeV to 10 GeV for eRHIC (J. Kewisch, BNL)

Building the Detector-Accelerator Interface (B. Parker, BNL)

Toy Model of a Detector for EIC (E. Barrelet, in2p3/cnrs)

Shielding Against Synchrotron Radiation at HERA (D. Pitzl, DESY)

Luminosity Study (D.K. Hassell, MIT-Bates)

A 3 Beams Insertion Preliminary Consideration (A. Verdier, CERN)

Second Plenary Session

IR Group Summary Talk (W. Krasny, CERN)

Ring-Ring Working Group Summary (C. Tschalaer, MIT-Bates)

Linac Ring Working Group (I. Ben-Zvi, BNL)

Participants

Volume II: Physics Opportunities and Detector Issues

Preface

Agenda

First Plenary Session

Collider Summary of EIC Accelerator Workshop (S. Ozaki and T.Roser, BNL)

Physics of Nucleon Spin (R. Jaffe, MIT)

Recent Excitement from RHIC (G.Bunce, BNL)

Experimental Status of Spin DIS (G.K.Mallot, CERN)

Experimental Status of eA, μA, and ep Physics (J. Moss, LANL)

Physics of Saturation: AA, eA, pA (D. Kharzeev, BNL)

Nonperturbative Structure of the Nucleon (T.Thomas, Univ. Adelaide)

Recent RHIC Results with AA (M. Baker, BNL)

Lessons from HERA Collider Program on Physics and Detectors (A. Caldwell, Columbia, Univ.)

About the Workshop (A. Deshpande, BNL)

Second Plenary Session

Experimental Observables in eA and Polarized ep at Future Colliders (A. De Roeck, CERN)

eA Physics: Theoretical Issues (M. Strikman, Penn State)

pA Physics at RHIC (J.C Peng, LANL)

Parallel Session I: eA Physics at EIC

e-A Parallel Session Summaries (J. Marian-Jalilian, BNL)

e-A Parallel Session Summaries (A.Bruell, MIT)

Single Hadron Transverse Momentum Distribution as a Probe of Gluon Saturation (J. Qiu, Iowa State)

Hard Diffraction in eA Collisions (Y. Kovchegov, Univ. Washington)

Phenomenology of Generalized Parton Distributions (A.V. Belitsky, Univ. Maryland)

Energy Dependence of QCD Cross Sections. Saturation Effects from HERA to RHIC to LHC (H. Weigert, Univ. Regensburg, Germany

High Partonic Density Effects QCD Expected at EIC (K. Tuchin, Univ. Washington)

Exclusive Processes at EIC: Feasibility Study (A. Sandacz, SINS, Poland)

Nuclear Shadowing in DIS on Nuclei: Leading Twist vs. Eikonal Approaches (V. Guzey, Univ. of Adelaide)

Analysis of HERA Data at Low x (K. Kowlaski, Columbia, BNL and DESY)

Higher Twist Effects in Nuclei (R. Fries, Duke Univ.)

Nuclear Shadowing in Non-linear Small x pQCD (A. Freund, Univ. Regensberg)

Parallel Session II: ep Physics at EIC

Polarized ep Physics: Summary (A. Deshpande, BNL/RBRC and W. Vogelsang, BNL)

Polarized Gluon Distribution from Present and Prospective future g_1 Measurements (J. Lichtenstedt, Tel Aviv Univ.)

g_1 at Low x and Low Q^2 with Polarized ep Colliders (S. Bass, ECT, Italy)

Probing the Spin Structure of the Photon at the EIC (M. Stratman, Regensburg Univ., Germany)

The Case for a Large Polarized Anitquark Flavor Asymmetry $\Delta\bar{u}(x) - \Delta\bar{d}(x)$ (C. Weiss, Regensburg Univ., Germany)

What Do We Learn from Lambda Polarization in SIDIS (M. Anselmino, Univ. di Torino and INFN, Italy)

Conditional Parton Distribution Functions and Nucleon Structure (M. Strikman, Penn State)

Accurate Tests of QCD Factorization at Electron Ion Collider (P. Nadolsky, SMU)

Deep Virtual Compton Scattering: Experimental Aspects (B. Fox, RBRC and BNL)

Quark-Hadron Duality in Electron-Nucleon Scattering (W. Melnitchouk, TJNAF)

Future Transversity Measurement (M. Grosse-Pederkamp, RBRC)

An Initial Study on Measuring F^p_2 at the EIC (A. Vogt, NIHKEF, Netherlands)

Fragmentation Functions from Semi-Inclusive DIS Pion Production and Implications for the Polarized Parton Densities (S. Kretzer, Michigan State Univ.)

Parallel Session III: Detector and IR Design for EIC

Overview (N. Saito, Kyoto Univ., Japan)

Recent R&D Activities on an Accordion-type Calorimeter (E. Kistenev, BNL)

Rear Detection Systems and Luminosity Measurement at H1 and Zeus (U. Schneekloth, DESY,)

Constraints on the H1/Zeus Interaction Regions from the HERA Luminosity Upgrade (U. Schneekloth, DESY)

Forward Physics and Detection Systems at HERA (H. Kowalski, Columbia, BNL and DESY)

Particle Identification at H1 (D. Milstead, Univ. Liverpool, England)

Particle Identification at Belle (T. Iijima, KEK, Japan)

EIC Detector Studies (J. Chwastowski, Institute Of Nuclear Physics, Poland)

Silicon Tracking for PHENIX Upgrade (Y. Goto, RBRC)

Discussion: Detector Design Working Group (B. Surrow, BNL)

Third Plenary Session

12 GeV Upgrade at Jefferson Lab (R. Ent, TJNAF)

The Future of Lepton-Nucleon Scattering: A Brief Summary of the Durham (HERA-3) Workshop, December 2001 (M. Klein, DESY, Zeuthen)

Tesla-N Plans (V. Korotkov, DESY, Zeuthen)

Final Plenary Session

Plans and Discussion (R. Milner, MIT Bates)

QCD and other Fundamental Interactions (V. Hughes, Yale Univ.)

New Directions in QCD and the Electron Ion Collider (S. Brodsky, SLAC)

Participants

Preface

Electron Ion Collider Workshop
February 26 to March 2, 2002
Brookhaven National Laboratory

The fifth in the series of Electron Ion Collider Workshops was held at Brookhaven National Laboratory on February 26 – March 2, 2002. The first two days, Feb. 26th & 27th, were dedicated to the accelerator and the interaction point design issues (hence forth called the EIC Accelerator Workshop). On February 28th, March 1st and 2nd the focus shifted to the physics of polarized e-p scattering, un-polarized e-A scattering, and the detector issues (from now on called the EIC Physics Workshop). The aim of the Workshop was to refine the physics goals of this proposed collider facility identified in previous meetings (see list below) and to begin dedicated efforts on the design of the accelerator, interaction region, and proposals for detectors in view of the physics case.

In the EIC Accelerator Workshop feasibility of various collider options, including the ring-ring geometry and linac-ring geometry for the electron-ion and polarized electron-proton collisions along with their implications for the interaction point (IP) design, were studied. The performance potentials for various options were considered, and technical risks involved were evaluated. The EIC Physics Workshop advanced the physics discussions started in previous EIC workshops (listed below), along with many new ideas for measurements that could be pursued with a Collider at BNL. Finally, working groups were formed to focus on various tasks, namely, the accelerator and IP development, detailed studies of various physics processes of interest in conjunction with realistic Monte Carlo simulations and Detector studies. The goal of this effort is to move towards a collaboration that will fully develop an electron-hadron collider design within the next 3 years.

In all ~50 people attended the Accelerator Workshop (Feb. 26-27, 2002), while ~130 people attended the EIC Physics workshop (Feb. 28 – March 2, 2002). Both had plenary as well as parallel sessions. For the Accelerator Workshop Chris Tschalaer (MIT/Bates) convened the group dedicated to the Ring-Ring collider design, Ilan Ben-Zvi (BNL) convened the group for the Linac-Ring design, while Witek Krasny (CERN/in2p3) convened a group focused on the interaction point design. For the EIC Physics Workshop Jamal J. Marian (BNL), Antje Bruell (MIT) & Raju Venugopalan (BNL) convened the e-A physics working group (WG), Abhay Deshpande (RBRC) and Werner Vogelsang (BNL/RBRC) convened the polarized e-p physics WG, while Naohito Saito (RIKEN/Kyoto U.), Bernd Surrow (BNL) and Abhay Deshpande (RBRC) convened the WG dedicated to the detector issues.

The Workshop proceedings are separated into two volumes. Volume I includes the summaries and slides from the presentations of the Accelerator Workshop, while Volume II includes summaries and selected slides from the EIC Physics Workshop. The authors were requested to summarize their presentations in two or three pages and to include a selection of the most important slides from their presentation. In a few cases, when the authors did not oblige, the responsibility of selection of slides was borne by the editors of these volumes. In addition to the

paper volumes, the proceedings are also available on CDs as PDF files and will be available in the near future on the EIC web pages at http://www.bnl.gov/eic.

This Workshop benefited immensely from the enthusiastic support and active involvement in the scientific organization and program development by the Electron Ion Collider Steering Committee and the Local Organizing Committees. Doris Rueger, the Workshop Secretary, was instrumental for the success of these workshops. She was well supported by Marcy Chaloupka. Sue Davis did an incredible job of putting together the EIC White Paper in time for the workshop and getting these proceedings in order and in their final form. We would also like to thank Pat Yalden of BNL's Photography and Graphic Arts department for doing a wonderful job on the Workshop posters and the cover pages of the proceedings. Last but not least, we appreciate the financial support from Brookhaven Science Associates without which this workshop would not have been possible.

Abhay Deshpande & Satoshi Ozaki
May, 2002

Electron Ion Collider Steering Committee:
J. Cameron (IUCF), R. Holt (ANL), V. W. Hughes (Yale), P. Jacobs (LBNL), R. Milner (MIT/Bates), G. Garvey (LANL), P. Paul(BNL), J. C. Peng (UIUC).

Local Organizing Committee for EIC Accelerator Workshop:
S. Ozaki (Chair), S. Peggs, T. Roser, C. Tschalaer(MIT-Bates)

Local Organizing Committee for EIC Workshop:
A. Deshpande (Chair), W. Guryn, J. J. Marian, L. McLerran, B. Surrow, R. Venugopalan (Co-Chair), W. Vogelsang

Previous Electron Ion Collider Workshops:

1. Physics with a High Luminosity Polarized Electron Ion Collider, EPIC 99, April 1999, IUCF, Bloomington, IN
2. The eRHIC Workshop, April 2000, Yale University, New Haven, CT
3. The eRHIC Workshop, July 2001, BNL, Upton, NY
4. Physics with an Electron Polarized Ion Collider, EPIC 2000, September 2000, MIT, Boston, MA

AGENDA

Workshop on the Electron Ion Collider
February 28, March 1, 2, 2002
Brookhaven National Laboratory
Web page: http://www.bnl.gov/eic

Thursday, February 28, 2002

PLENARY SESSION - PHYSICS SEMINAR ROOM, Building 510

07:30 – 09:00	**Registration:** Physics Lobby (Coffee and Danish Available)	
	Session Chair: John Cameron (IUCF)	
09:00 – 09:20	Welcome	T. Kirk, Assoc. Director
09:20 – 10:00	Vision of future EIC Collider & Summary of EIC Accelerator Workshop	S. Ozaki and T. Roser (BNL)
10:00 – 10:40	Physics of Nucleon Spin	R. Jaffe (MIT)
10:40 – 11:00	*Coffee – Physics Lobby*	
11:00 – 11:40	Experimental Status of Spin DIS	G.K. Mallot (CERN)
11:40 – 12:20	RHIC Spin: Recent Excitement	G. Bunce (RBRC, BNL)
12:20 – 13:00	Experimental Status of eA and pA Physics	J. Moss (LANL)
13:00 – 14:30	*Lunch – Available at Berkner Cafeteria*	
	Session Chair: Larry McLerran (BNL)	
14:30 – 15:10	Physics of Saturation: eA/pA/AA	D. Kharzeev (BNL)
15:10 – 15:50	Nonperturbative QCD in Nuclear DIS	T. Thomas (U. Adelaide)
15:50 – 16:10	*Coffee in Physics Lobby*	
16:10 – 16:50	Recent RHIC Results with AA	M. Baker (BNL)
16:50 – 17:30	Lessons from HERA Detector/Physics	A. Caldwell (Columbia U.)
17:30 – 17:45	Discussion	A. Deshpande (RBRC)
18:00 – 18:45	*Reception Hosted by Brookhaven Science Associates: Berkner Hall*	
18:45	*Banquet Hosted by Brookhaven Science Associates: Berkner Hall*	

AGENDA

Workshop on the Electron Ion Collider
February 28, March 1, 2, 2002
Brookhaven National Laboratory
Web page: http://www.bnl.gov/eic

Friday, March 1, 2000

PLENARY SESSION: PHYSICS SEMINAR ROOM – Building 510

08:00 – 09:00	*Coffee and Danish available in Physics Lobby*	
	Session Chair: Sam Aronson (BNL)	
08:30 – 09:10	Experimental Observables in eA and Polarized ep at Future Colliders	A. De Roeck (CERN)
09:10 – 09:50	e-A Physics: Theoretical Issues	M. Strikman (Penn State)
09:50 – 10:10	*Coffee in Physics Lobby*	
10:10 – 10:50	p-A/d-A physics at RHIC	J. C. Peng (LANL)
11:00 –16:30	**PARALLEL SESSIONS: Lunch will be available in the Lobby, all sessions are in the Physics Building 510**	
Location	**Topic**	**Convenors**
Small Seminar Room	Session I: e-A Physics at EIC	A. Bruell (MIT), J. Jalilian-Marian (BNL), R. Venugopalan (BNL)
Large Seminar Room	Session II: e-p Physics at EIC	A. Deshpande (RBRC), N. Makins (Illinois), W. Vogelsang (RBRC/BNL)
2-160	Session III: Detector & IR design for EIC	N. Saito (RBRC) B. Surrow (BNL), A. Deshpande (RBRC)

PLENARY SESSION: COMPLEMENTARY FUTURE PROJECTS
PHYSICS SEMINAR ROOM – Building 510

Session Chair: Roy Holt (ANL)

16:30 – 17:00	JLAB Upgrade	R. Ent (JLAB)
17:00 – 17:30	Summary of HERA III Workshop	M. Klein (DESY, Zeuthen)
17:30 – 18:00	Tesla-N plans	V. Korotkov (DESY, Zeuthen)

AGENDA

Workshop on the Electron Ion Collider
February 28, March 1, 2, 2002
Brookhaven National Laboratory
Web page: http://www.bnl.gov/eic

Saturday, March 2, 2002

PLENARY SESSION: PHYSICS SEMINAR ROOM – Building 510

08:00 – 09:00	*Coffee and Danish available in Lobby*	
	Session Chair: Gerry Garvey (LANL)	
09:00 – 09:40	Summary of eA physics WG	Convenors
09:40 – 10:20	Summary of ep physics WG	Convenors
10:20 – 10:40	*Coffee in the Lobby*	
10:40 – 11:20	Summary of the Detector & IR WG	Convenors
11:20 – 13:00	A Physics Overview	R. Venugopalan (BNL)/ A. Deshpande
	Plans and discussions	R. Milner (MIT-Bates)
13:00 – 14:30	*Lunch Available in Berkner Cafeteria*	
	Session Chair: Peter Bond (BNL)	
14:30 – 15:50	Perspectives on QCD	
	Experimental Effort on QCD in Future	V. W. Hughes (Yale)
	Electron-Ion Collisions and New Directions in QCD	S. Brodsky (SLAC)
15:50 – 16:10	*Coffee/Soda Available in Lobby*	
16:10 – 16:30	Conclusion of Workshop & Comments	P. Paul, Interim Director
16:30	Workshop Ends	

PARALLEL SESSION AGENDA: e - A

Workshop on the Electron Ion Collider

February 28, March 1, 2, 2002
Brookhaven National Laboratory
Web page: http://www.bnl.gov/eic

Friday, March 1, 2002

Small Physics Seminar Room - Building 510

Convenors:	A. Bruell (MIT), J. Jalilian - Marian (BNL), R. Venugopalan (BNL)	
11:00 – 11:10	Welcome	J. Jalilian - Marian
11:10 – 11:35	Inclusive DIS at EIC (Theory)	J. Qiu
11:35 – 12:00	Diffraction in DIS at EIC (Theory)	Y. Kovchegov
12:00 – 12:45	Inclusive and Final State Hadronic Observables at EIC (Exp)	A. Bruell
12:45 – 13:30	*Break to pick up lunch in the Lobby*	
13:30 – 13:55	Evolution in the Saturation Region	I. Balitsky
13:55 – 14:20	Energy Dependence of QCD Cross Sections. Saturation Effects from HERA to RHIC to LHC	H. Weigert
14:20 – 14:45	High Partonic Density Effects at EIC (Theory)	K. Tuchin
14:45 – 15:10	Exclusive Processes at EIC – Feasibility Study (Exp.)	A. Sandacz
15:10 – 15:25	*Coffee in Physics Lobby*	
15:25 – 15:50	Leading Twist Shadowing	V. Guzey
15:50 – 16:15	Diffractive DIS at EIC (Exp.)	H. Kowalski
16:15 – 16:30	Discussion	Led by J. Jalilian-Marian

PARALLEL SESSION AGENDA: e - p

February 28, March 1, 2, 2002
Brookhaven National Laboratory
Web page: http://www.bnl.gov/eic

Friday, March 1, 2000

Large Physics Seminar Room – Building 510

Convenors:	A. Deshpande (RBRC), N. Makins (Illinois), W. Vogelsang (RBRC/BNL)	
11:00 – 11:10	Overview	A. Deshpande
11:10 – 11:30	Delta g from DIS	J. Lichtenstedt
11:30 – 11:55	g_1 at Low x and Low Q^2 with Polarized e – p Colliders	S. Bass
11:55 – 12:20	Probing the Spin Structure of the Photon at the EIC	M. Stratmann
12:20 – 13:00	*Pick up Lunch in Lobby*	
13:00 – 13:25	The Case for a Large Polarized Antiquark Flavor Asymmetry $\Delta\bar{u}(x) - \Delta\bar{d}(x)$	C. Weiss
13:25 – 13:50	What Do We Learn from Lambda Polarization in SIDIS?	M. Anselmino
13:50 – 14:10	Conditional Parton Distribution Functions and Nucleon Structure	M. Strikman
14:10 – 14:25	*Coffee available in Lobby*	
14:25 – 14:50	Experimental Tests of DGLAP Factorization	P. Nadolsky
14:50 – 15:15	Polarization Phenomena in DVCS and Hard Meson Production	A. Belitsky
15:15 – 15:35	DVCS Experimental Aspects	B. Fox
15:35 – 16:00	Quark-Hadron Duality in Electron Nucleon Scattering	W. Melnitchouk
16:00 – 16:25	Measuring Transversity	M. Grosse-Perdekamp

PARALLEL SESSION AGENDA: DETECTOR DESIGN

February 28, March 1, 2, 2002
Brookhaven National Laboratory
Web page: http://www.bnl.gov/eic

Friday, March 1, 2000

Physics Conference Room 2-160 – Building 510

Convenors:	N. Saito (RBRC), B. Surrow (BNL) and A. Deshpande (RBRC)	
11:00 – 11:20	Welcome and Orientation	N. Saito
11:20 – 11:50	Rear Detection Systems and Luminosity Measurements at H1 and Zeus	U. Schneekloth
11:50 – 12:05	Constraints on the H1/ZEUS Interaction Regions from the HERA Luminosity Upgrade	U. Schneekloth
12:05 – 12:30	*Pick up Lunch in Physics Lobby*	
12:30 – 13:15	Forward Detection Systems at H1 and ZEUS	H. Kowalski
13:15 – 14:00	e/h Separation and Means of Particle ID	D. Milstead
14:00 – 14:45	Particle ID at Belle	T. Iijima
14:45 – 15:30	EIC Detector Studies	J. Chwastowski
15:30 – 15:55	Silicon Tracking for PHENIX Upgrade	Y. Goto
15:55 – 16:30	Discussion • Geant Detector Simulation Framework for EIC • Participation in Detector Design Studies • Organizational Issues of Detector Working Group • Outline of Roadmap toward a CDR for EIC Physics case → detector requirements Constraints from accelerator/injection region Choice of Detector Technology Detector Simulation Detector/Physics Studies Documentation	B. Surrow

Electron Ion Collider Workshop

Accelerator

Satoshi Ozaki

February 28-March 2, 2002

Building 510, Brookhaven National Laboratory

EIC Accelerator Workshop

Tuesday and Wednesday, February 26-27

Study feasibility of various collider options for the electron-ion and polarized electron-proton collisions, and assess their performance potentials, and evaluate technical risks involved.

Now is the time to review the options, with an idea that future R&D efforts can be focused on the promising few options.

Expectations:

- This Workshop can provide several options on which to build physics cases in the Electron Ion Collider workshop.
  Summary of the accelerator workshop by T. Roser
- This workshop should act as a catalyst to begin the R&D collaborations towards the realization of an electron-ion collider.
- The work here should lead to future workshops, hopefully scheduled in conjunction with next EIC Workshops.

How to Succeed in Business

Mounting a major research facility project

- Develop well defined physics goals
- Establish importance of physics and compelling reason why a new facility is needed.

  Must be able to convince people outside of your local field
- Build up a strong community support.

  Workshop like this will be very important.
- Establish technical basis for accelerator and detectors through focused R&D.

  Because of complexity and scale of the facility, inter-laboratory and international collaboration is essential
- Convince the funding agency

Example with RHIC

RHIC Project History:

1983: The Project Conceived as Part of US NSAC Long Range Plan

1985: The Workshop on Experiments and Detectors for a RHIC (BNL)

1986: CDR Submitted to DOE & Collider R&D Began

1987: The 2nd Workshop on Experiments and Detectors for a RHIC (LBL)

1988: The 3rd Workshop on Experiments and Detectors for a RHIC (BNL)

1989: Detector R&D Initiated

1991: The Construction Began

1992-5 : Four Detectors Approved, One-by-One

1999: Construction Completed and Functionality Verified

2000: Commissioning Completed and Physics Program Began

2001: Physics Results at the Quark Matter Conference 2001

17 + years later

Summary of the 2002 EIC Accelerator Workshop

Linac - ring working group

Ring - ring working group

Interaction region working group

BROOKHAVEN NATIONAL LABORATORY

Thomas Roser
EIC Workshop 2002
February 28, 2002

Purpose of the Workshop

Study feasibility of various collider options for the electron-ion and polarized electron-proton collisions.

Ring on Ring Option

Ring on Ring Option with Top-off Linac

Energy-Recovery-Linac on Ring Option

Assess their performance potentials, and evaluate technical risks involved.

Now is the time to review the options, with an idea that future R&D efforts can be focused on a promising few options.

The Facility Requirements

- Collider geometry capable of e-A and polarized e-p Collisions
- Range of $s^{1/2}$ for e-A as high as possible: (~ 63 GeV/u)
- Range of variable $s^{1/2}$ for e-p: 30 – 100 GeV
  $\Leftarrow$(Beam Energy)$_{Max}$: (E_e)10 GeV, (E_p) 250 GeV, (E_A) 100 GeV/u
- E_p/E_e, E_A/E_e: preferably independent of $s^{1/2}$ for detector geometry?

- Range of Ion Species: As wide as possible, p to U?
- Polarization: 70% $\times$ 70%

- Luminosity: 10^{33} $cm^{-2}s^{-1}$ per nucleon
- Integrated Luminosity for Significant Physics:
  For inclusive physics (Yale workshop): ~2 fb^{-1}
  For exclusive and semi-inclusive: ~5 –10 times more

- e^+p, in addition to e^-p, requirement?
  To be addressed by Electron Ion Collider Workshop

Questions to be Answered by Working Groups

Each working group should answer the following questions.

What is the likely performance achievable with each option?

What are advantages and disadvantages of each option?

What is the impact of each option on the IR design?

What is a showstopper, if any?

What is the path forward?

White paper EIC options

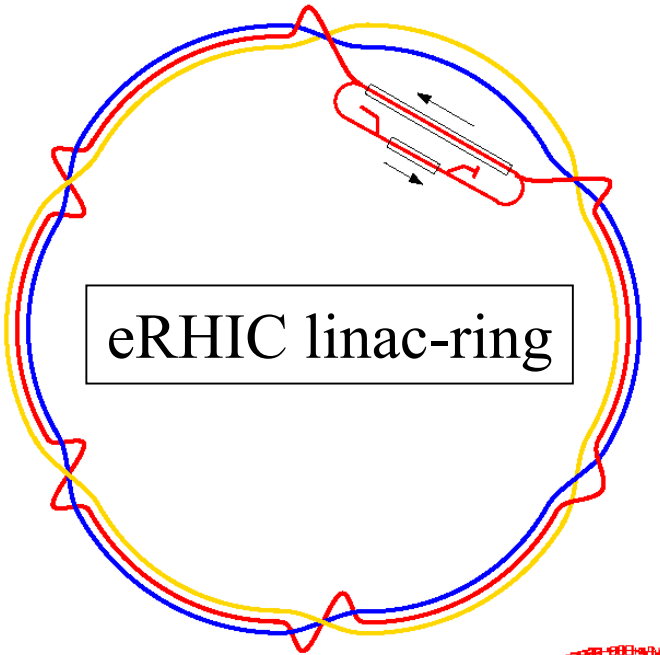

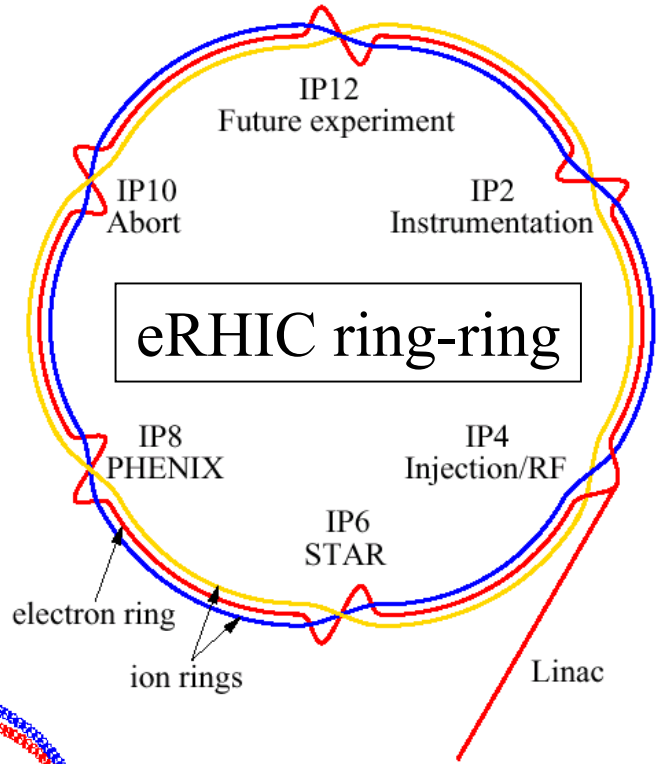

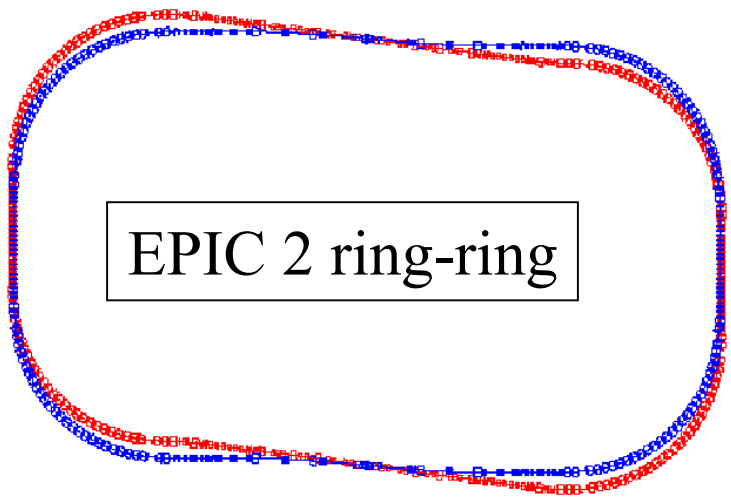

Ultimate EIC Performance

Beam-beam parameters:

$$\xi_e = \frac{N_i}{\epsilon_e}\left(\frac{r_e Z}{4\pi\gamma_e}\right)$$

$$\xi_i = \frac{N_e}{\epsilon_i}\left(\frac{r_i (v/c)_i}{4\pi Z}\right)$$

Electron-ion luminosity:

$$L = F_c\, \xi_e \xi_i\, \sigma_e'^{*} \sigma_i'^{*} \left(\frac{4\pi\gamma_e\gamma_i}{r_e r_i}\right)$$

At beam-beam limit ($\xi_e \sim 0.06$, $\xi_i \sim 0.003$) and angular apertures set by IR design, the only way to increase luminosity is to increase the collision frequency F_c (more bunches)

Linac-ring option: Higher ξ_e (high luminosity or lower e-current and synchrotron radiation)
Electron polarization can be reversed
No need for spin rotators at IR
Parameters ~ energy independent
Higher cost

White paper parameters

	THERA	EPIC 2	eRHIC	eRHIC	HER
Scenario	linac-ring	linac-ring	linac-ring	ring-ring	(SLAC)
Ion specie	protons	protons	protons/gold	protons/gold	–
Luminosity, [10^{32}cm^{-2}s^{-1}]	.041	21	4.6/.036	3.5/.086	–
Dipole bend radius, [m]	608	$\sim$ 50	243	243	165
RMS beam size, σ^* [μm]	10	25	21/60	40/50	157
Bunch spacing, [ns]	211	6.7	35.5	35.5	4.2
IONS					
Ion energy, [GeV/u]	1,000	50	100/250	250/100	–
Ion rms emittance, [μm]	1.0	2.0	0.8/1.0	0.8/1.0	–
Ion average current, [A]	.071	2.4	.14/.68	.42/.42	–
Ion IP beta, β_e^* [m]	.10	.10	.15/.39	.53/.27	–
Ion b-b parameter, ξ_i	.0023	.004	.0046/.0015	.004/.004	–
Laslett SC tune shift	.0003	.024	.001/.003	.003/.003	–
ELECTRONS					
Electron energy, [GeV]	250	5	10	10	9
Electron emittance, [nm]	.2	6	3	18	49
Electron beam current, [A]	.000084	.264	.135/.135	.12/.37	1.5
Electron beam power, [GW]	.023	1.32	1.35/1.35	1.2/3.7	13.5
Synch. rad. power, [MW]	–	$\sim$ .29	.49/.49	.43/1.3	7.2
Electron IP beta, β_e^* [m]	.50	.10	.15/1.2	.089/.139	.05/.50
Electron b-b parameter, ξ_e	.23	.35	.11/.57	.06/.06	.055

All EIC options require e-cooling of ions

Electron cooling of high energy proton or ion beams:

- Feasibility supported by study produced at BINP
- Bunched electron beam requirements for 100 GeV/u gold beams:
  E = 54 MeV, <I> ≤ 100 mA, electron beam power: ≤ 5 MW!
- Requires high brightness, high power, energy recovering superconducting linac, almost identical to IR FEL at TJNAF
- First linac based, bunched electron beam cooling system used at a collider
- First high p_t electron cooler to avoid recombination of e^- and Au^{79+}

New ideas (Y. Derbenev):

- Use circulator ring for e-cooling of very intense ion beams
- Cooling is improved if cooling decrements are equal in all 3 dimensions
- E-cooling can produce flat beams and very short ion bunches which can improve collider luminosities

The RHIC Electron Beam Cooler

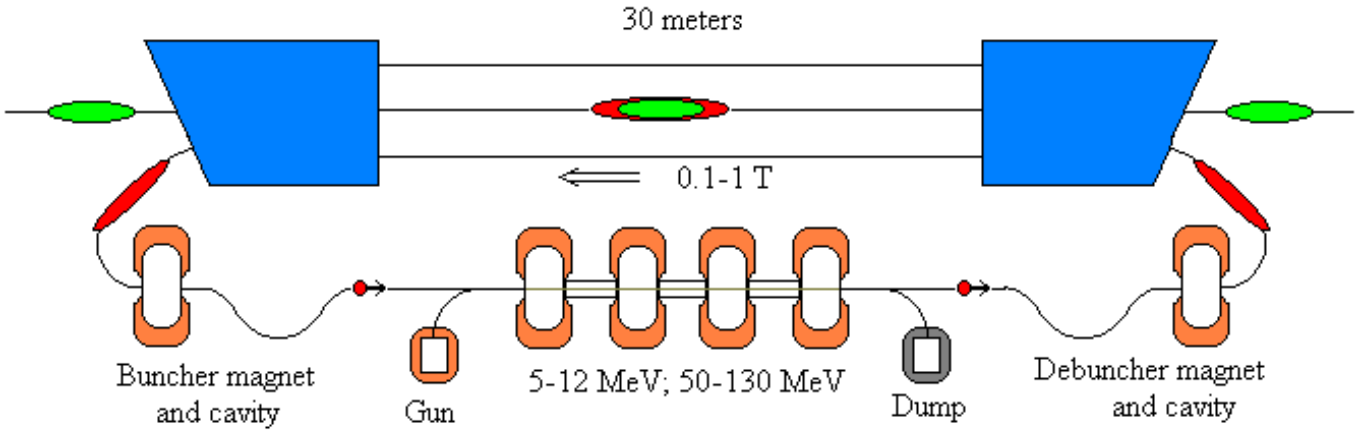

<u>R&D issues:</u>

High intensity photocathode electron gun

High efficiency energy recovering sc linac with magnetized electron beam

Efficient electron beam transport and debunching/bunching

High precision (10 ppm) solenoid for 30 m cooling section.

RHIC Luminosity and Emittance with Cooling

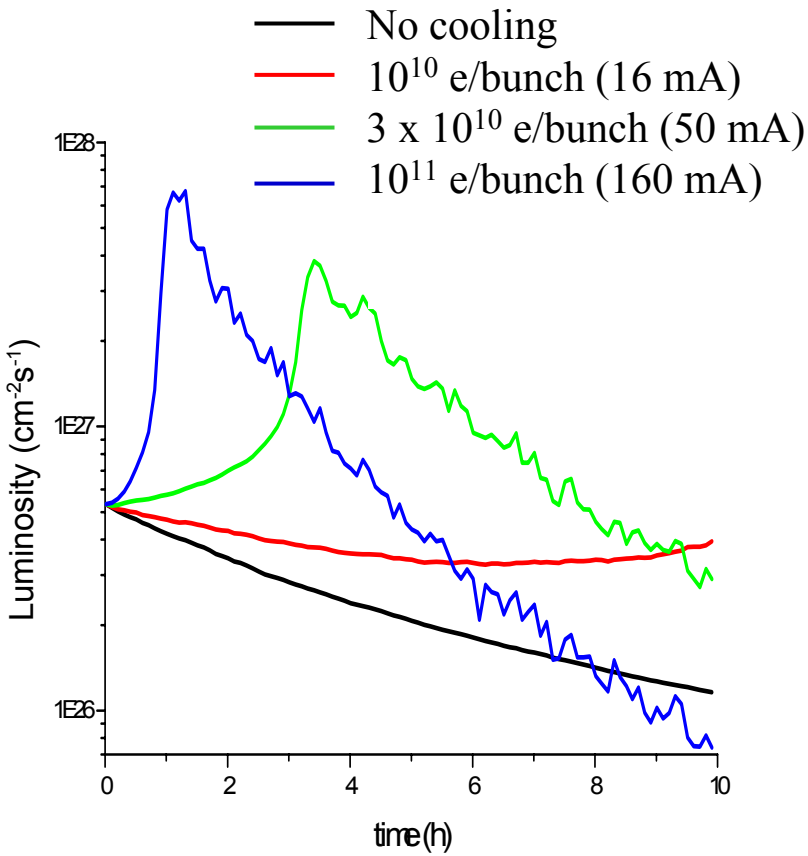

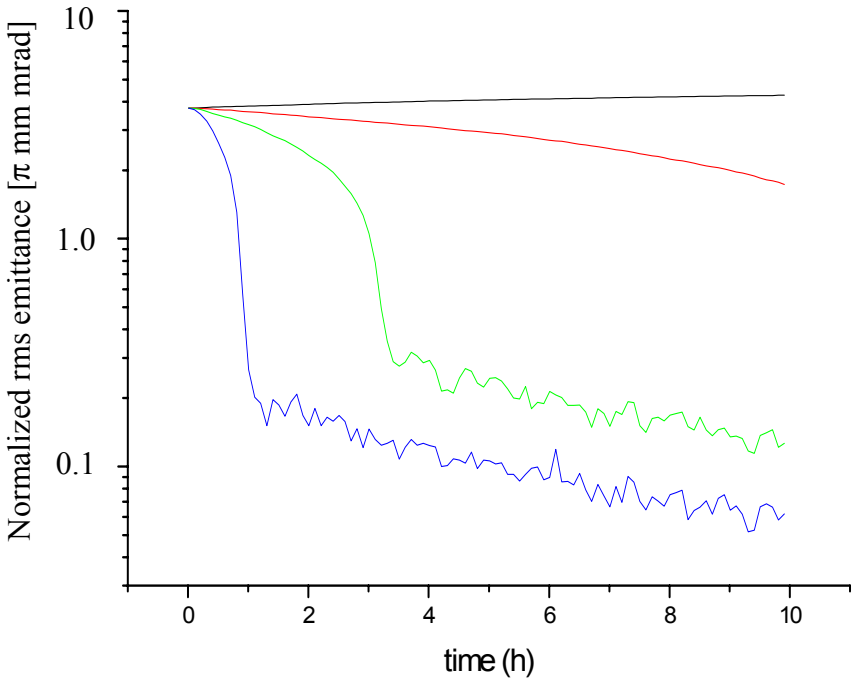

Energy Recovering Linac (ERL) for EIC

- Develop on-line absorbers for Higher Order Mode (HOM) power
- Need simulations and design of Beam Break-Up (BBU) feedback
- Develop and improve codes for BBU, beam dynamics, kink instability,..
- Energy recovery experiment at CEBAF to address high energy ratio

High current ERL tests:

Jlab FEL: 200 MeV, 10 mA

BNL: 50 MeV, 50 mA

Cornell: 100 MeV, 100 mA

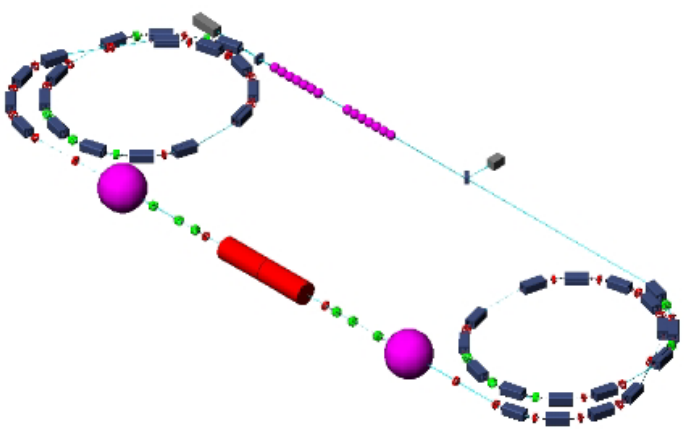

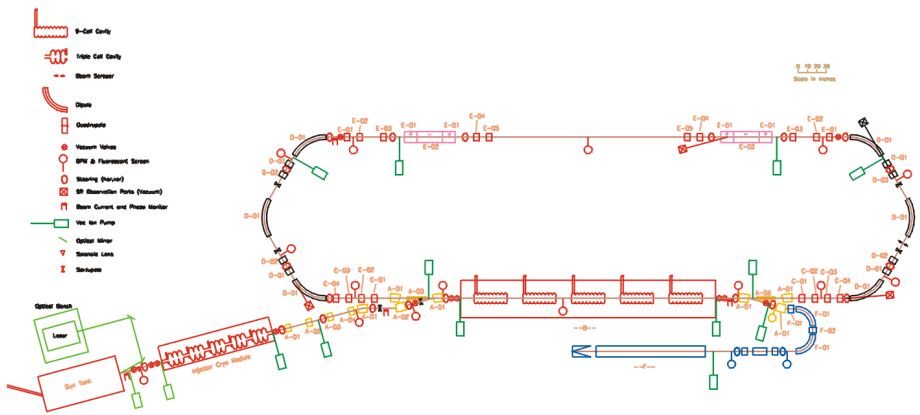

Linac Circulator Ring Option (Y. Derbenev)

Full energy electrons
are stored for ~100 turns
in circulator ring.

Linac current is much lower!

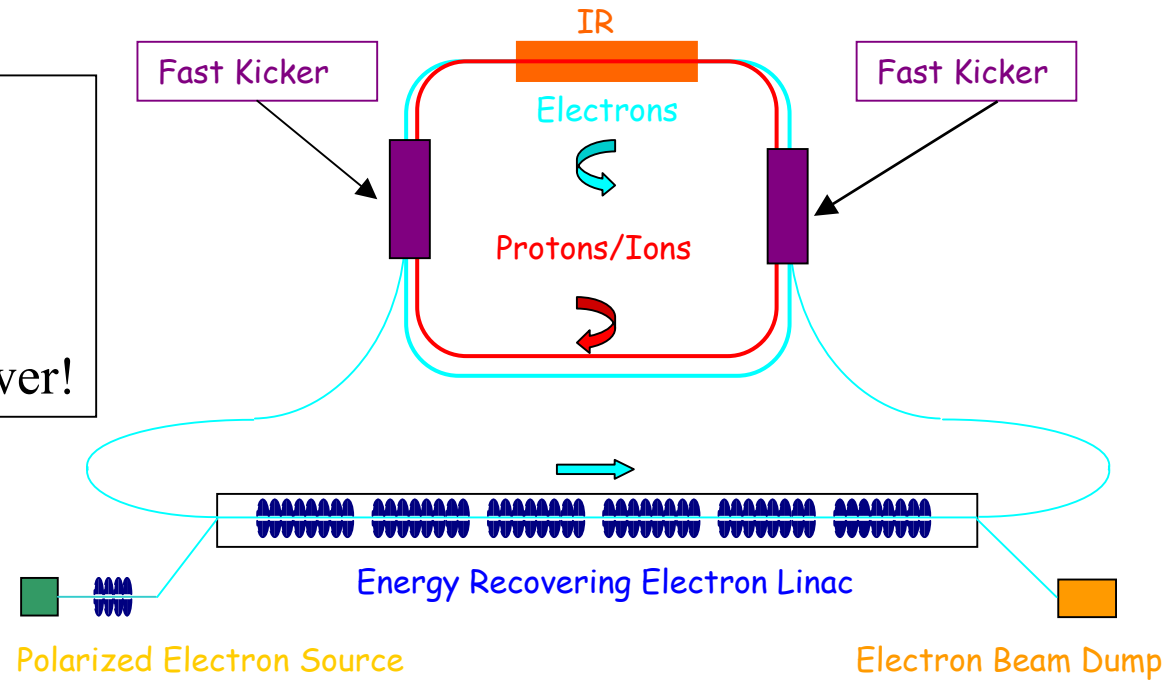

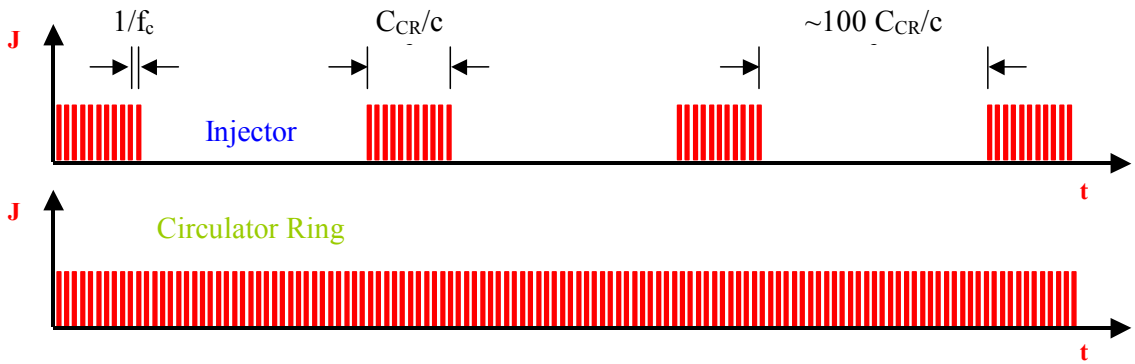

Linac Ring WG conclusions (I. Ben-Zvi)

- No showstoppers for 10 GeV ERL have been found
- 135 mA, 80% polarized electron source requires 200 W laser.
- Need R&D on laser and to demonstrate high current source
- Circulator ring could greatly reduce average current requirements
- Parameters for Linac-Ring EIC:

	Proton	Au
Luminosity [10^{31}]	100	1
σ*		
Ion parameters:		
#/bunch [10^{9}]	200	1.2
Emittance [μm]	0.9	0.5
Laslett tune shift	0.006	0.0053
Beam-beam parameter	0.004	0.004
Beta* [cm]	31	21
Electron parameters:		
#/bunch [10^{10}]	2.9	4.8
Emittance [nm]	6.0	6.0
Beam-beam parameter	0.38	0.18
Beta* [cm]	17	19

ELIC Layout

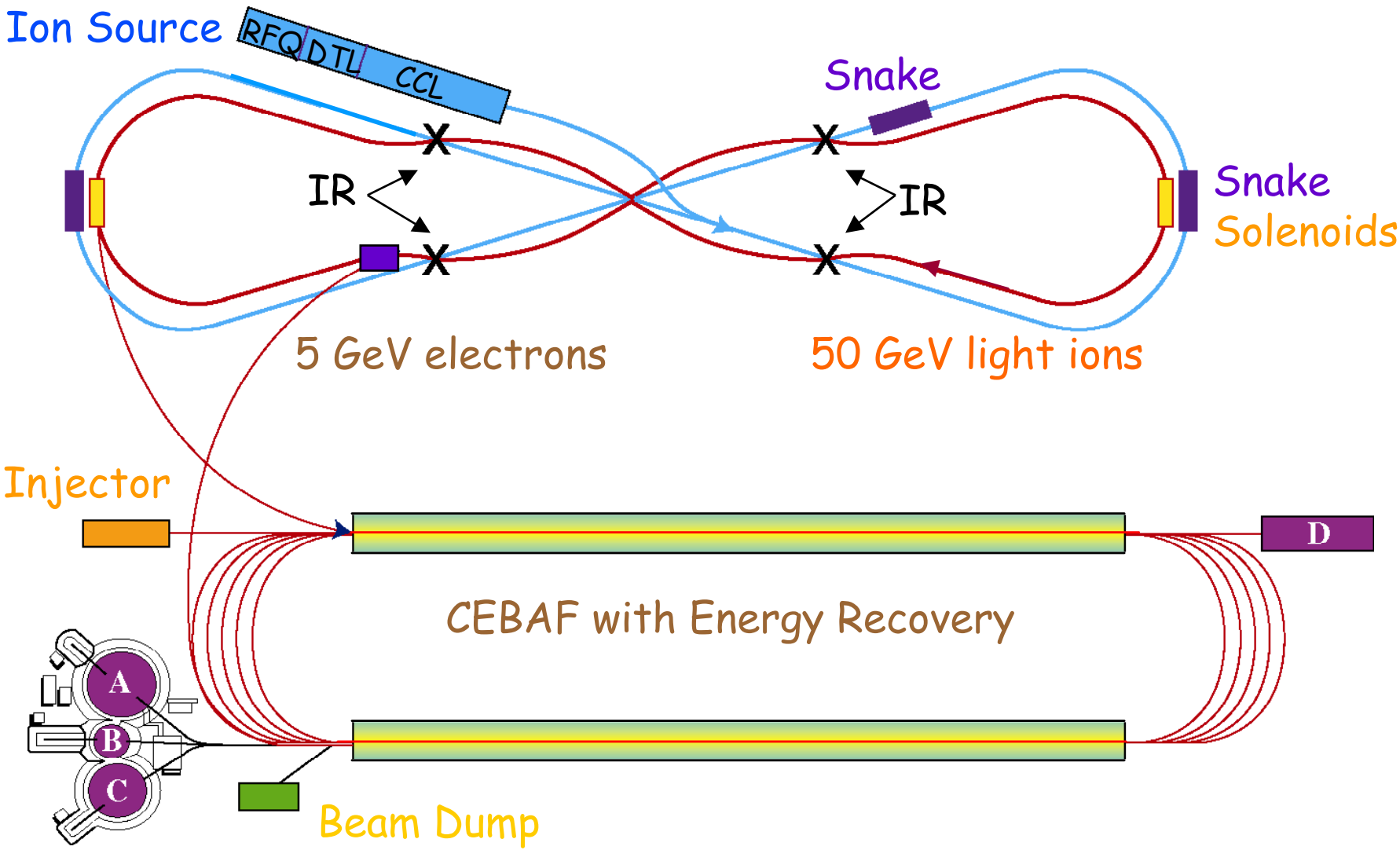
Ion Source
RFQ
DTL
CCL
Snake
IR
IR
Snake
Solenoids
5 GeV electrons
50 GeV light ions
Injector
D
CEBAF with Energy Recovery
A
B
C
Beam Dump

Parameter Choices

We have developed self-consistent parameters for 4 point designs (PDs):

- PD0: Max peak luminosity without cooling and
  parameters based on demonstrated performance to date
- PD1: Max luminosity of 1×10^{33} cm^{-2} sec^{-1}
  Electron cooling required
- PD2: Max luminosity of 1×10^{34} cm^{-2} sec^{-1}
  Electron cooling required -> short ion bunches
  Circulator ring
  Crab crossing
- PD3: Max achievable luminosity
  Electron cooling required -> short ion bunches
  Circulator ring
  Crab crossing
  Traveling focus ?

Assumptions

E_e=5 GeV, E_i = 50 GeV, ε_n^e = 10 μm, ε_n^i = 2 μm (w/out cooling)

Equal beam sizes for electrons and ions are assumed at the IP

5 – 10 GeV electron ring (Y. Shatunov)

- Spin rotators: solenoid + weak horizontal bend
- Short self polarizing time using “super bends”
- ¼ of RHIC circumference

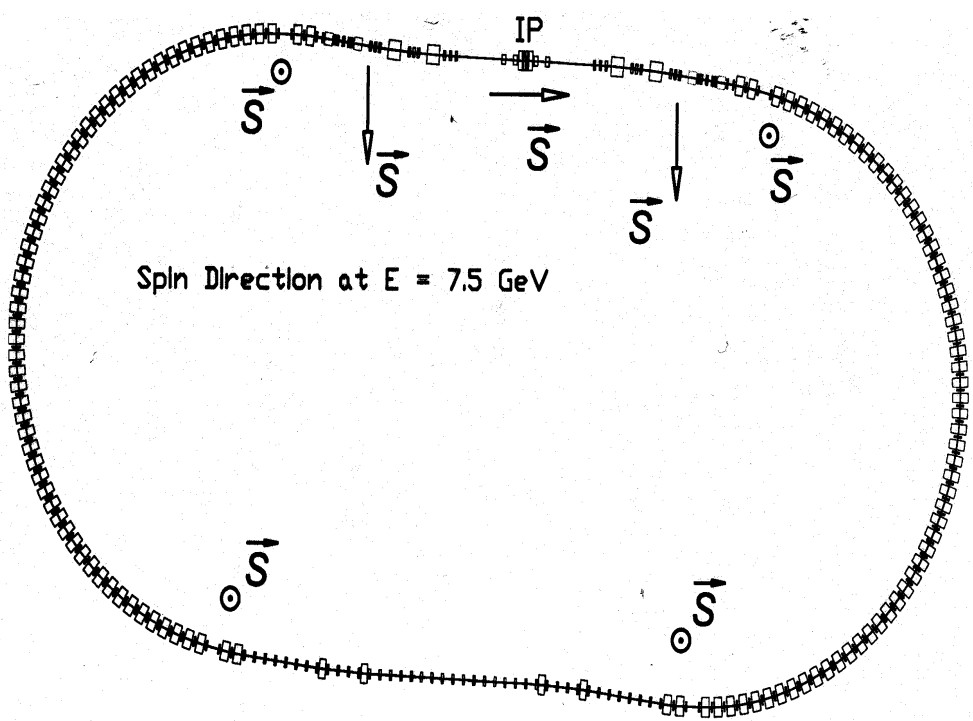

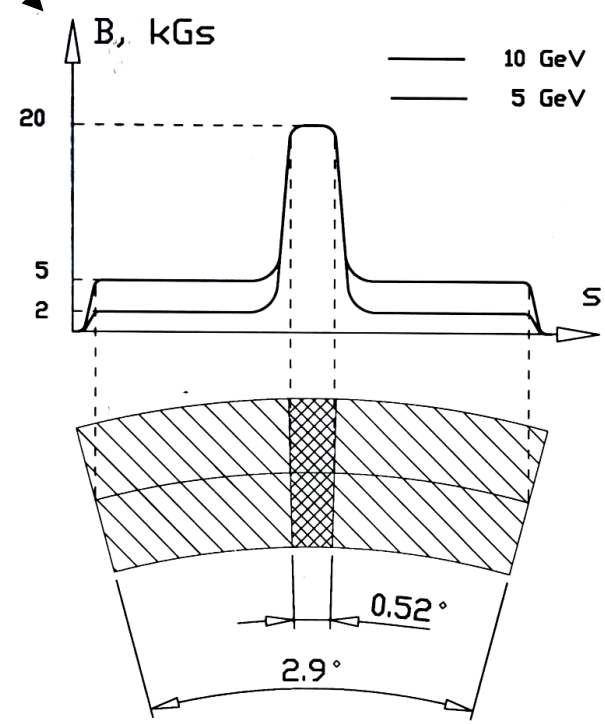

Ring-ring parameter (Y. Shatunov)

	Units	Electron ring	Proton ring
Circumferences	m	958.25	3833
Energy	GeV	5–10	25–200
Arc radius	m	97.98	610
Bending radius	m	63.59	243
Number of bunches		90	360
Bunch spacing	m	10.65	10.65
Bunch population		$1 \cdot 10^{11}$	$1 \cdot 10^{11}$
Beam currents	A	0.45	0.45
Harmonic number		1170	2520
RF frequency	MHz	365.7	196.9
Accelerating voltage	MV	30	1.5
Energy losses/turn	MeV	2.83–21.26	
Total radiated power	MW	1.27–9.57	
Beam emittances, $\varepsilon_{x,z}$	$\mu m \cdot mrad$	43–65	48–6
Beta function at IP	cm	10	10
Beam size at IP, $\sigma^*_{x,z}$	μm	65–80	68–24
Momentum spread		$1.0–1.6 \cdot 10^{-3}$	$1.1–0.4 \cdot 10^{-3}$
Bunch length, σ_l	cm	1–2	10–5
Beam-beam parameter, ξ		0.046–0.023	0.009–0.002
Lasslett tune shift, $\Delta\nu$			0.2–0.009
Luminosity	$cm^{-2}s^{-1}$		$0.45–1 \cdot 10^{33}$

Ring Ring WG conclusions (C. Tschalaer)

Cost effective path to eRHIC:

- 5-10 GeV e-ring (Y.Shatunov) with 2 GeV linac injector.
- Polarization build-up time ~ 15 min., collide with 10 – 100 GeV/n Au or 25 – 250 GeV pol. Protons, 30 ns between bunch crossings
- $L \sim 1 \times 10^{33}$ cm^{-2} s^{-1}
- To improve self-polarization: upgrade to 10 GeV linac with polarized source, inject and store every second or minute
- To get higher luminosity upgrade to energy-recovering linac using the e-ring as circulator ring (1-100 turns)

Work to do:

- Integrate e-ring into RHIC and detector/IR design
- Develop e-ring optics incl. IR and spin track including beam-beam effects
- Test self polarization and spin tracking codes at Bates SHR

PEP II IR (U. Wienands)

Strong separation bend and high luminosity → reduced detector acceptance

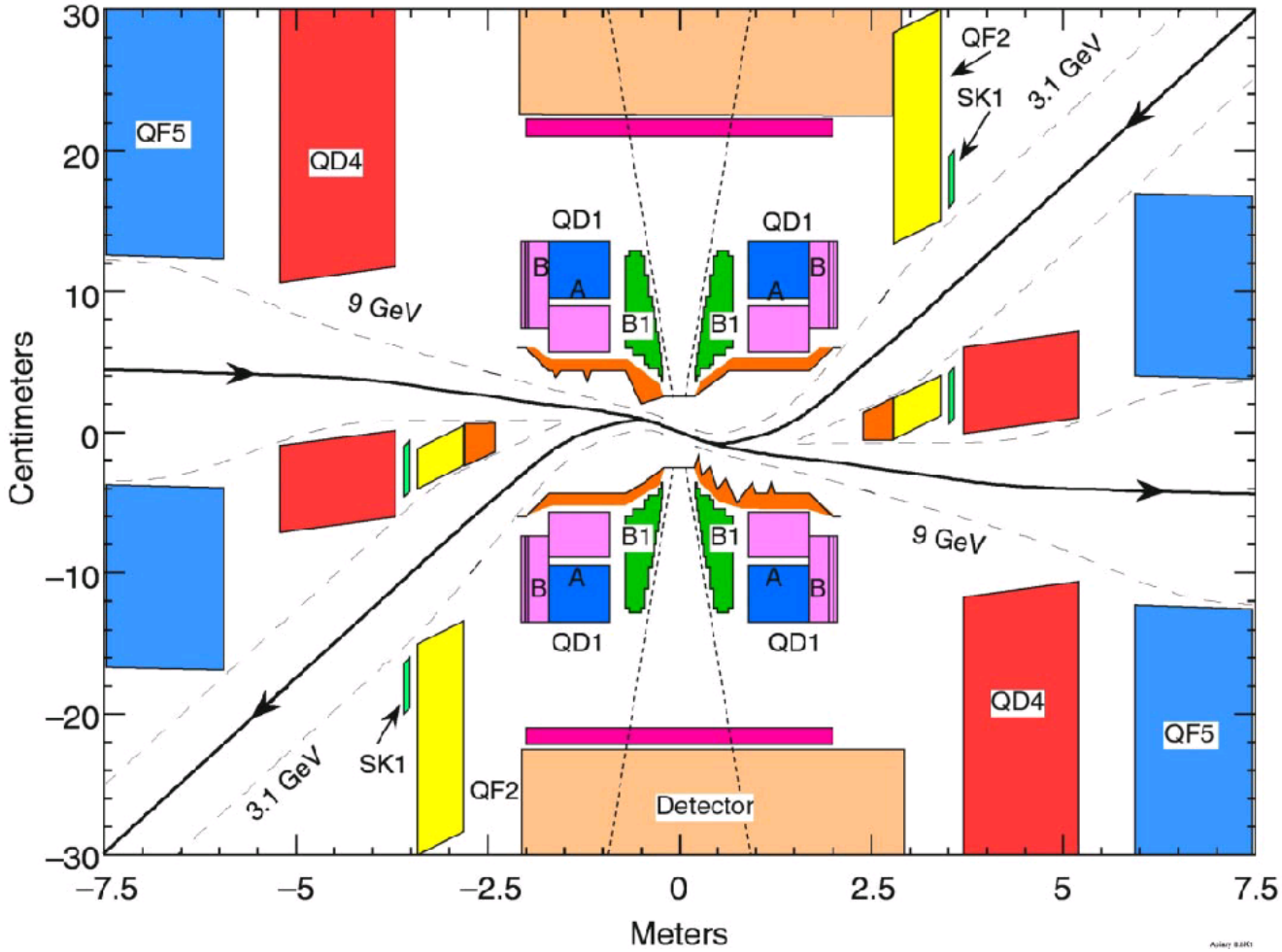

HERA II IR (U. Schneekloth)

Weaker separation bend → improved detector acceptance

Total power 18kW (26kW at 30GeV)

Critical energy up to 115 keV (150 at 30 GeV)

"No" upstream collimators

Radiation fan must pass through IR

Main background source: back-scattering from absorbers 11 to 27 m right of IP

Small central beam pipe

Top view of interaction region

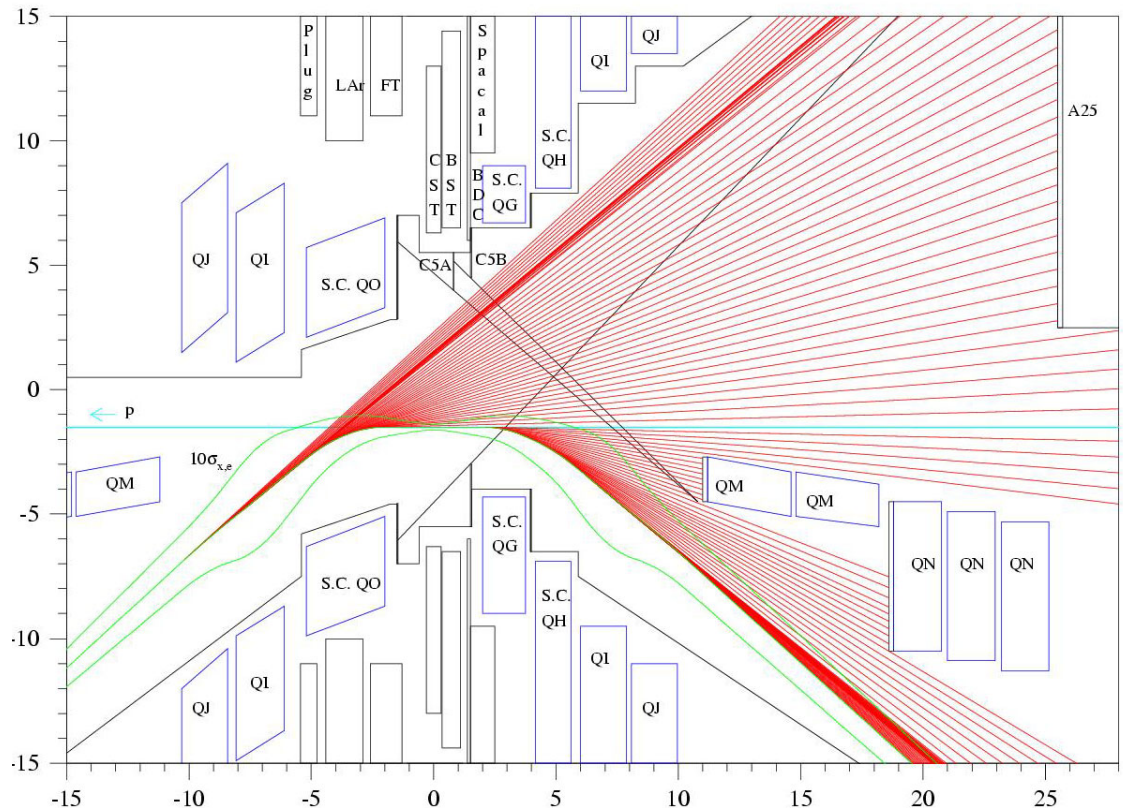

Details: talk by D.Pitzl

eRHIC IR with "weak – strong" bends (B. Parker)

- "Three beam" IR
- E-beam collides head on with blue at IP
- Small vertical deflection inside detecto separates electrons from circulating beams
- Ions bent by 1T field inside a Lambertson dipole
- Long drift downstream of Lambertson gives spectrometer lever arm
- Keep Lambertson short to pass synchrotron radiation.
- Small vertical kicks to Blue/Yellow beams compensate before triplets – proton spin should be OK

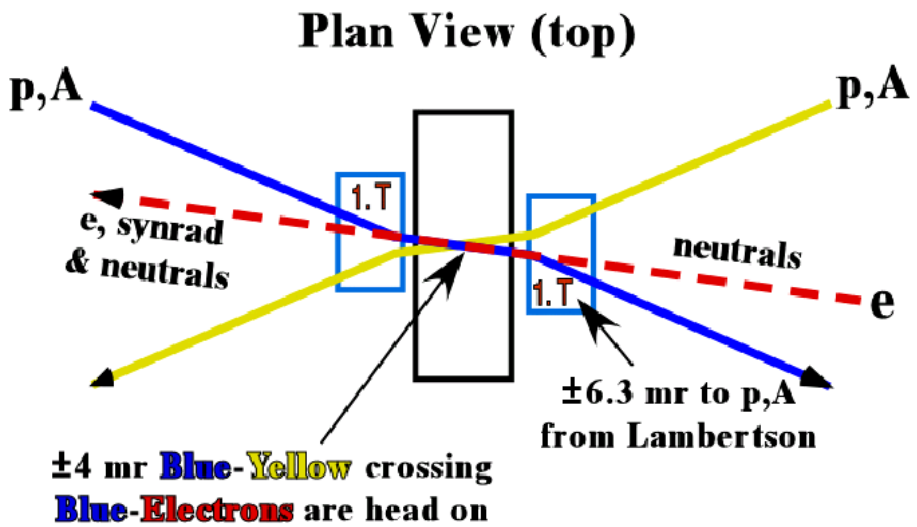

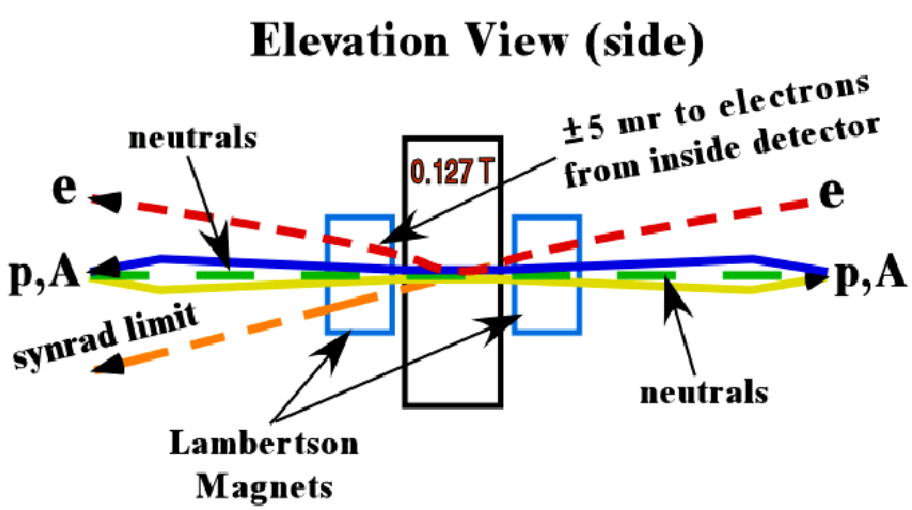

Conclusion: eRHIC Update

- Collisions only at one interaction region (IP12 ?)
- e-ring outside of RHIC tunnel with ¼ of RHIC circumference
- e-ring built to support polarization build-up or circulator ring for full energy (energy recovering) linac
- Existing RHIC IPs fully negotiable for electron-ion collisions

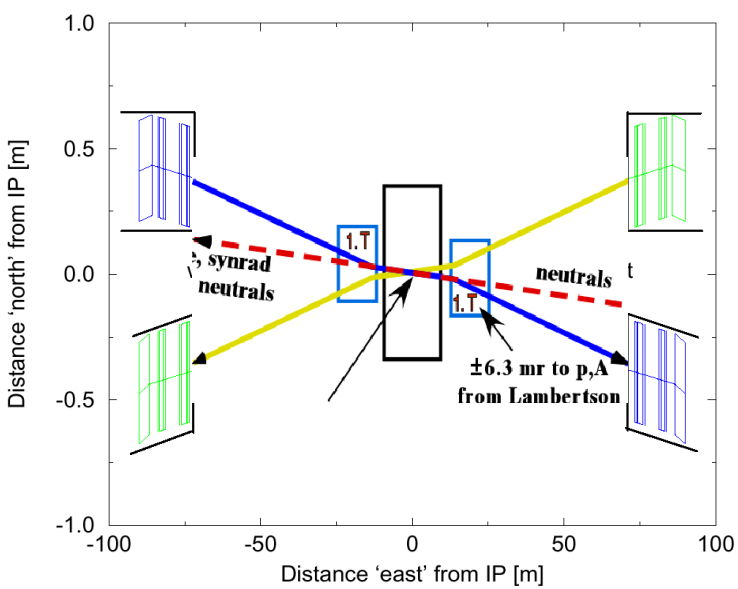

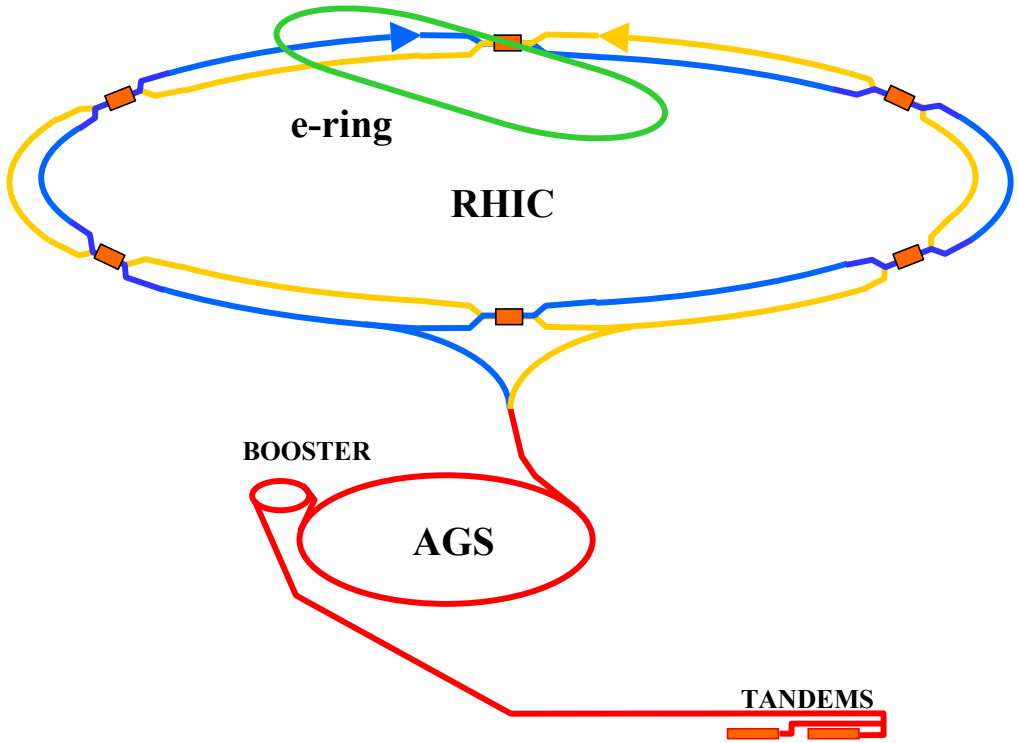

Physics of the Nucleon Spin

Workshop on the Electron Ion Collider
February 28, March 1, 2, 2002
Brookhaven National Laboratory

R.L. Jaffe

Summary

- Major questions about spin, flavor, and chiral structure of the nucleon accessible in DIS.
- Present facilities have work to do (JLab, Mainz, Bonn, SLAC, HERMES @ DESY, COMPASS @ CERN)
- Great expectations from RHIC Spin
- Future will require:
  - ⋆ High Polarization
  - ⋆ Large energy range
  - ⋆ High duty factor
  - ⋆ High quality measurements on final hadrons
  - ⋆ High luminosity
- EIC!

Highlights at all energy scales (at existing facilities)

- Bates, Mainz, Bonn and JLAB
  - ⋆ Gerasimov-Drell-Hearn-Hosata-Yamamoto Sum Rule
  - ⋆ Strangeness magnetic moment, charge radius, and axial charge.
  - ⋆ Quark orbital angular momentum via Deeply Virtual Compton Scattering (DVCS).
- •• Hermes, Compass (CERN)
  - ⋆ Polarized quark distributions at $x \gtrsim 0.1$.
  - ⋆ Flavor structure of quark spin via semi-inclusive DIS.
  - ⋆ First look at transversity and possibly at polarized gluon distribution.
- ••• RHIC
  - ⋆ Polarized quark and gluon distributions at intermediate and small x.
  - ⋆ Flavor structure of quark spin via semi-inclusive DIS and $W^{\pm}$ production.
  - ⋆ Transversity!
- BELLE (and other e^+e^- colliders)
  - ⋆ Fragmentation functions necessary for filtration

Focus on the Nucleon

★ The Bjorken Sum Rule
A model for understanding in QCD.

★ The Polarized Quark and Gluon Distributions in the Nucleon
Where are stand.

★ Quark and Gluon Spin Distributions at low x.
Expectations for a new regime.

★ The Hermes Azimuthal Asymmetry and Transversity!
Using fragmentation to isolate new spin information.

★ The Structure of the Angular Momentum
What can be measured?

★ The GDHHY Sum Rule
Close to an answer.

Polarized Quark and Gluon Distributions in the Nucleon

- Quark singlet and non-singlet helicity distributions
  - ⋆ Well-defined (textbook examples)
  - ⋆ Measured for $0.008 < x < 0.70$ with varying precision by SLAC, EMC, SMC, Hermes. . .
- Gluon distribution is well defined (despite controversy of 1990's)
  - ⋆ Gluon distribution unknown except for indirect effect on evolution of $g_1(x, Q^2)$
  - ⋆ Gluon spin may account for a significant fraction of the nucleon's angular momentum

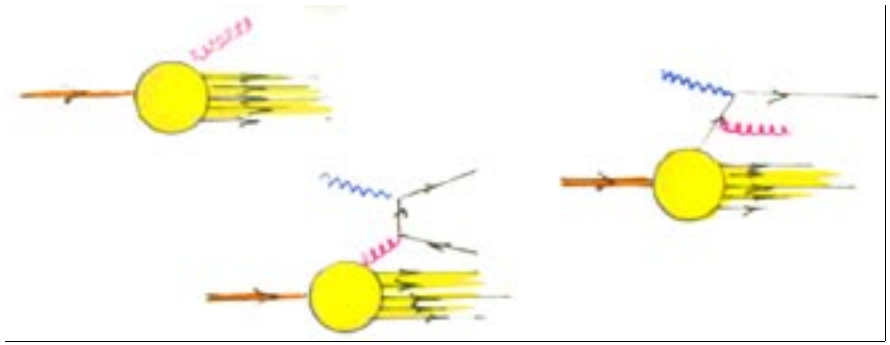

The Gluon Distribution

$$\Delta G\,(x_{\rm bj}, Q^2) \;=\; i\int \frac{d\xi^-}{4\pi x_{\rm bj} P^+}\, e^{i x_{\rm bj} P^+ \xi^-} \otimes \langle PS|\, F^{+\lambda}(0)\mathcal{I}(0,x^-)\tilde{F}^+_\lambda(\xi^-)\Big|_{Q^2}|PS\rangle$$

Manohar

- ⋆ where $\mathcal{I}(0,\xi^-) = \mathbf{P}\{e^{i\int_0^{x^-} dy^\mu A_\mu(y)}\}$
- ⋆ and $\tilde{F}_{\mu\nu} = \frac{1}{2}\epsilon_{\mu\nu\lambda\tau}F^{\lambda\tau}$
- ⋆ Define first moment Analytic continuation in n equivalent to direct integration of $\Delta G(x_{\rm bj})$

$$\Delta G(Q^2) = \frac{1}{2P^+}\int d\xi^-\epsilon(\xi^-)\langle PS|\, F^{+\lambda}(0)\mathcal{I}(0,x^-)\tilde{F}^+_\lambda(\xi^-)\Big|_{Q^2}|PS\rangle$$

where $\epsilon(x) = \begin{cases} 1 & \text{for } x>0 \\ -1 & \text{for } x<0 \end{cases}$

- ⋆ So in general gauges, the operator corresponding to gluon spin is nonlocal!
- ⋆ However, in $A^+ = 0$ gauges it reduces to local operator

$$\Delta G \xrightarrow{A^+=0} \frac{1}{P^+}\langle PS|A^1F^{+2} - A^2F^{+1}|PS\rangle$$

- ⋆ Identical to generator M_G^{+12} obtained from symmetry analysis, which confirms parton analysis.
- ⋆ Also identical to anomalous (Kogut-Susskind) current in $A^+ = 0$ gauge, which explains mistaken identification of ΔG with anomalous current.

- Measure $\Delta G(x_{\rm bj}, Q^2)$
  - ⋆ Attempts to extract ΔG are inherently limited because ΔG only enters DIS in higher order.
    - sensitive only to low moments
    - highly parameterization dependent
    - miss structure – eg. nodes?
  - ⋆ Directly by studying
    - two jet
    - two hadron
    - $c\bar{c}$ production in $e\,\vec{p} \to e'$ hadrons X
  - ⋆ By studying gluon scattering processes at $\overrightarrow{\text{RHIC}}$
    - Prompt photon production
    - Hadron production at high $p_\perp$ including π production.
    - $\vec{p}\,\vec{p} \to$ jet jet X
    - $\vec{p}\,\vec{p} \to \chi_2\; X$ and other charmonium channels

HERMES Azimuthal Asymmetry and Transversity!

Observations

- Azimuthal asymmetry observed at HERMES in $e\vec{p} \to e'\pi X$ with target polarization parallel to lepton beam.

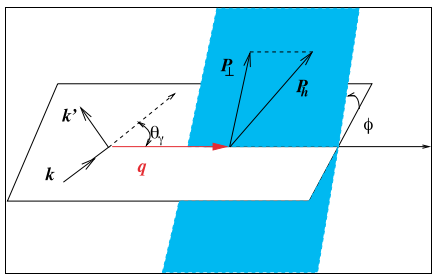

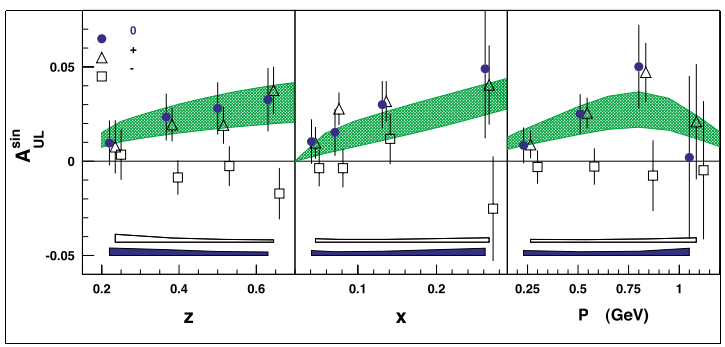

Note approximate with u-quark dominance. Should be $\pi^+ : \pi^0 : \pi^- :: 2 : 1 : 0$. Data show $\pi^+ \sim \pi^0 \gg \pi^-$

Important implications

- Collins angle asymmetry in DIS

  A leading twist effect expected to probe transversity in transversely polarized targets.

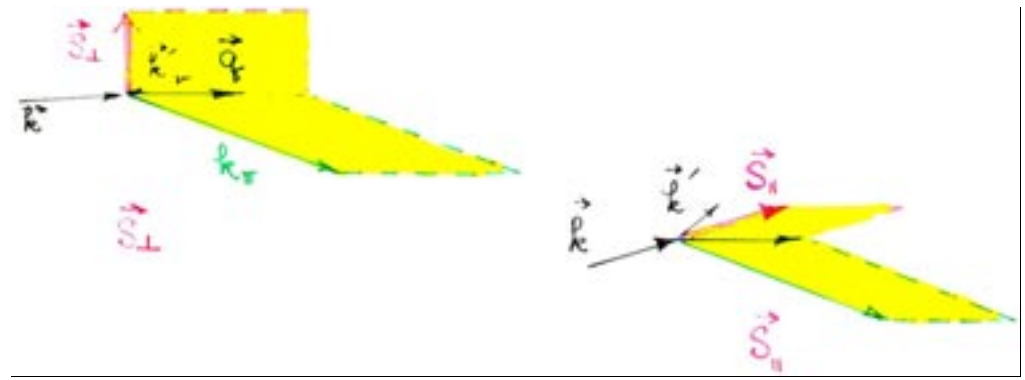

$$\vec{k}_\pi \times \vec{q} \cdot \vec{s}$$

- Collins fragmentation function: $C(z) = H_1^\perp(z)$ measures $\ell = 1$ correlation function between pion and fragmenting quark's transverse spin.

- Collins function is chiral-odd and therefore selects chiral odd distribution functions in the QCD factorized description of single particle electroproduction:

DISTRIBUTION
$\otimes$
HARD-SCATTERING
$\otimes$
FRAGMENTATION

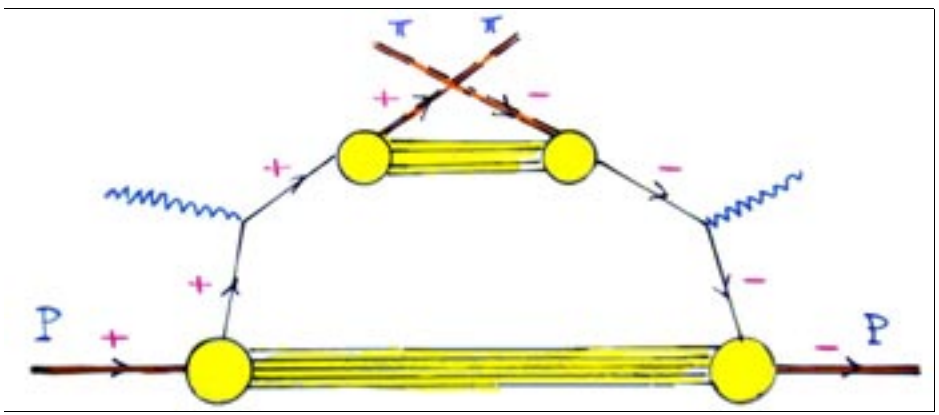

- So – IF HERMES is seeing the Collins asymmetry – then it is a new and very valuable tool for studying chiral odd distribution functions, notably the TRANSVERSITY

A dose of skepticism

- The Collins effect is time-reversal odd ($\vec{k} \times \vec{p} \cdot \vec{s}_\perp$) would vanish in the absence of a strong final state interaction phase $\equiv$ a phase between π and X. Must survive summation over unobserved X!!
- HERMES effect is observed with a longitudinally polarized target, for which the Collins effect is kinematically suppressed to twist three and competes with other twist three azimuthal asymmetries. It's not clear which effect is being seen at HERMES.
- Final state phase space at HERMES is not large. Assumption of factorization can be questioned.

A dose of enthusiasm

- The effect was predicted by theorists. Korotkov, Nowak & Oganesian hep-ph/0002268
- Data shows $\approx$ pion charge systematics expected from u-quark dominance.
- E704 is also a twist-three effect and large.

Tests in the future

Fortunately there are several immediate tests of the Collins function interpretation of the HERMES asymmetry which can be carried out at existing facilities.

- Turn the HERMES target transverse: then the Collins asymmetry is leading twist and should be confirmed. However: Transverse asymmetry could differ from longitudinal symmetry by twist three effects. So there is no *a priori* connection between $\parallel$ and $\perp$.

- Look for Collins asymmetry in at BELLE. If factorized QCD explanation of HERMES asymmetry is correct, then $e^+e^- \to (\pi^+X)(\pi^-X')$ MUST show a similar azimuthal correlation. (cf. M. Grosse-Perdekamp and RIKEN/BNL collaboration).

- Why care? No one knows how to understand Collins asymmetry or what it tells us about QCD. Its utility lies in its ability to filter for transversity. It can be used to extract the quark transversity distribution in the nucleon using DIS and $\vec{p}\vec{p}$.

What is the quark transversity distribution in the nucleon? $-\ \delta q(x, Q^2)$

- Transverse spin at leading twist $\equiv$ *transversity*
  - Twist-2, dominant parton distribution, on the same footing as $q(x)$, $\Delta q(x)$ but so far unknown!
  - Inaccessible in inclusive DIS
  - Expected to be roughly the same magnitude as $q(x)$ and $\Delta q(x)$
  - Attempts to measure δq require more sophisticated QCD analysis of parton processes
  - Must be measured in processes with at least two hadrons

- Recent extensive review of transversity: Transverse Polarization of Quarks in Hadrons. Barone, Drago, &Ratcliffe hep-ph/0104283

- Sketch of transversity
  - Requires transverse polarization.
  - Soffer's Inequality $|2\delta q^a| \leq q^a + \Delta q^a$
  - Normalization – tensor charges δq_a

$$\int_{-1}^{1} dx \delta q_a(x, Q^2) \sim \langle PS_\perp | \bar{q} \frac{\lambda_a}{2} \sigma^{0\perp} \gamma_5 q | PS_\perp \rangle \Big|_{Q^2}$$

From lattice studies:

$\delta q(\mu^2 = 2\text{GeV}^2) = 0.56 \pm 0.09$hfillS. Aoki et al., hep-ph 9608115

$\delta q(\mu^2 = 4\text{GeV}^2) = 0.76 \pm 0.0$ Göckeler et al., hep-ph 9711245

$\delta q(\mu^2 = ?\text{GeV}^2) = 0.31 \pm 0.12$ Blum, Ohta, & Sasaki, hep-lat 0011011

Compare experiment $\Delta q_{\text{EXPT}} \approx 0.2 \pm 0.1$

Transversity appears to be more "quark-model–like", valence dominated. . .

  - Models typically $\delta q \sim \Delta q$ at the input scale Q_0^2
  - Evolution: No gluonic transversity, all anomalous dimensions are positive $\Rightarrow$

δq evolves rather quickly to zero with increasing Q^2

The Structure of the Angular Momentum

What can be measured?

- Interesting theoretical questions: Hope to access quark orbital angular momentum forces one to consider off-forward parton distributions.
- Experimental hopes on Deeply Virtual Compton Scattering, which is a low energy (JLAB?) process.
- In some sense

$$\begin{aligned} \frac{1}{2} &= \int_0^1 dx \left[\tfrac{1}{2} \Delta\Sigma(x, Q^2) + \Delta G(x, Q^2) \right. \\ &+ \left. \mathcal{L}_Q(x, Q^2) + \mathcal{L}_G(x, Q^2) \right] \end{aligned}$$

- After considerable struggle, we know
  - What $\Delta\Sigma(x, Q^2)$ is and have measured it.
  - What $\Delta G(x, Q^2)$ is and how to measure it

- No useful angular momentum sum rule.

  - ⋆ Partonic formulation

    Bashinsky& Jaffe, Hagler& Schafer

    Harindranath & Kundu

    Standard parton densities of gauge invariant observables in Bjorken-x.

    Unfortunately $\mathcal{L}_Q$ and $\mathcal{L}_G$ cannot be measured.

  - ⋆ Rest Frame (DVCS) formulation

$$\frac{1}{2} = \frac{1}{2}\Delta\Sigma(Q^2) + L_Q(Q^2) + J_G(Q^2)$$

Ji, Hoodbhoy & Ji

$\Delta\Sigma$ is integral of usual DIS quark spin distribution

L_Q is measureable in DVCS, but is not integral of $\mathcal{L}(x)$

J_G cannot be decomposed into orbital and spin pieces in a gauge invariant way.

Recent Excitement from RHIC ($\vec{p} \cdot \vec{p}$)

Gerry Bunce & Thomas Roser

We have just completed the first run with polarized proton collisions in RHIC, as well as the first-ever run colliding polarized protons at high energy. A lot of hard work has led to an excellent first run–congratulations to all! Here is a summary of where we think we got to in the spin run, which ended at 6am Friday Jan. 25.

The run included the new high intensity polarized source, additional forward arms for the AGS polarimeter for low energy measurements, AGS tools for polarization (partial Siberian Snake, rf dipole, AGS pp polarimeter), 4 Siberian Snakes in RHIC, first pp collisions in RHIC, 2 p-carbon CNI polarimeters in RHIC (each ring), spin-flipper (rf dipole in RHIC), work on greatly reduced orbit variations in RHIC and device to control betatron tune on ramp.

For the experiments, the run included STAR: commissioning new forward π^0 calorimeter, beam-collision counters, and emcalorimeter modules and high tower energy trigger; PHENIX: commissioning additional beam counters and new triggers, including high-p_T π^0, charged particle, and muon triggers, DAQ with 1 kHz rate for these triggers; luminosity scalers sorted by crossing and by spin type; pp2pp Experiment: 2 Roman Pot stations (4 pots) with silicon tracking for pp elastics, and beam-beam inelastic counters; test setup near 0 degrees to measure asymmetries of photons and neutrons produced very forward ("photon polarimeter").

Polarized source: regularly had above 70% polarization, and intensity of several $\times 10^{11}$ polarized protons per pulse.

AGS Polarization: after tuning Booster, got full polarization into AGS at injection; ramp used backup motor generator, with half the normal ramp rate, increasing spin resonance strengths in AGS by factor 2; achieved typical polarization of 25% to 30% at extraction to RHIC in last 2 weeks.

RHIC Polarization: measured full polarization in RHIC at injection; measure polarimeter asymmetries between $80\% - 100\%$ of injection asymmetry at 100 GeV; in most cases, asymmetry after ramp to 100 GeV is maintained over multi-hour stores (8 hours frequently). A 14 hour store for the pp2pp Experiment which ended had the same measured polarization at the end as at the beginning (25%).

RHIC Luminosity: typically at goal with $\beta^* = 3m$ focus, 1.5×10^{30} cm^{-2} s^{-1}, in last 2 weeks of run. Decided not to squeeze to $\beta^* = 1$m due to lack

of time left in run. This luminosity uses 4×10^{12} polarized protons in 55 bunches in each ring, with alternating polarization in each bunch.

RHIC Polarimetry: p-carbon Coulomb Nuclear Interference polarimeter typically measured $2 - 3 \times 10^{-3}$ asymmetries with statistical error of 10% of itself, in 1 minute. $A_{raw} = 0.003$ corresponds to about 25% polarization.

Absolute polarization: known only at 24 GeV. Plan to accelerate to 100 GeV, and then to decelerate back to 24 GeV to carry known analyzing power from 24 GeV to 100 GeV was not completed. Beam lost at about 50 GeV on downramp–need measurements of transfer functions of magnets for this cycle.

Spin flipping in RHIC: successful, flipped spin twice in test.

Betatron tune control: succeeded with several ramps locking the tune. (Important, since the tunes must be controlled closely to maintain polarization. This was done successfully by hand for most of this run. Measured loss of polarization typically traced to changes in tunes.)

Vertical polarization: used for entire run. No longitudinal spin was tried due to lower polarization (2-spin asymmetries such as A_{LL} have figure of merit $P^4 \times L$.).

Experiments: data were taken for A_N for the following (this list is partial; successful measurements require successful control of systematic errors, yet to be studied by the experiments):

For $\sqrt{(s)} = 200$ GeV pp:

- very forward (p_T up to 0.5 GeV/c, x_F above 0.2) photon, neutron, π^0 A_N
- forward (p_T 1 to 2 GeV/c or so, x_F above 0.2) photon, π^0 A_N
- forward muons A_N
- mid-rapidity π^0, jets, photons, electrons, charged hadrons, p_T to 8 GeV/c or so A_N
- proton-proton CNI A_N and slope

For fixed target using polarimeter with carbon fiber target:

- proton-carbon CNI A_N and slope vs. t for $-t = .005 - .04$

First looks at these reactions show good signals for the processes, and possible physics asymmetries.

To summarize, we believe (or hope!) there will be a number of excellent A_N measurements at root(s)=200 GeV, using the first ever collisions of polarized protons. The AGS polarization was low, at least partly due to using a back up motor generator with a slow ramp. We did not do longitudinal polarization, due to the lower polarizations. The commissioning was very successful, including sustained use of the high intensity polarized H^- source, use of alternating polarization sign bunches in RHIC for polarimetry and physics, many studies of AGS polarization issues, high transfer of polarization to RHIC and up to 100 GeV (although uncalibrated polarization at 100 GeV), tune control on ramp, maintaining polarization over long stores in RHIC (often 8 hours or more), spin-flipping in RHIC, luminosity at goal for $\beta^* = 3\text{m}$.

Experimental

Status

of

Spin DIS

GEHARD MALLOT
CERN

EIC 2002 BNL
28 FEBRUARY 2002

The Nucleon spin puzzle

- Nucleon spin:

$$\boxed{\frac{1}{2} = \frac{1}{2}\Delta\Sigma + \Delta g + \langle L_z \rangle}$$

$$\Delta q = q^{\uparrow} - q^{\downarrow} + \bar{q}^{\uparrow} - \bar{q}^{\downarrow}$$

- quarks spins: $\Delta\Sigma = \Delta u + \Delta d + \Delta s$
- gluons spins: Δg
- orbital angular momentum of q & g: L_z
- Naïve: $\Delta\Sigma = 1$

EMC 1987:

$$\boxed{\Delta\Sigma = 0.12 \pm 0.17}$$

$$\Delta s = -0.19 \pm 0.06$$

THE PLAYERS

All started 1972 at SLAC with E80 and E130!

SMC 1992–1996
CERN μ^+ beam: 100–190 GeV
targets: butanol, ammonia
twin target

SLAC 1992–1999, E142, E143, E154, E155, E155x
SLAC e^-: 28–48 GeV
targets: ^{3}He, butanol, ammonia, ^{6}LiD
rapid change of beam polarisation

Hermes 1995–
Desy $e^\pm$: 27 GeV
targets: ^{3}He, H, D; internal gas storage cell
rapid change of target polarisation

COMPASS 2001 -
CERN μ^+ 100 - 190 GeV
^{6}LiD, NH_3 increased acceptance, particle ID

Kinematic ranges

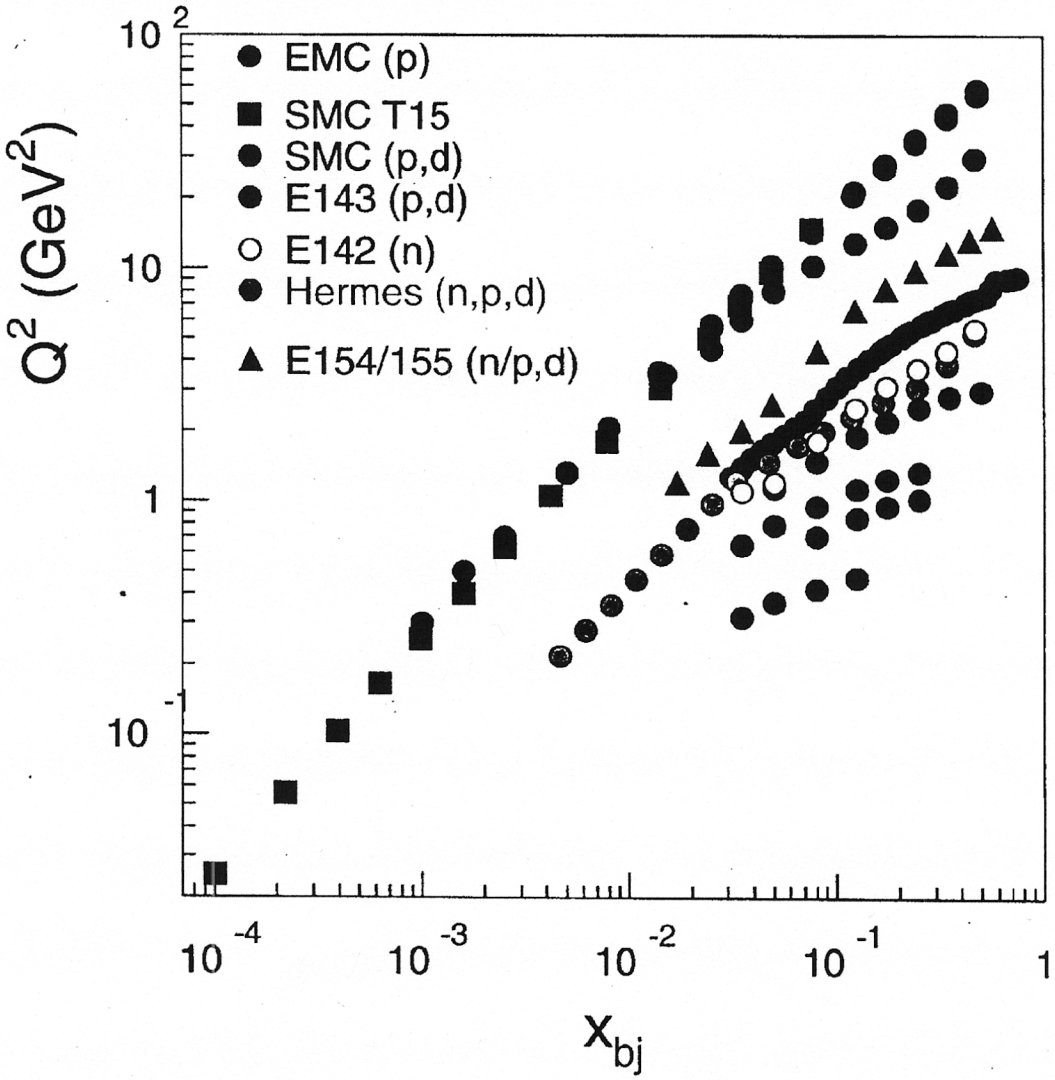

g_1^d/F_1^d WORLD DATA

- no Q^2 dependence visible
- execellent statistical precision

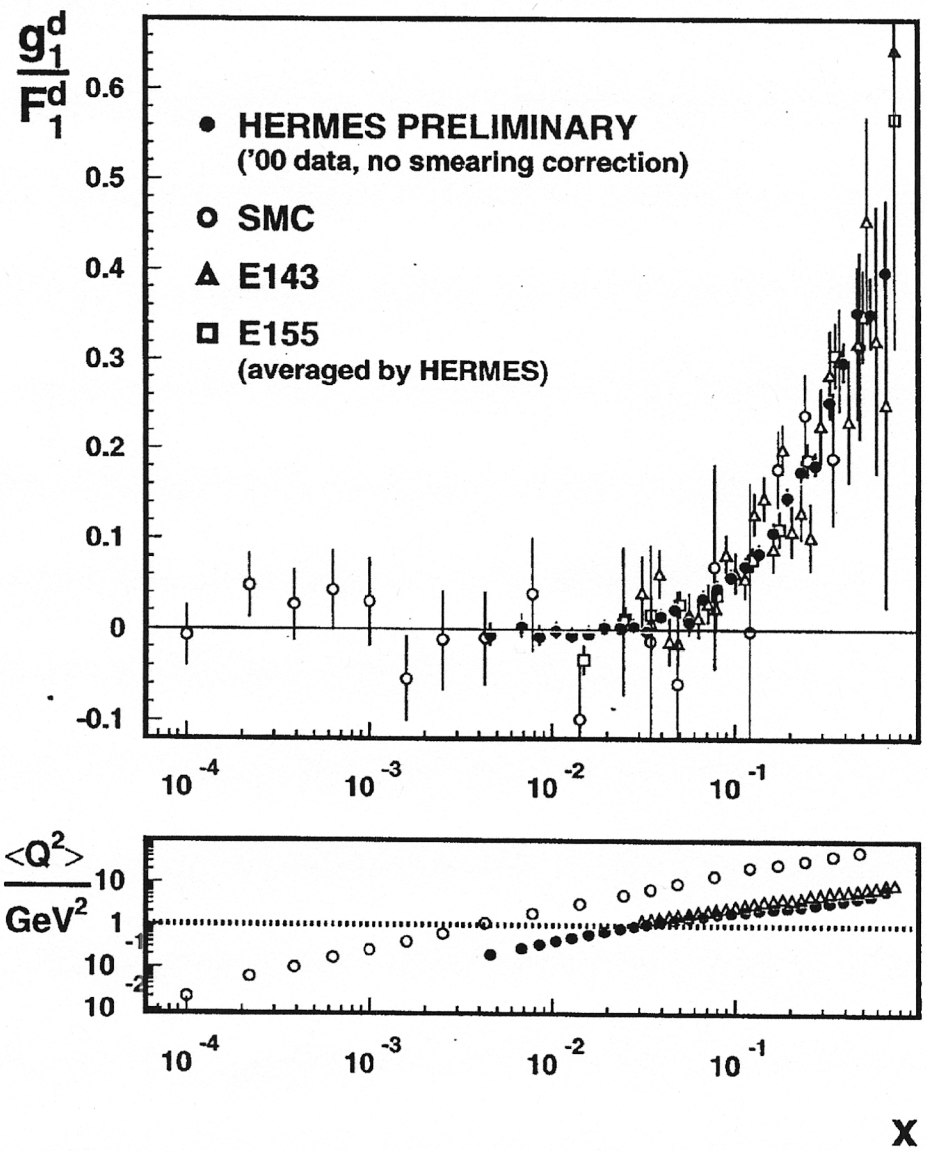

xg_1 WORLD DATA

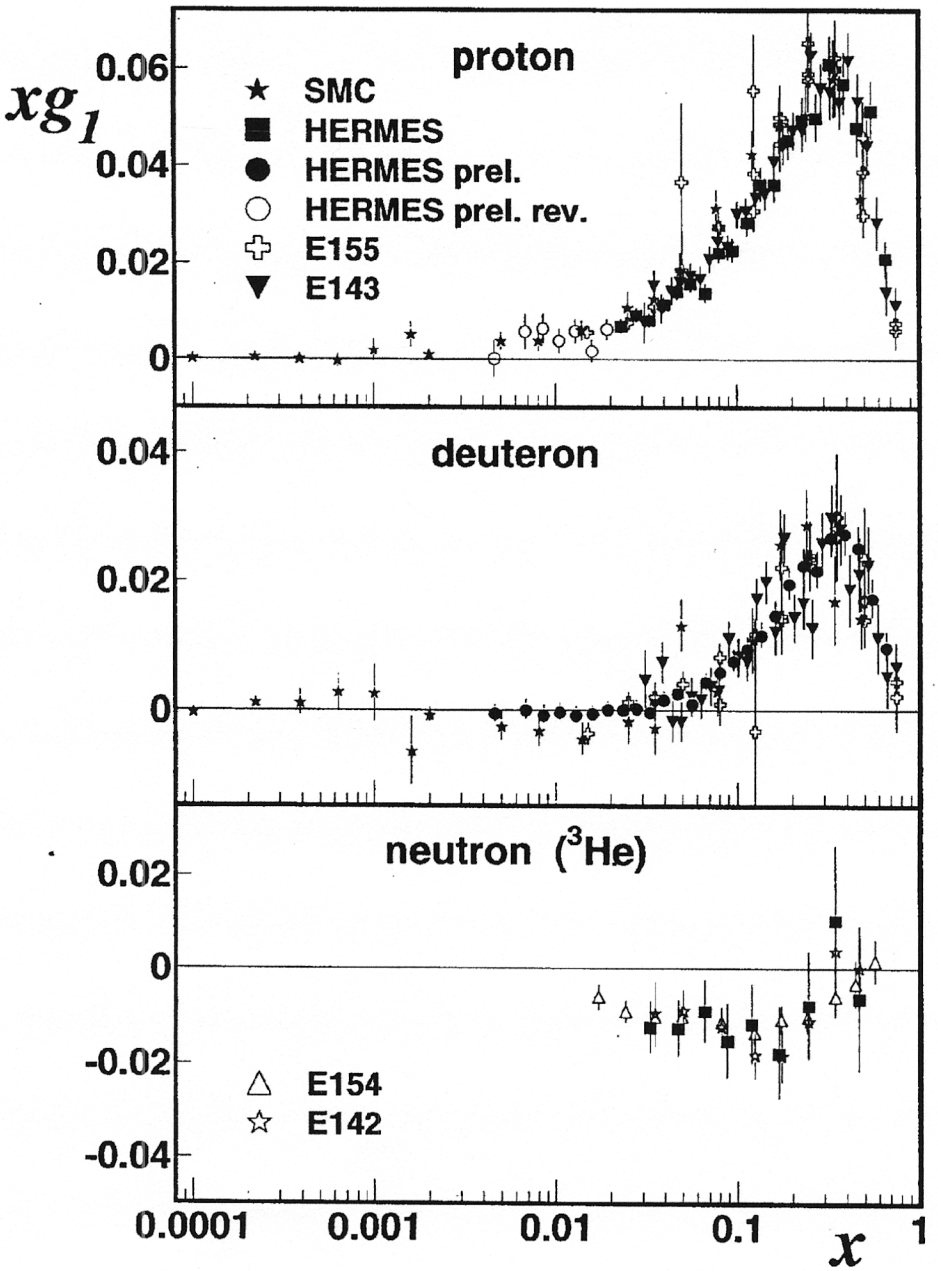

SMC NLO FIT

- distribution functions

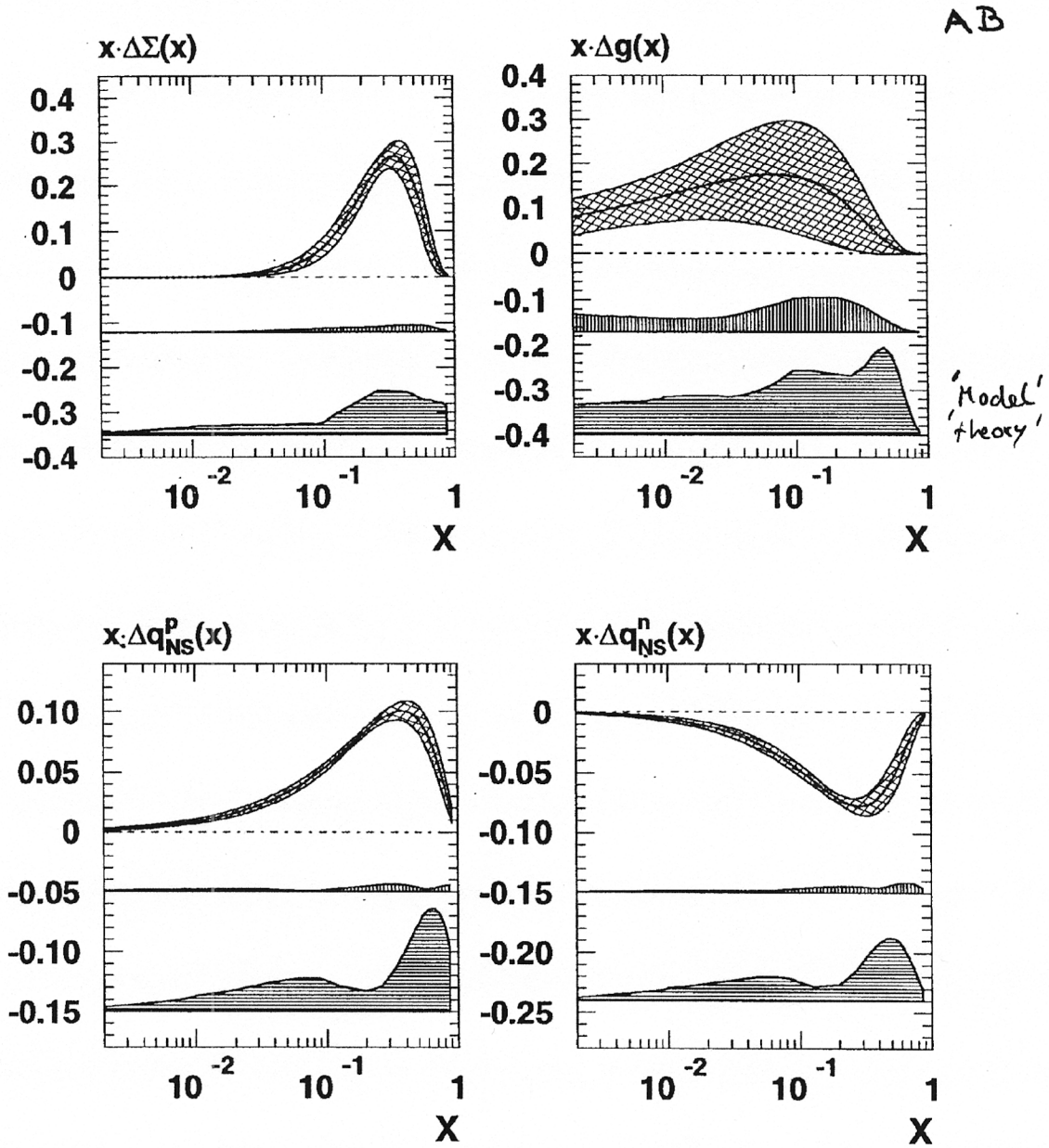

QCD Analyses

- Good Fits to data in NLO
- Δ u and Δ d well determined
- Δ g and Δ $\bar{s}$ hardly constrained
- Moments

  Δ g>0Preferred ~0.7 @ Q^2= 1 GeV^2

  $\Delta \Sigma_{AB} \cong 0.3 - 0.4$ AAC : uncertainty in Δ $\bar{q}$ jet at low x

  $a_0 \cong 0.1 - 0.2$

- Impact of recent data limited although excellent quality

  ⇒ More data in SLAC and HERMES kinematics will not improve Δ g, Δ $\bar{q}$ much

  ⇒ Needed: Data at large Q^2 and small x
  Direct measurements of Δ g and Δ s

STRUCTURE FUNCTION xg_2

- —— twist-2 term: g_2^{WW}
- -- -- bag model calculations

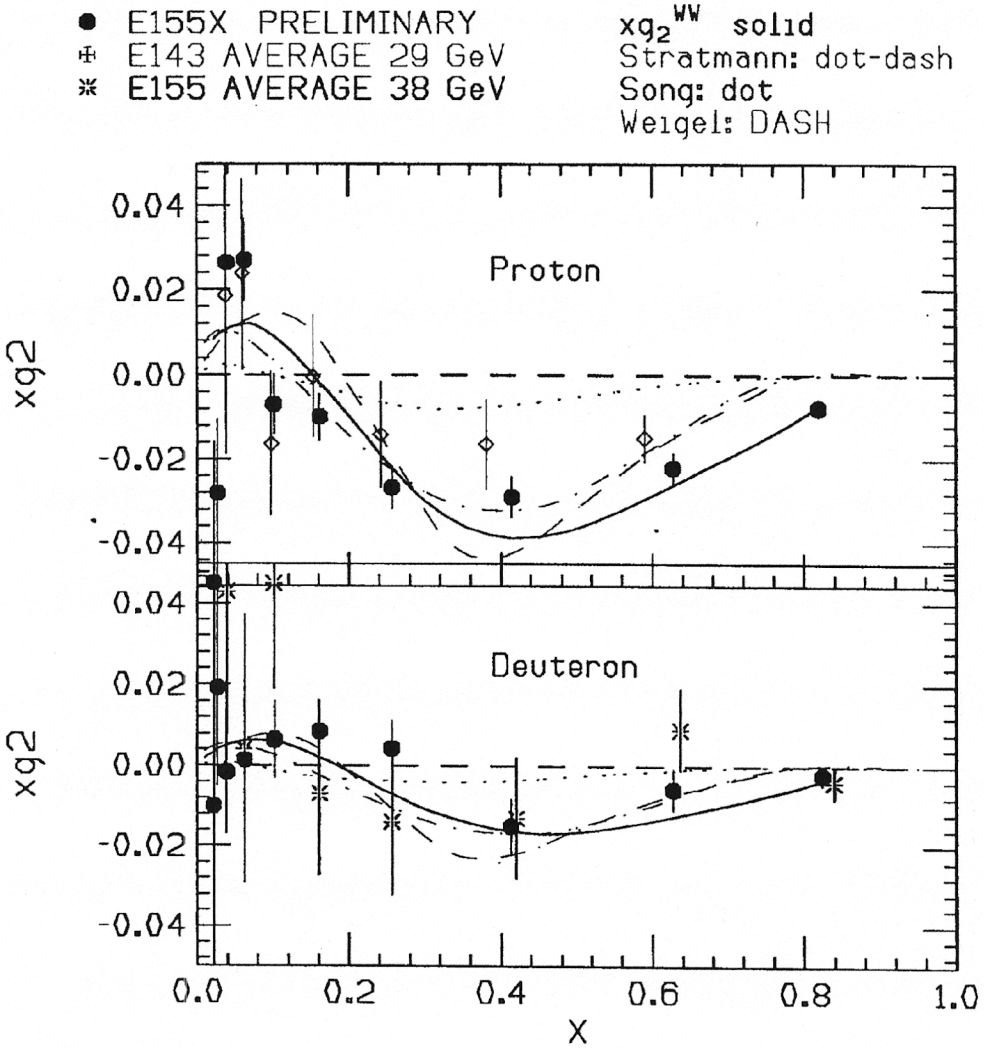

SEMI-INCLUSIVE ASYMMETRIES

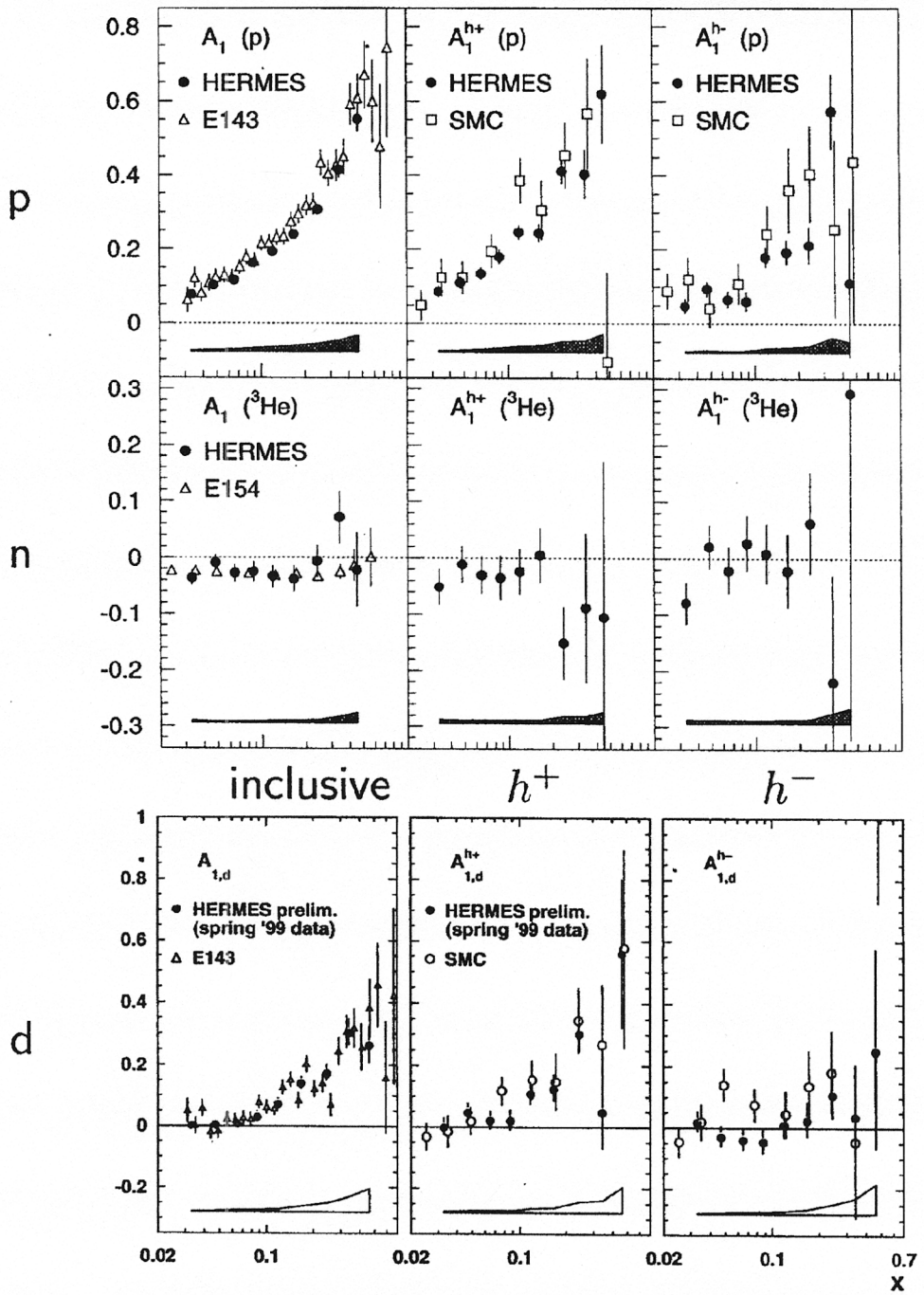

- low-x SMC data not shown

HINTS FOR TRANSVERSITY

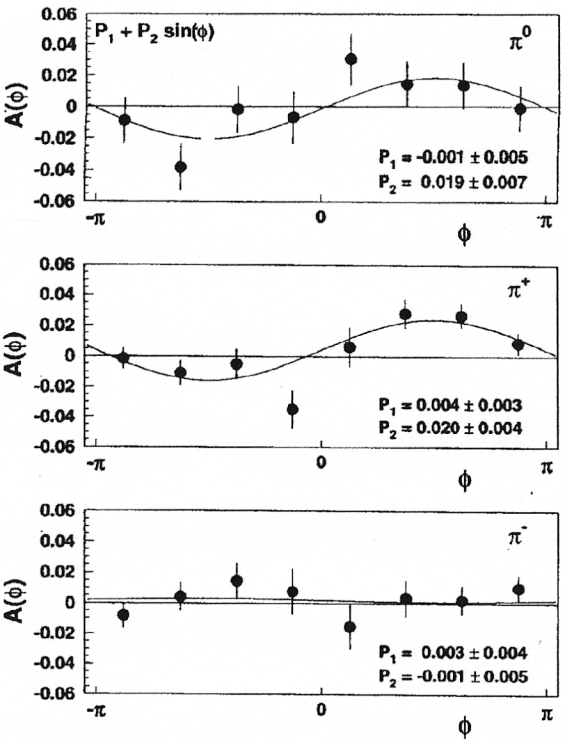

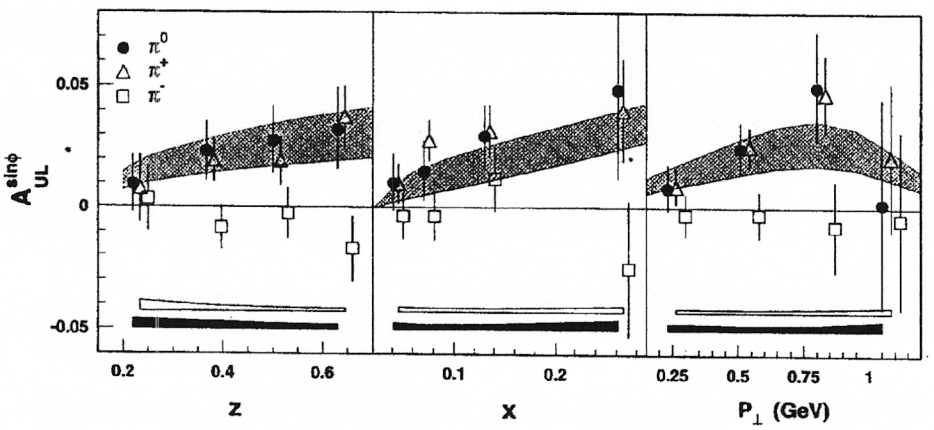

HIGH p_T h^+h^- & K^+K^- PAIRS

- Hermes preliminary 1996 – 2000

h^+h^-

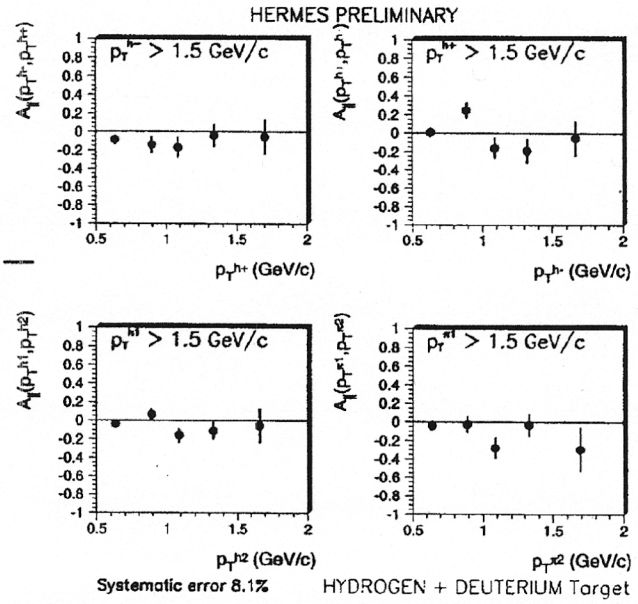

$\pi^+\pi^-$

K^+K^-

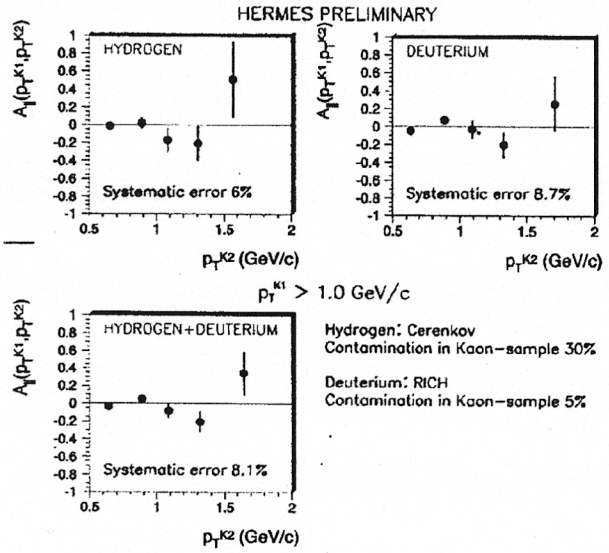

Observation of DVCS

- Hermes beam spin asymmetry in M_p region
  Missing mass spectrum and azimuthal distribution

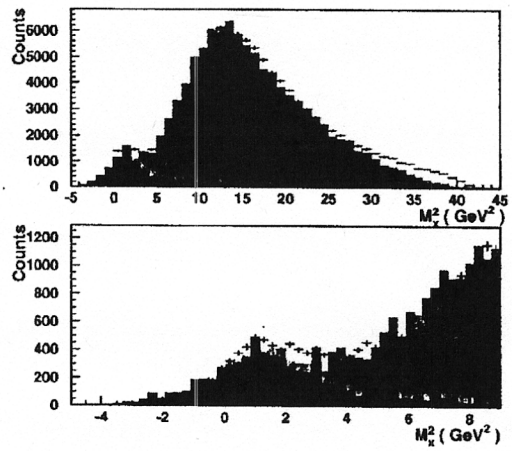

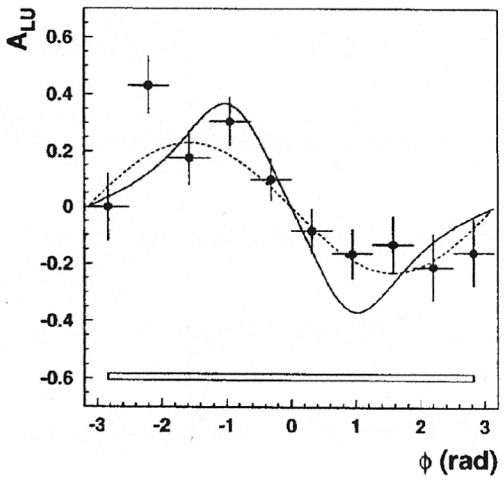

- Extract $\sin(\phi)$-moment, $A_{LU}^{\sin\phi} = \frac{2}{N}\sum_{i=1}^{N}\frac{\sin\phi_i}{(P_l)_i}$

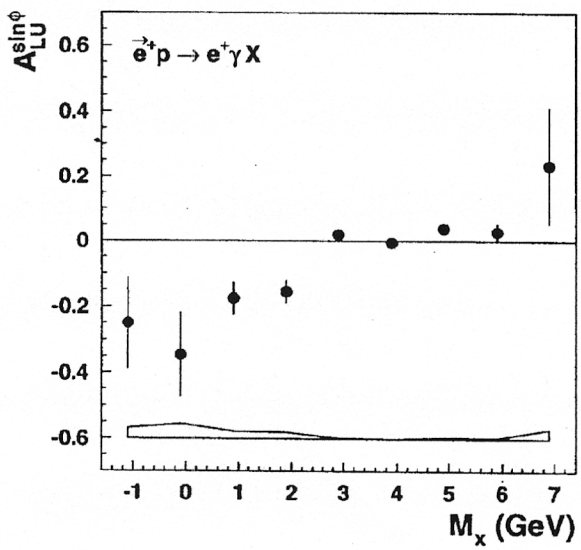

Hermes PRL87,182001

CLAS PRL87,182002

Status of the COMPASS experiment (tracking)

1998 Start of construction at CERN

2000 First stage of commissioning, few detectors

2001 Complete commissioning, first data taking

Status tracking detectors:

detector	# planes	fraction
SciFi	18	100 %
silicon	16	50 %
GEM	40	70 %
Micromegas	12	50 %
Drift	16	50 %
straws DL	15	27 %
MWPC	31	100 %
muon wall 1 DL†	8	10 %
muon wall 2 DL†	9	10 %

† prototype readout, inner muon identification by MWPC

Average:about 70 % operated in 2001!

COMPASS 2001 Data Taking

- Commissioning till October 10
- Smooth data taking for about two weeks with $2x10^8$ muons/spill, 160 GeV
- Complete 2001 – detector
- 14 TByte of data with 30 KByte/event
- About 500 M events collected
- Reconstruction started
- Computing farm with 200 CPU set up
- Well on track for 2002 data taking May 27-September 10.

Summary

- Excellent data on DIS: p, d, n
- Good description by QCD, however x, Q^2 of data too small range
- Δg and Δs are hardly constrained
- First glimpse of h_1
- Semi-inclusive Δu, Δd well determined

  $\Delta \bar{q}$: $\Delta \bar{u} - \Delta \bar{d}$, $\Delta \bar{s}$, Δs ?

  hardly constrained
- GPDs: seen tip of the iceberg!

  Cannot be mapped in the kinematic variables (combination, special values) measurable go exclusive
- New player, COMPASS on track for 2002

Experimental status of eA, μA, and pA physics

J. M. Moss, Los Alamos

EIC Workshop
Brookhaven 2/28/2002

What I will try to cover

eA, μA — mostly in the deep-inelastic region

pA — mostly to dileptons in the final state

Of the above — mostly nuclear dependence experiments

Outline

- History/sociology of early experiments
- Shadowing
- Quark energy loss
- Nuclear transparency revisited
- The pion cloud, spin, and isospin

Collaborations between nuclear and high-energy physicists in the 1980s

- The EMC effect

- Prospect of new facilities — CEBAF, RHIC, kaon factories

- new interests in electroweak experiments – rare decays, neutrinos

Facilities/Experiments

- SLAC, end-station spectrometers, E139, E140, NE*xx* series
- Fermilab

  E665: 500 GeV μ + A, DIS

  E772/E789/E866: 800 GeV p +A -> dimuons

  E769, E791, and others: A dependence of charm
- CERN-SPS

  EMC/NMC/SMC…: 100-200 GeV μ + A, DIS

  NA3, NA10, NA34…: 100-450 GeV p,π +A->dileptons

  WA82, WA92: A dependence of charm
- HERA:

  HERMES, 27 GeV e^+ + jet targets

demographics

During the 1980s and early 1990 nuclear physicists joined with particle physicists in the US and Europe to create new collaborations, refurbish and rebuild spectrometers, and create completely new experimental capabilities.

Most of the time, if the experimental vision was compelling enough, these collaborations were successful, and led to further experiments based on the original collaborating groups

Shadowing

- NMC data, early 1990s
- HERMES diffractive ρ^0 production
- 1990s, new developments in theory
  - Phenomenology of shadowing — connections to diffraction, impact of HERA data
  - Shadowing and energy loss combined for description of low-x Drell-Yan data

Shadowing in DIS

from Geesaman, Saito, Thomas ARNPS 45, 337 ('95)

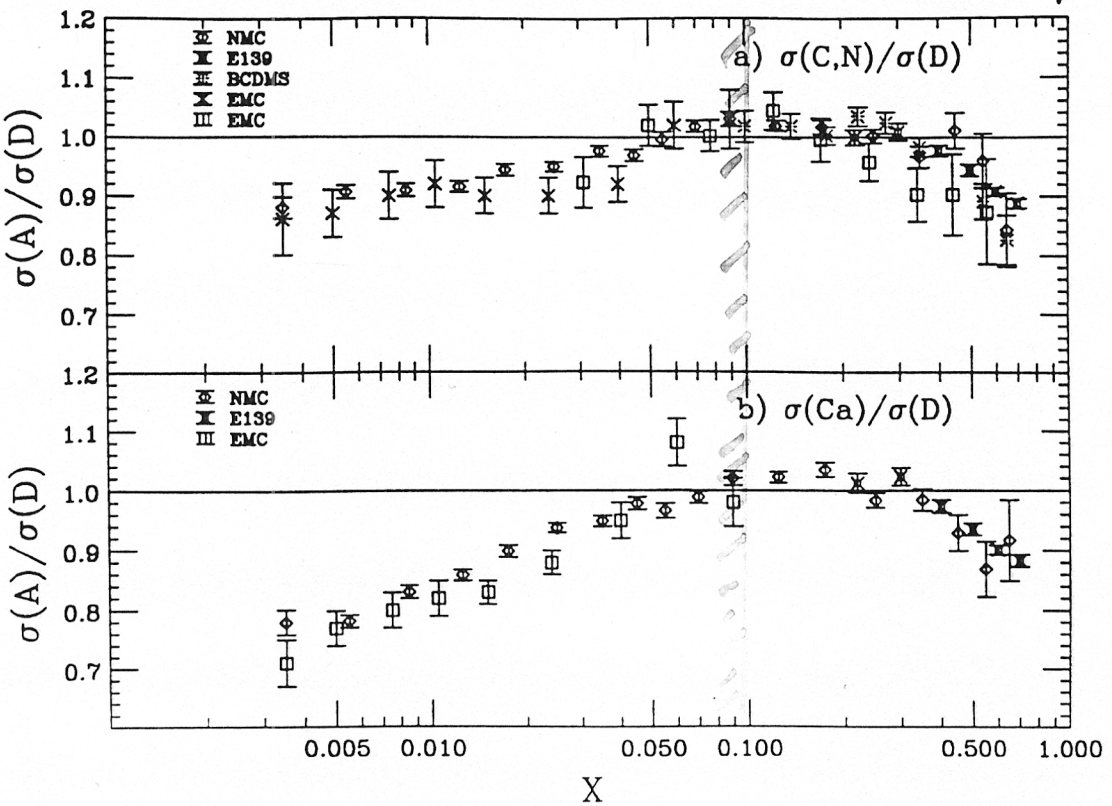

Figure 3 Ratios of the deep inelastic cross section on targets of (*a*) carbon and nitrogen and (*b*) calcium to those of deuterium (2, 6, 132, 138, 139).

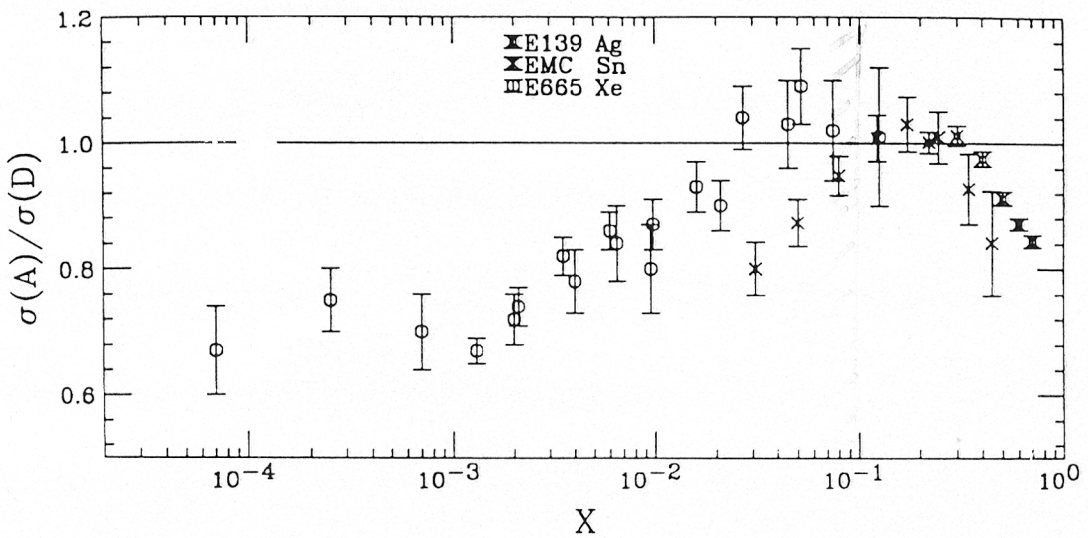

Figure 4 Ratios of the deep-inelastic cross section on targets of tin, xenon, and silver to those of deuterium (2, 6, 145, 146).

Shadowing I

Infinite momentum frame

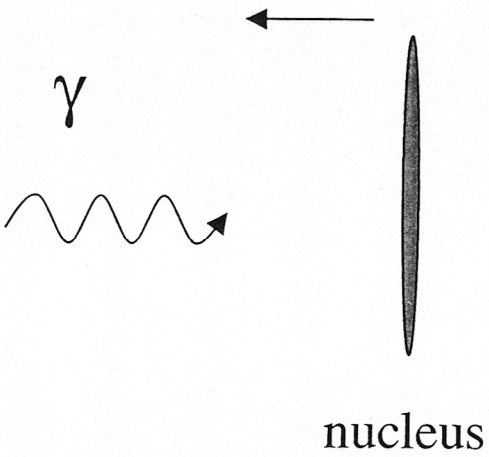

Inside the nucleus the inter-nucleon spacing is contracted

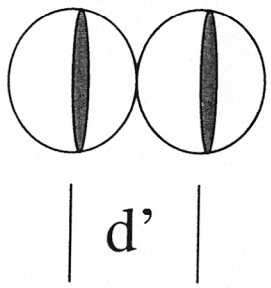

$d' = d(m_n/P)$

The longitudinal localization, δ, of partons is: $(\delta)(xP) \sim 1$

Thus partons from different nucleons overlap when $\delta > d'$

$$x < 1/d \bullet m_n$$

Shadowing II

Target rest frame

Focus on hadronic fluctuations of the photon

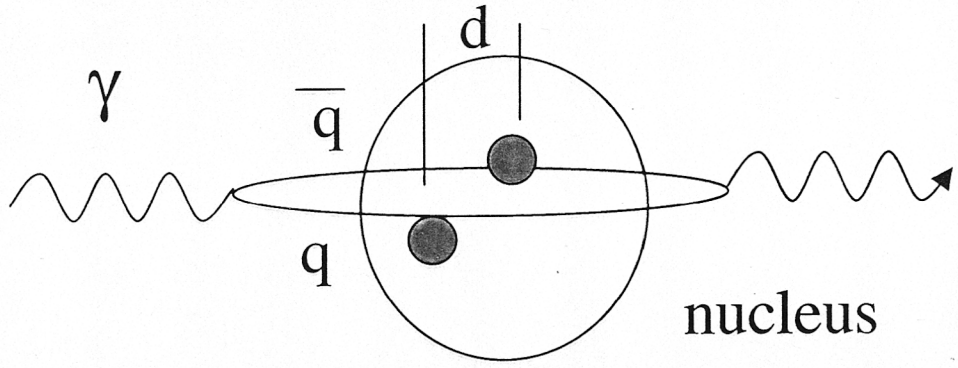

Coherence length of the fluctuation is $l_c \sim 1/x \bullet m_n$

Shadowing when $l_c > d$ $\qquad x < 1/d \bullet m_n$

Same physics?

Inf. Mom. frame: partons in the nucleus

Target rest frame: partons in the photon

Answer: yes/no

Yes: Shadowing: the suppression of a cross section on a heavy target must be, and is, Lorentz invariant.

No: Words and concepts that are used to describe the effect are not necessarily Lorentz invariant.

— target rest frame - No $\bar{q}$s !
Nayak, Peng, Raufeisen, preprint

--- CTEQ, standard $q\bar{q}$ Drell-Yan

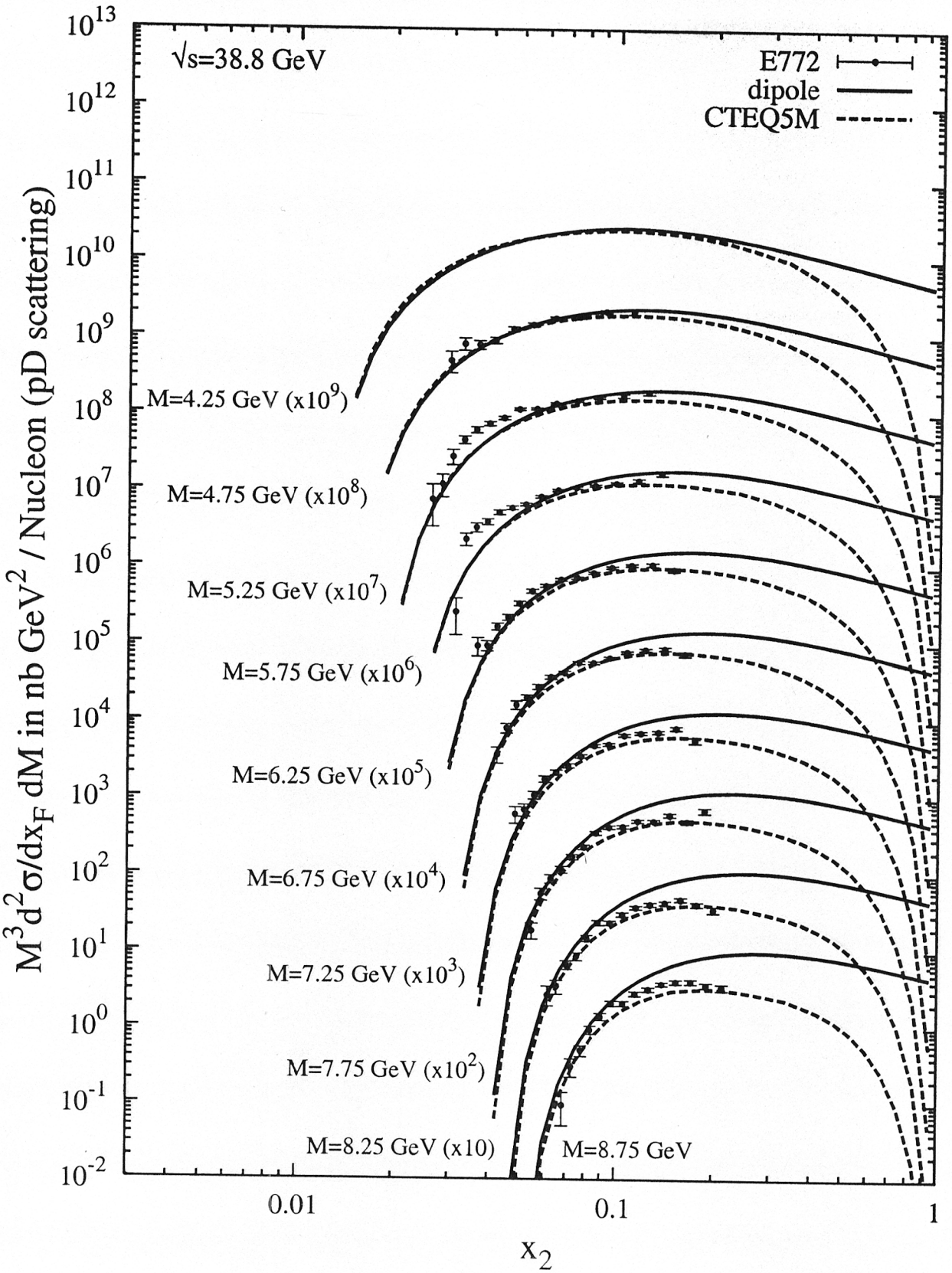

arXiv:hep-ph/9707466 v1 25 Jul 1997

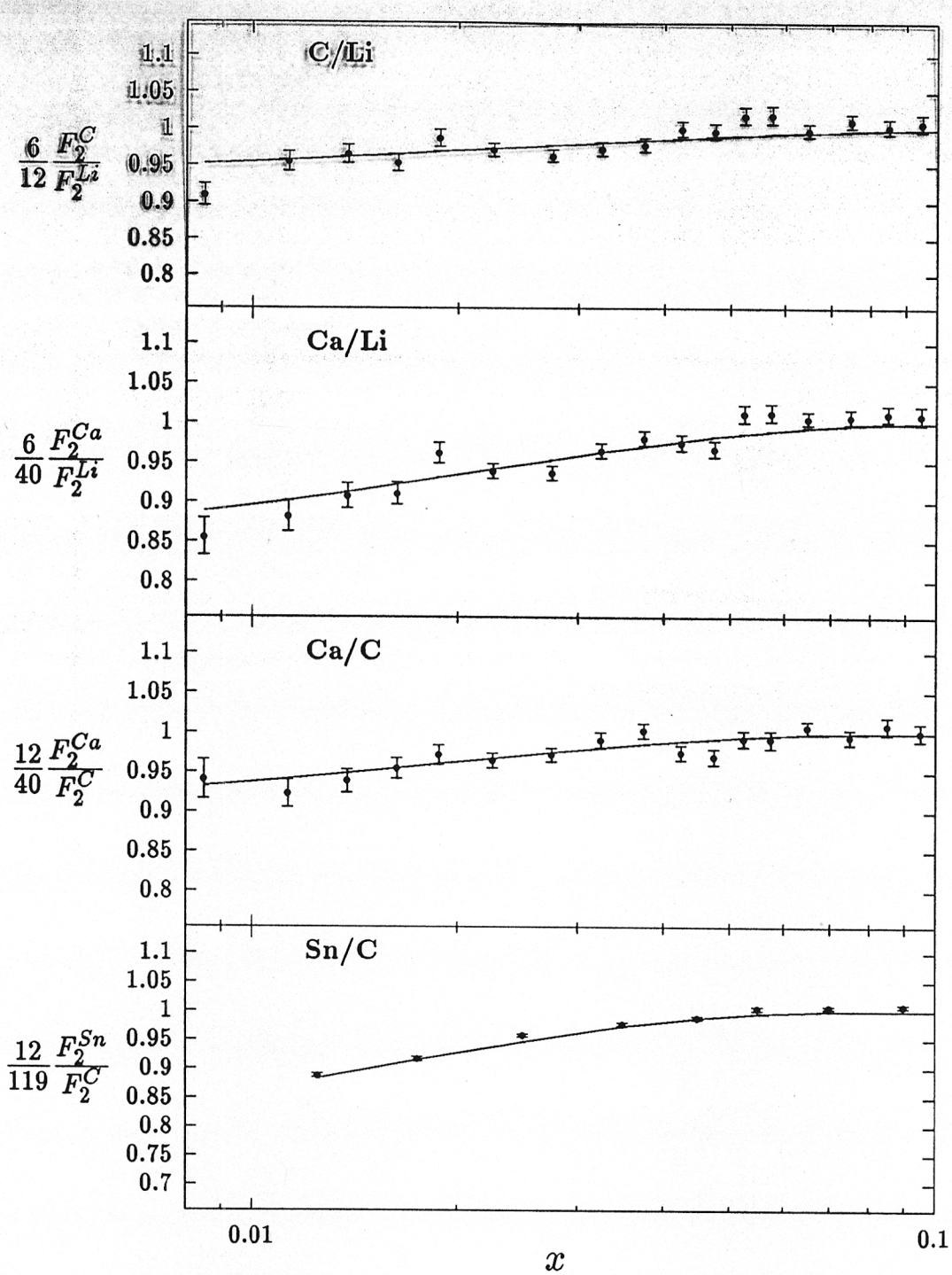

Fig. 4

Capella et al.

Uses $F_2^{Diffractive}$ determined by HERA data

Shadowing or energy loss in the DY process?

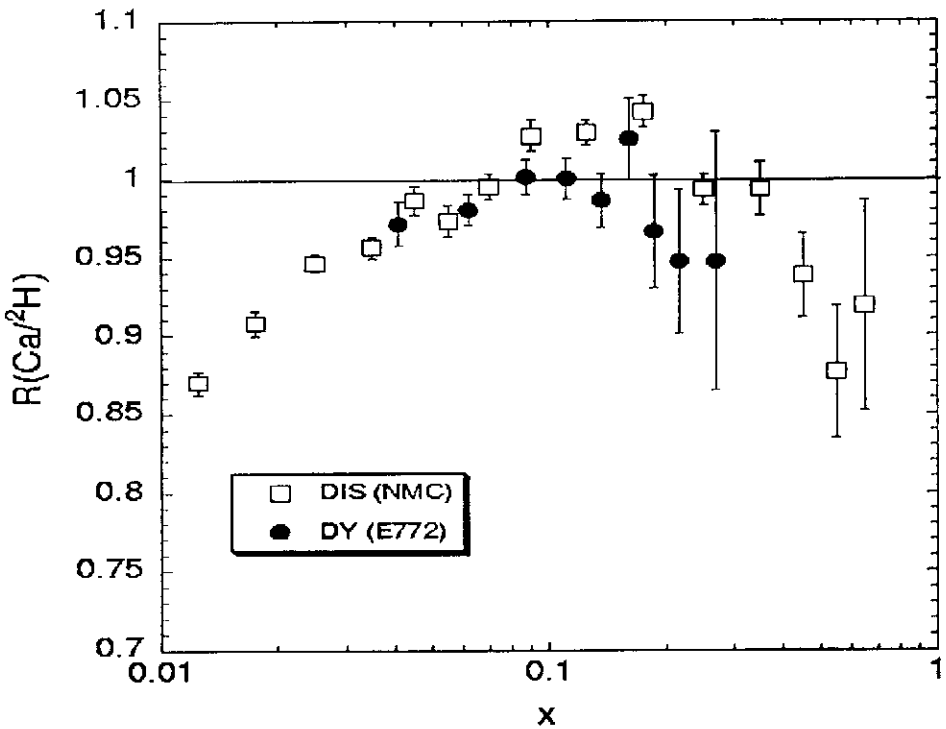

Vacuum energy loss of quarks: $-dE/dz = 2.73$ GeV/fm

Johnson et al, PR C 65, 025203(2002).

Induced energy loss – the LPM effect

- theoretical analysis 1990s -> $$-\frac{dE}{dz} = \frac{1}{4}\alpha_s N_c \langle p_t \rangle^2$$

Baier, Schiff, Zakharov, ARNPS 50, 37(2000)

- pt broadening for Drell-Yan exps. Indicate small effect: $-dE/dz_{max} \sim 0.2$ GeV/fm for W.

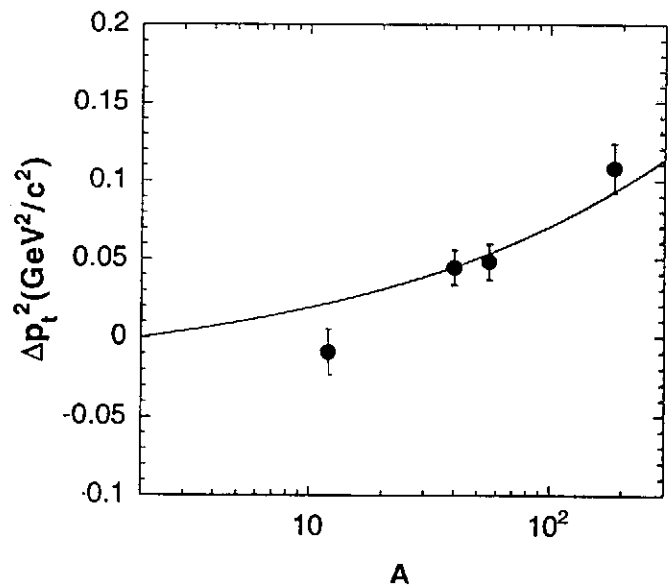

- "jet quenching" evidence from PHENIX gold-gold collisions.

E. Wang & X. N. Wang, hep-ph 0202105

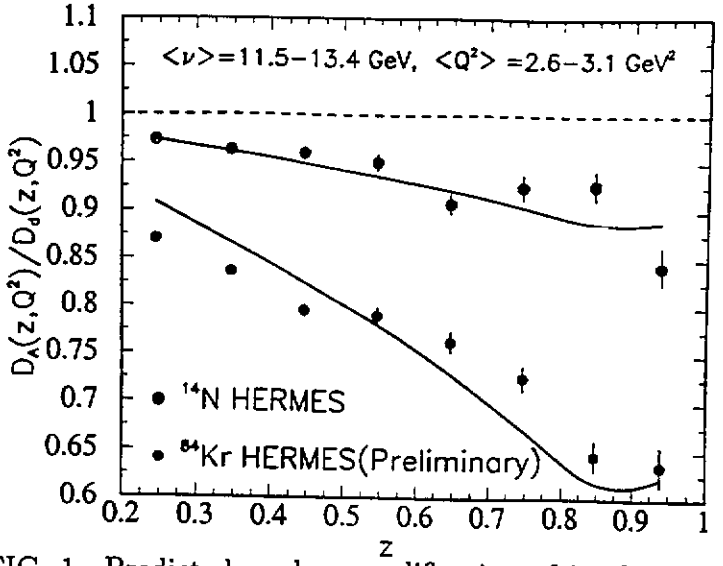

FIG. 1. Predicted nuclear modification of jet fragmentation function is compared to the HERMES data [10] on ratios of hadron distributions between A and D targets.

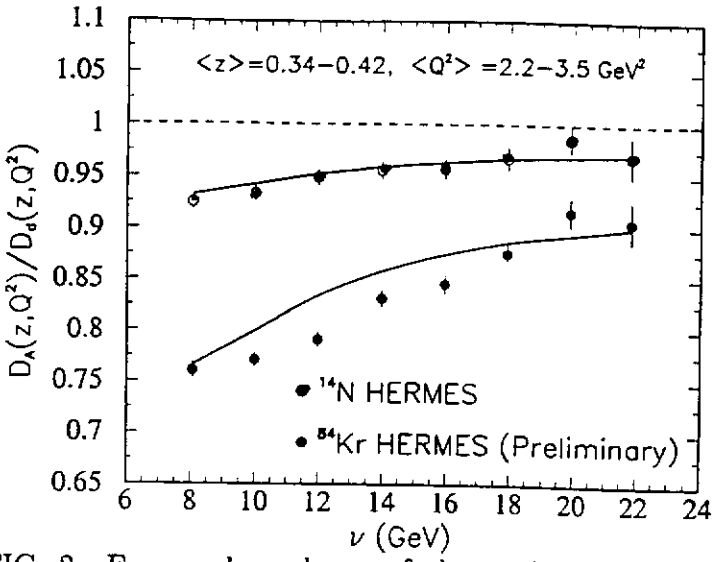

FIG. 2. Energy dependence of the nuclear modification compared with the HERMES data [10].

One parameter fit: quark-gluon correlation strength

But, $\tilde{C}$ can be related to $\langle p_t^2 \rangle$ found in Drell-Yan production

— Very good agreement —

$\tilde{C}\alpha_s^2 = 6.5\times10^{-3}$ (DY) ; $\tilde{C}\alpha_s^2 = 8.6\times10^{-3}$ (e,e'h)

Color transparency

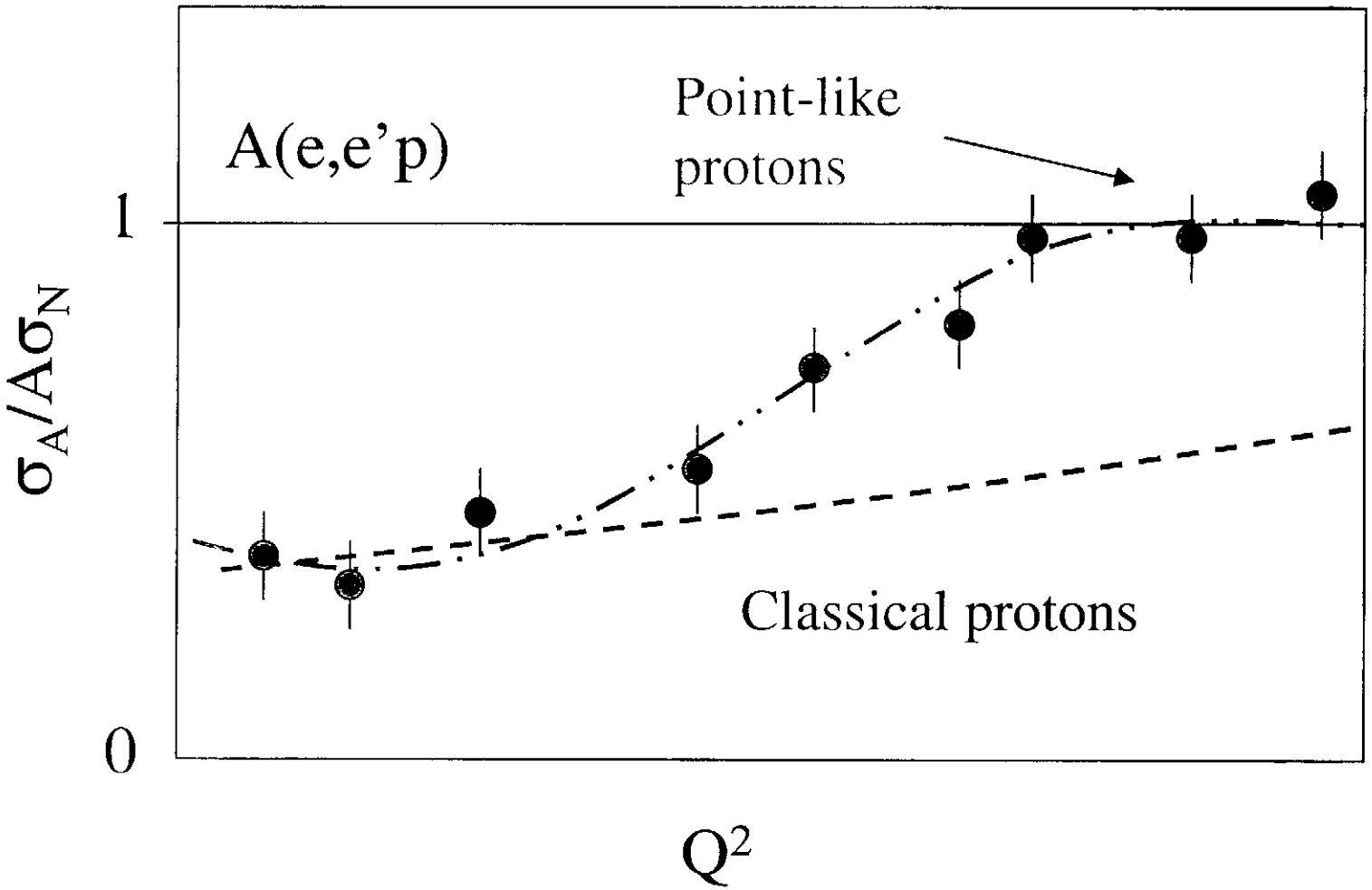

SLAC NE18 (1995)

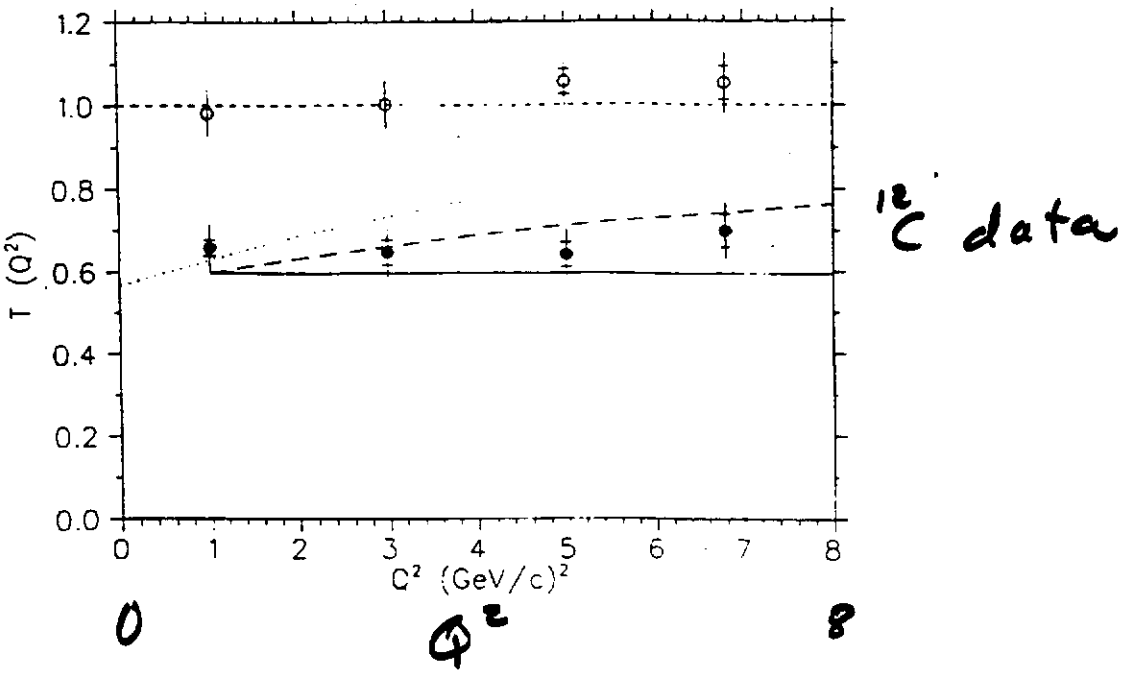

In summary, the ^{12}C$(e, e'p)$ cross section has been measured over the range $-25 < E_m < 140$ MeV and $0 < p_m < 250$ MeV/c in the momentum transfer range $Q^2 = 1$ to 6.8 (GeV/c)^2. This extends the Q^2 range of these measurements by over an order of magnitude. The distribution of strength is consistent with the impulse approximation for scattering from a single nucleon. The measured transparency ratios are essentially independent of Q^2, indicating the absence of large color transparency effects in this energy range.

Short history of color transparency

- 1980s theoretical concepts – Bertsch, Brodsky, Goldhaber, & Gunion; Mueller & Brodsky; Franfurt, Miller, & Strickman, Ralston et al., etc.

- late 1980s ~ 1995: experiments give negative or ambiguous results

- 2001, Fermilab E791: 500 GeV π^- —> dijets. scales as $A^{4/3}$

Diffractive dissociation of pions in nuclei

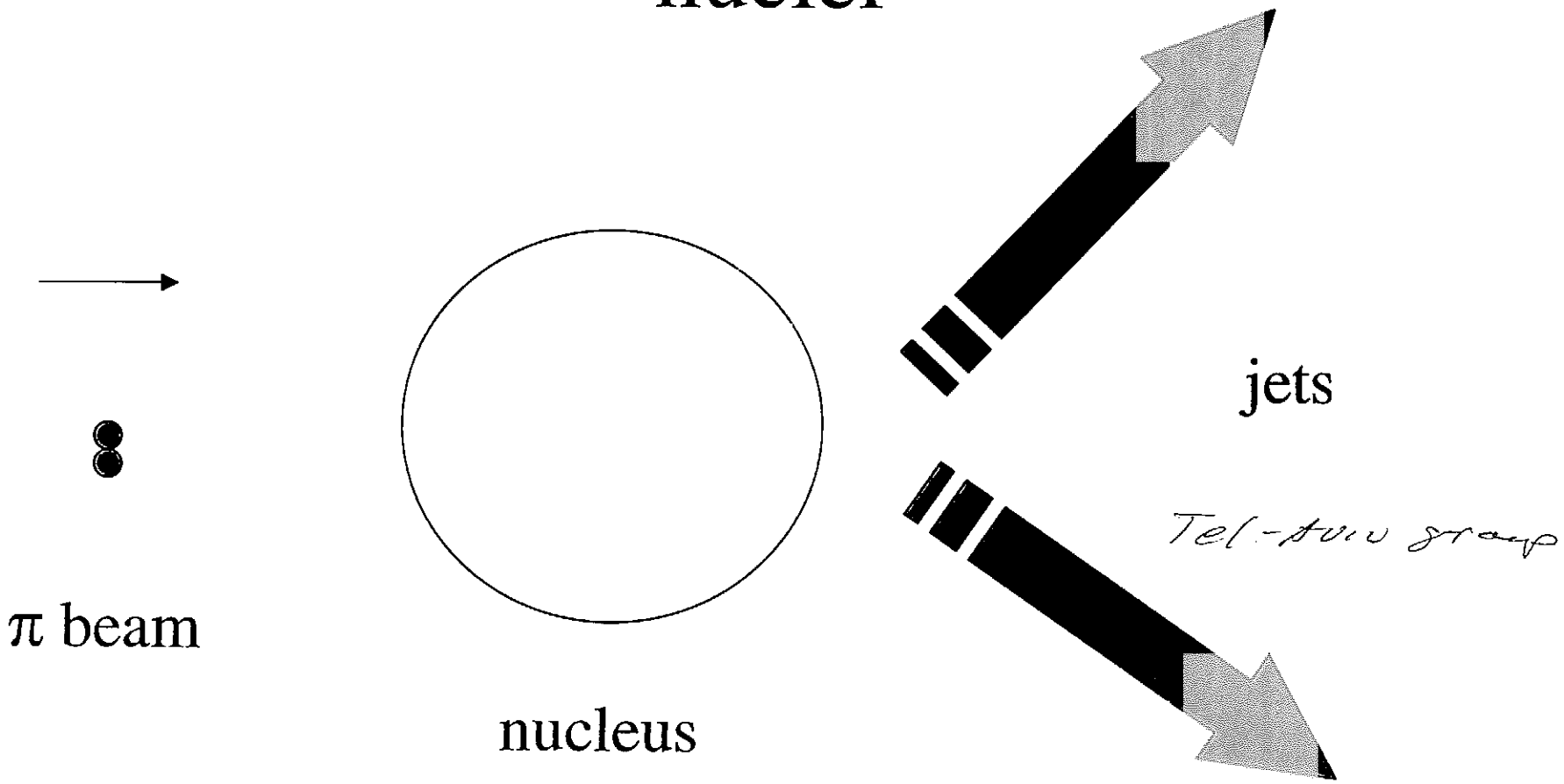

E791: 500 GeV π^- → dijets

PRL 86, 4773 ('01)

fruitful discussions. We gratefully acknowledge the staffs of Fermilab and of all the participating institutions. This research was supported by the Brazilian Conselho Nacional de Desenvolvimento Científico e Technológio, the Mexican Consejo Nacional de Ciencia y Tecnologica, the Israeli Academy of Sciences and Humanities, the United States Department of Energy, the U.S.-Israel Binational Science Foundation, and the United States National Science Foundation. Fermilab is operated by the Universities Research Association, Inc., under contract with the United States Department of Energy.

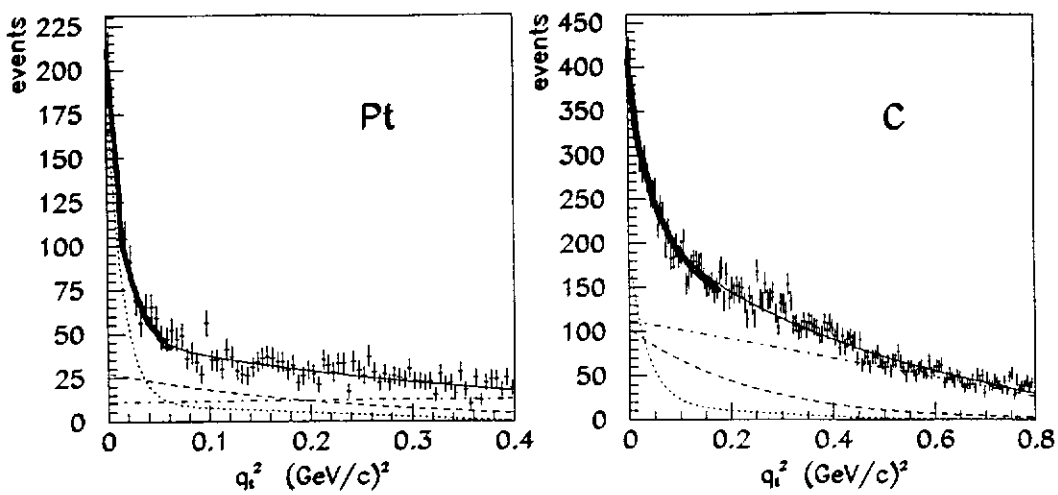

FIG. 3. q_t^2 distributions of di-jets with $1.5 \leq k_t \leq 2.0$ GeV/c for the platinum and carbon targets. The lines are fits of the MC simulations to the data: coherent nuclear dissociation (dotted line), coherent nucleon/incoherent nuclear dissociation (dashed line), background (dashed-dotted line) and total fit (solid line).

TABLE I. The exponent in $\sigma \propto A^{\alpha}$, experimental results for coherent dissociation and the Color-Transparency (CT) predictions.

k_t bin GeV/c	α	$\Delta\alpha_{stat}$	$\Delta\alpha_{sys}$	$\Delta\alpha$	α (CT)
1.25 – 1.5	1.64	±0.05	+0.04 −0.11	+0.06 −0.12	1.25
1.5 – 2.0	1.52	±0.09	±0.08	±0.12	1.45
2.0 – 2.5	1.55	±0.11	±0.12	±0.16	1.60

experiment theory

DIS and the pion field

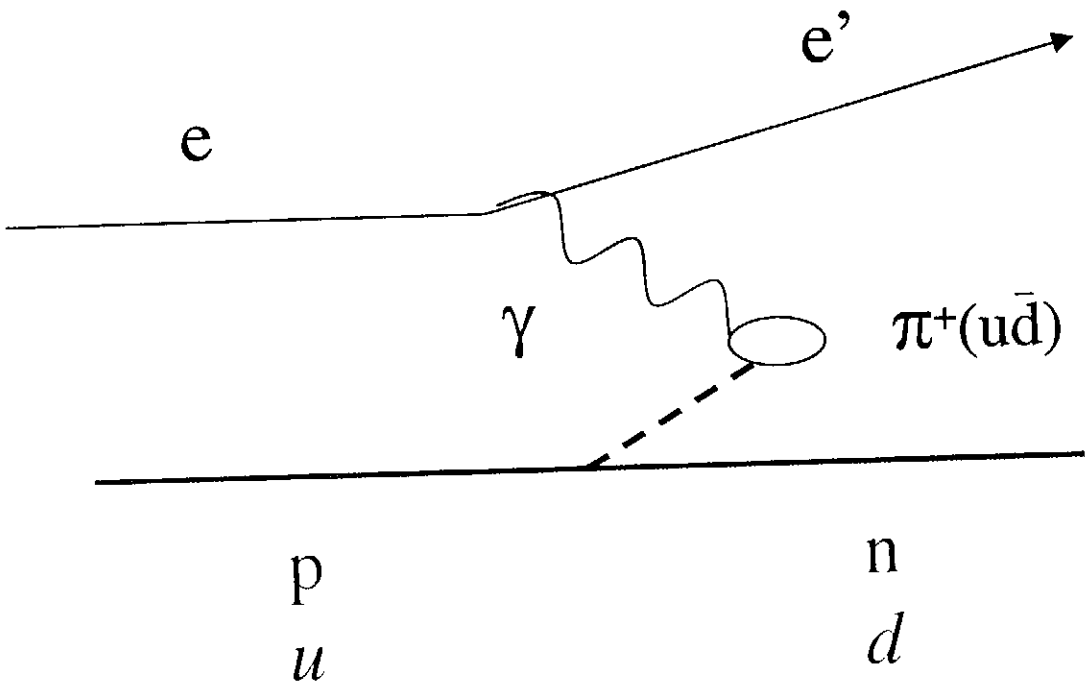

pion folding (Sullivan) model
Chiral-quark model

$\bar{d} - \bar{u}$ Comparison with Hermes

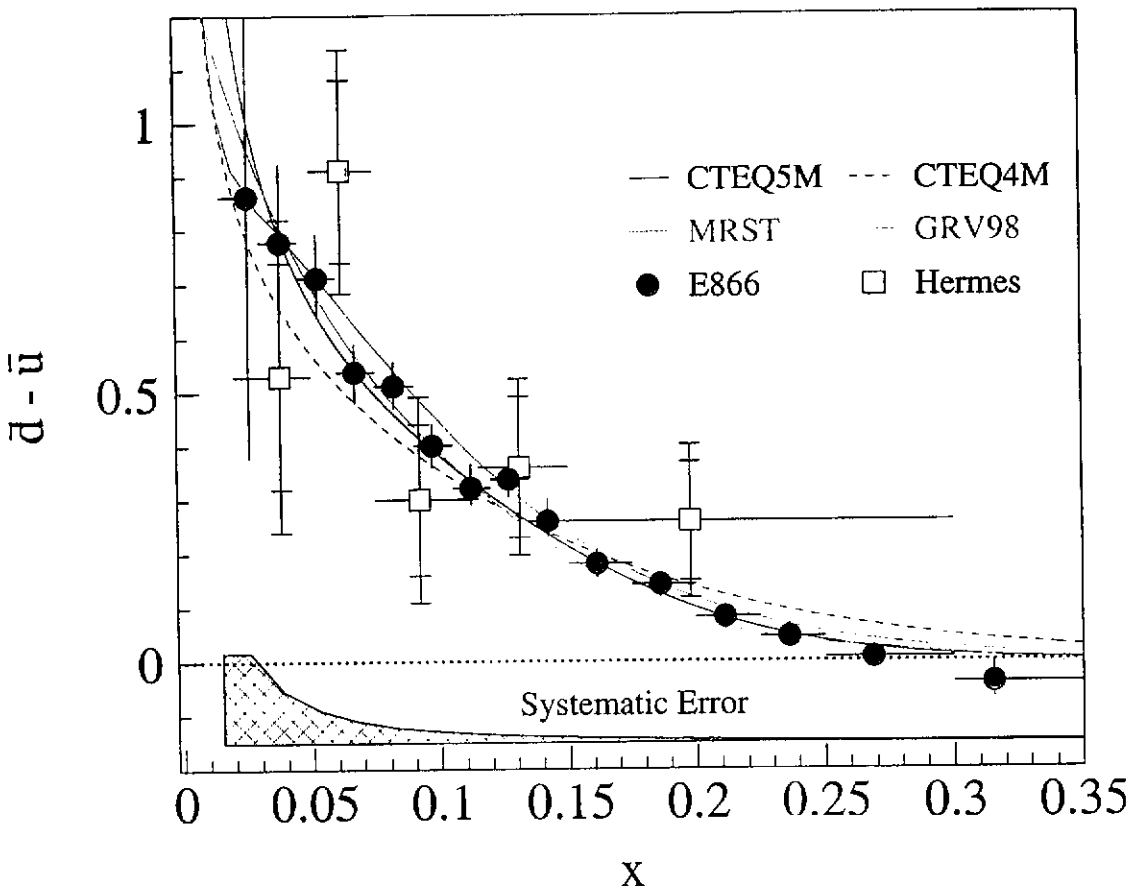

- Semi-inclusive Deep-Inelastic scattering
- HERMES Collaboration, K. Ackerstaff *et al.*, Phys. Rev. Lett. **81** 5519 (1998)

$$N^{\pi^\pm} \propto \sum_i e_i^2 \left[q_i(x) D_{q_i}^{\pi^\pm} + \bar{q}_i(x) D_{\bar{q}_i}^{\pi^\pm} \right]$$

Sum rules

Bjorken sum rule

$$B \equiv \int_0^1 B(x) = \int_0^1 (g_1^p(x) - g_1^n(x))dx = \boxed{\frac{1}{6}\frac{g_A}{g_v}}$$

Gottfried sum rule

$$G \equiv \int_0^1 G(x)dx = \int_0^1 \frac{1}{x}(F_2^p(x) - F_2^n(x))dx =$$

$$\boxed{\frac{1}{3} - \frac{2}{3}\int_0^1 (\bar{d}_p(x) - \bar{u}_p(x))dx}$$

NMC('91): G < 1/3

Sum rules in the NR quark model

$$\frac{G_{NR}}{B_{NR}} = \frac{\frac{1}{3}}{\frac{1}{6}\cdot(\frac{5}{3})} = \frac{6}{5} \qquad \text{but} \qquad \frac{G_{\exp}}{B_{\exp}} = \frac{0.255}{\frac{1}{6}(1.27)} = 1.20$$

In the pion folding model, one can show:

$$\boxed{G(x) = \kappa(a,b)B(x)} \qquad \kappa \sim 6/5;\ \text{not x-dependent}$$

Not a trivial relationship; pion struct. funct. does not contribute to G(x), B(x)

– Signal, Schreiber, and Thomas (1991).

g_1-F_2 comparison

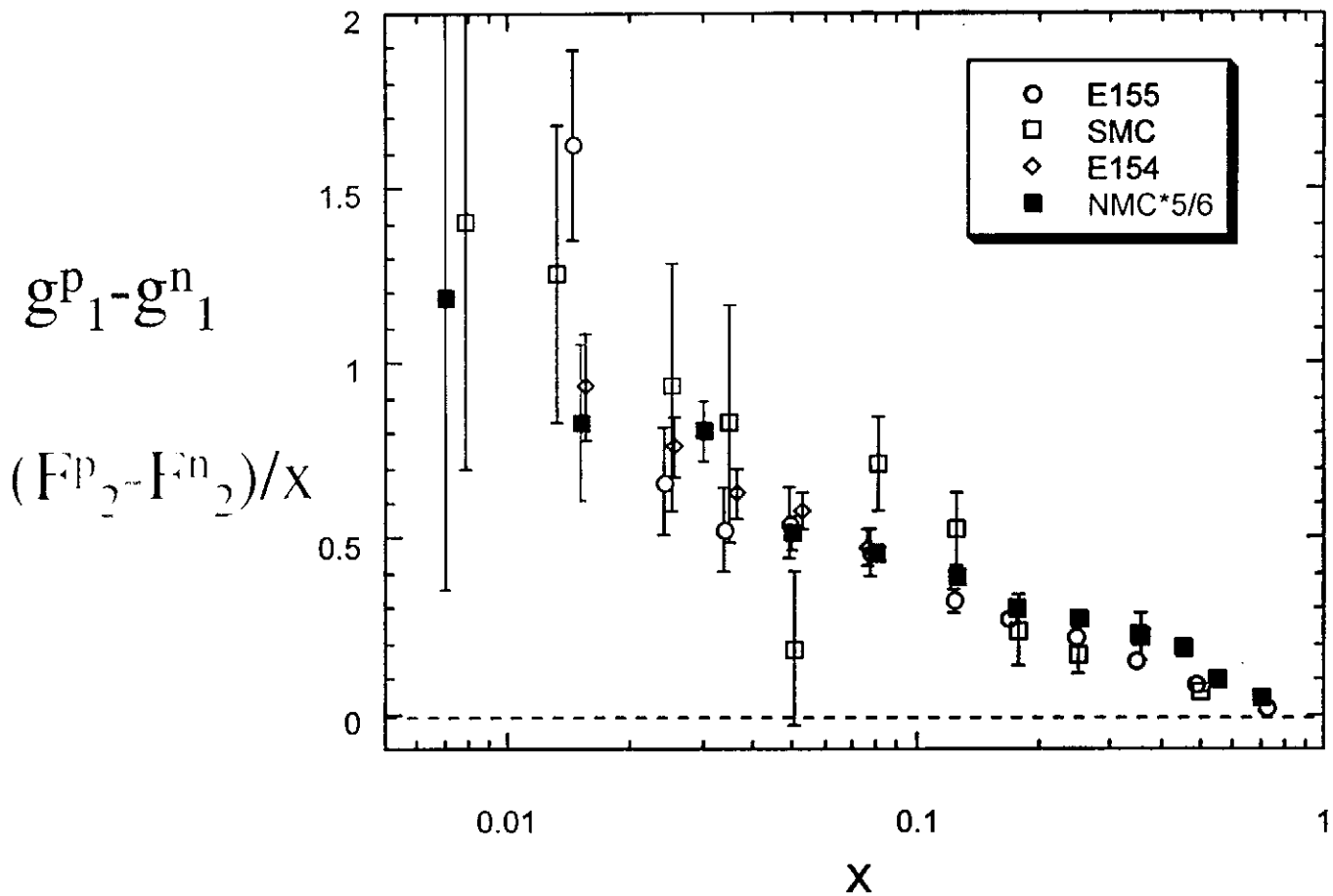

Fitted g_1

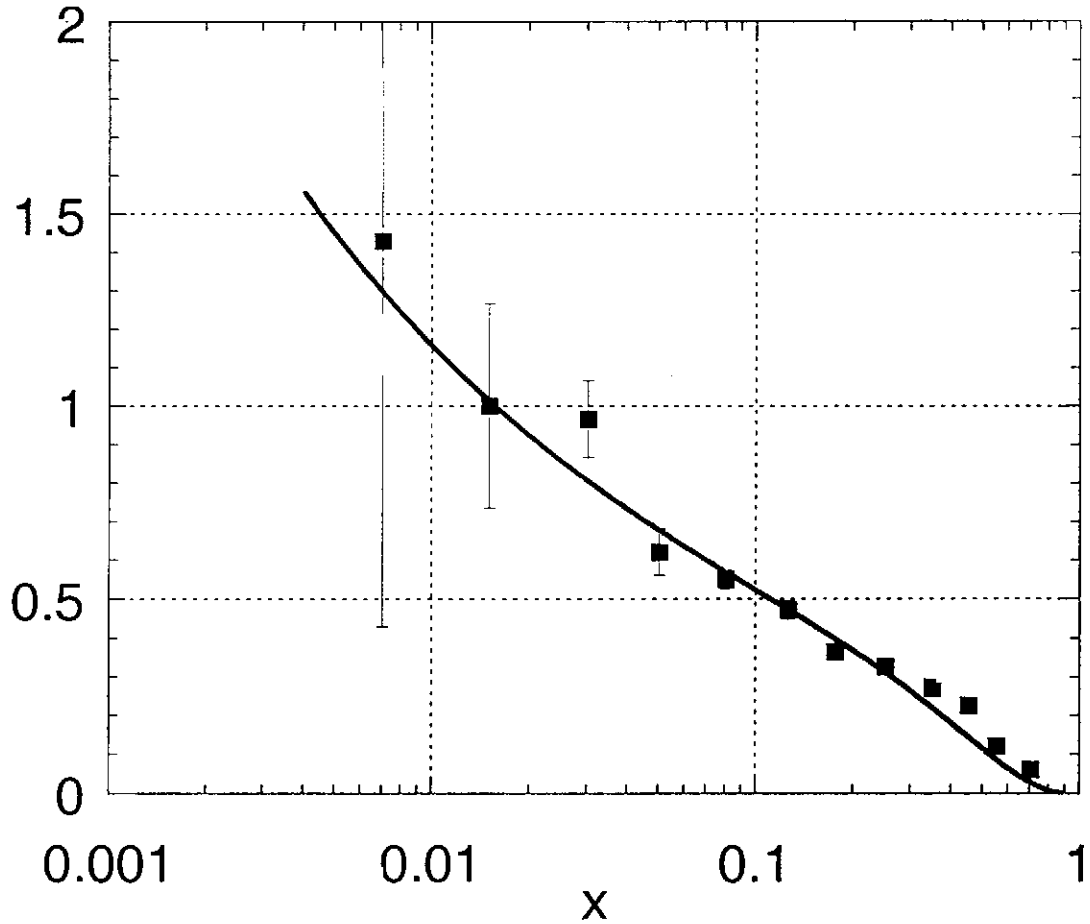

Fitted g_1

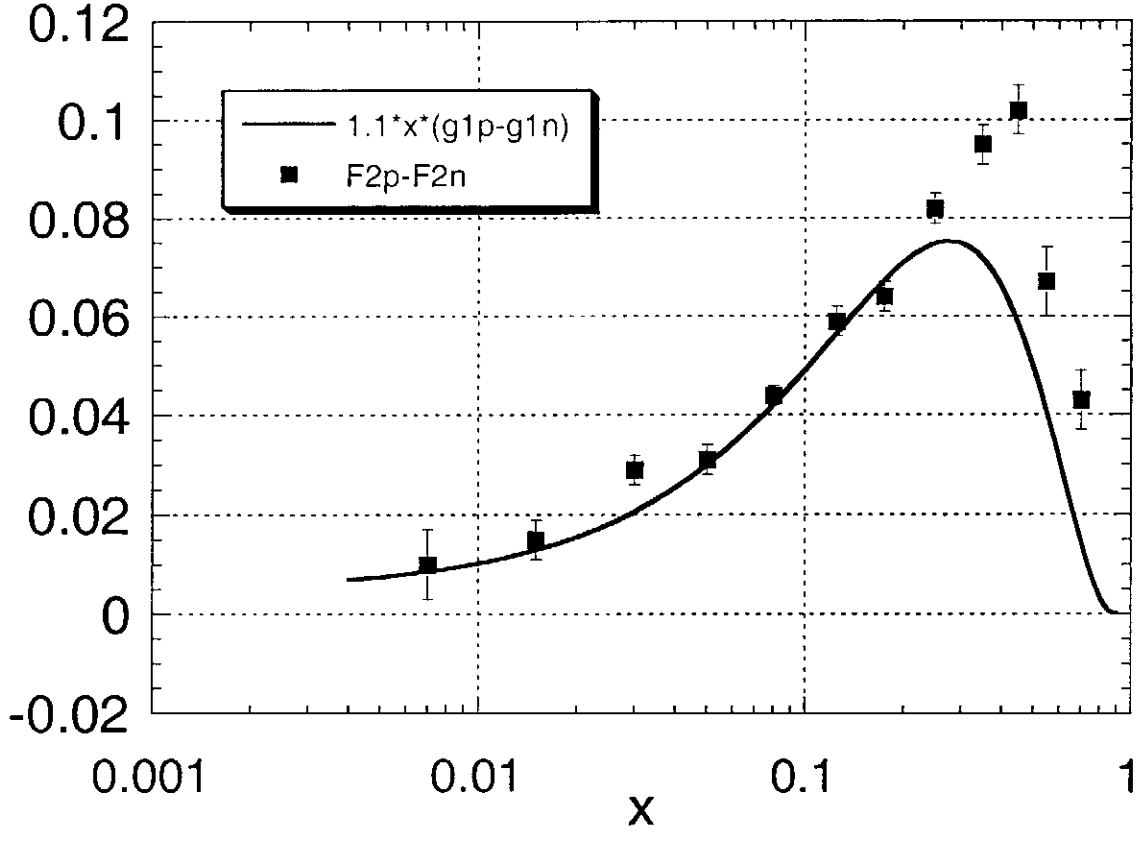

Summary

- Clever phenomenologies of nuclear shadowing — connections to diffraction, HERA results

  gluon shadowing

- parton energy loss in nuclear matter — beginnings of an experimental science?

- nuclear transparency — interesting results from diffractive dissociation. Still need A(e,e'p)

- pion cloud seen in $\bar{d}/\bar{u}$ asymmetry. Is that all that's needed for non-singlet structure functions?

The Physics of Saturation: AA, pA, eA

Dmitri Kharzeev

Physics Department, Brookhaven National Laboratory
Upton, NY 11973, USA

In this talk I first review the physics of QCD phenomena which occur at high parton density – the gluon saturation and the Color Glass Condensate. Then I discuss the ways to study this physics in relativistic nucleus–nucleus collisions, pA collisions, and in electron–ion collisions.

Gluon saturation at present seems to provide a good description of hadron multiplicities in nuclear collisions at RHIC, including their centrality, energy, and rapidity dependences. If this approach survives additional experimental tests, we would be able to conclude that saturation, at least in heavy nuclei, sets in already at RHIC energies. This would allow to reconstruct initial conditions in heavy ion collisions – a necessary pre-requisite for the understanding of thermalization and the search for the quark–gluon plasma. On the other hand, this would open new prospects for the study of gluon saturation phase in pA and eA collisions.

The measurements in eA collisions play a special role in these studies due to the clean initial state and well-defined kinematics. To utilize the great potential of the eA program fully, they should allow for a reconstruction of the final hadronic state, and not be constrained to the traditional measurements of the structure functions. Several examples of such measurements, and of their physical importance, are given.

Physics of AA collisions

- conventional view before RHIC:

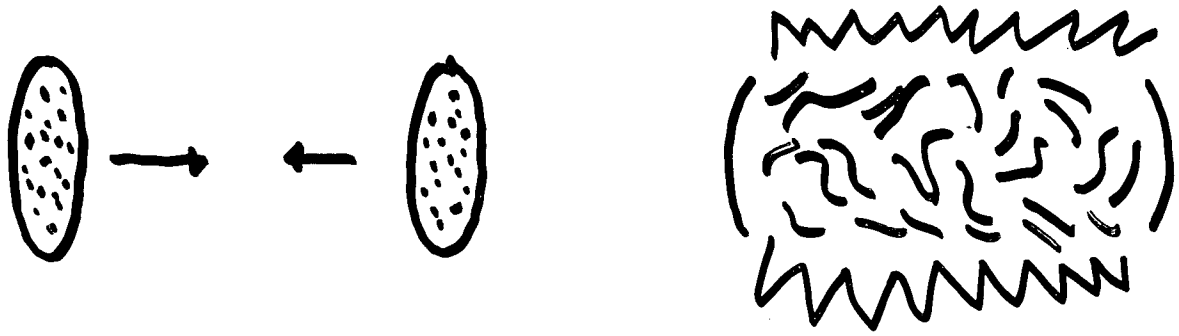

"EVERYTHING HAPPENS IN THE FINAL STATE"

new, emerging view:

"A LOT OF ACTION IS GOING ON EVEN BEFORE THE NUCLEI COLLIDE

What is special about eA:

"clean" probe, well-defined kinematics

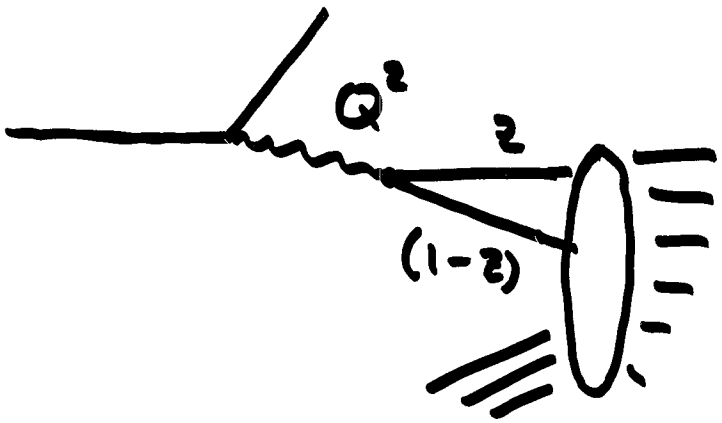

transverse size controlled by Q^2 (and z)

$$r_\perp^2 \sim \frac{1}{Q^2 z(1-z)}$$

longitudinal size (coherence length) controlled by Bjorken x:

$$\ell_c \sim \frac{1}{m_N x}$$

When $\ell_c > 2R_A$, all partons in A contribute coherently $\Rightarrow$ access to high parton densities ($A^{1/3}$) at moderate energies

Interesting measurements:

Jets

examples:

A) measure rapidity distribution of forward jets

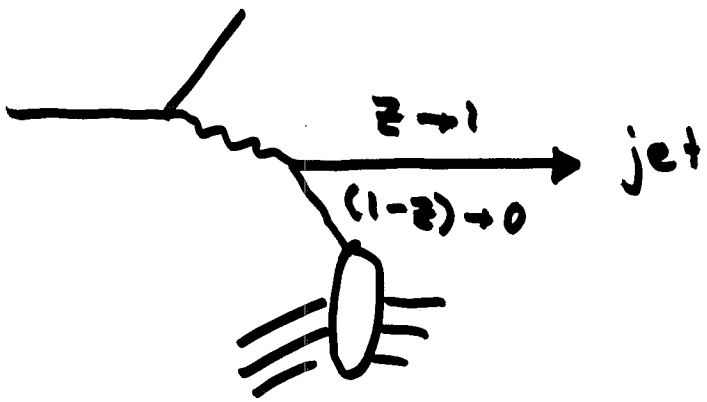

$$r_\perp \sim \frac{1}{\sqrt{Q^2 z(1-z)}}$$

dilute regime: "aligned jets" $z \to 1$

saturation: $\alpha_s r_\perp^2 \rho_g \sim 1$ even for $z \sim 1/2$

no aligned jets ??

B) diffractive production of dijets:

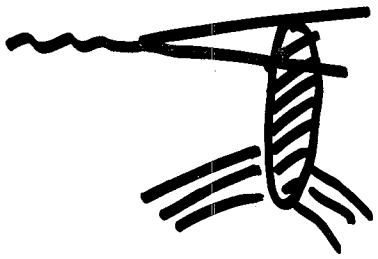

small configurations
(transparency)
or
the nuclear edge?

=> study A dependence

The structure of the final state

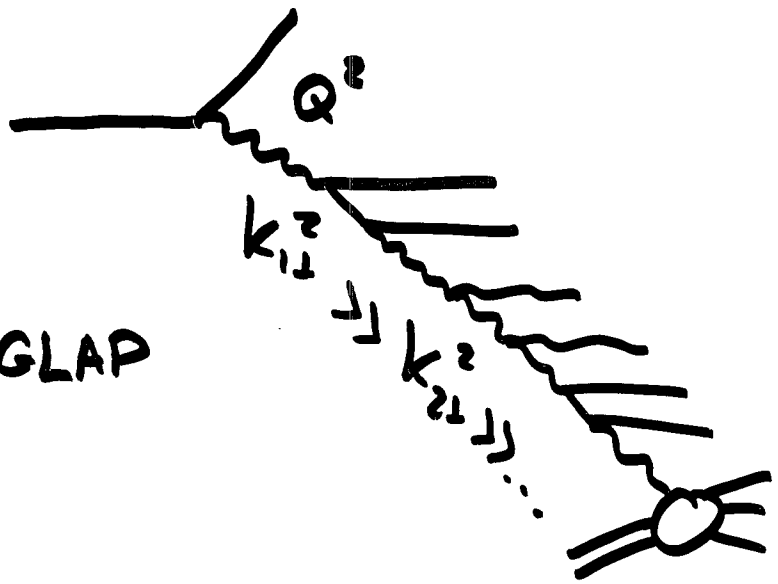

DGLAP

saturation?

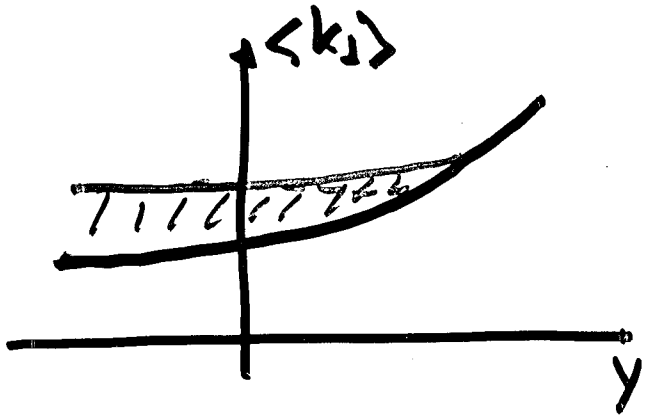

- production of heavy quarks and quarkonia

  $c\bar{c}$: J/Ψ, χ, D, ...

  extract gluon densities,
  study propagation of heavy quark in nuclear matter

  polarized nuclear DIS

  σ_L, σ_T, ...

  $\Rightarrow$ study A-dependence

$\Downarrow$

THE PHYSICS OF THE INITIAL STATE

(intense, coherent gluon fields)

IS VERY INTERESTING AND COMPLEX

IT

A) DESERVES A DEDICATED PROGRAM BOTH IN pA AND <u>eA</u>

B) NEEDS TO BE EXPLORED IN DETAIL TO EXPLOIT FULLY THE POTENTIAL OF AA PROGRAM

Non-perturbative structure of the nucleon

Anthony W. Thomas [a]

[a]Special Research Centre for the Subatomic Structure of Matter
and Department of Physics and Mathematical Physics,
The University of Adelaide, Adelaide SA 5005, Australia

There are many vital questions concerning the non-perturbative structure of the nucleon for which RHIC is well suited to give answers. We outline some of the essential issues in hadronic physics which can and should be addressed.

1. INTRODUCTION

We concentrate on the most significant open questions concerning nucleon structure and the way non-perturbative QCD works. In particular, we examine some of the outstanding questions that need to be tested in the deep-inelastic regime, including the flavor and spin-flavor asymmetries and what these might teach us.

2. SPIN AND FLAVOR DEPENDENCE OF PARTON DISTRIBUTION FUNCTIONS

The best known ambiguity in the unpolarised valence distribution is the asymptotic d/u ratio. For several decades this was believed to be proportional to $(1-x)$ [1,2]. Indeed, in spite of the fact that this behaviour is in disagreement with the expectation based perturbative QCD (pQCD) [3] that the ratio d/u should tend to $1/5$ as $x \to 1$, it is built into most standard parton distribution functions (PDF's). However, a careful relativistic treatment of binding, Fermi motion and off-shell corrections in the deuteron by Melnitchouk and Thomas in 1996 [4] suggested that the SLAC data [5] was in fact consistent with the pQCD expectation. A similar conclusion has been reached by others (e.g. Ref. [6]), but one would really like a demonstrably model independent proof for such a fundamental property of the nucleon.

One exciting possibility, which can be carried out after the Jefferson Lab 12 GeV upgrade, is to use the charge symmetry of the ^{3}H-^{3}He system to extract F_{2n}/F_{2p} and hence d/u up to $x \sim 0.85$ [7]. A direct measurement of the ratio of ν to $\bar{\nu}$ deep inelastic scattering at large-x on hydrogen would yield a totally unambiguous ratio. However, asymmetries in W-production in pp and pD collisions may also yield significant constraints. In combination with the JLab measurement in the very large-x region, this could yield quantitative information on possible new physics, such as six-quark configurations in the A=3 system.

2.1. The light quark sea

In an extremely important series of experiments at CERN, HERA and Fermilab [8–10], it has been clearly established that there is an excess of $\bar{d}$ over $\bar{u}$ quarks in the proton. This was actually anticipated on the basis of chiral symmetry almost a decade before the NMC experiment [11], but only recently has the unambiguous role of chiral symmetry, in terms of a leading non-analytic (LNA) contribution to $\bar{d} - \bar{u} \sim m_\pi^2 \ln m_\pi$, been established [12]. Such behaviour cannot be cancelled by any other mechanism, unless by chance at one particular quark mass. This realization has led to important advances in connecting moments of PDF's calculated in lattice QCD to data [13,14].

On the other hand, there has been an alternative suggestion concerning the non-perturbative origins of $\bar{d} - \bar{u}$ for more than a decade [15]. Actually this explanation has its roots in the Pauli correction of Field and Feynman [16], but the modern view is far deeper. We briefly review the

recent work on related problem in 1+1 dimensions by Tsushima *et al.* [17].

The problem of fermions moving in scalar and vector potentials in 1+1 dimensions has been widely studied since the work of Jackiw and Rebbi [18]. In particular, one has the fascinating possibility of fermions with fractional charge. Our concern is with a fermion moving in a purely scalar potential. In 1+1 dimensions one can explicitly examine the vacuum structure, which differs from the vacuum in the absence of the scalar potential. In particular, in terms of free fermion states, some of the higher states in the Dirac sea of the scalar potential will be unoccupied, while an equal number of positive energy states will be occupied. In the context of deep inelastic scattering, the process of normal ordering amounts to the statement that a deep inelastic probe will see the difference between the structure of the target and the free vacuum. Thus the change in the sea, even in the absence of valence quarks (of course, that would not be stable by itself but this is a thought experiment), amounts to the statement that the empty scalar potential looks like a sea of $q - \bar{q}$ pairs to an incident probe. Of course, this intrinsic sea carries no net spin or flavor.

On the other hand, if one considers a valence quark bound in this scalar potential, one needs a complete set of free positive *and* negative energy fermion levels to fully describe its wave function (unless the system is totally non-relativistic). A consequence of adding a valence quark to the interacting vacuum described above is that it will not only fill some positive energy free states but some of the vacant negative energy levels. Of course, the valence normalisation from the positive energy states alone is not complete. How do we interpret this? It is simple: the addition of the valence quark removes some of the intrinsic antiquark sea (of the same flavor), the corresponding sea quarks then make up the missing valence normalisation. The result is a system with a valence quark and some of the intrinsic sea, of the same flavor, suppressed.

If we take this result over to 3+1 and the proton, it is obvious that because we add two valence u-quarks and only one valence d, the intrinsic sea will now contain an excess of $d - \bar{d}$ pairs. It has so far proven difficult to make a quantitative estimate of the effect in models like the bag, but indications in the original work [15] suggested that the integral of $\bar{d} - \bar{u}$ should be between 0.05 and 0.20 – certainly the right order of magnitude. This leaves us with two mechanisms for the experimental observation and it is clearly very important for our understanding of hadron structure to determine how much should be attributed to each one.

The key to this separation is that the clear link between the reduction of the sea and the quantum numbers of the valence quarks provides a signature of the origin of the effect. Using an SU(6) wave function for a polarised proton, one finds that the valence u-quarks have predominantly positive polarisation, whereas the valence d's are only slightly, but negatively polarised. Hence one expects that the intrinsic sea produced by the Pauli effect should have $\Delta\bar{u}$ positive and a little larger (by a factor 5/3 - 1/3, for exact SU(6) symmetry) than the Pauli contribution to $\bar{d} - \bar{u}$, whereas $\Delta\bar{d}$ should be very small in magnitude (1/3 of the Pauli contribution to $\bar{d} - \bar{u}$, for exact SU(6) symmetry) and negative. In comparison, the sea produced by chiral symmetry is unpolarised. Thus a determination of $\Delta\bar{u}$ and $\Delta\bar{d}$, together with the existing information on $\bar{d} - \bar{u}$, should allow us to unambiguously understand the origins of the non-perturbative, light-quark sea of the nucleon.

2.2. The strange sea

Because the strange quark is much heavier, the Pauli effect discussed above for $\Delta\bar{q}$ should be relatively small. On the other hand, considerations of chiral SU(3) show that there is an unambiguous difference between the shape of $s(x)$ and $\bar{s}(x)$ [12]. This was first pointed out by Signal and Thomas [19] and later by Brodsky and Ma [20] (although the s-wave $\bar{K}N$ coupling used there needs revision). Prompted by improvements in the determination of the strange quark PDF's in recent neutrino experiments [21], as well as the determination of the strangeness form factors of the nucleon, there has also been quite a bit of theoretical activity on the problem of $s(x) - \bar{s}(x)$ recently [22–24].

For the present, it is probably fair to say that there is no convincing experimental evidence for such an asymmetry. Nevertheless, it must be there at some level and it is again a crucial property of the nucleon that really ought to be pinned down. It is the archetype upon which we can begin to build an understanding of the role of heavier quarks in light hadrons.

3. CONCLUSION

The least understood part of the standard model is QCD in the non-perturbative regime and the physics issues outlined here need to be pursued vigorously.

Acknowledgements

It is a pleasure to acknowledge the collaborations with many colleagues at CSSM and elsewhere which have led to the results presented here. I would particularly like to express my appreciation to Gerald Dunne, Wally Melnitchouk, Tony Signal, Andreas Schreiber, Fernando Steffens and Kazuo Tsushima. This work was supported by the Australian Research Council and the University of Adelaide.

REFERENCES

1. A. W. Thomas and W. Weise, "The Structure of the Nucleon," *289 pages. Hardcover ISBN 3-527-40297-7 Wiley-VCH, Berlin 2001.*
2. F. E. Close, Phys. Lett. B **43** (1973) 422.
3. G. R. Farrar and D. R. Jackson, Phys. Rev. Lett. **35** (1975) 1416.
4. W. Melnitchouk and A. W. Thomas, Phys. Lett. B **377** (1996) 11 [arXiv:nucl-th/9602038].
5. L. W. Whitlow, E. M. Riordan, S. Dasu, S. Rock and A. Bodek, Phys. Lett. B **282** (1992) 475.
6. U. K. Yang and A. Bodek, Phys. Rev. Lett. **82** (1999) 2467 [arXiv:hep-ph/9809480]; W. Melnitchouk, I. R. Afnan, F. Bissey and A. W. Thomas, Phys. Rev. Lett. **84** (2000) 5455 [arXiv:hep-ex/9912001].
7. I. R. Afnan, F. Bissey, J. Gomez, A. T. Katramatou, W. Melnitchouk, G. G. Petratos and A. W. Thomas, Phys. Lett. B **493** (2000) 36 [arXiv:nucl-th/0006003].
8. P. Amaudruz *et al.* [New Muon Collaboration], Phys. Rev. Lett. **66** (1991) 2712.
9. A. Baldit *et al.* [NA51 Collaboration], Phys. Lett. B **332** (1994) 244.
10. E. A. Hawker *et al.* [FNAL E866/NuSea Collaboration], Phys. Rev. Lett. **80** (1998) 3715 [arXiv:hep-ex/9803011].
11. A. W. Thomas, Phys. Lett. B **126** (1983) 97.
12. A. W. Thomas, W. Melnitchouk and F. M. Steffens, Phys. Rev. Lett. **85** (2000) 2892 [arXiv:hep-ph/0005043].
13. W. Detmold, W. Melnitchouk, J. W. Negele, D. B. Renner and A. W. Thomas, Phys. Rev. Lett. **87** (2001) 172001 [arXiv:hep-lat/0103006].
14. D. Dolgov *et al.* [LHPC collaboration], arXiv:hep-lat/0201021.
15. A. W. Schreiber, A. I. Signal and A. W. Thomas, Phys. Rev. D **44** (1991) 2653.
16. R. D. Field and R. P. Feynman, Phys. Rev. D **15** (1977) 2590.
17. K. Tsushima, A. W. Thomas and G. V. Dunne, "Distortions in the negative energy Dirac sea: Violation of the Gottfried sum rule and Delta(anti-u) in proton," arXiv:hep-ph/0107042.
18. R. Jackiw and C. Rebbi, Phys. Rev. D **13** (1976) 3398.
19. A. I. Signal and A. W. Thomas, Phys. Lett. B **191** (1987) 205.
20. S. J. Brodsky and B. Q. Ma, Phys. Lett. B **381** (1996) 317 [arXiv:hep-ph/9604393].
21. A. O. Bazarko *et al.* [CCFR Collaboration], Z. Phys. C **65** (1995) 189 [arXiv:hep-ex/9406007].
22. W. Melnitchouk and M. Malheiro, Phys. Lett. B **451** (1999) 224 [arXiv:hep-ph/9901321].
23. X. D. Ji and J. Tang, Phys. Lett. B **362** (1995) 182 [arXiv:hep-ph/9507465].
24. F. G. Cao and A. I. Signal, Phys. Lett. B **474** (2000) 138 [arXiv:hep-ph/9907560].

Moments of Parton Distributions

- **Can only compute low moments on lattice:**

$$< x^n > \;=\; \int_0^1 dx x^n [q(x) + (-)^{n+1}\bar{q}(x)]$$
$$\sim \;< N|\bar{\psi}\gamma_{\{\mu_1} D_{\mu_2} ... D_{\mu_{n+1}\}}\psi|N >(1)$$

- **Compute $< x^n >$ for $u - d$**

$\Rightarrow$ **NO "disconnected diagrams"**

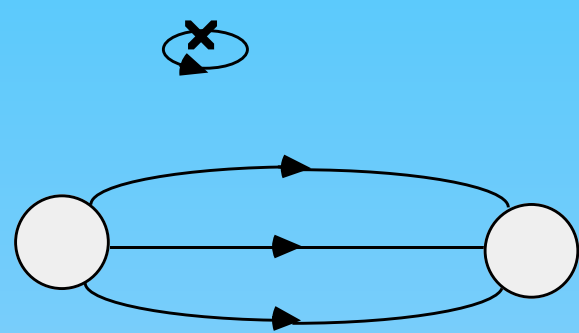

- **Until now, discrepancies with data of 50 % or more.....**

SPECIAL RESEARCH CENTRE FOR THE SUBATOMIC STRUCTURE OF MATTER

Chiral Behaviour

- **For Gottfried sum rule violation:**

$\bar{d} - \bar{u}|_{\rm LNA} \sim c_{\rm LNA} m_\pi^2 \ln m_\pi$

Thomas, Melnitchouk & Steffens, PRL 85 (2000) 2892

- **For $u - d$:**

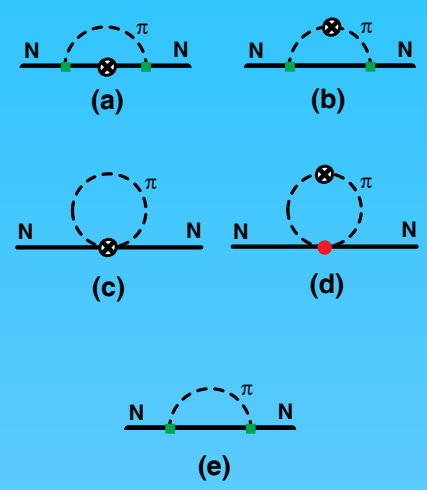

- $< x^n >= a_n + b_n m_\pi^2 + a_n c_{\rm LNA} m_\pi^2 \ln \frac{m_\pi^2}{m_\pi^2 + \mu^2}$
- $c_{\rm LNA}$ **from chiral perturbation theory**

Ji & Chen and Arndt & Savage

- **reproduces CBM calculation over full range of m_π^2**
- μ **is scale at which chiral behaviour turns off: expect $\sim$ 500 MeV**

Moments of $u - d$

- **Chiral extrapolation is essential:**

Detmold, Melnitchouk, Negele, Renner & Thomas,

hep-latt/0103006: $a + bm_\pi^2 + ac_{\rm LNA} m_\pi^2 \ln(m_\pi^2/(m_\pi^2 + \mu^2))$

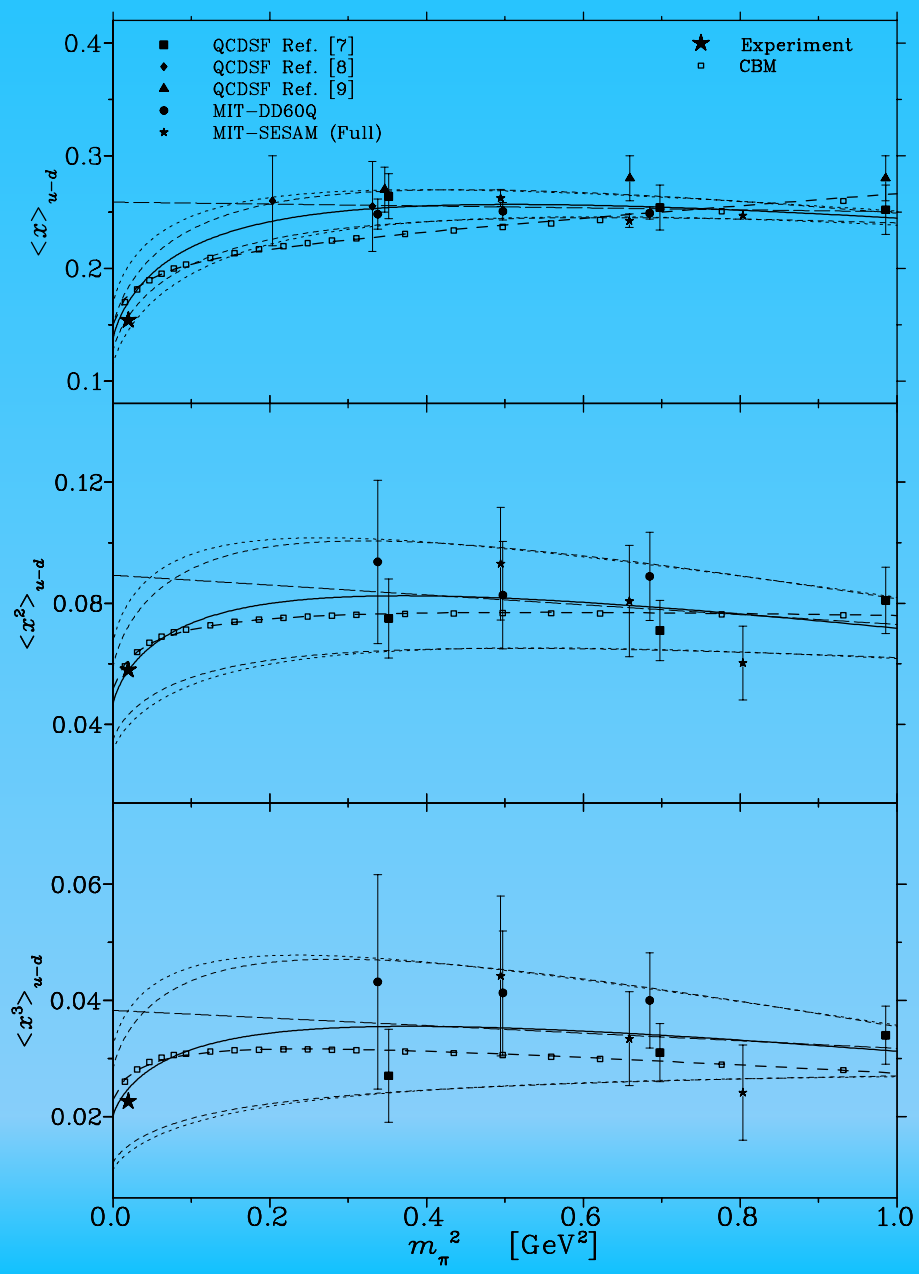

Comparison with Data

- Can use lowest 4 moments to reconstruct x-dependence of $u_v(x) - d_v(x)$

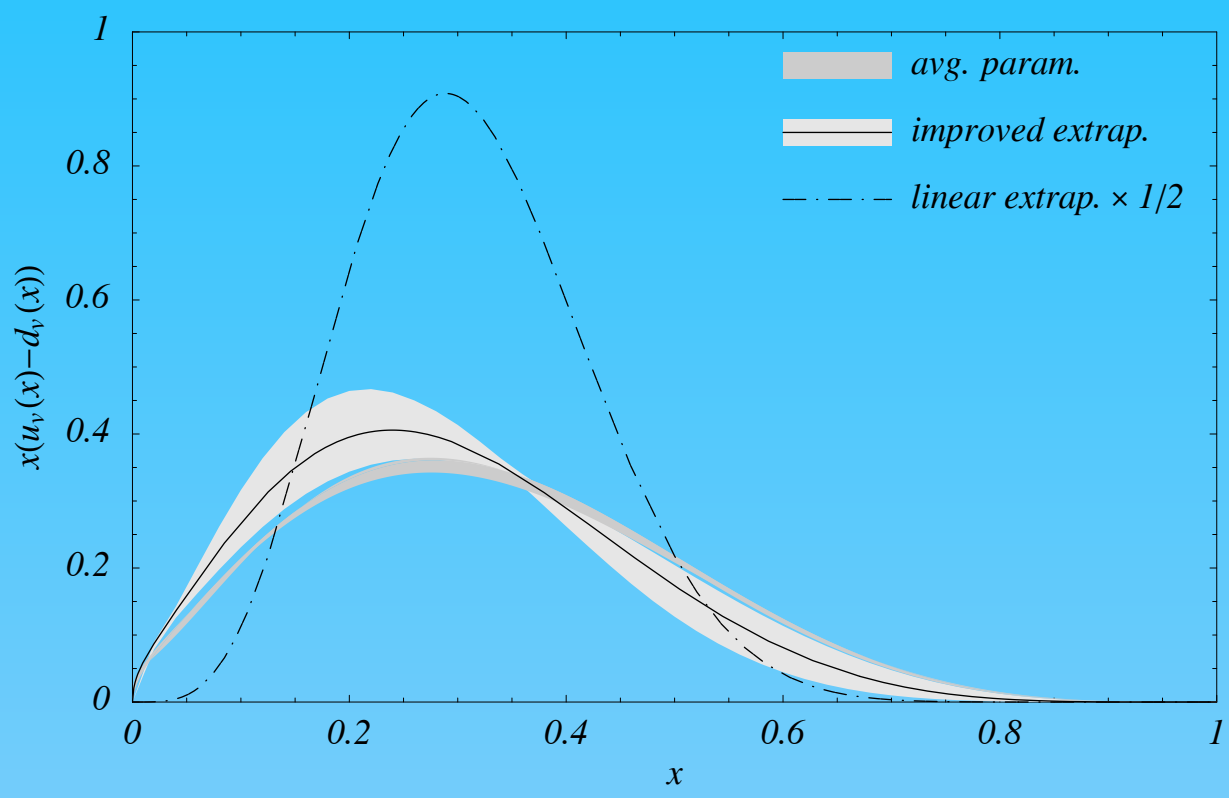

Detmold, Melnitchouk....

- Dark shading is world data
- Light shading chiral extrapolation

OVERVIEW

- **Lattice data $\bar{m} > 60$ MeV:**

— **(i.e. $m_\pi \geq$ 400–500 MeV)**

— **Hadron properties smooth, slowly varying functions of the constituent quark mass ($M \sim M_0 + c\bar{m}$):**

— $M_{N,\Delta} \sim 3M \ (\sim a + bm_\pi^2)$

— $M_{\rho,\omega} \sim 2M \ (\sim a' + \frac{2}{3}bm_\pi^2)$

— $\mu_H \sim 1/M$

- **BUT at small $\bar{m}(< 60$ MeV):**

— **(i.e. $m_\pi \leq$ 400–500 MeV)**

— **Chiral Symmetry $\Rightarrow$**

— **rapid, non-analytic variation with $\bar{m}$:**

— $\delta M_H \sim \bar{m}^{3/2}$

— $\delta\mu_H \sim \bar{m}^{1/2}$

— $\delta < r^2 >_{\rm ch} \sim \ln \bar{m}$

- **Models (like CBM) yield a natural explanation of transition from LNA to smooth behaviour**

Recent RHIC Results with AA

Mark D. Baker
Brookhaven National Laboratory
(April 11, 2002)

The latest results from RHIC are presented and summarized. The system created in heavy ion collisions is found to be a hot and rapidly expanding bulk system composed of up to 7500 particles (5000 measured charged particles). These events are the most violent ever created under laboratory conditions, and yet the particle production is modest compared to many models, indicating that initial state effects are the dominant source of entropy production and setting limits on the contribution of hard processes. The intriguing possibility of a relationship between the gluon structure function measured in deep inelastic collisions and the energy, centrality, and pseudorapidity dependence of particle production in heavy ion collisions is explored. A plausible description of the trajectory of these collisions in temperature and baryon chemical potential is discussed - indicating that these collisions might be described in terms of deconfined matter which expands, cools and freezes out into hadrons along a universal hadronization curve. Finally, the transverse momentum distribution of hadrons produced at RHIC does not scale as expected when compared to p+A and p+p collisions. This may be the first evidence of energy loss of jets in hot, dense matter, and when refined and extended, should provide information about the hot, dense, and presumably deconfined initial state.

Relativistic heavy ion collisions provide a laboratory for studying the strong interaction, described by Quantum Chromodynamics (QCD), under conditions of high parton density and high energy density. This regime is interesting because it probes nonlinear dynamics (e.g. parton saturation), and nonperturbative effects (e.g. the onset of color deconfinement and chiral symmetry restoration). Following successful AuAu runs at $\sqrt{s_{NN}}$ of 130 and 200 GeV as well as short runs at 56 and 19.6 GeV, the RHIC experiments have begun to successfully characterize these systems and to probe QCD at high density [1–17]. Due to space limitations, many important topics have been left out these proceedings (as well as the talk). The full talk is available on the web [18]. The most up-to-date information on physics and publications can be found at the RHIC or experiment websites [19].

The first, simple, but fundamental, heavy ion observable to be measured was the pseudorapidity density $dN_{ch}/d\eta$ of charged particles produced in a collision. This number is proportional to the entropy density at freezeout. Since total entropy cannot decrease with time, even in non-equilibrium systems, the pseudorapidity density provides a strong constraint on the initial state parton density and any further entropy produced during the subsequent evolution. The number of charged particles produced at midrapidity per pair of participating nucleons is shown vs center of mass energy in slide 1 for the most central AA collisions up to $\sqrt{s_{NN}} = 200$ GeV as well as for non-single-diffractive $p + \bar{p}$ collisions [1]. Early predictions for the charged particle pseudorapidity density varied by more than a factor of two, as indicated by the theoretical bands [20]. The total charged particle production is measured to be about 5000 particles [4,21]. A more robust test of the models is provided by ratios of particle production at different energies in the same experiment, allowing some systematic errors to cancel out. Slide 2 shows the ratio of particles produced at midrapidity between 200 and 130 GeV [4], where the band represents a 90% confidence level systematic error band. This solidly rules out one of the most prominent pre-RHIC predictions: the default HIJING model [22,23]. This model assumed a large amount of hard scattering, followed by a large amount of gluon radiation from jet quenching, with little reabsorption of that gluon radiation by the medium. This measurement sets strict limits on the amount of these final state hard processes which can be occurring in these collisions.

One model which does describe the data is the Kharzeev-Levin parton saturation model [24], based on the McLerran-Venugopalan model [25]. This Kharzeev-Levin model is particularly interesting in the context of this workshop since it relates gluon structure functions and low-x scaling relations from HERA to the energy, pseudorapidity, and centrality dependence seen in heavy ion collisions. Slides 3 and 4 show a fit to the 130 GeV data and the relatively successful prediction of the 200 GeV data shape and centrality dependence [3,4,21]. This model also assumes approximate parton-hadron duality, again implying that the multiplicity distribution reflects the initial state.

Turning to another set of observables, heavy ion collisions at 130 GeV show evidence of collective behavior, which can be seen from the elliptic flow [11,15] or from the mass dependence of the effective temperature (the p_T slopes of the particle spectra). The effective temperature vs. particle mass is shown in slide 5 [26], indicating a kinetic temperature similar to that seen at CERN (roughly 150 MeV), but a much larger collective expansion velocity. This expansion velocity effect is so large that protons and anti-protons have been shown to outnumber pions at p_T's near 3 GeV/c [27]. In addition to these kinetic "temperatures", particle ratios allow the estimation of a temperature at which the chemical composition (particle mix) freezes out. These temperatures are found to be in the range

170-200 MeV as seen in slide 6 [28].

While these measurements provide a snapshot of the temperature and expansion velocity of the system as it freezes out, we can also estimate the energy density or temperature of the initial state. Slide 7 shows how this is assembled. The energy density comes from a simple geometric estimate originally written down by Bjorken [29] which uses measurements of the number of particles produced at mid-rapidity [4] and the energy per particle [7]. This leads to an energy density of 5–25 GeV/fm^3 for $\sqrt{s_{NN}}$ = 130 GeV and 6–29 GeV/fm^3 for $\sqrt{s_{NN}}$ =200 GeV. In order to convert the energy density to a temperature, we have to assume the number of degrees of freedom of the system. If we accept the lattice estimate [30], which indicates a deconfined, but interacting system, for both CERN-SPS and RHIC energies, we would estimate an initial temperature between 250–350 MeV for RHIC @ $\sqrt{s_{NN}}$ = 130 GeV and 220–290 MeV for CERN-SPS energies. It should be noted that if we instead assume a smaller number of degrees of freedom, appropriate for a hadronic system, our estimated energy density would correspond to an even higher temperature (400–600 MeV for $\sqrt{s_{NN}}$ = 130 GeV). It would be difficult to reconcile hadronic matter at these high temperatures with our understanding of QCD, although the data does not unambiguously rule this possibility out.

Slide 8 shows the theoretical QCD phase diagram with the estimated freezeout values of heavy ion collisions. It is interesting to note that the apparent universal freezeout curve traced out by heavy ion collisions also seems to describe hadronization in e^+e^- collisions. The freezeout behaviour of AuAu collisions at RHIC — a bulk system with collective motion and thousands of particles — is consistent with the freezeout of hadrons from string fragmentation. This is very suggestive that this universal curve is fundamental to QCD. The fact that these collisions have finally reached a "bulk matter" state validates the description of all of these collisions in approximate thermodynamic terms.

Finally we turn, in Slides 9 and 10, to the possible evidence for "jet quenching". The production of neutral pions in peripheral collisions is well described by binary collision scaling from NN collisions. However, in central collisions, the production of neutral pions is suppressed relative to this scaling estimate [8]. Similar suppression is also seen in unidentified hadron spectra [8,26]. There are at least two possible explanations for this scaling violation: jet energy loss due to gluon radiation in dense matter (quenching) or parton saturation effects leading to a centrality-dependent scaling violation. More data in AA at higher transverse momentum and better reference data for pA (or dA) and pp are needed to resolve this question. Nevertheless, this measurement indicates that RHIC is able to probe the hot, dense, presumably deconfined initial state and measure its properties.

The AA program at RHIC has provided a wealth of data already, allowing us to characterize heavy ion collisions. Connections have been drawn to pp, pA, DIS, and even e^+e^- collisions which should allow us to explore high density (low x) QCD. First hints have been provided that for AA collisions, we may be probing properties of a deconfined initial state. Further measurements at RHIC should lead to an improved understanding of dense, hot strongly interacting matter and of QCD.

Acknowledgements: The author would like to thank Peter Steinberg, Axel Dress and Jamie Nagle for slides that went into this talk.

---

[1] B. B. Back *et al.* (PHOBOS), Phys. Rev. Lett. **85** (2000) 3100.
[2] B. B. Back *et al.* (PHOBOS), Phys. Rev. Lett. **87** (2001) 102301.
[3] B. B. Back *et al.* (PHOBOS), Phys. Rev. Lett. **87** (2001) 102303.
[4] B. B. Back *et al.* (PHOBOS), Phys. Rev. Lett. **88** (2002) 22302.
[5] B. B. Back *et al.* (PHOBOS), Phys. Rev. C **65** (2002) 031901.
[6] K. Adcox *et al.* (PHENIX), Phys. Rev. Lett. **86** (2001) 3500.
[7] K. Adcox *et al.* (PHENIX), Phys. Rev. Lett. **87** (2001) 052301.
[8] K. Adcox *et al.* (PHENIX), Phys. Rev. Lett. **88** (2002) 022301.
[9] I.G. Bearden *et al.* (BRAHMS), Phys. Rev. Lett. **87** (2001) 112305.
[10] I.G. Bearden *et al.* (BRAHMS), Phys. Lett. **B523** (2001) 227.
[11] C. Adler *et al.* (STAR), Phys. Rev. Lett. **86** (2001) 402.
[12] C. Adler *et al.* (STAR), Phys. Rev. Lett. **86** (2001) 4778.
[13] C. Adler *et al.* (STAR), Phys. Rev. Lett. **87** (2001) 082301.
[14] C. Adler *et al.* (STAR), Phys. Rev. Lett. **87** (2001) 112303.
[15] C. Adler *et al.* (STAR), Phys. Rev. Lett. **87** (2001) 182301.
[16] C. Adler *et al.* (STAR), Phys. Rev. Lett. **87** (2001) 262301.
[17] C. Adler *et al.* (STAR), Phys. Rev. Lett. **87** (2001) 262302.
[18] www.phobos.bnl.gov/Presentations/EIC_Mar02.ppt.
[19] www.bnl.gov/RHIC, www.phobos.bnl.gov, www.phenix.bnl.gov, www.star.bnl.gov, www.rhic.bnl.gov/brahms.
[20] N. Armesto and C. Pajares, Int. J. Mod. Phys. **A15** (2000) 2019.

[21] I.G. Bearden *et al.* (BRAHMS), nucl-ex/0112001.
[22] M. Gyulassy and X. N. Wang, Phys. Rev. **D44** (1991) 3501.
[23] X. N. Wang and M. Gyulassy, Phys. Rev. Lett. **86** (2001) 3496.
[24] D. Kharzeev and E. Levin, nucl-th/0108066 (2001).
[25] L. McLerran, R. Venugopalan, Phys. Rev. **D49** (1994) 2233, 3352.
[26] C. Adler *et al.* (STAR), Nucl. Phys. **A698** (2002) 64c.
[27] K. Adcox *et al.* (PHENIX), Nucl. Phys. **A698** (2002) 39c.
[28] N. Xu, M. Kaneta, Nucl. Phys. **A698** (2002) 306c.
[29] J.D. Bjorken, Phys. Rev. **D27** (1983) 140.
[30] F. Karsch, Nucl. Phys. **A698** (2002) 199c.

RHIC results at 200 GeV

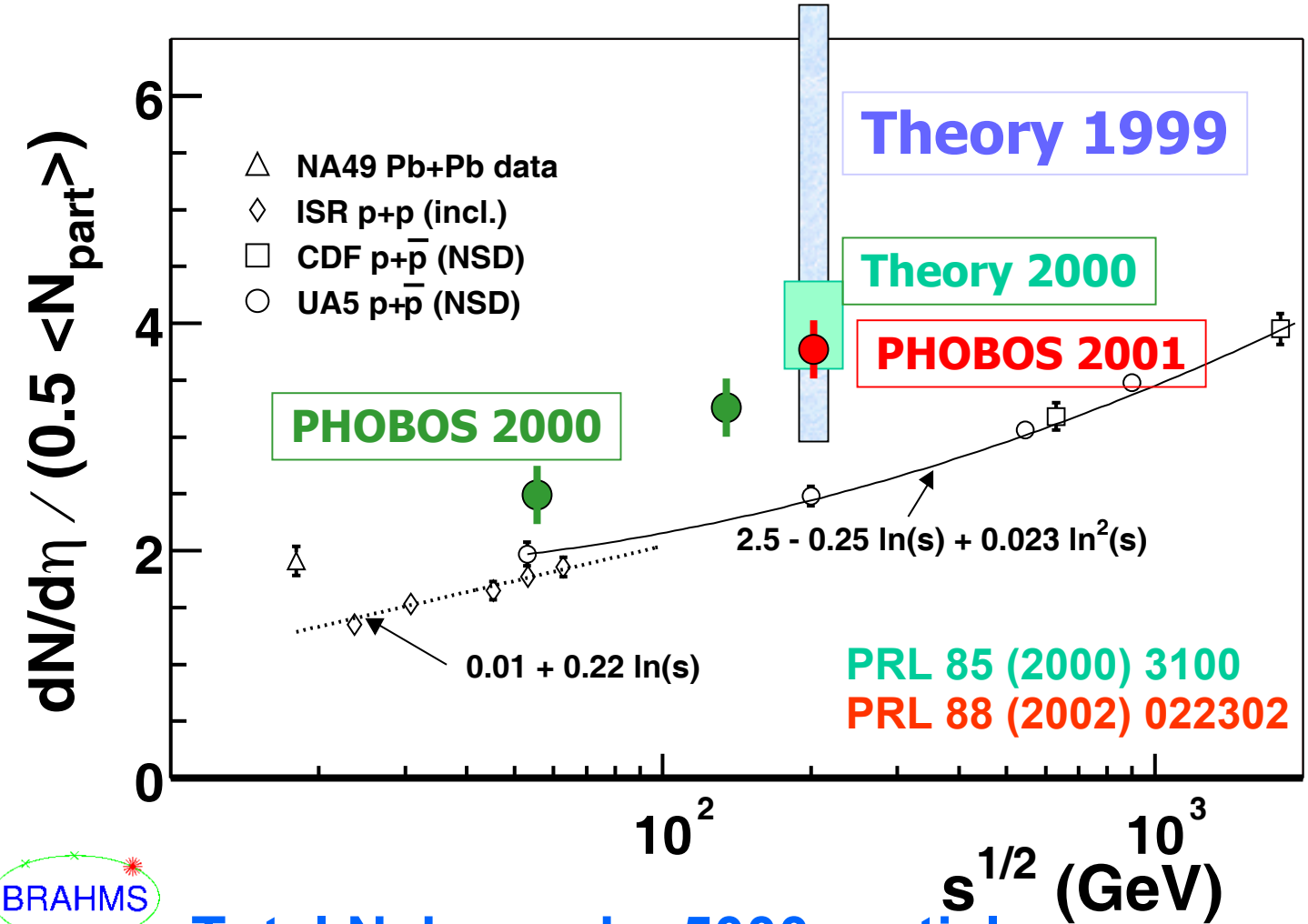

Total Ncharged ~ 5000 particles

Energy Dependence

PRL 88 (2002) 022302

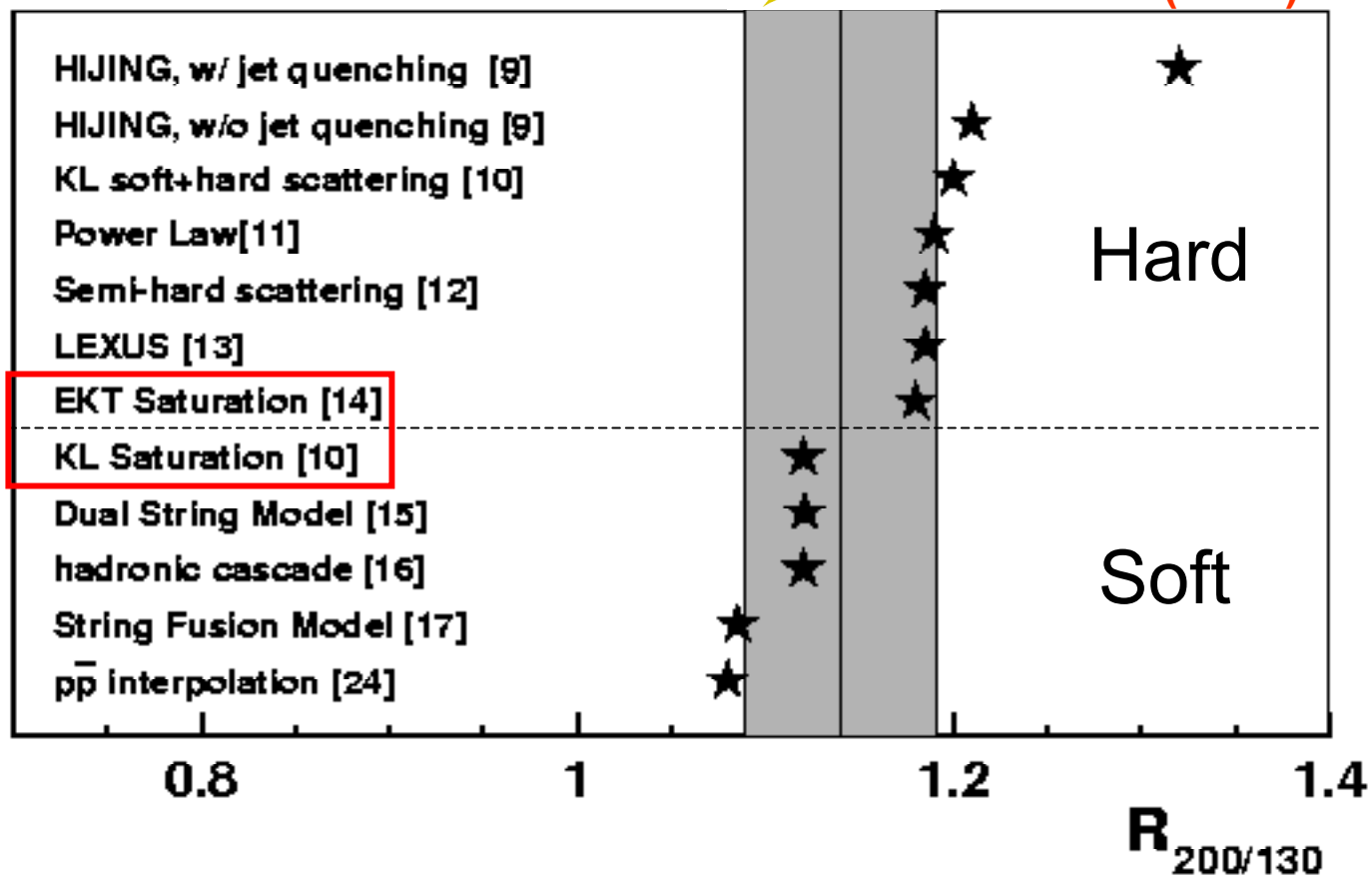

- Data favors models with minimal entropy production

Parton Saturation may connect eA to AA

- Saturated initial state gives predictions about final state.

$$\Rightarrow N_h = c \times N_g$$

$$\frac{dN}{d\eta} \cong cN_{part}\left(\sqrt{s}\right)^{\lambda} f(\lambda|y|, Q_s)$$

λ~0.25 from fits to HERA data:
$xG(x) \sim x^{-\lambda}$

Kharzeev & Levin, nucl-th/0108006

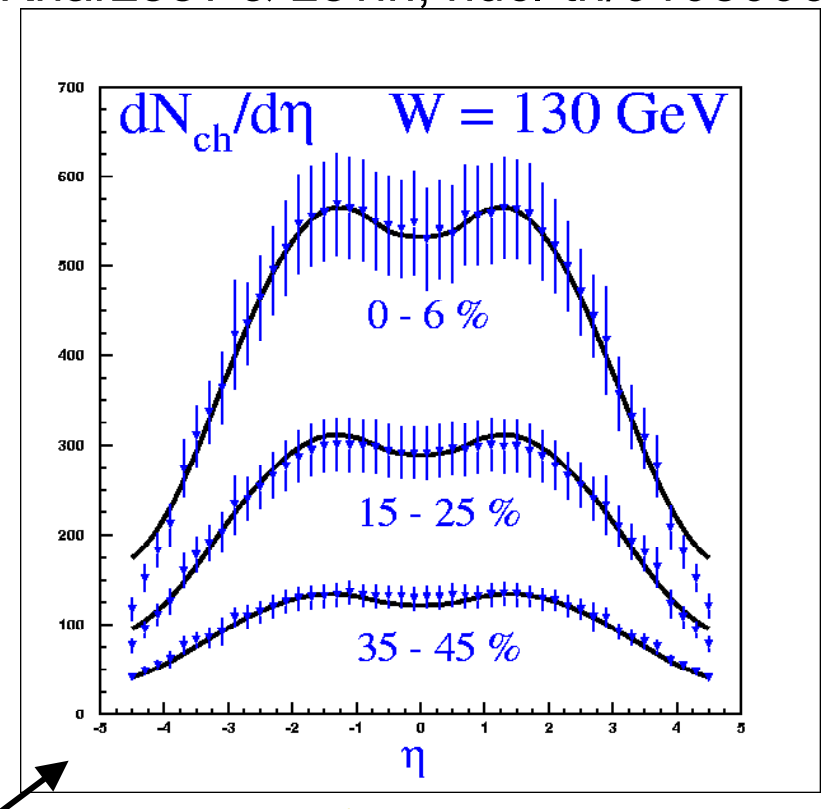

PHOBOS PRL 87 (2001)

Fit PHOBOS data at 130 GeV to set c, Q_s

Saturation Works at 200 GeV

L. McLerran, DNP 2001

nucl-ex/0112001

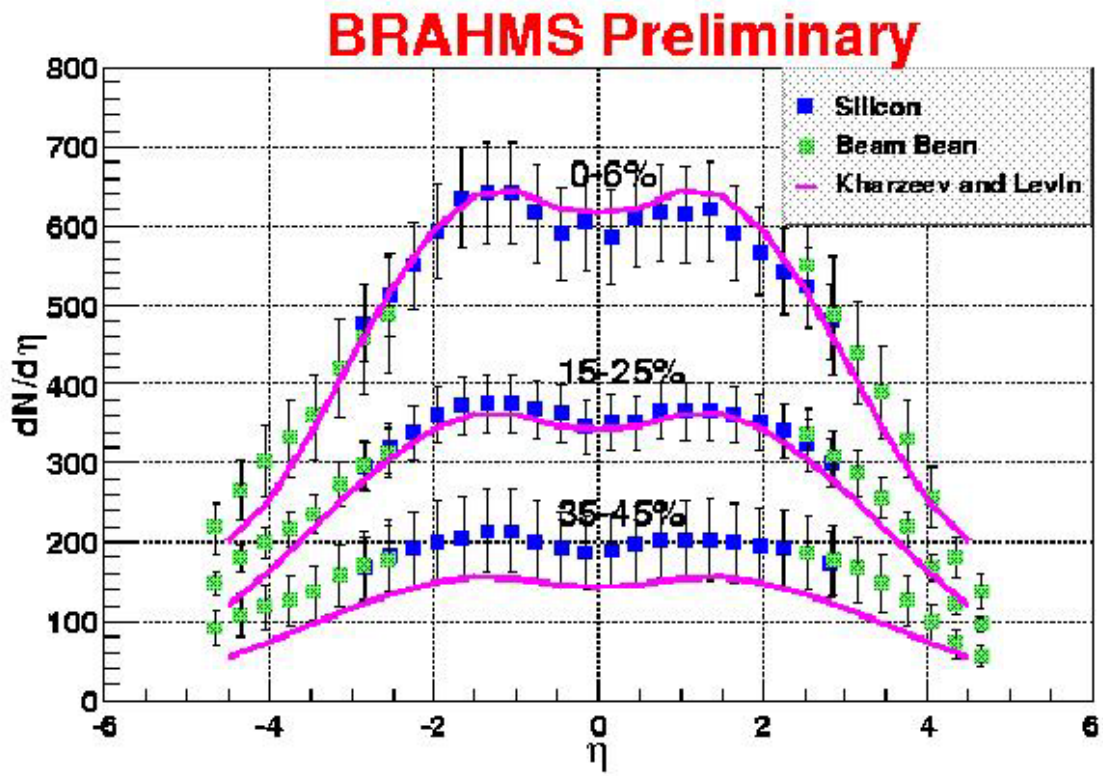

η

- Saturation models describe the data
  - Initial state parton density might be high enough to reach saturation regime

RHIC shows rapid expansion & a high temperature

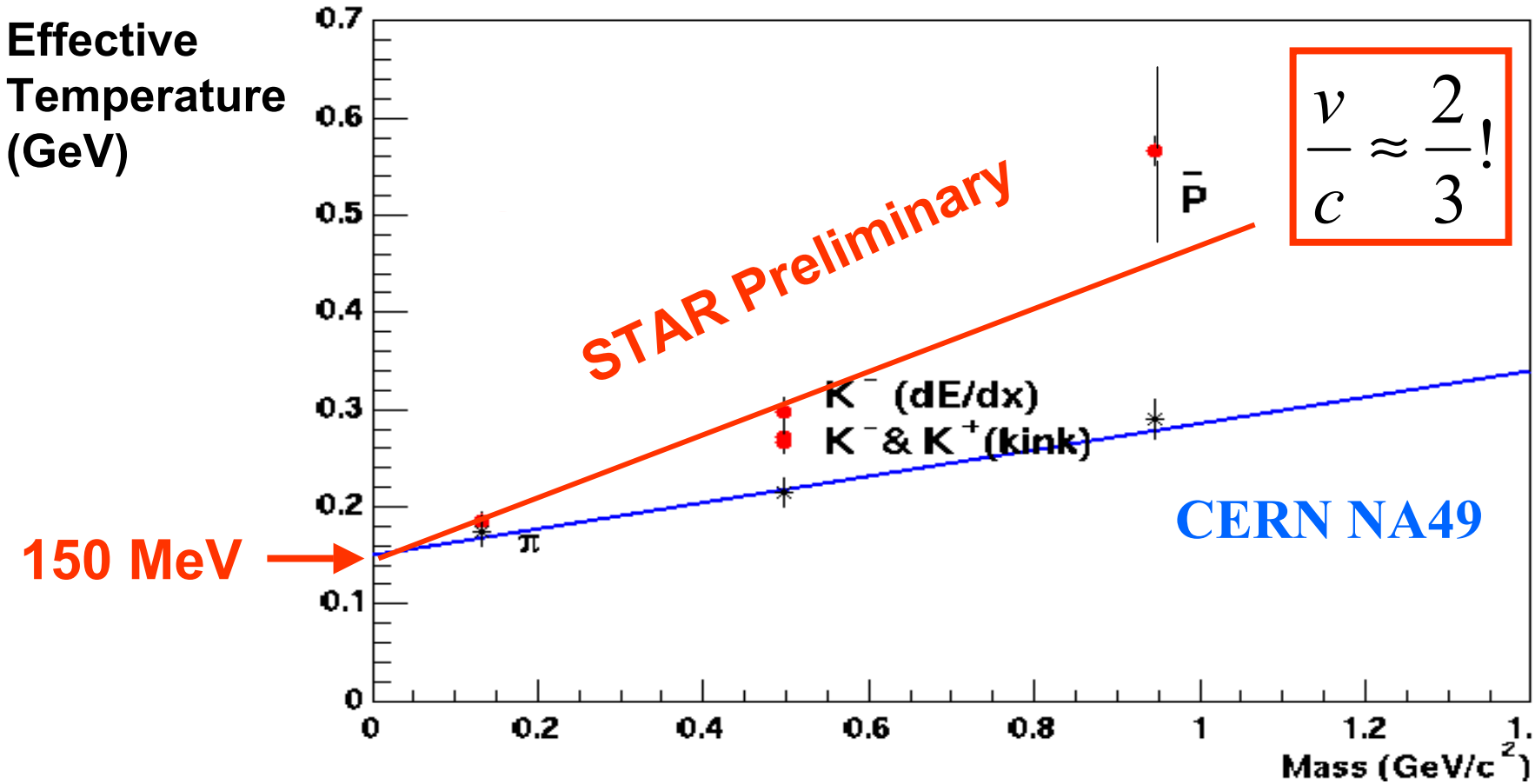

PHENIX: p's and pbar's outnumber π's at p_t of 3 GeV/c!

Another "Thermometer"

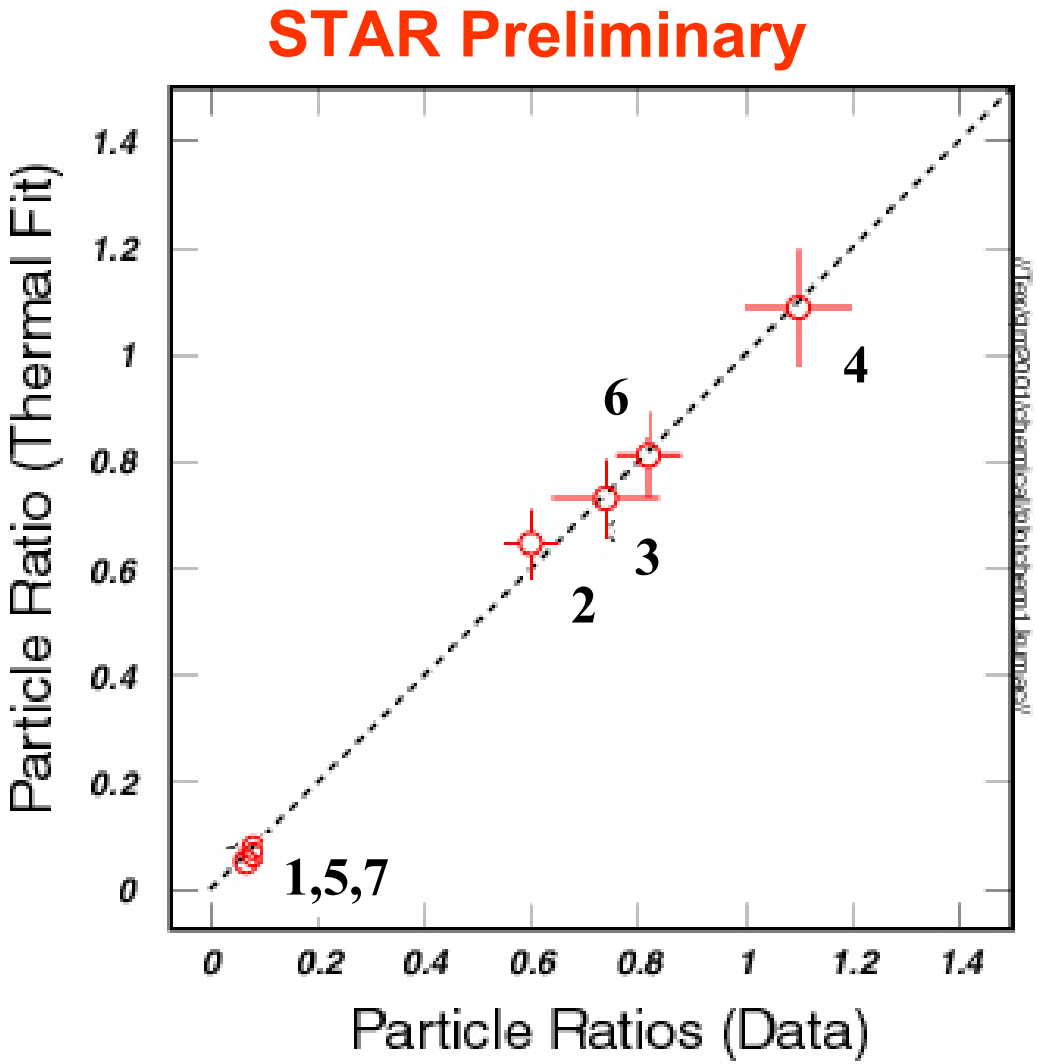

T ~ 170-200 MeV

1. $K^- / (h^+ + h^-)$
2. $\bar{p} / p$
3. $\bar{\Lambda} / \Lambda$
4. K^+ / K^-
5. K_0^* / h^-
6. $\bar{\Xi}^- / \Xi^-$
7. $\bar{p} / \pi^-$

Energy Density Estimate (Bj)

$$\varepsilon_{Bj} = \frac{1}{\pi R^2}\frac{1}{c\tau_0}\left(\frac{dE_T}{dy}\right)$$

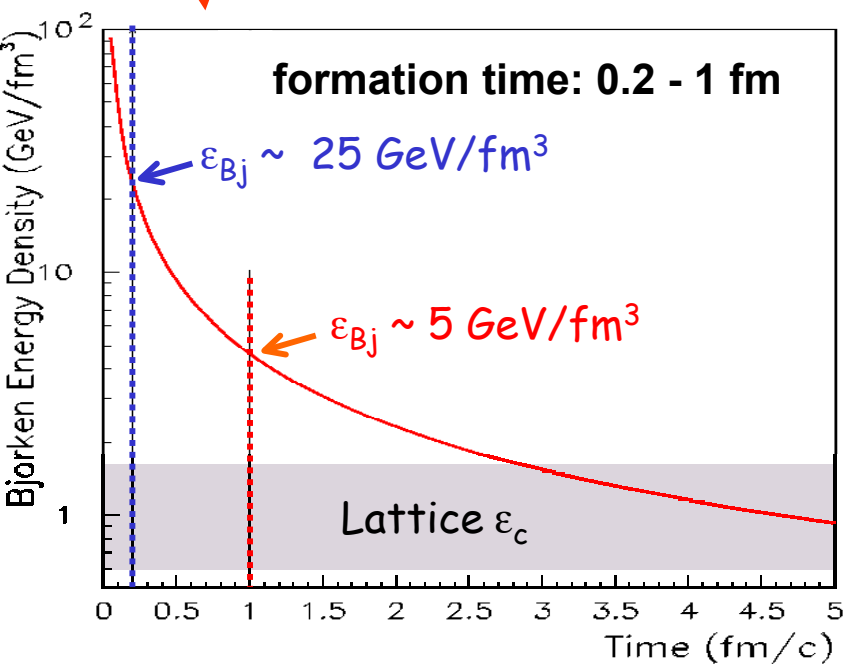

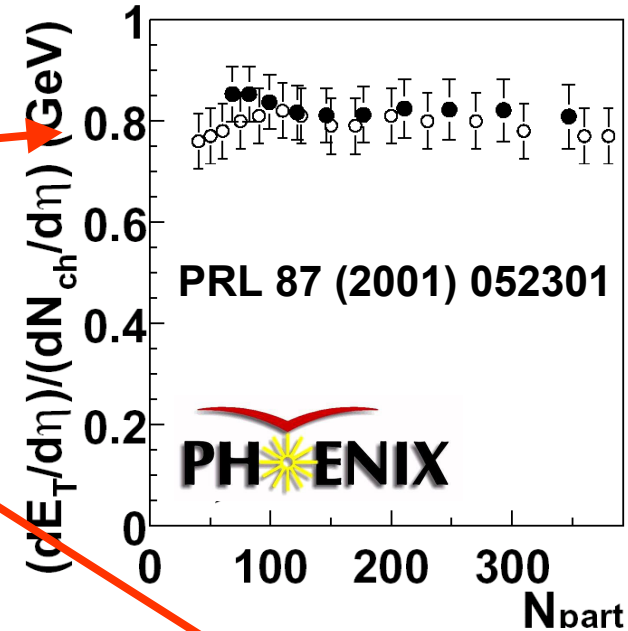

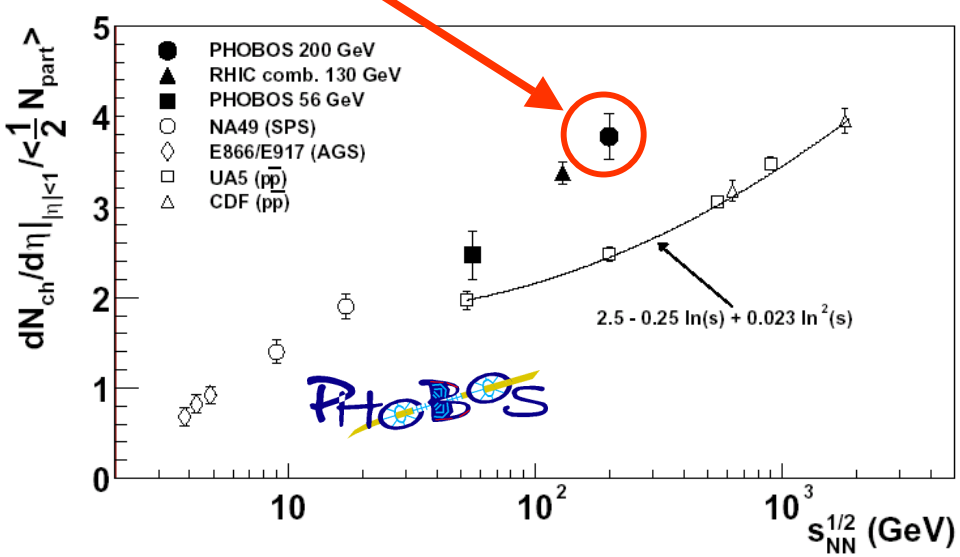

Putting it all together

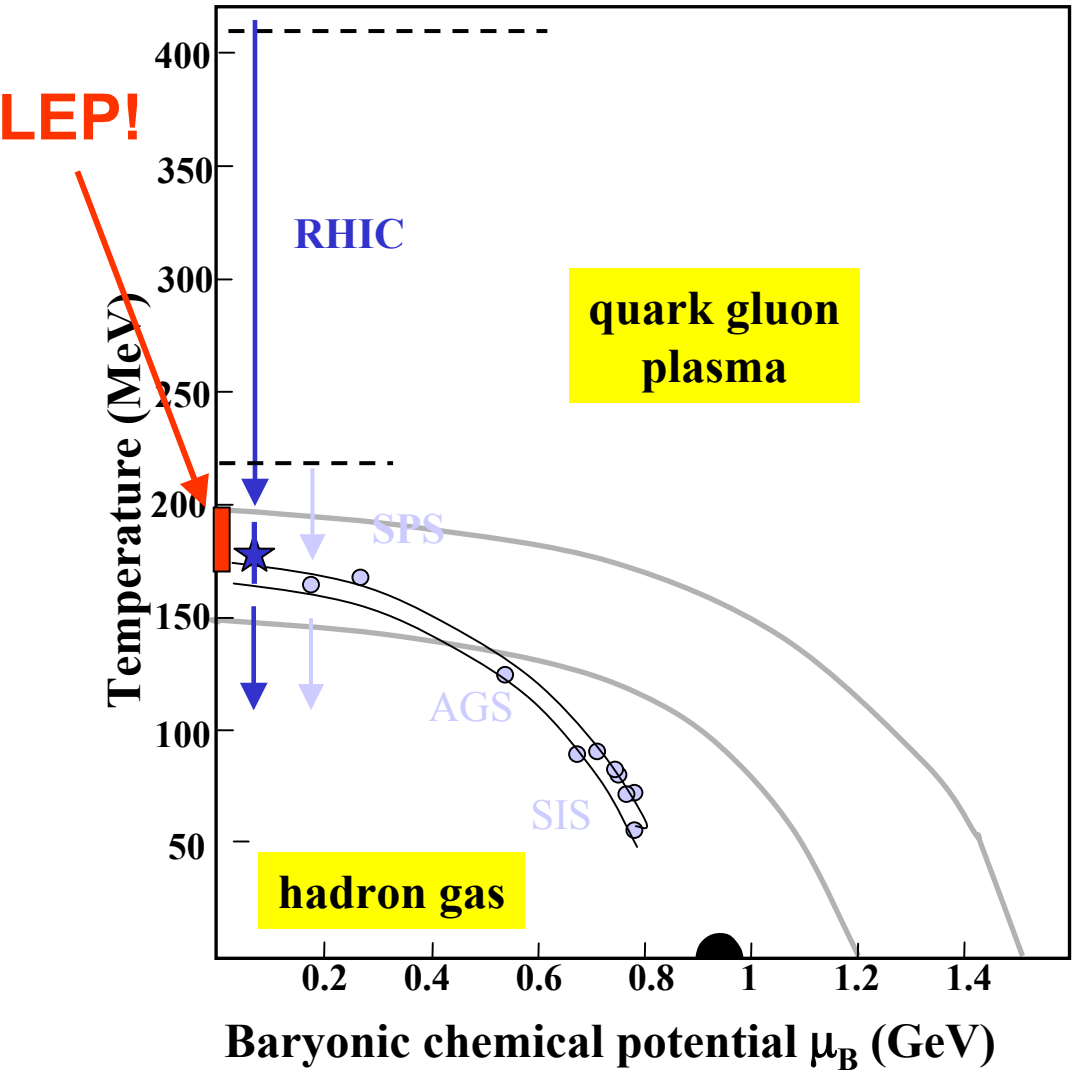

- Universal curve!
- RHIC:
  - "bulk" matter
  - high energy density
    $\varepsilon_{initial}$ ~ 5-25 GeV/fm^3
    (lattice $\Rightarrow$ T_i >250 MeV)
  - freezeout near T_C
  - early collective expansion
    v_t ~ 0.65 c

Suppression of High p_T Hadrons

- AuAu data
  - central (0-10%) and peripheral (60-80%)
- compared to N-N reference
  - peripheral collisions
    - described at high p_T
  - central collision
    - suppressed at high p_T

PHENIX, PRL 88 (2002) 022301

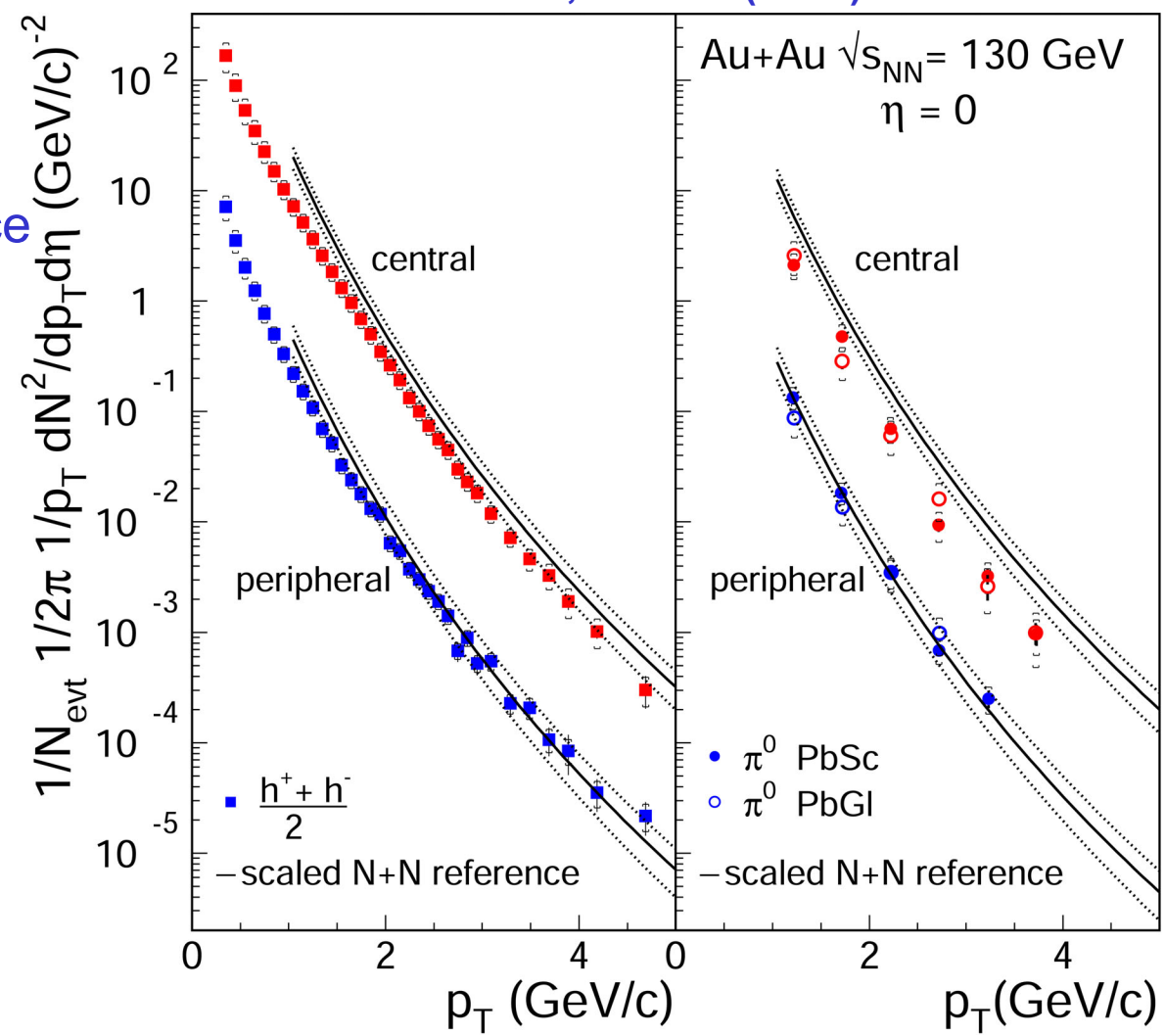

Scaling failure: might be quenching

PHENIX, PRL 88 (2002) 022301

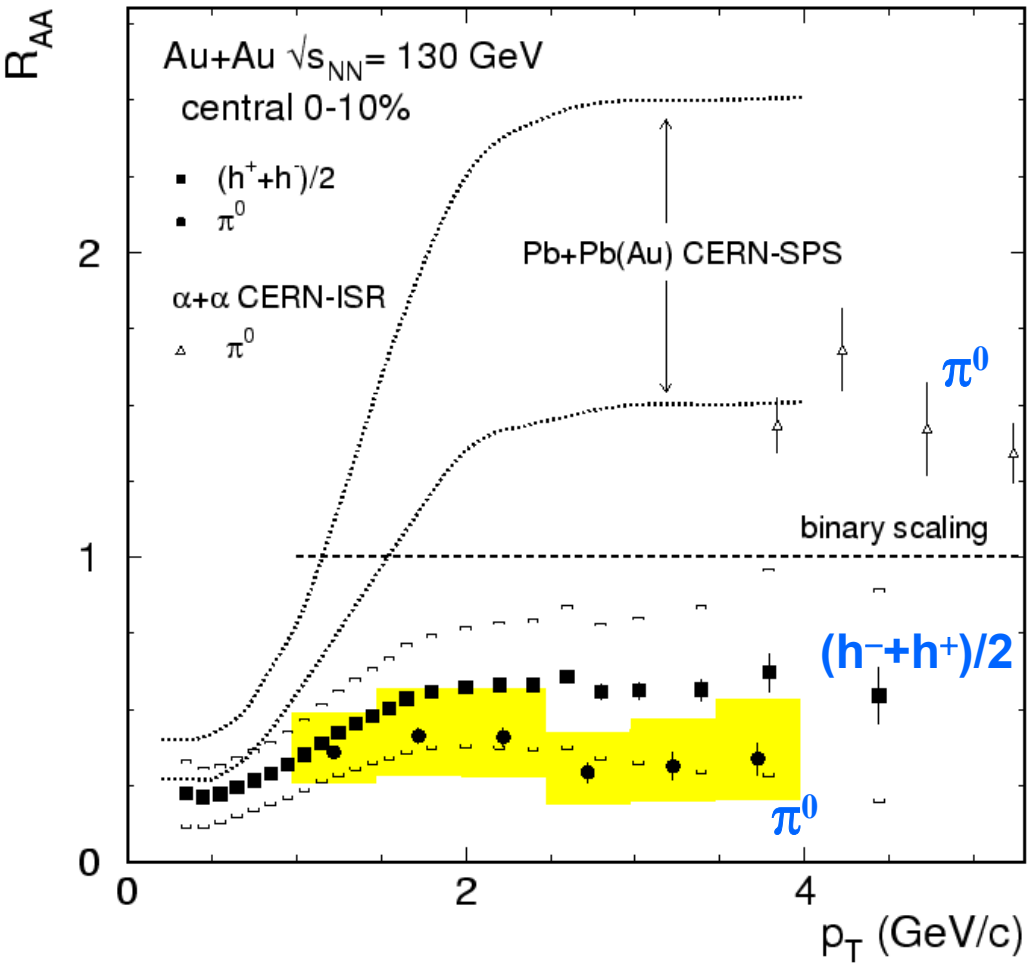

But it could be parton saturation

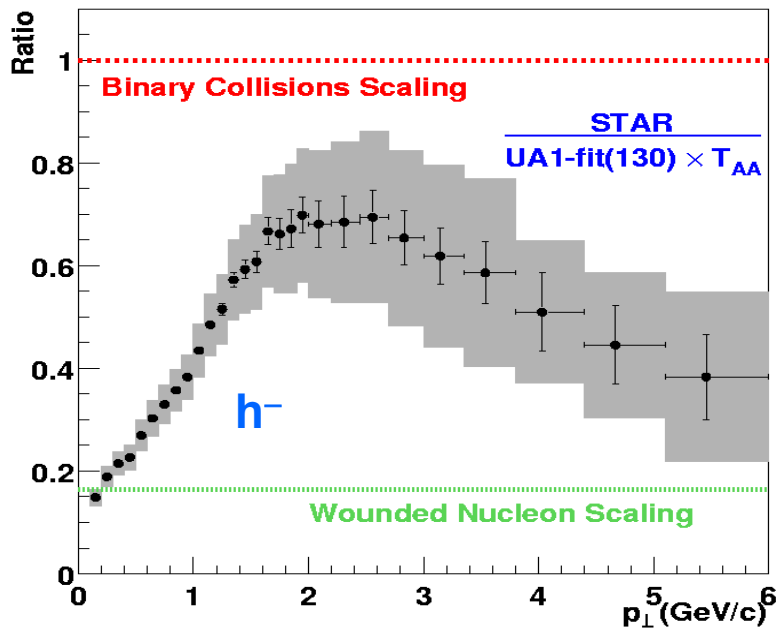

Lessons from the HERA Collider Program on Physics & Detectors

Allen C. Caldwell, Columbia University

1 Introduction

The HERA accelerator has provided a wealth of results on proton and photon structure, diffractive and exclusive production of different states, jet and particle production, α_S measurements, limits on exotic particle production, etc [1]. The most important results to date are the measurement of the steep rise of the structure function F_2 at small-x [2], and the measurement of a large diffractive cross section [3]. These measurements are of fundamental importance and have generated intense activity in trying to understand their physical origin. My main point in this talk is that these results were obtained with detectors not optimized for these measurements. A second round of experiments designed with this physics in mind, at the EIC and/or with further HERA running (HERA3), could lead us to a much better understanding of the physics opened up by the HERA data. I will discuss the structure function and diffractive data in more detail below, but will not have time to cover any other aspects of the HERA physics program.

2 Physics Goals of HERA Colliding Beam Experiments

The original physics goals for the HERA experiments can be summarized with a few quotes from ZEUS Technical Proposal (March 1986):

- "HERA [is] first and foremost an electron quark collider ..."
- "The measurement of the proton structure functions gives access to three domains of physics: electron and quark substructure; properties of the electroweak current; QCD interactions"

under QCD interactions, we find

- "Measurements of the quark and gluon structure functions and their logarithmic dependence with Q^2 should allow a precise measurement of the strong interaction parameter, α_S"
- In addition, we find some comments on the search for exotic particles and photoproduction experiments.

There is no mention at this time of low-x physics or diffraction. The experiments H1 and ZEUS were not designed for this type of physics. Small-x physics, due to kinematics, is small-Q^2 physics, and small Q^2 implies primarily small electron scattering angles. The granularity, acceptance and resolution of the detectors were not optimized in this region. Both H1 and ZEUS upgraded their detectors in this 'rear' direction, with significant improvements in position and energy resolution, and increased kinematic coverage, but a new detector could offer much improved measurements.

Diffractive physics, $eP \rightarrow ePX$, requires an outgoing scattered proton. ZEUS, and eventually H1, equiped the forward region with proton spectrometers. These had small acceptances limiting their usefulness for diffractive measurements. In fact, the large diffractive cross section at HERA was discovered by seeing a rapidity gap in the main detectors in the proton direction. A new detector with strong emphasis on diffractive measurements could have great impact on our understanding of this physics.

3 Structure Function Measurements

An extract of early HERA data is shown in Fig. 1.

The HERA data demonstrated the now well-known rise of F_2 with decreasing x. The rise in F_2 depends strongly on Q^2. An early question was 'how low in Q^2 does this rise persist' ? The H1 and ZEUS detectors employed upgrades to address this question. A summary of the the rise of F_2 at small-x is made by fitting F_2 to the form $Ax^{-\lambda_{eff}}$ for $x < 0.01$ for fixed Q^2, and is shown in Fig. 2.

There is a change in slope in the region $0.5 < Q^2 < 1$ GeV^2. At low Q^2, the photon behaves as a hadron as far as energy dependence is concerned. An important question raised by the HERA data is whether the transition to a steeper energy dependence, in particular the Q^2 value at which this transition takes place, can be understood. Note that the region around $Q^2 \approx 1$ GeV^2 is not measured precisely at HERA, since the main detectors have no acceptance at this Q^2, and special detectors installed later measure at lower Q^2. Special runs, such as the 'shifted vertex' runs help, but they dont yield precise results. There is therefore a lack of data exactly in the region of the transition in energy dependence.

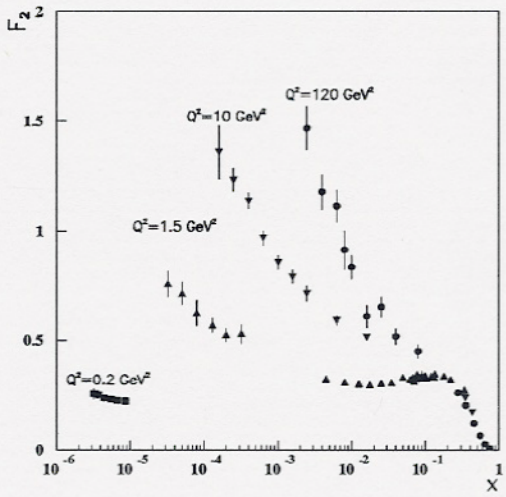

Figure 1: Some of the early HERA data on the proton structure function F_2.

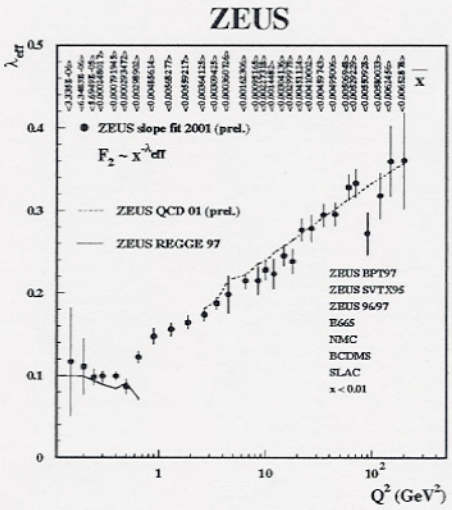

Figure 2: Effective power of F_2 at small-$1/x$ versus Q^2.

4 Gluon Density

The behavior of F_2 is shown versus Q^2 at fixed x in Fig. 3. At large-x, the gluon density is small, and $dF_2/d\ln Q^2$ is used to extract α_S. At small-x, scaling violations are dominated by the gluon density. In LO pQCD, $dF_2/d\ln Q^2 \propto \alpha_S x g(x, Q^2)$. The gluon density from a full NLO DGLAP fit is given in Fig. 4.

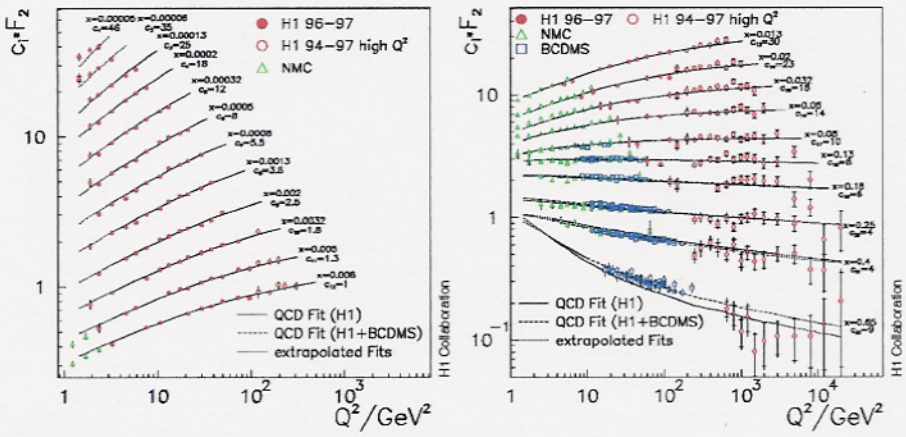

Figure 3: Proton structure function F_2 plotted versus Q^2 at fixed x.

At smaller Q^2, it is observed that the fits yield a vanishing NLO gluon density at small-x, while the quark density is still rising. These results are non-intuitive, and may signal the presence of screening or other types of corrections. Note that the DGLAP fits work at all Q^2 (the χ^2/DF do not deteriorate much when going to lower Q^2), yet it is not expected to be valid below $Q^2 < O(1)$ GeV^2. Physical intuition or other constraints, such as comparing pdfs order by order, is needed to decide if the results are sensible. Again, precision data in the region $Q^2 \approx 1$ GeV^2 would be very useful. Also, a measurement of F_L in this region could play a big role in understanding the behavior of the gluon density.

5 Diffraction in DIS

The diffractive events were initially seen in the HERA data as excess events with large rapidity gaps - i.e., events with no hadronic activity in the direction of the proton beam. These measurements were made with the main detectors. Events were also analyzed where

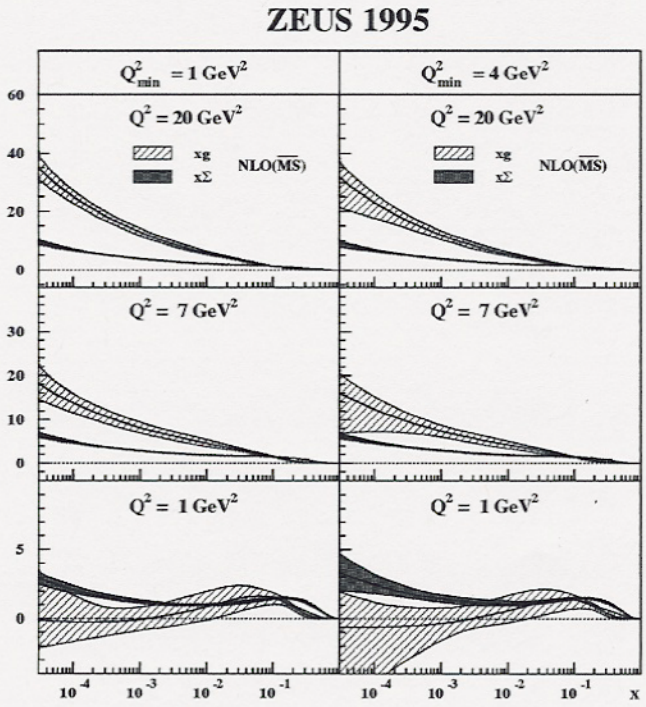

Figure 4: The gluon and quark momentum densities plotted versus x for different Q^2.

the outgoing proton was also measured, yielding a measurement of the t-dependence of the diffractive cross section. The 4-dimensional diffractive cross section $d\sigma/dx_P dQ^2 dt d\beta$ was also measured in large bins. However, the bulk of the data is integrated over t, e.g., as shown in Fig. 5. These data have high precision and yield a wealth of information. However, events where the proton has dissociated cannot be clearly separated, and models must be used to perform a subtraction, leading to substantial systematic uncertainties. In addition, the physics contained in the t distribution is very important. The ideal measurement would therefore be a full $F_2^{D(4)}$ measurement.

A striking observation is that the diffractive and DIS cross sections have very similar energy dependences. This is seen in Fig. 6.

This is a non-trivial observation which has generated a lot of theoretical activity, such as the development of the Golec-Biernat & Wüsthoff model of small-x DIS [4]. A full understanding of diffraction will undoubtedly require the measurement of the full 4-dimensional diffractive cross section, which would require high acceptance forward proton spectrometers.

6 Comments

- I have left out a large part of HERA collider physics (jet production, heavy quark physics, high-x parton densities, EW parameters, searches, ...)
- The most important measurements to date are the steep rise of the structure function at small-x, and the observation of a large diffractive cross section.
- The detectors were not designed for this purpose. Upgrades and clever ideas have allowed the measurement of many important features, but structure function measurements near $Q^2 = 1$ GeV^2 are not very accurate, no dedicated running for F_L has been done, and diffractive measurements are typically integrated over t and have large proton dissociation contributions.
- HERA II, with integrated luminosities of 1 fb^{-1}/expt and polarized lepton beams will greatly enhance the high Q^2 physics. This is achieved by putting accelerator magnets in the interaction regions. The minimum Q^2 is now about 4 GeV^2, and diffractive measurements with $X_P < 0.01$ will also be more difficult.
- A new phase of running, HERA III, would yield a wealth of new results. By HERA III, we mean running with heavier nuclei, which should give a new view on small-x physics; polarization of the nucleus leading to spin structure function measurements at small-x; and precision measurements of $F_2, F_L, F_2^{D(4)}, F_L^{D(4)}$ in the intermediate Q^2 range $0.1 - 50$ GeV^2.

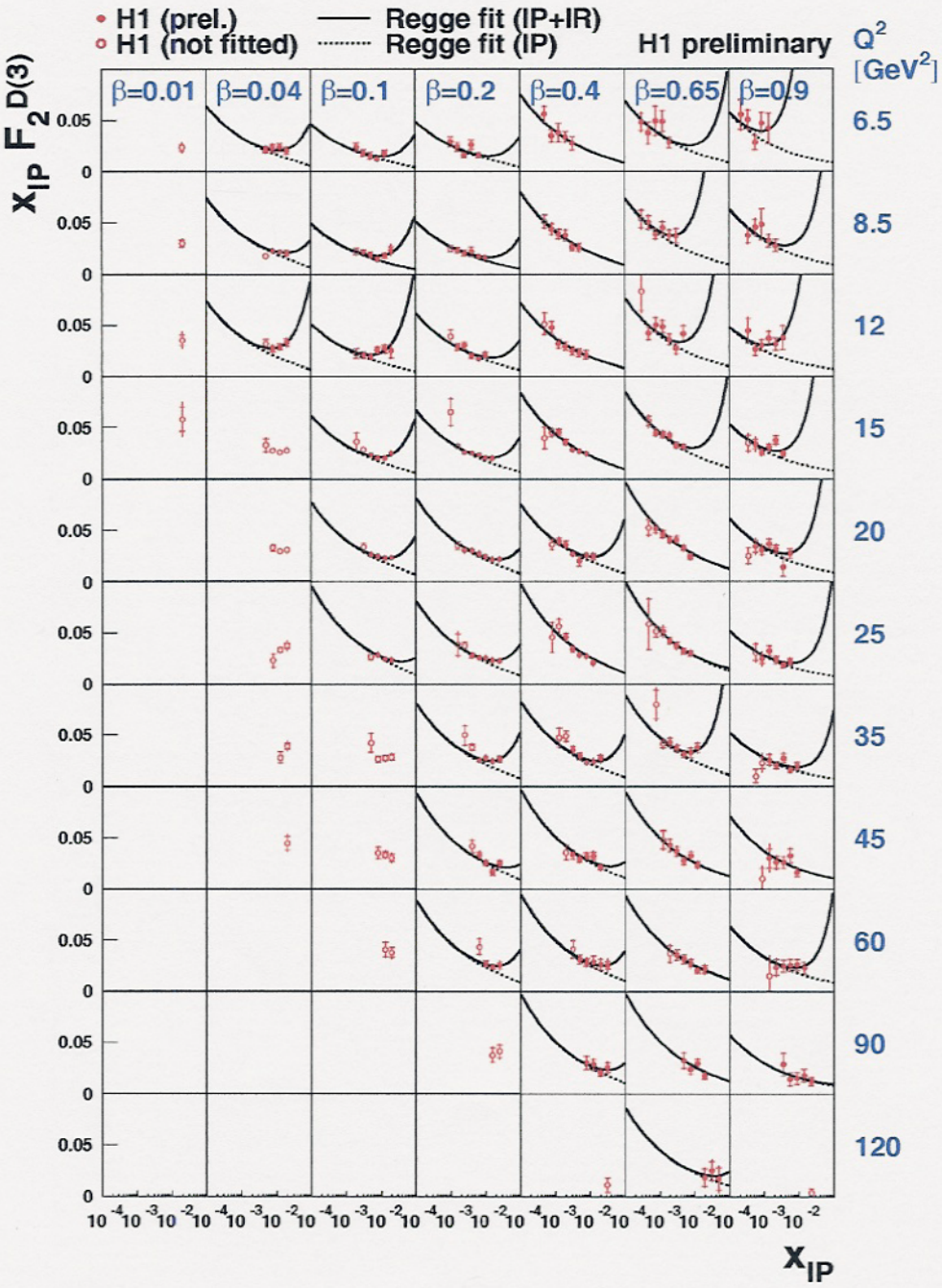

Figure 5: The diffractive structure function $F_2^{D(3)}$ at HERA.

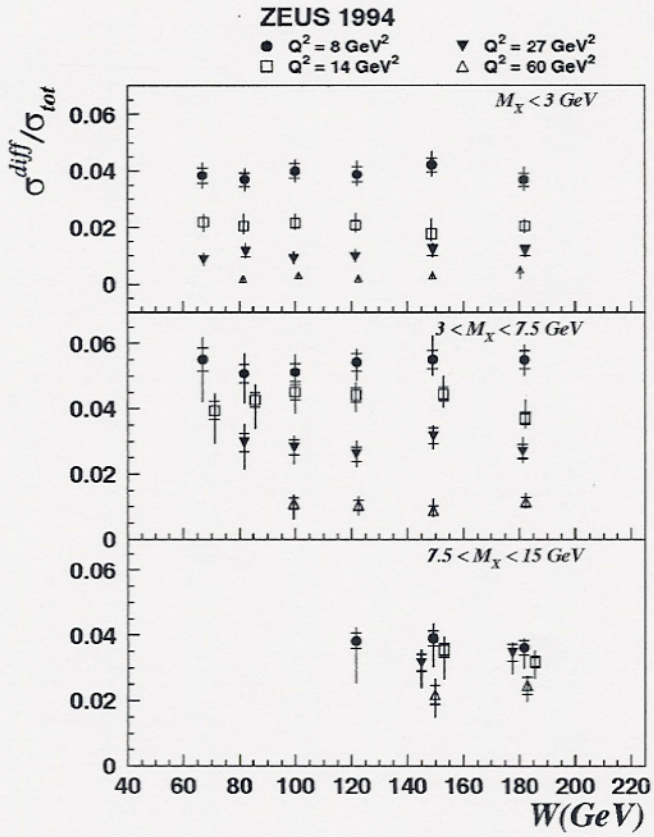

Figure 6: The ratio of the diffractive to total $\gamma^* P$ cross sections as a function of the $\gamma^* P$ center-of-mass energy for different Q^2 and masses of the diffractive final state.

The physics program should be complementary to what can be achieved with the EIC.

References

[1] H. Abramowicz and A. Caldwell, Rev. Mod. Phys. **71**, 1275 (1999).

[2] H1 Collab., I. Abt et al., Nucl. Phys. B 396 (1993) 3; ZEUS Collab., M. Derrick et al., Phys. Lett. B 316 (1993) 412.

[3] ZEUS Collab., M. Derrick et al., Phys. Lett. B 315 (1993) 481; H1 Collab., T. Ahmed et al., Phys. Lett. B 348 (1995) 681.

[4] K. Golec-Biernat and M. Wusthoff, Phys. Rev. D60 (1999) 114023.

A few words about this workshop

Abhay Deshpande
RIKEN-BNL Research Center

For the Local Organizing Committee

A.Deshpand, W. Guryn, L. McLerran, N. Saito, B. Surrow, R. Venugopalan, W. Vogelsang

The Structure

- **Day 1 ➔ *What have we learnt so far?***
  Summary of accelerator workshop ➔ **Focus on EIC**
  Review present experimental & theoretical status of pol.e-p/μ-p
  and e-A/μ–A/p-A physics & other related topics
  Lessons from HERA on detectors, acceptances ….
- **Day 2 ➔ *What can be achieved at the EIC?***
  Polarized e-p, e-A & p-A physics & correlations
  Parallel sessions: e-A, pol.ep & detector ➔ **Focus on EIC**
  Near & distant future plans at other laboratories
- **Day 3 ➔ Focus on EIC ➔ *How do we get there?***
  Parallel session summaries
  Discussion: Future of EIC and move towards a coherent effort
  Comments on QCD: Experiment & Theory 🡐➔ EIC ???

The Parallel Sessions➔ Working Groups

- **Unpolarized e-A Physics Working Group (PWG)**

  Progress on some studies begun earlier

  New ideas for measurements & simulations for EIC

  Discussion: Working Group plans & Communication with DWG
- **Polarized e-p Physics Working Group (PWG)**

  Review & progress of some studies from previous EIC WS

  New studies: Semi inclusive DIS, DVCS, Transversity….

  Discussion: Working Group plans & Communication with DWG
- **Detector Working Group (DWG)**

  Lessons from HERA regarding Forward & Rear Detectors

  Luminosity measurement at HERA ➔ Expectation at EIC?

  Ideas on Particle ID systems explored so far ➔ Ideas for EIC?

  Discussion: Working Group plans & communication with Accelerator/IR Working Group & PWG

Proceedings!

- ***Yes there will be proceedings!***
- **Plenary Session Speakers:**
  3 page summaries + 10 most important slides
- **Parallel Session Speakers:**
  2 page summaries + 5 most important slides
- **Expect submissions by email by March 15th, 2002**
- Proceedings mailed to participants in approximately a month
  on CD-ROMs
  Will also be available separated by talks on the Web Page
  Accessible from **http://www.bnl.gov/eic**
- We do NOT plan large scale production of paper copies of the proceedings, but if they are absolutely necessary, please contact me.

Experimental Observables in eA and Polarised ep at Future Colliders

A. De Roeck[a]

[a]CERN, 1211 Geneva 23, Switzerland

We discuss some of the experimental observables and physics opportunities at polarized ep and eA colliders. Recent studies for such colliders include HERA, EIC and THERA. This informal text accompanies the selection of transparencies given at the end.

1. Introduction

Polarised ep and eA physics has traditionally been studied with fixed target experiments. The commissioning of the first electron-proton collider HERA (27.5 GeV electrons on 820 GeV protons) eight years ago opened up a completely new kinematical domain in deep inelastic scattering (DIS), and was instrumental for exploring this field in collider mode. Apart from the possibility to extend the kinematic range, colliding beam configurations have several important advantages including:

- Better angular momentum separation of the scattered lepton and the nuclear fragments
- Better resolution of the electromagnetic probe
- Easier to tag rapidity gaps
- Possibility to measure the nuclear fragments

A disadvantage is the beampipe which allows part of the event to escape undetected unless an important effort is made to integrate detectors with the machine elements.

Several projects are being evaluated for an eA/polarised ep collider. So far the most complete studies have been done for HERA, which has already a polarised electron beam (see Table 1). When upgraded with Siberian snakes, HERA could operate with polarized electron and proton beams, each polarized to about 70%, accumulating a luminosity of 500 pb^{-1} when integrated over several years. The Electron Ion Collider (EIC) –if built at BNL– will need a polarized electron accelerator, added to the RHIC polarized proton rings, and will probably also need a dedicated experiment. THERA (=TESLA on HERA) will need TESLA to be built at DESY (or tangential to the TEVATRON) and polarized protons in the proton ring. All machines above could also operate in eA mode, with RHIC having already ion beams. The advantage of the EIC is its large reachable luminosity, imperative for many studies. At HERA the luminosity is (just) enough for most topics but its advantage lies in its larger kinematical reach. THERA reaches even further in the x and Q^2 plane, but its relatively low luminosity of 40 pb^{-1}/year may be a handicap for many studies.

Table 1
Possible future ep/eA-collider facilities (x_{min} for (Q^2=1 GeV^2))

Machine	Lumi/y. pb^{-1}(ep)	$\sqrt{s}(ep)$ TeV	x_{min}	Q$_{max}$ GeV^2
HERA	150	0.32	10^{-5}	10^5
Electron-Ion Collider (EIC)	4000	0.03-0.1	10^{-4}	10^4
THERA	40 (250)	1-1.6	10^{-6}	10^6

The kinematics of the scattered electron and (QPM) quark at the EIC with a 10 GeV electron beam on a 250 GeV proton beam is shown in Fig. 1. Low Q^2 values can already be reached with modest electron scattering angles, but well outside the beampipe. The energy of the scat-

tered quark in the detector will be relatively modest. Hence one can expect that the kinematics will mostly be determined from the scattered electron, e.g. by a low noise crystal calorimeter or SPACAL, and by a very precise tracker in a large (perhaps 2T) field. Hence values of $\Delta p/p \simeq 0.005p$ or better can be reached. The Jacquet Blondel method (or alike methods using the hadronic final states) which is limited at low y by $\mathrm{E}_{noise}/\mathrm{E}_{beam}$ may be less powerful than at HERA.

A typical list of experimental variables includes

- Scattered electron to measure the kinematics of DIS
- Scattered electrons at small (zero degree) angles to tag photoproduction events
- Central hadronic final state for kinematics, jet studies, quark flavour tagging, fragmentation studies
- Central hard photons and particles/vector mesons (DVCS...)
- Zero degree photons for control of radiative corrections and nuclear de-excitations
- Missing E_T for e.g. scattering with neutrinos in the final state.
- Tagging of forward particles (diffraction/target dependence)
- Tagging of forward nuclear fragments.

Furthermore it is desirable to have changeable beam energies, polarised beams other than protons (e.g deuterons), a spectrum of nuclear beams, and high luminosity.

2. Unpolarized ep/ed scattering (brief)

HERA already covers a large area for this physics. The additions an EIC could make result from the high lumi, variable CMS energy, deuteron beams, and designing an optimal detector and IP-detector layout for this physics from the start.

Key measurements include

- Deuteron beams to study the nuclear structure (d/u for $x \to 0$, $\overline{d}(x) - \overline{u}(x)$, α_s...)
- $F_L, \sigma_L(p) - \sigma_L(n)$
- Flavour separation (charm, strangeness)
- Curvature of $dF_2/dlnQ^2$
- Precise direct determination of the gluon ($0.001 < x < 0.5 - 1$)
- Exclusive reactions, t-dependence
- Transition region $Q^2 = 0 \to$ few GeV^2.
- Nucleon fragmentation

3. Polarized ep/ed scattering

Key measurements include

- Polarised structure functions of the proton and the neutron at low-x, low Q^2 and the Bjorken and other sum rules
- Contribution of the gluon to the spin of the proton (adding to pp-RHIC, HERMES and COMPASS in the near future)
- Quark flavour contributions to the proton (semi-inclusive, g_5,...)
- Spin structure of other hadrons
- Spin structure of the "resolved photon"
- Orbital momentum of quarks (gluons) $\to$?DVCS?
- Quark transversity distributions
- Spin effects in fragmentation (e.g via Λ production)
- Exclusive reactions

A measurement of $g_1(x, Q^2)$ is shown in Fig. 2 for both HERA an EIC. The measurements for the latter have a very high precision thanks to the large luminosity of this machine. Such measurements allow for Bjorken sum rule verifications to the level of order 1%, and for significant low-x measurements in search of BFKL.

Table 2
The expected statistical uncertainty in the determination of the first moment of the gluon distribution at $Q^2 = 1$ GeV^2

Analysis Type	$\delta(\int \Delta G \, dx)$
1. g_1 fixed target	0.2
2. g_1 fixed target + EIC	0.08
3. combined 2 & EIC jets	0.04

Note that g_1 will be a challenge in terms of controling the false asymmetries, and also for the DAQ system which will have to manage an event rate to tape of order 1 KHz if one wants to make use of full event band width.

Another important target is a direct measurement of ΔG. Several methods, shown to work at HERA, can be used: jet and high p_t hadron production, charm production both in DIS and photoproduction, etc.

The most promising process is di-jet production. The underlying idea is to isolate boson-gluon fusion events, i.e. a process where the gluon distribution enters at the Born level. The result for HERA is shown in Fig. 3. At an EIC the measurable range is reduced to $0.01 < x < 0.3$. Here it will be important to start at low p_T jets (3 GeV/c) and cover an as large as possible η range (-2,3). The result is shown in Fig. 4, compared with other future measurements. The reach at THERA is $0.0005 < x < 0.1$ but an event sample of several hundred pb^{-1} will be needed.

The first moment of ΔG can be extracted from QCD fits to g_1 data. The improvement due to inclusion of EIC di-jet and g_1 data is shown in Table 2. The first two rows give the values quoted before, namely for the NLO QCD analysis without and with projected EIC data for g_1. The third row shows the total improvement using all available information.

Recently some considerable attention was given to the measurement of the quark transversity distributions. These can be accessed via semi-inclusive spin asymmetries. An example for EIC is shown in Fig. 5.

Another new kid on the block is the study of the DVCS process, otherwise called 'micro surgery of hadrons', and leading to the extraction of so called skewed parton distributions. First studies have started on this topic, showing about 50 K events/fb^{-1} are produced within the acceptance cuts for the EIC kinematics.

In present fixed target experiments information on the flavour decomposition can be obtained from semi-inclusive measurements, i.e. measurements where a final state hadron is tagged. This will be possible at EIC as well, and optimally will need particle identification capabilities for the central detector. At ep colliders one has the additional option to study quark flavours in a more inclusive, and therefore fragmentation function independent mode, via charged current interactions, which allows to measure the g_5 spin structure function. A measurement of the appropriate asymmetries for EIC is shown in Fig. 6. The asymmetries are very large and significant measurements can be produced at EIC down to $x = 0.04$. These charged current measurements, with both e^+ and e^- beams, can be used to extract e.g. the Δu and Δd distributions.

Photoproduction processes have been shown to be sensitive probes for the polarized parton structure in the proton AND in the photon. Jet and high p_T track measurements will allow for the first time measurements of the polarised photon structure.

It can be further pointed out that a measurement of the total polarized photoproduction cross section $\Delta\sigma_{\gamma p}(\nu)$ as function of the photon-proton CMS energy ν would contribute to a better understanding of the Drell-Hearn-Gerasimov sum rule. In particular the Regge behaviour of the energy dependence of the polarized cross section can be tested. The sensitivity which could be reached with EIC is about one order of magnitude larger than the one for HERA.

Target fragmentation studies (e.g. detecting fast forward pions or charmed mesons) will allow to study the spin structure of other baryons than the proton and neutron (e.g. Δ^{++}).

It would be very advantageous to have also polarised deuterons. Recent ideas suggest that the acceleration of polarised deuterons could perhaps be even easier –possibly without the need of (many) Siberian snakes – than for protons. If

this becomes a real option the detectors should prepare for maximal forward tagging of the spectators, allowing for the simultaneous measurement of the (polarised and unpolarised) proton and neutron structure.

Disadvantages of using deuterons include a reduction by a factor of two in reach at low-x (but the possibility to obtain measurements at higher x values); the luminosity could be smaller than for ep (estimated to be a factor 5 for HERA); energy smearing of the target by several tens of GeV. An example of a new analysis of ΔG is given in Fig. 7.

4. eA scattering

Using nuclei, an eA collider can make important and novel contributions to QCD. Key measurements include

- Influence of the nuclear medium on the quark distributions within nucleons/nuclear shadowing; measure F_2^A/F_2^D.
- Gluon distributions in nuclei (via charm, jets, scaling violations of F_2)
- Parton saturation at low-x/color glass condensates
- Longitudinal structure function for nuclei (varying energies)
- Colour transparency and opacity (vector mesons)
- p_t broadening in nuclear media
- Jet quenching effects
- Diffractive phenomena (rapidity gaps)
- Hadron formation in nuclei
- Nuclear fragments and excitations

Many of these (parton distributions, jet quenching) are of direct relevance for better understanding of a new state of matter formation in heavy ion collisions. Thus eA can be considered as a calibration for pA and AA

Fig. 8 shows the F_2^A/F_2^D measurement perspectives at the EIC (and HERA) for a rather modest luminosity of 1 pb^{-1}/A per nuclei. At the EIC one can expect 10-100 times higher lumi values.

Fig. 9 shows several methods to measure/access the gluon distribution in nuclear matter: using jet rates, scaling violation or heavy vector meson resonance production. Again the precision shown is typical for HERA, but can be a factor 3-10 better at the EIC. Non-linear parton effects are expected to be amplified by a factor $\mathrm{A}^{(1/3)}$, hence with nuclei such new effects could show up at higher x values.

One of the important measurements at HERA was deep inelastic diffractive scattering and the study of diffraction, either via gaps or leading protons. Does the fraction of DIS events with a gap depend on A? Fig. 10 shows the precision that could be reached (for HERA), which would be more than sufficient to discriminate between different models.

Finally one of the strong advantages of a collider is the opportunity to see nuclear fragments. These fragments are quantised in energy and pseudo rapidity and can thus be identified. This is shown in Fig. 11. It stresses that one needs to equip the proton beam direction with detectors. A detector configuration which would optimize for the measurements above, actively integrated with the beam elements at the interaction point has been proposed by W. Krasny et al.

5. Summary

The EIC is a golden opportunity: Let's make use of it!

6. Acknowledgement

Thanks to S. Bass, D. Barber, G. Conteras, G.A. Deshpande, M. Grosse- Perdekamp, M. Hoffstaeter, J. Lichtestadt, W. Krasny, G. Radel, A.Sandacz, M. Stratmann and M. Strikman

Kinematics of electron and quark

Fig.1

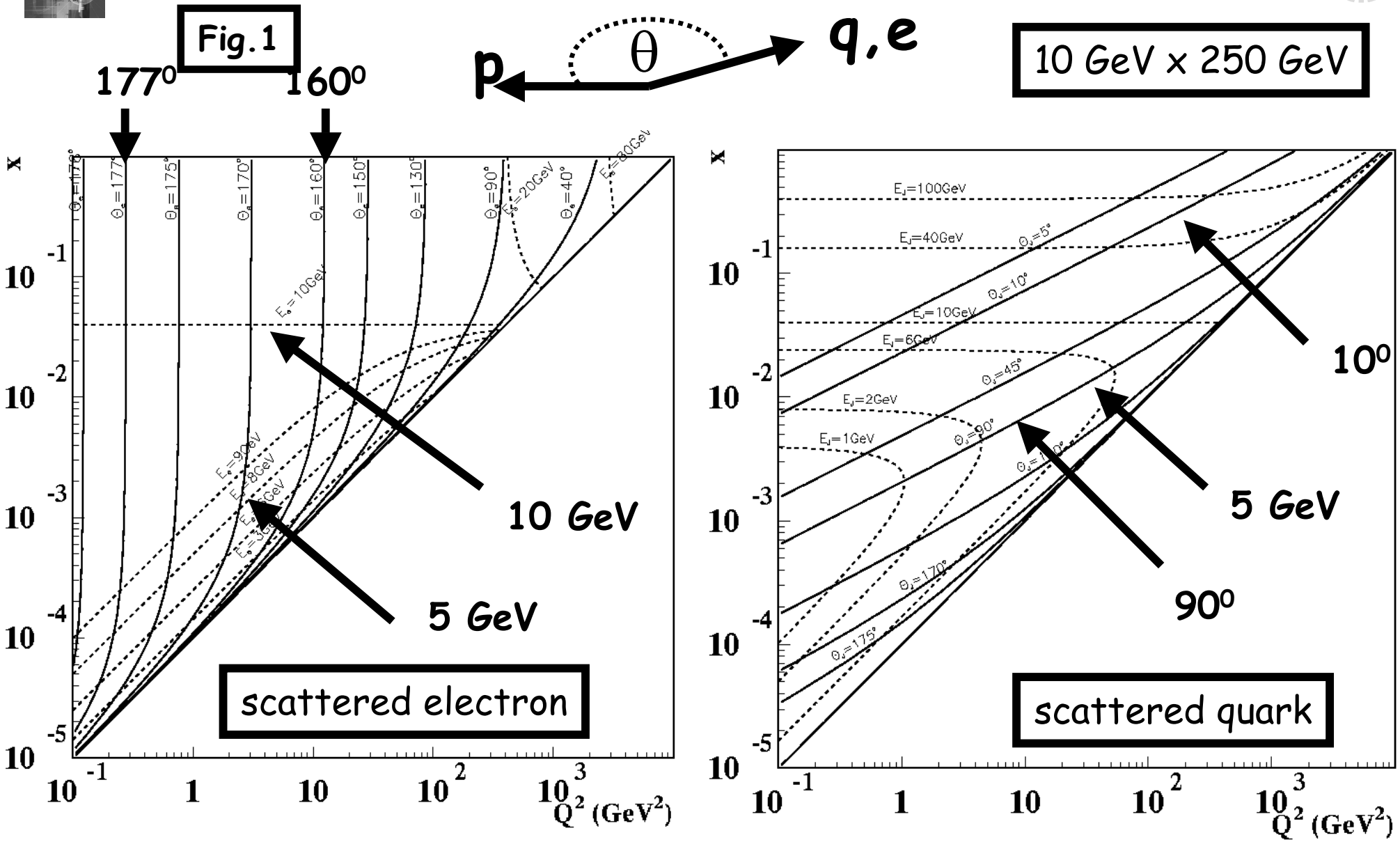

Polarised Structure Function

A. Deshpande et al.

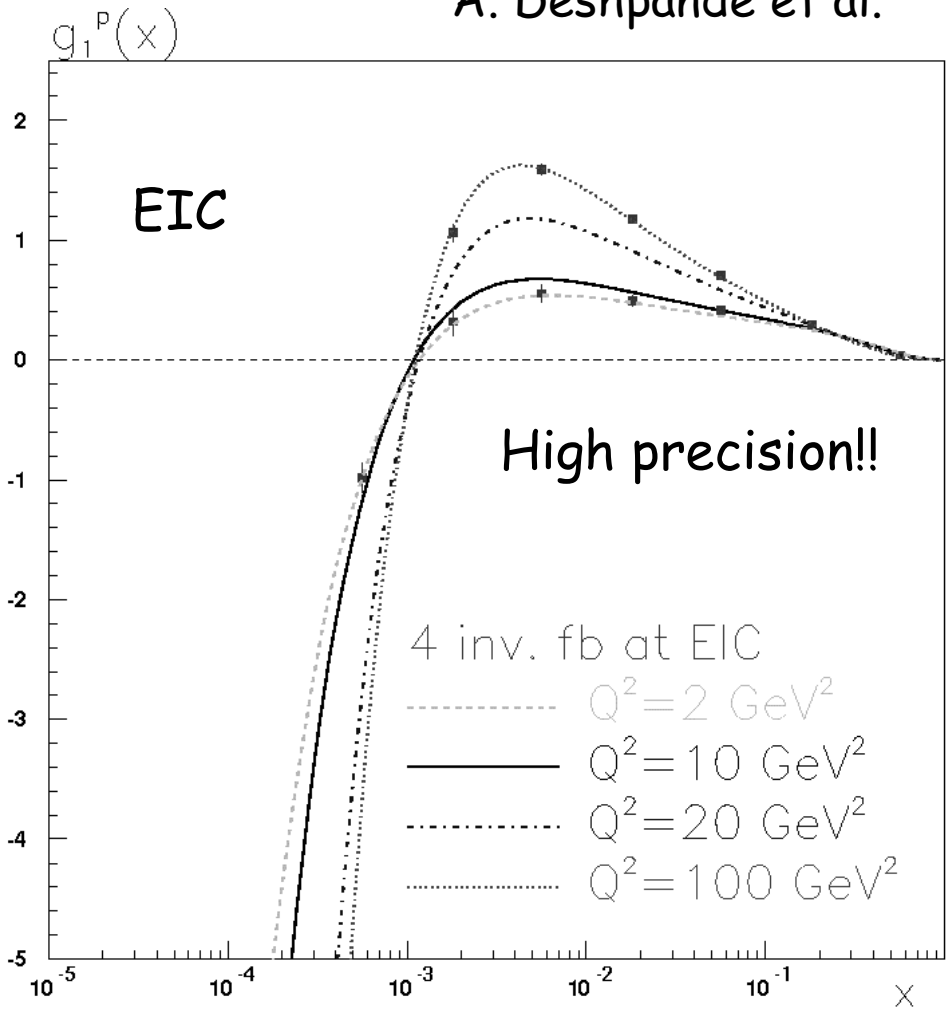

Fig.2

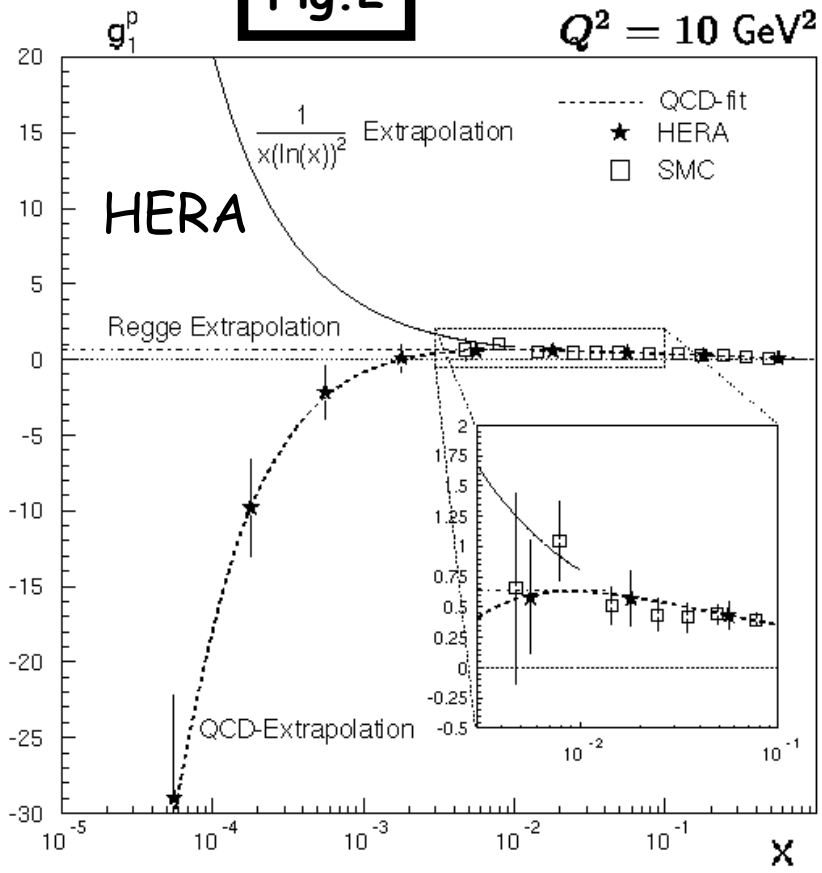

Lower x reach, but precision limited

T.Sloan, G.Igo

$\Rightarrow$ BJORKEN SUMRULE $\int_0^1 dx(g_1^p - g_1^n)(x, Q^2)$ ~ 1% precision at eRHIC

Polarised Gluon Distribution

- From QCD fits to $g_1(x,Q^2)$ data
- From final states: e.g. 2-jet events
- Also from tracks, multiplicities
- (charm at EIC?)

G. Radel, ADR

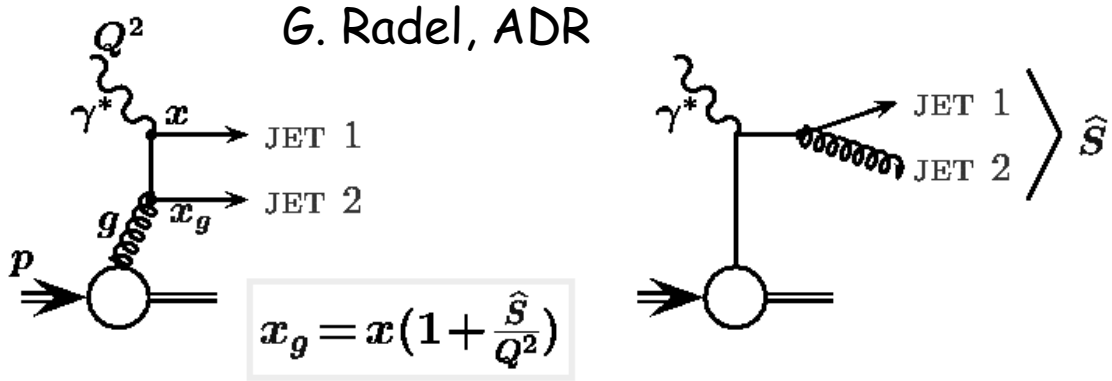

$$x_g = x\left(1+\frac{\hat{S}}{Q^2}\right)$$

"BOSON GLUON FUSION (BGF)" SIGNAL

"QCD-COMPTON" BACKGROUND

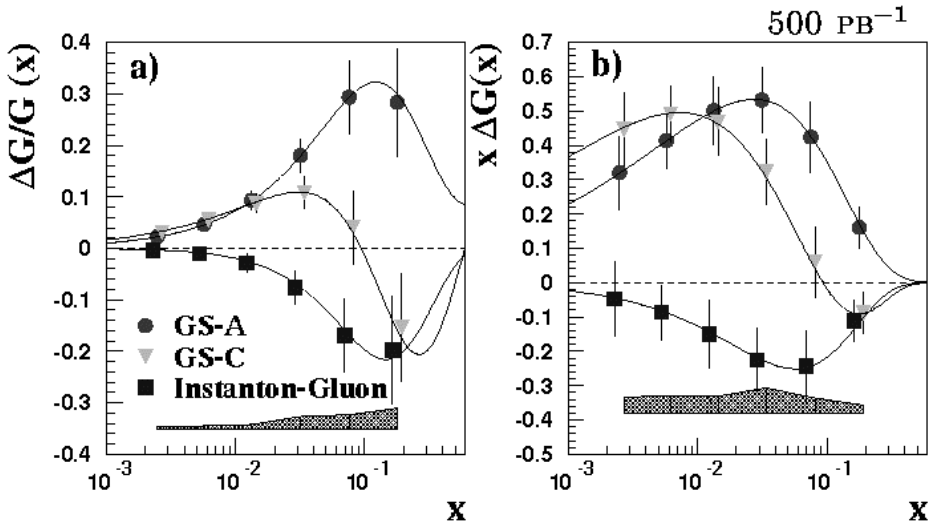

Hera

SELECTION:

- $5 < Q^2 < 100$ GeV^2
- $0.3 < y < 0.85$
- $p_T^{JET} > 5$ GeV
- $|\eta_{LAB}^{JET}| < 2.8$

DETECTOR EFFECTS INCLUDED

$\eta = -\ln\tan(\theta/2)$

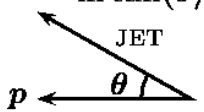

Fig.3

$\Rightarrow$ Needs jet or high p_t track measurements

Expected World Data on ΔG(x)

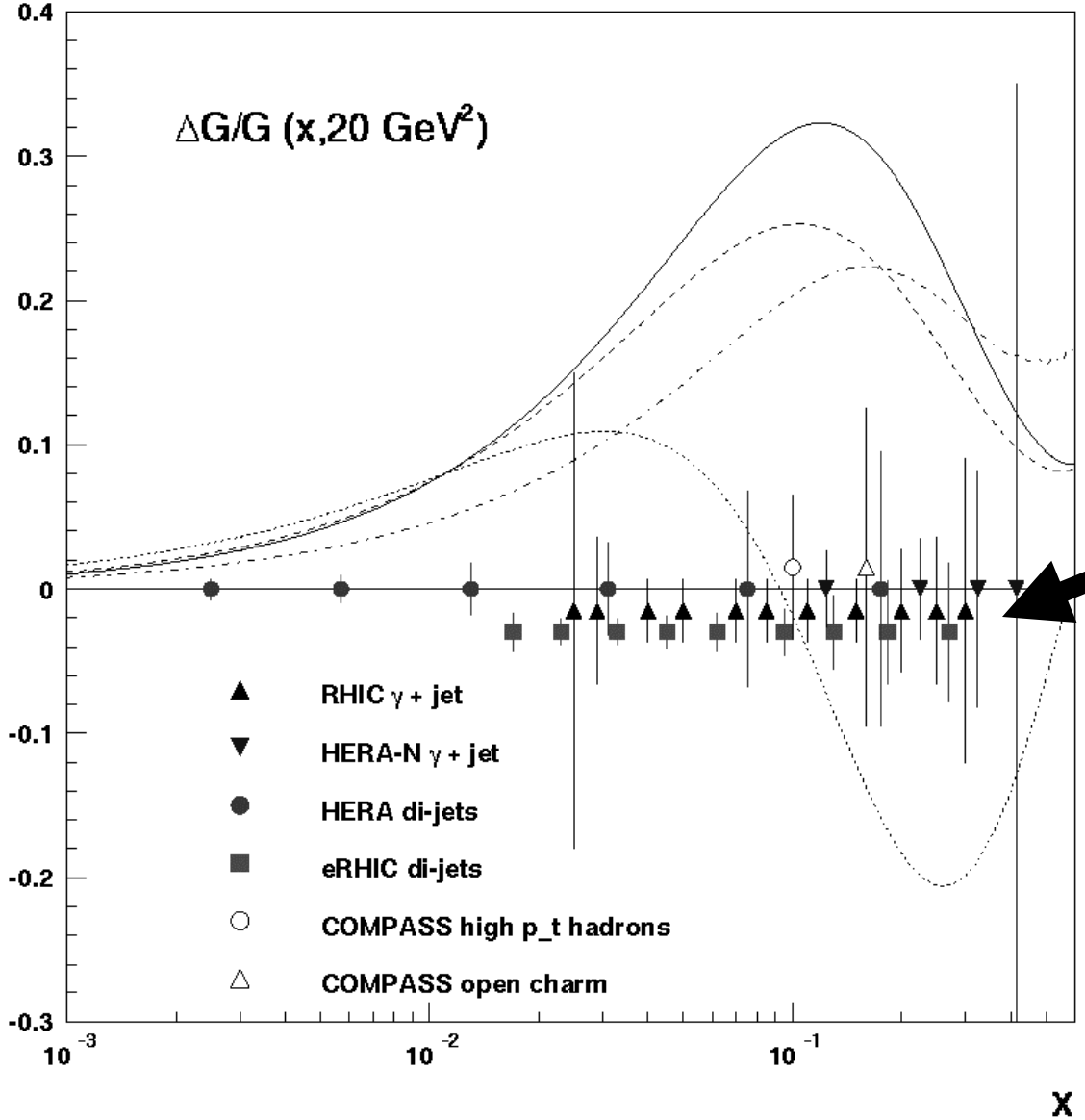

G. Radel, ADR

Fig.4

EIC DATA
$4fb^{-1}$

Good precision
Clean measurement
Range 0.01 <x< 0.3
Constrains shape!!

Transversity

Measure helicity flip amplitudes
$\Rightarrow \delta(x,Q^2)$ quark transversity

No mixing with gluon term in the QCD evolution

Measure single spin semi-incl. asymmetries
DIS+ pion in central detector
Acceptance required $|\eta|<3.5$

$$A_T(x,z) \sim \frac{\sum_q e_q^2 \delta q(x) H_1^{\perp q}(z)}{\sum_q e_q^2 q(x) D_1^q(z)}$$

M. Grosse Perdekamp

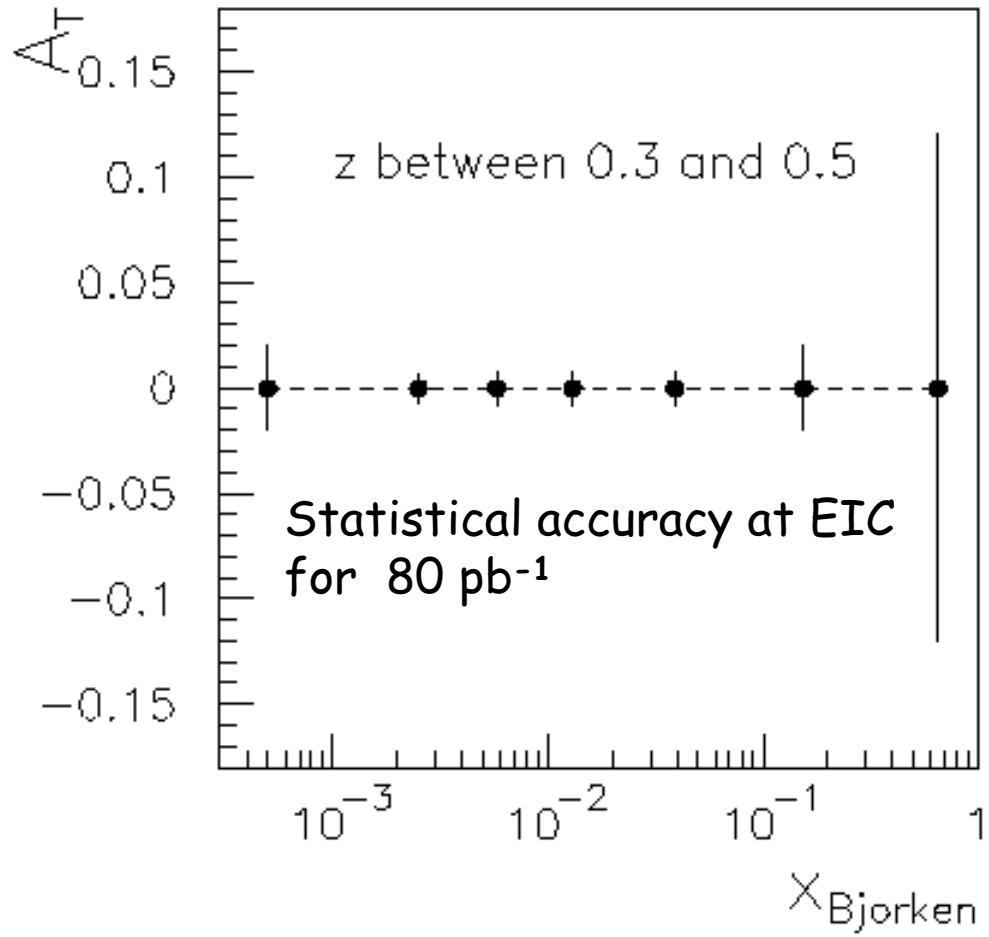

$H_1^{\perp}/D_1^u$ = Collins/fragmentation function
From e+e- data (LEP, B-factory)?

Fig.5

Parity Violating Spin Structure Function

Results for EIC (2 fb^{-1})

G. Contreras, ADR

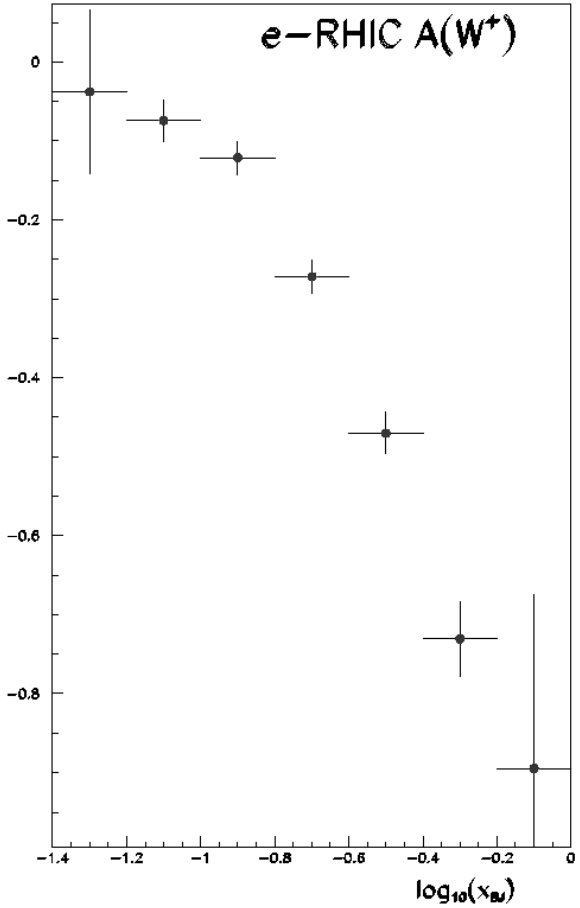

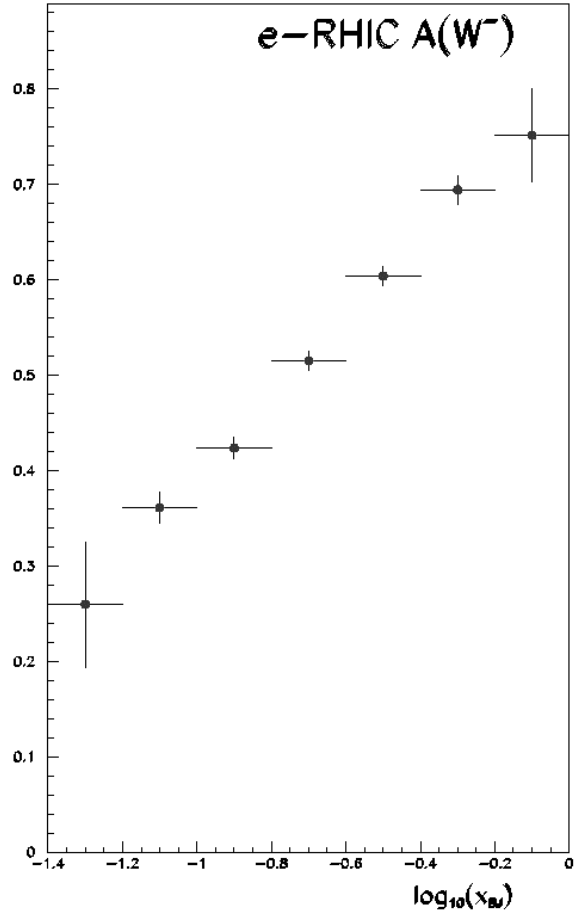

"Hermetic" Detector Required

Fig.6

Full Δu and Δd disentangling will need BOTH e^+ and e^- beams

Polarised Deutrons

Study for HERA: Δg from jets

G. Radel, ADR

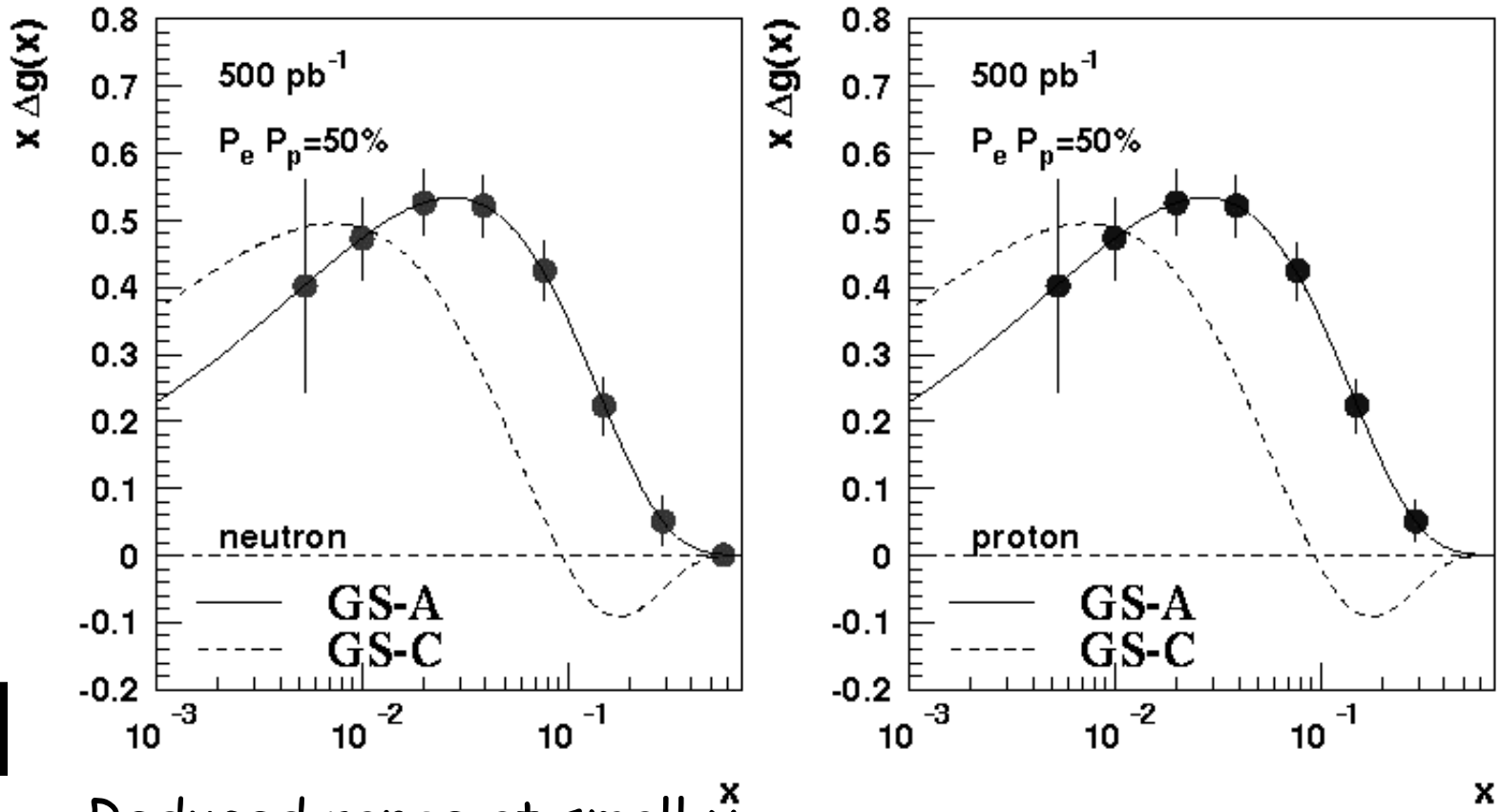

Fig.7

Reduced range at small x

Neutron data may allow to extend the high x range

(proton/neutron tagging assumed)

The Ratio F_2^A/F_2^D EIC perspectives

T. Sloan

systematic
error dominated
by radiative corrections
and luminosity
measurement

Fig.8

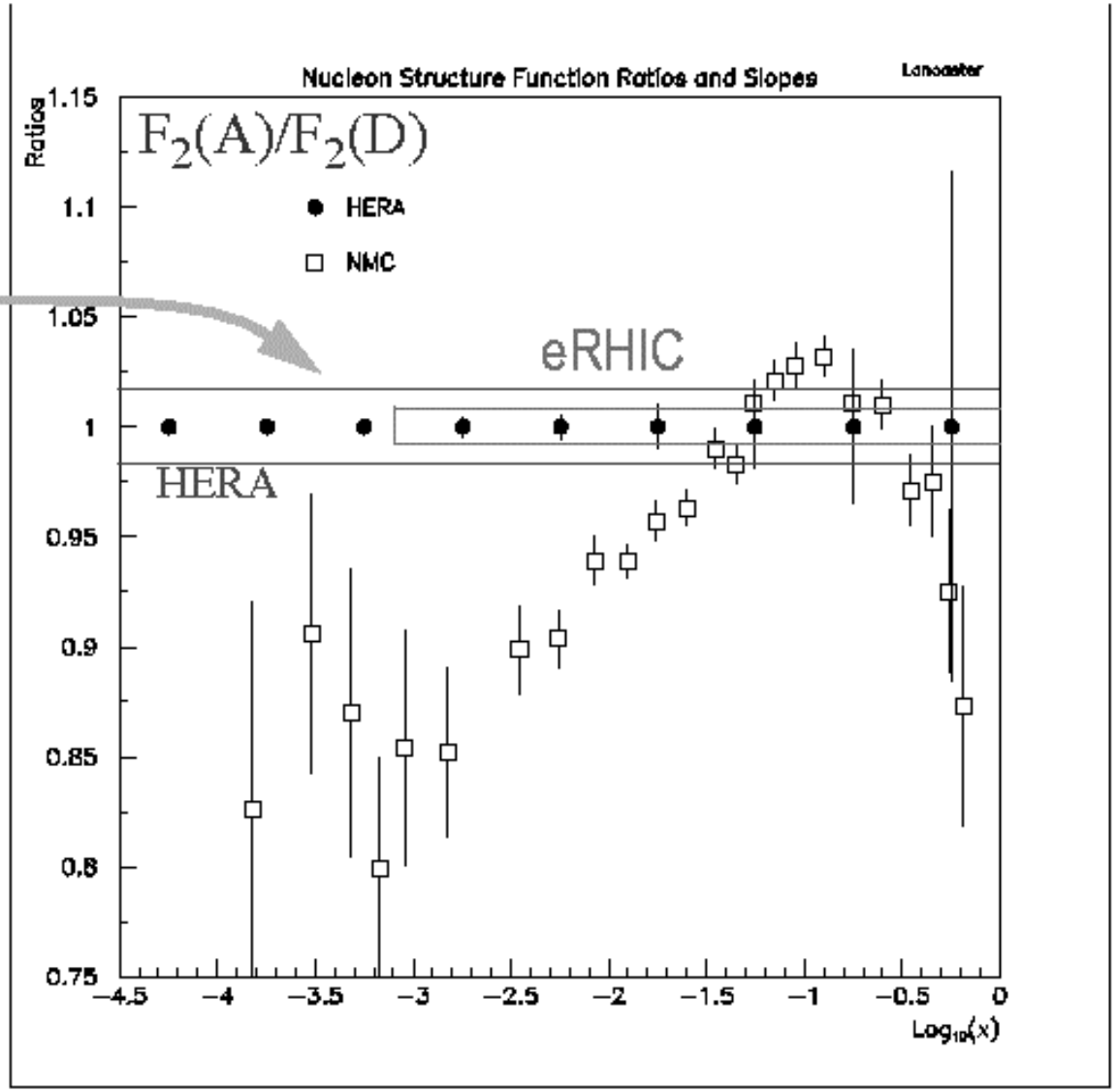

For HERA lumi:

- luminosity 1 pb^{--1} per nuclei
- isoscalar nuclei

Lumi at EIC 10-100 times larger

Methods to access the gluon

M. Arneodo et al.

... jet rates

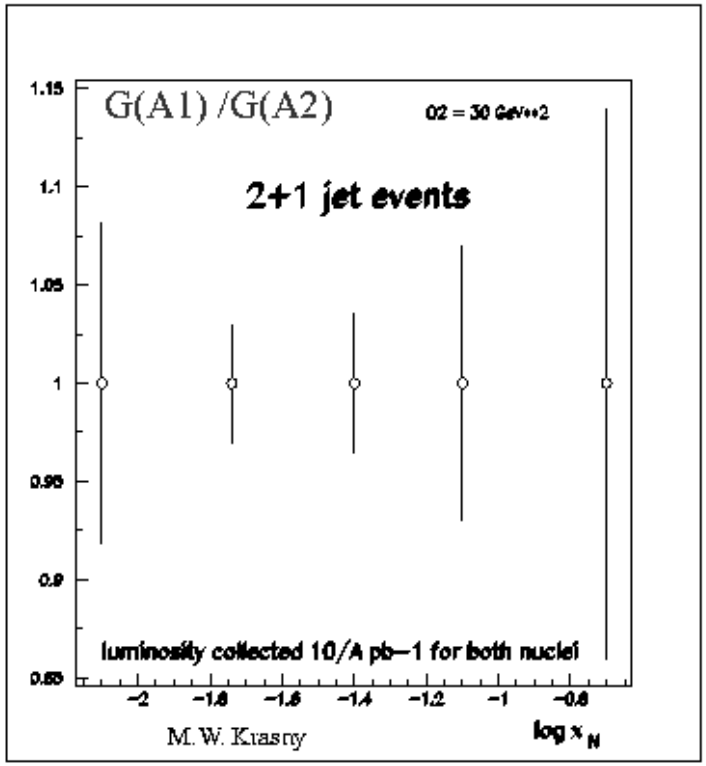

HERA

... $F_2(A)$ Q^2 -slopes (approx.)

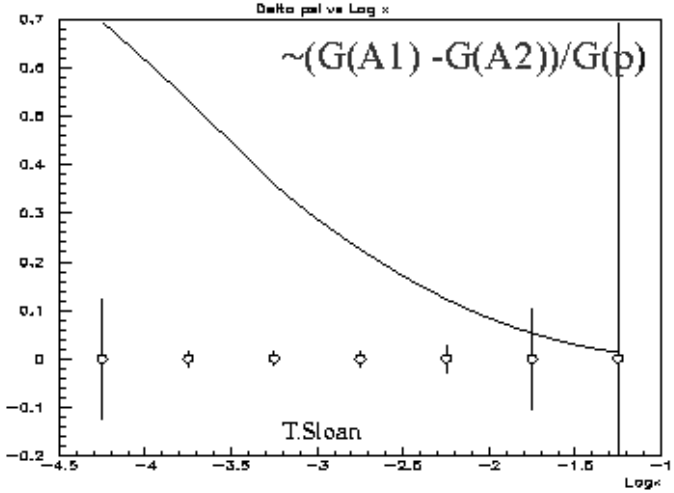

HERA

Fig.9

...inelastic J/Ψ production

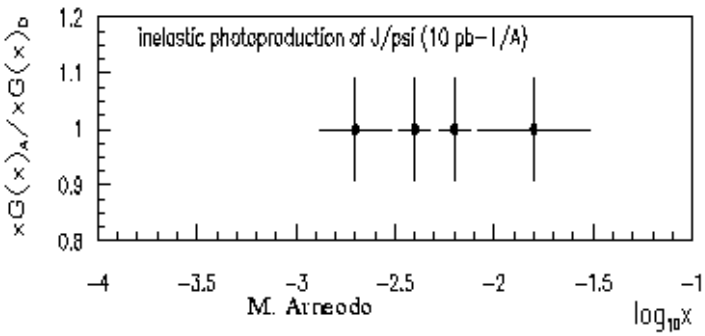

EIC: 3-10 times more precise

Diffractive measurements

M. Strikman

Either via gaps
or tagging leading
protons

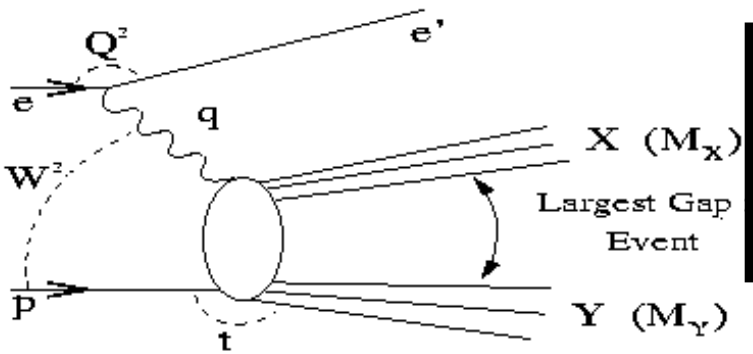

Does the fraction of DIS events with a gap depend on A?

F^D_{2A}, vector mesons…

Fig.10

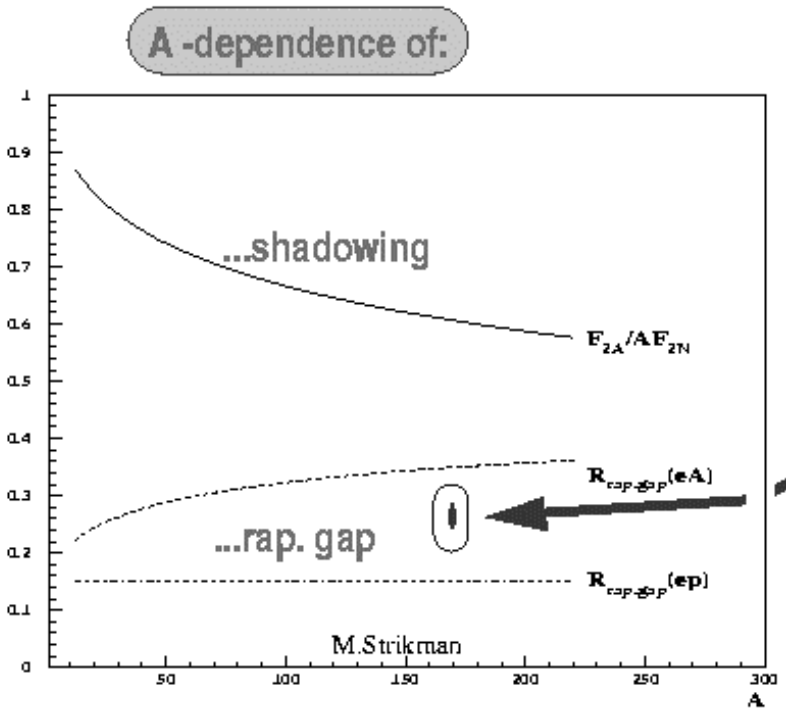

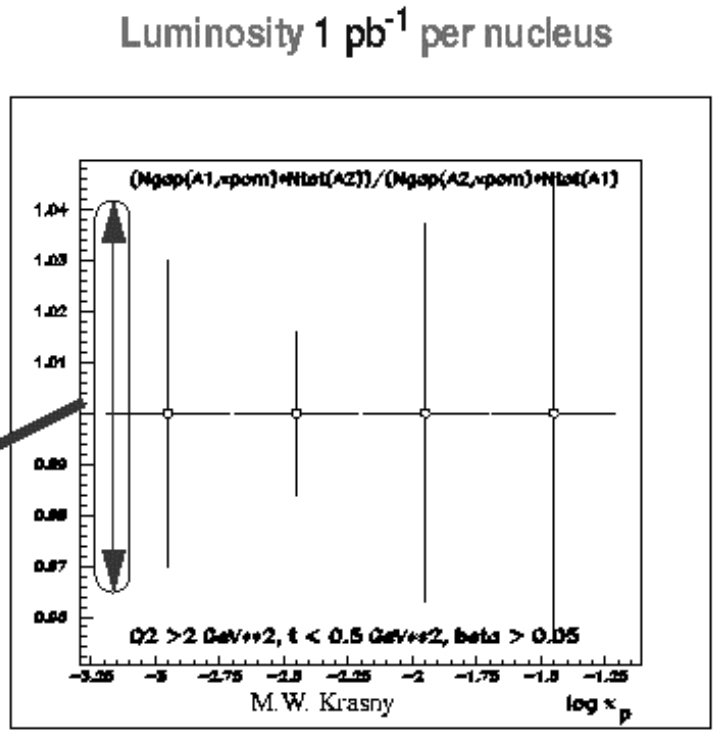

Nuclear Fragments

Beam colliding mode

M. Krasny, J. Chwastowski

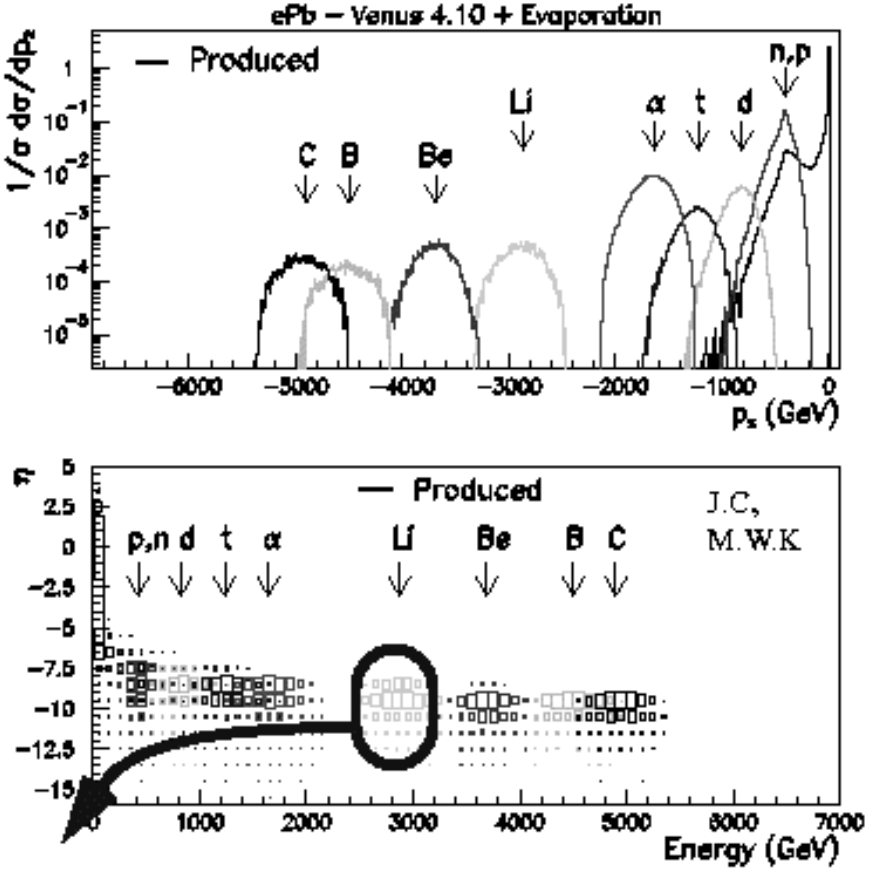

Quantised energy of nuclear fragments recognition of fragment type on the base of energy measurement

One of the strong advantages of a collider:
the different fragments are 'quantised' in energy and η can thus be identified

⇒ need to equip the proton beam direction with detectors

Zero degree photon detector allows to measure nuclear excitations in collisions

Fig.11

e-A Physics: Theoretical issues

M. Strikman
Department of Physics, Pennsylvania State University,
University Park, PA 16802, USA

The electron - nucleus scattering in the EIC energy range especially in the collider mode provides unique tools for addressing a number of fundamental issues of QCD. This includes the issue of existence of new phases of QCD, transparency of the extended systems to the propagation of small dipoles like J/ψ, the x - range one needs to reach to observe a breakdown of the linear DGLAP evolution equations, possibility of reaching the black body limit for interactions with heavy nuclei, leading twist shadowing of quark and gluon fields in nuclei, modifications of quark and gluon fields in nuclei at medium $x \sim 0.1 \div 0.2$ which could be related to the origin of the nuclear forces, parton propagation through nuclear media.

I. UNITARITY AND BLACK BODY LIMIT

Experiments at HERA have established a fast increase of the gluon densities with decrease of x already for the virtualities $\geq 2GeV^2$. Can the increase of parton densities - continue forever? One can easily see that this impossible by comparing the cross section of the inelastic interaction of a small dipole of a transverse size d with the S-channel unitarity constrain [1]:

$$\sigma_{inel}^{\text{“}q\bar{q}''+A}(x,d^2) = \frac{\pi^2}{3} d^2 x G_A(x,\lambda/d^2)\alpha_S(\lambda/d^2) \leq \pi R_A^2, \tag{1}$$

where $\lambda \sim 4-9$. For central impact parameters *effectively* $\sigma_A^{inel} \leq \pi R_A^2/1.5$. This condition (which can be also formulated in terms of the impact parameter amplitudes) implicitly assumes that the coherence length is large enough so that $x \ll 1/(2m_N R_A)$. For the case of the scattering of color octet dipoles the condition is a factor of 9/4 stronger. A numerical analysis [2] indicates that for heavy nuclei unitarity becomes a problem already at rather large x in a wide range of Q^2 even when a significant gluon shadowing is included.

It is instructive to consider the limiting case when most of configurations in the virtual photon wave function interact with a heavy target with the geometrical cross section $2\pi R_A^2$. In this limit which was first introduced by Gribov [4] the Bjorken scaling is grossly violated: $F_{2A}(x,Q^2) \propto \ln(x_0/x) \cdot 2\pi R_A^2$. Though this limit is difficult to reach, a number of precursors of this limit would be possible to observe at EIC. The most striking manifestations of BBL in (virtual) photon diffraction include strong enhancement of the large mass tail of the diffractive spectrum as compared to the expectations of the the triple Pomeron limit, dominance of production of dijet -like final states (with trijet / dijet ratio similar to $e^+e^- \to hadron$ process [3]. Also, for all Q^2 where the BBL is applicable one can predict in a model independent way the cross section of vector meson production:

$$\frac{d\sigma^{\gamma_T^*+A\to V+A}}{dt} = \frac{M_V^2}{Q^2}\frac{d\sigma^{\gamma_L^*+A\to V+A}}{dt} = \frac{(2\pi R_A^2)^2}{16\pi}\frac{3\Gamma_V M_V^3}{\alpha(M_V^2+Q^2)^2}\frac{4\ \left|J_1(\sqrt{-t}R_A)\right|^2}{-tR_A^2}. \tag{2}$$

This should be compared to much faster (by a factor Q^{-4}) drop of the cross sections in the leading twist (LT) limit. Inclusive production of leading hadrons in the current fragmentation region will also change drastically in the BBL as compared to the LT. In the LT a single parton parton with largest $z \sim 1$ and $p_t^2 \ll Q^2$ dominates fragmentation (the rest is the DGLAP evolution of the fragmentation function). In BBL quark and antiquark with $p_t^2 \approx Q^2$ and known z-distribution ($\langle z \rangle = 1/2$) fragment independently. Hence the leading particle spectrum in BBL is strongly suppressed. The inclusion of the $q\bar{q}g$ states in the virtual photon wave function (due to the QCD evolution) will further amplify the effect. In addition a broadening of p_t spectrum is expected [3].

II. LEADING TWIST SMALL X RANGE

General structure of the strong interaction dynamics leads to existence of a deep connection between phenomenon of nuclear shadowing and and diffraction in the scattering on nucleons [5] In particular, using the QCD factorization theorem for diffraction [6] we found a model independent relation between diffractive quark and gluon structure functions in DIS and the corresponding nuclear parton densities [7]. The recent studies of the problem using current information

Using several diverse parameterizations of diffractive parton distributions, extracted in leading twist QCD analyses of the HERA diffractive deep inelastic scattering (DIS) data, we recently make predictions for leading twist nuclear shadowing of nuclear quark and gluon distributions in DIS on nuclei [10]. We found that the diffractive data are precise enough to allow unambiguous predictions for the leading twist gluon, quark shadowing. In the case of the interaction of small dipoles with nuclei, in particular for the longitudinal structure function F_L^A the predictions are strikingly different from predictions of the eikonal models.

The LT shadowing mechanism for inclusive scattering leads also to prediction of a large probability of the diffractive processes ($\sim 30-40\%$ for $A \sim 200$)) [11].

The main difference with BBL is absence of an increase of the average transverse momenta of produced hadrons – diffraction into dijets constitutes a small portion of the diffraction and distribution over emission angle is more narrow. Also in difference from BBL the suppression of the leading hadron spectrum is absent for large z, it starts at rapidities related to the rapidity range occupied by diffraction [7].

EIC will be able to perform a detailed study of the color transparency phenomenon in the production of vector mesons as well as pions. Such studies are crucial for determining the Q^2 range were hard exclusive processes $\gamma_L + N \rightarrow$ "*meson*" + "*baryon*" could be used for the measurement of the generalized parton distributions in nucleons. The QCD factorization theorem [8,9] leads to

$$\frac{\left.\frac{d\sigma^{\gamma_L+A\rightarrow V+A}}{dt}\right|_{t=0}}{\left.\frac{d\sigma^{\gamma_L+p\rightarrow V+p}}{dt}\right|_{t=0}} = \left(\frac{G_A(x,Q^2)}{G_N(x,Q^2)}\right)^2 \tag{3}$$

It implies that EIC should be able to observe both the regime of color transparency for $x \sim 0.02-0.05$ where gluon shadowing in nuclei is small as well as the regime of color opacity for $x \leq 0.005$ where large gluon shadowing effects are expected.

III. THE $X \geq 0.1$ PHYSICS AND THE ORIGIN OF NUCLEAR FORCES

Understanding of microscopic nuclear structure is of crucial importance for many phenomena including the structure of neutron stars. Hence it is important to establish (i) whether nucleons are good quasiparticles for high resolution probes, (ii) what is the origin of intermediate and short-range nuclear forces: do nucleons exchange mesons or quarks (gluons)?, (iii) density dependence of interplay between nucleonic and nonnucleonic degrees of freedom.

Currently there is only limited experimental information on the gluon distributions in nuclei. Theoretical expectations of the gluon nuclear shadowing in combination with analysis of the experimental data on the ratio of the nuclear structure functions suggest that the gluon distributions in nuclei should be enhanced at $x \sim 0.1 \div 0.2$ [12–14]. This is consistent with the indications from the NMC measurements of the ratio of the Sn/C yields of the inelastic J/ψ production as well as the scaling violation for $F_2(Sn)/F_2(C)$. However the accuracy of the data is not sufficient to make firm conclusions. Studies at EIC will cover much larger Q^2 range and have larger luminosity and hence will be able to provide a decisive answer. It is worth noting that the enhancement is occurring the x-range which is dual to the longitudinal distances relevant for the short-range and medium range interactions between nucleons. Hence it would provide critical information for understanding relative role of meson and quark/gluon exchanges in nuclei. EIC will be able to resolve a long standing question of the presence of an enhancement of the gluon and valence quark densities at $x \sim 0.1 \div 0.2$ in a series of inclusive and semiinclusive measurements.

EIC kinematics provides unique opportunities for study of quark-gluon structure of nuclei in semiinclusive processes. The cleanest case which will be studied anyway with a large integrated luminosity for the purposes of extracting quark distributions in (un)polarized neutrons is the tagged structure functions of the deuteron: $e + {}^2\vec{H} \rightarrow e + N + X$. Defining the light-cone fraction for the produced nucleon as $\alpha = 2p_N/p_{^2H}$ we can distinguish two kinematic ranges: (a) $\alpha \approx 1$ - study of quasifree nucleon structure functions, (b) $\alpha \geq 1.2$ - study of the bound nucleon wave functions - search for EMC -like deviations of bound and free nucleon parton densities both for unpolarized and for polarized case !!! Also, selecting $\alpha_\Delta \geq 1$ in the process $e + {}^2\vec{H} \rightarrow \Delta + X$ will allow to look for Δ-like white clusters if they are present in the deuteron with probability $\geq 10^{-3}$. At the same time the process $e + {}^2\vec{H} \rightarrow p + p + X$ for $\alpha_{N_1}, \alpha_{N_2} < 0.8$ is sensitive to meson exchanges. For extensive discussion of various strategies see [12].

IV. CHALLENGES IN PARTON PROPAGATION THROUGH NUCLEI

A significant theoretical progress was made recently in the understanding of the parton propagation through nuclei, see review in [15]. Experimental situation was rather ambiguous for some time. The FNAL Drell-Yan data [16] observed a small p_t broadening which was consistent with the pQCD theoretical expectations. At the same time one of the procedures suggested by the authors allowed energy losses as large as 3 GeV/fm which was clearly inconsistent with pQCD expectation: $-\frac{dE}{dL} = \frac{\alpha_s N_c}{4}\Delta p_t^2(L)$.

A very recent analysis of the CERN Drell-Yan data clearly ruled out the large energy loss scenario [17]. At the same time the analysis [18] of the HERMES data indicates that (i) the energy losses for scattering off carbon and krypton are approximately energy independent for $\nu = 8 \div 22 GeV$, (ii) dependence of energy losses on A is consistent with linear increase of energy losses with distance which leads to the scaling of the fragmentation functions $D_A(z, Q^2)$ of the form:

$$1 - D_A(z, Q^2) \propto \int d^2b \int_{-\infty}^{\infty} dz_1 \int_{z_1}^{\infty} dz_2 \theta(z_2 - z_1)\rho_A(r_1)\rho_A(r_2)(z_2 - z_1). \tag{4}$$

The fitted total energy loss is $\Delta E(^{14}N) = 0.4 GeV$, $\Delta E(^{84}Kr) = 1.35 GeV$ which corresponds to $\Delta E(A = 200) = 2.6 GeV$. This is consistent with the analysis of the Drell-Yan data from CERN: $\Delta E(A = 195) = 10.75 GeV$. Hence the interactions of partons with nuclei remain small even at high energies.

Smallness of the final state interactions is indicated also by the analysis of the FNAL data [19] on the soft neutron emission in DIS off lead [20]. An extreme assumption that only recoil nucleons $T_N \leq 600 MeV$ reinteract in nuclei explains both the shape of the spectrum and the absolute multiplicity.

Small energy losses present a challenge for the observation of the parton propagation effects at EIC. Few possibilities include (i) study of the jet production at rapidities close to the nuclear fragmentation region, (ii) study of the p_t broadening in the current fragmentation region as this effect does not die out with increase of energy, (iii) study of planarity of the multijet events.

In summary, EIC will allow a qualitative progress in our understanding of the QCD dynamics of high energy interactions, physics of high parton densities, and the microscopic nuclear structure.

---

[1] L. Frankfurt, W. Koepf and M. Strikman, Phys. Rev. D **54**, 3194 (1996)
[2] L. Frankfurt, V. Guzey and M. Strikman, J. Phys. G **27**, R23 (2001)
[3] L. Frankfurt, V. Guzey, M. McDermott and M. Strikman, Phys. Rev. Lett. Phys. Rev. Lett. **87**, 192301 (2001)
[4] V. N.Gribov, Zh. Eksp. Teor. Fiz. **57** (1969) 1306.
[5] V.N. Gribov, Sov. J. Nucl. Phys. **9**, 369 (1969)
[6] J. C. Collins, Phys. Rev. D **57**, 3051 (1998) [Erratum-ibid. D **61**, 019902 (1998)]
[7] L. Frankfurt and M. Strikman, Eur. Phys. J. **A 5** (1999) 293.
[8] S. J. Brodsky, L. Frankfurt, J. F. Gunion, A. H. Mueller and M. Strikman, Phys. Rev. D **50**, 3134 (1994)
[9] J. C. Collins, L. Frankfurt and M. Strikman, Phys. Rev. D **56**, 2982 (1997)
[10] L. Frankfurt, V. Guzey, M. McDermott and M. Strikman, JHEP **0202**, 027 (2002)
[11] L. L. Frankfurt and M. I. Strikman, Phys. Lett. B **382**, 6 (1996).
[12] L. L. Frankfurt and M. I. Strikman, Phys. Rept. **160**, 235 (1988).
[13] L. L. Frankfurt, M. I. Strikman and S. Liuti, Phys. Rev. Lett. **65**, 1725 (1990).
[14] K. J. Eskola, Nucl. Phys. B **400**, 240 (1993).
[15] R. Baier, D. Schiff and B. G. Zakharov, Ann. Rev. Nucl. Part. Sci. **50**, 37 (2000)
[16] M. B. Johnson *et al.* [FNAL E772 Collaboration], Phys. Rev. Lett. **86**, 4483 (2001)
[17] F. Arleo, arXiv:hep-ph/0201066.
[18] E. Wang and X. N. Wang, arXiv:hep-ph/0202105.
[19] M. R. Adams *et al.* [E665 Collaboration], Phys. Rev. Lett. **74**, 5198 (1995) [Erratum-ibid. **80**, 2020 (1995)].
[20] M. Strikman, M. G. Tverskoii and M. B. Zhalov, Phys. Lett. B **459**, 37 (1999)

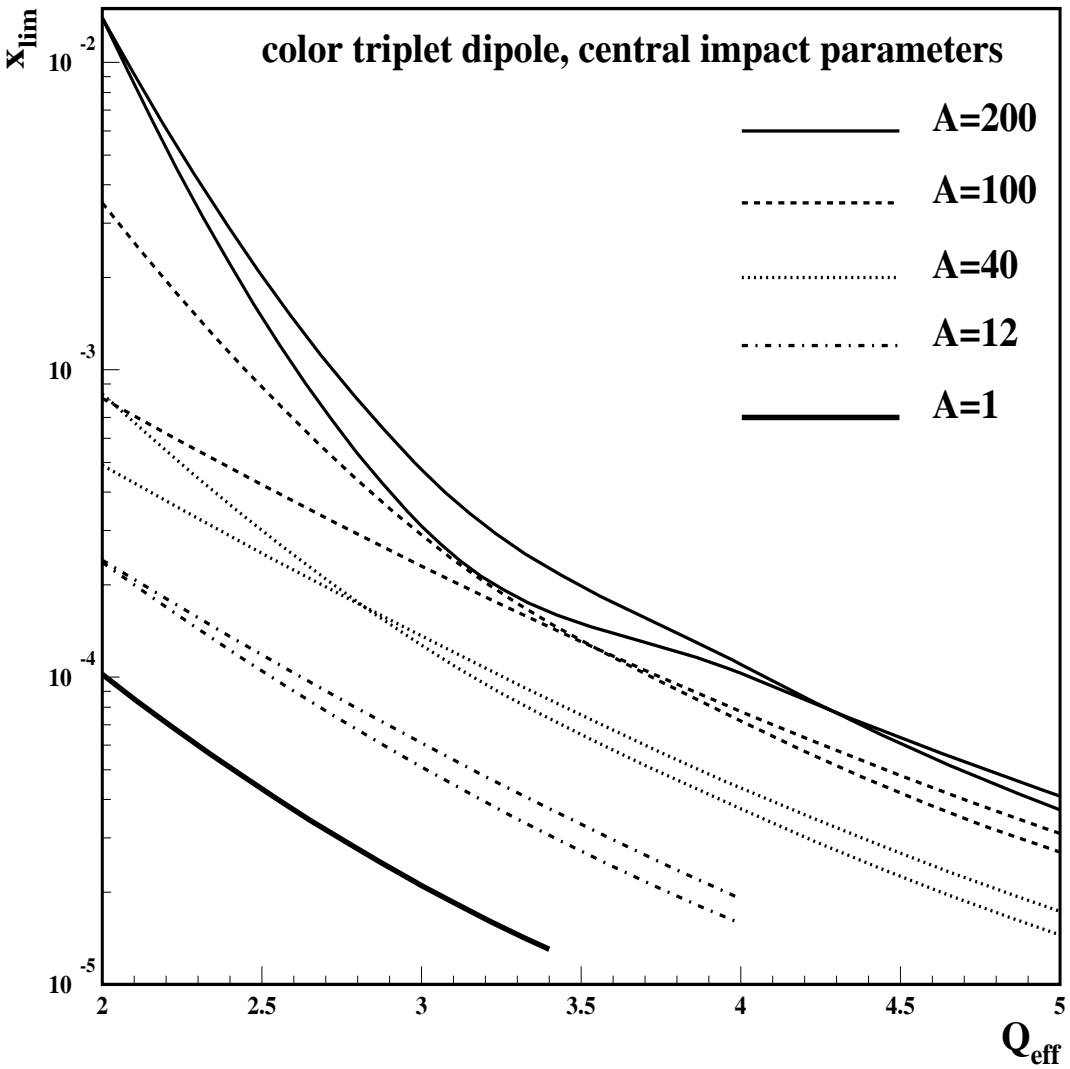

The unitarity boundary for the inelastic $q\bar{q}$-nucleus cross sections for nuclei with A=12, 40, 100, and 200 for the central impact parameters. The unitarity boundary for the inelastic $q\bar{q}$-nucleon cross section is presented as a thick solid line. Guzey & FS 2000 & FGS+McDermott 2001

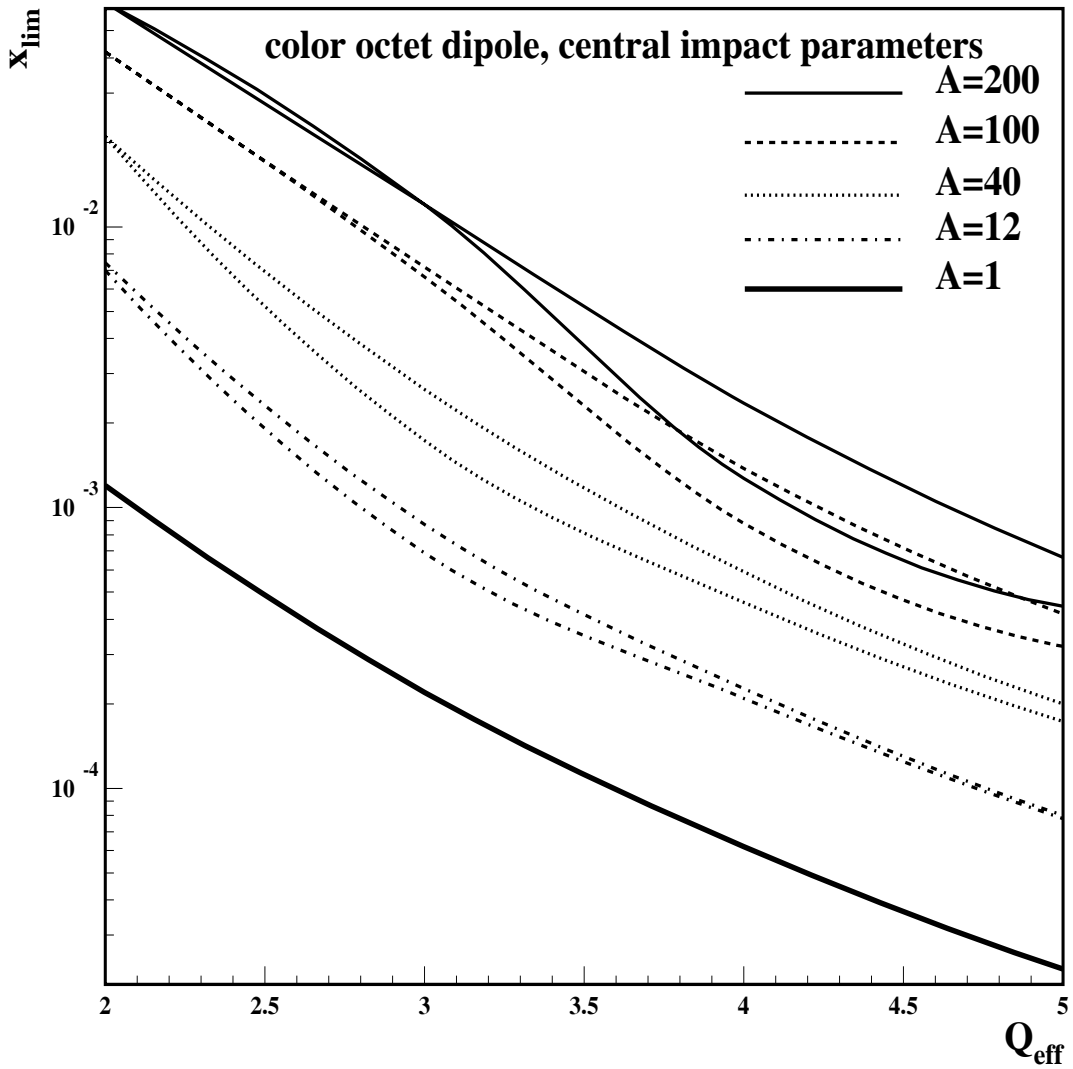

The unitarity boundary for the inelastic $q\bar{q}g(gg)$ (color octet)-nucleus cross sections for nuclei with A=12, 40, 100, and 200. The unitarity boundary for the inelastic $q\bar{q}g$-nucleon cross section is presented as a thick solid line.

Predictions for F_2^A and g_A

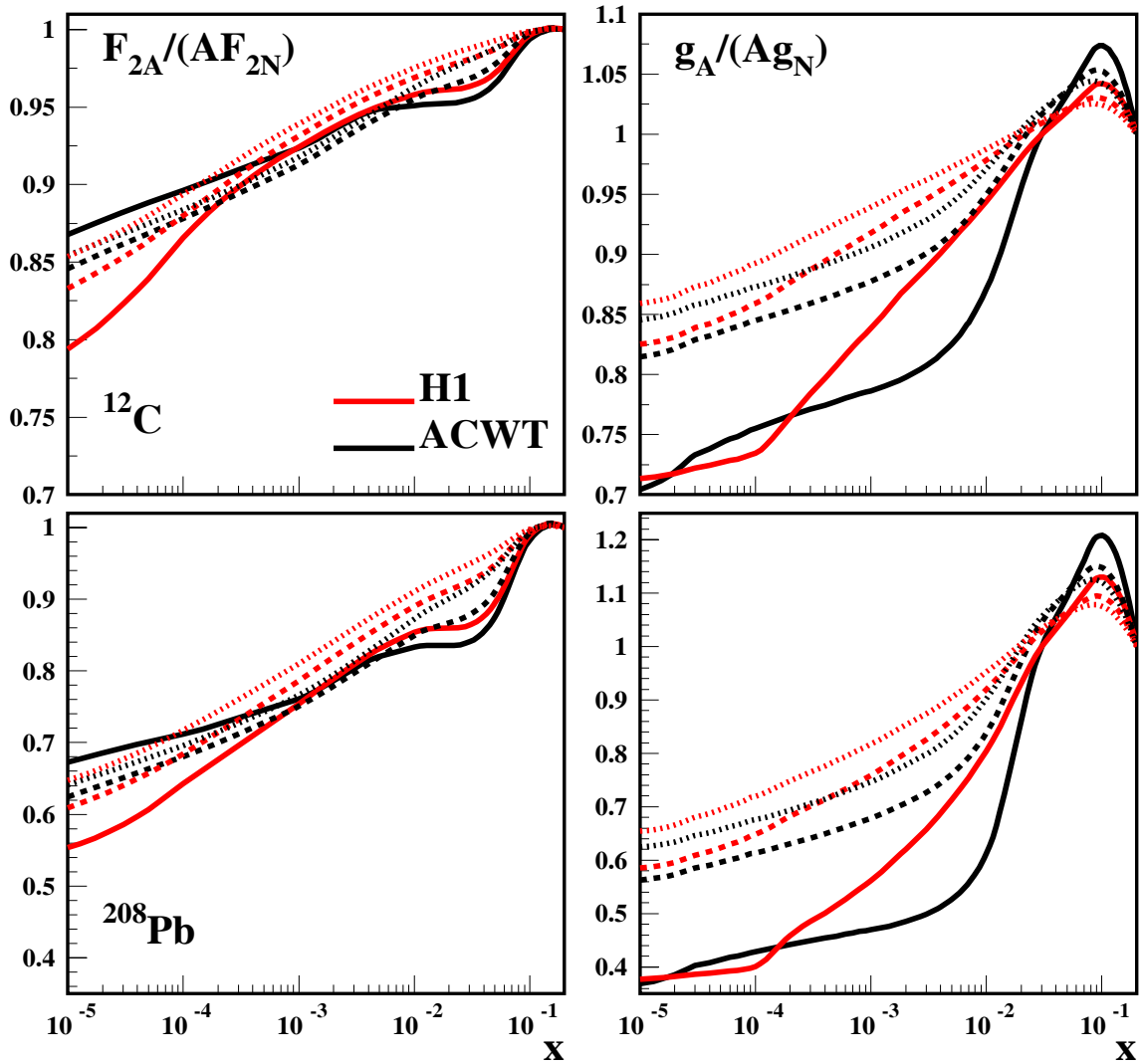

- NLO calculation (with CTEQ5M for $f_{j/N}$)
- Valence quarks are shadowed as the sea quarks; charm quarks are **not** modified at the input scale $Q_0 = 2$ GeV
- Predictions with H1 and ACWT are virtually the same for $10^{-4} < x < 10^{-2}$: F_2^D is measured in this range and fitted well by both parameterizations

Final states in DIS at small x - Summary of observables - LT versus BBL

◇ *Inclusive / large mass diffraction.*

In the BBL $\sigma_{diff}/\sigma_{tot} = 1/2$. Increase of $\sigma_{diff}/\sigma_{tot}$ with A is expected also in LT.

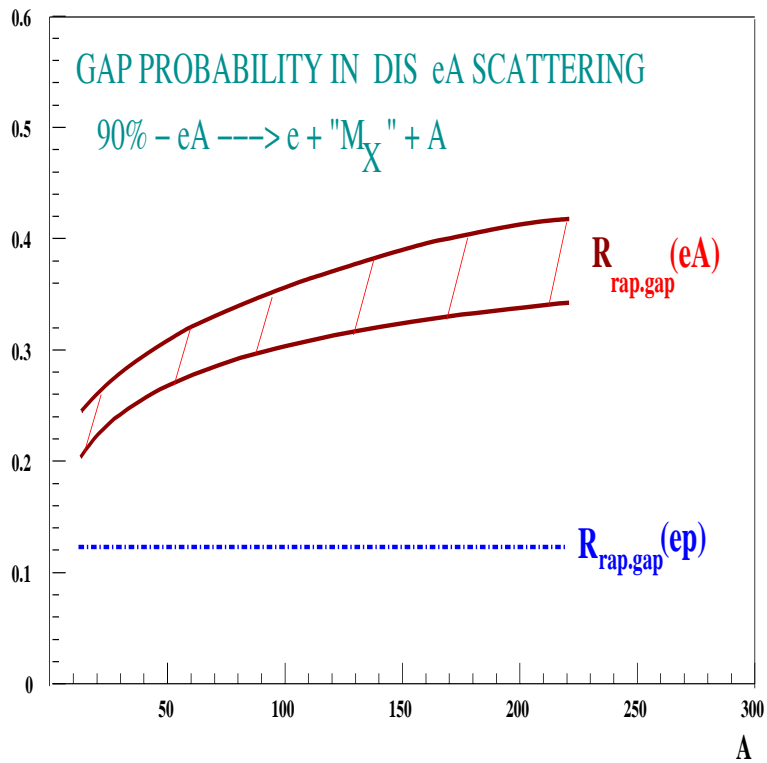

◇ ◇ ◇ Inclusive production of leading hadrons

The mechanism of fragmentation in LT: a single parton parton with largest $z \sim 1$ and $p_t^2 \ll Q^2$ dominates fragmentation (the rest is the DGLAP evolution of the fragmentation function).

The mechanism of fragmentation in BBL: quark and antiquark with $p_t^2 \approx Q^2$ and known z-distribution ($\langle z \rangle = 1/2$) fragment independently since for large $p_t^2 \to$ small α_s) Hence the leading particle spectrum in BBL is strongly suppressed. The inclusion of the $q\bar{q}g$ states in the virtual photon wave function (due to the QCD evolution) will further amplify the effect.

Perfect experimental observable. Study leading spectrum of hadrons as a function of neutron deposition in the forward calorimeter. DGLAP - no correlation. BBL - strong correlation. Also for the central impact parameters BBL onset is at substantially larger x. Cannot trigger on centrality in diffraction.

p-A Physics at RHIC

Jen-Chieh Peng

Department of Physics, University of Illinois
Urbana, IL 60801

The role of proton-nucleus (p-A) collisions in the study of strong interactions has a long history. At RHIC, p-A studies have been recognized since the beginning as important elements of the program. It is now timely to take a close look of the p-A physics opportunities at RHIC, since p-A experiments are ready to be done in the near future. Furthermore, the prospect of a future e-A collider has generated much interest to study the connections between p-A and e-A physics.

It is important to realize that RHIC, for the first time, allows us to study p-A interaction in a collider mode. The center-of-mass energy reached in p-A collisions at RHIC is roughly an order of magnitude higher than any existing fixed-target experiments. Moreover, the large-acceptance collider detectors can simultaneously measure many particles produced in the collisions. This could provide qualitatively new information not accessible in previous fixed-target p-A experiments.

The role of p-A physics at RHIC was reviewed at a Workshop conducted in October 2000 at BNL. The program of this Workshop is shown in Fig. 1. In this talk I will focus on the following physics topics discussed at the p-A Workshop:

- p-A comparision with A-A, p-p, and e-A.
- Quark and gluon distributions in nuclei.
- Shadowing and saturation effects at small-x.
- Hard diffractive processes with forward-tagging.

It has long been recognized that p-A collisions serve an important role in the search for quark-gluon plasma (QGP) in relativistic heavy-ion collisions. Since QGP is in general not expected to be produced in p-A collisions, a comparison of the A-A with p-A data at identical kinematic conditions is crucial for identifying signatures for QGP formation. This was clearly demonstrated in the AGS and SPS heavy-ion programs, which relied heavily on the p-A measurements for interpreting the A-A results. For example, the p-A measurements were crucial for identifying new phenomena in A-A collisions such as J/Ψ-suppression, enhancement of strange particle production, and the excess of low-mass lepton pairs. This important role of p-A collisions is clearly valid at RHIC too.

A comparison of the J/Ψ production in p+p, p+Au (or d+Au), and Au+Au at RHIC is crucial for understanding the origins of J/Ψ-suppression observed at SPS. At RHIC energies. Υ resonances can also be produced. The polarization of Υ resonances has been measured recently [1]. As shown in Fig. 2, the $\Upsilon(2S+3S)$ states were observed to possess large polarization, in striking contrast with the $\Upsilon(1S)$ state. The polarization of J/Psi and Υ might be an interesting observable at RHIC.

The need for p-A data is nicely illustrated by the recent A-A results from RHIC. Figure 3 shows the PHENIX data on the suppression of large-p_T hadrons in Au+Au collision [2]. While this effect can be well explained by an enhanced partonic energy loss rate in a dense medium [3], other explanation such as gluon saturation [4] can not be ruled out. In Fig. 3, the prediction of the energy-loss model for d+Au collision is shown. This prediction could be readily tested in upcoming d-A experiments at RHIC.

In addition to their connection to A-A physics, the p-A measurements are important in their own right. Many outstanding questions in hadron physics can be addressed with p-A experiments at RHIC. For example, what are the quark and gluon contents of nuclei? How are they different from those in a free nucleon? The famous EMC effect clearly showed that the F_2 structure function in a nucleus is different from the F_2 structure function in a free nucleon. However, the deep-inelastic scattering data provide no information on the flavor dependence of the nuclear modification of the parton distributions. These data also shed little light on the gluon distribution in nuclei.

The p-A program at RHIC can provide new information on the antiquark and gluon distributions in nuclei. As is well demonstrated from a series of Fermilab experiments [6], proton-induced Drell-Yan process is sensitive to antiquark distributions in nuclei. For 100 GeV (250 GeV) protons colliding with 100 GeV·A nuclear beams at RHIC, one will be able to reach values of x down to 1×10^{-3} (5×10^{-4}). This will extend the current reach in low x by roughly two orders of magnitude. Figure 4 shows the kinematic coverage in x and the expected statistical accuracy for a two-month run at PHENIX. Qualitatively new information on the sea-quark content in nuclei, such as shadowing and non-linear saturation effects, could be revealed. In principle, saturation effects for high-density partons at small x could also be searched for in the p-p or e-p collisions. However, by using a heavy nucleus in e-A or p-A collisions, the onset of the saturation effects can occur at a much larger value of x due to the $A^{1/3}$ enhancement factor for the partonic density.

The nuclear dependence of the gluon distribution is practically unknown [5]. At RHIC, the gluon content of the nucleus at a wide range of x could be measured using a variety of hard processes, including direct-γ production, γ-jet production, di-jet production, heavy-quark production, high-p_T single-muon production, and low-mass high-p_T dimuon production (see Fig. 5). Indeed, any hard processes suitable for extracting gluon polarization information in the RHIC-spin program would also be ideal for probing the nuclear gluon distributions in p-A collisions. These results will provide new information on the gluon content of nuclei, which is closely connected to one of the physics goals of a possible future e-A collider.

As shown in Fig. 5, one can measure the gluon distributions down to $x \sim 0.01$ by using, for example, the γ-jet production. To reach even smaller x, better detector coverage at forward rapidity is needed. Another process sensitive to the gluon distribution is the J/Psi production. Fig. 6 shows the kinematic coverage (in p_T and x_2) and the expected statistical accuracy for measuring the nuclear-dependence parameter α ($\sigma_A \propto A^\alpha$). Also shown in Fig. 6 are the data obtained at the Fermilab experiment E866 [7]. Of particular interest is the fact that RHIC can reach x_2 values down to ~ 0.001. This could give some interesting first information on gluon shadowing at small x, provided that other nuclear effects are understood and taken into account.

An exciting feature at RHIC is that the detectors allow a measurement of other particles emitted in coincidence with the lepton pairs. In particular, it might be possible to measure "diffractive" Drell-Yan process in which Drell-Yan dileptons are accompanied by an energetic

neutron or proton carrying a large fraction of the incident proton beam momentum. Such a process is the hadronic analog of the diffractive DIS process observed recently at HERA [8]. In this HERA experiment (Fig. 7), the DIS was tagged by a forward-going neutron or proton. These tagged DIS process can be interpreted as virtual photons scattering off the pion cloud (or Pomeron) of the proton beam. The pion structure function can be deduced from this measurement, as shown in Fig. 7.

It is natural to extend the HERA measurement to other hard-processes tagged by forward-going nucleons. Of particular interest is the tagged Drell-Yan experiment (see Fig. 8), which could provide a direct test of the meson-cloud model which can successfully explain the $\bar{d}/\bar{u}$ asymmetry of the nucleon sea [9, 10]. A simulation for the $p + p \rightarrow n + \mu^+\mu^- + X$ for the PHENIX detector, where the muon pairs are detected in the muon arms and the neutrons are detected by a small-angle calorimeter (such as the Zero Degree Calorimeter), has been carried out and the result is shown in Fig. 9. As shown in Fig. 10, there could be many extension of this idea. For example, one could consider tagging on forward-going Δ or Λ. The Λ-tagging is of special interest since it can shed light on the strange-quark contents of the proton. Another extension is the measurement of double-helicity asymmetry, A_{LL}, in diffractive $\vec{p} + \vec{p}$ Drell-Yan process. Since the underlying process involves proton-pion interaction, A_{LL} is expected to be zero. Double diffractive Drell-Yan process, which involves pion-pion interaction, can also be contemplated. Finally, it is natural to extend diffractive Drell-Yan measurement to diffractive J/Ψ production.

In concluion, a p-A program at RHIC will provide critical inputs for understanding the A-A data at RHIC, as well as generating new information on antiquark and gluon structures of nuclei. The RHIC p-A program is clearly complementary to the e-A program at EIC. First measurements of the d-A collision at RHIC is anticipated to happen soon.

References

[1] C. N. Brown et al., Phys. Rev. Lett. 86 (2001) 2529.

[2] K. Adcox et al., Phys. Rev. Lett. 88 (2002) 022301.

[3] E. Wang and X. N. Wang, hep-ph/0202105.

[4] D. Kharzeev and E. Levin, Phys. Lett. B523 (2001) 79.

[5] T. Gousset and H. J. Pirner, Phys. Lett. B375 (1996) 349.

[6] P. L. McGaughey, J. M. Moss and J. C. Peng, Annu. Rev. Nucl. Part. Sci. 49 (1999) 217 (hep-ph/9905409).

[7] M. J. Leitch et al., Phys. Rev. Lett. 84 (2000) 3256.

[8] C. Adloff et al., Eur. Phys. J. C6 (1999) 587.

[9] E. A. Hawker et al., Phys. Rev. Lett. 80 (1998) 3715; J. C. Peng et al., Phys Rev. D58 (1998) 092004.

[10] G. T. Garvey and J. C. Peng, Prog. Part. Nucl. Phys. 47 (2001) 203.

Workshop on pA Physics at RHIC
(BNL, October 28-29, 2000)

Introduction, Purpose of the Workshop	S. Aronson
pA Physics and Relation to AA at RHIC	X. N. Wang
Color Glass Condensate	R. Venugopalan
QCD and pA Physics at RHIC	M. Strikman
eA Physics	W. Krasny
pA Physics and Relation to eA	G. Garvey
Recent Results from pA	B. Cole
Results from CDF	A. Bhatti
Comments on experimental study of CGC	R. Seto
Polarized pA Physics at RHIC	H. En'yo
Diffractive Production, Luminosity, and Forward Tagging in pA at RHIC	S. White
Small-X and Diffractive Production at RHIC	J. Peng
Gluon Shadowing and Direct γ Production	P. Stankus
Comments on pA opportunities at RHIC	H. Huang
Cronin effect via p_T enhancement in pA	G. Fai
Plan for pA Measurements at PHENIX	M. Brooks
Plan for pA Measurements at STAR	P. Jacobs
Plan for pA Measurements at BRAHMS	F. Videbaek
Plan for pA Measurements at PHOBOS	A. Carroll
pA Accelerator Issues	D. Trbojevic
Discussions (run plans, detector issues, other physics topics, input to long-range plan etc.	All Participants

Figure 1: Program of the Workshop on pA Physics at RHIC.

- At RHIC energies, Υ production can also be measured.

- J/Ψ and Υ polarization might be an interesting observable at RHIC.

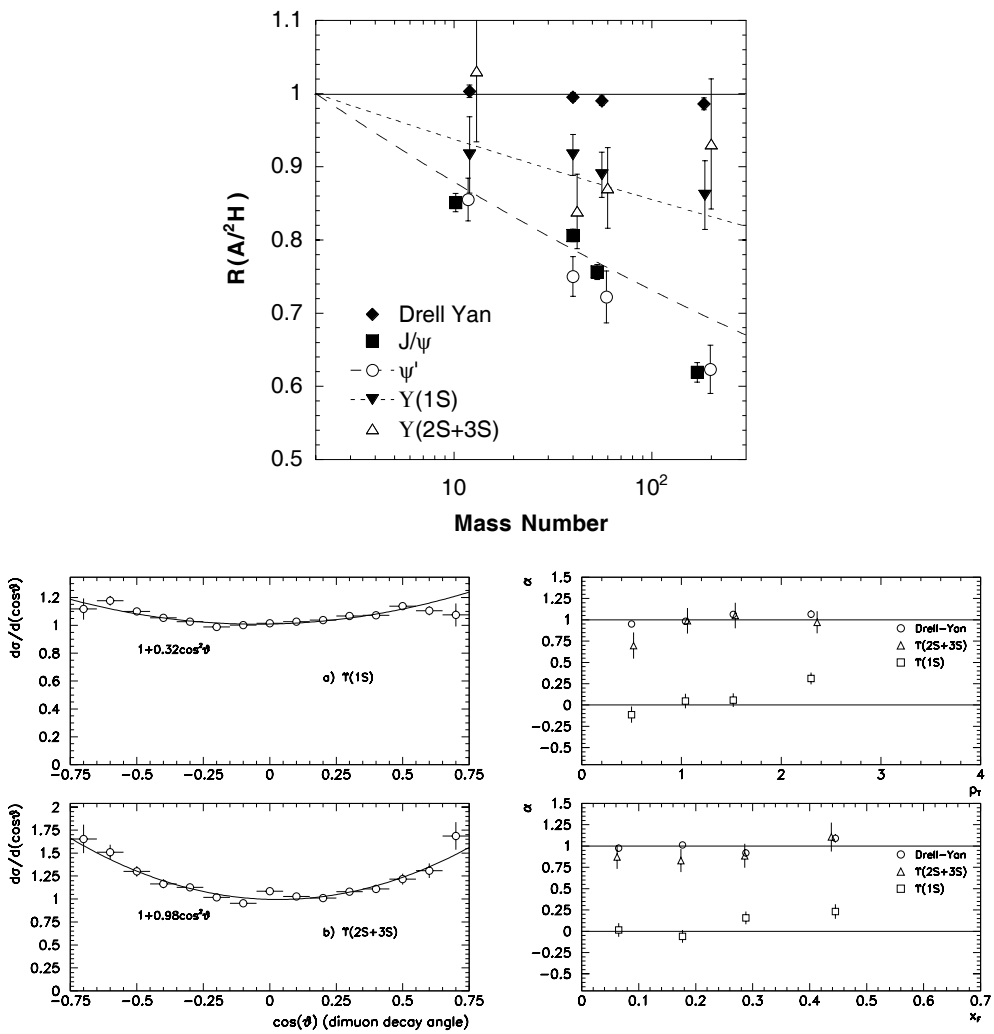

Figure 2: Nuclear dependence of Drell-Yan and quarkonium production. Polarization measurements of the Υ resonances are also shown.

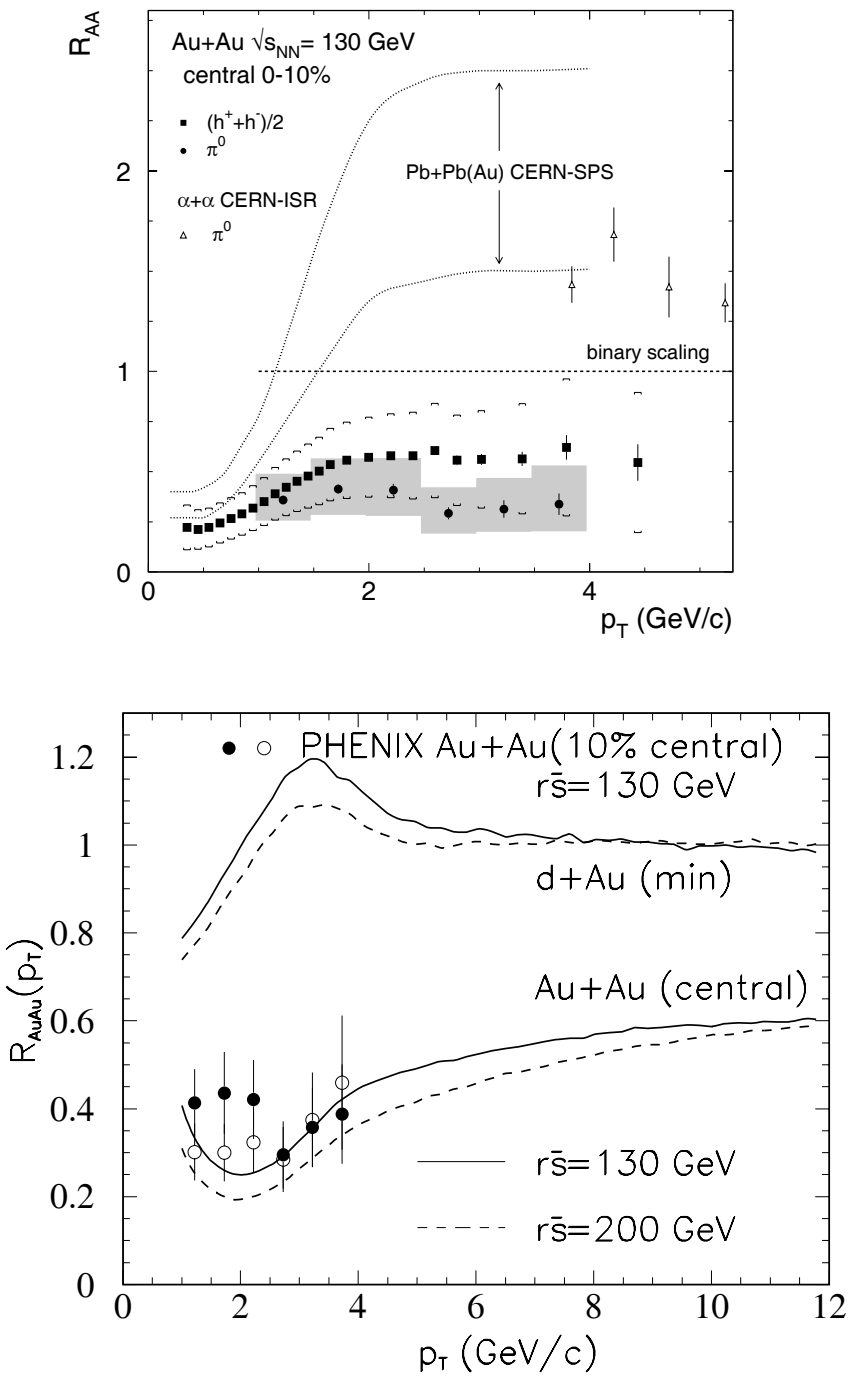

Figure 3: Upper panel: suppression of high-p_T single hadron production observed at PHENIX. Lower panel: predictions from Ref.3 for $Au + Au$ and $d + Au$ in an energy-loss model.

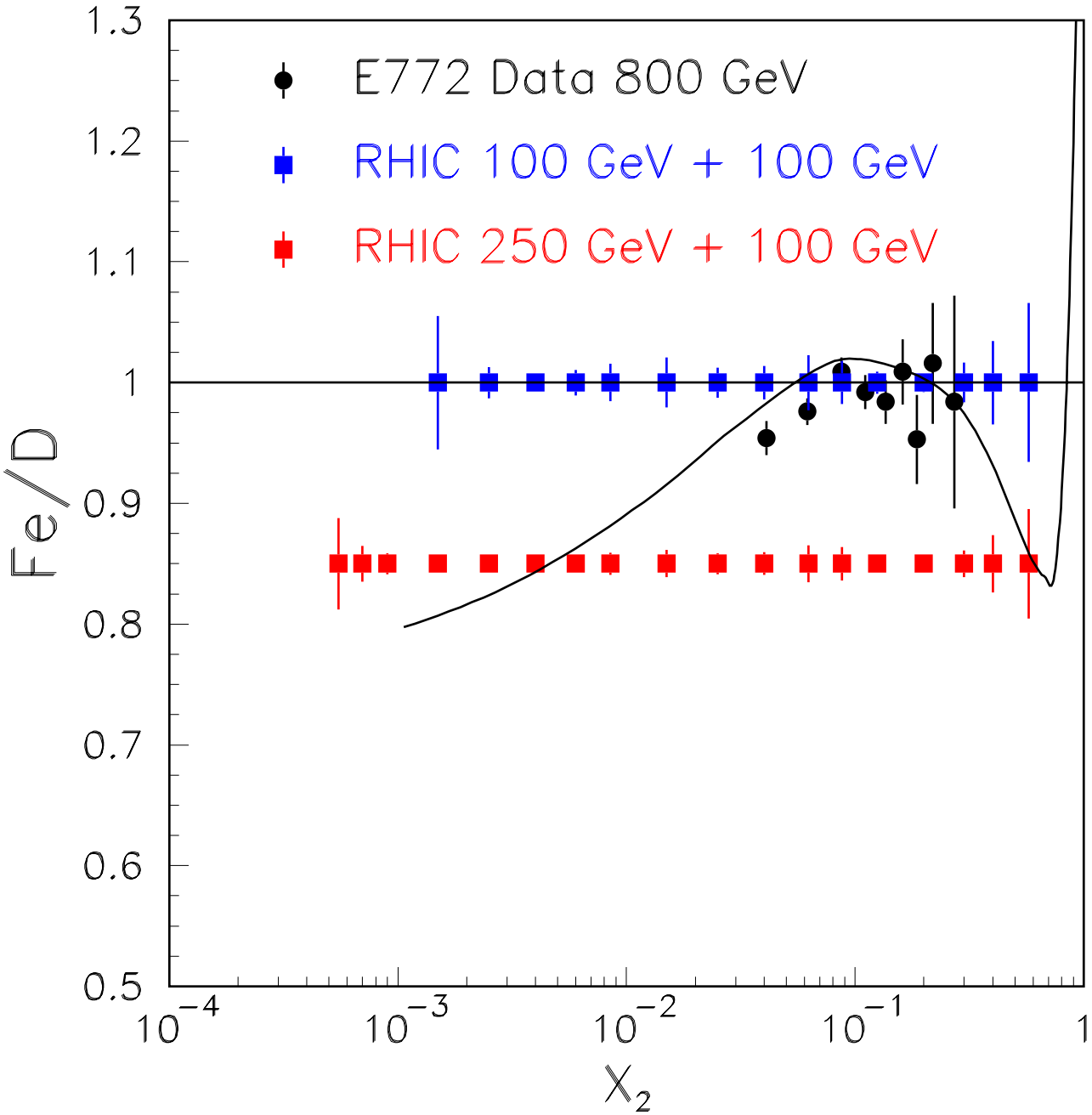

Figure 4: Projected statistical accuracy for Fe/D Drell-Yan cross section as a function of x_2 in a 2-month run at PHENIX. The E772 data are also shown. The solid curve is the EKS98 parametrization for parton distributions in nuclei.

At RHIC, many hard-processes in p-A collisions are sensitive to gluon distributions in nuclei (identical to the tools used to determine $\Delta G(x)$ in RHIC-Spin)

- γ - jet
- direct-γ
- dijet/dihadron
- open charm
- High-p_T lepton-pairs

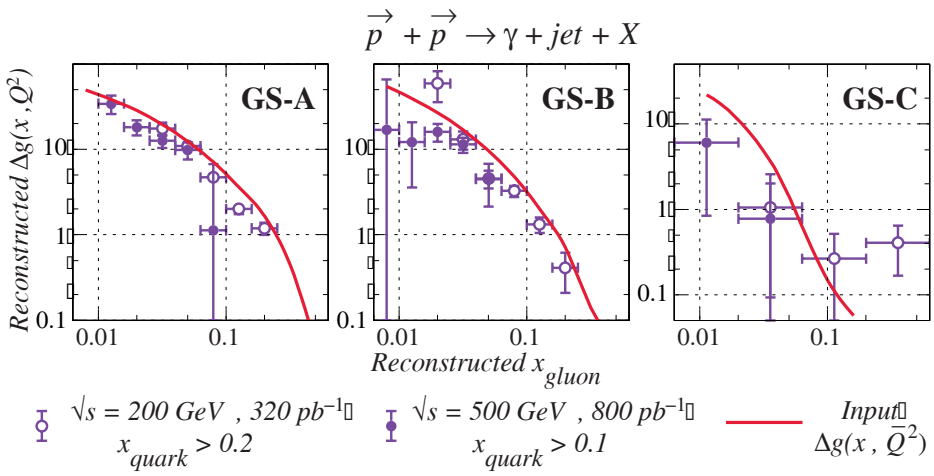

Gluon distributions in nuclei could be probed down to $x \sim 10^{-2}$

It would be very interesting to reach $x \sim 10^{-3}$ to search for gluon saturation effect at low-x

Figure 5: A variety of hard processes can probe the gluon distributions at RHIC. The same process suitable for measuring the polarized gluon distributions can also be used for measuring gluon distributions in nulcei. The kinematic coverage for the photon-jet process at the STAR experiment is also shown.

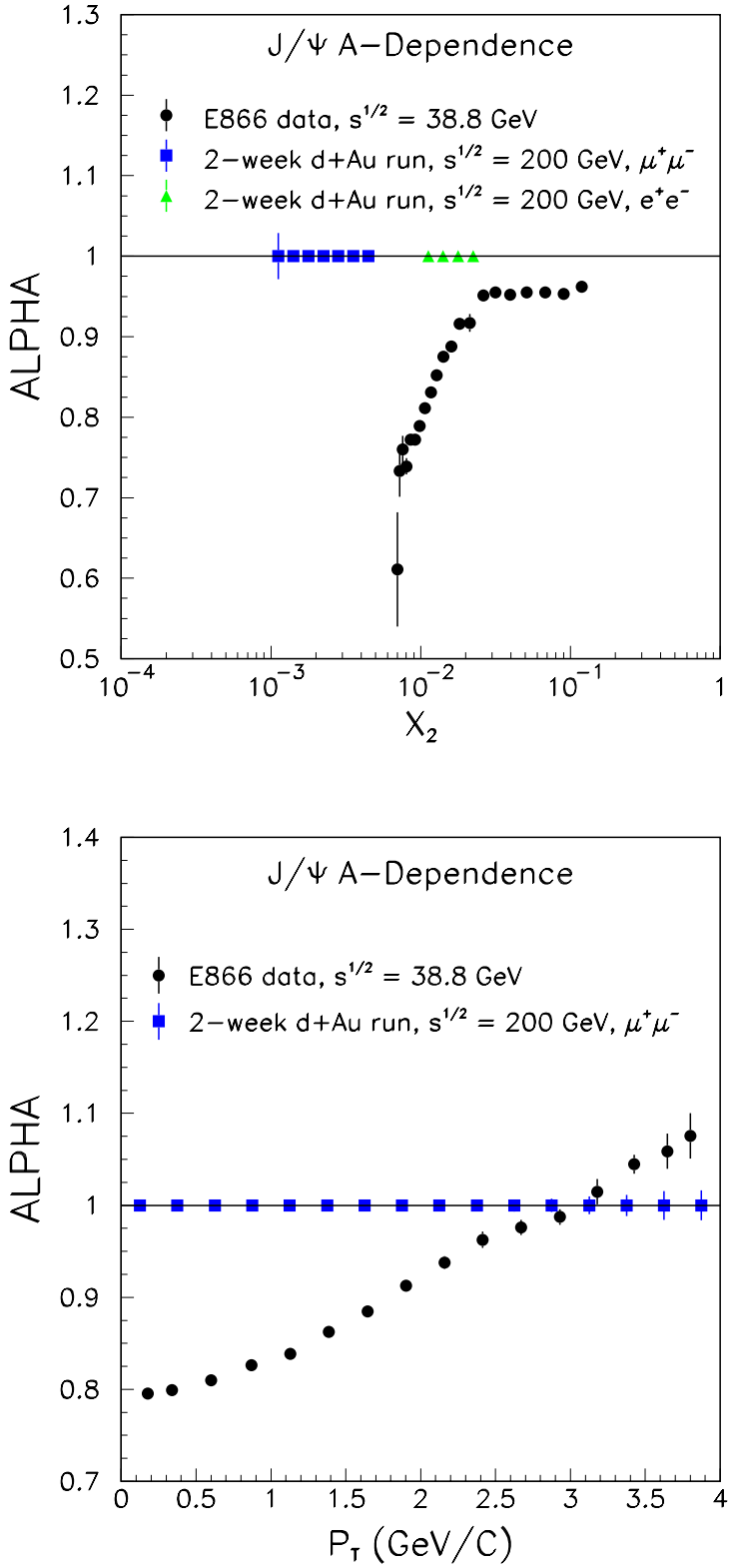

Figure 6: Expected statistical accuracy for measuring the nuclear dependence parameter α from a two-week $d + Au$ run the PHENIX. Data from a fixed-target experiment at $s^{1/2} = 38.8$ GeV are also shown.

Can one probe the meson cloud directly?

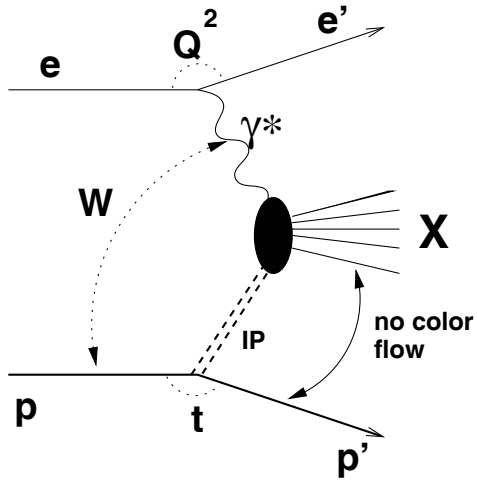

Virtual pion-electron scattering was studied at HERA by tagging forward-going proton/neutron

Pion structure functions at $10^{-4} < x < 10^{-2}$ were measured

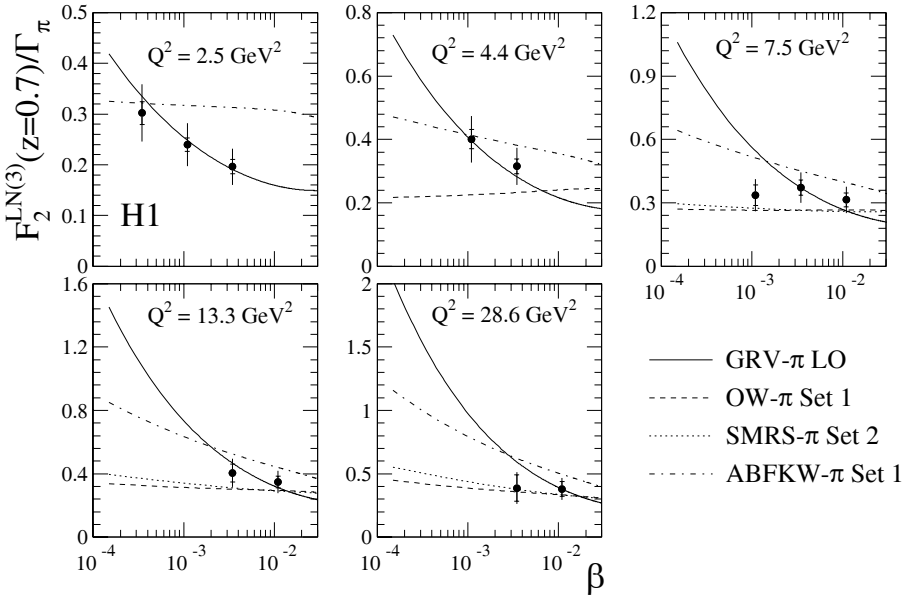

Can one study analogous processes at RHIC?

Figure 7: Deep-inelastic scattering tagged by forward-going nucleons. Extraction of pion structure function by the H1 collaboration using the tagged DIS process.

Tagged Drell-Yan production at RHIC?

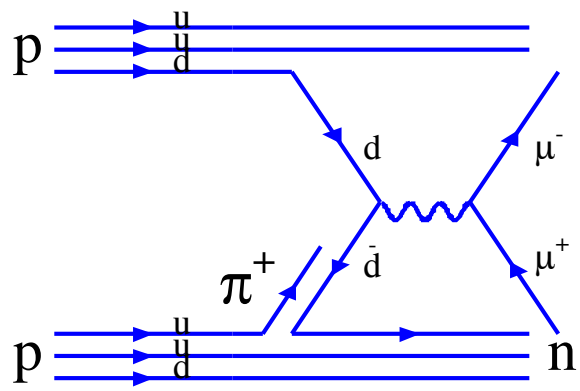

One can tag on forward-going proton, neutron, Δ, Λ in coincidence with lepton-pair detection

Assuming factorization, then

$$d\sigma^{DY}/dy\ dm\ dx_F\ (p + p \to n + \mu^+\mu^- + X) =$$

$$d\sigma^{DY}/dm\ dx_F\ (p + \pi^+ \to \mu^+\mu^- + X) \cdot f_{MB}(y)$$

$f_{MB}(y)$ is the probability for $p \to \pi^+ + n$, where n carries a fraction y of the proton momentum

Tagged D-Y production could provide information on the antiquark distribution in the mesons and on $f_{MB}(y)$

Figure 8: Consideration for measuring tagged Drell-Yan production at RHIC.

Can one detect Drell-Yan events tagged by forward-going nucleons at RHIC?

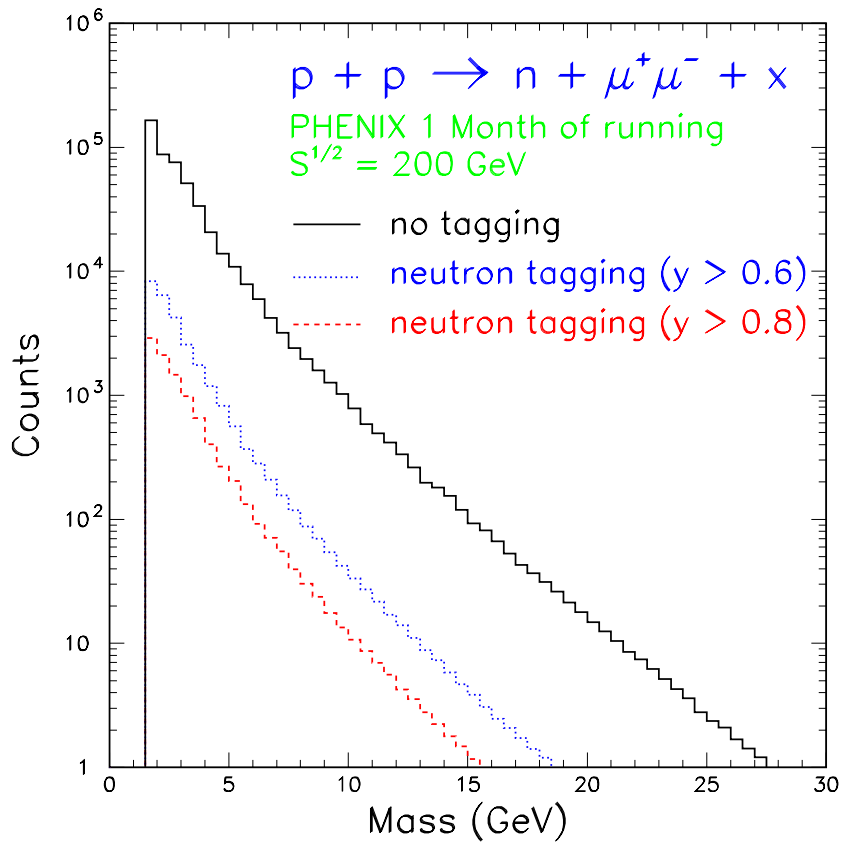

y: fraction of the proton beam momentum carried by the tagged neutron

Figure 9: The solid curve corresponds to dimuon event distributions for a one-month $p+p$ PHENIX run at $\sqrt{s} = 200$ GeV. The dotted and dashed curves correspond to the yields for $p+p \to n+\mu^+\mu^- + X$ with $Y > 0.6$ and $Y > 0.8$, respectively, where Y is the fraction of proton beam momentum carried by the neutron.

Other possible tagged Drell-Yan measurements

1. $p + p \to \Lambda + l^+ l^- + x$
   - probe the $p \to \Lambda + K^+$ component, and the strange quark contents in the proton

2. $\vec{p} + \vec{p} \to n + l^+ l^- + x$
   - measure helicity asymmetry A_{LL} due to meson cloud (expect $A_{LL} \sim 0$)

3. $p + A \to A + l^+ l^- + x$
   - test of pion-excess model in nuclei via the A-dependence measurement

4. Doubly-tagged Drell-Yan: $p + p \to p + p + l^+ l^- + x$
   - meson-meson annihilation?

Other hard-diffractive processes at RHIC?

1. Tagged J/Ψ production?

2. Tagged jet production?

Figure 10: Other possible tagged hard-processes at RHIC.

e-A Parallel Session Summary

Jamal Marian-Jalilian

EIC Workshop
BNL
February 28 – March 2, 2002

QCD is now accepted as the theory of strong interactions. Hard scattering or short distance phenomena are successfully described by perturbative QCD methods. However, these phenomena constitute only a small part of the QCD phase space. The semi-hard region of QCD, where hard and soft QCD meet, is poorly understood even though it may significantly contribute or even dominate many interesting QCD processes such as total cross sections and particle production. The semi-hard region of QCD can be understood as the limit where $x \to 0$. Therefore, exploring the small x limit of QCD will help us understand many of these interesting QCD phenomena.

Gluons are the most abundant partons at small x. They grow very fast with increasing energy (decreasing x) until this growth is inhibited, i.e. saturated by self interactions. The number of gluons per unit area and rapidity, designated $Q_s(x)$, is large ($Q_s \gg \Lambda_{QCD}$) at small x which allows a weak coupling ($\alpha_s(Q_s) \ll 1$) approach. These saturated gluons are said to form a *Color Glass Condensate* since gluons are colored and their occupation number is large. The Glass refers to the fact the there are two distinct time scales involved with these saturated gluons are their mathematical properties are similar to those of Glass. Therefore, a hadron or nucleus at very high energy can be described as a Color Glass Condensate (CGC). The CGC determines the initial conditions of a high energy hadronic or nuclear collision and can be studied in pp, pA, AA,ep and eA collisions.

Nuclei are the ideal environment in which to study the properties of the Color Glass Condensate. Nuclei enhance high gluon density effects by $A^{1/3}$. To achieve similar gluon densities in ep collisions, one would need at least two orders of magnitude higher center of mass energies. Deep inelastic scattering of electrons off nuclei, as in the proposed EIC, would enable us to establish and study the properties of the Color Glass Condensate. This knowledge is necessary and important to our understanding of the outcome of the heavy ion program at RHIC.

The properties of the Color Glass Condensate can be studied through different processes. The most common ones are the fully inclusive ones, such F_2 and F_L structure functions measured at different x and Q^2. EIC will enable us to measure the nuclear structure functions in a wide kinematic region and with unprecedented accuracy. The kinematic region covered by EIC and a comparison to the kinematic region covered by the fixed target experiments is shown in Figure (1) as well as some data on F_2 from NMC and $E665$ experiments. Measuring the structure functions at small x and intermediate $Q^2 \sim 1 - 5$ will shed light on the nature of shadowing and its Q^2 dependence. The current fixed target experiments can not unequivocally determine this Q^2 dependence (at small x) due to their limited kinematic reach. EIC will widen the Q^2 reach by at least an order of magnitude. V. Guzey's talk [1] (given by M. Strikman) concentrated on the common, leading twist picture of shadowing while the talk by A. Freund [2] considered the higher twist contributions to nuclear shadowing and the role of the Color Glass Condensate. EIC will go a long way toward clarifying the physics of shadowing.

J. Qiu, in his talk [3], pointed out that the Color Glass Condensate and saturation effects will modify the x and Q^2 dependence of the average p_t in hadron production. This average p_t is generated by initial state soft gluon radiation which can be re-summed. The saturation scale Q_s^2 will result in softening of the average p_t spectrum. The subject of

quantum evolution of the structure functions were covered in talks by I. Balitski [4] and H. Weigert[5]. I. Balitski showed new evolution equations for the gluon structure function in the kinematic region where gluon density is high. The same equations were obtained by Weigert and collaborators using a different formalism. Weigert used numerical methods to solve these equations and showed that one can fit the HERA data on F_2 at small x.

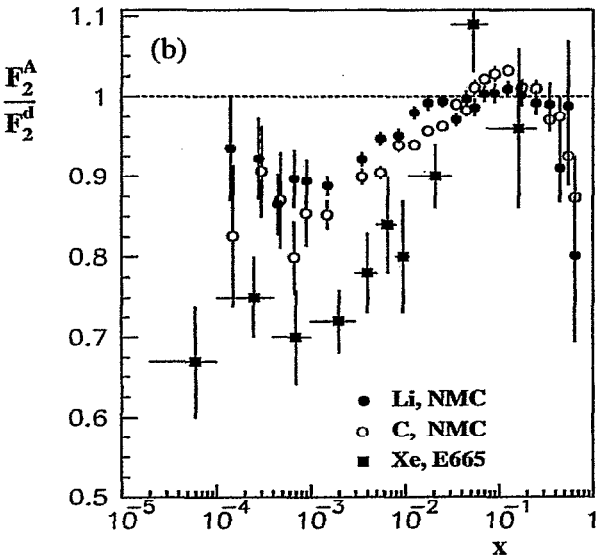

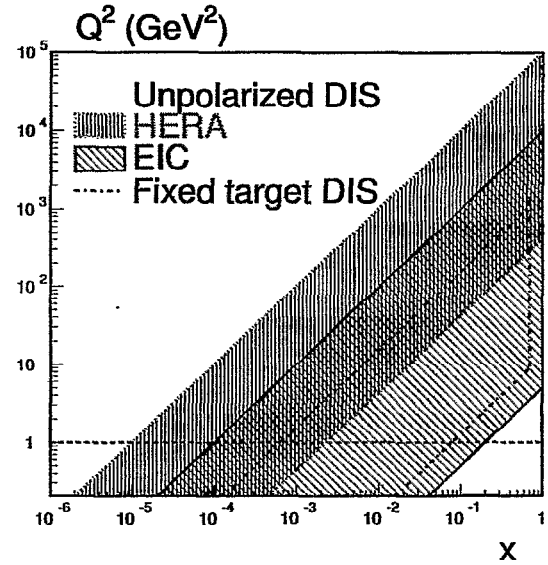

Figure 1: Nuclear shadowing and the kinematic region of EIC and fixed target experiments.

Less inclusive signatures of the Color Glass Condensate such as diffraction and gluon production were covered in talks by Y. Kovchegov [6] and K. Tuchin [7]. It was shown by Y. Kovchegov that the Color Glass Condensate description of diffractive cross sections can explain the near constancy of the ration of diffractive to total cross sections as a function of energy as measured by HERA. K. Tuchin showed that the Color Glass Condensate predicts an interesting behavior for the ratio of longitudinal to transverse diffractive structure functions which is markedly different from the standard dilute QCD parton model predictions. Finally, R. Fries [8] showed that higher twist effects which are behind the Color Glass Condensate picture, also effect the final state fragmentation functions.

EIC will enable us to explore some of the most interesting, but least understood regions of QCD phase space. It will reach the high gluon field strength domain of QCD where many novel phenomena such as gluon saturation and unitarization are expected to occur.

It will shed light on the nature of particle production, rapidity gaps and total cross sections and many other interesting phenomena at high energies. It will help us understand and measure the partonic structure of nuclei at high energy with unprecedented accuracy. This is urgently needed for the existing heavy ion experiments.

References

[1] Talk in the eA parallel session.

[2] Talk in the eA parallel session.

[3] Talk in the eA parallel session.

[4] Talk in the eA parallel session.

[5] Talk in the eA parallel session.

[6] Talk in the eA parallel session.

[7] Talk in the eA parallel session.

[8] Talk in the eA parallel session.

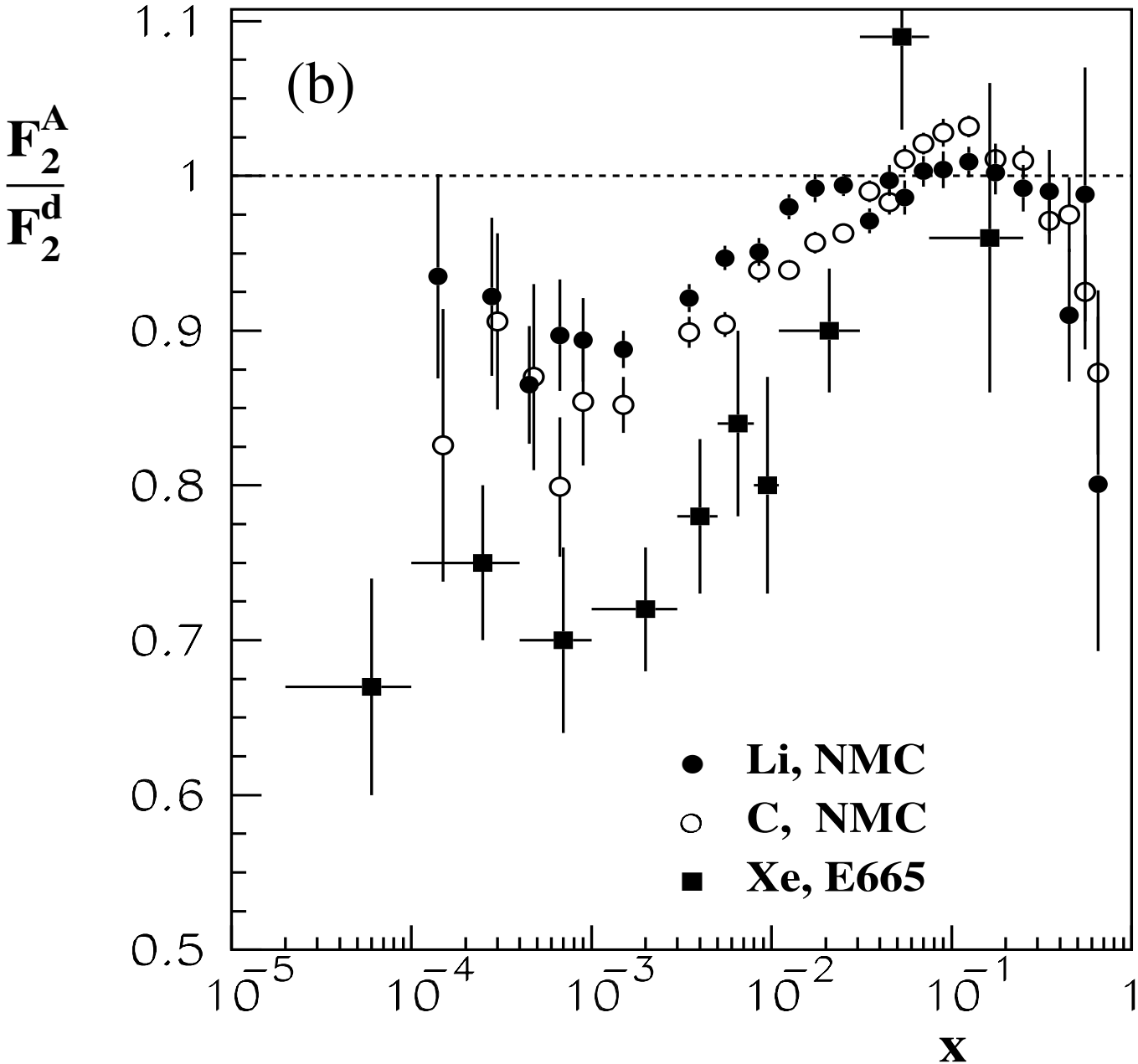
(b)
F_2^A / F_2^d
1.1
1
0.9
0.8
0.7
0.6
0.5
10^{-5}
10^{-4}
10^{-3}
10^{-2}
10^{-1}
1
x
Li, NMC
C, NMC
Xe, E665

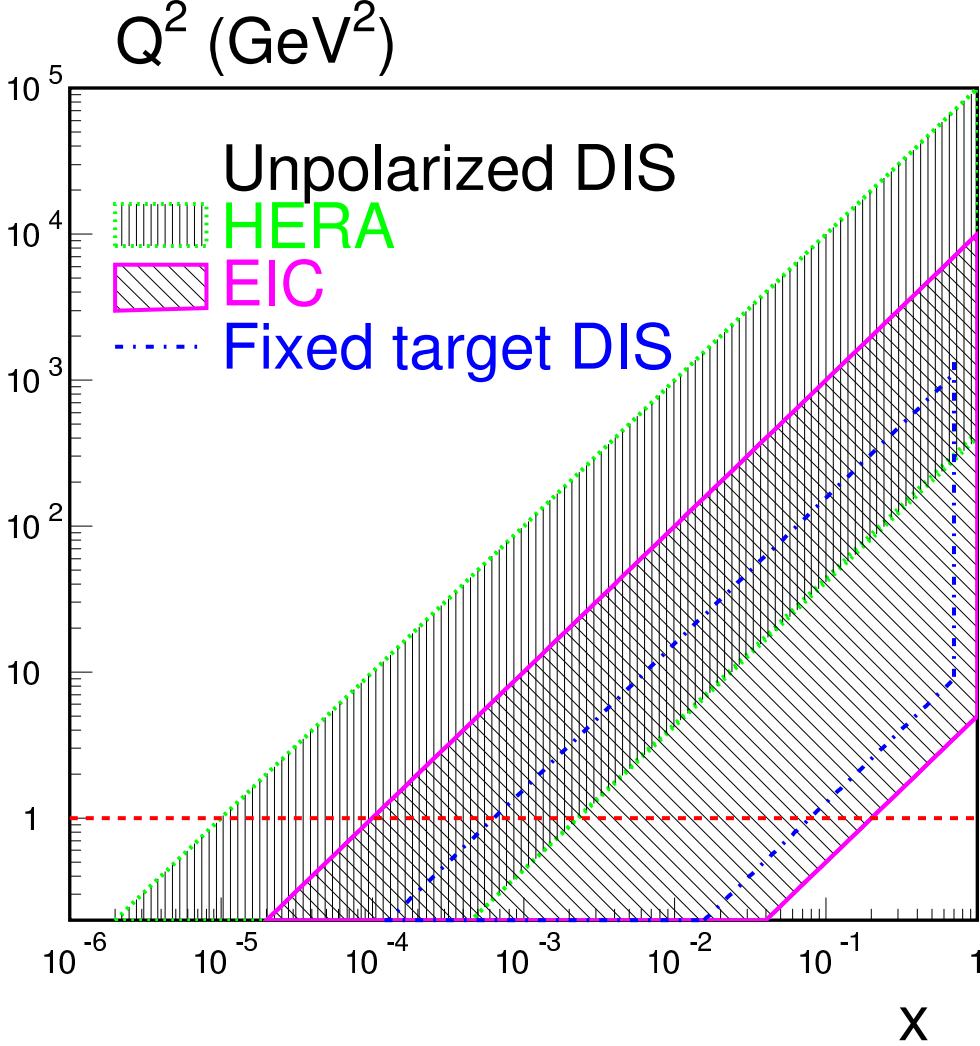
Q2 (GeV2)
Unpolarized DIS
HERA
EIC
Fixed target DIS
10 5
10 4
10 3
10 2
10
1
10 -6
10 -5
10 -4
10 -3
10 -2
10 -1
1
x

e-A Parallel Session Summary

A. Bruell

EIC Workshop
BNL
February 28 – March 2, 2002

Summary: Parallel Session on eA-Physics

- **What do we know?**
  - Very little!!!
  - x, A (and Q^2) dependence of $F^A{}_2/F^D{}_2$
    But: limited Q^2rand for fixed x
    systematic uncertainties
    low x (x<0.01) only at low Q^2
    $\Rightarrow$ constraints on q^A/q^D
    (almost) no constraints on G^A/G^D
  - Drell – Yan from fixed target experiments
    $\Rightarrow$ some constraints on $q^A{}_s/q^D{}_s$
  - J/ψ production
    $$\Rightarrow \quad \frac{\sigma_{J/\psi}(Sn)}{\sigma_{J/\psi}(C)} = 1.12 \pm 0.08$$
  - Medium effects in hadronization
    Separately for $\bar{k}$, k and p
    Measured as a function of ν, z and A
    $\Rightarrow$ Qualitative interpretation: parton energy loss!!

- **What's Needed?**
  - $F^A{}_2/F^D{}_2$ over wide range in x and Q^2
  - Flavor decomposition
  - Shadowing in G(x)
    - High p_t jet production
    - Charm production
  - Better understanding of fragmentation process and its modification int eh nuclear media
  - Diffraction in eA
  - Experimental observables to test saturation

$\Downarrow$

High Potential

(There is more than enough room for surprises.)

x- and A-dependence of the EMC effect

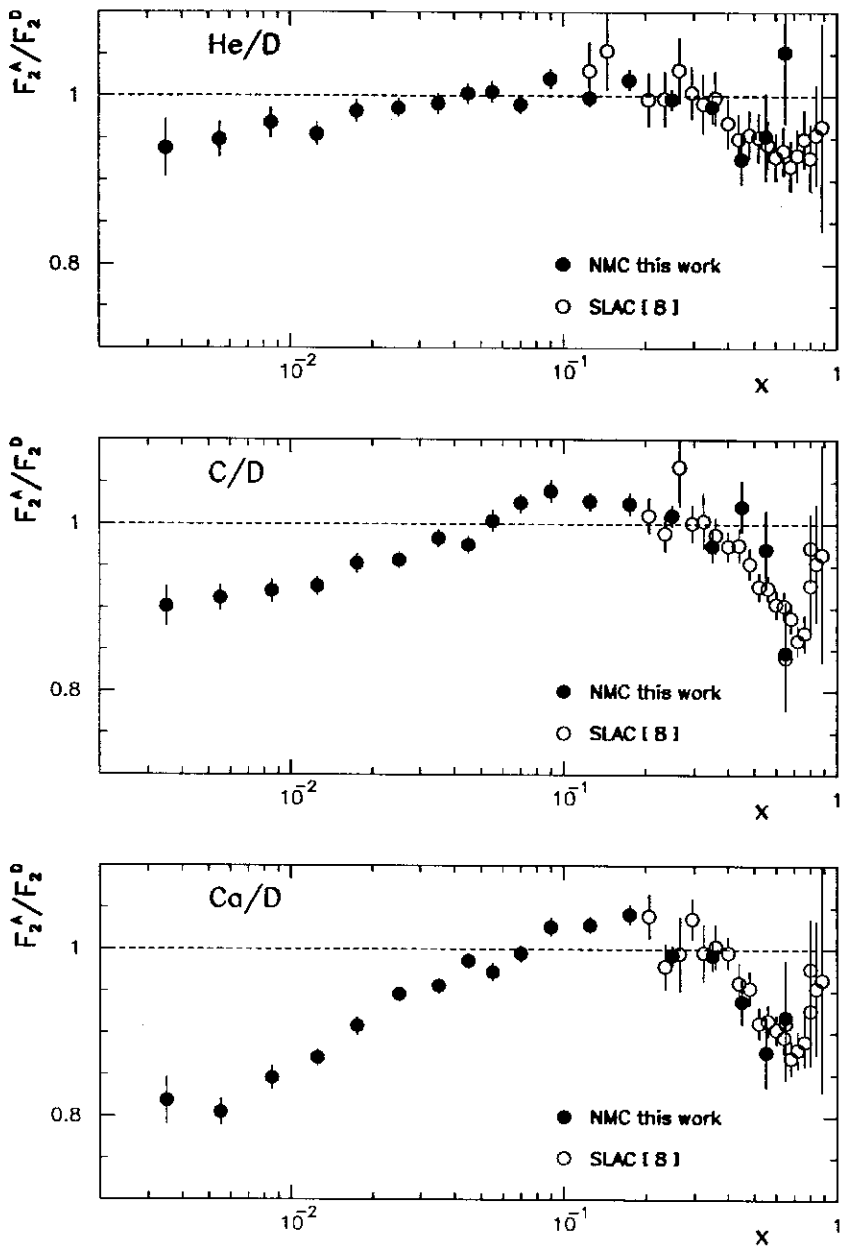

$F_2^A \neq F_2^D$ for all values of x
effect increasing with atomic number A

Parametrisations of the A-dependence

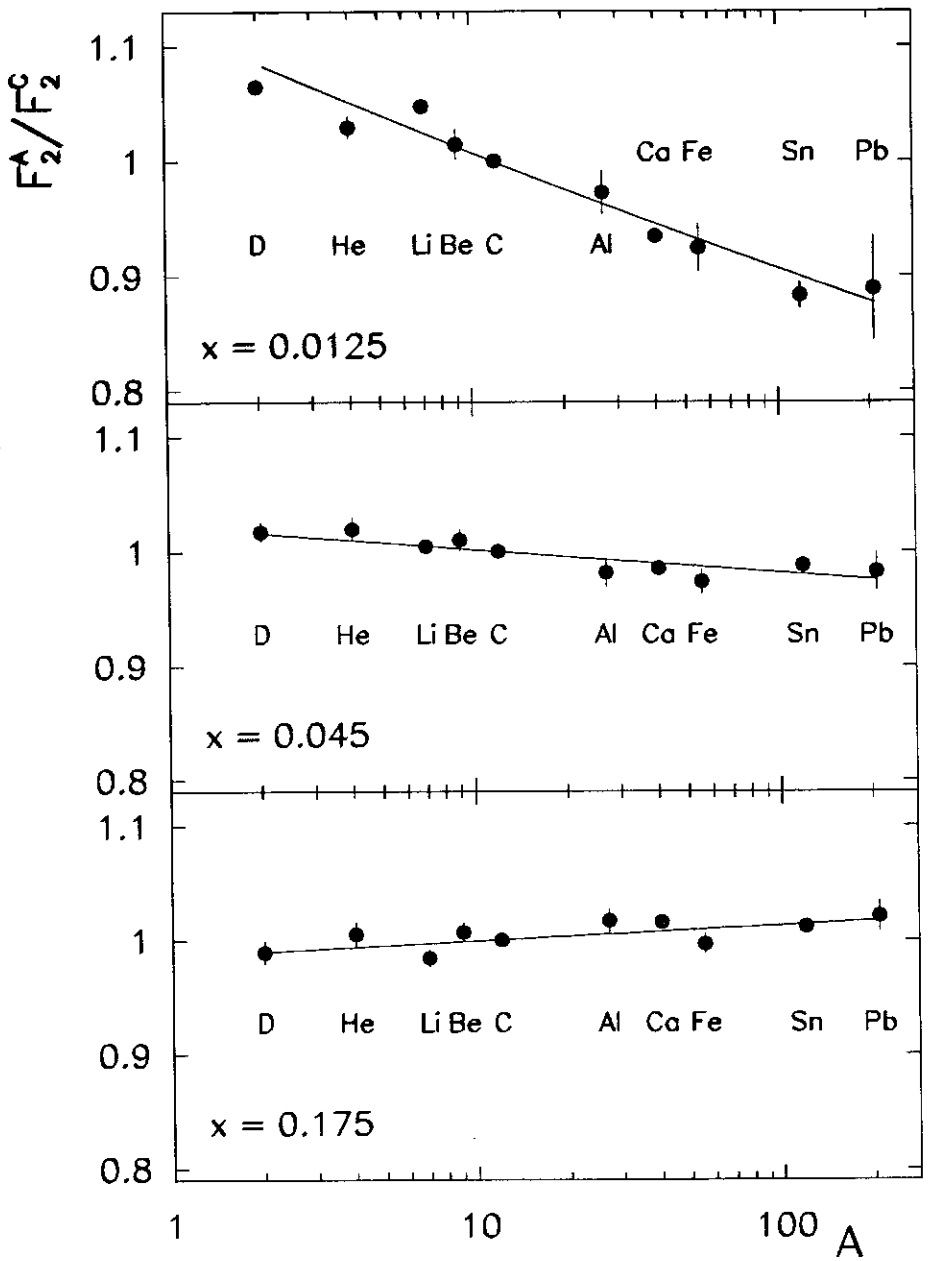

Simple power dependence A^α describes the data well

Q^2 dependence of the EMC effect

- Data on F_2^{Sn}/F_2^C collected at 4 different beam energies (NMC)

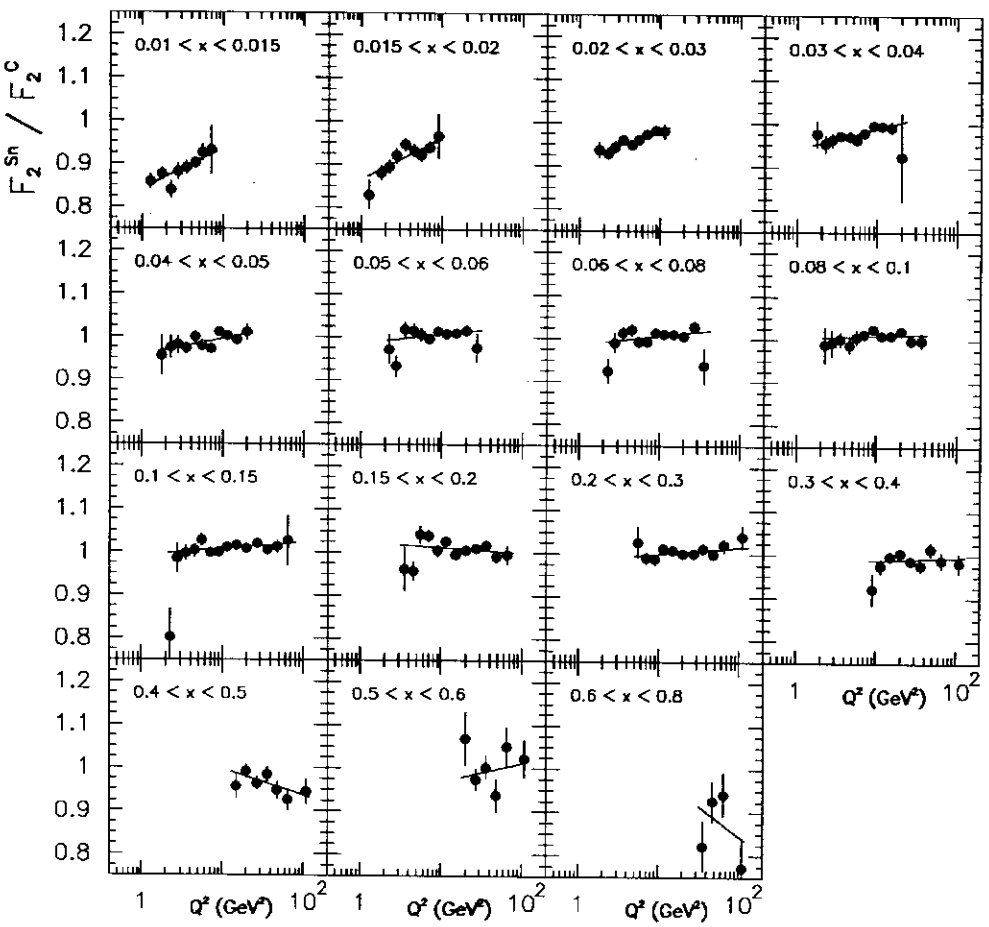

Small and positive Q^2 dependence at low values of x

Q^2 dependence of the EMC effect

- Data on F_2^{Sn}/F_2^C collected at 4 different beam energies (NMC)

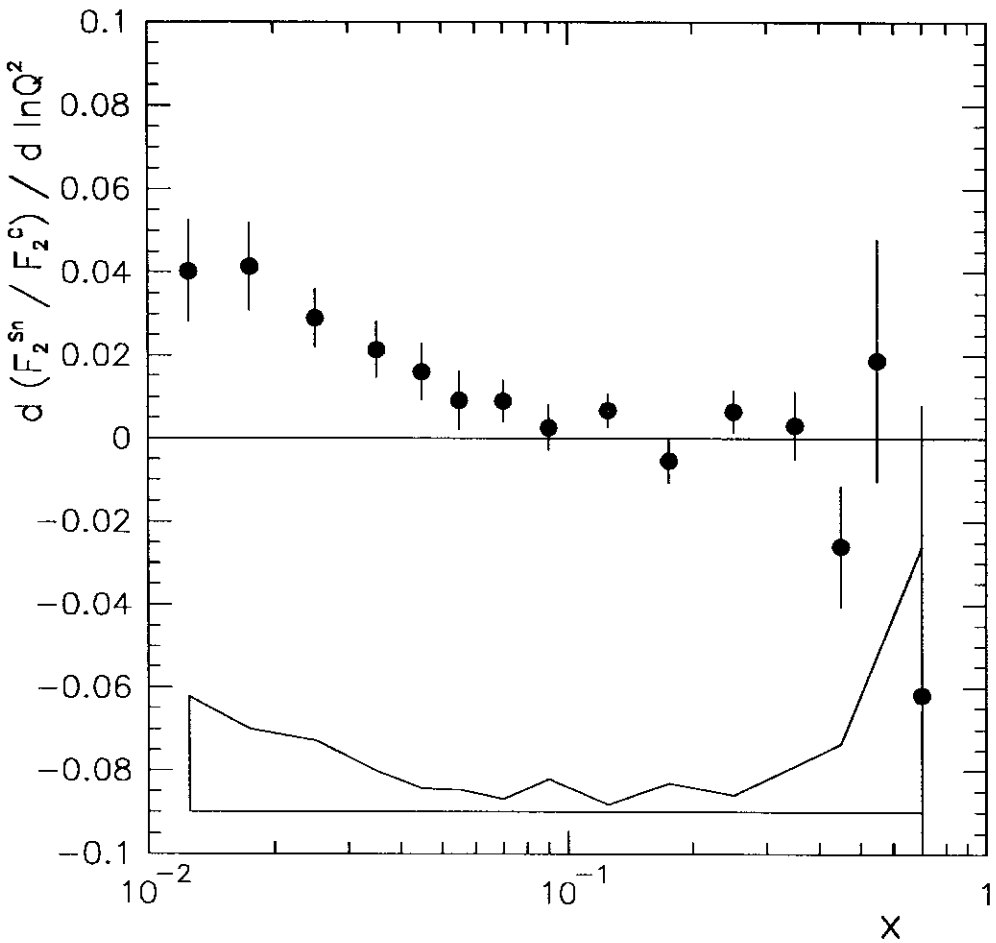

Small and positive Q^2 dependence at low values of x

$$\Delta G = G^{Sn}(x) - G^{C}(x)$$

from $\Delta R = R^{Sn} - R^{C}$

$$R(x, Q^2) = \frac{F_L + 4M^2x^2/Q^2\, F_L}{F_2 - F_L}$$

$$F_L = \frac{\alpha_s}{2\pi} x^2 \int \frac{d\omega}{\omega^3}\left[\frac{8}{3}F_2 + \frac{40}{9}\left(1 - \frac{x}{\omega}\right)\omega G\right]$$

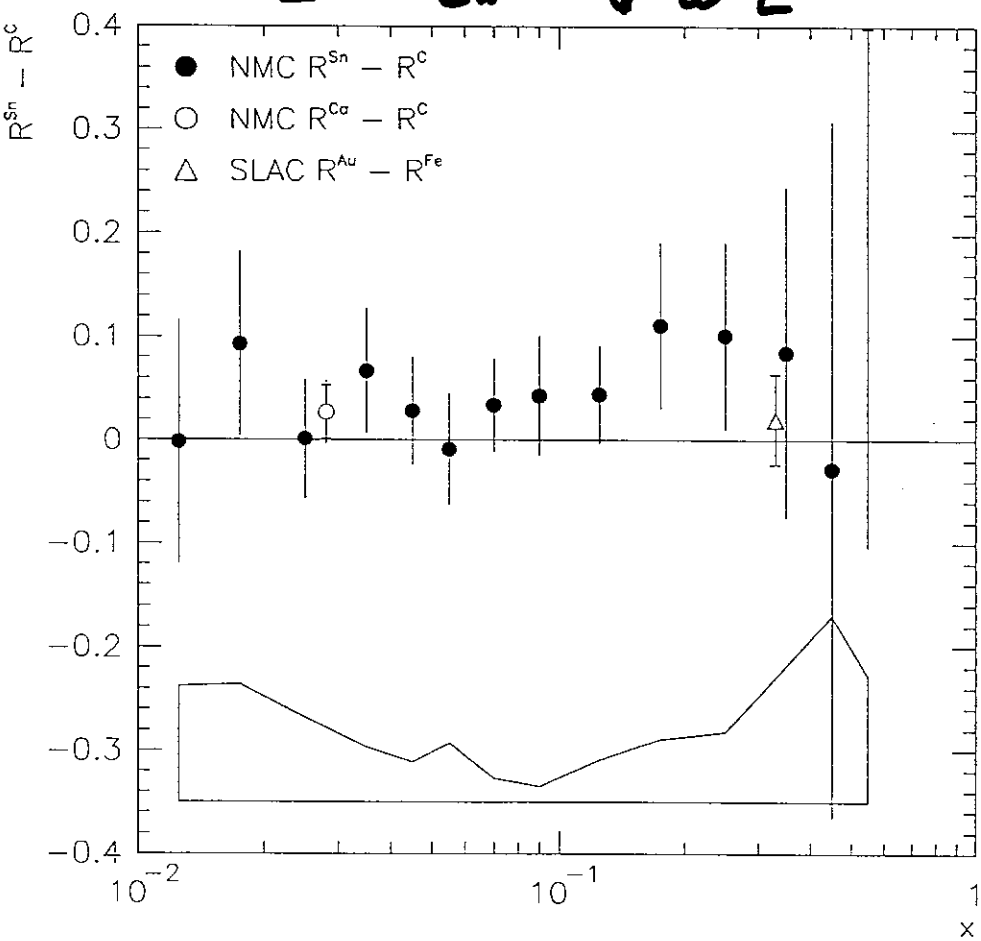

$$\Delta R = 0.039 \pm 0.018 \pm 0.026$$

(at $Q^2 = 10\ \mathrm{GeV}^2$)

$\Longrightarrow$ no significance for $G^{Sn}(x) \neq G^{C}(x)$

Frankfurt + Strikman

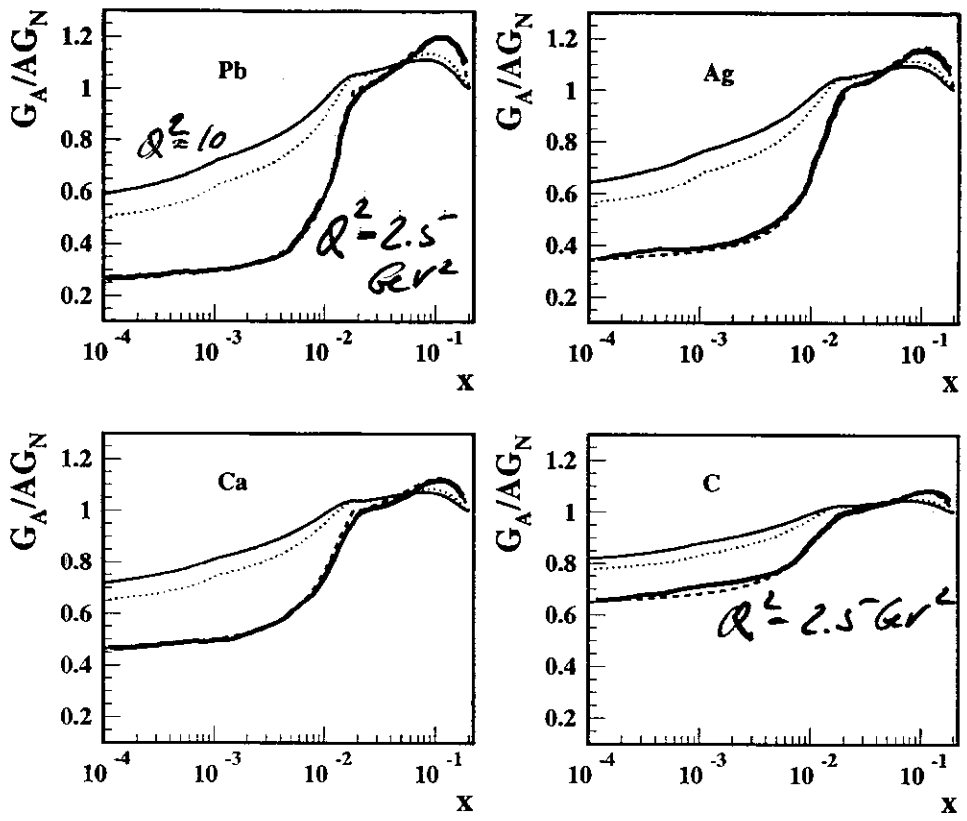

FIG. 4. Dependence of G_A/AG_N on x for Q=2,5,10 GeV (dashed, dotted, solid curves) calculated in the quasieikonal model.

Dipole description of DIS

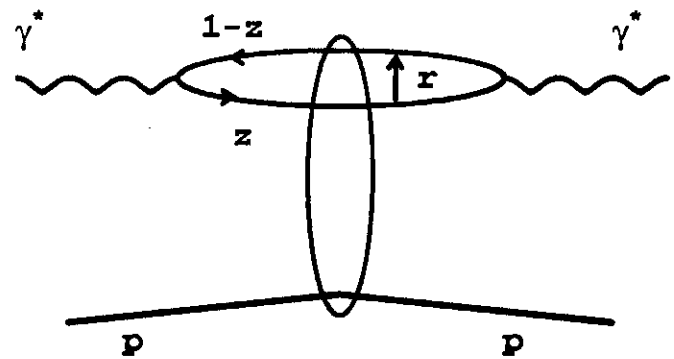

$$\sigma_{tot}^{\gamma^* p} = \int d^2\hat{\vec{r}} \int_0^1 dz\, \Psi(Q^2, z, \vec{r})^* \sigma_{q\bar{q}}(x, r^2) \Psi(Q^2, z, \vec{r})$$

$$\frac{d\sigma_{VM}^{\gamma^* p}}{dt}\Big|_{t=0} = \frac{1}{16\pi} \Big| \int d^2\vec{r} \int_0^1 dz\, \Psi_{VM}^*(Q^2, z, \vec{r})\ \sigma_{q\bar{q}}(x, r^2) \Psi(Q^2, z, \vec{r}) \Big|^2$$

$$\frac{d\sigma_{diff}^{\gamma^* p}}{dt}\Big|_{t=0} = \frac{1}{16\pi} \int d^2\vec{r} \int_0^1 dz\, \Psi^*(Q^2, z, \vec{r}) \sigma_{q\bar{q}}^2(x, r^2) \Psi(Q^2, z, \vec{r})$$

$\Psi(z, \vec{r})$	$\gamma \rightarrow q\bar{q}$ QCD wave function
$\sigma_{q\bar{q}}(x, r^2)$	cross section for scattering of $q\bar{q}$ pair on proton (dipol cross section)

GBW Model

K. Golec-Biernat, M. Wuesthoff

$$\sigma_{qq}(x, r) = \sigma_0 [1 - \exp(-\frac{r^2}{4 R_0^2})]$$

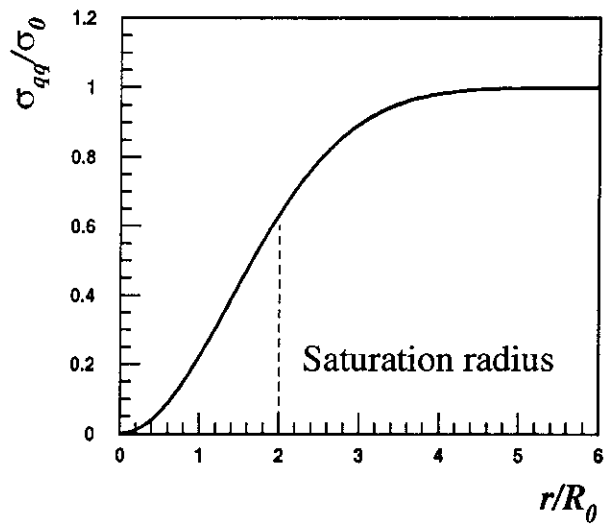

for $r \ll 2 R_0$ $\quad \sigma_{qq} = \sigma_0 \frac{r^2}{4 R_0^2}$

for $r \gg 2 R_0$ $\quad \sigma_{qq} = \sigma_0$

Size of r determined by the wave function:
perturbative region $r \ll 2R_0$
saturation region $r \gg 2R_0$

from DIS data: $\sigma_{qq} \sim x^{-0.3}$ in the perturbative region

=> Assumption $\quad R_0^2(x) = \frac{1}{GeV} \left(\frac{x}{x_0} \right)^{\lambda}$

Parameters fitted to DIS data:
$\sigma_0 = 23$ mb $\quad \lambda = 0.29 \quad x_0 = 0.0003$

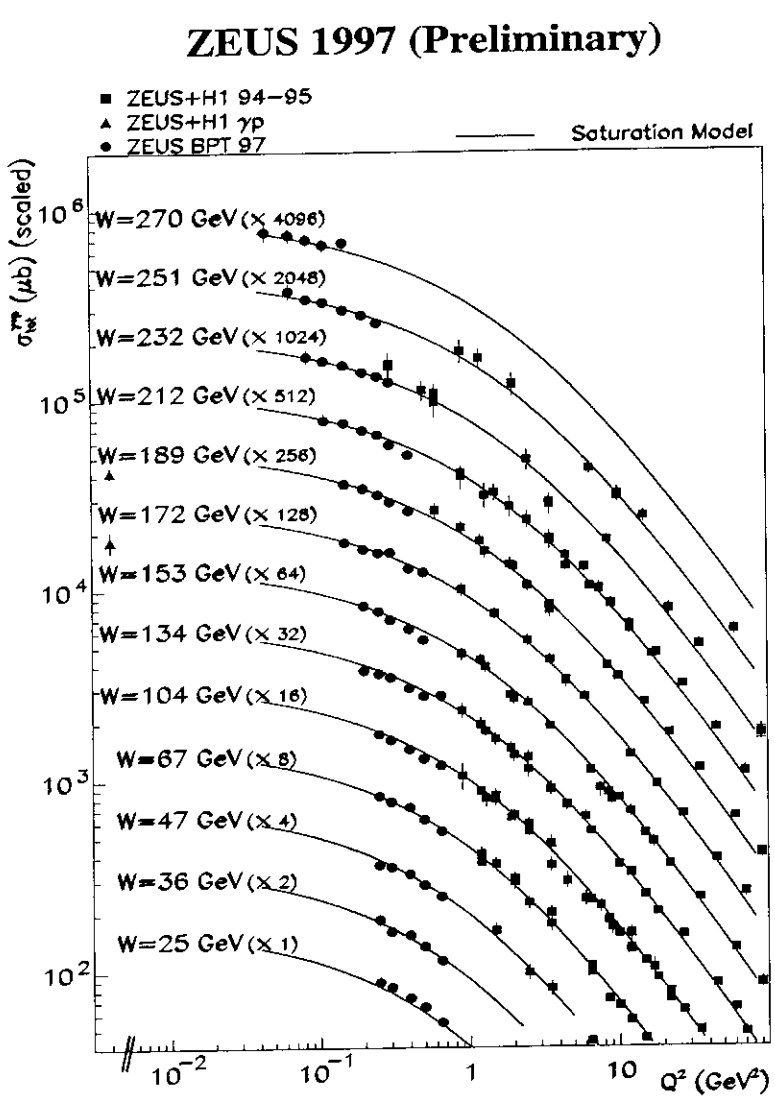

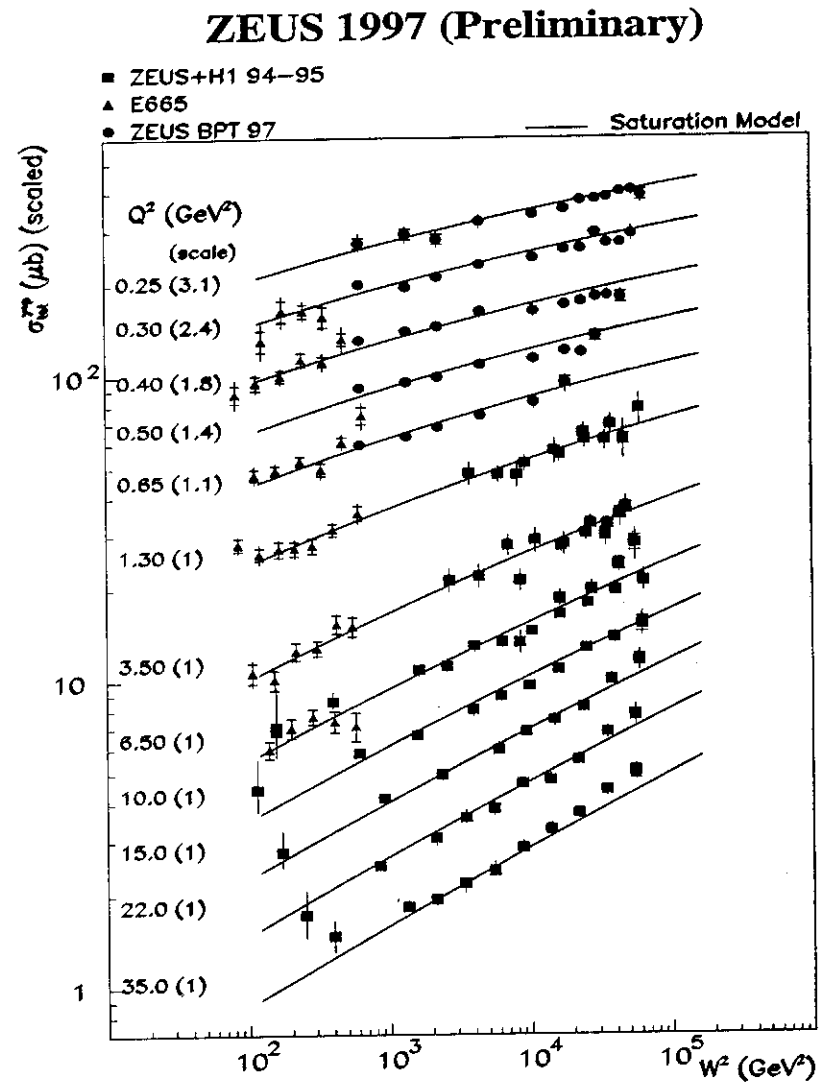

Parameters fitted to HERA DIS data: $\chi^2/N \sim 1$

$\sigma_0 = 23$ mb $\quad \lambda = 0.29 \quad x_0 = 0.0003$

Saturation Model
Predictions for Diffraction

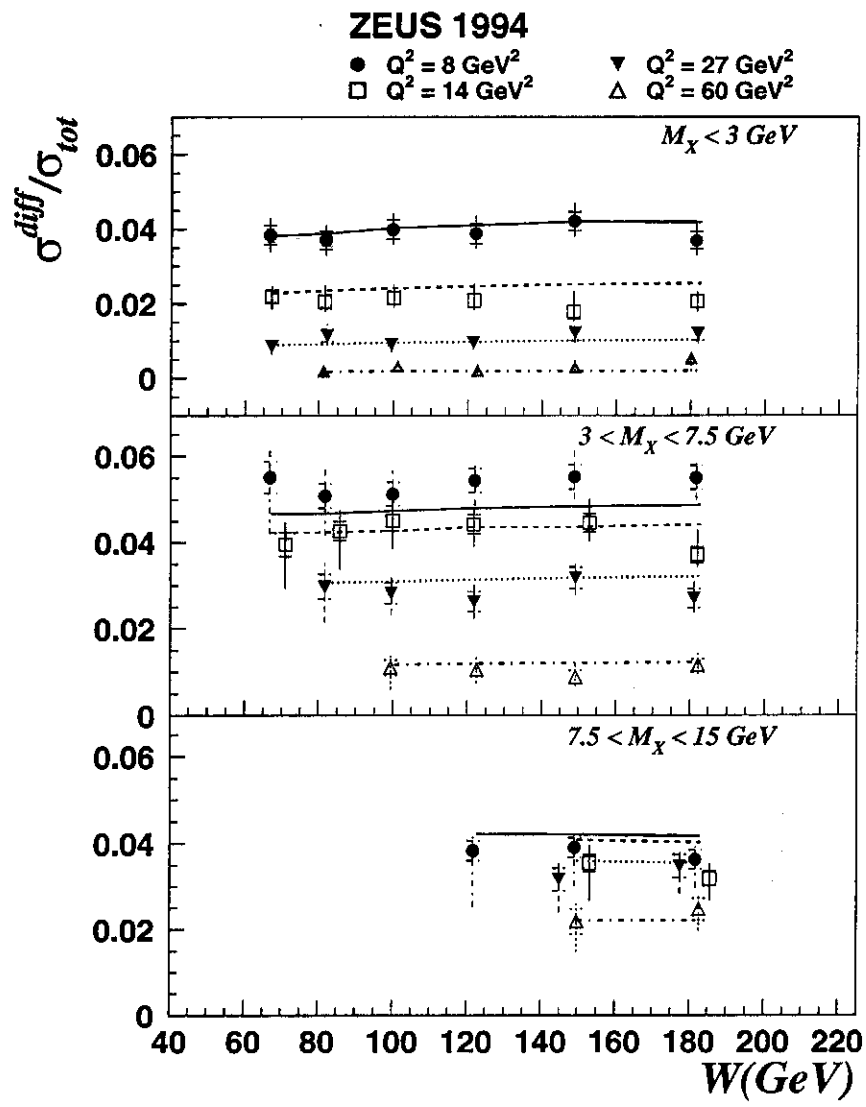

J/Ψ Diffractive Photo-production

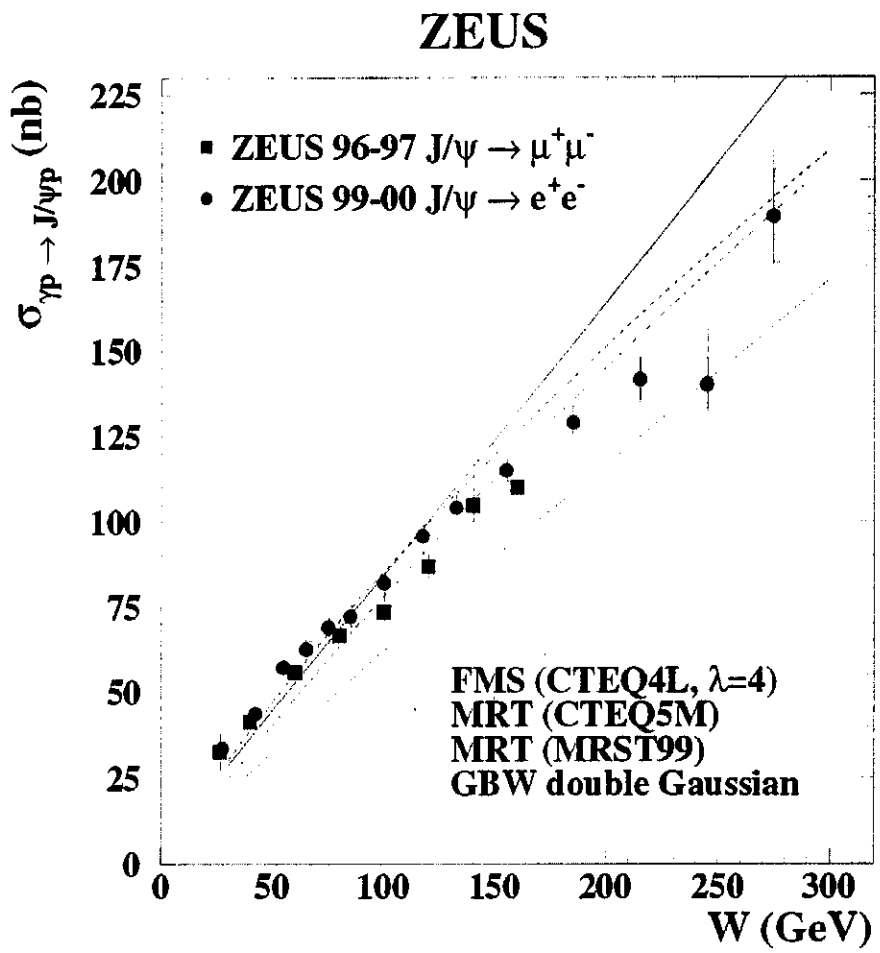

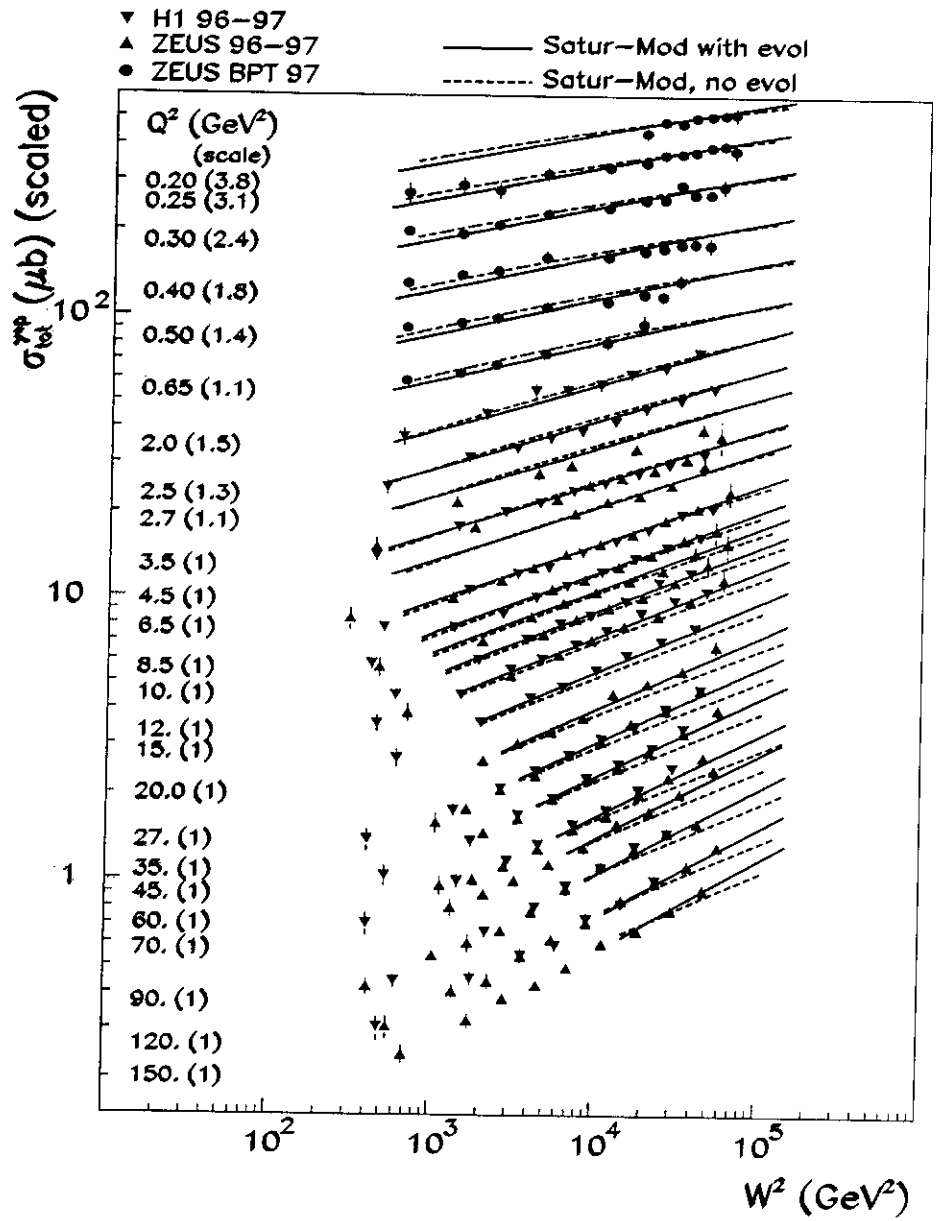

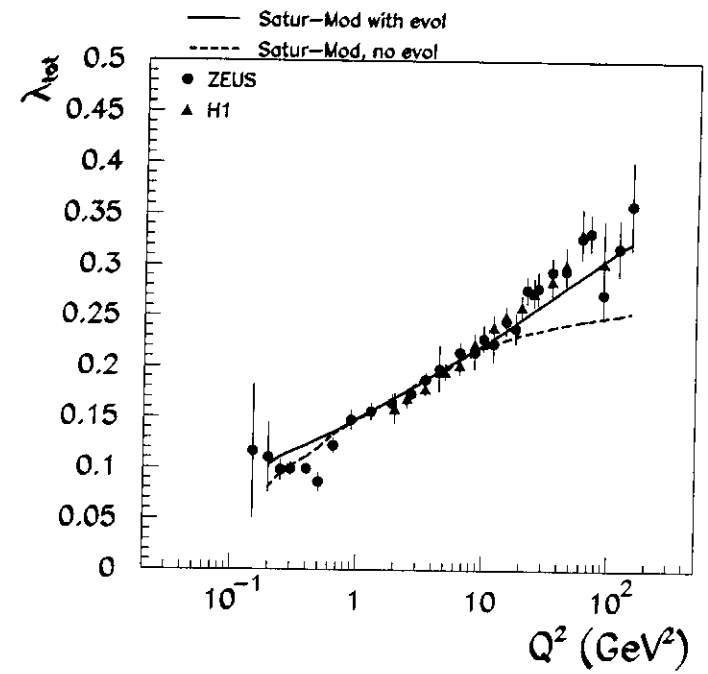

Fits to new data

$m_q = 140$ *MeV*

Original *GBW* Saturation Model $\chi^2/N \sim 2.4$

Saturation Model with evolution $\chi^2/N \sim 1.2$

$\sigma_0 = 23$ mb $\lambda = 0.28$ A=1.2

$C = 0.26$ $Q_0^2 = 0.5$ GeV^2

Single Hadron Transverse Momentum Distribution as a Probe of Gluon Saturation

Jianwei Qiu
Department of Physics and Astronomy, Iowa State University
Ames, Iowa 50011, U.S.A.

Abstract

In this talk, I argue that single hadron transverse momentum distribution in semi-inclusive electron-ion deeply inelastic scattering can be a good probe of gluon saturation phenomenon.

1. Introduction

It was pointed out recently that the initial-gluon distribution in high energy nuclear collisions can be described by the formation of a so-called Color Glass Condensate (CGC) [1]. The gluon multiplicity per unit rapidity and transverse area at very high energies has been shown to depend on the initial gluon density which saturates at small x [2, 3]. The first results of the charged multiplicity measurements at RHIC seem to be consistent with a picture of gluon saturation [4].

Since soft gluon interactions between colliding hadrons in heavy ion collisions can take place long before two ions collide. Such long range interactions can alter the initial gluon distributions at small x for global observables such as multiplicity distributions. In order to study gluon saturation phenomena within a heavy nucleus without influence from other hadrons, we propose to measure single hadron transverse momentum distribution in semi-inclusive electron-ion deeply inelastic scattering as a probe of gluon saturation at small x.

2. Semi-Inclusive Kinematics at Electron-Ion Collider

For studying single hadron transverse momentum distribution in semi-inclusive deep inelastic scattering (DIS) at electron-ion collider (EIC), $e(\ell) + A(p) \Longrightarrow e(\ell') + h(p') + X$, it is most convenient to choose the γ^*-hadron frame [5]. In this frame, the virtual photon and hadron momenta are chosen as $q^\mu = (0, 0, 0, -Q)$ and $p^\mu = \frac{Q}{2x_B}(1, 0, 0, 1)$, respectively. The observed hadron momentum is defined as $p'^\mu = \frac{zQ}{2}(1 + \frac{Q_T^2}{Q^2}, \frac{2Q_T}{Q}, 0, \frac{Q_T^2}{Q^2} - 1)$, with $z = \frac{p\cdot p'}{p\cdot q} = x_B \frac{2p\cdot p'}{Q^2}$, $Q_T = \sqrt{-q_T^\mu q_{T_\mu}}$, and $q_T^\mu \equiv q^\mu - \frac{q\cdot p'}{p\cdot p'}p^\mu - \frac{q\cdot p}{p'\cdot p}p'^\mu$. The transverse momentum satisfies $q_T \cdot p = q_T \cdot p' = 0$. As usual, $Q^2 = -q^2$ and Bjorken variable $x_B = Q^2/2p\cdot q$.

In terms of collinear factorization, momenta of initial-state parton and final-state fragmentation parton are defined as $p_a^\mu = \xi\, p^\mu$ and $p_c^\mu = p'^\mu/\,\eta$, respectively. In deeply inelastic scattering at EIC, the center of mass collision energy between the virtual photon and colliding ion, $S_{\gamma^*-A} = (q+p)^2 \approx Q^2\left[\frac{1-x_B}{x_B}\right]$, is a function of Q^2 and x_B. That is, we can "scan" the collision energy by varying x_B and Q^2.

Due to invariant mass of the γ^*-parton system, $\hat{s}_{\gamma^*-p}$, parton momentum fraction ξ in semi-inclusive DIS, $\xi \approx x_B \left[1 + \frac{\hat{s}_{\gamma^*-p}}{Q^2}\right]$, can be very different from x_B. In order to probe soft gluon saturation, we need observables sensitive to small parton momentum fraction ξ.

3. Single Hadron Transverse Momentum Distribution

According to QCD factorization theorem, cross section for single hadron transverse momentum distribution can be expressed as [5]

$$\frac{d\sigma_{A\to h}}{dx_B dQ^2 dz dq_T^2} = \sum_{a,c} \int_z^1 \frac{d\eta}{\eta} D_{c\to h}(\eta) \int_{x_B}^1 \frac{d\xi}{\xi} f_{a/A}(\xi) \left[\frac{d\hat{\sigma}_{a\to c}}{d\hat{x} dQ^2 d\hat{z} dq_T^2}\right] \tag{1}$$

with parton level variables, $\hat{x} = \frac{Q^2}{2p_a\cdot q} = \frac{x_B}{\xi}$ and $\hat{z} = \frac{p_c\cdot p_a}{q\cdot p_a} = \frac{z}{\eta}$. If $Q^2 \gg Q_T^2$, the perturbatively calculated partonic hard part $\hat{\sigma}_{a\to c}$ becomes unstable due to initial-state and final-state soft gluon radiation which generates large logarithms, $\frac{1}{Q_T^2}\alpha_s^n \log^{2n-1}(Q^2/Q_T^2)$. Reliable QCD prediction for the distribution in small Q_T region, where the most data are, requires to resum these large logarithms to all orders in α_s.

Resummation of the large logarithms can be achieved by solving renormalization group equations in b-space, the Fourier conjugate of the Q_T-space [6]. It was shown recently that such a resummation formalism has an excellent predictive power if Q^2 and $\sqrt{S}$ are large enough [7]. Resummation for single hadron transverse momentum distribution at HERA was carried out and found to be consistent with existing data [8].

4. Nuclear Dependence of the Transverse Momentum Distribution

According to the resummation formalism, Soft gluon radiation broadens single hadron transverse momentum distribution. Larger the Q^2 is, more phase space for soft gluon radiation (or gluon shower) before the hard collision takes place and more broaden the transverse momentum distribution is. In addition, due to strong evolution of parton distribution at small x, soft gluon radiation is much stronger at high $\sqrt{S}$ or low x_B at EIC.

In nuclear medium, multiple scattering triggers more soft gluon radiation and induces the well-observed transverse momentum broadening in pA and AA collisions. Same broadening, which is proportional to the medium size, should take place in semi-inclusive eA collisions.

If there is no saturation, partons in a free nucleon and in a nucleus should have similar intrinsic transverse momentum. Therefore, the phase space for soft gluon shower (from intrinsic transverse momentum square to Q^2) should be the same in both cases, and therefore, only nuclear effects to the transverse momentum distribution come from initial-state nuclear shadowing and final-state multiple scattering. At a fixed $\sqrt{S}$ (i.e., at a fixed x_B at EIC), the averaged transverse momentum square $\langle Q_T^2 \rangle$ should decrease as Q^2 decreases, and stops at

intrinsic transverse momentum square plus whatever the amount broadening due to final-state multiple scattering. If there is saturation, saturation scale is believed to be much larger than the intrinsic momentum scale [1, 4]. Therefore, the averaged transverse momentum square $\langle Q_T^2 \rangle$ should be saturated at a much larger scale when Q^2 decreases at a fixed x_B.

At a fixed Q^2, the averaged transverse momentum $\langle Q_T^2 \rangle$ increases as x_B decreases (i.e., increase of effective collision energy) due to the stronger evolution of parton distribution at smaller x. If there is saturation, parton distributions stop evolving for x small enough. Therefore, when collision energy increases (or x_B decreases at EIC) while Q^2 is fixed, the averaged transverse momentum square $\langle Q_T^2 \rangle$ increases slower if there is gluon saturation in parton distributions.

5. Summary and Conclusions

With QCD resummation of all order logarithms, single hadron transverse momentum distribution can be calculated reliably, if collision energy, S_{γ^*-A}, between the virtual photon and heavy ion is large enough. We argued that the averaged transverse momentum distribution square $\langle Q_T^2 \rangle$ is a good observable to see gluon saturation in a large nucleus. The saturation effect can be seen by (1) decreases x_B while keeping a moderate Q^2; and (2) decreases Q^2 while keeping x_B small and fixed.

References

[1] L. McLerran and R. Venugopalan, Phys. Rev. D49, 2233 (1994); *ibid* 3352 (1994); J. Jalilian-Marian, A. Kovner, L. McLerran, and H. Weigert, Phys. Rev. D55, 5414 (1997); J. Jalilian-Marian, A. Kovner, A. Leonidov, and H. Weigert, Nucl. Phys. B504, 415 (1997); Phys. Rev. D59, 014014 (1999).

[2] L.V. Gribov, E.M. Levin, M.G. Ryskin, Phys. Rep. 100, 1 (1983); A.H. Mueller and J.-W. Qiu, Nucl. Phys. B268, 427 (1986).

[3] A. Kovner, L. McLerran, and H. Weigert, Phys. Rev. D52, 6231 (1995); *ibid* 3809 (1995).

[4] D. Kharzeev and M. Nardi, Phys. Lett. B507, 121 (2001).

[5] F.I. Olness, and D.E. Soper, Nucl. Phys. B371, 79 (1992); Phys. Rev. D54, 1919 (1996).

[6] J.C. Collins, D.E. Soper, and G. Sterman, Nucl. Phys. B250, 199 (1985).

[7] J.-W. Qiu and X.-F. Zhang, Phys. Rev. D63, 114011 (2001).

[8] P. Nadolsky, D.R. Stump, and C.P. Yuan, Phys. Rev. D61, 014003 (1999); Erratum, D64, 059903 (2001).

SOFT-GLUON RESUMMATION IN PQCD

- initial-state and final-state soft gluon radiations generate large logarithms: $\frac{1}{q_T^2}\alpha_s^n \log^{2n-1}(Q^2/q_T^2)$

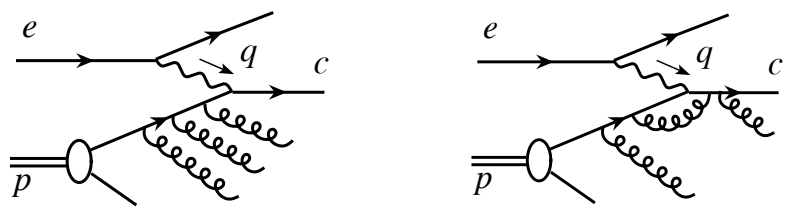

- resummation = sum large logarithms to all orders in α_s
- resummation leads to suppression in small q_T^2 region

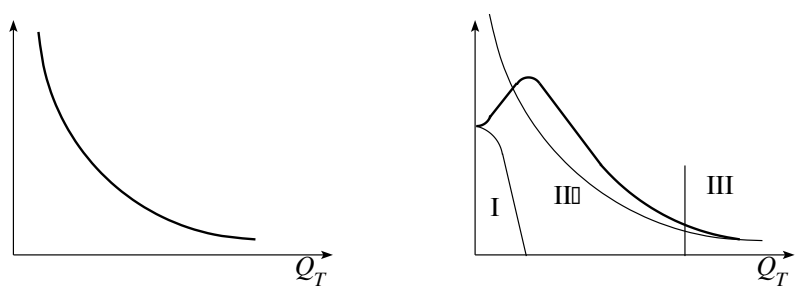

- Generic features of the resummed q_T-distribution:[a]
  - (I): dominated by intrinsic k_T (Gaussian type)
  - (II): pQCD soft-gluon resummation ($q_T \leq Q$)
  - (III): pQCD fixed order calculation ($q_T \sim Q$)
  - relative size of three regions depend on Q^2 and S
  - large Q^2 and large $S \Rightarrow$ smaller region (I)
  - smaller $Q^2 \rightarrow$ smaller logs $\rightarrow$ smaller region (II)

[a] X. Guo, J.Q., and X. Zhang, Phys. Rev. Lett. 84, 5049 (2000); Phys. Rev. D62, 054008 (2000).

b-SPACE RESUMMATION (OR CSS) FORMALISM[a]

- Resummation of all order logarithms is done in b-space, Fourier conjugate of the q_T-sapce

$$\frac{d\sigma_{A\to h}}{dx_B dQ^2 dz dq_T^2} = \frac{d\sigma^{(\mathrm{resum})}_{A\to h}}{dx_B dQ^2 dz dq_T^2} + \frac{d\sigma^{(Y)}_{A\to h}}{dx_B dQ^2 dz dq_T^2}$$

- $\sigma^{(Y)}$-term: small at low q_T, and dominant at large q_T
- Resummed part:

$$\frac{d\sigma^{(\mathrm{resum})}_{A\to h}}{dx_B dQ^2 dz dq_T^2} \propto \int \frac{d^2 b}{(2\pi)^2}\, \mathrm{e}^{i\vec{q}_T\cdot\vec{b}}\, W(b,x,z,Q)$$

$$= \int \frac{db}{2\pi} J_0(q_T b)\, b\, W(b,x,z,Q)$$

- Need non-perturbative contribution at large b:

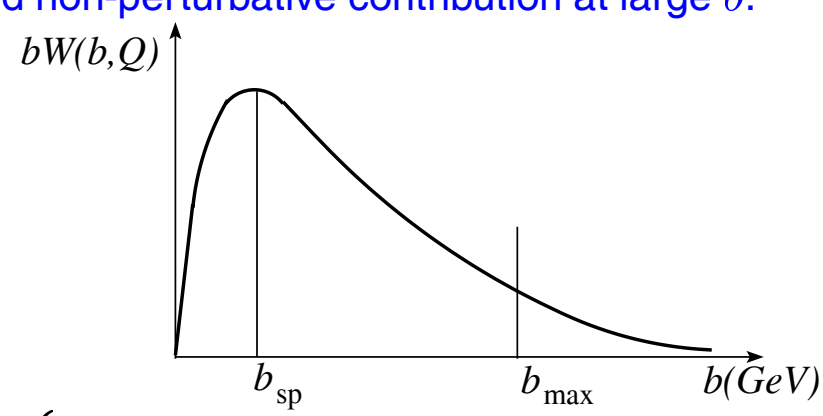

$$W = \begin{cases} W^{\mathrm{pert}}(b,x,z,Q) & b \le b_{max} \\ W^{\mathrm{pert}}(b_{max},x,z,Q)\, F^{NP}(b,Q;b_{max}) & b > b_{max} \end{cases}$$

- W^{pert} is perturbative, no-fitting needed[b]

---

[a] J.C. Collins, D.E. Soper, and G. Sterman, Nucl. Phys. B250, 199 (1985).

[b] J.Q. and X. Zhang, Phys. Rev. D63, 114011 (2001).

- perturbative part[a]

$$W^{\rm pert}(b,x,z,Q) = \sum_j e_j^2 \left[f_{a/A} \otimes C^{in}_{a\to j} \right] \times \left[C^{out}_{j\to c} \otimes D_{b\to h} \right] \times {\rm e}^{-S(b,Q)}$$

  - all large logarithms are summed into $S(b,Q)$, and $S(b,Q)$ is perturbative for b not too large
  - functions: $C^{in}_{a\to j}$ and $C^{out}_{j\to c}$ are perturbative[a]

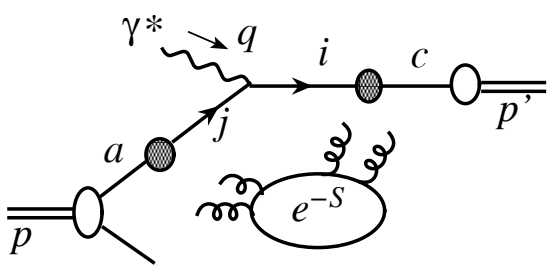

- Functional form of F^{NP} fixed by solving evolution equations with power corrections[b]

$$F^{NP} = \exp\left\{ -\log(Q^2 b^2_{max}/c^2) \left[g_1[(b^2)^\alpha - (b^2_{max})^\alpha] + g_2[b^2 - b^2_{max}] \right] - \bar{g}_2[b^2 - b^2_{max}] \right\}$$

  for $c \sim 1$ and $Q^2 > 1/b^2_{max}$.

- Predictive power:
  - universality of the limited parameters
  - predicted Q^2 and S dependence

[a] P. Nadolsky, D.R. Stump, and C.P. Yuan, Phys. Rev. D61, 014003 (1999).

[b] J.Q. and X. Zhang, Phys. Rev. D63, 114011 (2001).

3. Transverse momentum broadening in $e - A$

- b-space distribution:

$$b J_0(q_T b) \left[f_{a/A} \otimes C^{in}_{a\to j} \right] \left[C^{out}_{j\to c} \otimes D_{b\to h} \right] \mathrm{e}^{-S(b,Q)}$$

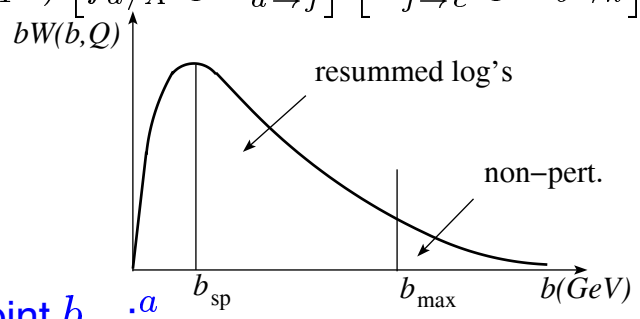

- saddle point b_{sp}:[a]
  - Sudakov form factor $\rightarrow$ $b_{sp} \propto (\frac{\Lambda_{\rm QCD}}{Q})^{\lambda}, \lambda \sim 0.5$
  - evolution of $f_{a/A}$ and $D_{c\to h}$ also moves b_{sp} smaller $\xi \Rightarrow \mu \frac{\partial}{\partial \mu} f_{a/A}(\xi) > 0 \Rightarrow$ lower b_{sp}
  - parton recombination reduces the evolution $\Rightarrow$ moves b_{sp} to the right $\Rightarrow$ more Gaussian like

- multiple scattering changes size of power corrections
  - increases the effective "intrinsic k_T"
  - reduces the phase space for soft-gluon shower

$\Rightarrow$ broadening the q_T distribution

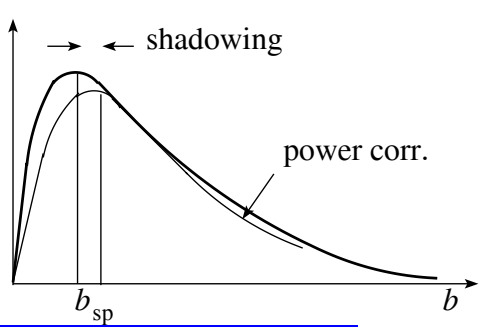

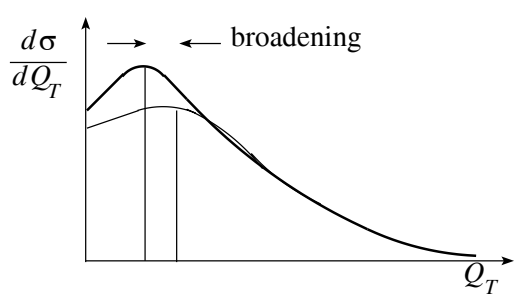

[a] J.Q. and X. Zhang, Phys. Rev. D63, 114011 (2001).

4. Probe gluon saturation at EIC

- large Q^2, larger phase space for soft-gluon shower $\Rightarrow \log(Q^2)$-type dependence for $\langle q_T^2 \rangle$

$$\langle q_T^2 \rangle \equiv \int dq_T^2\, q_T^2 \frac{d\sigma_{A\to h}}{dx_B\, dQ^2\, dz\, dq_T^2} \Bigg/ \frac{d\sigma_{A\to h}}{dx_B\, dQ^2\, dz}$$

- at small x_B (i.e. large $S_{\gamma^* - A}$), q_T-distribution is perturbative even at low Q^2

- saturation stops the evolution $\Rightarrow \mu \frac{\partial}{\partial \mu} f_{a/A}(\xi) \to 0$ $\Rightarrow$ increase b_{sp}
  - lower the q_T-distribution at $q_T = 0$
  - saturate the q_T-distribution at a much larger q_T

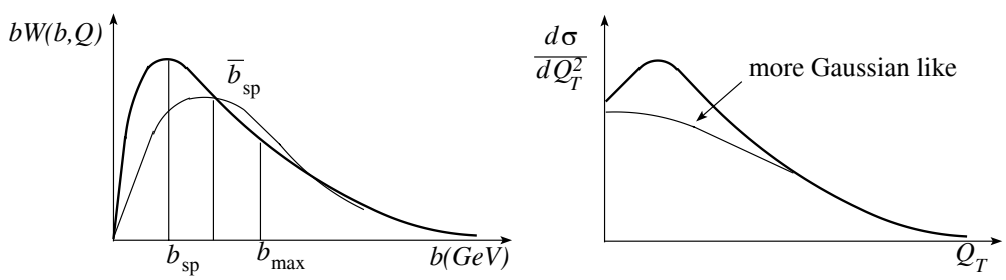

  - saturation in $\langle q_T^2 \rangle$ as a function of x_B

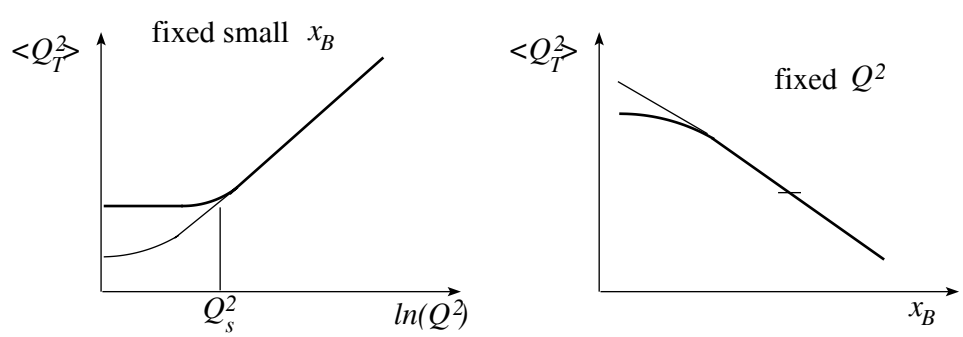

NT@UW-02-007

Hard Diffraction in eA Collisions

Yuri V. Kovchegov
Department of Physics, University of Washington, Box 351560
Seattle, WA 98195

Diffraction is an interesting and important process deeply related to the fundamental underlying dynamics of strong interactions in deep inelastic scattering (DIS). We will demonstrate in this talk that diffraction is tied to unitarization of the total DIS cross sections and to saturation of partonic structure functions. The strong classical gluonic fields arising in the nuclear wave function yield a diffractive cross section capable of explaining HERA data. Inclusion of quantum corrections gives the single diffractive DIS cross section in the full high parton density regime yielding some interesting non-trivial predictions for the Electron Ion Collider (EIC).

This talk is based on the work [1,2] done in collaborations with L. McLerran and E. Levin.

We will concentrate on the process of single diffractive dissociation in DIS, where a virtual photon interacts with the target proton or nucleus leaving it intact while breaking itself up into many quarks and gluons. These quarks and gluons turn into hadrons in the photon's fragmentation region leaving a rapidity gap adjacent to the target (see transparency #1).

Collinear factorization approaches based on DGLAP equation have been rather successful in describing the diffractive data at HERA. However, naive factorization approach suggests that if the total DIS cross section scales proportionally to the gluon distribution function $\sigma_{tot} \sim xG(x,Q^2)$ than the diffractive (elastic) cross section should scale as $\sigma_{diff} \sim [xG(x,Q^2)]^2$. Therefore the ratio of the two should scale as $\sigma_{diff}/\sigma_{tot} \sim xG(x,Q^2)$ and should be an increasing function of Bjorken-x, or, equivalently, center of mass energy. This conclusion contradicts the data reported by ZEUS [3] demonstrating that the ratio of $\sigma_{diff}/\sigma_{tot}$ is independent of energy throughout all of HERA kinematic region. To explain these data collinear factorization approaches make use of diffractive parton distribution functions. The DGLAP evolution for these diffractive distributions starts at rapidities above the rapidity gap. Therefore all the interesting diffractive physics leading to formation of rapidity gaps is included in the initial conditions for this evolution and is not addressed in much detail. We are going to present a different explanation of energy independence of $\sigma_{diff}/\sigma_{tot}$ involving strong gluon fields.

Let us consider quasi-elastic scattering process in the classical approximation developed in [4]. Virtual photon splits into $q\bar{q}$ pair which then rescatters on the nucleons in a nucleus by exchanging two gluons in the amplitude or in the complex conjugate amplitude with each of them. (For simplicity we are going to consider a nuclear target here. In case of a proton multiple sources of color charge in its wave function would play the role of the nucleons in our discussion here leading to the same conclusion [4].) The corresponding diagram is shown in transparency #2. Its contribution to diffractive (more precisely quasi-elastic) structure function in the large-Q^2 limit is [1]

$$F_2^D = \frac{N_c R^2}{3\pi^2} \sum_f Z_f^2 \int_{1/Q^2}^{\infty} \frac{dx_\perp^2}{(x_\perp^2)^2} \left[1 - \exp\left(-\frac{1}{4} x_\perp^2 Q_s^2\right)\right]^2 , \tag{1}$$

where we defined the *saturation* scale [4]

$$Q_s^2 = \frac{2\,\alpha_s\,\pi}{N_c\,R^2}\, x_{Bj} G_A(x_{Bj}, 1/x_\perp^2) \tag{2}$$

with $x_{Bj}G_A(x_{Bj},Q^2)$ the gluon distribution function of the whole nucleus or proton of radius R. The effect of the saturation scale Q_s^2 in Eq. (1) is to cut off the infrared part of $x_\perp^2$ integral

$$F_2^D \approx \frac{N_c R^2}{48\pi^2} \sum_f Z_f^2 \int_{1/Q^2}^{4/Q_s^2} dx_\perp^2 [Q_s^2]^2 \approx \frac{N_c R^2}{12\pi^2} \sum_f Z_f^2 Q_s^2, \tag{3}$$

which, using Eq. (2) leads to

$$F_2^D(x_{Bj}, Q^2) \approx \frac{\alpha_s}{6\pi} \sum_f Z_f^2 x_{Bj} G(x_{Bj}, Q^2). \tag{4}$$

Comparing Eq. (4) to the large Q^2 asymptotics of the total DIS structure function obtained in the same approximation [1]

$$F_2(x_{Bj}, Q^2) \approx \frac{\alpha_s}{3\pi} \sum_f Z_f^2 x_{Bj} G(x_{Bj}, Q^2) \ln \frac{Q^2}{Q_s^2} \tag{5}$$

we conclude that the ratio F_2^D/F_2 given by Eqs. (4) and (5) is independent of energy [1] in agreement with ZEUS data [3]. The physical principle of saturation cutting off the infrared part of the integral in Eq. (1) allowed the authors of [5] to produce a rather good fit to that data using a saturation-inspired model.

To improve the quasi-classical approximation of [1] one needs to include quantum evolution in diffractive structure functions similar to how it was done in [6] for the total DIS cross section. This was done in [2]. The lowest order diagram including quantum BFKL-type evolution for single diffractive dissociation is the triple-pomeron vertex diagram shown in transparency #3 (see Fig. 4). To include the multiple rescatterings effects one has to sum over all possible numbers of triple pomeron vertices. An example of such diagram is shown in Fig. 5 in transparency #4. Summation of all such diagrams leads to the following nonlinear equation for the diffractive cross section N^D of a dipole with transverse size $\mathbf{x}_{01}$, impact parameter $\mathbf{b}$ and rapidity Y scattering on a target with rapidity gap of the scattering being greater or equal to Y_0 [2]

$$N^D(\mathbf{x}_{01}, \mathbf{b}, Y, Y_0) = N_0^2(\mathbf{x}_{01}, \mathbf{b}, Y_0)\, e^{-\frac{4\alpha C_F}{\pi} \ln(\frac{x_{01}}{\rho})(Y-Y_0)} + \frac{\alpha C_F}{\pi^2} \int_{Y_0}^{Y} dy\, e^{-\frac{4\alpha C_F}{\pi} \ln(\frac{x_{01}}{\rho})(Y-y)}$$

$$\times \int_\rho d^2x_2 \frac{x_{01}^2}{x_{02}^2 x_{12}^2} [2\, N^D(\mathbf{x}_{02}, \mathbf{b} + \frac{1}{2}\mathbf{x}_{12}, y, Y_0) + N^D(\mathbf{x}_{02}, \mathbf{b} + \frac{1}{2}\mathbf{x}_{12}, y, Y_0)\, N^D(\mathbf{x}_{12}, \mathbf{b} + \frac{1}{2}\mathbf{x}_{02}, y, Y_0)$$

$$-4\, N^D(\mathbf{x}_{02}, \mathbf{b} + \frac{1}{2}\mathbf{x}_{12}, y, Y_0)\, N_0(\mathbf{x}_{12}, \mathbf{b} + \frac{1}{2}\mathbf{x}_{02}, y) + 2\, N_0(\mathbf{x}_{02}, \mathbf{b} + \frac{1}{2}\mathbf{x}_{12}, y)\, N_0(\mathbf{x}_{12}, \mathbf{b} + \frac{1}{2}\mathbf{x}_{02}, y)]. \tag{6}$$

Eq. (6) can be solved numerically to produce exact predictions for HERA and EIC [7]. It [2] it was solved for a simple toy model case. The result was a prediction illustrated in Fig. 6 of transparency #5. It predicts that in the case of saturation in the total cross section the diffractive cross section as a function of the gap size Y_0 (or, equivalently, the invariant mass M_X^2) would exhibit a maximum at some rather large Y_0 (small M_X^2). This prediction could be tested at EIC to verify our understanding of underlying strong interaction dynamics leading to diffraction.

---

[1] Yu. V. Kovchegov and L. McLerran, Phys. Rev. D **60**, 054025 (1999); Erratum-ibid. D **62**, 019901 (2000).

[2] Yu. V. Kovchegov and E. Levin, Nucl. Phys. **B577**, 221 (2000).

[3] ZEUS Collaboration, J. Breitweg et al , Eur. Phys. J. **C6**, 43 (1999).

[4] A.H. Mueller, Nucl. Phys. **B335**, 115 (1990); L. McLerran and R. Venugopalan, Phys. Rev. D **49**, 2233 (1994); **49**, 3352 (1994); **50**, 2225 (1994); Yu.V. Kovchegov, Phys. Rev. D **54**, 5463 (1996); **55**, 5445 (1997); J. Jalilian-Marian, A. Kovner, L. McLerran, and H. Weigert, Phys. Rev. D **55**, 5414 (1997); Yu. V. Kovchegov, A.H. Mueller, Nucl. Phys. **B 529**, 451 (1998).

[5] K. Golec-Biernat, M. Wusthoff, Phys. Rev. D **60**, 114023 (1999).

[6] Yu. V. Kovchegov, Phys. Rev. D **60**, 034008 (1999); D **61**, 074018 (2000).

[7] E. Levin, M. Lublinsky, Phys. Lett. **B521**, 233 (2001).

Single Diffractive Dissociation

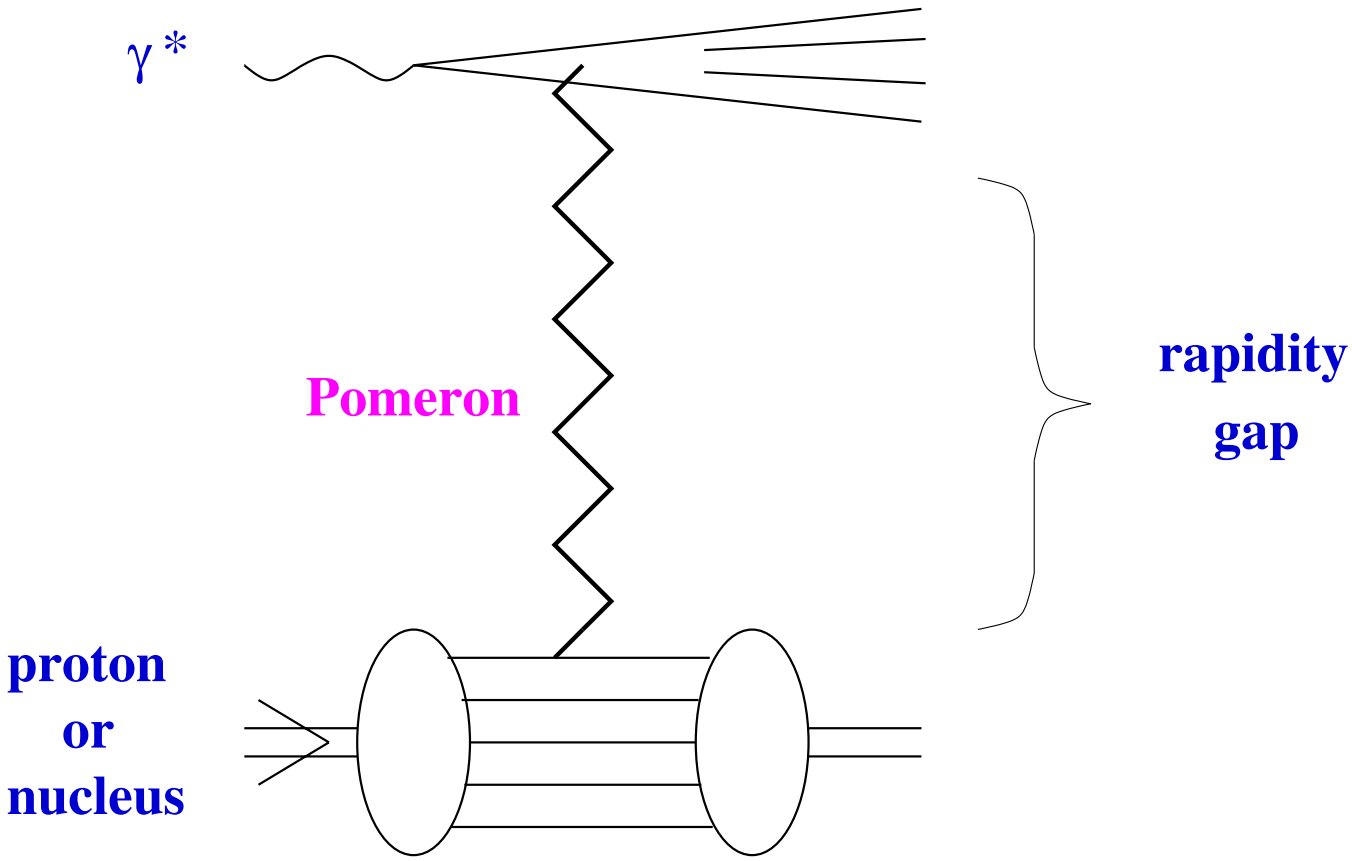

Figure 1: Single Diffraction in Deep Inelastic Scattering.

The target hadron or nucleus remains intact, while the virtual photon breaks up into pieces.

We will concentrate on this process.

SEEMS LIKE COLLINEAR FACTORIZATION DOES NOT WORK !!!

There are several explanations to this phenomenon, and people, in principle, still can get away with collinear factorization picture. However, the most natural and physically interesting next step is to include higher twist terms — multiple rescatterings.

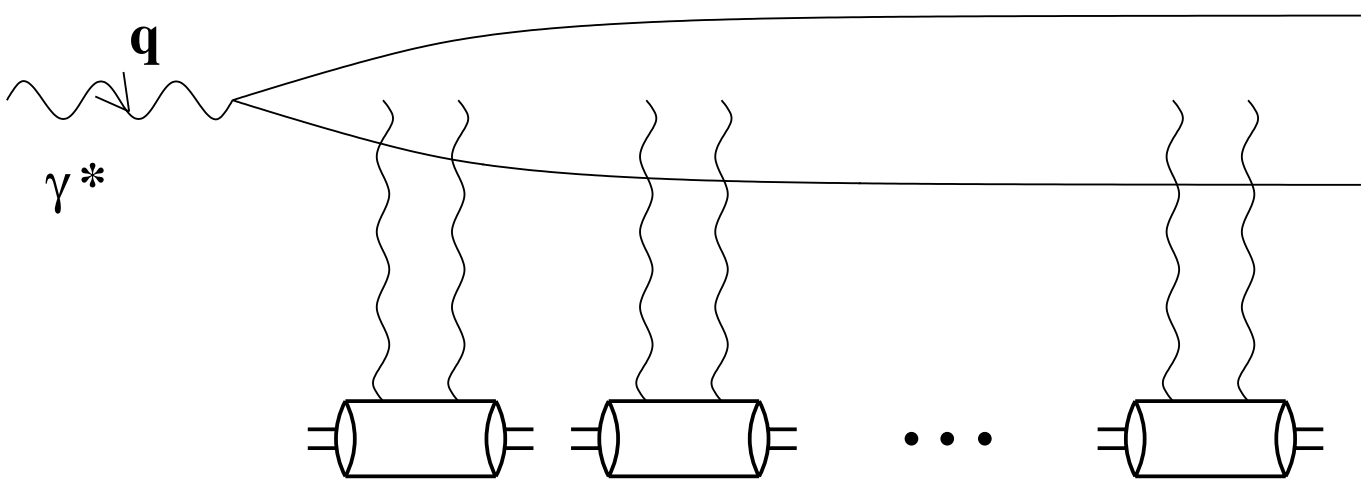

Figure 2: Single diffractive cross section enhanced by multiple interactions.

$$\frac{\sigma_{diff}}{\sigma_{tot}} \propto \frac{1}{2\ln Q^2}$$ (no energy dependence !!!)

Yu. K., L. McLerran, '99; K. Golec-Biernat, M. Wüsthoff, '99; W. Buckmüller, T. Gehrmann, M. McDermott, A. Hebecker, '97-'99; B. Kopeliovich '99

As energy increases the quantum fluctuations become important. They lead to pomerons – "things" responsible for steep rise of cross sections.

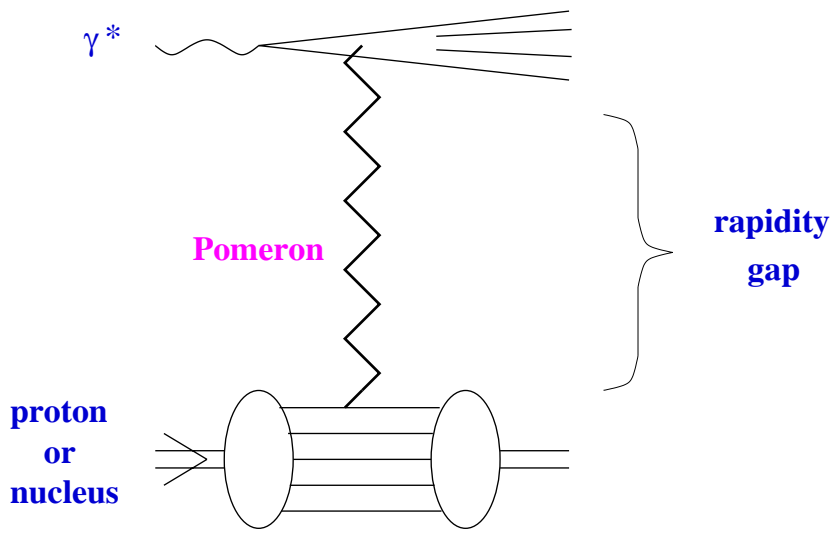

Figure 3: The amplitude of single diffractive dissociation with a pomeron exchange.

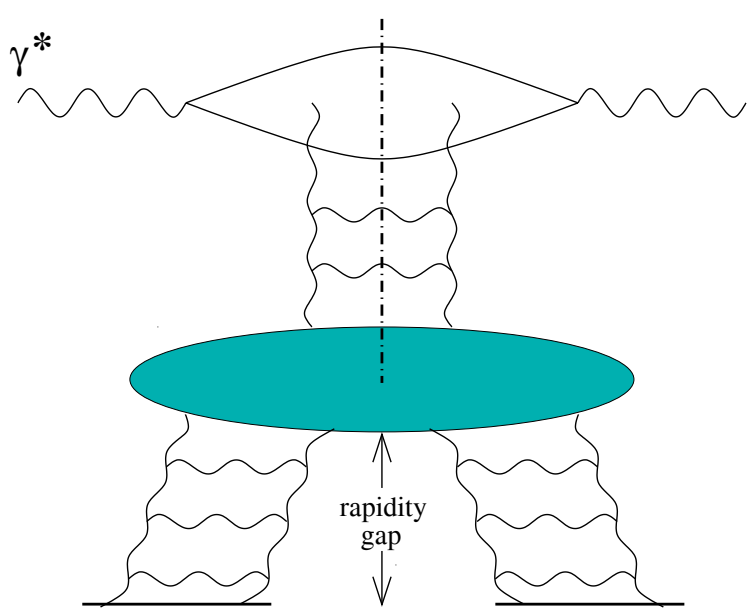

Figure 4: The cross section of the single diffractive dissociation now has a triple pomeron vertex in it (A.H. Mueller, ca 70's).

We can generalize this picture to the case of very high energies when there could be many pomerons:

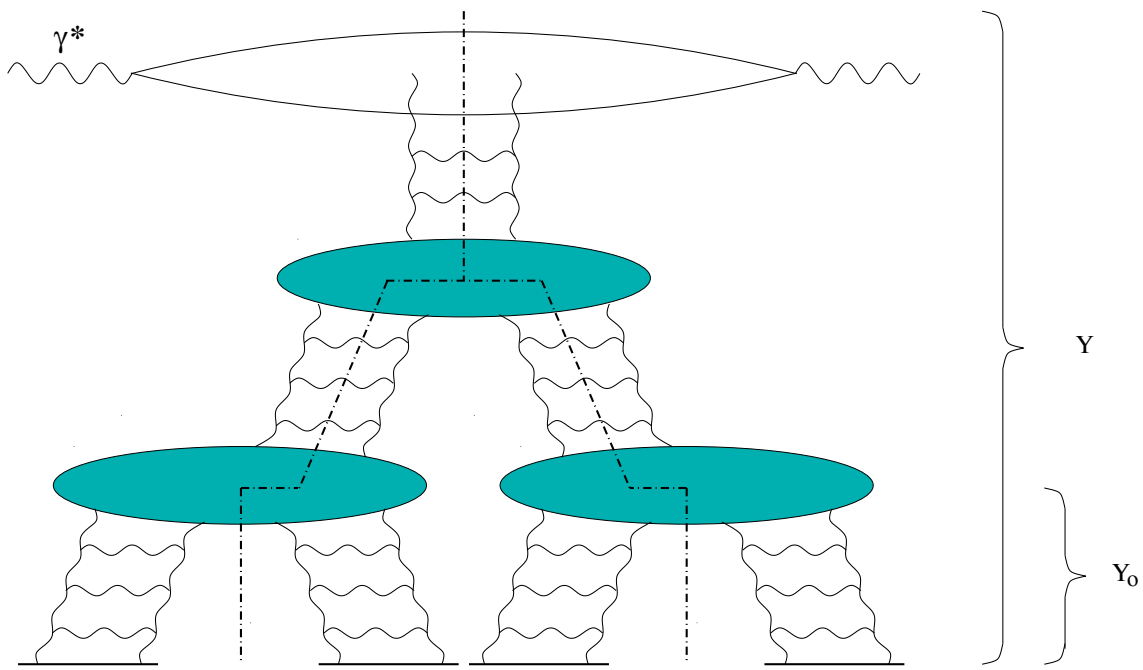

Figure 5: The cross section of the single diffractive dissociation enhanced by multiple pomeron exchanges.

Yu. K. , E. Levin, '99

Nothing is produced in the rapidity interval from 0 to Y_0, and lots of hadronic garbage will be observed in the rapidity interval from Y_0 to Y.

$$Y = Y_0 + \ln \frac{M_X^2}{Q^2}$$

Resummation of these multiple pomeron exchanges leads to an interesting behavior of the diffractive cross sections. Define

$$R(Y, Y_0) = M_X^2 \frac{\partial \sigma^D}{\partial M_X^2}$$

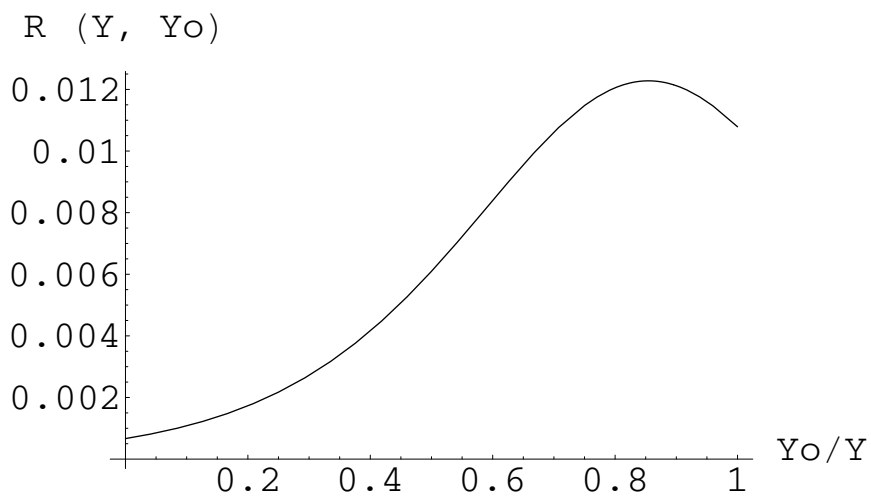

Figure 6: The cross section of the single diffractive dissociation plotted as a function of the size of the rapidity gap $Y_0 = Y - \ln \frac{M_X^2}{Q^2}$.

Saturation effects (multiple pomeron exchanges) make the cross sections turn over for very large rapidity gaps (small M_X^2)!!!

A test of whether saturation did set in or not!

Phenomenology of generalized parton distributions

A.V. Belitsky

Department of Physics
University of Maryland at College Park
MD 20742-4111, College Park, USA

Abstract

Generalized parton distributions are non-perturbative objects which parametrize long distance dynamics in a number of exclusive processes. They are hybrids of conventional parton densities, distribution amplitudes and hadron form factors, and also encode information on parton angular momenta in the nucleon which will shed a light on the nucleon spin structure. In this talk we discuss cross sections for leptoproduction of the real photon from the nucleon, which is sensitive to the deeply virtual Compton scattering amplitude where generalized parton distribution are accessible in a cleanest way. We discuss consequences of the target and lepton beam polarizations for measuring the generalized parton distributions on available experimental facilities such as CLAS at JLab and HERMES at DESY

On the quest for the missing proton spin

The spin of a composite particle is build from

- spins of its constituents
- orbital motion of its constituents

In QCD $\vec{S}_N = \langle N | \sum_{i=q,g} \int d^3x \, \vec{x} \times \vec{\Theta}_i | N \rangle = \vec{S}_q + \vec{L}_q + \vec{J}_g$

Momentum density (Θ_{0i} component of the energy-momentum tensor)

The sum rule for the proton spin

$$\frac{1}{2} = S_q + L_q + J_g$$

with the quark spin fraction

$$S_q = \frac{1}{2} \Delta\Sigma$$

FAQs

Q: How can one probe other sources of the nucleon spin?

A: Measure the off-forward matrix element of the energy-momentum tensor.

$$\langle N(P_2)|\Theta_{\mu\nu}|N(P_1)\rangle = \bar{u}(P_2)\left\{A(\Delta^2)\gamma_\mu P_\nu + B(\Delta^2)\frac{P_\nu \sigma_{\mu\rho}\Delta_\rho}{2M} + \ldots\right\}u(P_1)$$

The nucleon spin carried by quark and gluon angular momentum

$$J_{q,g} = \frac{1}{2}\left\{A_{q,g}(0) + B_{q,g}(0)\right\}$$

X.Ji '96

Q: Where to measure?

A: Graviton scattering would help!

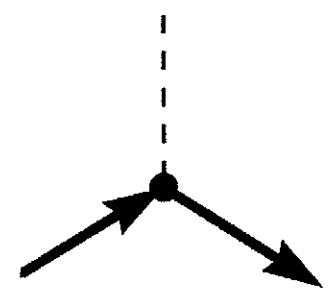

Q: Anything more feasible?

A: Yes, exclusive reactions with photoproduction of photons or hadrons!

Light-cone exclusive processes

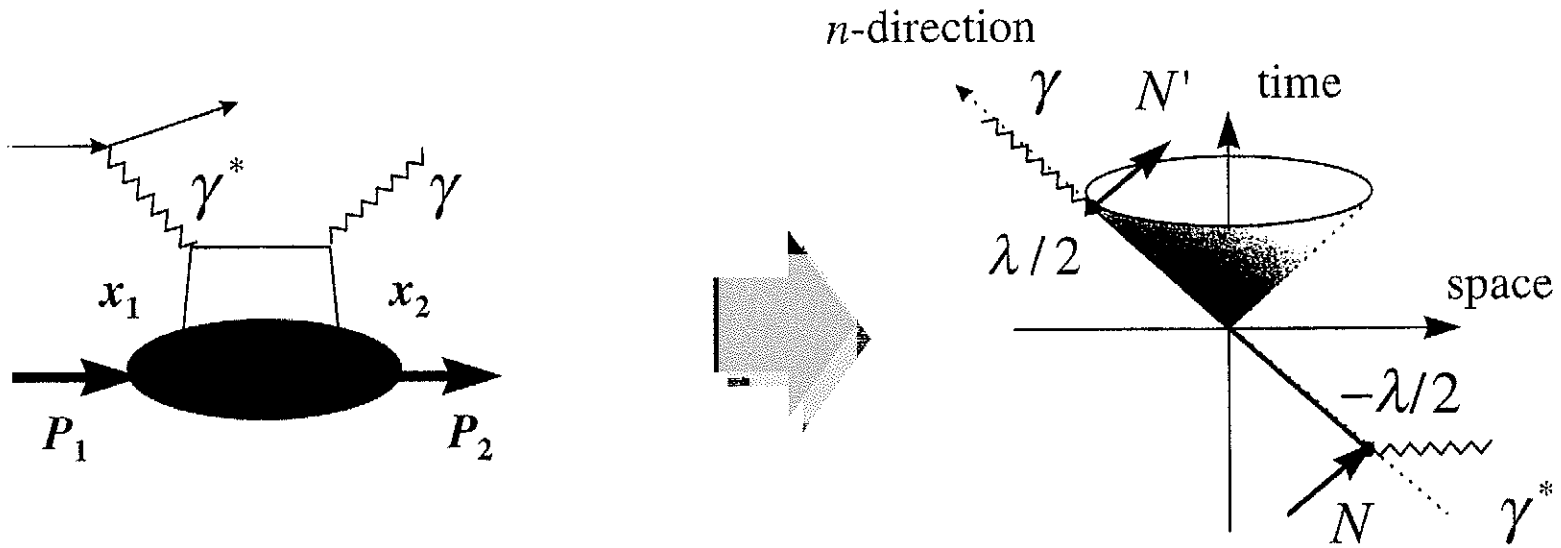

$$\left\langle P_2 \middle| \overline{\psi}(-\lambda/2n)\gamma_\mu \psi(\lambda/2n) \middle| P_1 \right\rangle = \cdots + \left\langle P_2 \middle| \overline{\psi}(0)\gamma_\mu \partial_\nu \psi(0) \middle| P_1 \right\rangle \lambda n_\nu + \cdots$$

The off-forward matrix element of the quark part $\Theta^q_{\mu\nu}$ of the energy momentum tensor is accessible. Similarly for the gluonic part.

Therefore, the total parton angular momentum $J_{q,g}$ is measurable.

Generalized parton distributions

Form factor decomposition of off-forward matrix element

$$\int \frac{d\lambda}{2\pi} e^{i\lambda x} \langle P_2 \,|\, \overline{\psi}(-\lambda/2)\gamma_+ \psi(\lambda/2) \,|\, P_1 \rangle$$

$$= H(x,\eta,\Delta^2)\overline{U}(P_2)\gamma_+ U(P_1) + E(x,\eta,\Delta^2)\overline{U}(P_2)\frac{i\sigma_{+\nu}\Delta_\nu}{2M}U(P_1)$$

Two momentum flows:

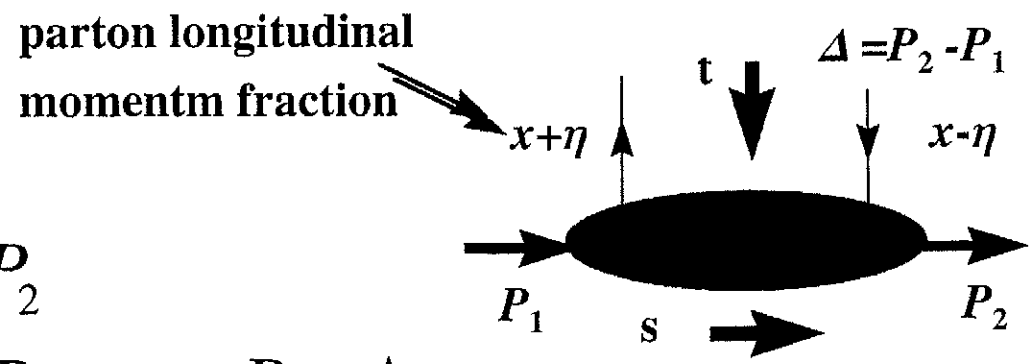

s-channel $P = P_1 + P_2$

t-channel $\Delta = P_2 - P_1 = -\eta P + \Delta_\perp$

Characteristic feature: non-zero momenum transfer; η is called skewedness

D.Muller et al.'94

X.Ji '96

Different versions:
A.V.Radyushkin '96
J.C.Collins et al. '97

Deeply virtual Compton scattering

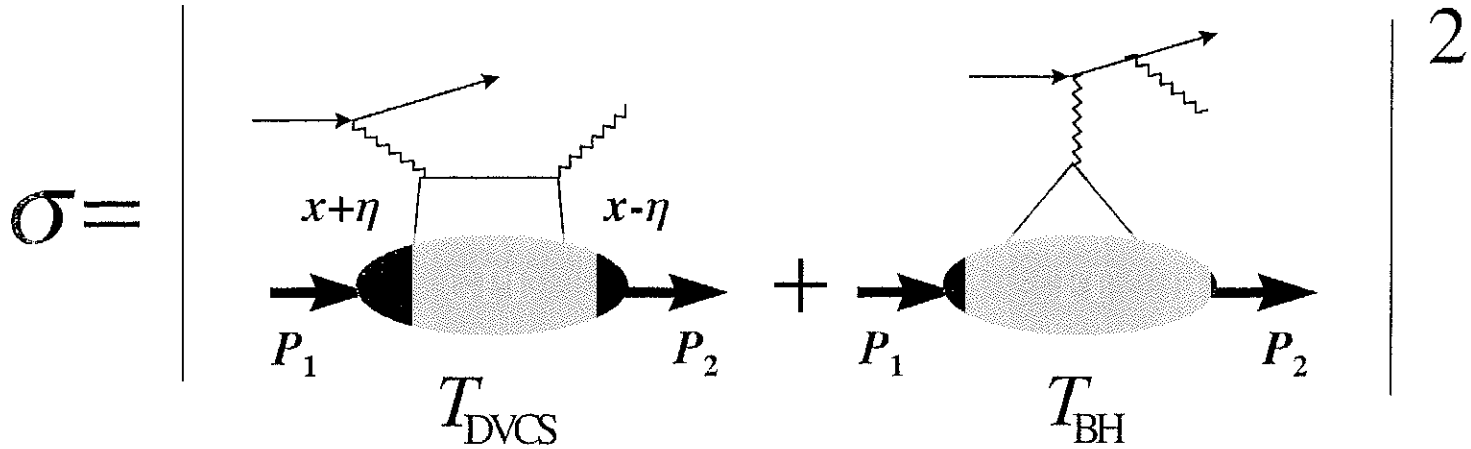

GPDs ⇄ Amplitudes ⇄ Cross Sections

?

$$T_{\mathrm{DVCS}} \sim \frac{\mathrm{Lepton\,Tensor}_1}{Q^2} \times \int_{-1}^{1} dx \frac{F(x,\xi,\Delta^2)}{\xi(1-x/\xi-i0)}$$

$$T_{\mathrm{BH}} \sim \frac{\mathrm{Lepton\,Tensor}_2}{\Delta^2} \times F(\Delta^2)$$

Cross sections → GPDs

Angular and polarization observables is a way to go.

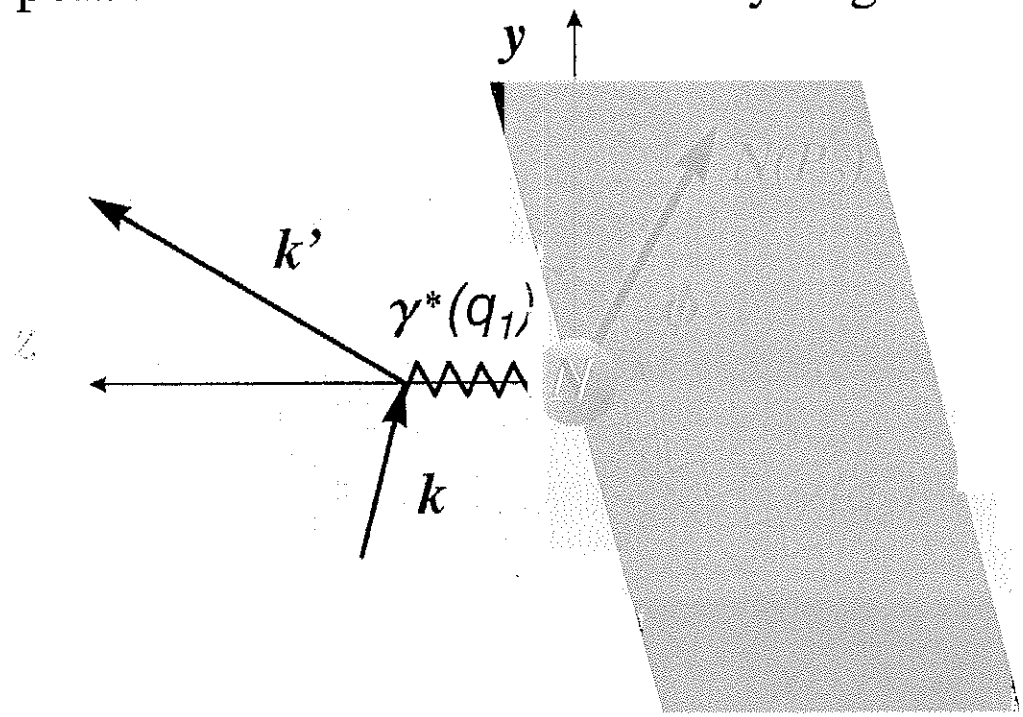

Variables: Q^2, x_B, Δ^2, y and ϕ, the azimuth between the lepton and photon (proton) scattering planes

$$\frac{d\sigma}{dx_B dy d|\Delta^2| d\phi} = \frac{\alpha_{em}^3 x_B y}{8\pi Q^2} \left| T_{BH} + T_{DVCS} \right|^2$$

Quark angular momentum

$$J_q = \frac{1}{2}\int_{-1}^{1} d\,x\, x\left\{H(x,\xi,0)+E(x,\xi,0)\right\}$$

$$= \frac{1}{2}\left\{(1+\kappa_p+\kappa_n/2)P^u_{\text{val}} + (1+\kappa_p+2\kappa_n)P^d_{\text{val}} + (1+\overset{?}{\kappa_{\text{sea}}})P_{\text{sea}}\right\}$$

magnetic moments momentum fractions

Models used in estimates

$$J_q = 0.3 + 0.09\overset{?}{\kappa_{\text{sea}}}$$

Model A:

$\kappa_{\text{sea}} = 0$

Model B

$\kappa_{\text{sea}} = -3$

Beam-spin asymmetry

$$A_{\mathrm{LU}} = \frac{d\sigma^{\uparrow}(\phi) - d\sigma^{\downarrow}(\phi)}{d\sigma^{\uparrow}(\phi) + d\sigma^{\downarrow}(\phi)}$$

$$A_{\mathrm{LU}} \approx \pm \frac{x_B}{y} \frac{s^I_{1,\mathrm{unp}}}{c^{\mathrm{BH}}_{0,\mathrm{unp}}} \sin(\phi)$$

(data from PRL 82 (2001) 182001)

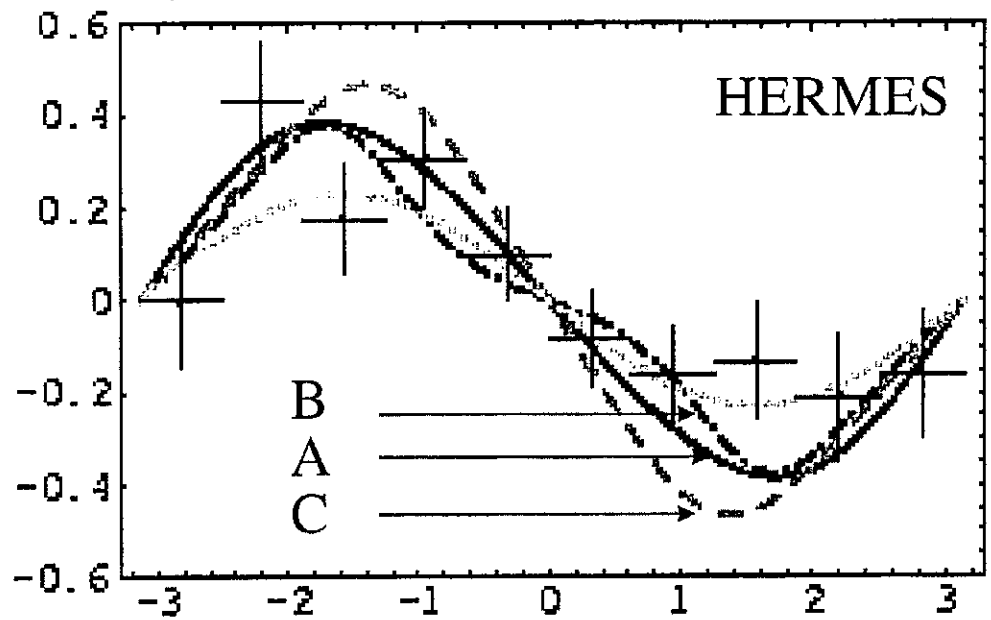

$$\phi_\gamma = \pi - \phi$$

$$s^I_{1,\mathrm{unp}} \sim F_1 H + \frac{x_{\mathrm{B}}}{2 - x_{\mathrm{B}}}(F_1 + F_2)\tilde{H} - \frac{\Delta^2}{4M^2} F_2 E$$

Sin-moment of the asymmetry:

Exp.: $A_{LU} = -0.23 \pm 0.04(\mathrm{stat}) \pm 0.03(\mathrm{syst})$

A: $A_{LU} = -0.27$

B: $A_{LU} = -0.16$

C: $A_{LU} = -0.37$

Energy dependence of QCD cross sections

Saturation effects from HERA to RHIC and LHC

Kari Rummukainen[1] and Heribert Weigert[2]

[1] *NORDITA, Blegdamsvej 17, 2100 Copenhagen Ø, Denmark*
[2] *Institut für theoretische Physik, Universität Regensburg, 93040 Regensburg, Germany*

We present a numerical study of the full nonlinear small x RG equations presented in [1]. Initial conditions are taken from the Golec-Biernat Wüsthoff ansatz and a successful comparison with HERA cross sections is obtained. Extrapolation to RHIC and LHC predict the presence of a perturbative saturation scale Q_s also at these experiments.

There has been a large amount of activity in recent years, trying to expose universal features in the energy dependence of ep, eA and AA collisions based on the idea of the presence of a dense gluonic medium that dominates the scattering events in all these types of experiment, caused by gluon radiation and optionally enhanced by the presence of many scattering centers in nuclei. Indeed collisions with heavy nuclei is the environment where the underlying idea of what is now often called a Color Glass Condensate was conceived. It states that at small x or large collision energies, the dominant degrees of freedom are gluon fields, which, to the probe in DIS or diffraction appear to be frozen in light cone time (x^+) and strongly Lorentz contracted in x^-. Their phase space density becomes large, of the order of $1/\alpha_s$ and brings with it a large scale, the saturation scale Q_s. Its presence gives rise to the hope that it is possible to extract the physics of saturation and unitarization in an expansion in powers of a small coupling, $\alpha_s(Q_s)$ after a resummation of the large density effects has been achieved.

To do so requires a radical change in methodology compared to what is usually employed in perturbative QCD where, as in the DGLAP treatment of scaling violations at large Q^2, large scales are used to prepare the system to look dilute and single out two particle correlators as the only important contribution. To be able to cope with density effects, all n-point functions have to be treated on the same footing and we need a different tool to simplify matters. This is done by identifying the kinematically enhanced degrees of freedom, which turn out to be gluonic and much simplified due to kinematics and resolution. Of all the components of $F^{\mu\nu}_{\text{target}}$ only F^{+i} are boost enhanced and hence we read off that only one component, the "+" component of the gauge field is important in this kinematic situation. It enters as

$$A^+(x) = \delta(x^-)\beta(x) + \text{fluctuations} \tag{1}$$

where only the kinematically suppressed "fluctuations" bring in x^+ dependence and structure in x^- beyond the first moment. It is easy to see that this single degree of freedom may be traded for path ordered exponentials along x^-, $U_{\boldsymbol{x}} := \mathsf{P}\exp -i\int_{-\infty}^{\infty} dz^- A^+$. In fact it is the latter form in which they enter cross sections in the small x limit. The formula for the total cross section there is of the (schematic[1]) form

$$\sigma_{\text{tot}} =$$

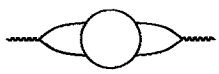

$$= \int d^2x d^2y\, |\psi^2|(\boldsymbol{x},\boldsymbol{y};Q^2)\, \langle \frac{\text{tr}(1-U_{\boldsymbol{x}}U^\dagger_{\boldsymbol{y}})}{N_c}\rangle \tag{2}$$

which naturally separates into a known photon wave function part and a dipole part, $\langle \frac{\text{tr}(1-U_{\boldsymbol{x}}U^\dagger_{\boldsymbol{y}})}{N_c}\rangle$, that carries all the accessible information about the QCD part of the scattering event as determined by the QCD action and the wave function of the target. The exponentials U encode naturally the multiple scattering taking place within the Lorentz contracted target whose internal structure the small x probe is unable to resolve. The form for dominant gluon fields given in Eq. (1) is indeed resolution dependent: the smaller x, the less our probe will be capable of resolving structures in x^- and hence the more modes in the target gluon field will be indistinguishable from a fully Lorentz contracted $\delta(x^-)$. Similarly for x^+ dependence: the smaller x, the more modes will appear to be frozen in x^+. All these features bring two mayor consequences for the averaging procedure $\langle\ldots\rangle$ in Eq. (2):

1. The average is dominated by the Lorentz contracted, frozen configurations of Eq. (1), hence a weight for these configurations is all we need to know about QCD and the wave function to determine σ_{tot}. We therefore write

$$\langle\ldots\rangle := \int \hat{D}[U]\ \ldots\ \hat{Z}[U] \tag{3}$$

where $\hat{D}[U]$ is a functional Haar measure and $\hat{Z}[U]$ is some functional weight for the $SU(3)$ valued configuration variables U.

[1] see e.g. [2, 3] for a fairly complete collection of explicit expressions.

2. $\hat{Z}[U]$ has to be x dependent to accommodate the fact that more and more of the QCD induced fluctuations assume the form Eq. (1) and hence fall under the purview of our averaging procedure Eq. (3).

Clearly this leads to a resolution motivated Wilson RG argument for the x dependence of $\hat{Z}[U]$ which can be addressed within perturbative QCD, provided that the large number of dominant gluons governed by $\hat{Z}[U]$ furnishes the scale Q_s alluded to.

This is addressed in the transparencies. The nature and generic features of the ensuing *functional* RG equation for $\hat{Z}[U]$ is discussed and the result of lattice simulations are shown. We are able to establish infrared safety of the evolution, measure the x dependence of the dipole amplitude $\langle \frac{\mathrm{tr}(1-U_x U_y^\dagger)}{N_c} \rangle$ using an initial condition motivated by the Golec-Biernat+Wüsthoff fit [2, 3] to HERA data. We are able to extract a power like growth of $Q_s = 1/R_s$ according to

$$R_s(x) = x^\lambda R_0 \qquad \lambda = 0.9\alpha_s \qquad \text{i.e.} \qquad \lambda = 0.18 \pm 0.02 \quad \text{at} \quad \alpha_s = 0.2 \tag{4}$$

very close the value resulting from the G-B-W fit. This has motivated us to try and compare our results to those same DIS data, with surprising success, all of which is shown in more detail on the seclection of transparencies appended.

This calculation is the first to give a first principle, one loop (fixed coupling!) calculation of evolution rates as in Eq. (4) without employing any additional approximations.

This constitutes considerable progress in our understanding. It tells us why we appear to see similar saturation scales at HERA and RHIC experiments: Simply rescaling the saturation scale in Eq. (4) from protons to nuclei according to $R_0^A = R_0^p/A^{1/3}$ we find that saturation scales for protons and nuclei coincide for x values that relate as $x_A = x_p A^{1/(3\lambda)}$: The x values necessary to see a certain saturation scale Q_s at large nuclei are smaller. λ in the vicinity of the value given in Eq. (4) are compatible with the idea that RHIC and HERA show comparable saturation scales.

Wider implications lie in the use of the distributions found above in the calculation of initial conditions for heavy ion collisions [4, 5] that would allow us to cross correlate all the experiments.

Obviously, this is only a beginning. There are more details to be extracted from the simulations, possibilities to refine initial conditions need to be explored. Size and features of two loop corrections, in particular running coupling effects that should allow us to show how α_s runs with Q_s need to be understood and the issues of A scaling have to be examined in experimental data.

There are limitations also: The machinery used in the above is applicable to central collisions only. Direct use of these results in diffraction is limited to a small subset of diffractive events. Extensions here are both intriguing and challenging. Nevertheless, the wide-ranging consequences to be explored right away, using the tools shown here is a strong motivator to continue work along these lines.

References

[1] H. Weigert, *Unitarity at small bjorken x*, `http://arXiv.org/abs/hep-ph/0004044` and *many* references therein.

[2] K. Golec-Biernat and M. Wusthoff, *Phys. Rev.* **D59** (1999) 014017, [`http://arXiv.org/abs/hep-ph/9807513`].

[3] K. Golec-Biernat and M. Wusthoff, *Phys. Rev.* **D60** (1999) 114023, [`http://arXiv.org/abs/hep-ph/9903358`].

[4] A. Kovner, L. D. McLerran, and H. Weigert, *Phys. Rev.* **D52** (1995) 6231–6237, [`http://arXiv.org/abs/hep-ph/9502289`].

[5] A. Krasnitz and R. Venugopalan, *Phys. Rev. Lett.* **84** (2000) 4309–4312, [`http://arXiv.org/abs/hep-ph/9909203`].

The need for an RG in $x_{\rm Bj}$

The need for an RG in $x_{\rm Bj}$

Kovner, Weigert
McLerran
Jalilian-Marian
Leonidov
Milhano

Balitsky

$$A^+ = \delta(x^-)\beta(\boldsymbol{x}) + \text{corrections}$$

- $x_{\rm Bj}$ determines
  - the resolution on $\delta(x^-)$
  - our idea of "constant in x^+" changes
- with smaller $x_{\rm Bj}$
  - x^- resolution worsens
  - more modes appear frozen in x^+

The method

The method

- lower cutoff & integrate out fluctuations
- $\alpha_s \Delta \ln(1/x)$ (1 loop)
- allow $A^+ = \delta(x^-)\beta(\boldsymbol{x})$ to be large

The result

The result

Weigert hep-ph/...

$$\frac{\partial}{\partial \ln(1/x)} \hat{Z}[U] = \alpha_s \left\{ \frac{1}{2} \nabla^a_{\boldsymbol{x}} \nabla^b_{\boldsymbol{y}} \hat{\chi}^{ab}_{\boldsymbol{xy}}[U] - \nabla^a_{\boldsymbol{x}} \sigma^a_{\boldsymbol{x}}[U] \right\} \hat{Z}[U]$$

$\nabla^a_{\boldsymbol{x}}$: functional Lie derivatives

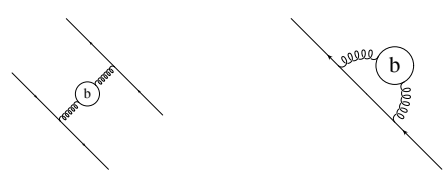

Fokker Planck $\int \hat{D}[U]\hat{Z}[U]$ conserved

probabilistic interpretation

The acttractive fixed point

Where evolution takes you: The attractive fixed point

Weigert

- Compact form: $\sigma^a_{\boldsymbol{x}}[U] = \frac{1}{2}\nabla^b_{\boldsymbol{y}}\hat{\chi}^{ab}_{\boldsymbol{xy}}[U]$

$$\frac{\partial}{\partial \ln(1/x)}\hat{Z}[U] = -\underbrace{\frac{\alpha_s}{2} i\nabla^a_{\boldsymbol{x}}\hat{\chi}^{ab}_{\boldsymbol{xy}}[U] i\nabla^b_{\boldsymbol{y}}}_{H_{\rm FP}}\ \hat{Z}[U]$$

- fixed point $\exists$: $\hat{Z}_\infty[U] = \text{const}$
- it is attractive: $H_{\rm FP} \geq 0$

Correlators at the fixed point

Correlators at the fixed point

Weigert

are determined by the Haar measure as $\hat{Z}_\infty[U] = \text{const}$:

$$\int \hat{D}[U]\ [U_{\boldsymbol{x}}]_{ij}[U^\dagger_{\boldsymbol{y}}]_{kl} = \begin{cases} 0 & \text{if } \boldsymbol{x} \neq \boldsymbol{y} \\ \frac{\delta_{jk}\delta_{il}}{N_c} & \text{if } \boldsymbol{x} = \boldsymbol{y} \end{cases}$$

Evolution erases all correlation lengths

$\sigma_{\rm dipole} = \langle \frac{{\rm tr}(1-U_{\boldsymbol{x}}U^\dagger_{\boldsymbol{y}})}{N_c} \rangle$

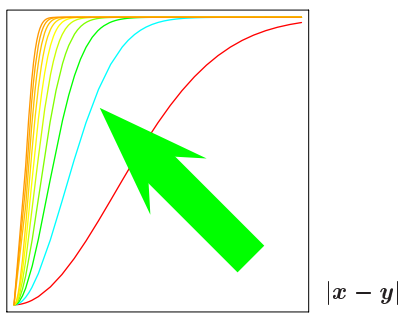

- $\sigma_{\rm dipole}$ saturates

Known limits

Known limits

- Large N_c: factorization: functional $\longrightarrow$ function

Balitsky-Kovchegov (BK)

$$\frac{\partial}{\partial \ln(1/x)}\langle N_{\boldsymbol{xy}}\rangle = \frac{\alpha_s N_c}{2\pi^2}\int d^2z\ \tilde{\mathcal{K}}_{\boldsymbol{xzy}}\langle N_{\boldsymbol{xz}} + N_{\boldsymbol{zy}} - N_{\boldsymbol{xy}} - \underbrace{N_{\boldsymbol{xz}}N_{\boldsymbol{zy}}}_{\text{drives saturation}}\ \rangle$$

$\langle N_{\boldsymbol{xy}}\rangle = \sigma_{\rm dipole}$

- small density: $\longrightarrow$ BFKL (drop nonlinear term in BK)
  - no saturation
  - no IR safety

$SU(3)$ evolution

Rummukainen & Weigert

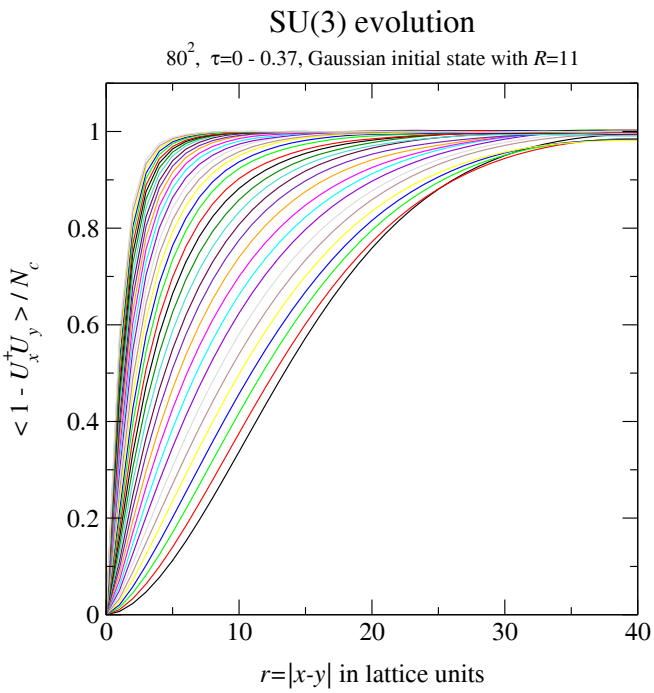

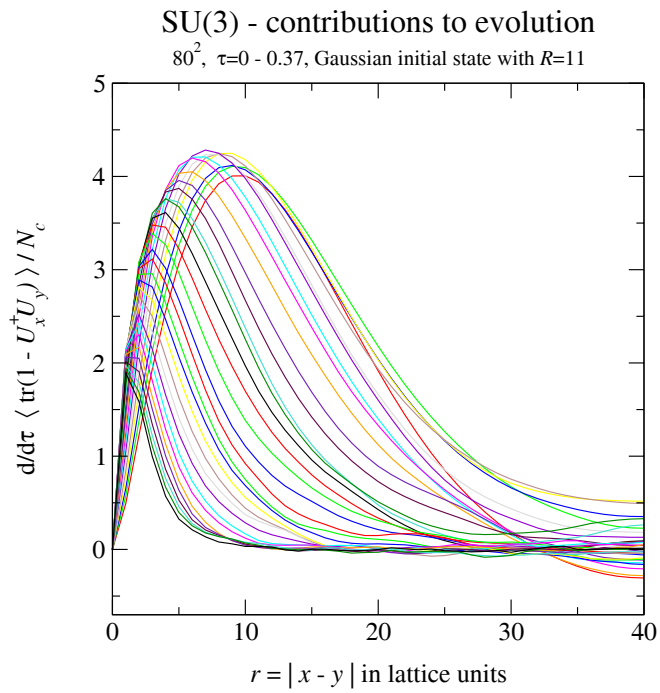

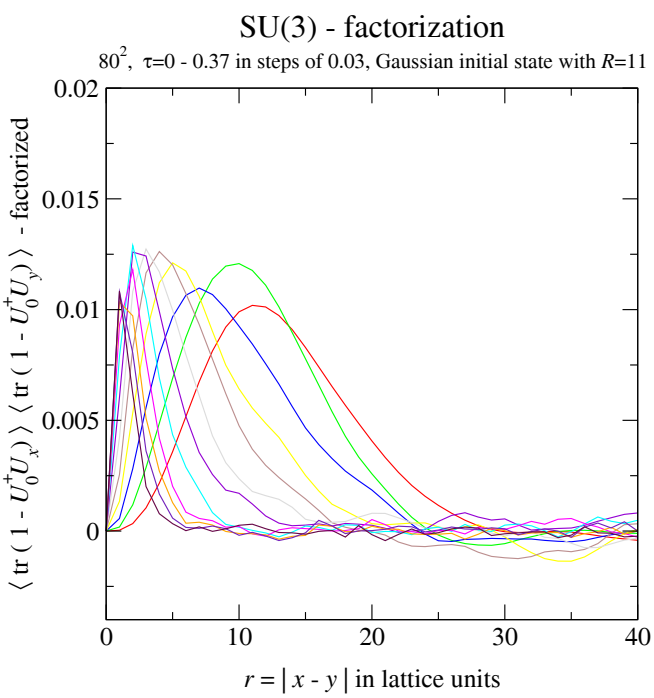

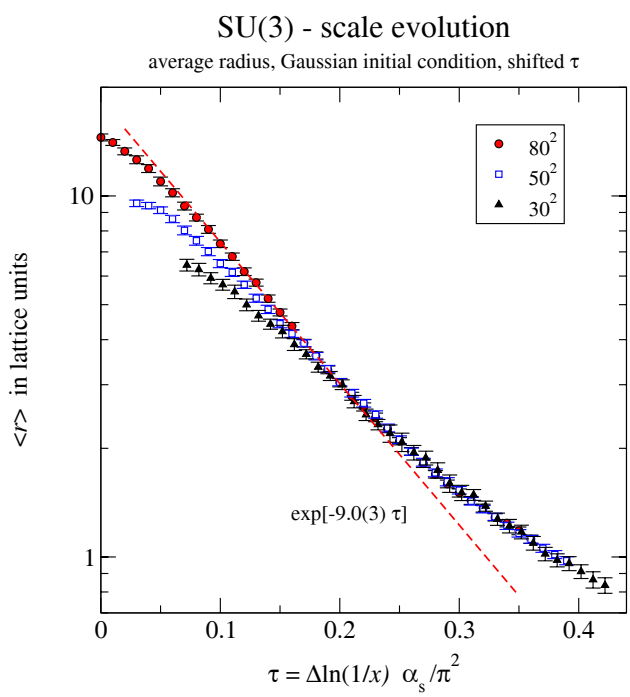

BFKL and BK

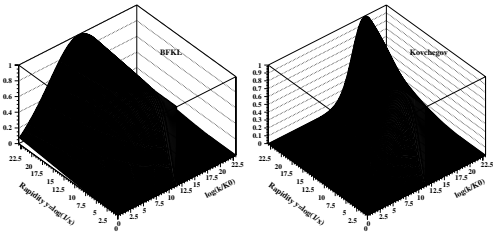

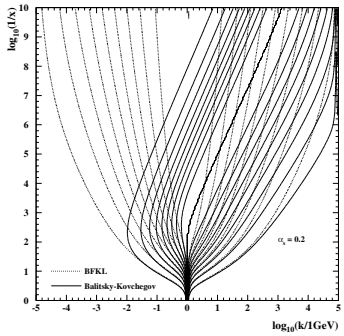

- BFKL: no saturation, no IR safety

$$\frac{\partial}{\partial \ln 1/x} N_{xy} = \frac{\alpha_s N_c}{2\pi^2} \int d^2 z \tilde{\mathcal{K}}_{xzy} \Big\{ \big(N_{xz} + N_{zy} - N_{xy} \big) - N_{xz} N_{zy} \Big\}$$

- BK:

  growing momentum scale

$$Q(x_{\mathrm{Bj}}) = x^{-\lambda} Q_0 \qquad \boxed{\lambda = 0.39} \qquad \alpha_s = 0.2$$

Full Langevin Simulation

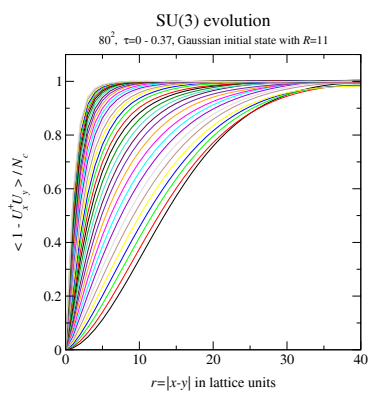

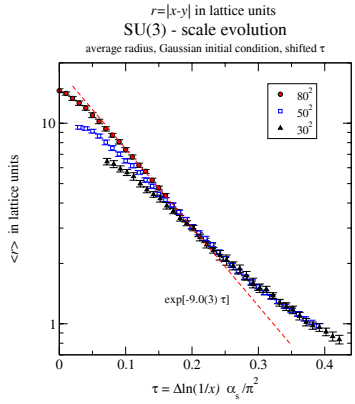

- Full Langevin:

  ∞-ly many coupled Eqns.

  All n-point functions

$$R((x_{\mathrm{Bj}}) = x^{\lambda} R_0$$

$$\lambda = \eta \alpha_s N_c \qquad \boxed{\lambda = 0.18 \pm 0.02} \qquad \alpha_s = 0.2$$

G-B+W HERA fits

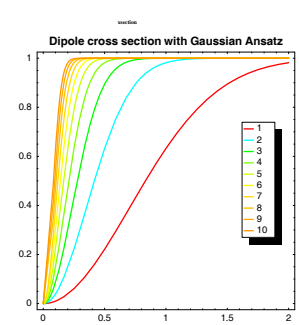

- G-B+W fits to HERA data

$$\sigma_{\mathrm{tot}}(x_{\mathrm{Bj}}, Q^2) = \int d^2x d^2y \ldots$$
$$= \int d^2(x-y)\ Q^2 \mathrm{wf}^2((x-y)^2 \cdot Q^2)\ \sigma_{\mathrm{dipole}}((x-y)^2 \cdot Q_s^2(x_{\mathrm{Bj}}))$$

$$Q(x_{\mathrm{Bj}}) = x^{-\lambda} Q_0 \qquad \boxed{\lambda = 0.144}$$

Comparing to HERA data

Rummukainen & Weigert

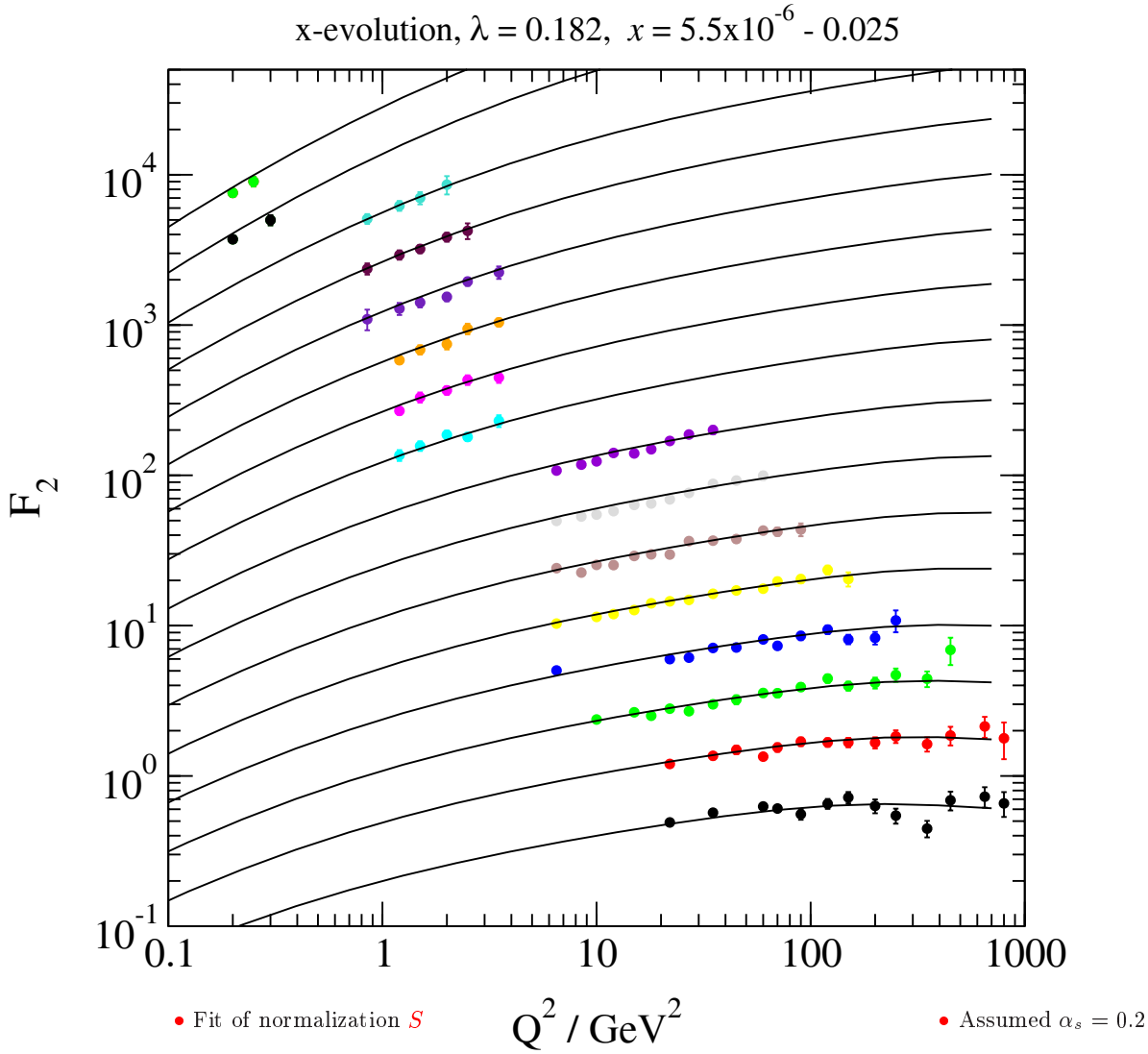

G-B+W in comparison

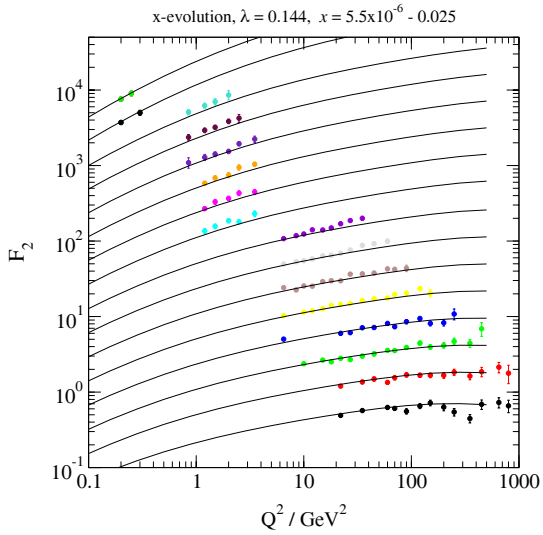

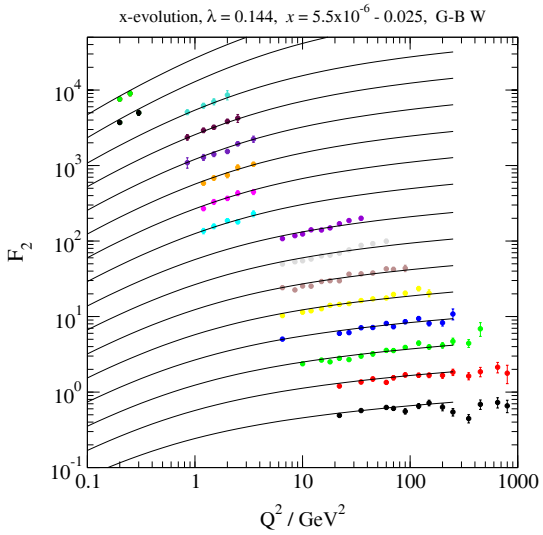

High parton density QCD effects expected at EIC

Kirill L. Tuchin

Institute for Nuclear Theory, University of Washington, Box 351550
Seattle, WA 98195

March 7, 2002

In DIS at high energies and/or on large nuclei the density of partons becomes so large that their mutual interactions becomes important. This leads to the nonlinear evolution described by Balitsky–Kovchegov nonlinear evolution equation. Initial condition to this equation is given by the Glauber-Muller formula which sums all rescatterings of the $q\bar{q}$ pair inside heavy nucleus at some fixed energy such that $\alpha_s \ln s < 1$. Approximate solutions of the BK equation show that there exists typical momentum scale (saturation scale) $Q_s(x, A)$ at which nonlinear evolution becomes essential. It is believed that at sufficiently high energy and/or large nuclei the saturation scale is much larger than $\Lambda_{\rm QCD}$ so that the perturbative approach is justified.

The main question is: does the data show any signs of the nonlinear physics? In other words what do we want to learn from the data?

- Value of x at which initial condition for the nonlinear evolution must be set.
- Dependence of the saturation scale on x and A.
- In what kinematical region $xG(x, Q^2) = xG(Q/Q_s(x))$, i.e. where the "geometric scaling" is applicable?

The main goal is to find observables which depend strongly on the high parton density effects. Measurements of such observables provide inside into the physics of saturation.

To estimate the onset of saturation at intermediate energies the *eikonal model* has been suggested by E. Gotsman, E. Levin and U. Maor. The idea is to use the initial condition for the nonlinear evolution equation as a first approximation to the exact scattering amplitude:

$$N(x, \underline{r}, \underline{b}) = 1 - e^{-\frac{A\alpha_s\pi^2}{2N_c}\underline{r}^2\, xG(x,4/\underline{r}^2)S(\underline{b},A)}$$

where xG satisfies DGLAP evolution equation.

Advantages of the eikonal model.

1. At high Q^2 it gives correct matching with DGLAP,
2. It gives a natural estimation of the saturation scale, $Q_s(x, A)$
3. It provides the correct anomalous dimensions for all high twist contributions at $N_c \gg 1$ and $\alpha_s \ln(1/x) \gg 1$
4. It includes impact parameter $\underline{b}$ dependence which is important for DIS on nucleus
5. It describes HERA experimental data well (E. Gotsman, E. Levin, U. Maor, M. Lublinsky, E. Naftali, K. T.). In particular, it describes simultaneously
   - slope $\frac{\partial F_2}{\partial \log Q^2}$ vs x and Q^2.
   - energy dependence of J/Ψ production.

   whereas, all DGLAP parameterizations fail to do that!

Using the eikonal model we calculate the following observables:

1. the ratio $\frac{F_L}{F_T}(x, Q^2, A)$ of the longitudinal to transverse structure functions for inclusive DIS and for diffraction in DIS. It's maximum is intimately connected to the saturation scale.
2. contribution of higher twists to the inclusive and diffractive structure functions; the breakdown of OPE is a clear signature of the saturation region.
3. energy, momentum and atomic number dependence of the diffractive to inclusive cross section ratio.

It is also instructive to study energy dependence of the inclusive gluon production in various high energy regions and compare with the result of explicit diagram summation.

Estimates of higher twists. $A = 238$.

E. Gotsman, E. Levin, U. Maor, L. McLerran, K. T., 2000

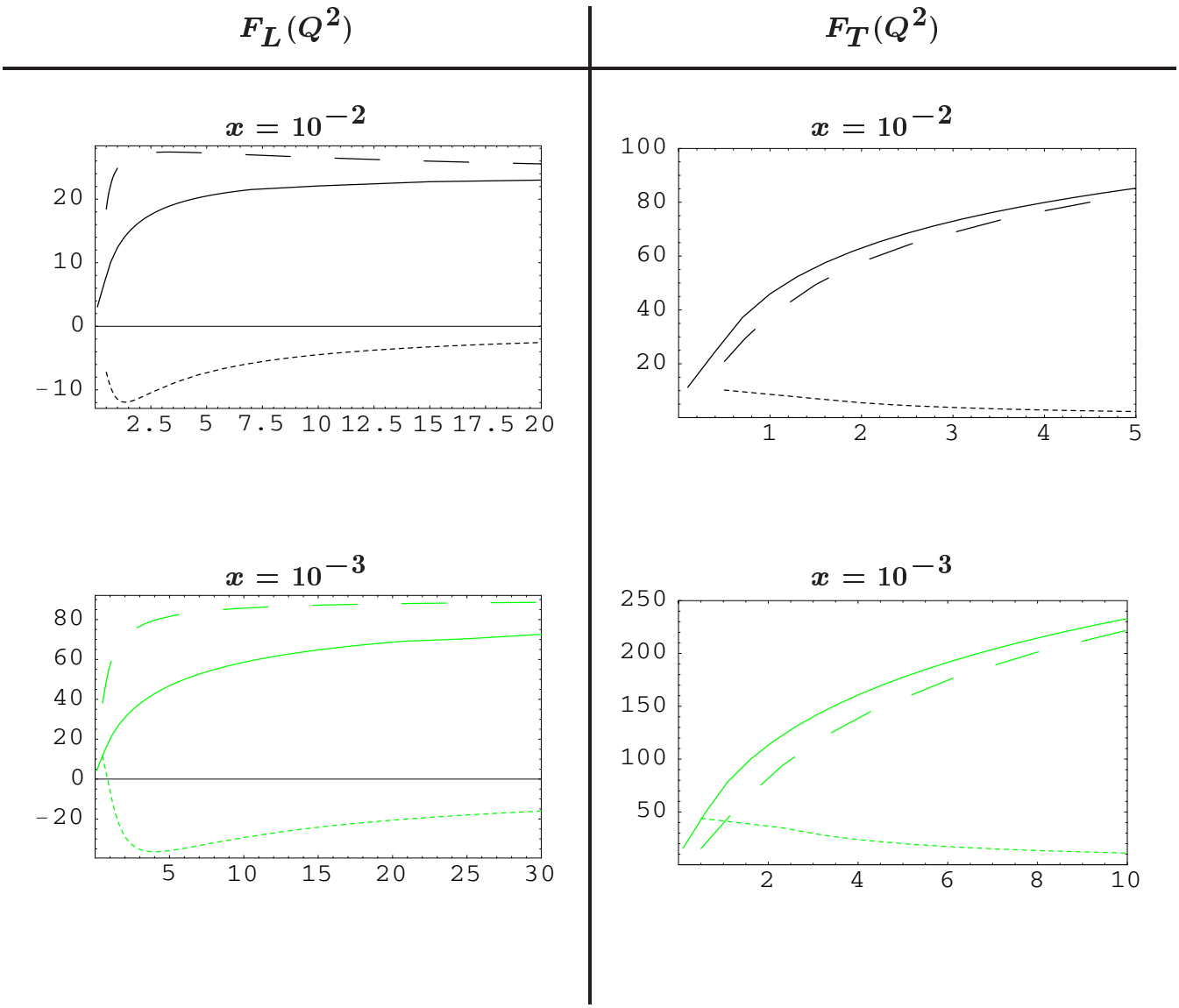

—— exact structure function

- - - leading twist

• • • next-to-leading twist

Estimates of higher twists. $A = 238$.

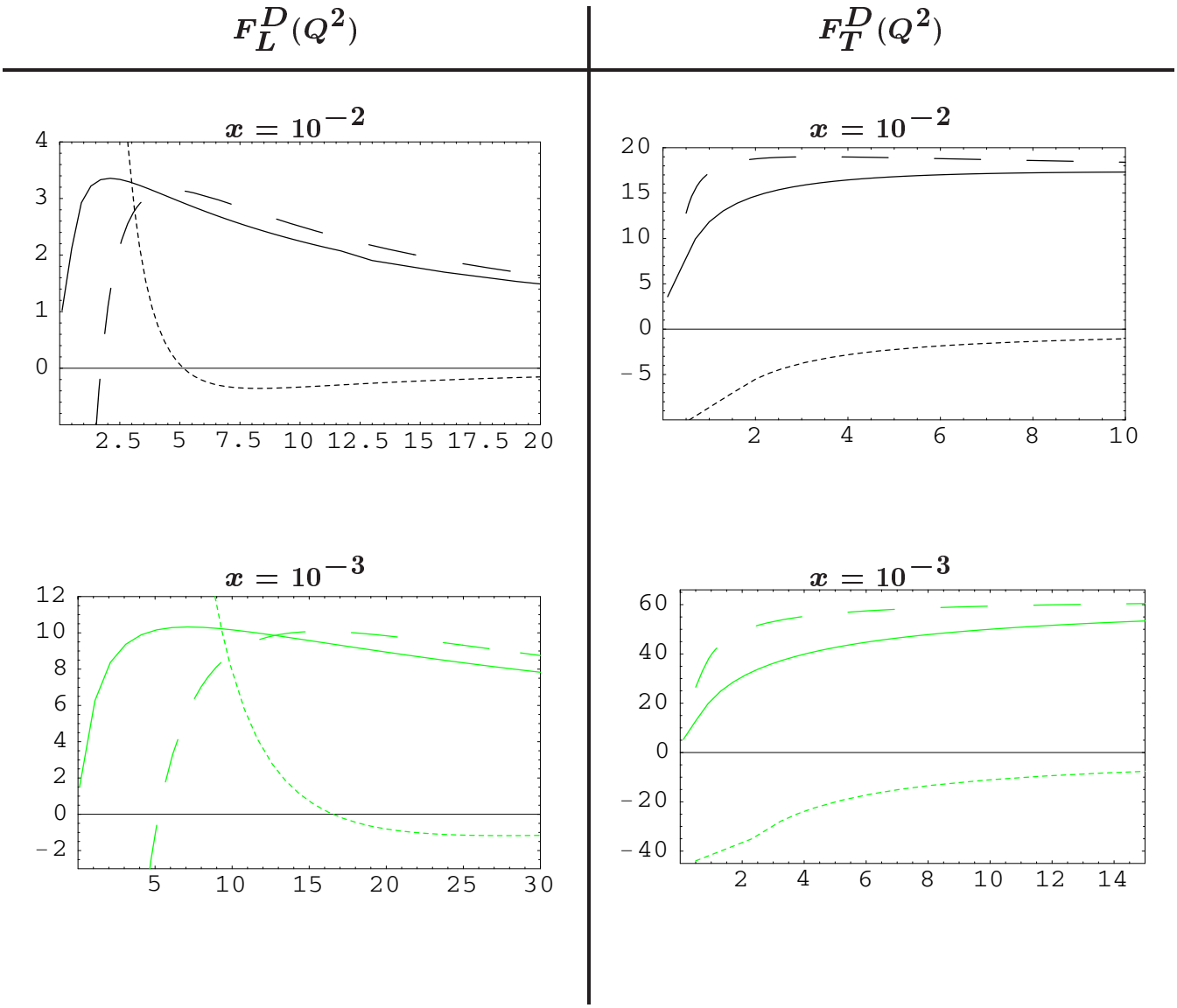

OPE breaks down at $Q \leq Q_s$. No DGLAP.

Ratios of structure functions.

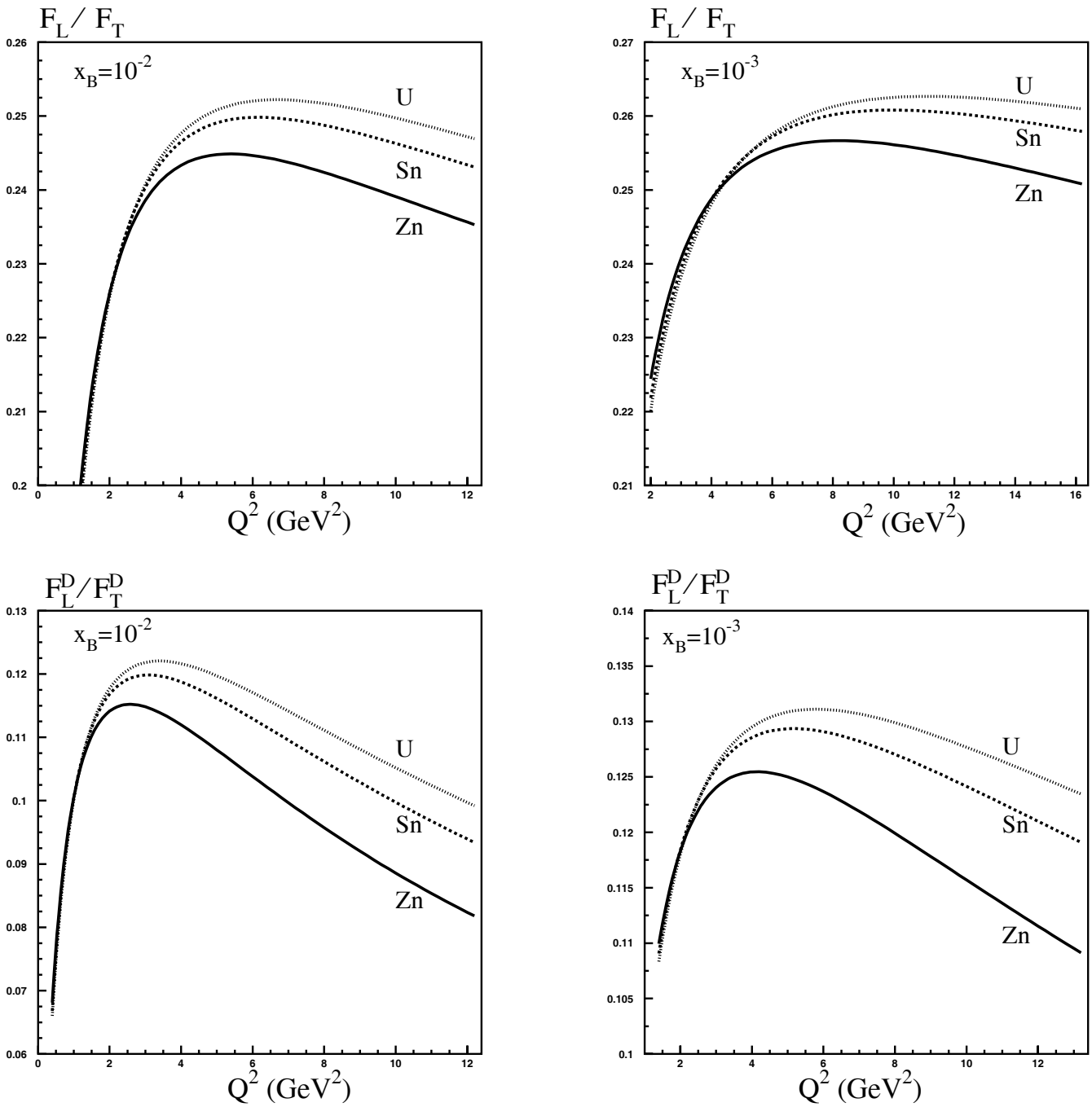

Maximum $\propto Q_s^2(x, A)$.

Diffraction.

E. Gotsman, E. Levin, M. Lublinsky, U. Maor, K. T., 2000

$$R = \frac{\sigma_{\rm diff}(x, Q^2)}{\sigma_{\rm tot}(x, Q^2)}$$

A=200

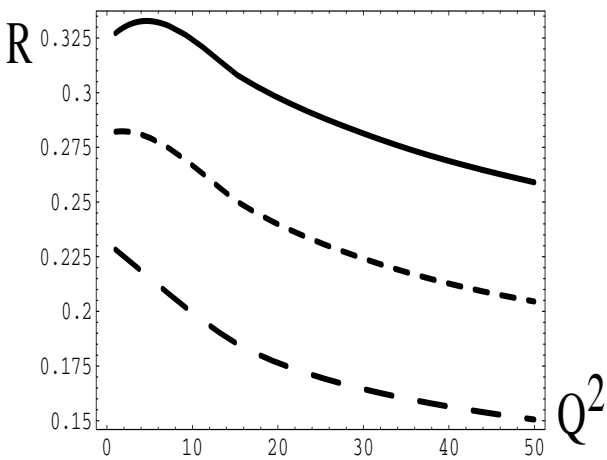

$Q^2 = 1$GeV^2

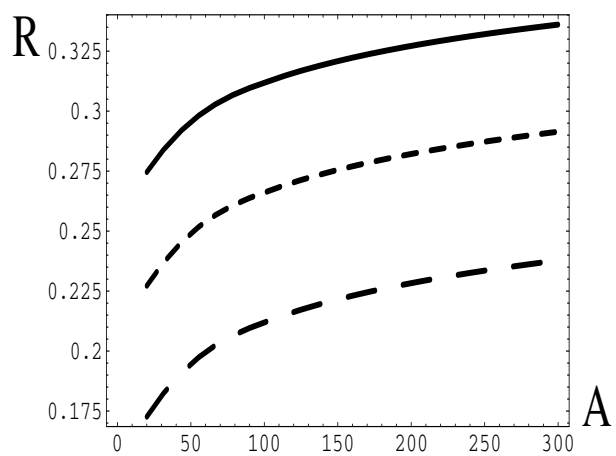

$Q^2 = 1$ GeV^2

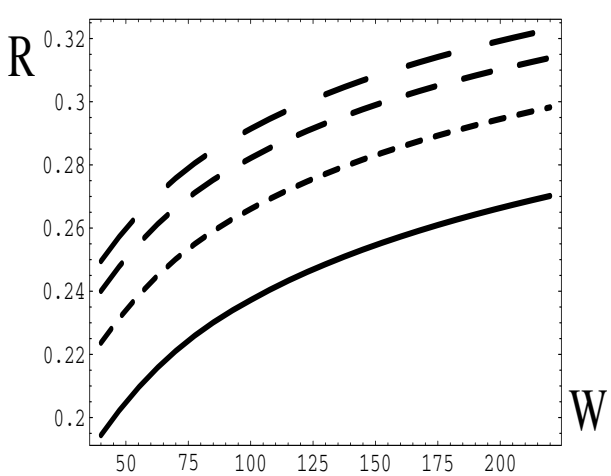

$Q^2 = 12$ GeV^2

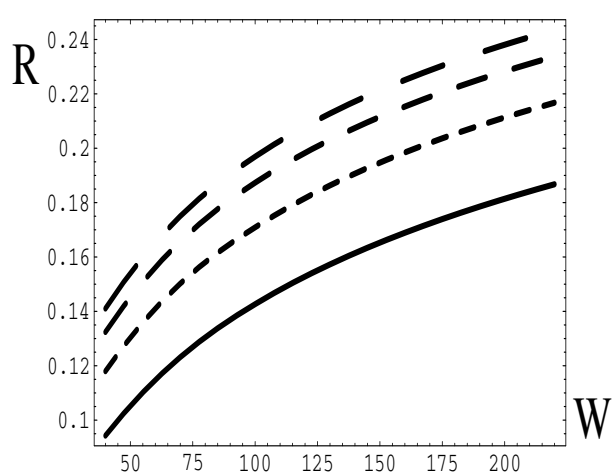

i. Evidence of geometric scaling: R does not depend on W,

ii. When SC dominate: $R \to 1/2$.

Energy dependence of inclusive spectrum in asymptotic regions.

Yu. Kovchegov, K. T., 2002

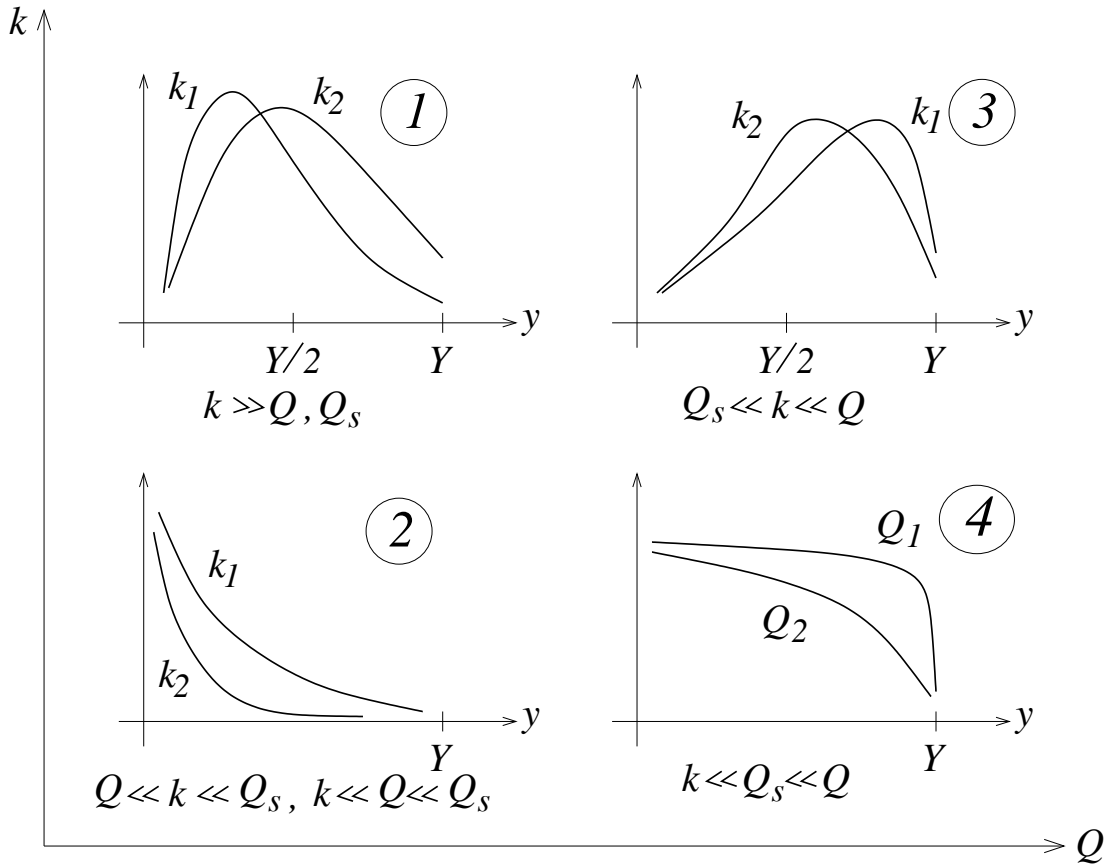

Distinguishes different kinematical regions in DIS.

Exlusive Processes at EIC - Feasibility Study

A. Sandacz
Sołtan Institute for Nuclear Studies, ul. Hoża 69, Warsaw, PL 00681, Poland
E-mail: sandacz@fuw.edu.pl

Abstract

We examine the potential of the EIC to study color transparency and color opacity via exclusive vector meson production in eA collisions. It is demonstrated that the EIC will allow comprehensive testing of these important predictions of perturbative QCD.

Color transparency (CT) is a phenomenon of perturbative QCD, whose characteristic feature is that small color-singlet objects interact with hadrons with small cross sections [1, 2, 3, 4]. Cross section for the interaction of such small object, or small size configuration (SSC), with a hadron target has been calculated in QCD using the factorization theorem [5, 4, 6, 7]. These QCD calculations confirmed the hypothesis of F. Low [1] on smallness of the cross section for the interaction of SSC with a hadron, if the gluon density in the hadron is not very high (moderately small x). They also predict a related phenomenon of *color opacity* when the gluon density becomes very large (at small x) and SSC interacts with the hadron with large cross section [2, 4].

The prerequisite for observing CT is to select a sample containing SSC's via a hard process (i.e. with large Q^2, high p_t, or large produced mass). To 'measure' the SSC-nucleon cross sections one should study absorption of the SSC propagating through nuclear matter. In order to clearly observe CT it is necessary that the SSC lives long enough to traverse distances larger than the size of the target nucleus. Another requirement is that SSC stays small while propagating through the nucleus. These requirements are quantified in terms of the coherence length and the formation length.

Experimental searches for CT started more than a decade ago and encompass various processes: large-t quasielastic (p, $2p$) scattering [8], large-Q^2 quasielastic (e, $e'p$) scattering [9], J/ψ photoproduction [10] and J/ψ muoproduction [11], exclusive ρ^0 leptoproduction [12, 13, 14] and coherent diffractive dissociation of the pion into two high-p_t jets [15].

Among these experiments only few have reported an evidence for CT. For the others an obstacle to clearly demonstrate CT was a relatively low energy of the projectile, and thus low coherence length and formation lentgh. A recent evidence for CT comes from Fermilab E791 experiment on the A-dependence of coherent diffractive dissociation of the pion into two high-p_t jets [15]. Also the E691 results on A-dependence of coherent J/ψ photoproduction [10] and the NMC measurements of A-dependence of coherent and quasielastic J/ψ muoproduction are consistent with CT. Measurements of the nuclear transparency for incoherent exclusive ρ^0 production by Fermilab experiment E665 give a hint for CT. However, due to the low statistics of that data at high Q^2, it was not possible to disentangle effects of decreasing coherence length at high Q^2 and to demonstrate CT unambiguously.

At EIC, taking advantage of its high energy, large luminosity and wide range of nuclear beams, a more precise systematic study could be realised. This will allow to unambigously demonstrate CT and also, for the first time, to observe color opacity. The program of such comprehensive study should include:

- measurements of A-, Q^2- and x-dependences of cross sections for exclusive production of *various* vector mesons (J/ψ, ρ, ϕ, ψ' or ρ');

• measurements of both *coherent* and *incoherent* cross sections (which should exhibit different A-dependences);
• analysis of event samples with the vector mesons beeing predominantly polarised either *longitudinally* or *transversely* (to study possible different dependences of the cross sections on A and on kinematical variables for different meson polarisations).

In the following we discuss results of simulations of hard exclusive J/ψ production, hard exclusive ρ^0 production and of J/ψ quasi-real photoproduction at EIC. We assumed 10 GeV electron beam and hadron beams of 100 GeV per nucleon. Both proton beam and heavy ion (gold/lead) beams were considered. For ep collisions we used the parameterisations of the cross sections measured at HERA, which were extrapolated down to EIC energies. To account for nuclear effects in eA collisions the VMD was assumed for ρ production and the complete CT for J/ψ production. Kinematical smearing was simulated using parametrisations of the resolutions of various kinematic variables as measured by the Central Tracking Detector of ZEUS. The accessible kinematic range at EIC was studied by varying the acceptance of the central detector.

The kinematics of the produced vector meson, J/ψ or ρ^0, and of the particles from its decay is shown in the first transparency. The vertical dashed lines at the plots in the right column represent various angular acceptances for the decay particles. The inner lines correspond to the angular coverage similar to that of the central tracking detectors in both HERA experiments, $20 < \theta < 160°$ ($-1.75 < \eta < 1.75$). (Here θ is the polar angle and η is the pseudorapidity of the decay particle in the laboratory system.) The outer lines correspond to the acceptance of a proposed Extended Central Tracking Detector (ECTD) for the EIC, with the wider angular coverage, $5 < \theta < 175°$ ($-3.1 < \eta < 3.1$). The increased coverage of the central detector allows to extend the acceptance for the exclusive channels towards the low x region.

The analysis of the simulated hard vector meson production indicates that with the ECTD the good acceptance may be achieved in the kinematical range $1 < Q^2 < 50\,\mathrm{GeV}^2$, $10 < W < 55$ GeV and $0.0003 < x < 0.16$ both for ρ^0 and J/ψ production. Therefore, the transition from color transparency to color opacity may be observed. On the other hand, if ZEUS-like central detector is used, the kinematical range will be more limited, with $W_{max} = 40$ GeV and $x_{min} = 0.001$. Note, that in addition to the wider kinematical coverage for the decay particles, the ECTD will improve tracking of the scattered electron, thus allowing a better constraints on the exclusivity of events.

Similarly, it was found that with the ECTD the kinematical range for J/ψ photoproduction will be $Q^2_{min} < Q^2 < 1\,\mathrm{GeV}^2$ and $10 < W < 65$ GeV, where $Q^2_{min} = M_e^2 y^2/(1-y)$. Here, for the most of events, both scattered electron and fast hadron(s), proton or ions, escape into the beam pipe. Assuming that only the central detector is used for tracking of the praticles in the final state, the kinematical variables W and t could be calculated approximately using the reconstructed four-momentum of J/ψ.

Both for hard production and for photoproduction, the effects of acceptance and kinematical smearing on t distributions were studied assuming that the final state particles momenta are measured only in the ECTD. Because the fast protons or ions escape into the beam pipe, one has to use a (quite accurate) approximation $t \simeq (\sum p_T)^2$, where the sum is over transverse momenta of all particles measured in the ECTD. The resulting smearing in t, which increases with $|t|$, is about 0.008 GeV^2 for hard J/ψ production and about 0.005 GeV^2 for ρ^0 production at $|t| = 0.05\,\mathrm{GeV}^2$. The smearing is sufficiently small to allow use of t cuts in order to select samples of coherent or incoherent (quasi-elastic) events. However, the smearing may prevent the precise measurement of the shape of the coherent peak.

Similarly, the acceptance and smearing effects were studied as a function of the angle θ^*, which is the polar angle of the positive decay particle in the parent vector meson helicity frame. The accurate determination of this angle is important for selection of event samples dominated either by longitudinally or transversely polarised vector mesons. For instance, for hard production of ρ^0 the cut $|\cos\theta^*| > 0.7$ results in a sample with the fraction of ρ^0_L equal about 0.8 and for the cut $|\cos\theta^*| < 0.4$ the same fraction is about 0.2. The resolution in $\cos\theta^*$, which is about 0.06 for ρ^0 decaying into two pions and about 0.08 for J/ψ decaying into two muons, will be adequate for such selections.

The estimates of rates were obtained assuming integrated luminosity $\int \mathcal{L}$ equal to 330 pb^{-1} for ep collisions and 10 pb^{-1} for eAu collisions. The total numbers of accepted events for hard exclusive ρ^0 production are 1.1 mln for the proton beam and 4.2 mln for the gold beam. For hard exclusive J/ψ production with J/ψ dacaying into either e^+e^- or $\mu^+\mu^-$ the corresponding numbers are 7000 and 210000 events. The event sample for J/ψ photoproduction will be about ten times larger than for hard J/ψ production; 80000 events for the proton beam and 2.2 mln for the gold beam.

The expected statistical accuracy of the differential cross section $\mathrm{d}^2\sigma/\mathrm{d}x\mathrm{d}Q^2$ for hard exclusive ρ^0 production measured at EIC is shown in the second transparency. The kinematical range is divided in (x, Q^2) bins with the relative statistical errors $\Delta\sigma/\sigma$ displayed for the proton (left-top corner of each bin) and for the gold beam (left-bottom). At the right-hand side of each bin the error $\Delta\alpha$ is shown, where α parametrizes A-dependence of the cross section; $\sigma_A = \sigma_0 A^\alpha$. (The values of α itself are in the range 0.6 - 2.0 depending on the process and on the strength of nuclear absorption.) Note, that in general the statistical error $\Delta\alpha$ at EIC will be within the range 0.0005 - 0.01, except for the region of the lowest x at high Q^2 values. For the sample of coherent events, with the cut $|t| < 0.02\,\mathrm{GeV}^2$ applied to the events from gold, the values of $\Delta\alpha$ will be practically about the same as those shown for the global sample. For the incoherent events, selected with the cut $|t| > 0.05\,\mathrm{GeV}^2$ for gold, the errors will be about 1.5 to 2 times larger. Also for J/ψ production the statistical precision will be high. In particular, for the photoproduction data divided between 6 bins in W, $\Delta\alpha$ will be about 0.002 in each bin.

At EIC the precision of α will be significantly higher than in previous experiments. For example, the statistical errors $\Delta\alpha$ for the coherent dissociation of pions into high p_t jets from E791 [15] are about 0.1, for the coherent J/ψ photoproduction measured by E691 [10] $\Delta\alpha = 0.06$ and for the NMC results on coherent J/ψ muoproduction [11] it is about 0.02.

Finally we summarize the requirements for a detector to study exlusive processes at EIC.

• Tracking.

A tracking detector to measure charged particles momenta with precision $\Delta p/p \leq 1\%$ in the extended central region, $5 < \theta < 175°(|\eta| < 3.1)$, will be an essential element of the experimental setup. Such a detector will allow to determine the position of the interaction vertex and of the momenta of scattered electron and produced particles. We propose to measure the scattered electron momentum in the tracking detector rather than to determine it from calorimetric measurements.

• Hermetic detector.

An almost 4π acceptance both for charged and neutral particles is needed. This is important for studies of exclusive processes which have significantly smaller cross sections than inclusive and semi-inclusive processes. A significant background may be expected for exclusive events, unless one is be able to observe full event topology and tag background events.

• Separation of electrons, muons and hadrons.

The minimum requirement for particle identification is to realise the separation of electrons, muons and hadrons using EM calorimeters and muon detectors.

• Leading particle spectrometer (LPS).

Momentum measurement of a leading particle, proton or nucleus, which usually escapes into the accelerator beam pipe, may be possible with the Roman pot spectrometer. Such measurements will provide independent determination of t, which will be more acurate than that from the central detector. In addition, the LPS will allow to suppress events from nucleon dissociation and other non-exclusive processes.

The characteristic t values for different processes as well as the corresponding polar angles of the leading particles in the laboratory system are shown in the third transparency. For exclusive production on protons or light nuclei the leading particles are scattered at small angles of few milliradians, which could be accessed with the Roman pots. For the coherent exclusive production on heavy nuclei the leading nuclei are emitted at much smaller angles of few μrad and therefore can not be detected by the LPS.

Although it is possible to study the exclusive processes with a central detector only, an option of having in addition the LPS will significantly enhance the quality of the data for the proton and light ions beams. The advantage of having the LPS is the significant reduction of the non-exlusive background as well as a possibility of direct measurement of the differential cross sections $d\sigma/dt$.

In conclusion, the proposed comprehensive studies of exclusive production of vector mesons in eA and ep collisions at EIC will be a decisive step towards experimental verification of the predictions of perturbative QCD on color transparency and color opacity.

References

[1] F.E. Low, Phys. Rev. **D 12** (1975) 163.
[2] G. Bertsch *et al*, Phys. Rev. Lett. **47** (1981) 297.
[3] S.J. Brodsky, L.L. Frankfurt, J.F. Gunion, A.H. Mueller, M.I. Strikman, Phys. Rev. **D 50** (1994) 3134.
[4] L.L. Frankfurt, G.A. Miller and M.I. Strikman, Phys. Lett. **B304** (1993) 1; L.L. Frankfurt, G.A. Miller and M.I. Strikman, Ann. Rev. Nucl. Part. Sci. **45** (1994) 501.
[5] B. Blättel, G. Baym, L.L. Frankfurt and M.I. Strikman, Phys. Rev. Lett. **70** (1993) 896.
[6] L.L. Frankfurt, W. Köpf and M.I. Strikman, Phys. Rev. **D54** (1996) 3194.
[7] L.L. Frankfurt, A.V. Radyushkin and M.I. Strikman, Phys. Rev. **D55** (1997) 98.
[8] A.S. Carroll *et al*, Phys. Rev. Lett. **61** (1988) 1698.
[9] N.C.R. Makins *et al*, Phys. Rev. Lett. **72** (1994) 1986; T.G. O'Neil *et al*, Phys. Lett. **B351** (1995) 87.
[10] M.D. Sokoloff *et al*, Phys. Rev. Lett. **57** (1986) 3003.
[11] NMC, P. Amaudruz *et al*, Nucl. Phys. **B371** (1992) 553; NMC, M. Arneodo *et al*, Phys. Lett. **B332** (1994) 195.
[12] E665 Collab., M.R. Adams *et al*, Phys. Rev. Lett. **74** (1995) 1525.
[13] NMC, M. Arneodo *et al*, Nucl. Phys. **B429** (1994) 503.
[14] HERMES Collab., K. Ackerstaff *et al*, Phys. Rev. Lett. **82** (1999) 3025.
[15] E791 Collab., E.M. Aitala *et al*, Phys. Rev. Lett. **86** (2001) 4773; E791 Collab., E.M. Aitala *et al*, Phys. Rev. Lett. **86** (2001) 4768.

Kinematics of VM exclusive production at eRHIC

10 GeV x 100 GeV $\quad Q^2 > 1\ \mathrm{GeV}^2$

$ep \to ep J/\psi$

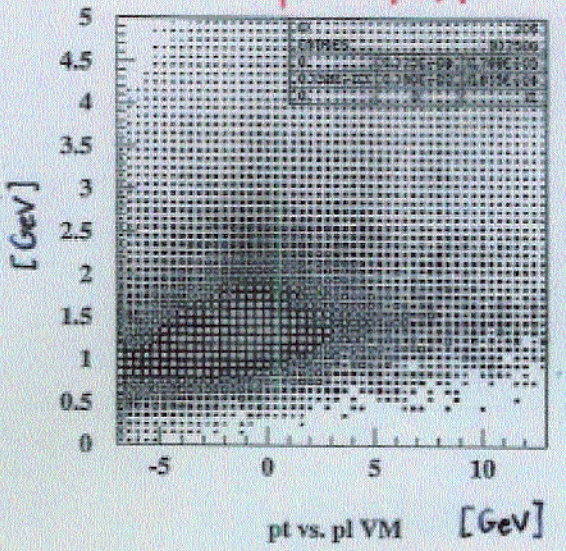

p_T vs. p_L (J/ψ)

$J/\psi \to \mu^+\mu^-$

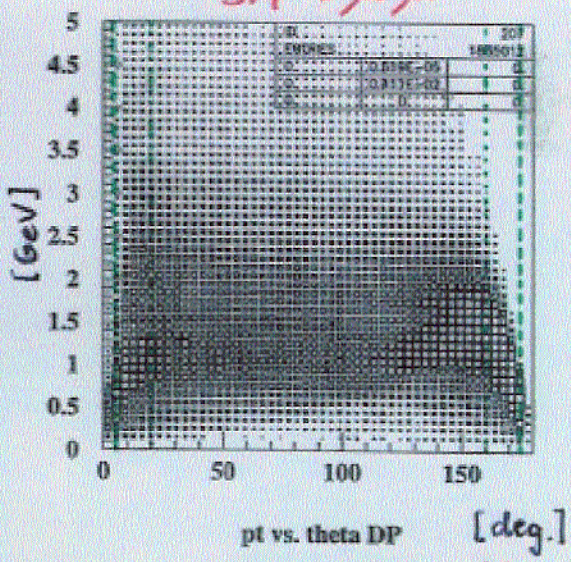

p_T vs. Θ $(\mu^\pm)$

$ep \to ep\rho^0$

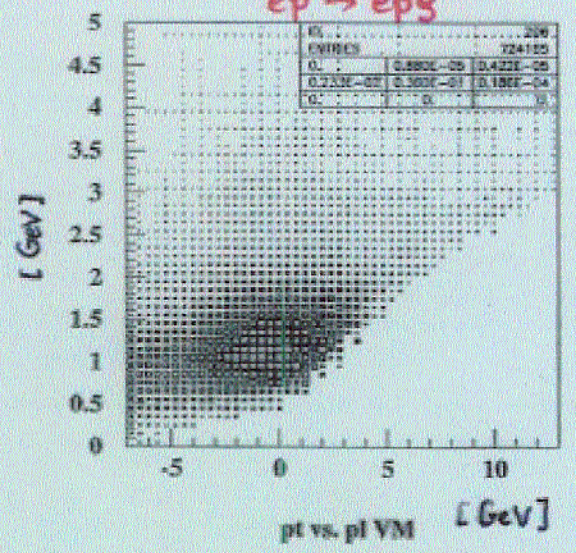

p_T vs. p_L (ρ^0)

$\rho^0 \to \pi^+\pi^-$

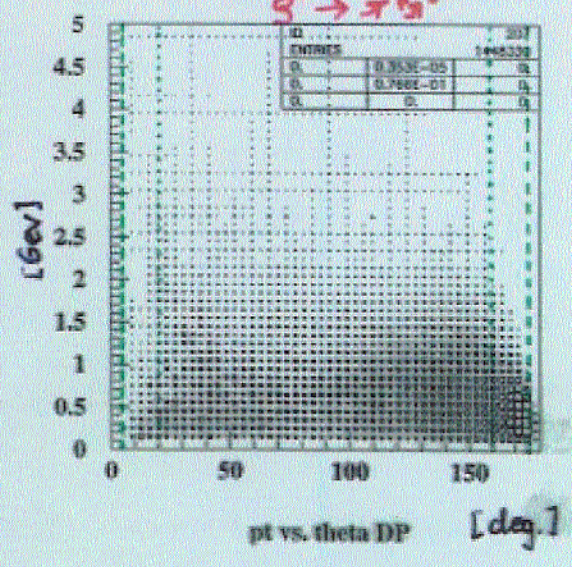

p_T vs. Θ $(\pi^\pm)$

Expected statistical precision

hard exclusive ρ^0 production

Assumed $\int \mathcal{L}$: $\boxed{\begin{array}{l} 330 \ \mathrm{pb}^{-1} \\ 10 \ \mathrm{pb}^{-1} \end{array}}$ for ep / for eAu

$\leftarrow Q^2 \ [\mathrm{GeV}^2] \rightarrow$

x ↓	1	2	4	8	15	25	50
0.0003 – 0.001	0.2 / .0005 / 0.1	0.8 / .0020 / 0.4	—	—	—	—	—
0.001 – 0.0025	0.2 / .0004 / 0.1	0.4 / ① .0008 / 0.2	1.0 / .002 / 0.5	13.0 / ② .028 / 6.8	—	—	—
0.0025 – 0.005	0.3 / .0005 / 0.1	0.4 / .0008 / 0.2	0.8 / .002 / 0.4	2.1 / .004 / 1.1	15.0 / 0.032 / 7.8	—	
0.005 – 0.01	0.3 / .0005 / 0.1	0.5 / .0010 / 0.2	0.8 / .002 / 0.4	1.8 / .004 / 1.0	4.2 / .009 / 2.2	15.0 / .032 / 7.6	
0.01 – 0.025	0.4 / .0009 / 0.2	0.4 / ③ .0009 / 0.2	0.8 / .002 / 0.4	1.6 / ④ .003 / 0.9	3.4 / .007 / 1.8	6.1 / ⑤ .013 / 3.3	
0.025 – 0.16	—	1.4 / .003 / 0.7	1.0 / .002 / 0.6	1.6 / .003 / 0.9	2.9 / .006 / 1.6	4.8 / .010 / 2.6	

$\frac{\Delta\sigma}{\sigma}$ [%] for ep

$\frac{\Delta\sigma}{\sigma}$ [%] for eAu

$\Delta\alpha$

$\sigma_A = \sigma_0 A^{\alpha}$

Total numbers of accepted events:

1.1 M for ep 4.2 M for eAu

Requirements for the detector

Tracking

vertex + momenta of scattered electron
and decay particles

in the region $-3.1 < \eta < 3.1$
with $\Delta p/p \lesssim 1\%$

Hermeticity

4π acceptance for charged and neutral part.

To suppress significant background

$e/\mu/h$ separation

Leading Particle Spectrometer (LPS)

Why needed

- independent and precise determination of t
- suppresion of nucleon dissociation
  and other backgrounds

Where applicable

process (10 GeV + 100 GeV/nucl.)	$\langle t \rangle$ [GeV^2]	$\langle \theta_{LP}^{lab} \rangle$
$ep \to e\rho^0 p$	0.15	4 mrad
$ed \to e\rho^0 d$ (interf. region)	~0.4	3 mrad
$e\,{}^4He \to e\rho^0\,{}^4He$ (double scatt reg.)	~0.3	1.3 mrad
$e\,Au \to e\rho^0\,Au$	0.004	3 μrad

Nuclear shadowing in deep inelastic scattering on nuclei: leading twist versus eikonal approaches

V. Guzey, L. Frankfurt, M. McDermott, M. Strikman

In this talk I will present results of our recent studies on nuclear shadowing in deep inelastic scattering (DIS) on nuclei [1] from the point of view of the leading twist (LT) approach of Frankfurt and Strikman [2].

Nuclear shadowing is a depletion of the distribution of quarks and gluons in nuclei relative to free nucleons at small values of Bjorken x. At present almost all information about nuclear shadowing came from DIS on fixed nuclear targets. However, these data (predominantly the data on F_2^A) do not constrain the nuclear parton distributions enough, especially for $x < 5\times10^{-3}$, because such low values of x correspond to $Q^2 < 1$ GeV^2, where the perturbative QCD analysis of the data is not reliable. In addition, the limiting statistics and kinematical $x - Q^2$ coverage of the fixed target experiments do not allow to reliably extract the gluon distribution in nuclei, $g_A(x, Q^2)$. Hence, a new machine, a lepton-ion collider and measurements of new observables (e.g. F_L^A) are needed for an unambiguous determination of nuclear parton distributions, especially in the region of nuclear shadowing at small x.

Our treatment of nuclear shadowing is based on the connection between nuclear shadowing in scattering on nuclei and diffractive scattering on a single proton established by Gribov [3]. In essence, the theory by Gribov rests on the observation that when the energy of the projectile is sufficiently high, the projectile interacts with nucleons of a nuclear target by dissociating into diffractive states rather than by elastic scattering. Frankfurt and Strikman [2] showed that the same logic can be carried over to DIS: in the limit of low nuclear density (i.e. for sufficiently light nuclei), the nuclear shadowing correction to the inclusive structure function F_2^A can be unambiguously expressed in terms of the proton diffractive structure function $F_2^{D(4)}$. Since $F_2^{D(4)}$ obeys the leading twist QCD evolution equation, so does the shadowing correction to F_2^A. Hence the name the leading twist approach.

The QCD factorization theorems enables one to present F_2^A and $F_2^{D(4)}$ in terms of the same hard scattering coefficients and parton distributions. Consequently, one predict nuclear shadowing for each parton flavor separately:

nuclear shadowing for the parton of flavor j, $f_{j/A}$, is given by the diffractive distribution of the parton j of the proton, $f^D_{j/N}$.

In the present analysis [1] we used 4 different parameterization of $f^D_{j/N}$, which describe reasonably well the HERA diffractive data. Since the best description of the data is provided by the H1 fit [4], our predictions for nuclear shadowing made using this fit should be considered as the "standard" scenario. We presented our predictions for the ratios $\bar{u}_A/(A\bar{u}_N)$ (sea up quarks), $g_A/(Ag_N)$, $c_A/(Ac_N)$ (charm quarks), $F_2^A/(AF_2^N)$ and $F_L^A/(AF_2^L)$ (longitudinal structure function) for $10^{-5} \leq x \leq 0.2$ and $2 \leq Q \leq 10$ GeV for a range of light and heavy nuclei. Despite a theoretical uncertainly in the slope of the gluon diffractive distribution, we are able to make several interesting and striking predictions:

- Nuclear shadowing for gluons is larger than that for sea quarks and structure function F_2^A.
- Longitudinal structure function F_L^A discriminates well between the LT and eikonal approaches: we predict a slow (logarithmic) Q^2-dependence of significant (larger than F_2^A) nuclear shadowing, while the size of nuclear shadowing within the eikonal approach is smaller in several times and vanishes much faster with Q^2. The trends for F_2^A are similar but less dramatic. We recommend to measure F_L^A and other gluon-sensitive observables at EIC.
- Nuclear shadowing and saturation of parton distributions at small x are related. In our analysis of nuclear shadowing we had to impose unitarity constraints on the growth of the gluon diffractive distribution (and thus nuclear shadowing for gluons). Conversely, any quantitative analysis of saturation requires a good understanding of nuclear shadowing.

References

[1] L. Frankfurt *et al.*, JHEP **202** (2002) 27.

[2] L. Frankfurt and M. Strikman, Eur. Phys. J. A **5** (1999) 293.

[3] V.N. Gribov, Sov. Phys. JETP **29** (1969) 483.

[4] H1 Collab., Z. Phys. C **76** (1997) 613.

Generalization to nuclear parton distributions in any nucleus

The result for the deuteron can be generalized to nuclear parton distributions in any nucleus in 3 steps.

1. Shadowing correction from the interaction with any **two nucleons** (main contribution, model-independent)

$$\delta F_2^{A(2)} = \frac{A(A-1)}{2} 16\pi Re \left[\frac{(1-i\eta)^2}{1+\eta^2} \int d^2b \int_{-\infty}^{\infty} dz_1 \int_{z_1}^{\infty} dz_2 \times \right.$$

$$\left. \int_x^{x_{I\!P},0} dx_{I\!P} F_2^{D(4)}(\beta, Q^2, x_{I\!P}, 0) \rho_A(b, z_1) \rho_A(b, z_2) e^{i x_{I\!P} m_N (z_1 - z_2)} \right]$$

- The nucleus is heavy enough that its recoil can be safely neglected $\rightarrow F_2^{D(4)}$ is evaluated at $k_t^2 \approx t \approx 0$
- The deuteron charge form factor is replaced by the nuclear one. The integration over k_t^2 gives the integral of the product of nuclear densities, ρ_A, with two nucleons at the same impact parameter b.
- The longitudinal momentum transfer to the nucleus is accounted for by $e^{i x_{I\!P} m_N (z_1 - z_2)}$

2. Factorization theorem for inclusive processes (Collins, Soper, Sterman, NP B 308 (1988) 833) and for hard diffraction (Collins, PR D 57 (1998) 3051):

$$F_2(x, Q^2) = \sum_i \int_0^x dz C_{2,i}(x/z, Q^2, \mu^2) f_i(z, \mu^2)$$

$$F_2^{D(4)}(x, Q^2, x_{I\!P}, t) = \sum_i \int_0^{x_{I\!P}} dz C_{2,i}(x/z, Q^2, \mu^2) f_i^D(z, \mu^2, x_{I\!P}, t)$$

Here f_i is the inclusive parton distribution; f_i^D is the diffractive parton distribution.

Shadowing correction to nuclear distribution $f_{i/A}$, $\delta^{(2)} f_{i/A}$:

$$\delta f_{j/A}^{(2)} = \frac{A(A-1)}{2} 16\pi Re \left[\frac{(1-i\eta)^2}{1+\eta^2} \int d^2b \int_{-\infty}^{\infty} dz_1 \int_{z_1}^{\infty} dz_2 \times \right.$$

$$\left. \int_x^{x_{I\!P},0} dx_{I\!P} f_{j/N}^D(\beta, Q^2, x_{I\!P}, 0) \ \rho_A(b, z_1) \ \rho_A(b, z_2) \ e^{i x_{I\!P} m_N (z_1 - z_2)} \right]$$

Important: Since $f_{j/N}^D$ obey the DGLAP evolution equation, so does $\delta f_{j/A}^{(2)}$. Hence, a slow, logarithmic, or **leading-twist Q^2-dependence** of nuclear shadowing is expected.

3. Interaction with 3 and more nucleons is accounted for the by attenuation factor. Our final equation for sea quarks and gluons, $\delta f_{j/A} = f_{j/A} - A f_{j/N}$:

$$\delta f_{j/A} = \frac{A(A-1)}{2} 16\pi Re \left[\frac{(1-i\eta)^2}{1+\eta^2} \int d^2b \int_{-\infty}^{\infty} dz_1 \int_{z_1}^{\infty} dz_2 \times \right.$$

$$\int_x^{x_{I\!P,0}} dx_{I\!P} f^D_{j/N}(\beta, Q^2, x_{I\!P}, 0)\ \rho_A(b, z_1)\ \rho_A(b, z_2) e^{i x_{I\!P} m_N (z_1 - z_2)} \times$$

$$\left. e^{-(A/2)(1-i\eta)\sigma^j_{eff} \int_{z_1}^{z_2} dz \rho_A(z)} \right]$$

The value of $x_{I\!P,0}$ determines the transition between shadowing and enhancement.

- $x_{I\!P,0} = 0.1$ for sea quarks. No antishadowing for sea quarks (Frankfurt, Strikman, Liuti, PRL 65 (1990) 1725) and $x_{I\!P,0}$ could be arbitrary large, but this doesn't affect results due to damping factor $e^{i x_{I\!P} m_N (z_1 - z_2)}$.

- $x_{I\!P,0} = 0.03$ for gluons. Motivated by the analysis (Gousset and Pirner, PL B 375 (1996) 349) of the NMC data. Antishadowing for $0.03 < x < 0.2$ is introduced by requiring

$$\int_{10^{-5}}^{0.2} dx x g_A/A = \int_{10^{-5}}^{0.2} dx x g_N$$

Predictions for F_2^A and g_A

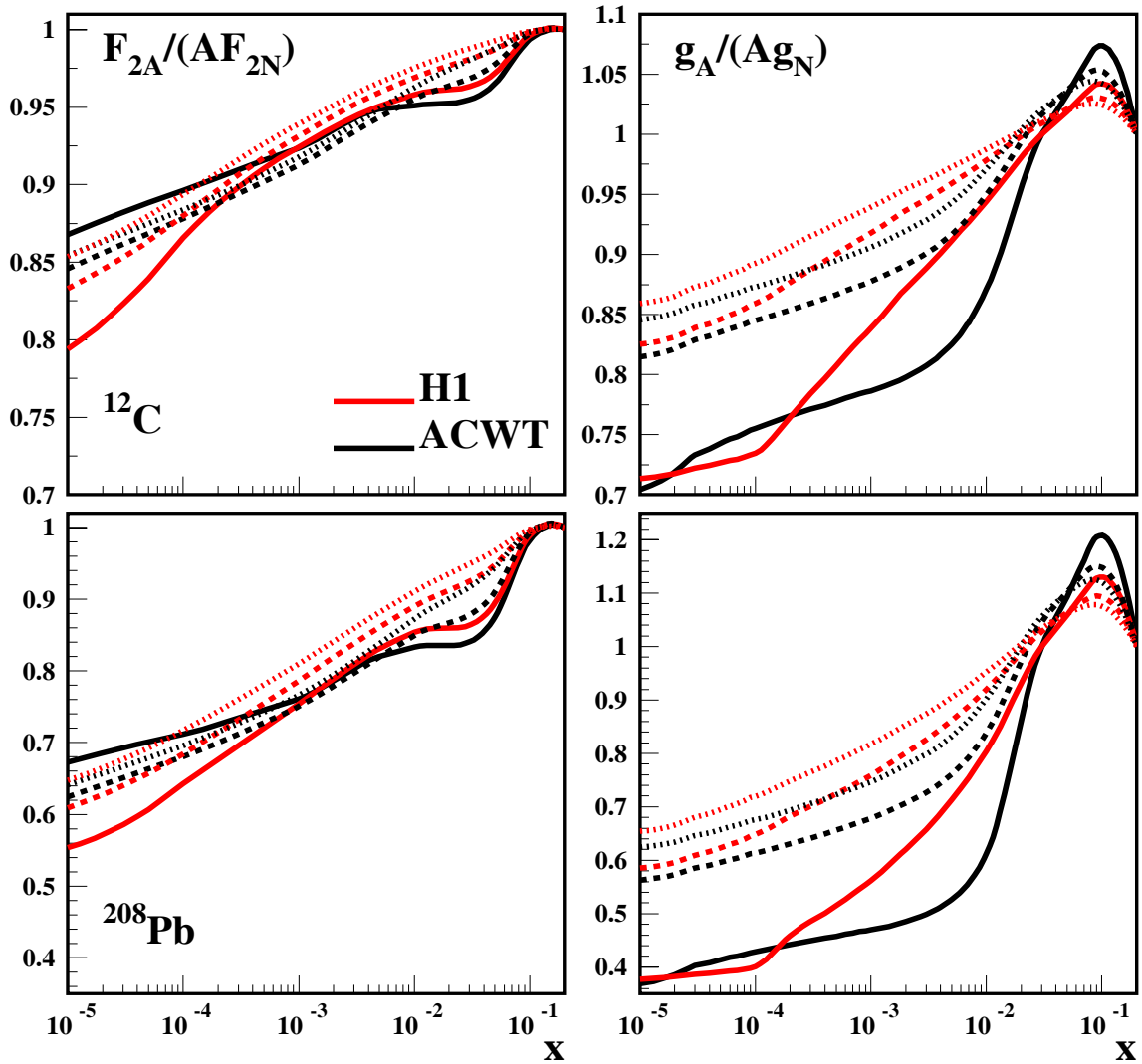

- NLO calculation (with CTEQ5M for $f_{j/N}$)
- Valence quarks are shadowed as the sea quarks; charm quarks are **not** modified at the input scale $Q_0 = 2$ GeV
- Predictions with H1 and ACWT are virtually the same for $10^{-4} < x < 10^{-2}$: F_2^D is measured in this range and fitted well by both parameterizations

Predictions for F_L^A

Longitudinal structure function F_L^A at small x is sensitive to the gluon distribution in the nucleus

$$F_L^A(x,Q^2) = \frac{2\alpha_s(Q^2)}{\pi}\int_x^1 \frac{dy}{y}\left(\frac{x}{y}\right)^2\left(\sum_{i=1}^{n_f} e_i^2\left(1-\frac{x}{y}\right)y\,g_A(y,Q^2)+\frac{2}{3}F_2^A(y,Q^2)\right)$$

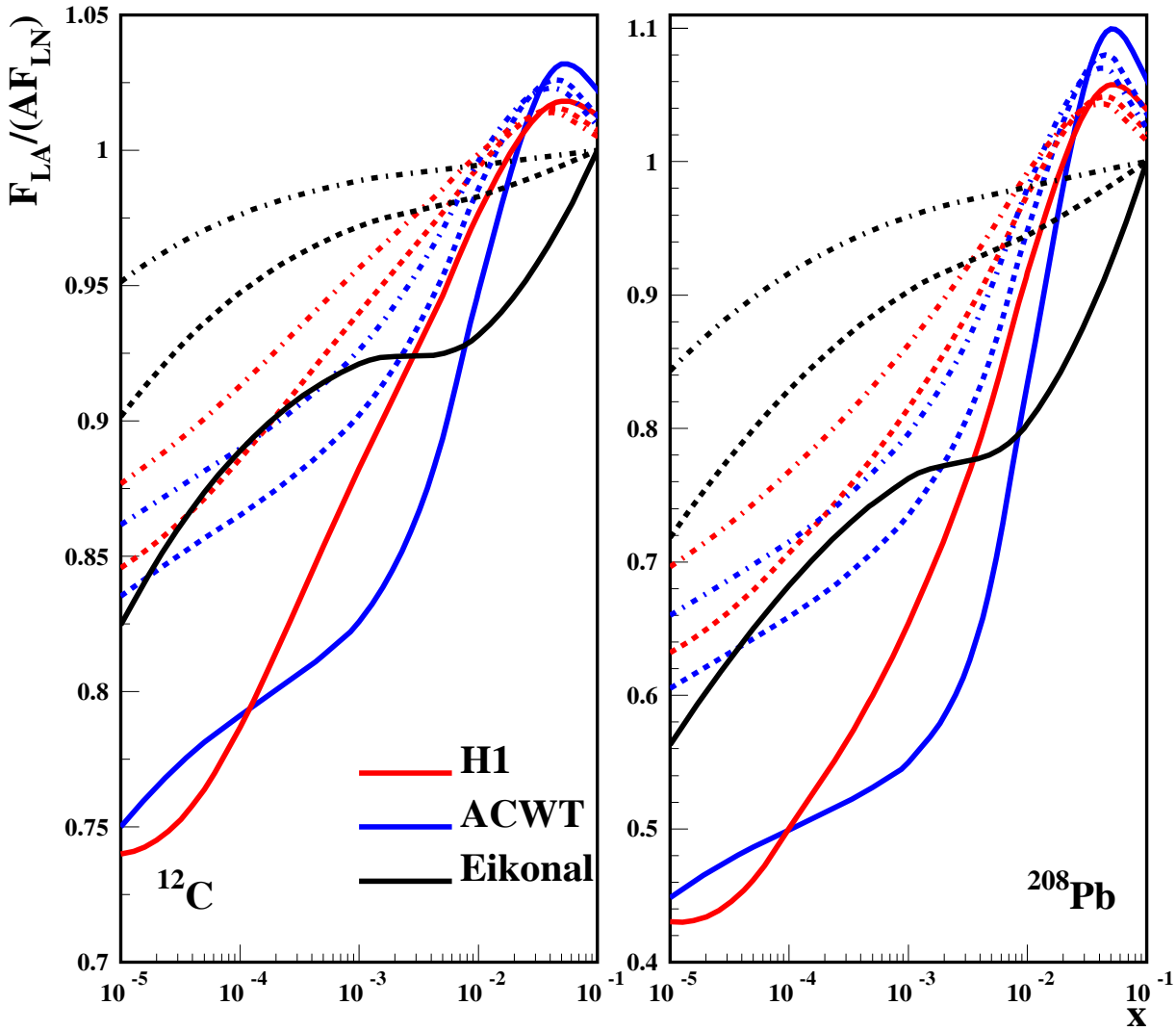

PROCEEDINGS

Analysis of HERA data at low x

Henri Kowalski*
Columbia/BNL/DESY
E-mail: kowalski@nevis.columbia.edu

ABSTRACT: We discuss HERA data on the high energy behavior of the total $\gamma^* p$ cross section and on diffraction in DIS. A natural link between inclusive and diffractive $\gamma^* p$ processes is provided by the dipole description of DIS. In the dipole picture the hard and soft interaction regions can be connected by the saturation hypothesis which leads to a good description of HERA measurements. An extension of the saturation ansatz by the evolution effects improves sizably the agreement with data.

Let us first recall that at HERA the electrons collide with protons by emitting highly energetic photons which then hit the proton. One of the most important measurements at HERA is the determination of the total $\gamma^* p$ cross section as a function of the photon virtuality, Q^2, and of the energy of the $\gamma^* p$ system, W.

Beginning at the top of our cross section plot (see transparencies) with small Q^2-values (large transverse sizes) the photon resembles a hadron, e.g. a ρ-meson. As the Q^2-values increase the photon shrinks and becomes more and more point-like. Following the rise of the total cross section in W as a function of Q^2 we observe a striking change. At small Q^2 the behavior is still very much the same as in hadron-hadron scattering, however with increasing Q^2, the rise in W becomes stronger. If we parameterize the W-dependence by a power law, $\sigma_{tot}^{\gamma^* p} \sim (W^2)^{\lambda_{tot}}$, this behavior is translated into the Q^2 dependence of the exponent λ_{tot}. QCD calculations allow the results of the small-distance part (large Q^2 values) to be interpreted in terms of QCD radiation.

Another important observation of HERA is the measurement of the diffractive $\gamma^* p$ cross section. Before HERA it was not expected that diffractive final states in deep inelastic scattering would play a significant role: the energetic virtual photon smashes the proton into pieces, the final state contains large numbers of particles or jets, and it was expected that the $q\bar{q}$-pair created by the photon could hardly be separated from the rest of the final state. In contrast to this expectation, a sizable and approximately constant fraction of diffractive events was observed as a function of W.

The observation of diffractive processes at HERA leads to a dipole picture of DIS. In the dipole description the probability for the incoming virtual photon to fluctuate into

*Speaker.

quark-antiquark pair is given by the photon wave-functions $\psi(Q^2, z, \vec{r})$ (z denotes here the momentum fraction of the photon carried by the quark and $\vec{r}$ the transverse size of the quark-antiquark pair). The emission of the gluon cloud and its interaction with the proton is described by the dipole cross section, $\sigma_{q\bar{q}}(x, \vec{r})$, which is closely related to the (unintegrated) gluon distribution (see transparencies).

In the proton rest frame the total cross section can be written in the following form:

$$\sigma_{t,l}^{\gamma^* p}(x, Q^2) = \int d^2\vec{r} \int dz\, \psi(Q^2, z, \vec{r})^* \, \sigma_{q\bar{q}}(x, \vec{r}) \psi(Q^2, z, \vec{r}). \tag{1}$$

The Optical Theorem applied in the framework of the dipole picture allows to express the cross section of diffractive $q\bar{q}$ production in which proton remains intact as:

$$\frac{d\sigma_{Diff}^{\gamma^* p}}{dt}|_{t=0} = \frac{1}{16\pi} \int d^2\vec{r} \int dz\, \psi(Q^2, z, \vec{r})^* \sigma_{q\bar{q}}^2(x, r^2)\, \psi(Q^2, z, \vec{r}) \tag{2}$$

The total and diffractive cross sections are expressed by the same elements. This shows the general property that the structure functions related to these cross sections, F_2 and $F_2^{D(4)}$, are of the same fundamental importance. Hence simultaneous observation of the inclusive and diffractive DIS processes allows us to get a better insight into the proton structure.

In order to describe the data it is necessary to make specific assumptions about the dipole cross section. A good description of the HERA data has recently been obtained by a model built on the idea of saturation. The idea of saturation emerges from the study of the rise of the total $\gamma^* p$ cross section with energy. This rise can be explained in QCD by the emission of a single gluon cascade. The one-cascade picture can be valid only if the system of gluons is sufficiently dilute. When at very small x the gluon density of the single cascade becomes too high, interactions with other cascades will become important. This process, called saturation, leads to a damping of the growth of cross sections with energy. It can be modeled by a simple ansatz for the dipole cross section

$$\sigma_{q\bar{q}}(x, \vec{r}) = \sigma_0\, (1 - \exp[-\frac{r^2}{4R_0^2}]), \tag{3}$$

where R_0 denotes the (x-dependent) dipole size where saturation sets in ("saturation radius": $R_0^2 = R_0^2(x) = \frac{1}{Q_0^2}\left(\frac{x}{x_0}\right)^{\lambda_{GBW}}$ with $Q_0 = 1$ GeV). The model describes the damping of the rise of the cross sections at high energies for higher Q^2 (outside of the energy range accessible to HERA) as an effect of the diminishing saturation radius. At low Q^2 the dipole sizes are large compared to the saturation radius which leads to the typical hadronic rate of rise.

The model has also been used for diffraction (see transparencies). In particular, as a result of a subtle interplay between the photon wave function and the dipole cross section, it succeeds in reproducing the energy dependence.

An extension of the saturation ansatz (see transparencies) by the evolution effects leads to the excellent description of the HERA data and shows that saturation and evolution effects can cooperate successfully. For further informatiom and references see also a recent paper by J. Bartels, K. Golec-Biernat, H. Kowalski, hep-ph/0203258.

DGLAP evolution in the Saturation Model

J. Bartels, K. Golec-Biernat, H. Kowalski

In the Saturation Model for small *r*

$$\sigma_{qq}(x,r) \approx \frac{\sigma_0 r^2}{4R_0^2(x)}$$

Dipole cross section in the small-*r* region:

$$\sigma_{qq}(x,r) \approx \frac{\pi^2}{3} r^2 \alpha_s xg(x,\mu_0^2)$$

Modification of the model

$$\sigma_{qq}(x,r) \approx \sigma_0 (1-\exp(-\frac{\pi^2}{3\sigma_0} r^2 \alpha_s xg(x, C/r^2 + Q_0^2)))$$

with *xg(x,)* evolving according to DGLAP equations from:

$$xg(x, Q_0^2) = Ax^{-\lambda_g}(1-x)^6$$

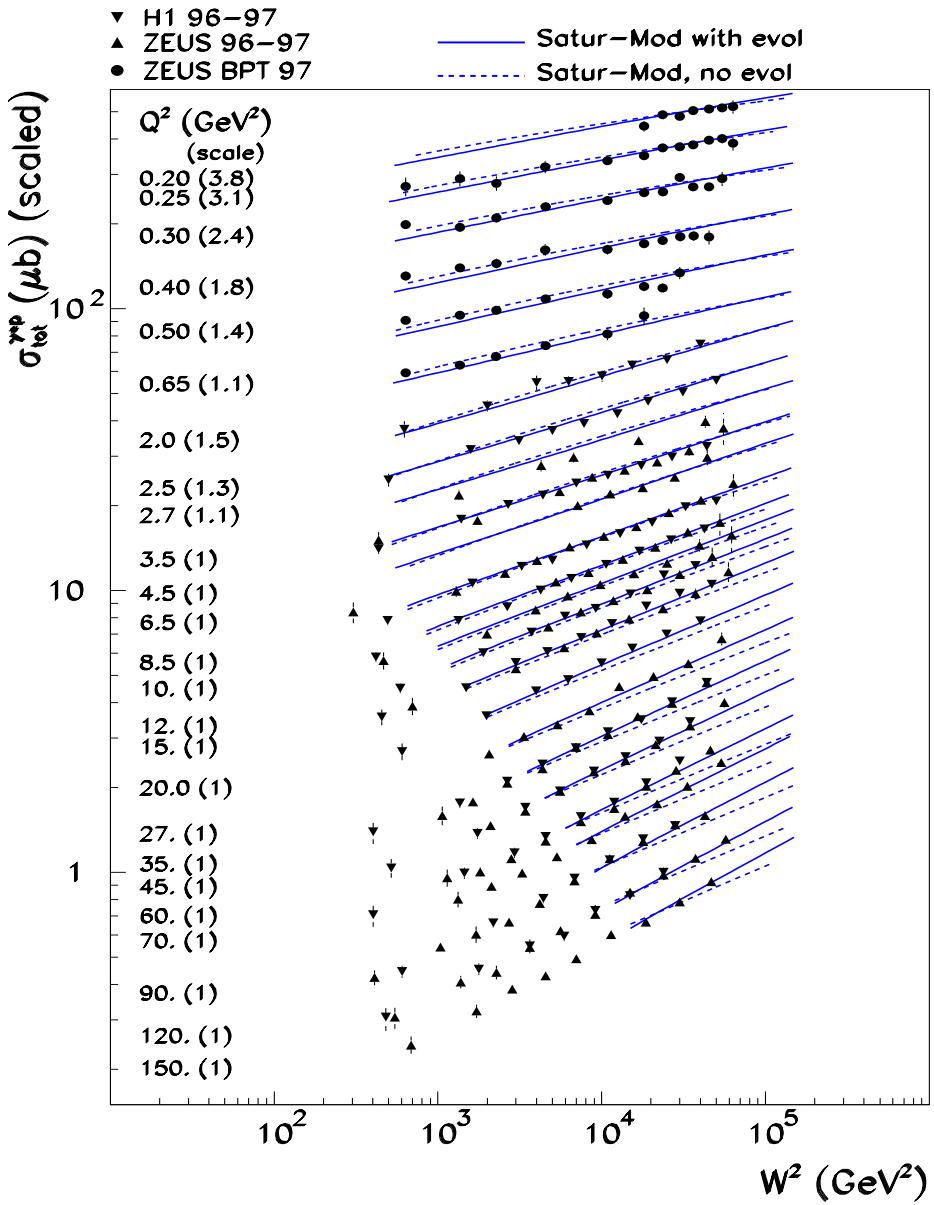

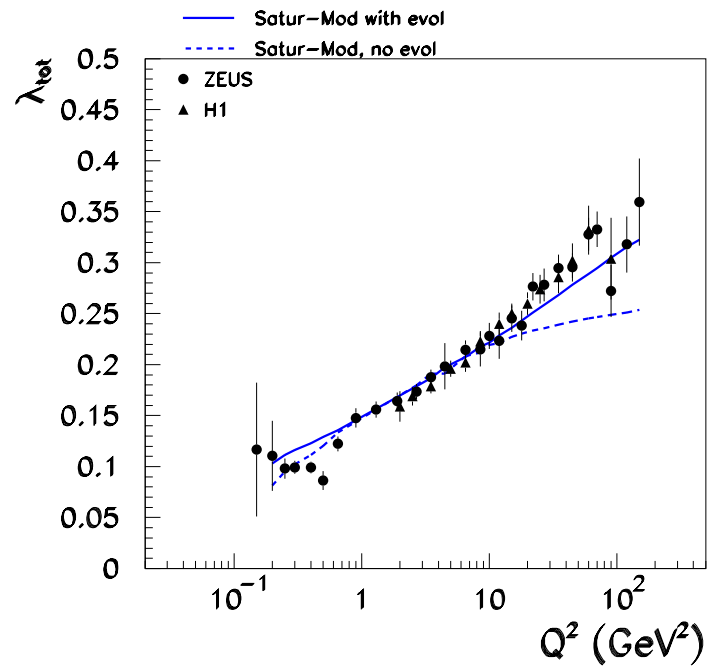

Fits to new data

$m_q = 140\ MeV$

Original *GBW* Saturation Model $\chi^2/N \sim 2.4$

Saturation Model with evolution $\chi^2/N \sim 1.2$

$\sigma_0 = 23$ mb $\lambda = 0.28$ A=1.2

$C = 0.26$ $Q_0^2 = 0.5$ GeV^2

Inclusive Diffraction

LPS - Method

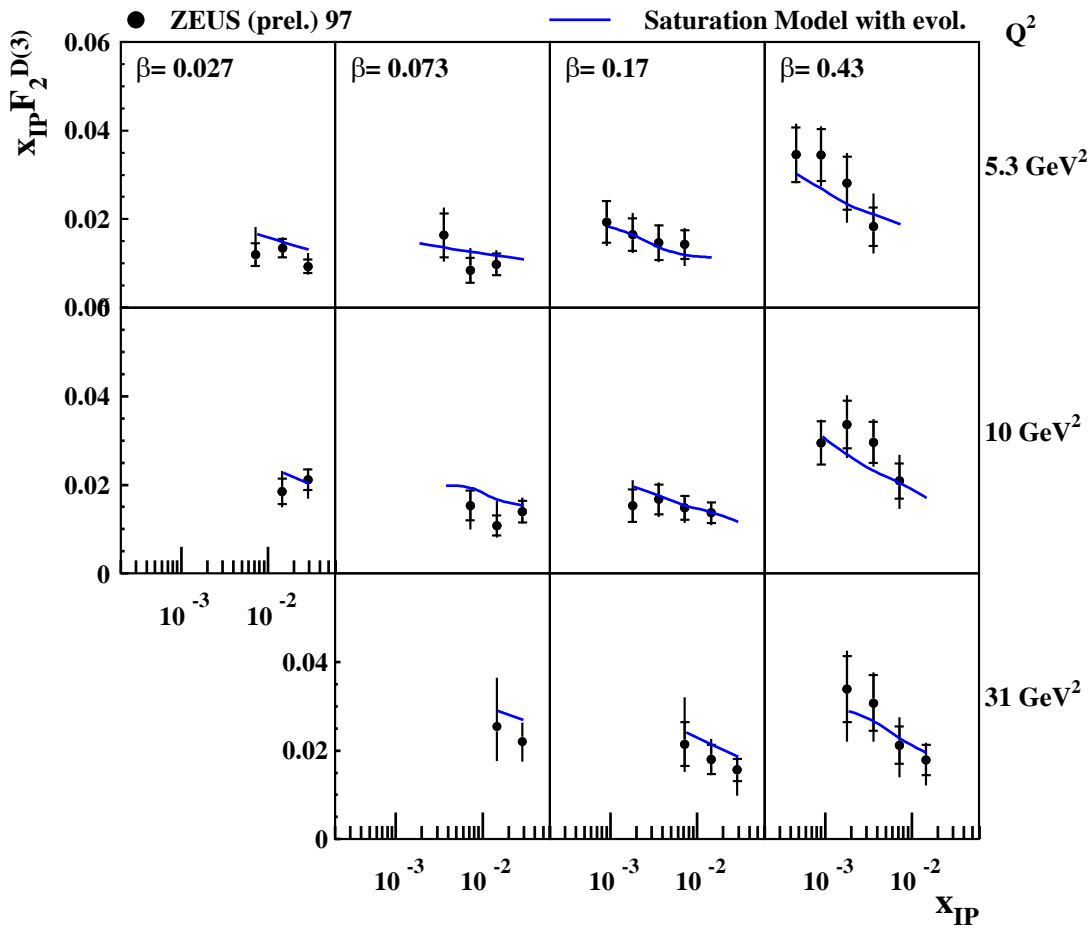

Gluon Amplitude $f(x,l^2)$ in the Saturation Model

Dipole cross section in momentum space:

$$\sigma_{qq}(x,\vec{r}) = \frac{2\pi}{3}\int \frac{d^2\vec{l}}{l^4}\alpha_s f(x,l^2)(1-\exp(-i\vec{l}\vec{r}))(1-\exp(i\vec{l}\vec{r}))$$

Doing the angular integration:

$$\sigma_{qq}(x,\vec{r}) = \frac{4\pi^2}{3}\int_0^\infty \frac{dl^2}{l^4}\alpha_s f(x,l^2)(1-J_o(lr))$$

Approximating: $1-J_o(lr) \approx l^2 r^2/4$ for $l^2 < 1/r^2$

we find for large l^2 :

$$\alpha_s(Q^2)xg(x,Q^2) = \int^{Q^2} \frac{dl^2}{l^2}\alpha_s(l^2)f(x,l^2)$$

$f(x,l^2)$ coincides with the un-integrated gluon distribution (for constant α_s)

$$\frac{\alpha_s f(x,l^2)}{l^4} = \frac{3}{8\pi^2}\int_0^\infty drrJ_0(lr)\{\sigma_{qq}(x,\infty)-\sigma_{qq}(x,r)\}$$

$$\frac{\alpha_s f(x,l^2)}{l^2} = \frac{3\sigma_0}{4\pi^2}R_0^2(x)l^2\exp\{-R_0^2(x)l^2\}$$

Saturation without evolution

Fit with m_q=140 MeV

σ_0 = 23 mb **λ = 0.28**
A=1.2 *C*= 0.26
Q_0^2 = 0.5 GeV^2
χ^2 /N = 1.17

Fit with m_q= 0 MeV

σ_0 = 23.8 mb **λ = -0.41**
A= 13.7 *C* = 11.1
Q_0^2 = 1.0 GeV^2
χ^2 /N = 0.97

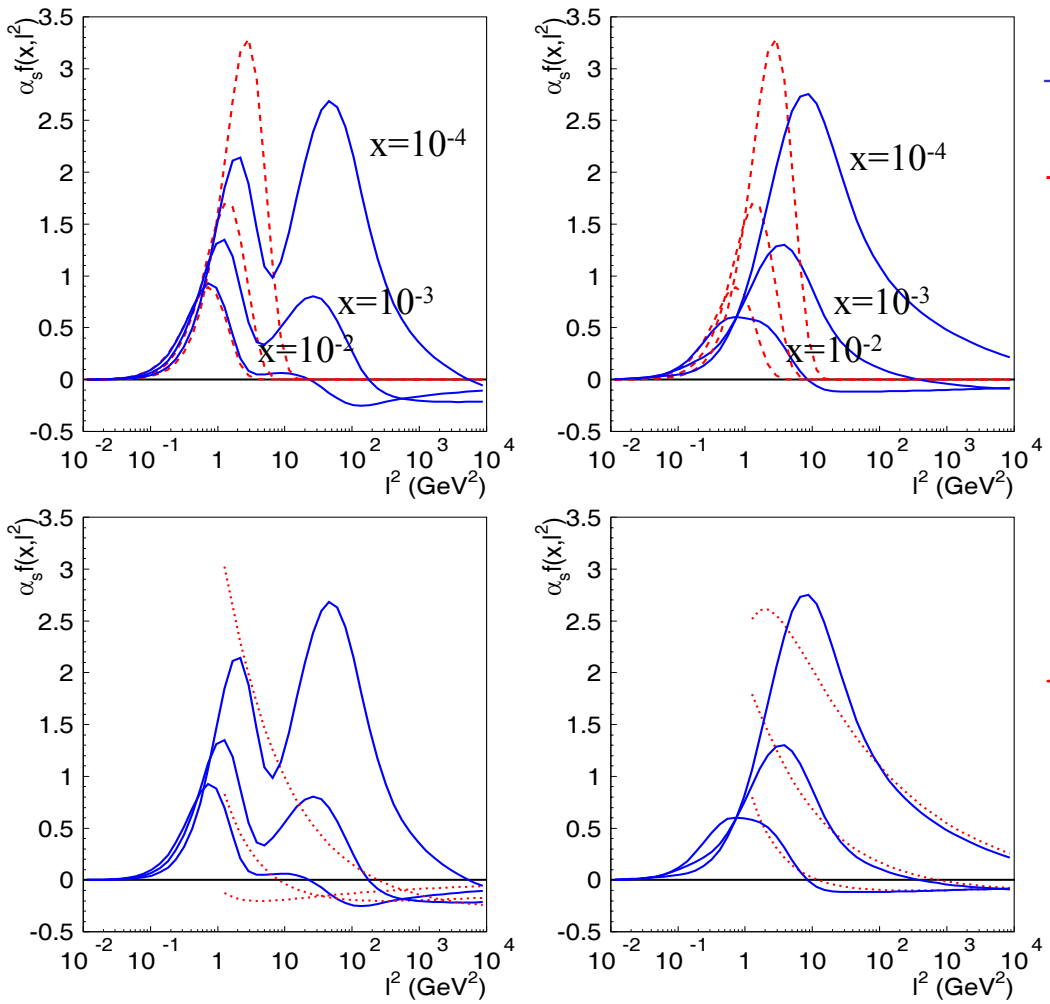

Gluon Amplitude

no evolution (orig. model)

no saturation

Higher Twist Effects in Nuclei

Rainer Fries

Duke University, Durham NC

Perturbative quantum chromodynamics (pQCD) is a successfull theory to explain scattering reactions involving hadrons at large momentum transfer. pQCD calculations are based on factorization theorems that allow a rigorous separation of short range (perturbative) and long range (non-perturbative) properties. The well known leading twist factorization theorem [1] tells us that the cross section for electron nucleon scattering can we written as $\sigma_{eN} = \sum_a \sigma_{ea} \otimes f_a$ where a is a parton species in the nucleon. Here σ_{ea} is the cross section of an electron scattering off a parton a which is perturbatively calculable and can be written as a series in α_s. On the other hand f_a is the parton distribution of parton a in the nucleon and encodes the non-perturbative part of the cross section. This factorization formula is valid at leading twist accuracy, i.e. modulo corrections of order λ^2/Q^2 where Q is the perturbative scale and λ a non-perturbative hadronic scale.

One notes that there is only one parton a at leading twist between the perturbative and the non-perturbative part, i.e. one is restricted to single scattering. Multiple scattering enters only as a higher twist correction. If one wants to study reactions involving heavy ions, the working assumption that leading twist is dominant already at intermediate values of Q, breaks down since multiple scattering becomes more important as one scatters off an extended nuclear medium. The origin of this behavior lies in the fact that the new matrix elements, which are introduced beyond the leading twist level, can show an anomalous scaling with the size of the nucleus. While ordinary parton distributions scale simply with the volume A of the nucleus (neglecting shadowing corrections), twist-n matrix elements can scale with powers of A as high as $A^{(4+n)/6}$. That happens if partons can stem from different nucleons in the nucleus.

In this spirit Liu, Qiu and Sterman [2] suggested that for large nuclei $A \gg 1$ it is sufficient to take into account only those higher twist matrix elements which show maximal nuclear enhancement and hence they proposed a reorganization of the twist expansion as a series in $\lambda^2 A^{1/3}/Q^2$. These matrix elements have a clear partonic interpretation as correlators between different partons. Parton distributions are matrix elements of single parton densities for quarks $\langle \bar{q}q \rangle$ and gluons $\langle FF \rangle$. At the level of nuclear enhanced twist 4 (double scattering) matrix elements with quark-quark $\langle \bar{q}q\, \bar{q}q \rangle$, gluon-gluon $\langle FF\, FF \rangle$ and quark-gluon correlators $\langle \bar{q}q\, FF \rangle$ appear. These new matrix elements are unknown at present and have to be extracted from experiment like ordinary parton distributions. However once this is done due to their universality property they are process independent and can be used to predict cross sections for other processes.

The future EIC facility would be an ideal tools to study nuclear enhanced multiple scattering and to probe the new higher twist matrix elements which can deepen our understanding of parton correlations in nuclei. There are three different scenarios under consideration where the effects of multiple interactions can be studied.

- There can be interactions between partons from different nuclei prior to the hard process [3]. This leads to modifications of the parton evolution equations which are analogous to those in the GLR equations. Here however one ist interested only in modifications arising from the nuclear environment the single nucleon is sitting in. Therefore one would be able to understand shadowing phenomena in terms of internucleon parton correlations.

- Multiple scatterings in the hard scattering process have been studied in a variety of different reactions [2, 4, 5]. The most simple though effective process for the EIC is jet production. This has been studied up to twist-4 accuracy. Furthermore there are recent activities to gain a deeper understanding by the resummation of higher twist corrections.

- X. Guo, X. Wang and E. Wang [6] recently have studied nuclear enhanced twist-4 corrections to the evolution of fragmentation functions. These medium modifications are different from the other two scenarios since they are not process independent. However they are a valuable tool to understand fragmentation in a nuclear medium and energy loss in nuclear matter.

To conclude there is a consistent pQCD formalism to understand multiple scattering in a nuclear environment. There is a strong case to study the new matrix elements associated with multiple scattering in order to get a handle on nuclear effects in numerous observables in $e+A$, $p+A$ and $A+A$ collisions. The EIC provides a unique opportunity to study nuclear enhanced higher twist matrix elements in clean observables like jet and particle production.

References

[1] J. C. Collins, D. E. Soper, G. Sterman, in: A. H. Mueller (ed.), "Perturbative Quantum Chromodynamics", World Scientific Publ., Singapore (1989).

[2] M. Luo, J. Qiu and G. Sterman, Phys. Lett. B **279**, 377 (1992); Phys. Rev. D **49**, 4493 (1994); Phys. Rev. D **50**, 1951 (1994).

[3] J. Qiu, Talk at the Workshop "Hard probes at LHC", Geneva, Oct. 2001.

[4] X. Guo, Phys. Rev. D **58**, 036001 (1998). R. J. Fries, B. Müller, A. Schäfer and E. Stein, Phys. Rev. Lett. **83** (1999) 4261; Nucl. Phys. **B582** (2000) 537.

[5] X. Guo, Phys. Rev. D **58**, 114033 (1998).

[6] X. Guo and X. Wang, Phys. Rev. Lett. **85**, 3591 (2000); Nucl. Phys. A **696**, 788 (2001). E. Wang and X. N. Wang, arXiv:hep-ph/0202105.

pQCD and Nuclear Collisions

- Now $e + A$, $p + A$ or $A + A$ collisions:
  Even for inclusive observables at typical momentum transfers the pure single scattering picture might me no langer valid.
  $\Longrightarrow$ Multiple scattering, in pQCD described by higher-twist matrix elements (multi-particle correlators), suppressed by powers of λ^2/Q^2.
  Only poorly known!

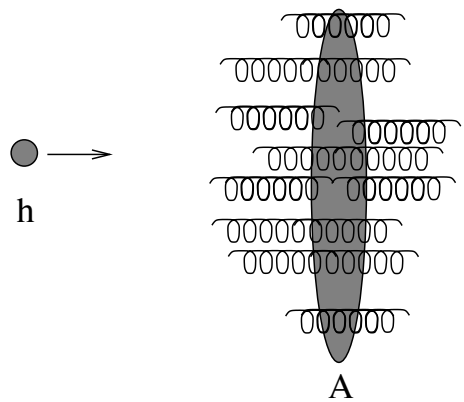

- *Why* are multiple scatterings important, despite power suppression?
  $\Longrightarrow$ Nuclear size must enter!

Appropriate expansion parameter is

$$\frac{\lambda^2 A^{1/3}}{Q^2}$$

"Nuclear Enhancement"

- Rearrange the twist expansion in this spirit.

J. Qiu and G. Sterman

Twist corrections & α_s corrections

Single scat.
(Twist-2)

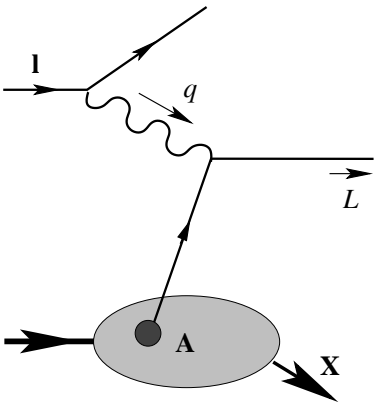

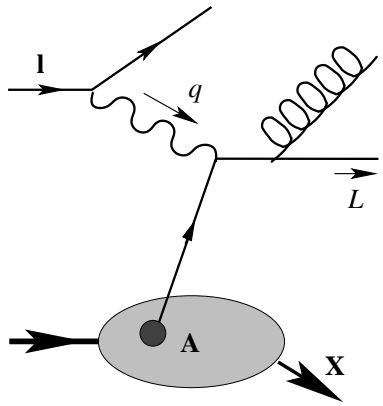

$\mathcal{O}(\ldots)$ $\quad 1 \quad$ α_s

Double
scat.
(Twist-4)

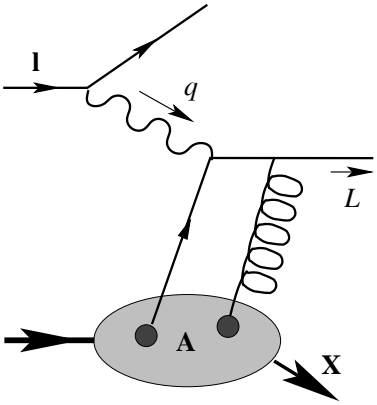

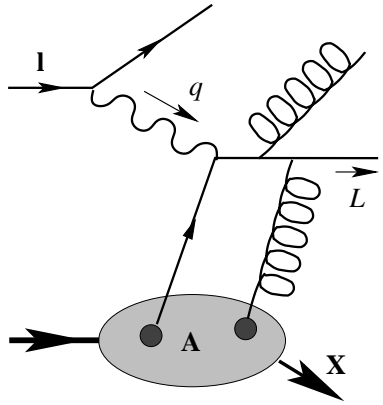

$\mathcal{O}(\ldots)$ $\quad \frac{\alpha_s \lambda^2 A^{1/3}}{Q^2} \quad$ $\alpha_s \left(\frac{\alpha_s \lambda^2 A^{1/3}}{Q^2} \right)$

$\ldots \quad \ldots \quad \ldots$

Different Types of Corrections

- Corrections to the hard scattering cross section.

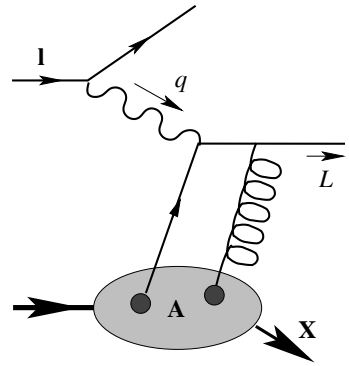

- Corrections factorized into the nuclear matrix elements: Modifications internal to the nucleus due to interactions between partons from different nuclei.

E.g. GLR type modification to the evolution equations $\Rightarrow$ nuclear modified PDFs.

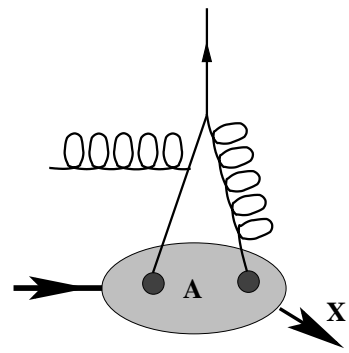

- Corrections to fragmentation functions. These in-medium modifications break factorization in the sense that they are no longer process independent.

X. Guo, X. Wang, E. Wang

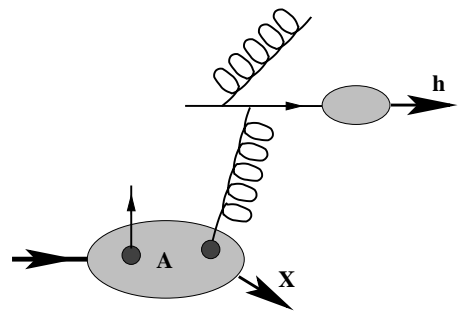

Probing Nuclei by Twist 4 Correlators

• Jet Tomography (X. Guo, X. Wang & E. Wang): Nuclear modifications to fragmentation functions and energy loss.

Here physics is sensitive to matrix elements in the soft hard interference region. Strong destructive interference between soft and hard poles $\Longleftrightarrow$ LPM interference pattern.

Comparison to Hermes data on fragmentation functions in N and Kr (E. Wang, X. Wang).

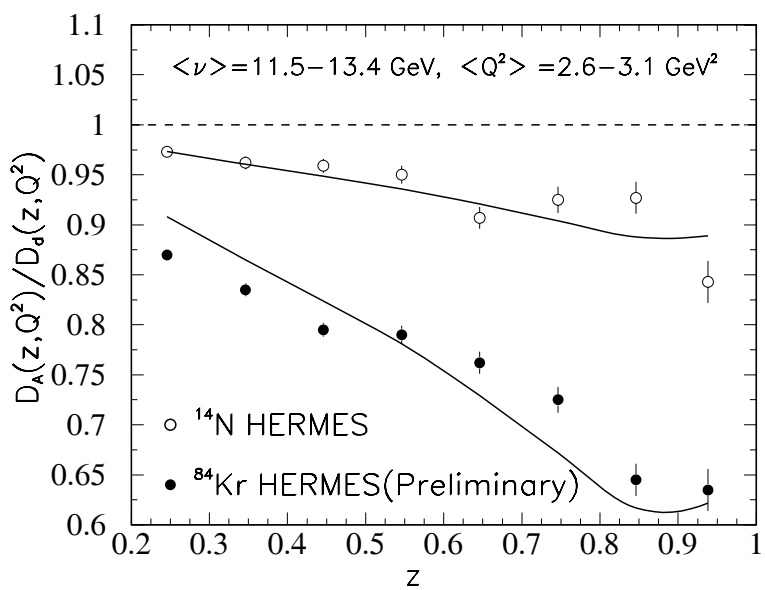

Energy loss shows the typical $A^{2/3}$ behavior, in accordance with previous work.

Beyond Double Scattering

- LO graphs for multiple scattering: introducing matrix elements $T_{qg^n} \sim \langle \bar{q}q(FF)^n \rangle$

- Assuming simple nuclear structure, one can relate matrix elements of different twist $\Longrightarrow$ resummation possible!

- Resumming higher twist cures the collinear limit of leading twist:

- Twist-2: $d\sigma \sim r\delta(p_\perp^2)$
- Twist-4; $d\sigma \sim s\delta'(p_\perp^2) + t\delta(p_\perp^2)$
- ...

Restoring a smooth transverse spectrum, but of course only the effects of internucleonic interaction! The typical transverse momentum gain should be of the order $p_\perp^2 \approx 4\pi^2\alpha_s\lambda^2 A^{1/3}/N_c$.

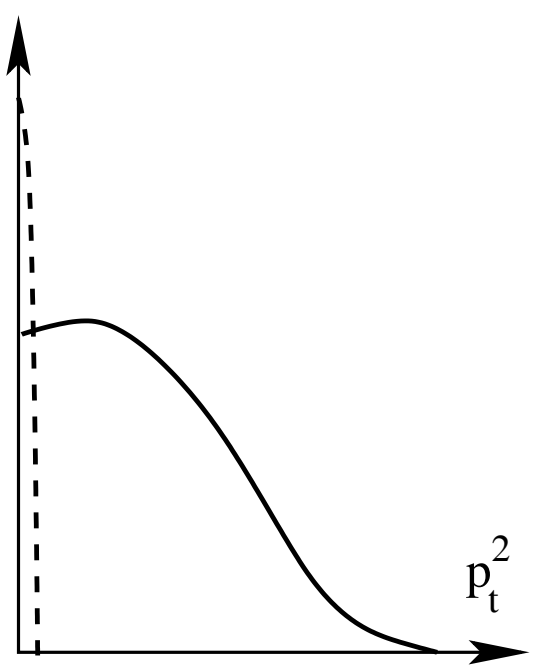

Nuclear Shadowing in non-linear small x pQCD

A. Freund[1], K. Rummukainen[2], H. Weigert[1] and A. Schäfer[1]
[1] *Institut für Theoretische Physik, Universität Regensburg, D-93040 Regensburg, Germany*
[2] *NORDITA, DK-2100 Copenhagen, Denmark*
(March 21, 2002)

In this talk we discuss inclusive eA scattering in the framework of the JIMWLK approach to non-linear, small x, pQCD, in particular the natural emergence of nuclear shadowing within the JIMWLK framework through simple scaling of the natural scaling variable τ, in this framework, by A^δ. We then compare our results to other popular approaches to nuclear shadowing like the eikonal approximation or leading twist calculations.

I. INTRODUCTION

The question of the onset of saturation/unitarization in inclusive QCD observables, in particular in the proton structure function $F_2(x,Q^2)$, has been the subject of active discussions for many years now (see a detailed discussion of this subject in [1,2] and references therein.). The most promising approach to properly include saturation/unitarization effects within the framework of QCD is the JIMWLK equation [1] which resums the leading $\ln(1/x)$ terms in *all* N-point correlators functions of the participating fields in the process in question, i. e. not just the leading correlators as in $k_\perp$-factorization. This leads to non-linearities in a RGE for the generating functional for these N-point correlators which slows down the rapid growth of structure functions at small x due to the presents of an infrared fixpoint which bounds the equation from below. When linearizing this JIMWLK equation one obtains the well-known BFKL equation (see [3] for details), which, however, gives to strong a growth in $F_2(x,Q^2)$, precisely because it does *not* have an infrared fixpoint bounding the equation from below. The JIMWLK approach is among other things *target independent*, which allows it to be used in ep as well as in eA scattering!

The basic picture in the approach to small x resummation is quite similar in all the various approaches: The virtual photon, in the infinite momentum frame split into a $q\bar{q}$ color-dipole (treated as eikonalized Wilsonlines) of, in principle, arbitrary size, which then punches through, and interacts with, the target, which it sees as a pancake of infinitesimal width but with the targets, gluonic spectator fields spread densely in the transverse plane. Since the dipole sees only a dense medium of gluons in the transverse plane, it does not know in what type of target these gluons reside and this leads to the statement of target independence of the predictions of this approach.

The above statement translates into a formula for the $\gamma^* p$ cross section or alternatively for F_2 (here for a proton target),

$$\begin{aligned}\sigma_{tot}(x,Q^2) =& N\int d^2\mathbf{z}\int_0^1 d\alpha|\psi_{\gamma^*}(\mathbf{z}^2\alpha(1-\alpha)Q^2)|^2 \\ &\times\sigma_{Dipole}(\mathbf{z}^2 Q_s(x,x_0,Q_0)) \\ &\text{with } \mathbf{z}=\mathbf{x}-\mathbf{y},\end{aligned} \tag{1}$$

where ψ_{γ^*} encodes the information about the color dipole and σ_{Dipole} contains the information about the interaction of the dipole with the spectator fields and which is obtained through the JIMWLK equation. As mentioned above, the JIMWLK equation can be recast as an equation for a generating functional of the Fokker-Plank type which in turn can be easily rewritten as a Langevin equation with white noise, at least in leading order of $\ln(1/x)$. This type of equation can be discretized and solved numerically [4]. $Q_s = (x/x_0)^\lambda Q_0$ is a saturation scale and λ is obtained from the numerical solution of the JIMWLK equation to be $\lambda = 0.182 \pm 0.02$ [4], very close to the value obtained within the Golec-Biernat/Wüsthoff saturation model [5] when fitting the HERA F_2^p data. N is a normalization constant which has to be fitted to data at a x_0 and Q_0.

II. NUCLEAR SHADOWING WITHIN JIMWLK AND OTHER APPROACHES.

Nuclear shadowing can be easily incorporated in this approach by realizing that the impact parameter integral will yield an A dependence via a simple rescaling of $\mathbf{z}$ and Q by A^δ where $\delta = 1/3$ if the distribution of spectator partons in the target were homogeneous. Since this is a priori not necessarily the case, we leave this parameter to be determined by data. Eq. (1) then turns into

$$F_2^A(\tau) = N(A)\left(\frac{x}{x_0}\right)^{2\lambda} F_2^p(x_0,\tau(x,Q^2,A,Q_0^2)) \tag{2}$$

with $\tau = \left(\frac{x}{x_0}\right)^{2\lambda}\left(\frac{Q}{A^\delta Q_0}\right)^2$ and where the normalization $N(A)$has to be determined for some x_0 and Q_0 from data. In fact normalizing the F_2^p one can use the same x_0 and Q_0 as for the normalization of F_2^p! Thus we have an unambiguous prediction for F_2^A which says that not only can the observed nuclear shadowing be explained by a

simple rescaling of the variable τ with A, but also that, after proper normalization, all F_2^A data should, plotted vs. τ, lie on the same line as the data for F_2^p. Thus we also predict geometric scaling in inclusive eA scattering.

The eikonal approach: The main equation of this approach is

$$\mathrm{Im}\ A_{e-A} \propto |\psi_{\gamma^* \to q\bar{q}}|^2 \otimes \exp\left(\sigma^{tot}_{q\bar{q}-N}\right), \qquad (3)$$

which basically says the following two things: a) the $q\bar{q}-N$ interaction does *not* change the transverse size or momentum fractions of the dipole and b) that no higher Fock components like $q\bar{q}g$ contribute to the cross section.

The leading twist approach: Gribov observed that if $R_{\text{strong interactions}} \ll R_{\text{N-N in A}}$ then there is a *direct* relationship between nuclear shadowing in $N-A$ collisions and σ^{diff}_{N-N}. Furthermore, there is a generalization [6] to calculate the leading twist component of nuclear shadowing for each nuclear parton distribution separately through the factorizable, *diffractive* $F_2^{D(4)}$:

$$\delta F_2^A = AF_2 - F_2^A$$
$$= \frac{16\pi A(A-1)}{2}\mathrm{Re}\Big[\frac{(1-i\eta)^2}{1+\eta^2}\int d^2b \int dz_1 \int_{z1} dz_2 \int_x dx_{I\!P}$$
$$F_2^{D(4)}(\beta, Q^2, x_{I\!P}, k_\perp^2 = 0)\rho(b,z_1)\rho(b,z_2)e^{(x_{I\!P} m_N (z_1 - z_2))}\Big] \qquad (4)$$

In the following we compare the JIMWLK and the leading twist approach with one another as well as with data (here only NMC data for $x \leq 0.05$ was used.). We will plot $F_2^A(t)$ vs. τ, normalized to F_2^p, where, for the leading twist approach [7], we choose the same value for λ, x_0 and Q_0 as in the JIMWLK one: $\lambda = 0.182$, $x_0 = 2\times 10^{-4}$ and $Q_0 = 1$ GeV. δ was found from a fit to the data to be about $\delta \simeq 0.05$. This implies a weak A dependence in the data, implying a more granular structure of the nucleus. Note, however, that the bulk of the data on F_2^A is at small x is for light, not for heavy, nuclei! Thus it will be very interesting to see how the A dependence changes for larger nuclei at small x.

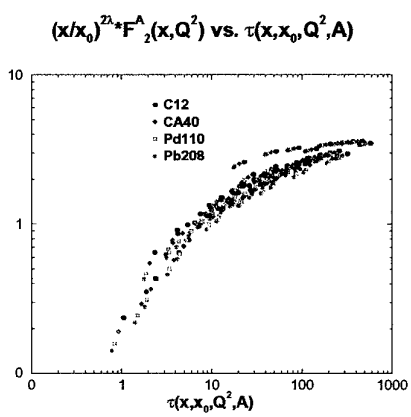

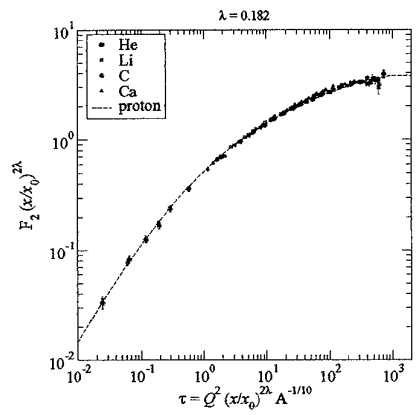

As can be seen from the figures, the F_2^A data indeed falls on the F_2^p curve as predicted by the JIMWLK approach and thus describes the data surprisingly well!

III. CONCLUSIONS

The JIMWLK approach makes an unambiguous prediction of the x behavior of eA cross sections where only the normalization of the cross section has to be fitted to data. Furthermore, nuclear shadowing appears naturally in this approach through simple rescaling of τ. It predicts that the eA data lie, after proper normalization, on the same curve as the data for small x ep scattering. Thus geometric scaling is predicted and indeed born out by a comparison with NMC data. A comparison with the leading twist approach shows a similar behavior in τ but a certain scattering of points, a different normalization and in addition a steeper slope in τ at small τ. Thus the two approaches are qualitatively similar, however, details of saturation and initial conditions seem to be different.

[1] H. Weigert, hep-ph/0004044.
[2] A. Stasto, K. Golec-Biernat, J. Kwiecinski, Phys. Rev. Lett. 86 (2001) 596.
[3] Jamal Jalilian-Marian, Alex Kovner, Andrei Leonidov, Heribert Weigert, Nucl. Phys. B504 (1997) 415.
[4] K. Rummukainen and H. Weigert, preprint in preparation.
[5] K. Golec-Biernat and M. Wüsthoff, Phys. Rev. D60 (1999) 114023.
[6] L. Frankfurt and M. Strikman, Eur. Phys. J. A5 (1999) 293.
[7] L. Frankfurt, V. Guzey, M. McDermott and M. Strikman, JHEP 0202 (2002) 027.

Comparisons of different approaches

Amongst many approaches:

- The Eikonal Approach (Cheng et. al $'69$):

$$\text{Im } A_{e-A} \propto |\psi_{\gamma^* \to q\bar{q}}|^2 \otimes \exp\left(\sigma^{tot}_{q\bar{q}-N}\right)$$

$$\downarrow$$

$$\sim \sum_{i=1}^{\infty} \left(\sigma^{tot}_{q\bar{q}-N}\right)^i$$

Basic assumptions:

  - $q\bar{q} - N$ interaction does not change the transverse size or momentum fractions of dipole!
  - No higher Fock components like $q\bar{q}g$

- The Leading Twist Approach (LT) (Frankfurt et. al $'99,'02$):

(see talk by V. Guzey)

  - Observation by Gribov: If $R_{\text{strong interactions}} \ll R_{\text{N-N in A}}$ then there is a direct realtionship between nuclear shadowing in $N - A$ collisions and σ^{diff}_{N-N}.
  - There is a generalization (Frankfurt/Strikman $'99$) to calculate leading twist component of nuclear shadowing for each nuclear parton distribution separately:

$$\delta F_2^A = AF_2 - F_2^A$$
$$= \frac{A(A-1)}{2} 16\pi \mathrm{Re}\Big[\frac{(1-i\eta)^2}{1+\eta^2}\int d^2b \int dz_1 \int_{z1} dz_2 \int_x dx_{I\!P}$$
$$F_2^{D(4)}(\beta, Q^2, x_{I\!P}, k_\perp^2 = 0)\rho(b,z_1)\rho(b,z_2)\exp^{\left(x_{I\!P} m_N (z_1 - z_2)\right)}\Big]$$
$$\downarrow$$

Factorization: $C \otimes PDF_{Diff}$ $\leftarrow$ Leading Twist

- The JIMWLK framework of non-linear small x resummation:

(see talk be H. Weigert)

- ∞ of non-linear DEQ resumming all N-point functions (NO TWIST EXPANSION!)
- infra-red stable!
- Non-linearities drive saturation $\leftarrow$ unitarization effect.
- Initial conditions contain saturation ($\leftarrow$ necessary for consistency)

$$\sigma_{tot}^A(x, Q^2) = N(A) \int d^2\mathbf{z} \int_0^1 d\alpha |\psi_{\gamma^*}(\mathbf{z}^2 \alpha(1-\alpha)(Q/A^\delta)^2)|^2$$
$$\times\, \sigma_{Dipole}^A(\mathbf{z}^2 Q_s(x, A, Q_0)) \quad \text{with } \mathbf{z} = \mathbf{x} - \mathbf{y}$$

- σ_{Dipole}^A is obtained from the JIMWLK small x evolution equation.
- only $N(A)$ has to be fitted to data!

rescaling argument $\mathbf{x}, \mathbf{y} \to \mathbf{x}/A^\delta, \mathbf{y}/A^\delta$ leads to:

$$\sigma_{tot}^A(x, Q^2) = N(A)\sigma_{tot}^p\left(x_0, \left(\frac{x}{x_0}\right)^{2\lambda}\left(\frac{Q}{A^\delta Q_0}\right)^2 = \tau(x, Q, A, Q_0)\right)$$

$$F_2^A(\tau) = N(A)\left(\frac{x}{x_0}\right)^{2\lambda} F_2^p(x_0, \tau(x, Q, A, Q_0))$$

- x_0, Q_0 is the x, Q to which one has to normalize σ_{tot} to.
- λ is determined from the evolution equation.
- Only the overall normalization has to be fitted to data!

General Predictions:

- Unambigous prediction of x behavior!
- As already noticed [Golec-Biernat et. al. '00] all data on F_2^p plotted vs. τ MUST lie on ONE curve.
- Same is true for F_2^A! Moreover, curve must coincide with the one for F_2^p for the correct A dependence $\leftarrow$ determination of δ!

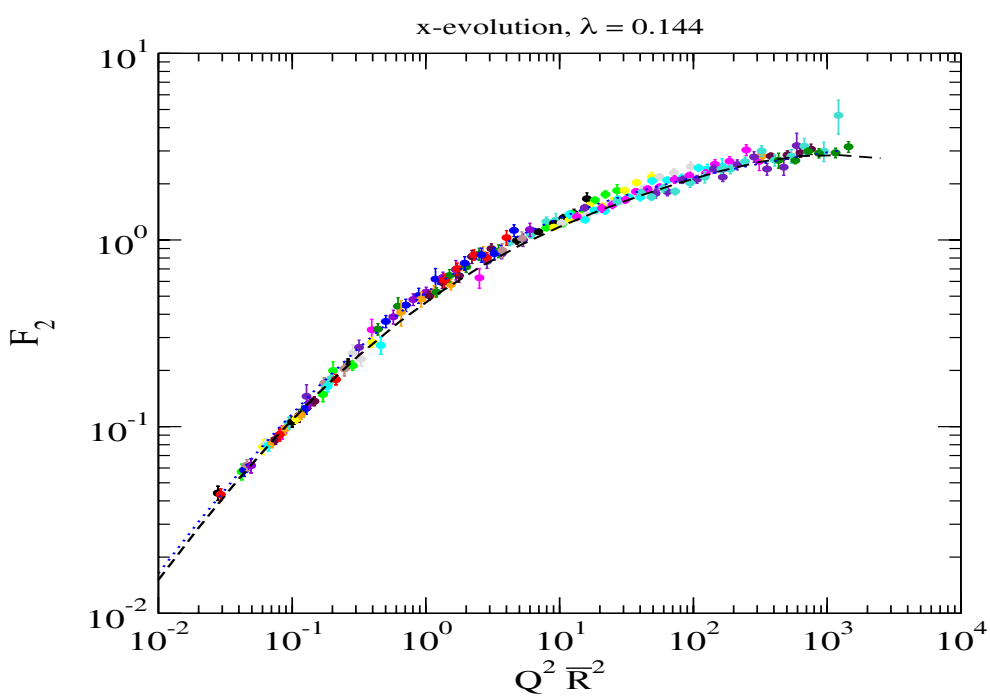

F_2^A comparison between JIMWLK, LT and data

For the leading twist approach we chose the same value for λ and x_0 as in the JIMWLK approach: $\lambda = 0.182$ and it was normalized at $x_0 = 2 \times 10^{-4}$, $Q_0 = 1$ GeV . δ was found to be about $\delta \simeq 0.05 \rightarrow$ weak A dependence!

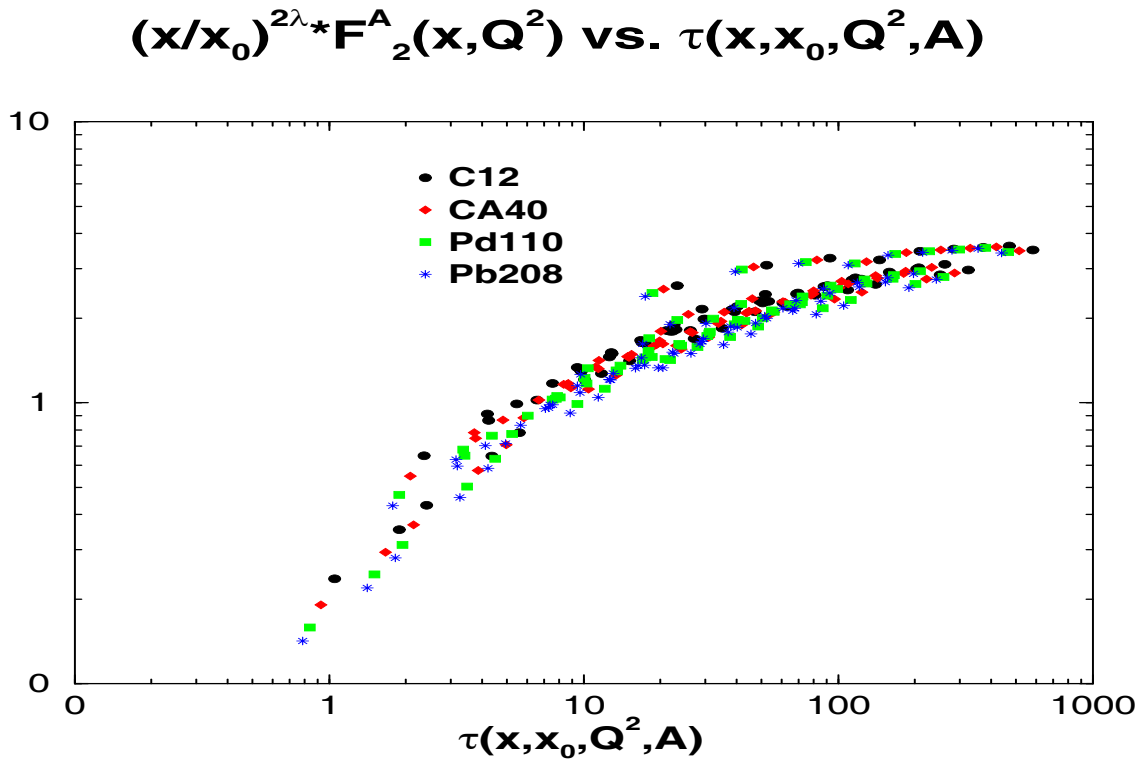

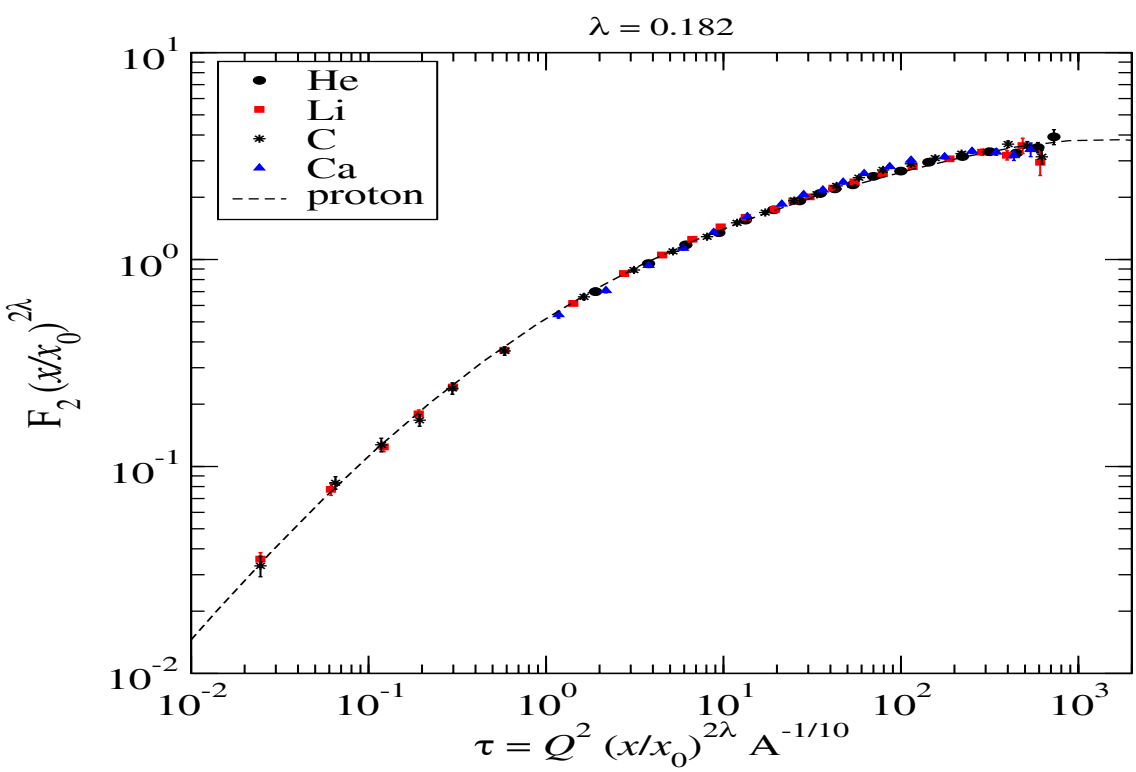

Conclusions & Outlook

- The JIMWLK approach makes unambigous prediction of the x behavior of $e - A$ cross sections only the normalization of the cross section has to be fitted once to data.

- Nuclear shadowing appears naturally in this approach through simple rescaling of the arguments! Plotted in the proper variable all $e - A$ data lie on one curve as for $e - p$ scattering. ($\leftarrow$ Geometric Scaling!). Very good agreement with data!!

- Comparsion with the leading twist approach shows similar behavior in τ but certain scattering of points plus different normalization. LT has steeper slope in τ at small τ. Behavior of F_2^A vs. Q^2 and x very similar in the two approaches. Final conclusion: Qualitatively similar. Details of saturation and initial conditions seem different.

- NLO corrections to the evolution function (Partly calculated by Balitsky/Belitsky $'01$) ? Does the Q^2 behavior change when coupling starts running ? Can one still speak of a running coupling in this language ?

- What happens in exclusive reactions like $e\ A \rightarrow e\ A\ \gamma$? Are nuclear shadowing effects different in the real part of the scattering amplitude (which includes virtual meson-like states in the t channel) compared with the imaginary part (does not contain virtual meson-like states in the t channel) ? ($\leftarrow$ currently under investigation!)

- A new, non-linear, QCD regime has been opened which needs new interpretations, new tools and new concepts. Underlying explanation of what we are seeing (like geometric scaling) similar to phenomena in other parts of physics/Biology/Chemistry which can be explained by self-organized criticality ????? We will see ...

Polarized ep Physics

A. Deshpande[a] and W. Vogelsang[a,b]

[a] RIKEN-BNL Research Center, Brookhaven National Laboratory, Upton, NY 11973-5000
[b] Nuclear Theory Group, Brookhaven National Laboratory, Upton, NY 11973-5000

The goal of this session was to analyze the physics possibilities that polarized ep collisions at the EIC would offer. A lot of work in this direction had already been done in the past, either directly as studies for EIC, or to study the physics case for a conceivable polarized collider mode of HERA. Studies for HERA can be easily adapted to the EIC situation. The talks in the session were partly meant to collect the results of previous HERA and EIC workshops, and to expand the previous studies. Moreover, because of the significantly higher luminosity planned at the EIC compare to the HERA, new topics in polarized and unpolarized ep physics were addressed for the first time. This led to a great variety in the topics covered in the presentations and demonstrated the impact EIC would have in the field of high-energy spin physics.

Since the speakers in our session have already summarized their talks in this volume, we refrain from doing this. Here we only list the topics that were discussed with very brief comments whenever necessary.

- **J. Lichtenstedt** reviewed our knowledge on the nucleon spin structure resulting from polarized DIS. He and **M. Stratmann** presented studies of polarized DIS at the EIC, highlighting the access to small-x one would gain and the increase in Q^2-lever arm with the resulting information on scaling violations and gluon polarization. **A. Vogt** contributed studies on unpolarized event rates and possibilities for precise measurements of F_2, in particular at large x.

- semi-inclusive DIS at the EIC would offer a number of exciting possibilities for studying nucleon structure. As **C. Weiss** explained, theoretical models favor a fairly large isospin SU(2) breaking in the polarized nucleon sea, and SIDIS measurements at the EIC would be ideal for pinning down the breaking. For this to be viable, fragmentation functions need to be known accurately, and **S. Kretzer** contributed a study of the capabilities of EIC to test and improve our knowledge on these. Staying with fragmentation, the importance of target fragmentation studies was

emphasized by **M. Strikman** who showed that they would give access to "conditional parton distributions" – a very rich and so far practically unexplored field. **M. Anselmino** showed how studies of Λ production and polarization would give information both on nucleon structure and spin effects in fragmentation. **W. Melnitchouk** explained how measurements of (spin) structure functions in the resonance region could give new insight into the old issue of quark-hadron duality. In particular, it would be an interesting question whether duality can also be observed in SIDIS. Semi-inclusive physics at the EIC would also offer new possibilities in "precision QCD". **P. Nadolsky** presented one case study for "q_T resummations" in SIDIS. Measurements of transverse-momentum distributions in SIDIS would not only provide detailed tests of QCD, but would also give insights into certain non-perturbative effects.

- As amply demonstrated by HERA, ep collider physics also allows unique access to the small-x and/or small-Q^2 regime. **Steven Bass** reviewed Regge predictions for the small-x behavior of g_1 and discussed how one might observe their onset at the EIC. He also discussed the impact EIC would have on the high-energy part of the Drell-Hearn-Gerasimov sum rule. **M. Stratmann** presented updated studies that show how one could pin down the parton content of polarized *photons* at the EIC. Clearly the EIC would be in a unique position here.

- **M. Grosse-Perdekamp** showed that the EIC would give precision information on transversity, making use of the Collins effect. Such studies would be extensions of ongoing efforts at HERMES.

- The EIC would also be optimal for measurements of deeply virtual Compton scattering (DVCS) and of hard exclusive meson production. **A. Belitsky** gave an overview of theoretical results in this field, emphasizing the importance of angular observables. **B. Fox** discussed the experimental situation today and the implications for the EIC.

The polarized gluon distribution from present and prospective future g_1 measurements

Jechiel LICHTENSTADT

School of Physics and Astronomy
The Raymond and Beverly Sackler Faculty of Exact Sciences
Tel Aviv University, 69978 Tel Aviv, ISRAEL *

We present an updated QCD analysis in next to leading order in α_s of all available g_1 spin structure function data. The first moment of the polarized gluon distribution is determined from the fit with a statistical error of 30%. The results of the fit are used to project measurements in the kinematic region of an electron-proton collider such as suggested by the e-RHIC project or a polarized HERA. The new data obtained from a collider like e-RHIC will improve our knowledge on the low x behavior of g_1 and will further reduce the error on the first moment of the polarized gluon distribution to about 10%. Including di-jet asymmetries data in a global fit will further reduce the error to about 6%.

1. INTRODUCTION

The measurement of the spin structure function of the proton g_1^p by the EMC [1] and the conclusion about the small fraction of the nucleon spin carried by the valence quarks has triggered a new series of experiments. The experiments aimed to reduce the statistical and systematic uncertainties on the measurements, to extend the kinematic range of the data and obtain data on both, the neutron and the proton and thereby test experimentally the Bjorken sum rule. Measurements were performed initially by the SMC at CERN [2] which extended the x range of the data down to $x = 5 \cdot 10^{-3}$ and by the E142 and E143 collaborations at SLAC [3,4]. The last g_1 data on the proton, deuteron and the neutron obtained by E155 and E154 at SLAC [5–7] as well as the HERMES [8,9] collaboration at DESY bring to a conclusion the second generation of polarized deep inelastic scattering experiments which followed EMC. The E155 and E154 data extend the former SLAC data of E143 and E142 [4,3] to lower x and provide a measurement at higher Q^2 values, thus adding important data to the global QCD analysis of g_1 data. The new HERMES data while not extending the kinematic region of the SLAC experiments provide an important and independent consistency check of the data.

The data cover now the entire kinematic range accessible by present day accelerators which are capable of providing polarized beams. Extending further the kinematic range will require new machines, possibly colliders of polarized beams.

On the theoretical side, the new data have induced much activity. In QCD the treatment of g_1 follows closely that of the unpolarized structure functions and parton distributions. The evolution of the parton distributions is given by the Altarelli-Parisi equations [10], for which the coefficient functions and the splitting functions have been computed to next-to-leading-order [NLO] in α_s [11,12] , thus allowing for a consistent QCD analysis in NLO of scaling violations in the spin dependent structure functions [13–16]. The polarized gluon distribution obtained from the fit provides the first information on the contribution of the polarized gluons to the nucleon spin. Such analyses were carried out by several theoretical groups [13–16] as well as by the SMC [17].

It is timely than, at the end of the second era of polarized deep inelastic scattering experiments,

*This work is supported by The Israel Science Foundation founded by The Israel Academy of Sciences and Humanities.

to repeat the QCD analysis performed on the g_1 data and include all the new (recent) data which were not available in the SMC analysis. Furthermore, one can use the results of such analysis to make projections of the expected measurements in proposed future machines. This approach has been used in the past to evaluate the impact of g_1 measurements in a polarized HERA [18–20].

2. QCD ANALYSIS OF g_1 DATA

The QCD analysis has been done following Ball Forte and Ridolfi [13] including all available g_1 data on the proton, deuteron and the neutron (from ^{3}He measurements) [1–9]. Using the DGLAP equations parton distributions, parameterized at an initial scale Q_0^2 are evolved to the Q^2 value of the experimental data at the measured x, thereby fitting the initial parameterization to the data. The form for each parton distribution at the initial scale (Q_0^2=1 GeV^2) was taken as:

$$\Delta f = N(\alpha_f, \beta_f, a_f, \rho_f)\eta_f x^{\alpha_f}(1-x)^{\beta_f}(1 + a_f x + \rho_f\sqrt{x})$$

where N is a normalization factor ($\int_0^1 N x^\alpha (1-x)^\beta (1 + ax + \beta\sqrt{x})\mathrm{d}x = 1$) and η_f is the first moment of the Δf. The analysis has been carried out in the AB scheme [13]. Our results [21] for the first moments of the singlet parton distribution and the polarized gluon distribution are:
$\eta_q = 0.40 \pm 0.02$ $(\Delta\Sigma \pm \delta(\Delta\Sigma))$
$\eta_g = 0.63^{+0.20}_{-0.19}$ $(\Delta g \pm \delta(\Delta g))$
Errors are statistical only.

It is interesting to note that the statistical error on the first moment of the polarized gluon distribution is about 30%. The systematic error is essentially the same as that determined in the QCD analysis performed by the SMC [17]. The results of the fits are compared to the data in the attached figures.

3. PROSPECTIVE MEASUREMENTS AT e-RHIC AND HERA

The results of the QCD analysis were used to project values of measurements in the extended kinematic region which may become possible in the future and examine their impact on the determination of Δg. Two future machines were considered:

- A new electron-proton collider at RHIC (e-RHIC) [22] with beam energies of E_p=250 GeV and E_e=10 GeV.

- Polarized HERA [23], with polarized electron (available) and proton beams of 27 and 820 GeV respectively.

The estimates were done assuming beam polarizations of 0.7 for both beams, and detector parameters similar to those of H1 at HERA. A total integrated luminosity of $\mathcal{L} = 12.6$ fb^{-1} was assumed for the expected e-RHIC data and $\mathcal{L} = 500$ pb^{-1} for HERA. If such machines are constructed these integrated luminosities should be obtainable in three years according to the design parameters.

The parton distributions from the QCD analysis were used to project the g_1 values at the extended kinematic region, and the statistical errors were estimated according to the detector and machine parameters. The projected *'data'* were then added to the real data and the QCD analysis was repeated to asses the uncertainty on the polarized gluon distribution deduced from the scaling violation in g_1.

The new g_1 data with its extended kinematic region will reduce significantly the uncertainty on the first moment of the polarized gluon distribution in the nucleon, Δg:

- Inclusion of projected HERA data with an integrated luminosity of $\mathcal{L} = 500$ pb^{-1} will result with:
  $\Delta g = 0.6 \pm 0.14$
  $\Delta\Sigma = 0.40 \pm 0.02$

- Inclusion of projected e-RHIC data with an integrated luminosity of $\mathcal{L} = 12.6$ fb^{-1} will result with:
  $\Delta g = 0.7 \pm 0.08$
  $\Delta\Sigma = 0.41 \pm 0.015$

The estimated errors are statistical only.

4. COMBINED ANALYSIS OF g_1 AND DI-JET ASYMMETRIES DATA

New experiments which measure processes in which Δg contributes in leading order, such as COMPASS at CERN or RHIC-Spin are underway. These data will provide us with a direct measurement of $\Delta g(x)$. Future facilities will enable measurements of two-jet asymmetries where Δg contributes in leading order as well. These data which will determine the shape of the gluon distribution, can also be included in the QCD analysis in a self-consistent way [20]. They will constrain the (presently) assumed shape of the polarized gluon distribution as well as reduce the uncertainty on its first moment. The expected uncertainties on the di-jet asymmetries were evaluated by Rädel and DeRoeck [24]. They are shown in the attached figures. Including such di-jet asymmetries in the QCD analysis, will further reduce the uncertainty on the first moment of the the polarized gluon distribution: $\Delta g = 0.6 \pm 0.04$

The expected uncertainties on the polarized gluon distribution which will be obtained from QCD analysis of present and future data are summarized in the attached table.

REFERENCES

1. EMC, J. Ashman *et al;* Nucl. Phys. **B 328** (1989) 1.
2. B. Adeva *et al;* Phys. Rev. **D58** (1998) 112001.
3. E-142 P. L. Anthony *et al;* Phys. Rev. **D 54** (1996) 6620.
4. E-143, K. Abe *et al;* Phys. Rev. **D 58** (1998) 112003.
5. E-155, P. L. Anthony *et al;* Phys. Lett **B 493** (2000) 19.
6. E-155, P. L. Anthony *et al;* Phys. Lett **B 463** (1999) 339.
7. E-154 K. Abe *et al;* Phys. Rev. Lett. **79** (1997) 26.
8. HERMES Coll. K. Ackestaff *et al;* Phys. Lett **B 404** (1997) 383.
9. HERMES Coll. A. Airapetian *et al;* Phys. Lett **B 442** (1998) 484.
10. V. N. Gribov and L. N. Lipatov, Sov. J. Nucl. Phys. **15** (1972) 438; **15** (1972) 675; G. Altarelli and G. Parisi Nucl. Phys. **B 126** (1977) 298; Yu. L. Dokshitzer, Sov. Phys. JETP **46** (1977) 641.
11. J. Kodaira *et al;* Phys. Rev. **D 20** (1979) 627; J. Kodaira, Nucl. Phys. **B 165** (1980) 129.
12. R. Mertig and W. L. van Neerven Z. Phys. **C 70** (1996) 637; W. Vogelsang, Nucl. Phys. **B 475** (1996) 47.
13. R. D. Ball, S. Forte and G. Ridolfi Phys. Lett. B378 (1996) 255
14. M. Glück et al., Phys. Rev. D53 (1996) 4775.
15. T. Gehrmann and W. J. Stirling Z. Phys. C65 (1995) 461; Phys. Rev D53 (1996) 6100.
16. G. Altarelli et al., Nucl. Phys. B 496 (1997) 337
17. SMC, B. Adeva *et al;* Phys. Rev. **D58** (1998) 112002.
18. R. Ball, et al., Workshop on Future Physics at HERA, G. Ingelman, A. DeRoeck and R. Klanner Ed. DESY Hamburg Germany 1995-1996.
19. A. Deshpande, V. W. Hughes and J. Lichtenstadt Workshop on Deep Inelastic Scattering off Polarized Targets J. Blümlein et al; Eds. DESY Zeuthen Germany. Sept 1997
20. A. De Roeck, A. Deshpande, V. W. Hughes, J. Lichtenstadt and G. Rädel, Eur. Phys. **J C 6** (1999) 121.
21. J. Lichtenstadt, Nucl. Phys. **B** (Proc. Suppl.) **105** (2002) 86. Workshop on the spin structure of the proton and polarized collide physics, D. Bass, A. DeRoeck and A. Deshpande Ed. Trento, Italy, July 2001.
22. The 2nd eRHIC Workshop, L. McLerran *et al;* Yale University April 2000. BNL-52592 Formal Report.
23. Workshop on Future Physics at HERA, G. Ingelman, A. DeRoeck and R. Klanner Ed. HERA, Hamburg Germany 1995-1996.
24. G. Rädel and A. De Roeck, Nucl. Phys. **B** (Proc. Suppl.) **105** (2002) 90.

QCD Analysis of Spin Structure Function Data from Present Data and Prospective Measurements

Jechiel LICHTENSTADT

School of Physics and Astronomy
The Raymond and Beverly Sackler
Faculty of Exact Sciences
Tel Aviv University, 69978 Tel Aviv, Israel

The Electron Ion Collider
Workshop

Brookhaven National Laboratory

Feb. 2002

NEW QCD fit in NLO of world data

- Use only data with $Q^2 > 1$ **GeV**^{2}
- Fit results at $Q^2 = 1$ GeV^2 (preliminary):

$\eta_q = 0.40 \pm 0.02 \quad (\Delta\Sigma \pm \delta(\Delta\Sigma))$
$\alpha_q = 1.6 \pm 0.2$
$\beta_q = 4.4 \pm 0.4$
$a_q = 0.0$ (Fixed)
$\rho_q = 0.0$ (Fixed)

$\eta_g = \mathbf{0.63^{+0.20}_{-0.19}} \quad (\ \Delta g \pm \delta(\Delta g))$
$\alpha_g = -0.15 \pm 0.21$
$\beta_g = 4.0$ (Fixed)
$a_g = 7.4 \pm 0.7$
$\rho_g = -5.6 \pm 0.3$

$\eta_{NS}^{p(n)} = (-)0.75 g_A + 0.25 a_8$
$\alpha_{NS}^p = -0.75 \pm 0.07$
$\beta_{NS}^p = 2.4 \pm 0.1$
$a_{NS}^p = 27.5 \pm 14.8$
$\alpha_{NS}^n = 0.01 \pm 0.1$
$\beta_{NS}^n = 2.5 \pm 0.4$

$\chi^2 = 194.5$ for 174 deg. of freedom

NLO Fit to World-Data
(Preliminary)

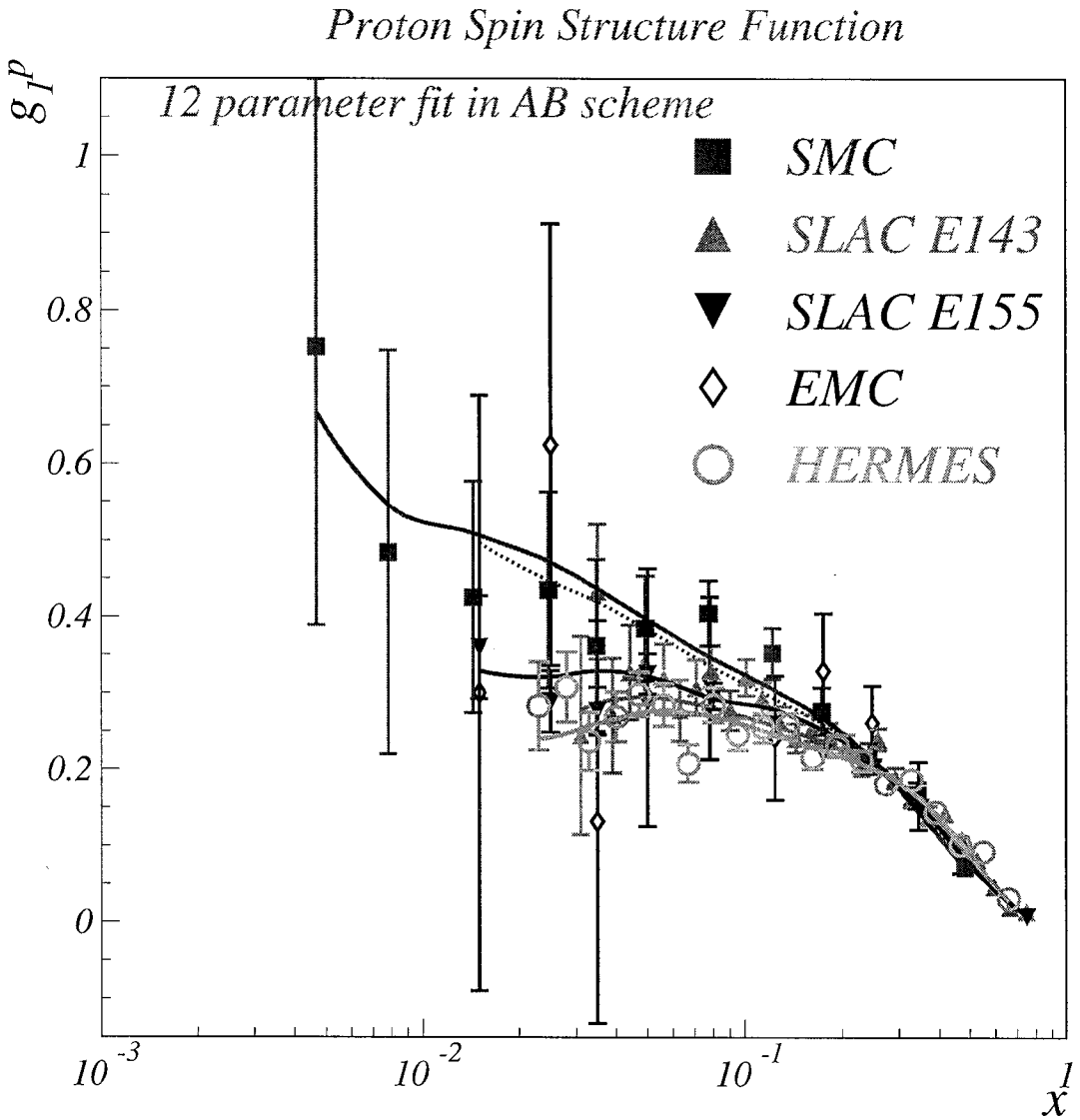

NLO Fit to World-Data (Cont.)

(Preliminary)

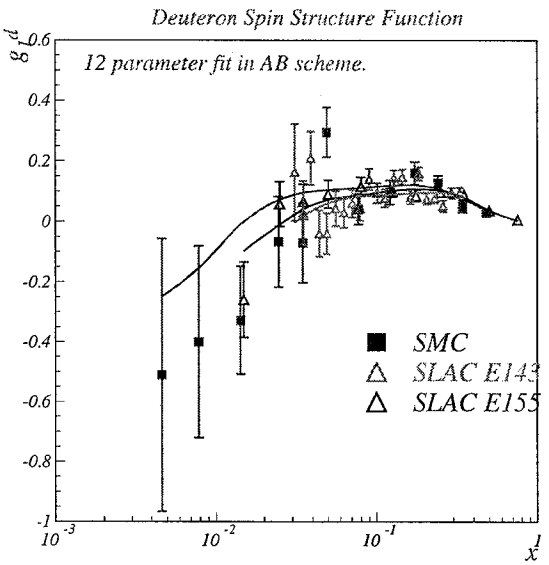

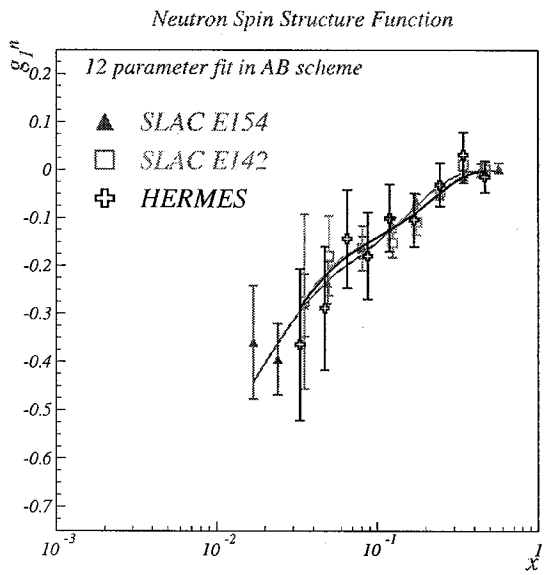

Parton Distributions

AB scheme

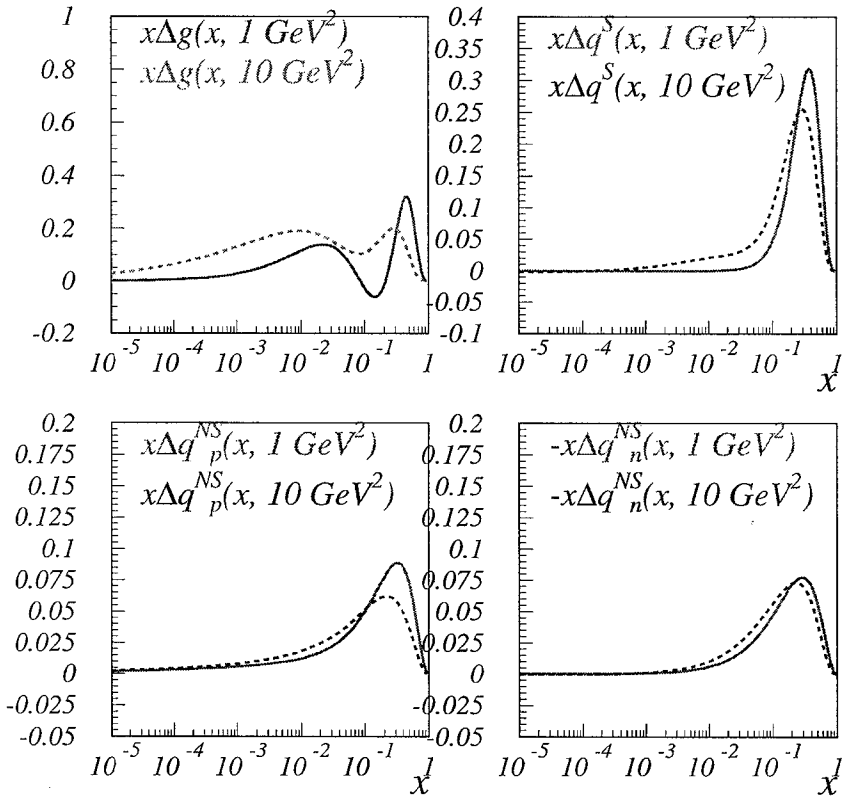

(PRELIMINARY)

Fit to world data and e-RHIC projections

Three years - 12.6 fb^{-1}

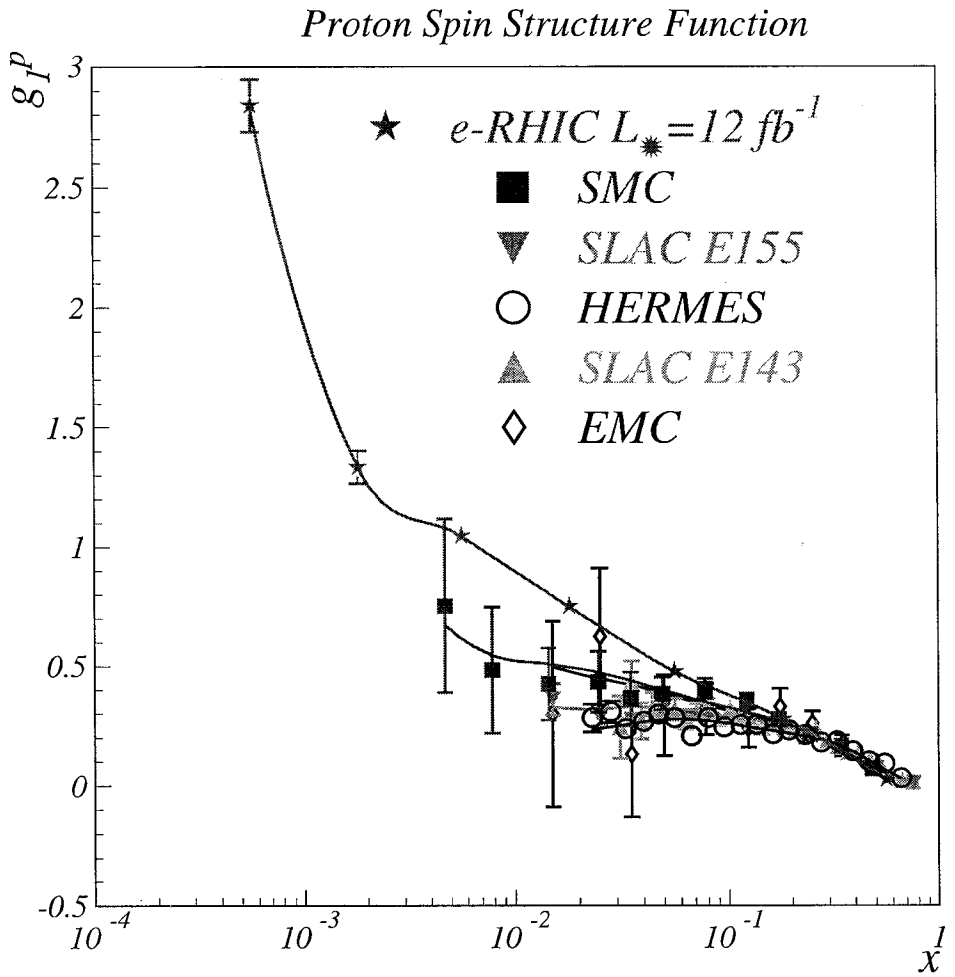

From QCD analysis (in NLO) at 1 GeV^2:

$$\eta_g = \int_0^1 \Delta g(x)\mathrm{d}x = 0.7\ ^{+0.08}_{-0.08}\ \text{(statistical)}$$

$$\eta_q = \Delta\Sigma = 0.41 \pm 0.015\ \text{(statistical)}$$

Combined analysis of g_1 and 2-jet data

A. Polarized gluon distribution Δg

From QCD analysis (in NLO) at 1 GeV^2:
$\mathcal{L} = \mathbf{12.6\ fb^{-1}}$

$$\eta_g = \int_0^1 \Delta g(x)\mathrm{d}x = 0.64 \pm 0.04 \text{ (statistical)}$$

$$\eta_q = \Delta\Sigma = 0.40 \pm 0.02 \text{ (statistical)}$$

B. Sensitivity to the shape of Δg

Polarized gluon distributions
Fits compared to $\Delta g(x)$ from 2-jet asymmetries

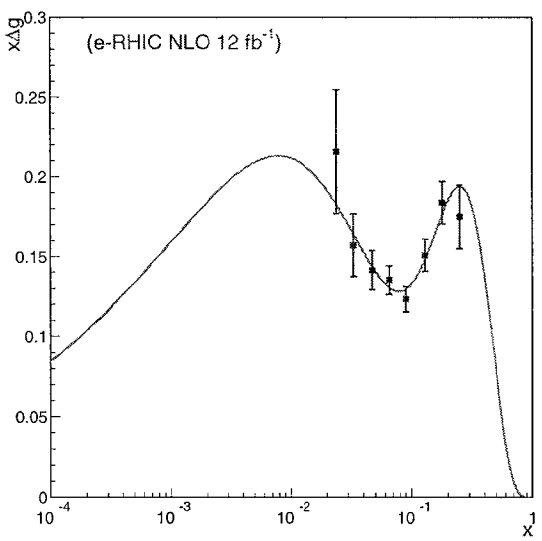

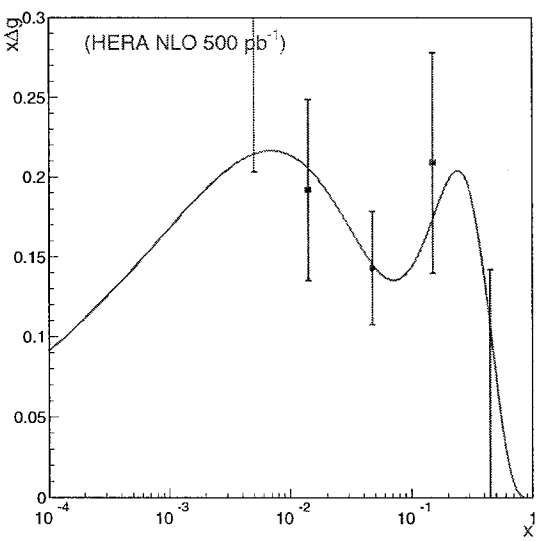

- **Experiments in a polarized collider (e-RHIC or pol-HERA) which will include also measurements of di-jet asymmetries are expected to determine the polarized gluon distribution with about 7% accuracy as well as constrain its shape.**

Data used	$\delta(\int \Delta g)$	$\delta(\int \Delta q_S)$
QCD Anal. g_1 data ("D")	± 0.20	± 0.02
"D" + e-RHIC g_1^p ($420 pb^{-1}$)	± 0.15	± 0.02
"D" + e-RHIC g_1^p ($4.2 fb^{-1}$)	± 0.10	± 0.02
"D" + e-RHIC g_1^p ($12.6 fb^{-1}$)	± 0.08	± 0.016
"D" + HERA g_1^p ($500 pb^{-1}$)	± 0.15	± 0.02
"D" + HERA g_1^p + Δg-jets	± 0.10	± 0.02
"D" + e-RHIC g_1^p + Δg-jets (12.6 fb^{-1})	± 0.04	± 0.014

g_1 at low x and low Q^2 with Polarized ep Colliders

S.D. Bass[a]

[a]ECT*, Strada delle Tabarelle 286, I-38050 Villazzano, Trento, Italy

Measurements of g_1 at low x and low Q^2 are expected to provide a sensitive probe of the transition from Regge to perturbative QCD dynamics, offering a new testing ground for models of small x physics. We discuss the potential of the EIC to investigate this physics — varying Q^2 between 0.01 and 1 GeV^2 — and to constrain the high-energy part of the Drell-Hearn-Gerasimov sum-rule for polarized photoproduction.

1. Physics issues and EIC

The transition region

The HERA measurements of the proton structure function $F_2(x, Q^2)$ at low x and low Q^2 (less than 1 GeV^2) [1] mark the transition between Regge "confinement physics" and perturbative QCD. For fixed Q^2 up to 0.65GeV^2 the measured large $s_{\gamma p} \sim Q^2/x$ behaviour of F_2 is consistent with the expectations of Regge phenomenology. For values of Q^2 greater than 1GeV^2 the F_2 data is well described by DGLAP evolution and rises faster with decreasing x than the soft Regge prediction. The "transition region" between photoproduction and deep inelastic scattering and the onset of perturbative QCD is a subject of much current interest.

The small x behaviour of nucleon structure functions $f(x, Q^2)$ is often described in terms of an effective intercept λ ($f(x, Q^2) \sim x^{-\lambda}$ at small Bjorken x) which changes between 0.1 and 0.35 for unpolarized data as we increase Q^2 from zero to about 100 GeV^2.

In the transition from photoproduction to deep inelastic values of Q^2 much larger changes are expected in the effective intercept for the g_1 spin dependent structure function compared to the spin independent structure function F_2 [2]. For example, the soft Regge prediction for the isotriplet part of g_1 has $g_1^{(p-n)} \sim x^{0.4}$ if we make the usual assumption of a straight line a_1 Regge trajectory running parallel to the (ρ, ω) trajectories. In contrast, the best fit to the SLAC "small x" data between $0.01 < x < 0.1$ has $g_1^{(p-n)}$ rising as $x^{-0.5}$. The soft Regge prediction is unstable to perturbative QCD evolution, which tends to shift the weight of the distribution to smaller Bjorken x as we increase Q^2. However, the size of the change in the effective intercept is both large and also almost required for $g_1^{(p-n)}$ to accomodate the large area fixed by the Bjorken sum-rule — that is, the size of $g_A^{(3)}$ – a non-perturbative constraint [3]. Similar large changes are expected in the isosinglet part of g_1 which is directly sensitive to polarized gluonic degrees of freedom.

Open questions which may be addressed with the EIC are: At which Q^2 does the effective intercept for g_1 start to grow ? What is the rate of growth with increasing Q^2 ? Where in Q^2 will perturbative QCD start to describe future g_1 data at small x ?

The more dramatic expected effects in g_1 will, if confirmed, yield new challenges for models which aim to describe the Regge to hard Q^2 transition.

Drell-Hearn-Gerasimov sum-rule

Polarized photoproduction measurements at the EIC would constrain our knowledge of spin dependent Regge theory and put an upper bound on the high-energy Regge contribution to the Drell-Hearn-Gerasimov sum-rule. This sum-rule relates the difference $(\sigma_A - \sigma_P)$ to the square of the anomalous magnetic moment of the target nucleon:

$$-\frac{4\pi^2\alpha\kappa^2}{2m^2} = \int_{\nu_{th}}^{\infty} \frac{d\nu}{\nu}(\sigma_A - \sigma_P)(\nu). \qquad (1)$$

Here ν is the LAB energy of the exchanged photon, m is the nucleon mass and κ is the anomalous magnetic moment. The DHG sum-rule is derived from fundamental principles plus a single assumption that the spin-dependent part of the forward Compton amplitude satisfies an unsubracted dispersion relation. Regge theory suggests that DHG integrand is expected to converge — failure would imply the presence of a $J = 1$ Regge fixed pole or "subtraction at infinity". Such an effect is outside perturbation theory. Failure of the DHG sum-rule would imply new non-perturbative phenomena at work in the spin structure of the proton.

It is intriguing that the present preliminary data from the Bonn-Mainz experiment for the proton target up to $E_\gamma = 1.8$GeV seem to be converging to a value about $-220\mu b$ or two standard deviations greater than the DHG prediction [4]. Phenomenological Regge based estimates [5] suggest that $25 \pm 10\mu$b (about 10%) of the sum-rule may come from $s_{\gamma p}^{1/2} > 2.5$GeV. These Regge estimates, if confirmed, would be sufficient to resolve the sum-rule but require a sign change in $(\sigma_A - \sigma_P)$ between E_γ about 1.8 and 3.0 GeV. SLAC experiment E-159 expect to measure the DHG integrand between $s_{\gamma p}^{1/2}$ between 3.3 and 9 GeV (E_γ between 5 and 40 GeV) in 2006. EIC could extend these measurements to $20 < s_{\gamma p}^{1/2} < 90$GeV. Further exploration and new measurements at higher-energy are clearly necessary!

Figure 5 attached shows an estimated of projected low Q^2 asymmetries assuming different proposed Regge behaviours in comparison with the expected precision achievable with both the EIC and polarized HERA colliders [2]. For EIC access to the low Q^2 region becomes easier. Due to the different beam energies electrons from DIS events with a Q^2 of 0.1 GeV^2 scatter at an angle of 2 degrees or more, which allows them to be accepted within the central detector. Special beam-pipe calorimeters and trackers are only required for the region $0.01 < Q^2 < 0.1$ GeV^2. The higher luminosity of RHIC and larger azimuthal acceptance will allow one to measure the asymmetries 10-15 times more precisely, but in a kinematic range where, for the same Q^2, x is 10 times larger than for HERA.

2. Summary

Exploration of the transition region between polarized photoproduction and deep inelastic scattering, $0 < Q^2 < 1$GeV^2, looks feasible with Polarized EIC and HERA. Polarized photoproduction measurements at these colliders would constrain our knowledge of spin dependent Regge theory and put an upper bound on the high-energy Regge contribution to the Drell-Hearn-Gerasimov sum-rule. Much larger changes in the effective intercept for the spin dependent structure function g_1 at small x than for spin independent F_2 are expected. A dedicated measurement at Polarized EIC or HERA would impose new constraints on QCD based models of the transition from Regge theory to perturbative QCD with increasing Q^2 at fixed low x.

With appropriate small angle tagging detectors in both the electron and proton direction at EIC very precise data on asymmetries can be collected, which will be important in the progress of this data driven field to the study of the strong interaction. Hence, having such detector coverage included in design of a new detector for measuring ep and eA collisions at EIC is strongly encouraged. The use of deuteron beams with spectator tagging could help to disentangle different exchange contributions in the Regge regime.

I thank A. De Roeck and M. Brisudova for collaboration on the issues discussed here.

REFERENCES

1. B. Surrow, hep-ph/0201025.
2. S.D. Bass and A. De Roeck, Eur. Phys. J C18 (2001) 538; hep-ph/0008289.
3. S.D. Bass, Eur. Phys. J A5 (1999) 17; hep-ph/9902280.
4. K. Helbing, NUcl. Phys. B (Proc. Suppl.) 105 (2002) 113.
5. S.D. Bass and M. Brisudova, Eur. Phys. J A4 (1999) 251; N. Bianchi and E. Thomas, Phys. Lett. B450 (1999) 439.

SDB, A D Roeck
EPJ C18 (2001) 531

g_1 at low x and low Q^2 with polarized ep colliders

Steven Bass

Physics issues

- Regge → perturbative QCD transition @ low Q^2

$$g_1 \sim x^{\alpha_{eff}}$$

$$\Delta\alpha_{eff}^{spin} \sim 5\,\Delta\alpha_{eff}^{(F_2)}$$

how fast? what Q^2?

- DHG sum-rule at $Q^2 = 0$

$$\int_{\nu_{th}}^{\infty} \frac{d\nu}{\nu}\,\Delta\sigma(\nu) = -\frac{2\pi^2\alpha\,\kappa^2}{m^2}$$

Assuming no "subtraction @ ∞" ($J=1$ Regge fixed pole)

Constrain high-energy part of sum-rule

BASS

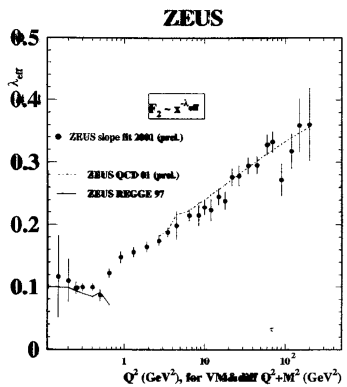

Figure 8: *ZEUS preliminary results on $\lambda_{eff} = \lambda(Q^2)$ as a function of Q^2. The estimates of the ZEUS Regge97 and ZEUS QCD01 parameterizations are also shown.*

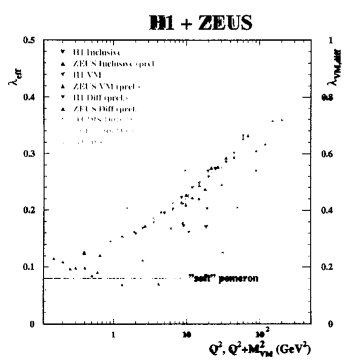

Figure 9: *Compilation of various slope analyses from the H1 and ZEUS Collaborations on the energy dependence of the respective cross-sections: inclusive results (Inclusive), vector-meson results (VM), inclusive diffractive results (Diff) and deeply-virtual Compton scattering results (DVCS).*

ZEUS

$$\sigma_{tot}^{\gamma^* p}(s,Q^2) = \frac{M_0^2}{M_0^2+Q^2}\left(A_R s^{\alpha_R - 1} + A_\rho s^{\alpha_\rho - 1}\right)$$

+0.5 1.102 ± .007

.52 ± .04 GeV^2

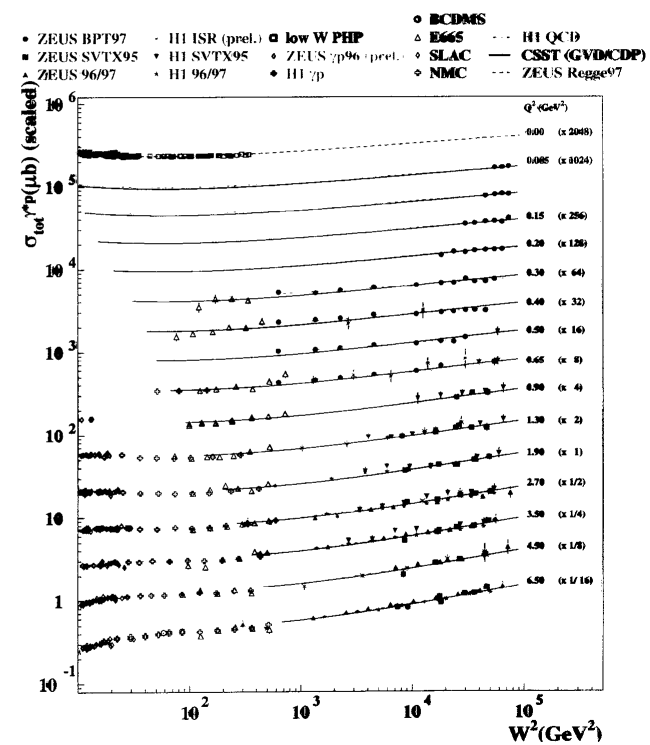

Figure 3: *$\sigma_{tot}^{\gamma^* p}$ as a function of W^2 for different values of Q^2.*

Isotriplet Structure Functions

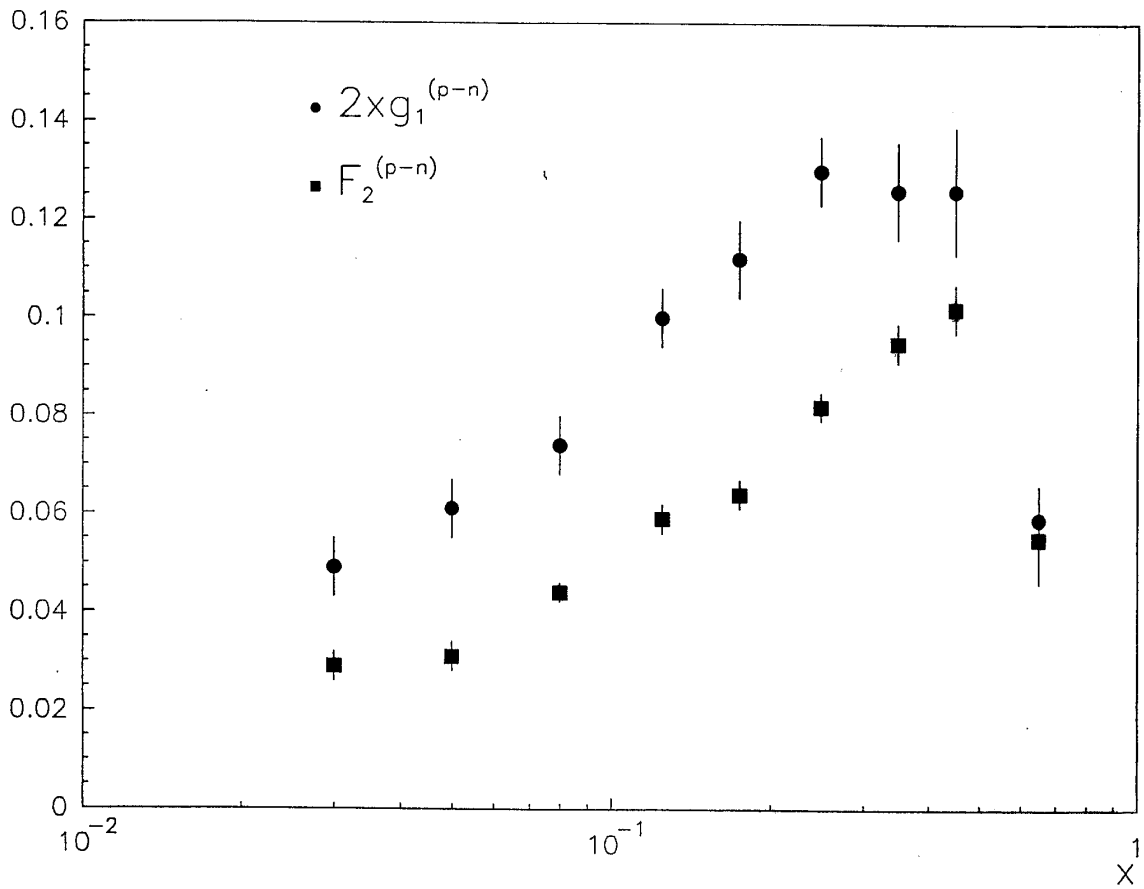

g_1^p E-143

g_1^n E-154

$\Big\}\ Q^2 = 5\ GeV^2$

F_2^{p-n} NMC $Q^2 = 4\ GeV^2$

Isotriplet Structure Functions

$$R_3 = \frac{2x\, g_1^{(p-n)}}{F_2^{p-n}}$$

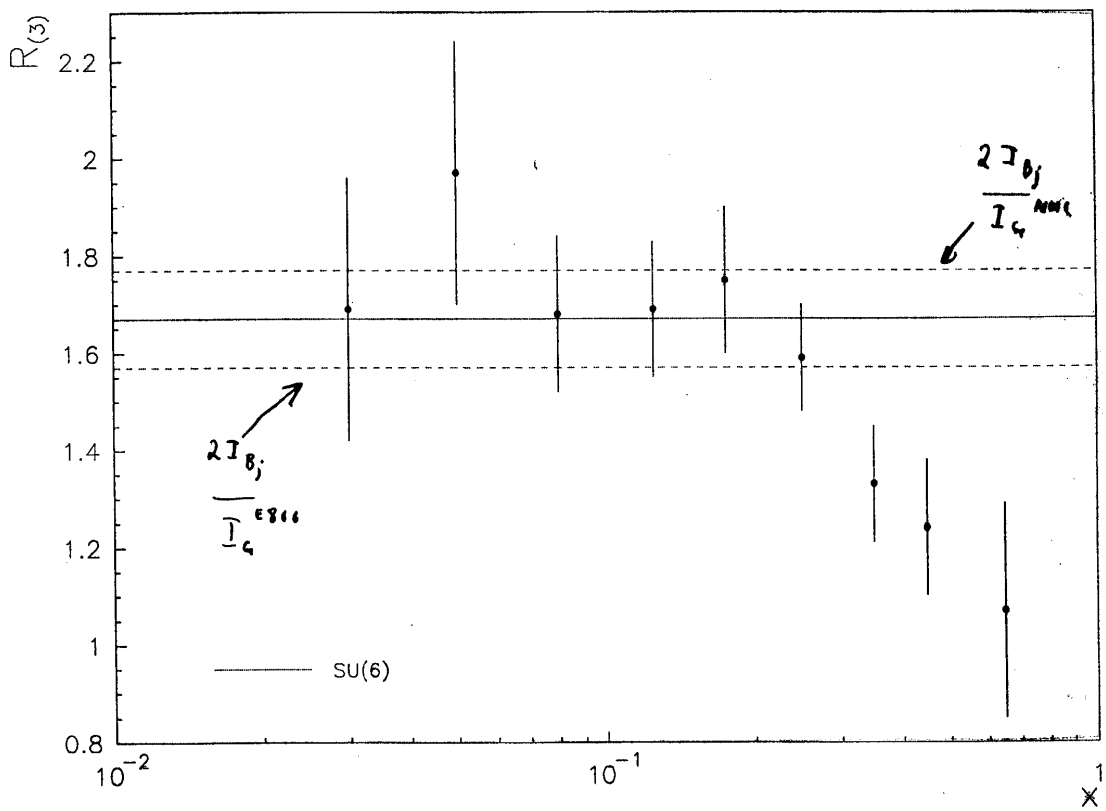

SU(6) predicts $\frac{5}{3}$

QCD Counting Rules predict $R_3 \to 1$ when $x \to 1$

Regge predicts $R_{(3)} \sim x$, $x \to 0$

Estimating asymmetries

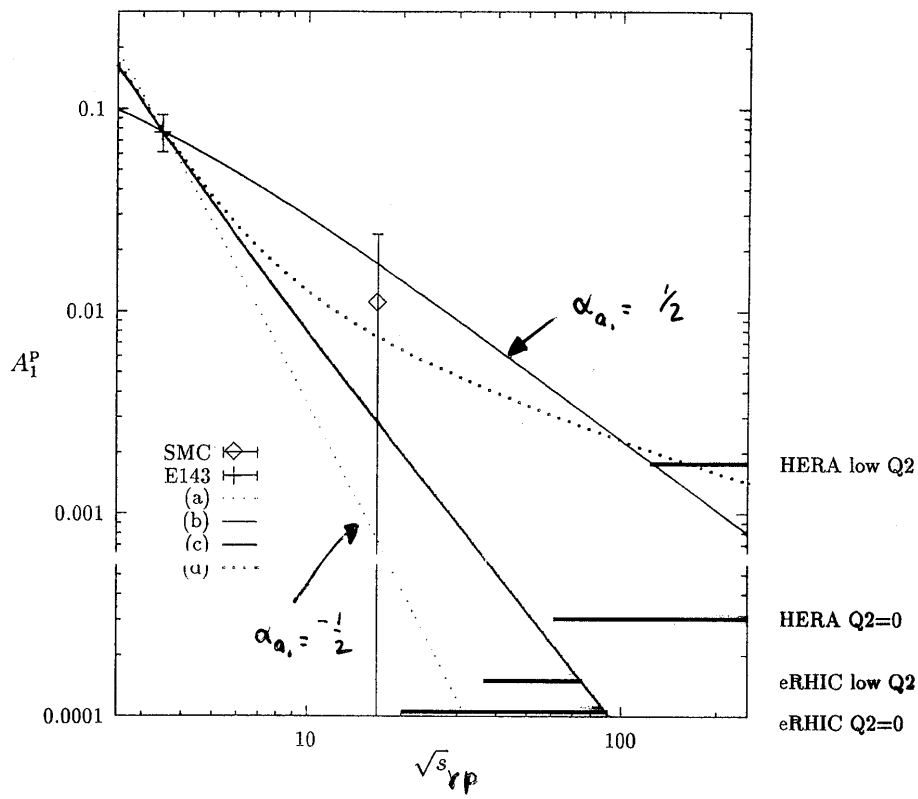

Reggé

$$\Delta\sigma = N_3\, s^{\alpha_{a_1}-1} + N_0\, s^{\alpha_{f_1}-1} + N_g \frac{\ln s/\mu^2}{s} + N_p \frac{1}{\ln^2 s/\mu^2}$$

Isotriplet

$N_3^p = -N_3^n$

Isosinglet

Probing the spin structure of the photon at the EIC†

Marco Stratmann[a] and Werner Vogelsang[b]

[a] Institut für Theoretische Physik, Universität Regensburg, D-93040 Regensburg, Germany
[b] RBRC and Physics Department, Brookhaven National Laboratory, Upton, NY 11973-5000

Nothing is known experimentally about the parton content of circularly polarized photons, defined by $\Delta f^\gamma(x,Q^2) \equiv f_+^{\gamma+}(x,Q^2) - f_-^{\gamma+}(x,Q^2)$, where $f_+^{\gamma+}$ ($f_-^{\gamma+}$) denotes the density of a parton f with helicity '+' ('−') in a photon with helicity '+'. The present round of spin experiments, HERMES, COMPASS, and RHIC, is not sensitive to these distributions either. The Δf^γ contain information different from that included in the unpolarized ones, f^γ, and their measurement is vital for a *complete* understanding of the partonic structure of photons. It has been demonstrated [1] that measurements of the structure function g_1^γ and of di-jet spin asymmetries at a future polarized linear e^+e^- collider can provide valuable information about Δf^γ. Also HERA, after an upgrade to polarization for both the electron and the proton beam, could be in the position to shed some light on the Δf^γ, the preferred tool being the study of "resolved"-photon contributions to the spin asymmetry for (di-)jet photoproduction [2]. This presentation extends the previous HERA studies to the case of the EIC with a c.m.s. energy of $\sqrt{S_{\rm ep}} = 100$ GeV. Again we will exploit the predictions of two very different models for the Δf^γ [3], and study the sensitivity of (di)-jet production to these unknown quantities. For the "maximal scenario" we saturate the positivity bound $|\Delta f^\gamma(x,Q^2)| \leq f^\gamma(x,Q^2)$ at a low input scale $\mu \simeq 0.6\,\mathrm{GeV}$, using the GRV f^γ densities. The "minimal scenario" is defined by a vanishing hadronic input at the scale μ.

The generic expression for polarized resolved photoproduction of two jets with laboratory system rapidities η_1, η_2 and transverse momentum p_T reads in LO

$$\frac{d^3\Delta\sigma}{dp_T d\eta_1 d\eta_2} = 2p_T \sum_{f^e,f^p} x_e \Delta f^e(x_e,\mu_f^2) x_p \Delta f^p(x_p,\mu_f^2) \frac{d\Delta\hat{\sigma}}{d\hat{t}}\,, \tag{1}$$

where $x_e \equiv p_T/(2E_e)\,(e^{-\eta_1}+e^{-\eta_2})$ and $x_p \equiv p_T/(2E_p)\,(e^{\eta_1}+e^{\eta_2})$. The Δf^p and Δf^e in (1) denote the spin-dependent parton densities of the proton and electron, i.e., photon, respectively, see [2]. The key advantage of *di*-jet as compared to single-inclusive jet production is that a measurement of *both* jet rapidities allows for fully reconstructing the kinematics of the underlying hard subprocess and thus for determining $x_\gamma = x_e/y$ on an experimental basis, with y being the fraction of the electron's energy taken by the photon. In this way it becomes possible to "scan" the x-shape of Δf^γ. However, unfolding the Δf^γ from a jet-measurement would in general be a very involved task, since many subprocesses and combinations of parton densities contribute to the cross section. It was shown [4] that the ratios of the dominant unpolarized

†Talk presented by Marco Stratmann

LO subprocesses are roughly constant w.r.t. the c.m.s. scattering angle, such that the jet cross section factorizes approximately into some "effective parton densities" times a single partonic cross section. In the polarized case the situation is somewhat less clear, but the approximation still works surprisingly well at a level of $5-10\%$ accuracy. The appropriate effective densities are given by [2] $\Delta f^{\gamma}_{\rm eff} = \sum_q(\Delta q^{\gamma} + \Delta\bar{q}^{\gamma}) + \frac{11}{4}\Delta g^{\gamma}$ (see also ref. [5]) such that the polarized double resolved jet cross section can be expressed as $\Delta\sigma^{2-\rm jet} \simeq \Delta f^{\gamma}_{\rm eff} \otimes \Delta f^{p}_{\rm eff} \otimes \Delta\hat{\sigma}_{qq'\to qq'}$. It is only for large p_T that deviations from the exact results become more pronounced.

In general the lower energy of the EIC, as compared to HERA, has both advantages and disadvantages: spin asymmetries are generally expected to be larger at the EIC since – for a given jet transverse momentum – the parton densities are probed at somewhat higher x. On the other hand, event rates will be lower, with ensuing larger statistical uncertainties (assuming similar integrated luminosities for HERA and the EIC). Also, the resolved photon component we are interested in here generally becomes the less important, the smaller the energy of the interaction is. Nevertheless, our results show the trend that the advantages of having lower energies outweigh the disadvantages, so that the EIC appears superior to HERA concerning the potential for determining the Δf^{γ}. This is in particular true if one keeps in mind that we have assumed only a rather modest luminosity for our simulation concerning the EIC.

References

[1] M. Stratmann and W. Vogelsang, Nucl. Phys. Proc. Suppl. **82** (2000) 400.

[2] M. Stratmann and W. Vogelsang, Z. Phys. **C74** (1997) 641;
J.M. Butterworth, N. Goodman, M. Stratmann, and W. Vogelsang, in DESY-PROC-1998, p. 120.

[3] M. Glück and W. Vogelsang, Z. Phys. **C55** (1992) 353; ibid. **C57** (1993) 309;
M. Glück, M. Stratmann, and W. Vogelsang, Phys. Lett. **B337** (1994) 373.

[4] B.L. Combridge and C.J. Maxwell, Nucl. Phys. **B239** (1984) 429.

[5] D. Indumathi *et al.*, Z. Phys. **C56** (1992) 427.

To study the sensitivity to Δf^γ at future experiments it is sufficient to construct two *extreme* models:

$$|\Delta f^\gamma| \leq f^\gamma$$

'max.' input

$$\Delta f^\gamma(x, Q_0^2) = f^\gamma_{\mathrm{GRV}}(x, Q_0^2)$$

pure VMD input at Q_0

'min.' input

$$\Delta f^\gamma(x, Q_0^2) = 0$$

pointlike for all Q

$Q_0 \sim 0.6$ GeV

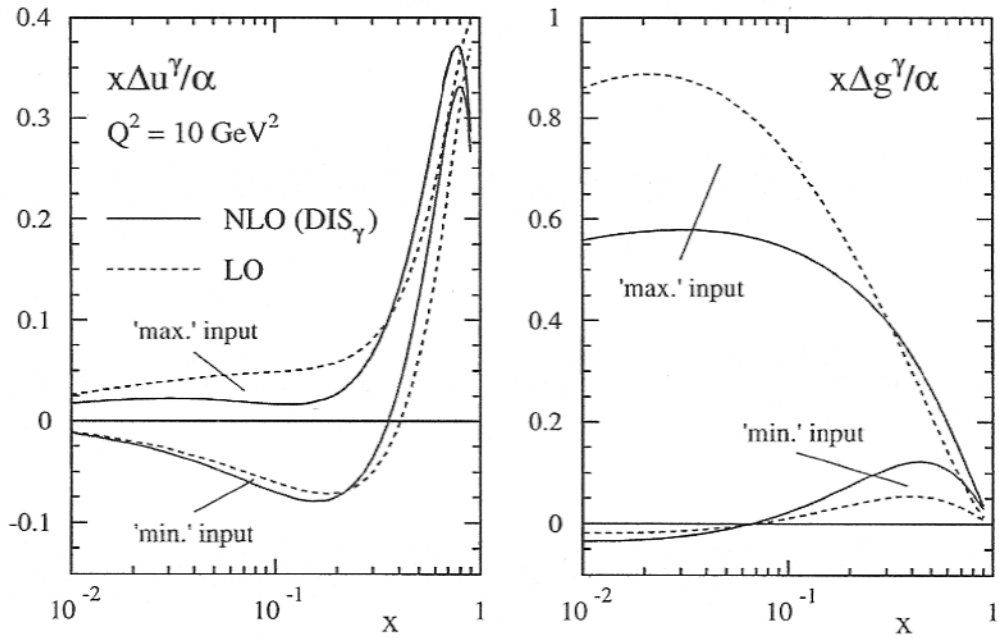

$\rightsquigarrow$ expect sizable (perhaps even sign) differences in spin asymmetries sensitive to our Δf^γ models

• Δf^γ @ future polarized $\vec{e}\vec{p}$ colliders

Δf^γ accessible via *resolved contr.* in photoproduction

general problem: suppression of unwanted direct-γ part

promising processes: Vogelsang, MS

· $\boxed{\vec{e}\vec{p} \to \text{jet} + X}$ (similar for $h^\pm + X$)

× only indirect direct/resolved 'separation' via

$(\Delta)\sigma_{\text{dir}}$ dominant $\eta_{\text{lab}} < 0$ $(\leftrightarrow x_\gamma \to 1)$
$(\Delta)\sigma_{\text{res}}$ for $\eta_{\text{lab}} > 0$ $(\leftrightarrow x_\gamma \ll 1)$

[positive η: proton direction]

✓ stable under NLO corrections de Florian, Frixione

· $\boxed{\vec{e}\vec{p} \to \text{jet}_1 + \text{jet}_2 + X}$

✓ reconstruction of x_γ possible:

define direct and resolved samples via x_γ-cut

old idea: Forshaw, Roberts

✓ LO QCD $\approx$ MC Butterworth, Goodman, WV, MS

extraction of Δf^γ from $\Delta\sigma/\sigma$:

· $\Delta\sigma/\sigma$ is complicated function of $\Delta f^{\gamma,p}$ and $(\Delta)\hat{\sigma}_{ij}$

idea: *effective* PDF's unpol.: Combridge, Maxwell

$\sigma_{\text{res}} \simeq f^\gamma_{\text{eff}} \otimes f^p_{\text{eff}} \otimes \hat{\sigma}_{qq' \to qq'}$ with $\boxed{f_{\text{eff}} = \sum(q + \bar{q}) + \frac{9}{4}g}$

· works fine in *pol. case* with $\ldots + \frac{11}{4}\Delta g$ WV, MS

• Di-jets @ $\vec{e}\vec{p}$ machines: overview & comparison

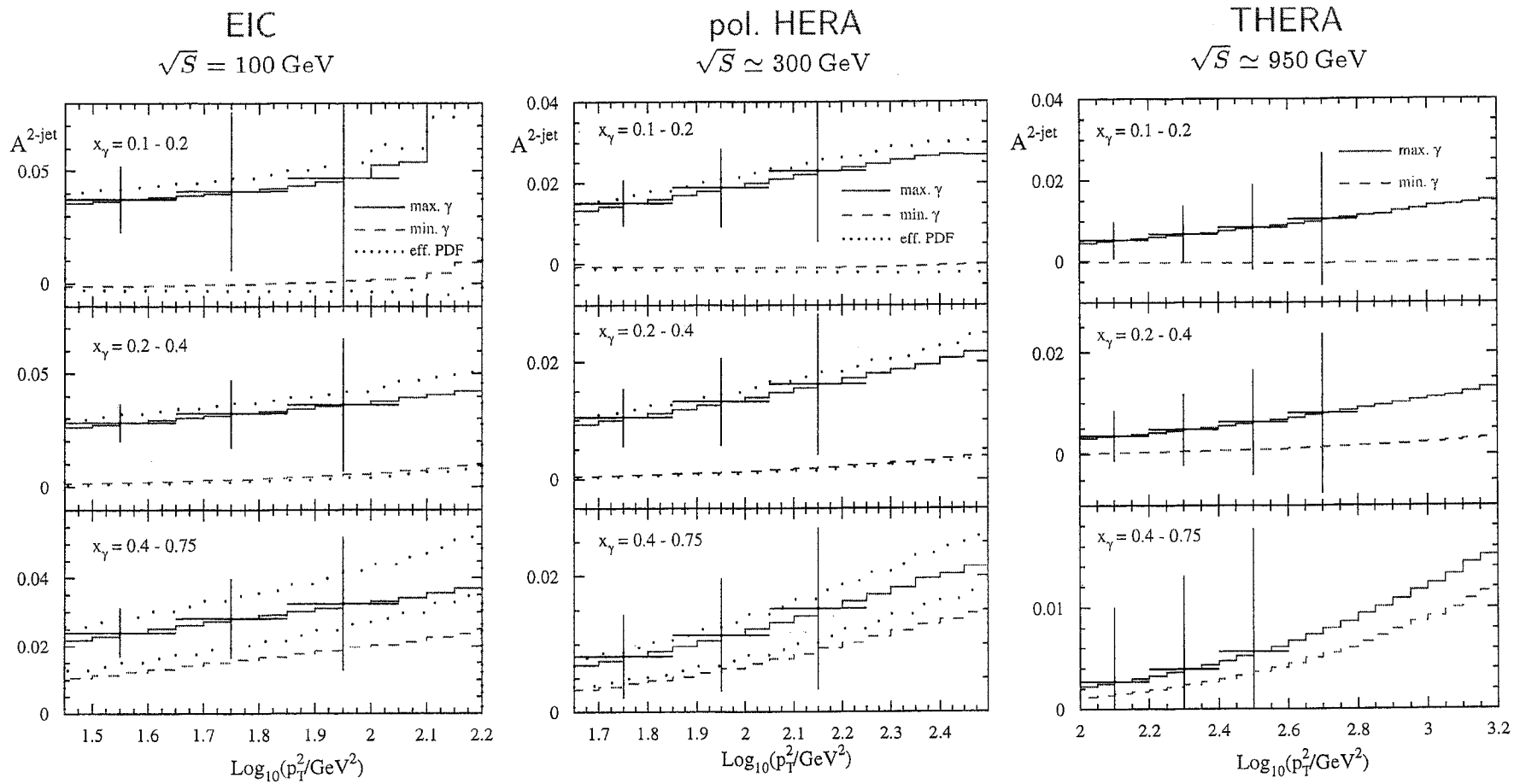

param. used: LO; Δf^p: GRSV; $\mu = p_T$; 'errors': $\mathcal{L} = 200\,\mathrm{pb}^{-1}$, $P_e = P_p = 0.7$; WW: $0.2 \leq y \leq 0.85$, $Q^2_{\max} = 4\ (1)\ \mathrm{GeV}^2$ (EIC)

$|\Delta\eta| \equiv |\eta_1 - \eta_2| \leq 1$, $0 < \frac{\eta_1+\eta_2}{2} < 2$ (EIC, pol. HERA) and $-1.5 < \frac{\eta_1+\eta_2}{2} < 1.5$ (THERA)

• 1-jet inclusive @ $\vec{e}\vec{p}$ machines: overview & comparison

EIC
$\sqrt{S} = 100\,\mathrm{GeV}$

pol. HERA
$\sqrt{S} \simeq 300\,\mathrm{GeV}$

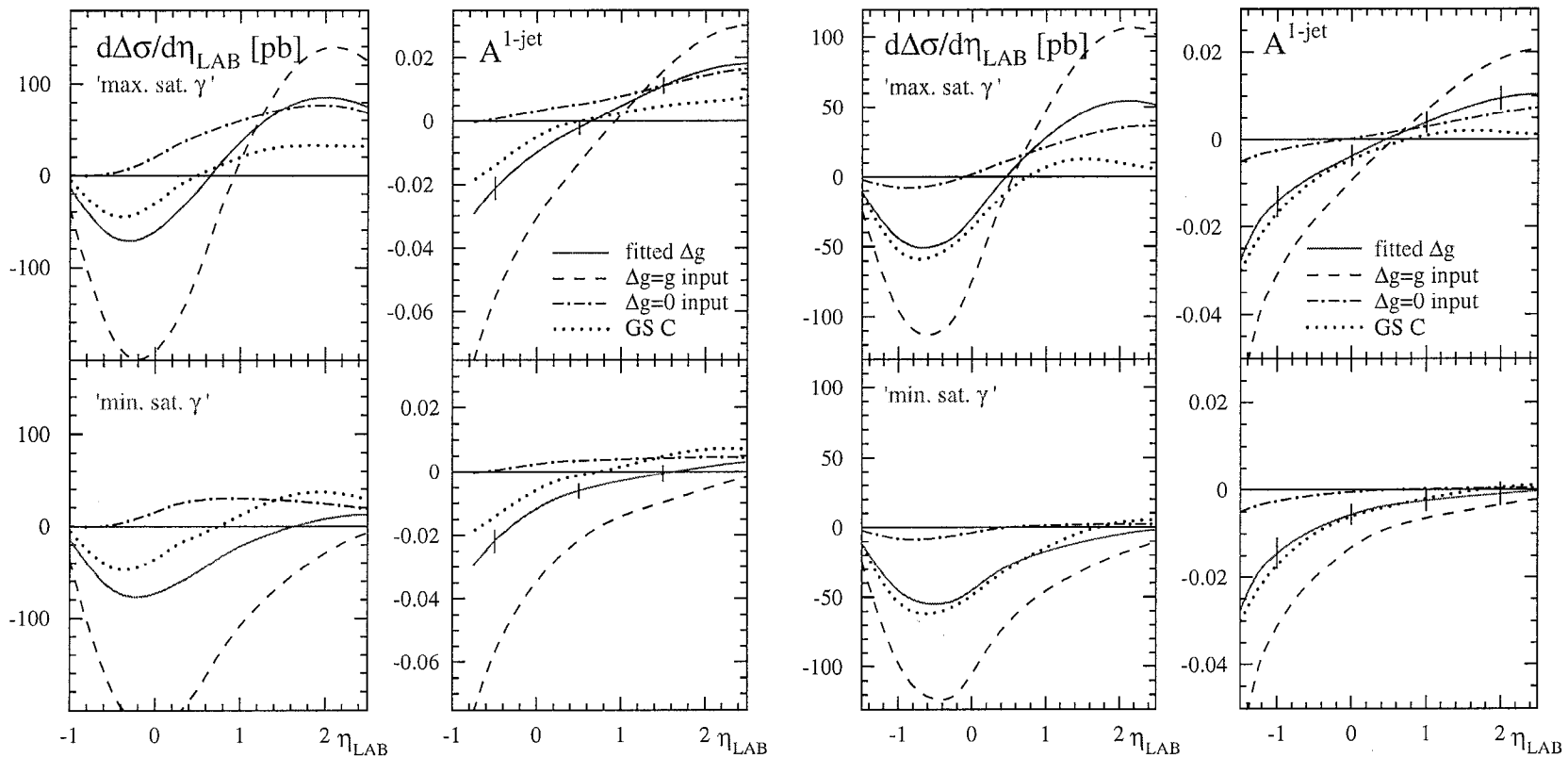

param. used: LO; Δf^p: GRSV; $\mu = p_T$; 'errors': $\mathcal{L} = 100\,\mathrm{pb}^{-1}$, $P_e = P_p = 0.7$
WW: $0.2 \leq y \leq 0.85$, $Q^2_{\max} = 4\ (1)\ \mathrm{GeV}^2$ (EIC); $p_T^{\min} = 8\ (5)$ GeV (EIC)

• Summary & comparison of results

collider	$\sqrt{S}$ [GeV]	promising processes	required lumi. [pb^{-1}]	mainly sensitive to	remarks
EIC	100	1-jet incl. di-jets	100 200	Δg^γ $\Delta f^\gamma_{\mathrm{eff}}$	dir. vs res. ✓
pol. HERA	300	1-jet incl. (1-had. incl.) di-jets	100 200 200	Δg^γ compl. combi. $\Delta f^\gamma_{\mathrm{eff}}$	dir. vs res. small $p_T^{\min}$ req. ✓
THERA	950	((di-jets))	$\gg$200	$\Delta f^\gamma_{\mathrm{eff}}$	large stat. errors
lin. collider TESLA	500	g_1^γ di-jets	100000 10000	Δu^γ $\Delta f^\gamma_{\mathrm{eff}}$	only in $\gamma\gamma$-mode ? better in $\gamma\gamma$-mode

· higher energies are *not* always helpful ($\rightarrow$ THERA): small asymmetries; large stat. errors

· $\gamma\gamma$-mode for next linear collider helpful (probably mandatory for g_1^γ measurement)

best process: di-jets (best enhancement of resolved contr.; access to x_γ; eff. PDF approx. works well)

best machine to pin down Δf^γ: EIC in $\vec{e}\vec{p}$ and TESLA ($\vec{\gamma}\vec{\gamma}$-mode)

[of course, pol. HERA would be also nice]

The case for a large polarized antiquark flavor asymmetry $\Delta\bar{u}(x) - \Delta\bar{d}(x)$

C. Weiss

Institut für Theoretische Physik, Universität Regensburg, D–93053 Regensburg, Germany

The polarized antiquark flavor asymmetry $\Delta\bar{u}(x) - \Delta\bar{d}(x)$ has become a focus of attention recently. It is expected that this asymmetry will be measured with good accuracy in polarized semi-inclusive DIS (HERMES, EIC), and in particular in Drell–Yan pair or $W^{\pm}$ production in polarized pp collisions at RHIC.

The polarized asymmetry is of great value for comparing different approaches to model parton distributions in the nucleon at a low scale. Considerable interest was caused by a calculation within the chiral quark–soliton model of the nucleon, based on the large–N_c limit of QCD, which suggests a large positive $\Delta\bar{u}(x) - \Delta\bar{d}(x)$, larger than the unpolarized asymmetry, $\bar{d}(x) - \bar{u}(x)$ [1]. In contrast, predictions based on rho meson contributions in the "meson cloud" picture of antiquark distributions tend to give a small $\Delta\bar{u}(x) - \Delta\bar{d}(x)$ of negative sign [2].

Here we show that a small negative asymmetry is by no means a necessary consequence of the "meson cloud" picture. In fact, a sizable positive $\Delta\bar{u}(x) - \Delta\bar{d}(x)$ is naturally obtained from πN–σN "interference type" contributions to the nucleon parton distributions, whose importance is suggested by chiral symmetry [3]. With this effect included, the predictions of the "meson cloud" picture are compatible with those of the chiral quark–soliton model. While we do not advocate to take too seriously the "meson cloud" picture, which is essentially qualitative and cannot be systematically improved, we nevertheless think that this point is interesting, as it resolves a long-standing discrepancy between models which both correctly describe the measured unpolarized flavor asymmetry $\bar{d}(x) - \bar{u}(x) > 0$.

We also summarize the experimental consequences of a large positive $\Delta\bar{u}(x) - \Delta\bar{d}(x)$. We study the influence of this asymmetry on the LO theoretical predictions for the double spin asymmetries in semi-inclusive DIS [3], and show that the present HERMES and SMC data do not yet allow for significant conclusions. A dramatic effect of $\Delta\bar{u}(x) - \Delta\bar{d}(x)$ is found in the LO theoretical predictions for the spin asymmetries in Drell–Yan pair and $W^{\pm}$ production at RHIC [4]. This makes us hopeful that an asymmetry of the magnitude predicted by the present model calculations can indeed be observed experimentally.

[1] D. I. Diakonov, V. Y. Petrov, P. V. Pobylitsa, M. V. Polyakov and C. Weiss, Nucl. Phys. B **480**, 341 (1996); Phys. Rev. **D56**, 4069 (1997).

[2] R.J. Fries and A. Schäfer, Phys. Lett. **B 443**, 40 (1998); K. G. Boreskov, A. B. Kaidalov, Eur. Phys. J. **C 10**, 143 (1999); Fu-Guang Cao and A. I. Signal, Eur. Phys. J. **C21**, 105 (2001); S. Kumano and M. Miyama, Phys. Rev. D **65**, 034012 (2002).

[3] B. Dressler, K. Goeke, M. V. Polyakov and C. Weiss, Eur. Phys. J. C **14**, 147 (2000).

[4] B. Dressler, K. Goeke, M. V. Polyakov, P. Schweitzer, M. Strikman and C. Weiss, Eur. Phys. J. C **18**, 719 (2001).

Pion cloud contributions to DIS [Sullivan 72, Thomas 83]

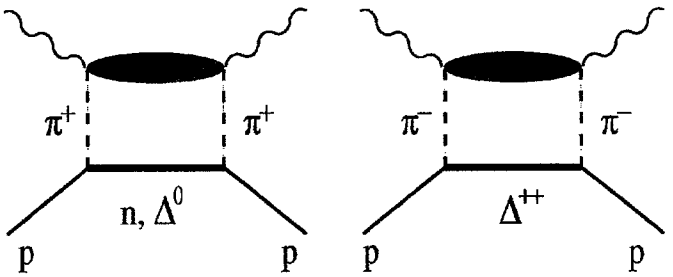

$\rightarrow \quad \bar{d}(x) > \bar{u}(x)$

Polarization?

- Sullivan mechanism does not contribute to $\Delta\bar{u} - \Delta\bar{d}$
- Fries, Schäfer 98: Rho meson contributions

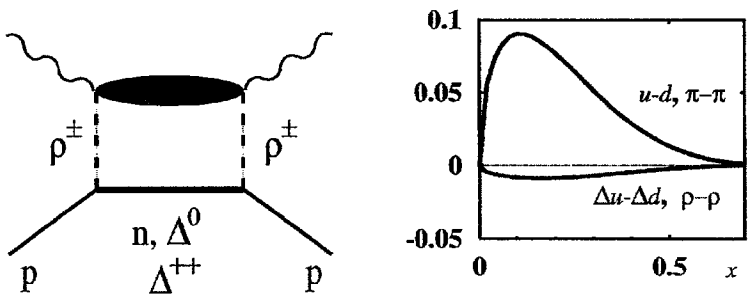

See also:

Boreskov, Kaidalov 99 Cao, Signal 01	ρ–π–Interference (small x!)
Kumano 01	g_2–type contribution to ρ structure function

- Dominant contribution to $\Delta\bar{u} - \Delta\bar{d}$: Pi–sigma–interference [Dressler et al. 00; Fries, Schäfer, Polyakov, CW 02]

Chiral symmetry: $\bar{q}\gamma_\mu\gamma_5\tau^a q \overset{\text{bosonization}}{\longleftrightarrow} \sigma \overleftrightarrow{\partial}_\mu \pi$

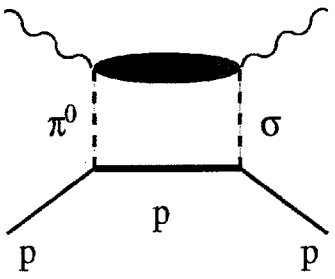

+ (π, σ interch.)

π–σ "transition" parton density

$g_{\pi\sigma}(x) \overset{\text{chiral symm.}}{\longleftrightarrow} v_\pi(x)$ valence dist'n in pion

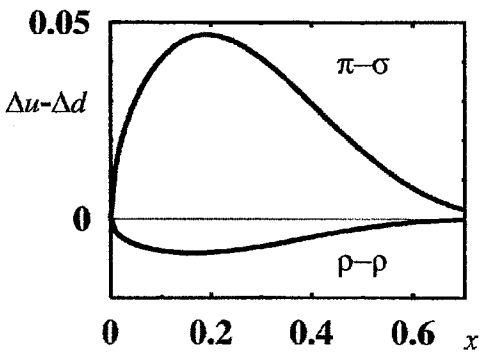

Parameters:
Bonn potential

Large positive $\Delta\bar{u} - \Delta\bar{d}$ from π–σ interference!

Comparison of model results

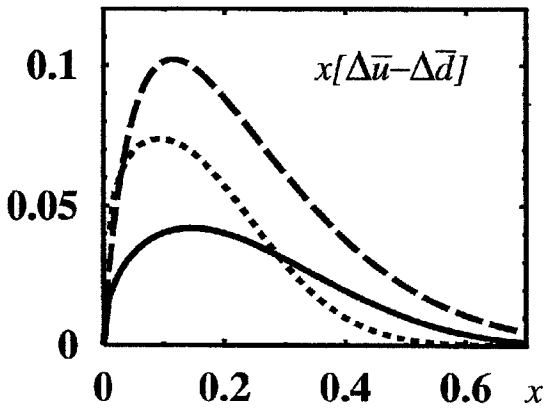

Dotted: "Pauli blocking" ansatz [Glück, Reya 2000]

Dashed: Chiral quark–soliton model [Diakonov et al. 1996]

Solid: πN–σN interference–type contribution in the meson cloud model [Fries, Schäfer, Polyakov, CW 2002]

"Emerging consensus" on large positive $\Delta\bar{u} - \Delta\bar{d}$

Implications for experiments [Dressler et al. 2000]

- Semi-inclusive DIS [HERMES, COMPASS, EIC]

  Double spin asymmetry for charged particle production [SMC, HERMES]

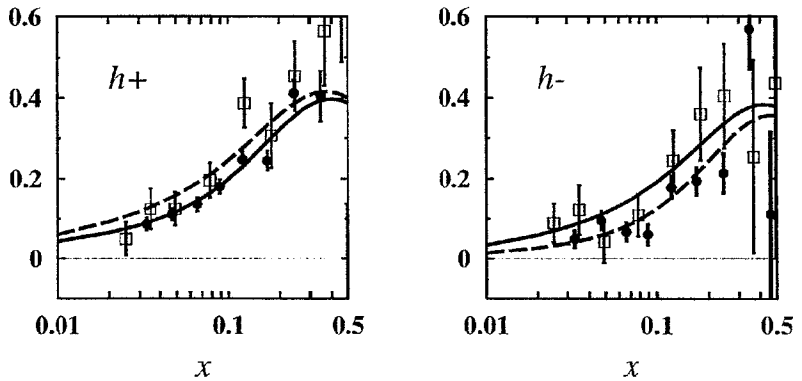

Dashed: Theoretical prediction (LO) based on GRSV95 parametrization with $\Delta\bar{u}(x) - \Delta\bar{d}(x) = 0$

Solid: Same with $\Delta\bar{u}(x) - \Delta\bar{d}(x) > 0$ from chiral quark–soliton model [Diakonov et al. 1996]

Large $\Delta\bar{u} - \Delta\bar{d}$ consistent with HERMES '98 results

NB: More precise data from HERMES to be released soon

- Drell–Yan/$W^{\pm}$ production [RHIC]

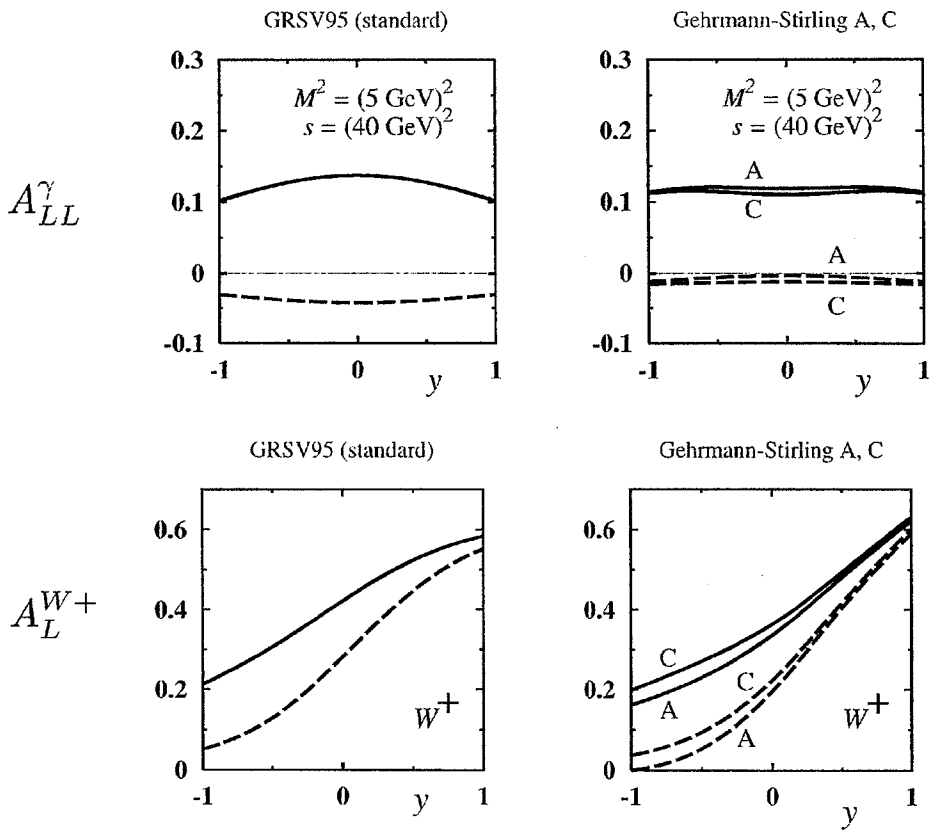

Dashed: Theoretical predictions (LO) based on parametrization with $\Delta\bar{u}(x) - \Delta\bar{d}(x) = 0$

Solid: Same with $\Delta\bar{u}(x) - \Delta\bar{d}(x) > 0$ from chiral quark–soliton model [Dressler et al. 2000]

Consequences of large $\Delta\bar{u}(x) - \Delta\bar{d}(x)$

- dramatic effect on spin asymmetries
- effect much larger than uncertainty in polarized gluon distribution (in LO)

What do we learn from Λ polarization in SIDIS?

Mauro Anselmino

Dipartimento di Fisica Teorica, Universita di Torino and INFN, Sezione di Torino, Via P. Giuria 1, 10125 Torino, Italy

Λ hyperons show naturally their polarization through the angular distribution of their weak decays, $\Lambda \to p\,\pi$: this makes them special particles, which may give access to new information.

We consider here the production of Λ's in semi-inclusive deep inelastic scattering (SIDIS), $\ell N \to \ell \Lambda X$. and discuss the leading order and leading twist expressions of polarization, considering the new knowledge which can be obtained and the novel tests of available information which can be performed.

The independent observables depend on elementary dynamics, distribution and fragmentation functions, both polarized and unpolarized. First access to separate q and $\bar{q}$ unpolarized and polarized fragmentation function is possible. Weak interaction contributions are also taken into account.

The transverse polarization of Λ's produced off transversely polarized protons could offer a good access to the so far unmeasured transversity distribution; transverse polarization from unpolarized initial states could offer a direct information on new polarizing fragmentation functions which might explain the longstanding problem of Λ transverse polarization in unpolarized processes.

The usefulness of studying the separate dependence on different kinematical variables and of combining RHIC pp data with DIS data is stressed.

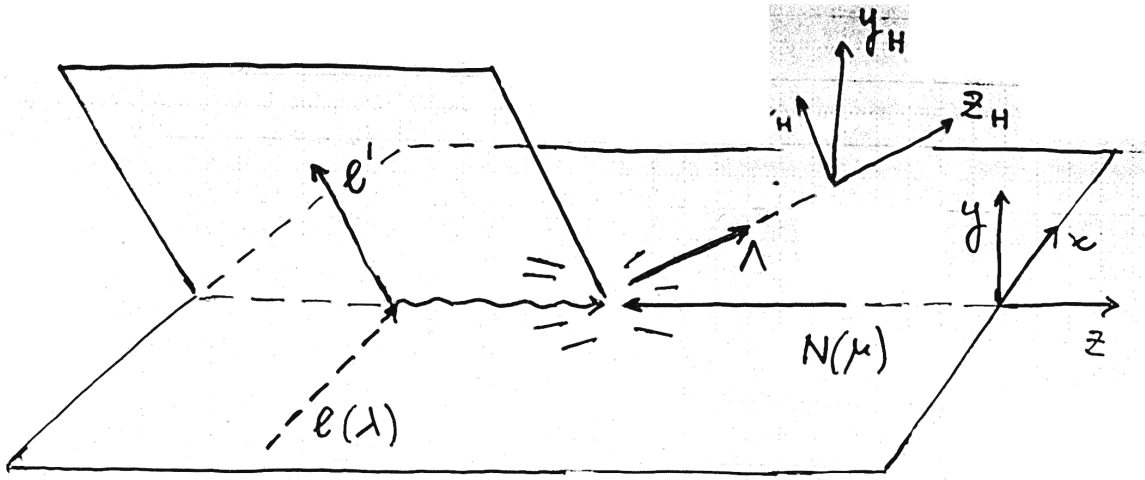

$\Lambda \to p\pi$ in helicity rest frame

Angular distribution of decay:

$$W(\theta_p, \varphi_p) = \frac{1}{4\pi}\left[1 + \alpha \vec{P}\cdot\hat{p}\right]$$

$$\alpha = 0.642 \pm 0.013 \implies P_{x_H}, P_{y_H}, P_{z_H}$$

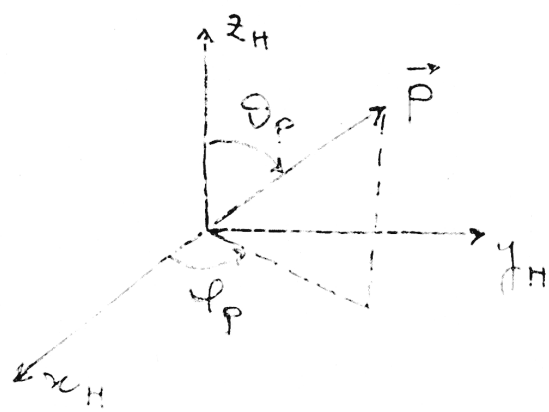

Unpolarized cross-section

$$d\sigma^H = \frac{1}{4}\left[d\sigma^H_{++} + d\sigma^H_{--} + d\sigma^H_{+-} + d\sigma^H_{-+}\right]$$

$$= \frac{1}{2}\left[d\sigma^H_{++} + d\sigma^H_{+-}\right] \equiv d\sigma^H_{00}$$

visual double-spin asymmetry

$$\Delta d\sigma^H \equiv d\sigma^H_{++} - d\sigma^H_{+-} \implies A^H_{\parallel} = \frac{\Delta d\sigma^H}{2\, d\sigma^H}$$

Spin-transfer from lepton

$$d\sigma^{H+}_{+0} - d\sigma^{H-}_{+0} = P^H_{+0}\, d\sigma^H = -P^H_{-0}\, d\sigma^H$$

Spin-transfer from nucleon

$$d\sigma^{H+}_{0+} - d\sigma^{H-}_{0+} = P^H_{0+}\, d\sigma^H = -P^H_{0-}\, d\sigma^H$$

Other quantities are related to these:

$$P^H_{++} = \frac{1}{1+A_{\parallel}}\left(P^H_{+0} + P^H_{0+}\right)$$

$$P^H_{+-} = \frac{1}{1-A_{\parallel}}\left(P^H_{+0} - P^H_{0+}\right)$$

$$\frac{d\sigma^H}{dx\,dy\,dz} = \frac{2\pi\alpha^2}{sx}\,\frac{1+(1-y)^2}{y^2}\sum_q e_q^2\, q(x)\, D_q^H(z)$$

$$A_{LL}^H = \underbrace{\frac{y(2-y)}{1+(1-y)^2}}_{\equiv\,\hat{A}_{LL}}\;\frac{\sum_q e_q^2\,\Delta q(x)\, D_q^H(z)}{\sum_q e_q^2\, q(x)\, D_q^H(z)}$$

$$P_{+0}^H = \hat{A}_{LL}(y)\,\frac{\sum_q e_q^2\, q(x)\,\Delta D_q^H(z)}{\sum_q e_q^2\, q(x)\, D_q^H(z)}$$

$$P_{0+}^H = \frac{\sum_q e_q^2\,\Delta q(x)\,\Delta D_q^H(z)}{\sum_q e_q^2\, q(x)\, D_q^H(z)}$$

$\Rightarrow$ P gives new information on D and ΔD

[$\sum_q \Rightarrow u, \bar{u}, d, \bar{d}, s, \bar{s}, \ldots$

Q^2 dependence from QCD evolution]

Special combinations

Define $d\tilde{\sigma}^H \equiv \frac{d\sigma^H}{dx\,dy\,dz}[d\hat{\sigma}]^{-1} = \sum_q e_q^2\, q\, D_q^H$

Assume charge conjugation + isospin invariance $\Rightarrow D_q^\Lambda = D_{\bar{q}}^{\bar{\Lambda}}$; $D_d^\Lambda = D_u^\Lambda$

<u>Unpolarized cross-sections</u>

$$d\tilde{\sigma}^{\Lambda+\bar{\Lambda}}\Big|_p - d\tilde{\sigma}^{\Lambda+\bar{\Lambda}}\Big|_n = \frac{1}{3}\left[u+\bar{u}-d-\bar{d}\right] D_u^{\Lambda+\bar{\Lambda}}$$

$$d\tilde{\sigma}^{\Lambda-\bar{\Lambda}}\Big|_p - d\tilde{\sigma}^{\Lambda-\bar{\Lambda}}\Big|_n = \frac{1}{3}\left[u_v - d_v\right] D_u^{\Lambda-\bar{\Lambda}}$$

$$\Rightarrow D_u^{\Lambda\pm\bar{\Lambda}},\ D_u^{\Lambda},\ D_u^{\bar{\Lambda}}$$

$$d\tilde{\sigma}^{\Lambda+\bar{\Lambda}}\Big|_p + d\tilde{\sigma}^{\Lambda+\bar{\Lambda}}\Big|_n = \frac{5}{9}\left[u+\bar{u}+d+\bar{d}\right] D_u^{\Lambda+\bar{\Lambda}} + \frac{2}{9}\left[s+\bar{s}\right] D_s^{\Lambda+\bar{\Lambda}}$$

$$d\tilde{\sigma}^{\Lambda-\bar{\Lambda}}\Big|_p - d\tilde{\sigma}^{\Lambda-\bar{\Lambda}}\Big|_n = \frac{5}{9}\left[u_v+d_v\right] D_u^{\Lambda-\bar{\Lambda}} + \frac{2}{9}\left[s-\bar{s}\right] D_s^{\Lambda-\bar{\Lambda}}$$

$$\Rightarrow \left[s+\bar{s}\right] D_s^{\Lambda+\bar{\Lambda}},\ \left[s-\bar{s}\right] D_s^{\Lambda-\bar{\Lambda}}$$

[M.A., Boglione, D'Alesio, Leader, Murgia]

Electro-weak effects in $lp \to l\Lambda X$

Now $d\hat{\sigma}_{++} \neq d\hat{\sigma}_{--}$; $d\hat{\sigma}_{+-} \neq d\hat{\sigma}_{-+}$

$$P^{\Lambda}_{\pm 0} = \frac{\sum_q q(x)\left[d\hat{\sigma}^q_{\pm +} - d\hat{\sigma}^q_{\pm -}\right] \Delta D^{\Lambda}_q(z)}{\sum_q q(x)\left[d\hat{\sigma}^q_{\pm +} + d\hat{\sigma}^q_{\pm -}\right] D^{\Lambda}_q(z)}$$

$$P^{\Lambda}_{0\pm} = \frac{\sum\left[q_{\pm}\left(d\hat{\sigma}^q_{++} + d\hat{\sigma}^q_{-+}\right) - q_{\mp}\left(d\hat{\sigma}^q_{+-} + d\hat{\sigma}^q_{--}\right)\right] \Delta D^{\Lambda}_q}{\sum\left[q_{\pm}\left(d\hat{\sigma}^q_{++} + d\hat{\sigma}^q_{-+}\right) + q_{\mp}\left(d\hat{\sigma}^q_{+-} + d\hat{\sigma}^q_{--}\right)\right] D^{\Lambda}_q}$$

$$P^{\Lambda}_{\pm\pm} = \frac{\sum\left[q_{\pm}\, d\hat{\sigma}^q_{\pm +} - q_{\mp}\, d\hat{\sigma}^q_{\pm -}\right] \Delta D^{\Lambda}_q}{\sum\left[q_{\pm}\, d\hat{\sigma}^q_{\pm +} + q_{\mp}\, d\hat{\sigma}^q_{\pm -}\right] D^{\Lambda}_q}$$

$\Rightarrow$ different combinations of polarized distributions, fragmentations and dynamics.

$$P^{\Lambda}_{00} = \frac{\sum q\left[d\hat{\sigma}^q_{++} + d\hat{\sigma}^q_{-+} - d\hat{\sigma}^q_{+-} - d\hat{\sigma}^q_{--}\right] \Delta D^{\Lambda}_q}{4 \sum q\, d\hat{\sigma}^q\, D^{\Lambda}_q}$$

[purely parity violating effect;
$\simeq 1\%$ for $Q^2 > 4000\ \mathrm{GeV}^2$ at HERA]

$[\, q_+ \equiv q^+_+ \qquad q_- \equiv q^+_- \,]$

Transverse Λ pol. in unpolarized DIS

$\ell p \to \ell \Lambda^{\uparrow} X$ [similar to $pp \to \Lambda^{\uparrow} X$]

Access to polarizing frag. functions

$$\Delta^N D_{\Lambda^{\uparrow}/q}(z, \vec{k}_\perp) = \hat{D}_q^{\Lambda^{\uparrow}}(z, \vec{k}_\perp) - \hat{D}_q^{\Lambda^{\downarrow}}(z, \vec{k}_\perp)$$

$$\sim D_{1T}^{\perp}$$

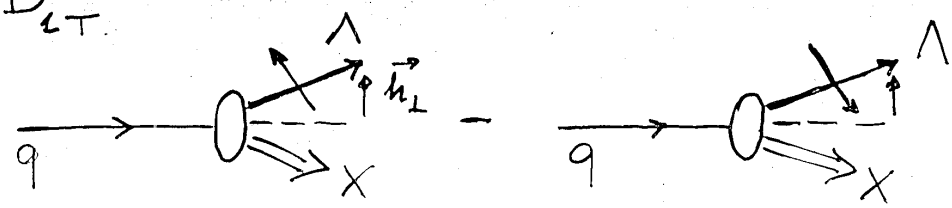

[Mulders, Tangerman;
M.A., Boer, D'Alesio, Murgia]

$$P_N^{\Lambda} = \frac{\sum_q e_q^2 \, q(x) \, \Delta^N D_{\Lambda^{\uparrow}/q}(z, k_\perp)}{\sum_q e_q^2 \, q(x) \, \hat{D}_q^{\Lambda}(z, k_\perp)}$$

$\ell p \to \ell \Lambda^{\uparrow} X$ (NOMAD)

$$P_N^{\Lambda} \simeq \frac{\Delta^N D_{\Lambda^{\uparrow}/u}}{D_u^{\Lambda}}$$

Conclusions

$$\left.\begin{array}{l} \ell N \to \ell \Lambda^{\uparrow} X \\ \ell N \to \ell \Lambda^{\uparrow} X \end{array}\right. \Rightarrow P(\Lambda)$$

$P(\Lambda)$ depends on parton densities, dynamics and quark fragmentation

Tests of existing knowledge + access to new independent information

Measure of h_L ?

Mechanism for Λ transverse polar. in unpolarized processes ?

Some data available (HERMES, NOMAD, SLAC), more to come (HERMES with transverse polarization, COMPASS, RHIC...)

<u>Combined data to get more information</u>

Conditional parton distribution functions and nucleon structure

Mark Strikman
Pennsylvania State University, University Park, PA 16802

Very little is known experimentally about hadron production in DIS in the target fragmentation region. The only notable exception is the diffractive studies at HERA and as well as studies of production of neutrons at $x_F^h \equiv p_h^-/p_N^- \geq 0.5$ (the plus direction is along the virtual photon momentum). Collins [1] has proved the QCD factorization theorem which states that the Q^2 dependence of the differential cross section of the process $\gamma^* + N \to X + h$ for fixed x_F^h, p_t is governed by the DGLAP evolution equations. Hence one needs to introduce parton distribution functions for fixed values of x_F^h, p_t. They are referred to as diffractive pdf's in the HERA studies where an evidence for factorization was observed for diffractive proton production. In a more general case of x_F^h not close to one and h being any fixes mass hadronic state (baryon, meson, system of mesons) it is natural to refer to these objects as *conditional pdf's*. They are also referred to as generalized fracture functions [2]. Study of such processes is important for understanding of color screening since in these processes at finite x a hard process leads to a creation of a color hole in the target rapidity which is compensated by the color in the current fragmentation region. Also, fragmentation of diguark (qqg,...) system into hadrons should be sensititve to the structure of the bound state.

Here is a sample of interesting issues related to these processes:

• It is important to check experimentally whether the soft factorization approximation $f_j^D(\frac{x}{x_{I\!P}}, Q^2, x_{I\!P}, t) = f_{flux}(x_{I\!P}, t)\phi(\frac{x}{x_{I\!P}}, Q^2)$ holds for the diffractive pdf's ($x_{I\!P} = 1 - x_F$). Violation of such factorization is expected both as a function of ($x_{I\!P}$ and t. In particular one may expect a weaker t dependence for the gluon induced diffraction due to a smaller gluon radius of the nucleon [3].

• Investigation of the correlation between the decay of the produced system (x_F distribution) and x_{Bj} will provide qualitatively new information about the structure of the bound state. In particular, within the picture of nucleon build of the valence quarks and sea partons one may expect a strong change of the x_F dependence of $d\sigma/dx_F$ from $\propto 1 - x_F$ at $x > 0.2$ to $\approx const(x_F)$ for $x \sim 0.1$ and $1/x_F$ for $x \leq 0.01$ [4]. Processes where a valence gluon ($x \geq 0.2$) is removed are of special interest since in this case one studies production of a leading baryon from a three quark color octet state.

• One expects an abundant production of baryon resonances in the fragmentation region including the ones which are rarely excited in low-energy $\pi(\gamma) - N$ scattering. In particular, for $x \sim 1$ the residual system is predominantly produced in a highly asymmetric state, hence one may expect an enhancement of production of rare baryon states like the 20-multiplet.

• Comparison of gluon and quark conditional pdf's for production of leading mesons will provide a new way for understanding the dominant mechanism of the low p_t leading meson production. If, for example, the minimal Fock state dominates, the gluon conditional pdf's will be strongly suppressed.

• Study of the polarization transfer in the scattering off the polarized nucleons would be possible using production of hyperons which are self analyzing and via investigation of the spin alignment of N^*, Δ-isobars. One could also try to use the Collins variables [5] with one or two of the particles chosen in the target fragmentation region. A comparison of conditional gluon and quark polarized pdf's will be especially revealing.

• It appears promising to search for new types of baryon states in the diffractive processes like $\gamma^* + p \to \rho * N^*$ at small x, since it is easy in these processes to exchange color over the distances $\sim 1/2m_N x$.

In conclusion, the study of the fragmentation processes in DIS provides new ways to probe nucleons, space-time picture of confinement, and look for new baryonic states. It would be crucial for success of such studies to have a detector with a good efficiency for a large range of x_F and with ability to detect the hyperon decays for large x_F.

References

[1] J. C. Collins, Phys. Rev. D **57**, 3051 (1998) [Erratum-ibid. D **61**, 019902 (1998)] [arXiv:hep-ph/9709499].

[2] M. Grazzini, L. Trentadue and G. Veneziano, Nucl. Phys. B **519**, 394 (1998) [arXiv:hep-ph/9709452].

[3] M. McDermott, L. Frankfurt, V. Guzey and M. Strikman, Eur. Phys. J. C **16**, 641 (2000) [arXiv:hep-ph/9912547].

[4] M. I. Strikman and L. L. Frankfurt, Yad. Fiz. **25** (1977) 1177.

[5] J. C. Collins, Nucl. Phys. B **396**, 161 (1993) [arXiv:hep-ph/9208213].

QCD factorization theorem for hadron production in DIS in the target fragmentation:

Collins 97

Differential cross section of the target fragmentation process $\gamma^* + N \to X + h$ for fixed $x_F^h \equiv p_h^- / p_N^- > 0, p_t$ evolves with Q^2 according to the DGLAP evolution equations.

Physics of factorization theorem: Soft interactions between "h" and the partons emitted in the $\gamma^* - parton$ interaction does not resolve changes of color distribution between the scale $Q_0 \gg soft\ scale$ and $Q^2 > Q_0$

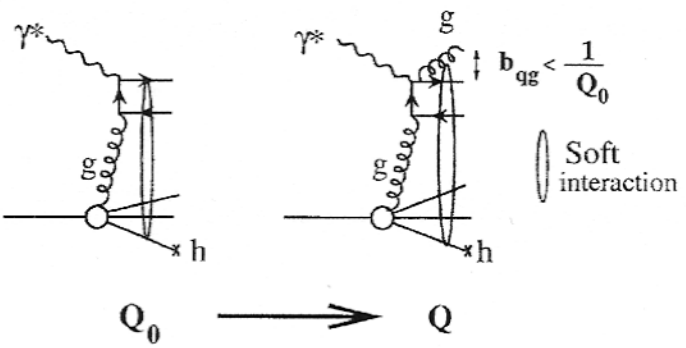

$\to$ Production of "h" when a parton at x, Q^2 is hit is the same as when an "ancestor" parton is hit at x, Q_0^2.

One defines $f_j^D(\frac{x}{x_{I\!P}}, Q^2, x_{I\!P}, t)$, the leading twist conditional pdf's for the processes where parton j with $x = x_{bj}$ is removed from the nucleon and a hadron with $x_{I\!P} = 1 - x_F^p$ is produced. So far most of the data for small x, and main focus in of diffractive pdf's (small $x_{I\!P}$

HERA data

(a) Approximate scaling for the diffractive structure functions $f_j(\beta, Q^2, x_{I\!P}, t)$ for $Q^2 \geq 4\ GeV^2$ and large probability of the rapidity gap:

$$P_q = \frac{\sigma(\gamma^* + p \to X + p)_{x_{I\!P} \leq 0.01, x \leq 10^{-3}}}{\sigma_{tot}(\gamma^* + p)} \approx 0.1$$

(b) Factorization theorem allows to define a probability

$P_j(x, Q^2) = \int f_j^D(\frac{x}{x_{I\!P}}, Q^2, x_{I\!P}, t) dt dx_{I\!P} / f_j(x, Q^2)$ of diffractive gaps for the hard processes induced by hard scattering off

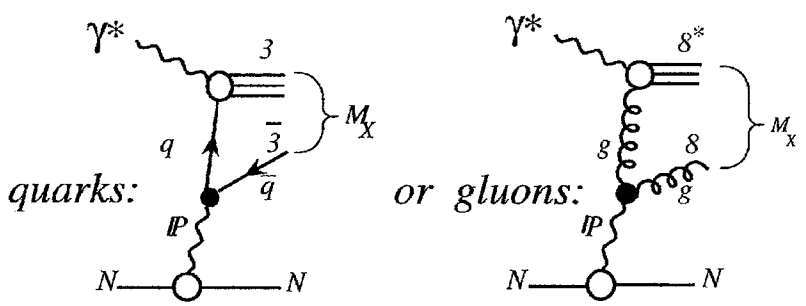

If the interaction in the gluon sector at small x reaches strengths close to the unitarity limit we should expect that P_g is rather close to $1/2$ and much larger than P_q.

Using pQCD expression for $\sigma^{inel}_{color\ octet\ dipole-N}$ we find :

$$P_g(x = 10^{-4}, Q^2 = 10GeV^2) \approx 1/3$$

Indeed, using the global fit of Alvero, Collins and Whitmore we find: $P_g \gg P_q, P_g(x \leq 10^{-3}, Q = 2) \approx 0.4$!! Other fits though different in details give similar probabilities.

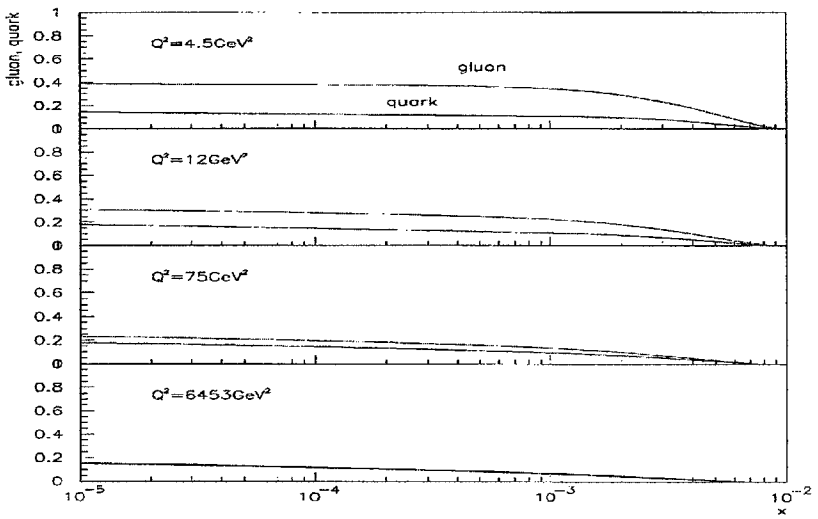

The ACW fit and the optic theorem $\sigma_{eff}(x,Q^2) \equiv \frac{16\pi d\sigma^{dif}/dt_{|t=0}}{\sigma} \Longrightarrow$ average cross sections for the configurations which contribute to quark ($3 \times \bar{3}$ dipole) and gluon ($8 \times 8^*$-dipole) induced diffraction.

$\sigma_{eff}^{q(g)}(x,Q)$ for $Q = Q_0 = 2GeV$:

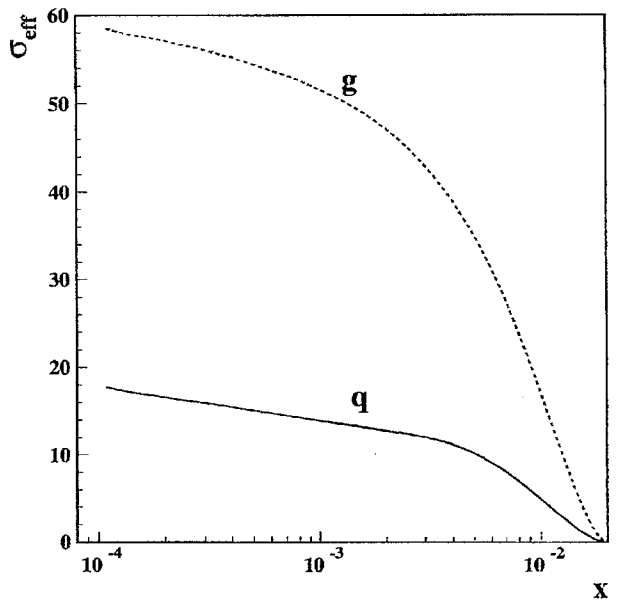

$\sigma_{eff}^{gluons}(x = 10^{-4}, Q = 4) \sim 30mb$ and even larger value of $\sigma_{eff}^{gluons}(x = 10^{-4}, Q = 2) \sim 50mb$ indicate presence of very (super) strong interactions in the gluon sector. These strong interactions should be due to some perturbative dynamics of strong gluon fields since the $\gamma + p \to J/\psi + p$ data indicate that pQCD for these Q occupies most of the phase volume.

This argument for super strong gluon interactions at small x is complementary to the unitarity argument based on perturbative calculation of "small color octet dipole"- nucleon interaction.

Conditional parton distribution functions & nucleon structure

M.Strikman, PSU

- ◇ Collins factorization theorem for fragmentation in DIS
- ◇ HERA data
- ◇ Examples of interesting observables/ phenomena for EIC

QCD factorization theorem for hadron production in DIS in the target fragmentation:

Collins 97

Differential cross section of the target fragmentation process $\gamma^* + N \to X + h$ for fixed $x_F^h \equiv p_h^- / p^- N < 0, p_t$ evolves with Q^2 according to the DGLAP evolution equations.

Physics of factorization theorem: Soft interactions between "h" and the partons emitted in the $\gamma^* - parton$ interaction does not resolve changes of color distribution between the scale $Q_0 \gg soft\ scale$ and $Q^2 > Q_0$

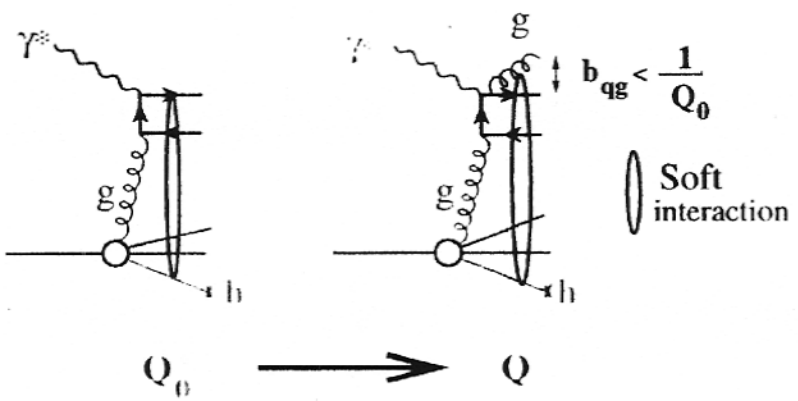

One defines $f_j^D(\frac{x}{x_{I\!P}}, Q^2, x_{I\!P}, t)$, the leading twist conditional pdf's for the processes where parton j with $x = x_{bj}$ is removed from the nucleon and a hadron with $x_{I\!P} = 1 - x_F^p$ is produced. So far most of the data for small x, and main focus in of diffractive pdf's (small $x_{I\!P}$)

HERA data

(a) Approximate scaling for the diffractive structure functions $f_j(\beta, Q^2, x_{I\!P}, t)$ for $Q^2 \geq 4\ GeV^2$ and large probability of the rapidity gap:

$$P_q = \frac{\sigma(\gamma^* + p \to X + p)_{x_{I\!P} < 0.01, x < 10^{-3}}}{\sigma_{tot}(\gamma^* + p)} \approx 0.1$$

(b) Factorization theorem allows to define a probability

$P_j(x, Q^2) = \int f_j^D(\frac{x}{x_{I\!P}}, Q^2, x_{I\!P}, t) dt dx_{I\!P} / f_j(x, Q^2)$ of diffractive gaps for the hard processes induced by hard scattering off

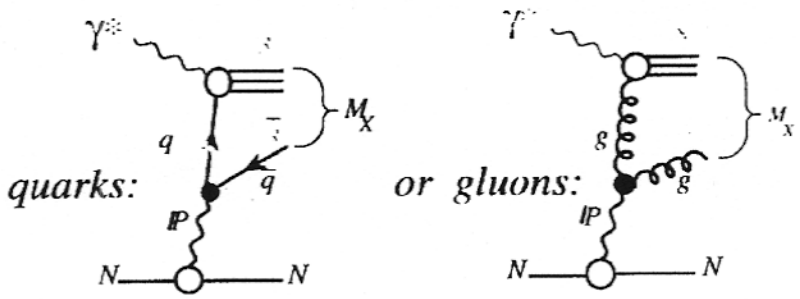

→ Production of "h" when a parton at x, Q^2 is hit is the same as when an "ancestor" parton is hit at x, Q_0^2.

If the interaction in the gluon sector at small x reaches strengths close to the unitarity limit we should expect that P_g is rather close to 1/2 and much larger than P_q.

Using pQCD expression for $\sigma^{inel}_{color\ octet\ dipole-N}$ we find :

$$P_g(x = 10^{-4}, Q^2 = 10GeV^2) \approx 1/3$$

Indeed, using the global fit of Alvero, Collins and Whitmore we find: $P_g \gg P_q, P_g(x \leq 10^{-3}, Q = 2) \approx 0.4$!! Other fits though different in details give similar probabilities.

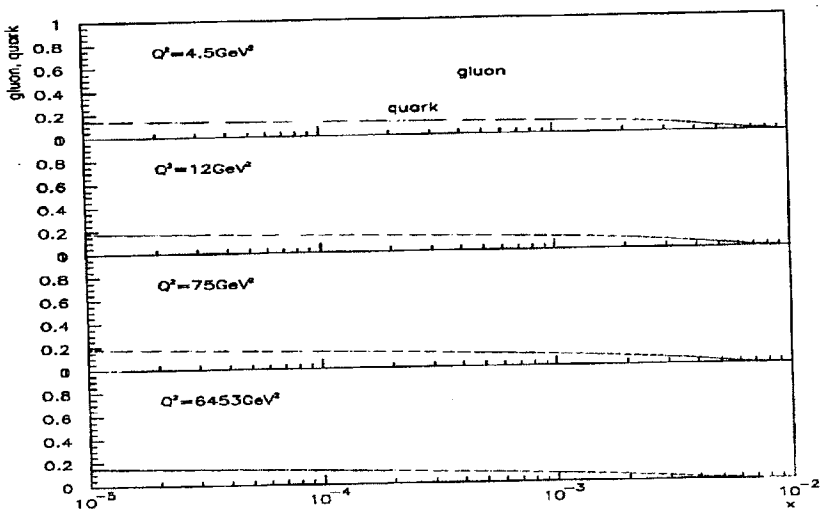

Open questions at small x.

Check soft factorization

$$f_i^D\left(\frac{x}{x_{I\!P}}, Q^2, x_{I\!P}, t\right) = f_{flux}(x_{I\!P}, t)\, \varphi\left(\frac{x}{x_{I\!P}}, Q^2\right)$$

No deep reasons for this. Especially t-dependence. Gluon radius of nucleon appears to be smaller than the quark one

FGMS 01-02

$\Rightarrow$ Naively t-slope for f_q^D larger than for f_g^D.

— · — · — —

Convenient variable is

$$x_F \equiv z = \frac{x_h}{(1-x)} \leq 1$$

Expect: distribution in z change qualitatively with increase of x_{Bj}.

FS 77,
FKS 97

(1) Small x $\qquad \frac{d\sigma}{dz} \propto \frac{1}{1-z}$ for large z

for $1-z \gg x$

(2) $x \sim 0.1$ $\qquad \frac{d\sigma}{dz} \sim \text{const}$

(scattering of $q\bar{q}$)

(3) $x \sim 0.3$ $\qquad \frac{d\sigma}{dz} \propto (1-z)$

removal of
valence quark

(4) $x \sim 1$

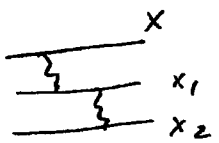

$\frac{x_1}{x_2} > 1$ / or $\frac{x_2}{x_1}$

likely $\simeq$ independent
fragmentation $\Rightarrow$ further
suppression of leading
nucleon spectrum

(5) gluon removal at $x \sim 0.2$

can one produce a leading baryon
from 3 colored quark state ?

$\Rightarrow$ studies will reveal correlations of partons in nucleon.

- Pion production at large z

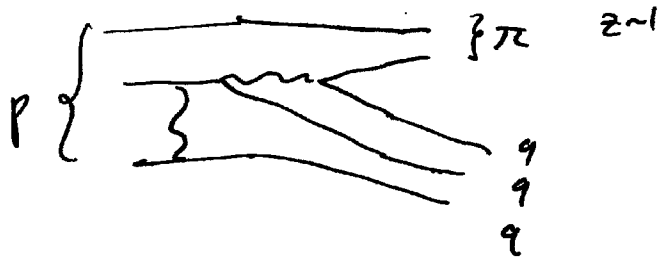

$z \sim 1$

Minimal Fox state

$\Downarrow$

gluon conditional pdf suppression.

- Baryon production – in soft physics meson resonances are very important.

removal of quark – potentially large orbital momenta $\Rightarrow$ production of excited states. Enhancement of 20-plet production (can discover these states).

- Polarized nucleon

  $\Rightarrow$ polarization of baryons – $\Delta^{++}, \Delta^{0}, N^{*}$
  - alignment effects, Λ, Σ selfanalyzin

- Collins-type observables for scattering of transversely polarized nucleons for the nucleon fragmentation region

- Excitation of gluon degrees of freedom in baryons in small x processes

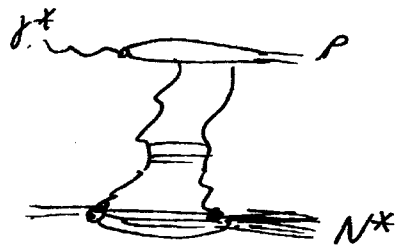

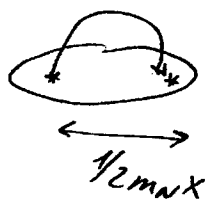

$\Sigma\Sigma\Sigma$ Study of conditional pdf's
new way to probe nucleons,
look for new baryonic states.

$\Rightarrow$ Need detector with good efficiency for large range of x_F.
Detection of hyperons is also highly desirable. (similar to Hard Exclusive pdf's).

Accurate tests of QCD factorization at Electron-Ion Collider

Pavel Nadolsky
Department of Physics, Southern Methodist University, Dallas, TX, 75275-0175

Although the attention of this Workshop is concentrated on experiments with nuclei and polarized protons, the goal of my talk is to point out a useful role that Electron-Ion Collider could play in tests of the QCD factorization *in unpolarized electron-proton collisions.* Of a particular interest would be studies of (a) inclusive deep-inelastic scattering $e + p \xrightarrow{\gamma^*} e + X$ at large values of Bjorken x; and (b) semi-inclusive hadroproduction in DIS (SIDIS) $e + p \xrightarrow{\gamma^*} e + H + X$ at $x \gtrsim 0.01$ and $Q \gtrsim 5 - 10$ GeV.

The proof of the factorization lies at the foundation of any perturbative QCD calculation involving observed individual hadrons. In general, the factorization states that, in the presence of a large momentum scale, the hadronic cross section can be expressed as a convolution of perturbatively calculable coefficient functions and unknown, but universal long-distance functions (*e.g.*, parton distributions).

It is useful to distinguish between two kinds of factorized observables. Coefficient functions for observables of the first kind (*e.g.*, inclusive DIS structure functions $F_i(x, Q^2)$) can be reliably calculated at a finite order of the strong coupling α_S. Coefficient functions for observables of the second kind cannot be reliably approximated at any finite order of the perturbative QCD due to the presence of logarithms of small or large dimensionless quantities at each order of the perturbative expansion. The convergence of the perturbative series for the coefficient functions of the second kind is restored by summing large logarithms through all orders of α_S using the procedure of refactorization.

Angular distributions of hadronic final states in SIDIS provide an example of observables of the second kind [1]. In the current fragmentation region of the $\gamma^* p$ c.m. frame (or any other frame related by a boost along the z direction), the fixed-order QCD fails when the polar angle θ of the final-state hadron approaches zero, due to the presence of large terms $\theta^{-2}\alpha_S^n \ln^m \theta^2/4, \quad 0 \leq m \leq 2n - 1$. The predictive power of the perturbative theory can be restored by applying the Collins-Soper-Sterman (CSS) refactorization formalism [2], which leads to a good agreement with the data [3]. In its essential aspects, the refactorization of the SIDIS angular distributions is similar to the resummation of angular distributions in e^+e^- hadroproduction and transverse momentum distributions in the Drell-Yan process. It reflects the physical picture that lies behind both types of factorization: the dominance of rare hard scattering events accompanied by the intensive soft and quasi-collinear QCD radiation along directions of external hadrons. While the inclusive DIS probes global features of this picture, SIDIS is well-suited for detailed studies of the multiple parton radiation, and its results improve understanding of strong interactions at colliders of all types.

In addition, the study of refactorization in SIDIS is more informative than in the Drell-Yan or e^+e^- hadroproduction processes, due to the enhanced reach of SIDIS in x and Q, separate dependence on the initial- and final-state longitudinal variables x and z, and possibility to choose between different final states for the same initial state. Deviations from the expected pattern of angular distributions may signal development of non-conventional dynamics. For instance, the onset of the "k_T-unordered" (BFKL) evolution at small x is likely to cause the broadening of angular distributions, which would be hard to describe in the CSS formalism or by using DGLAP showering programs. Remarkably, such broadening indeed seems to affect the HERA data on the transverse energy flow and charged particle production at $x \lesssim 0.005 - 0.01$ and $Q = 3 - 10$ GeV [3]. Hence, SIDIS at HERA may indicate that "naive" applications of the conventional QCD factorization are not always adequate at $x \lesssim 0.005$, notably for modeling of exclusive reactions at the LHC. Unfortunately, the resolution of HERA detectors is not sufficient for probing in detail the current fragmentation region at $x \gtrsim 0.01$, where the QCD factorization is expected to work well. Due to the high energy of HERA, this kinematical region corresponds to the final-state hadrons that escape close to the outgoing proton beam pipe, where the resolution is inadequate.

Let us now see what EIC could say on the above issues, starting from the inclusive DIS. According to

the recent global analysis of the hadronic data [4], the PDFs are determined to an accuracy of a few percent at $10^{-4} \lesssim x \lesssim 10^{-1}$ (cf. the attached transparencies, which show the PDF uncertainty bands found in the CTEQ6 analysis). At the same time, not much is known about the behavior of the PDFs at $x \gtrsim 0.3$, especially for sea quarks and gluons. For instance, at $x = 0.5$ the relative uncertainties for $u(x)$, $d(x)$ and $g(x)$ are about 6, 17, and 100%, respectively. The high-x gluons are mostly constrained by the CDF and D0 high-E_T jet data [5], which tend to prefer a harder gluon distribution compared to other data sets. Since the behavior of the high-E_T jet data was originally interpreted as a deviation from the Standard Model predictions (cf. the first reference in [5]), before a "PDF explanation" was suggested [6], it remains important to confirm the hardness of $g(x)$ by independent methods, *e.g.*, by measuring it in a different energy range.

The inclusive DIS at the high-luminosity EIC is naturally suited for studies of the valence quark PDFs at large x, and potentially for the determination of $g(x)$ through observation of scaling violations. By the time of their measurement, EIC data will be complemented by large-x results from the Drell-Yan process and $W^{\pm}$-production at RHIC, which test the magnitude and flavor composition of the sea quark PDFs. Combined together, the RHIC and EIC data will present a comprehensive and detailed picture of the proton structure at large x, thus meeting one of the Top Challenges of the perturbative QCD [7] at a qualitatively new level.

EIC may also have an edge on HERA in studying the multiple parton radiation in SIDIS at $x > 0.01$ and $Q > 1$ GeV. Due to the smaller energy of the EIC beams, hadrons produced in the current region will escape under larger angles to the beam pipe, and it will be easier to register them with a high angular resolution. Potentially, EIC could produce a wealth of data about the x, z, flavor and spin dependence of the multiple parton radiation, an attractive possibility that will not be available for a while at colliders of other types. Due to its large span in Q, EIC could be also used to study the development of collinear singularities in charm quark production [8], as well as to test the impact of the multiple parton radiation on SIDIS azimuthal asymmetries [9]. To conclude, DIS and SIDIS experiments at EIC could lead to significant progress in understanding of fundamentals of the perturbative QCD.

References

[1] R. Meng, F. I. Olness and D. E. Soper, Phys. Rev. D**54**, 1919 (1996).

[2] J. C. Collins and D. E. Soper, Nucl. Phys. B**193**, 381 (1981); B **213**, 545 (1981); J. C. Collins, D. E. Soper, and G. Sterman, Nucl. Phys. B**250**, 199 (1985).

[3] P. Nadolsky, D. R. Stump and C.-P. Yuan, Phys. Rev. D**61**, 014003 (2000); D**64**, 059903 (2001); D**64**, 114011 (2001).

[4] J. Pumplin, D. R. Stump, J. Huston, H. L. Lai, P. Nadolsky and W. K. Tung, hep-ph/0201195.

[5] CDF Collaboration, Phys. Rev. Lett. **77**, 438 (1996); Phys. Rev. D**64**, 032001 (2001); D**65**, 039903 (2001); D0 Collaboration, Phys. Rev. Lett. **82**, 2451 (1999); **86**, 1707 (2001); Phys. Rev. D**64**, 032003 (2001).

[6] J. Huston *et al.*, Phys. Rev. Lett. **77**, 444 (1996).

[7] http://www.hep.fsu.edu/~owens/qcd/QCD_list.html

[8] N. Kidonakis *et al.*, contribution to Les Houches Proceedings (2001).

[9] P. M. Nadolsky, D. R. Stump and C. P. Yuan, Phys. Lett. B**515**, 175 (2001); D. Boer, Nucl. Phys. B**603**, 195 (2001).

Uncertainties in $u(x)$ and $d(x)$ at $Q^2 = 10$ GeV^2

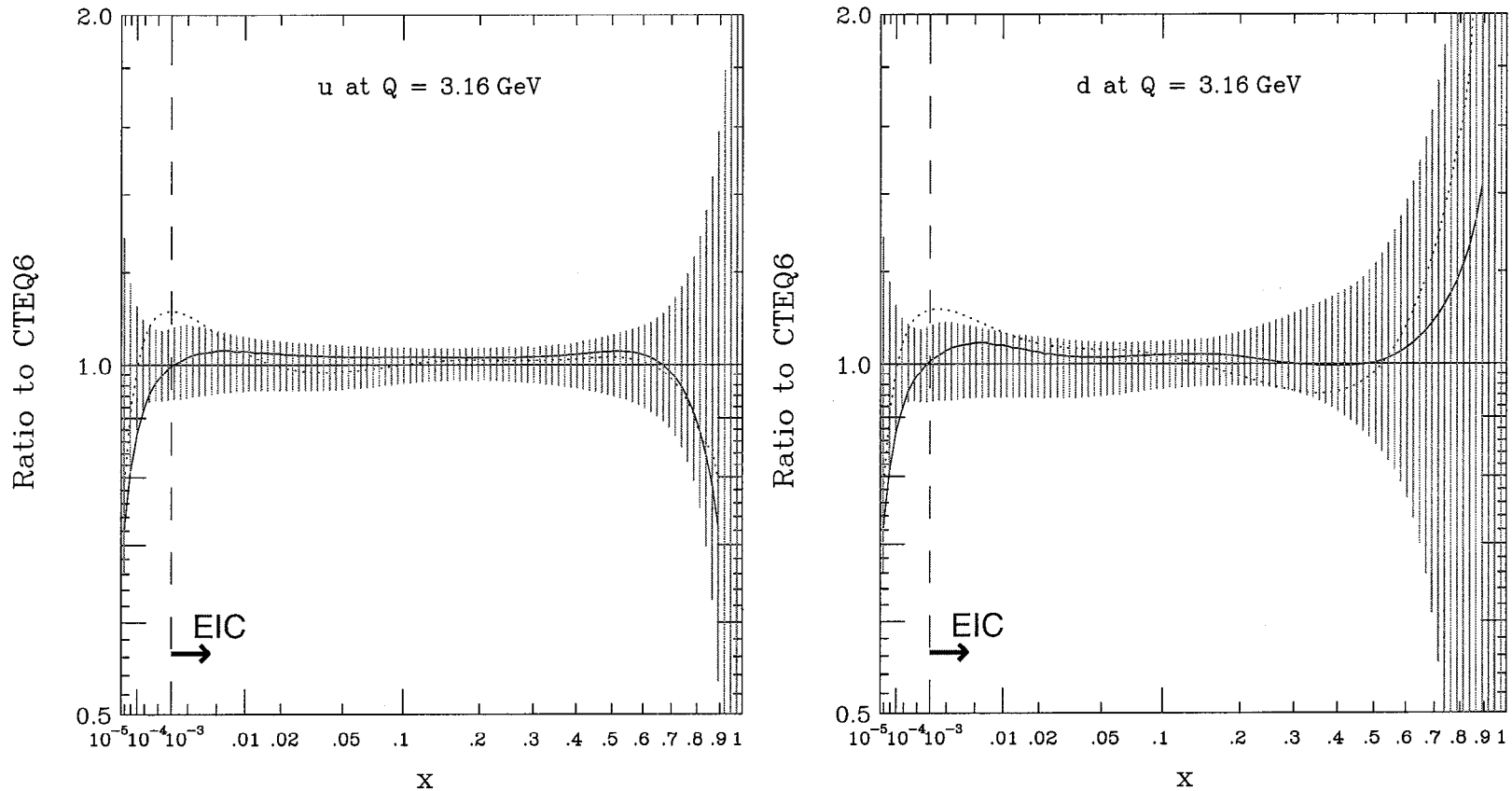

CTEQ5M1 (solid), MRST2001 (dotted)

Uncertainty in $g(x)$ at $Q^2 = 10$ GeV^2

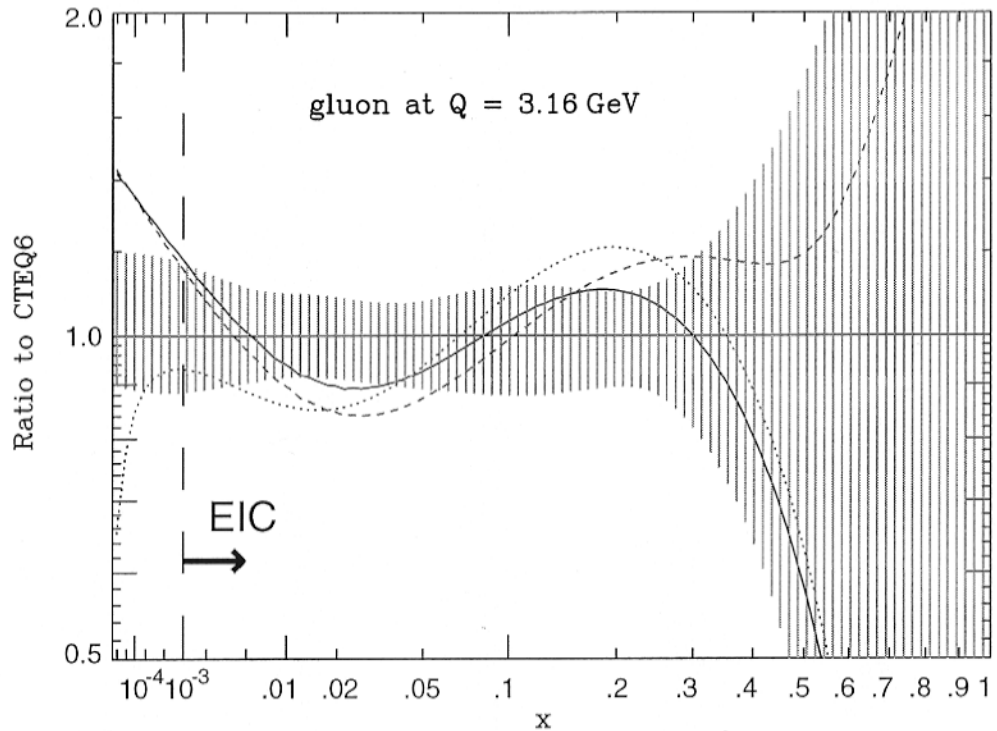

CTEQ5M1 (solid), CTEQ5HJ (dashed), MRST2001 (dotted)

Semi-inclusive DIS in $\gamma^* p$ c.m. frame

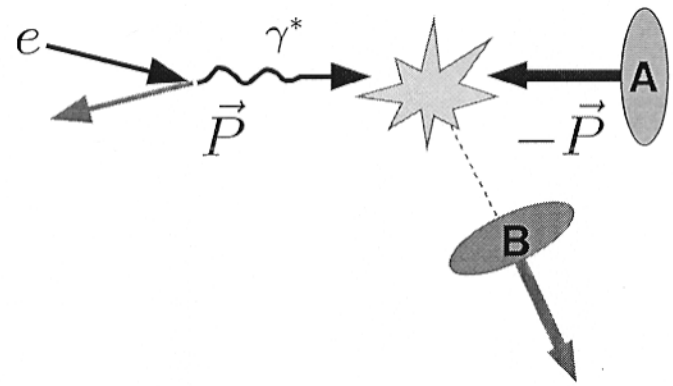

Incoming particles

Outgoing particles

$$0 \leq x \leq 1$$
$$0 \leq z \leq 1$$

No QCD radiation

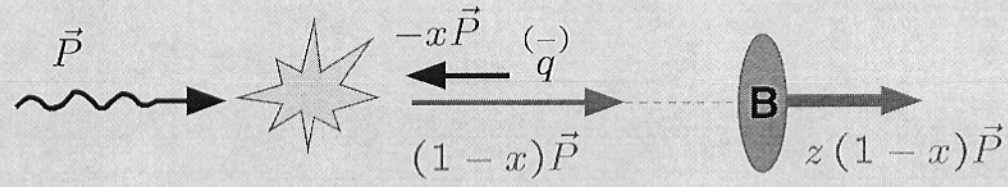

QCD radiation

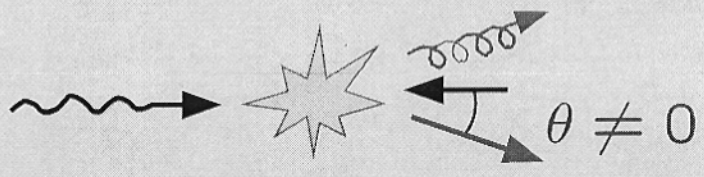

q_T dependence of E_T flow at small x

Data from *H1 Collaboration*

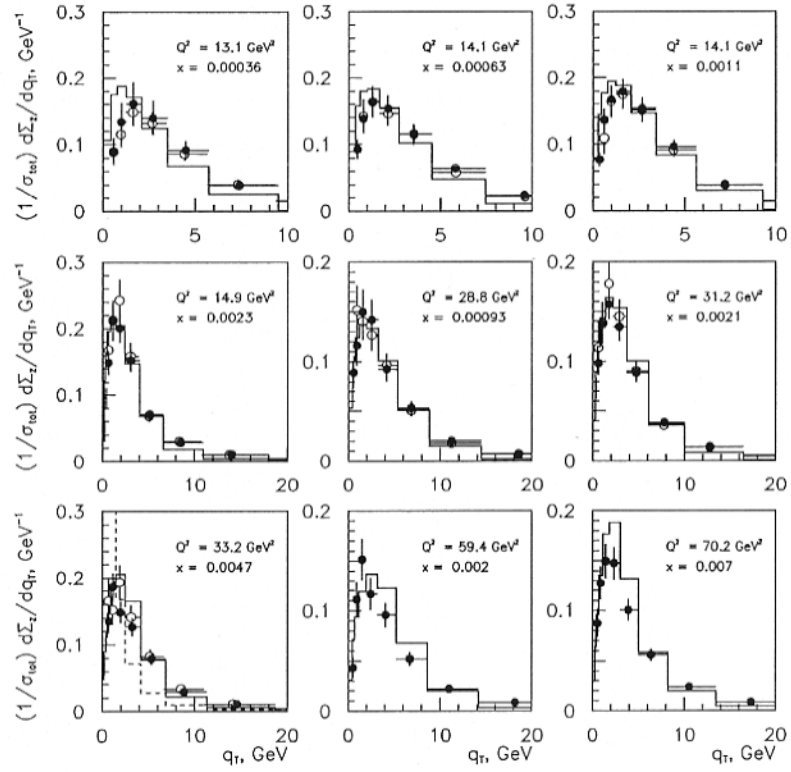

$13.1 < \langle Q^2 \rangle < 70.2 \quad \text{GeV}^2,$
$8 \times 10^{-5} < \langle x \rangle < 7 \times 10^{-3}$

Resummed z-flow: CTEQ5M1 PDFs,

$$S_z^{NP} = b^2 \left\{ 0.013 \frac{(1-x)^3}{x} + 0.19 \ln\left(\frac{Q}{2 \text{ GeV}}\right) \right\}$$

Possible interpretation:
rapid increase of "intrinsic" k_T when x decreases (first BFKL signs???)
No mechanism for such increase in the $\mathcal{O}(\alpha_s)$ part of the CSS formula

BFKL cross sections do not factorize

E_T flow at HERA at large x

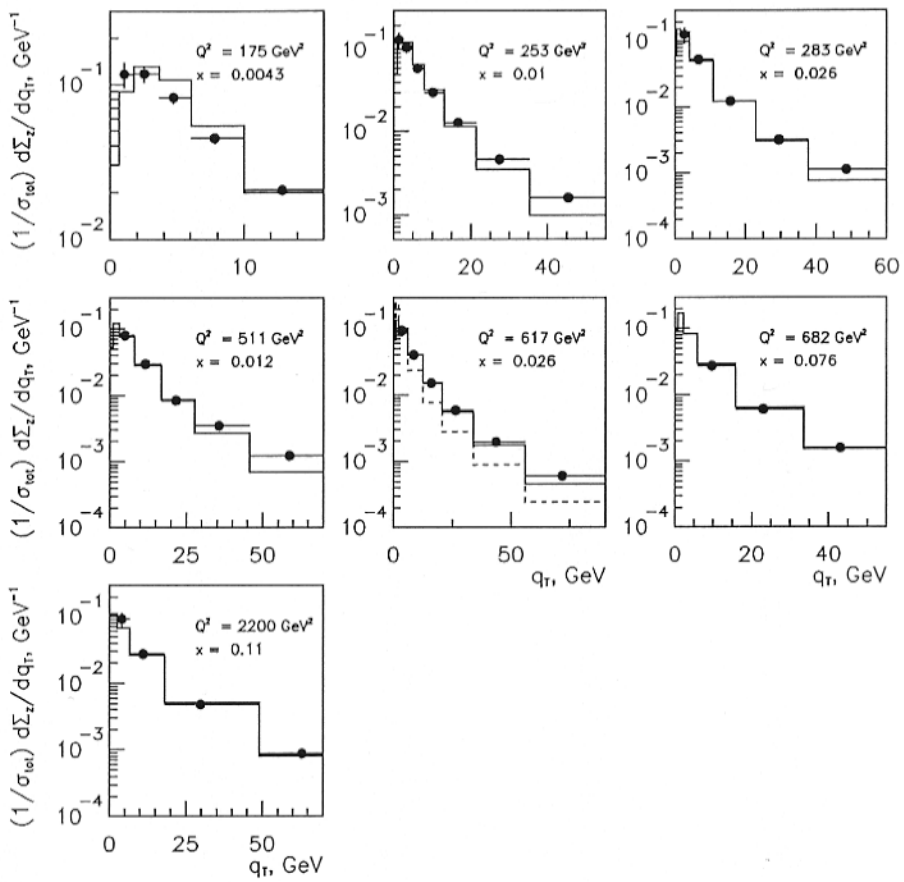

Resolution of the H1 detector not sufficient for studying the q_T distribution at large x

$$175 < \langle Q^2 \rangle < 2200 \quad \text{GeV}^2,$$
$$0.0043 < \langle x \rangle < 0.11$$

$\Rightarrow$Because of lower energy, resolution at EIC may be better than at HERA

Deeply Virtual Compton Scattering – Experimental Aspects

Brendan D. Fox
RIKEN-BNL Research Center
Brookhaven National Laboratory
Upton, NY 11973-5000, U.S.A.

For over three decades, deep inelastic lepton scattering (DIS) has been the principle method for probing the structure of the nucleon. This work has resulted in a precise determination of the parton momentum and, to a lesser extent, helicity distributions over a large kinematic regime. Following the demonstration of QCD factorization,[1,2] hard exclusive electroproduction of mesons and photons has arisen as a possible candidate for future efforts to study the nucleon. These processes are sensitive to a new set of structure functions, called skewed parton distributions functions (SPDs). These generalizations of the standard parton distribution functions describe the soft components of processes in which a nucleon recoils elastically after receiving a non-zero momentum transfer from a probe as a result of a hard interaction involving one of its quarks or gluons. In the limit of zero-momentum transfer, these functions are identical to the standard distribution functions. But, because they involve an additional degree of freedom (*i.e.* the momentum transfer), they are also sensitive to correlations in the quark/gluon wave functions. It is hoped that these correlations will be calculable via lattice QCD methods soon after results for the standard distributions functions become available.

During the last three years, current DIS experiments have begun to report the first cross section and azimuthal asymmetry measurements for exclusive processes involving pion, rho, or photon production. The latter, called deeply virtual Compton scattering (DVCS), is the process with the simpliest final state. As compared with meson production, DVCS has the advantage that there are no additional theoretical complications associated with the convolution of the meson wave function with the final nucleon state. But, the process is experimentally more difficult to study because it results in the same final state as the typically more dominant Bethe-Heitler (BH) process.

In a collider experiment, however, it is possible to isolate the DVCS contribution to exclusive photon production by looking at photons produced at backward angles relative to the detected, scattered lepton. At such angles, the BH contribution is small because the BH cross section is strongly peaked along either the incoming or scattered lepton direction. The ZEUS and H1 experiments at HERA/DESY have utilized this feature to extract the first measurement of the DVCS cross section from their 1997 positron-proton dataset. [4,5] Because of the high center of mass energy at HERA, these measurements are sensitive to low-x efforts and thus dominated by gluons. The results of these measurements are in good agreement with a model by Frankfurt *et. al*[6] in which the inter action is mediated by a quark-loop which couples the initial and final proton states via gluon exchanges. Despite breaking new ground, these measurements have a cloudy interpretation because the exclusivity of the reaction was not ensured by direct measurements in either experiment.

In a typically fixed target experiment with forward detectors, the BH cross section is an order of magnitude or more larger than the DVCS cross section. With such a large background, it is not possible to measure the DVCS cross section with reasonable precision. Such experiments, instead, can utilize the helicity or the charge of the lepton beam to isolate the contribution to the cross section from the quantum interference between the BH and the DVCS processes. These interference effects give rise to an azimuthal dependence to the cross section, the sine and

cosine moments of which are related to the SPDs in first order. The two experiments of this type presently operating, HERMES at HERA/DESY[7] and CLAS[8] at Jefferson Laboratory, have published the first measurements of the beam helicity dependence of the azimuthal asymmetry. Both of these experiments demonstrated that the sine moment of this quantity is sizeable (20%) and thus readily measureable. In addition, HERMES has recently reported a preliminary result on the charge dependence of the azimuthal asymmetry.[9] Because of the relative small center of mass energy of these experiments, these results are sensitive to quarks. However, as in the case of ZEUS and H1, neither experiment is presently able to guarantee the exclusivity of the data sample on an event-by-event basis.

During the near (next five years) future, ZEUS and H1 will likely report both a charge and a beam asymmetry in addition to improving upon their present cross section measurement. As a consequence, there will be complete set of observeables available at relatively high Q^2/low x. However, neither experiment has augmented their detectors to guarantee the exclusivity of the observation and thus the interpretation of these measurements will remain a bit problematic. In contrast, both HERMES and CLAS are actively upgrading their detectors to address this systematic weakness to refine their existing measurements. Since the amplitudes for DVCS, not just the interaction probabilities, can be extracted from a complete set of the asymmetry observables, this work will lead to a complete measurement at lower Q^2/mid to high x. And, finally, the COMPASS experiment at CERN intends to initiate a program to measure DVCS using muons. Together, these measurements will provide a first opportunity to verify the scale of factorization for the process and also constrain model calculations of the SPDs.

These efforts, along with the continued theoretical progress in this field, will have forged the groundwork for a future, precise measurement of SPDs. Such measurements should be possible at the Electron-Ion Collider (EIC) if the detectors include sufficient calorimetry and forward proton and lepton detections. This opportunity is especially attractive because EIC would likely provide the large kinematic coverage needed for a thorough investigation of SPDs.

References

1. J. C. Collins and A. Freund, *Phys. Rev.* D **59**, 074009 (1999).
2. A. V. Radyushkin and C. Weiss, *Phys. Rev.* D **63**, 114012 (2001).
3. A. V. Belitsky *et al.*, *Nucl. Phys.* B **593**, 289 (2001).
4. P. R. Saull for the ZEUS Collaboration, hep-ex/0003030.
5. C. Adloff *et al.*, *Phys. Lett.* B **517**, 47 (2001).
6. L. L. Frankfurt, *et. al*, *Phys. Rev.* D **59**, 119901E (1999).
7. A. Airapetian *et al.*, *Phys. Rev. Lett.* **87**, 182001 (2001), hep-ex/0106068.
8. S. Stepanyan *et al.*, *Phys. Rev. Lett.* **87**, 182002 (2001), hep-ex/0107043.
9. D. Gaskell for the HERMES collaboration, Spring 2002 APS Meetings.

How to measure OFPDFs?

- Meson Production

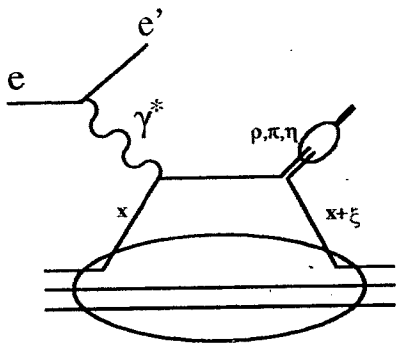

  - Easy to detect final state
  - Messy theory, need the meson wave function

- Deeply Virtual Compton Scattering (DVCS)

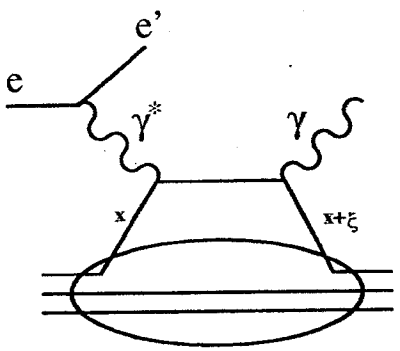

  - Clearer theory, all QED except for OFPDFs
  - Large background due to Bethe-Heitler (BH)

ZEUS/H1 - Method

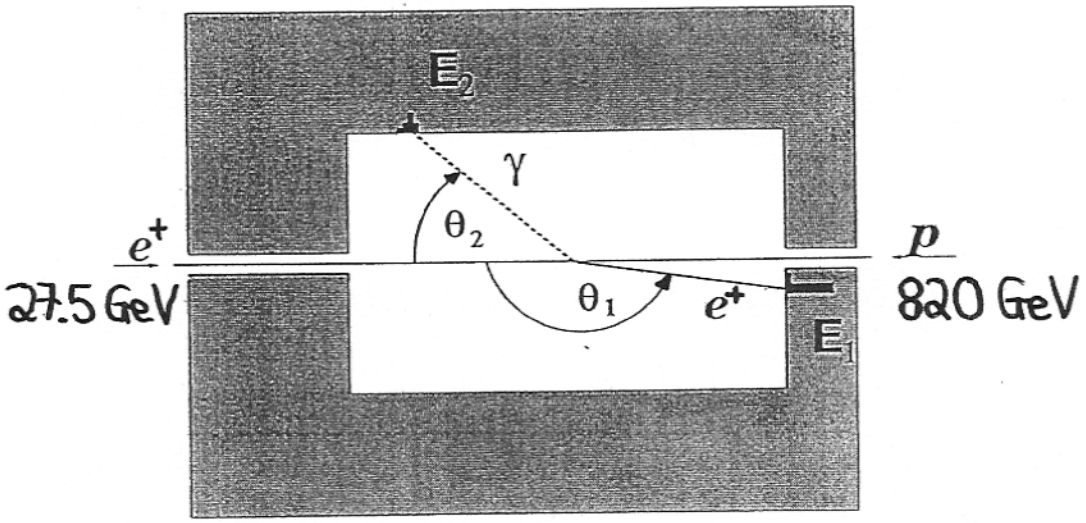

- Sample – $e^+\gamma$ and solo-γ events
  - two EM ($E_i > 2$ GeV) clusters
  - at most one EM cluster with track

- Cuts: $Q^2 > 6\ \mathrm{GeV}^2$
  $|\theta_\gamma - \theta_e| > 0.8$ radians
  $\theta_e < 2.8$ radians and $E_e > 10$ GeV
  $\theta_\gamma < 2.4$ radians and $E_\gamma > 2$ GeV
  $y_\gamma < 0.99$

- Use shower profile to sort $\pi^\circ \to \gamma\gamma$ from γ events

- Look at angular distribution of γ

ZEUS/H1 - Results

ZEUS 1996/97 Preliminary

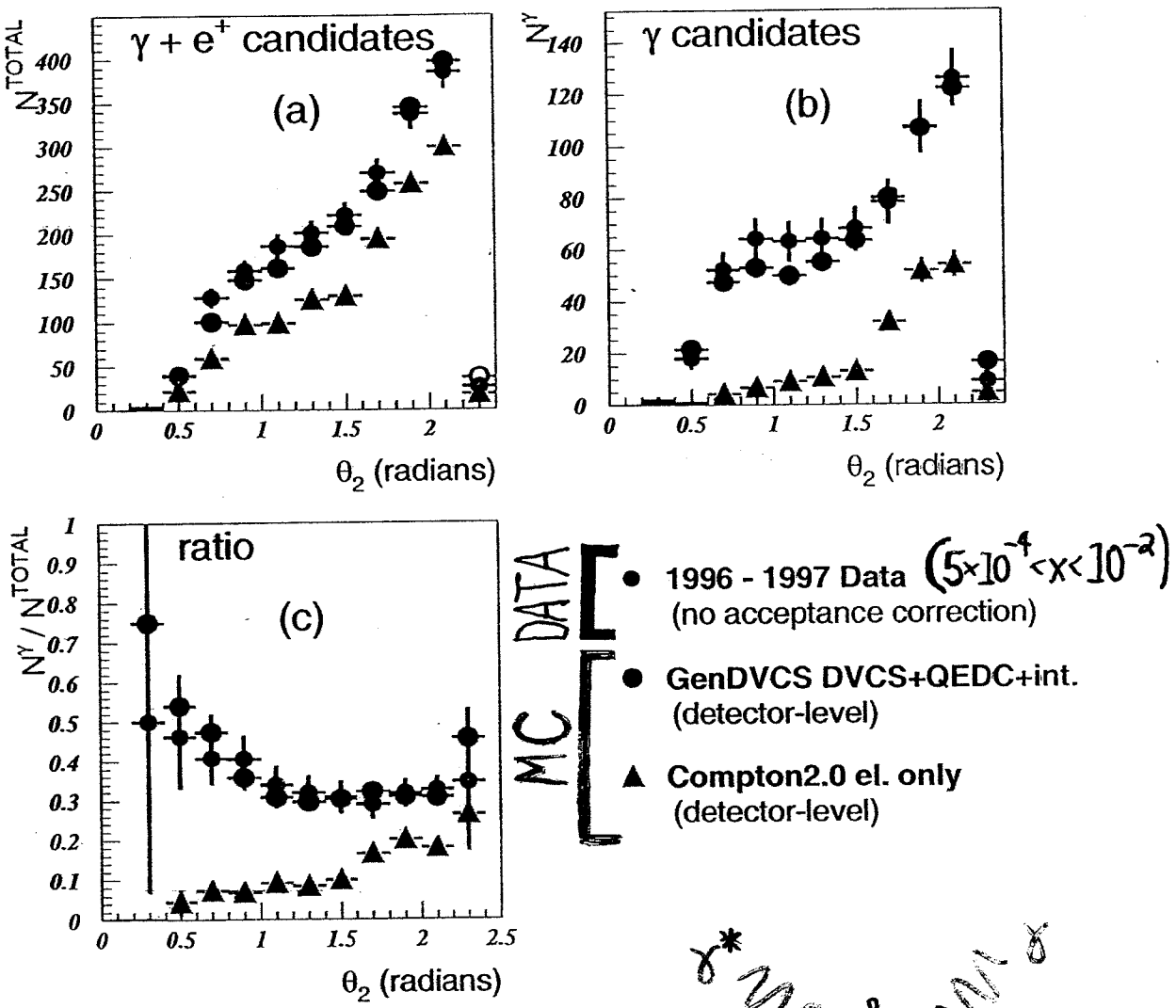

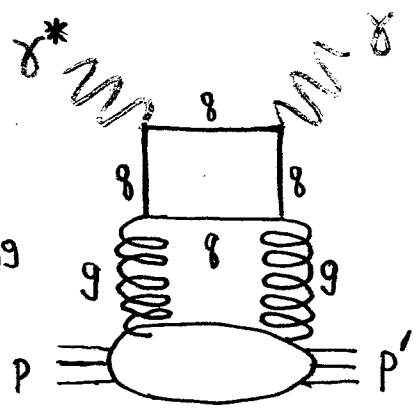

MC: L.L. Frankfurt, et al., PRD 59 (119901E), 1999

DATA: ZEUS Collaboration talk (preliminary release)

ZEUS/H1 - Results

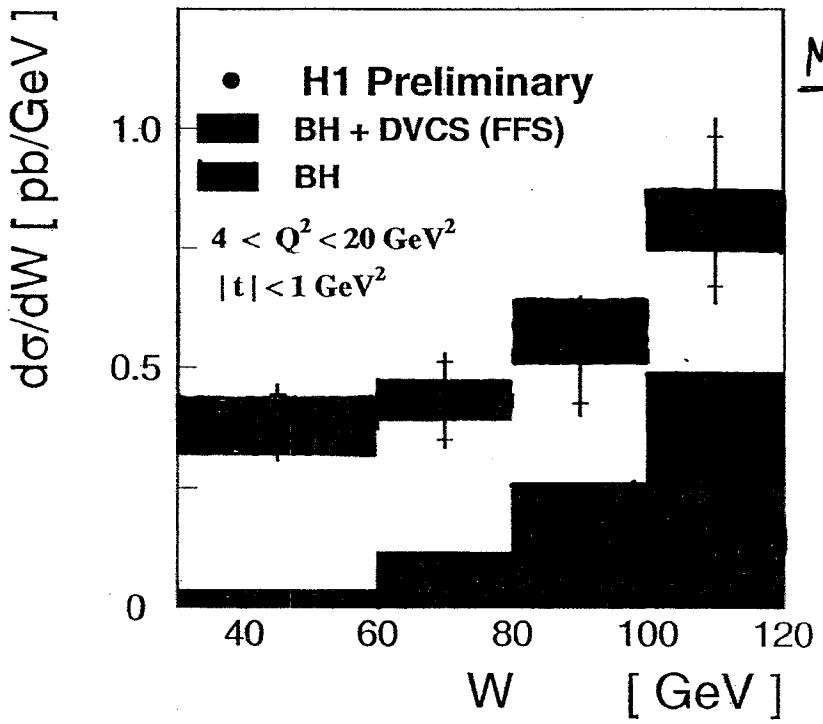

MC: Same Physics As ZEUS except $b_r \sim 7$ to $10\,GeV^{-2}$ instead of $4.5\,GeV^{-1}$

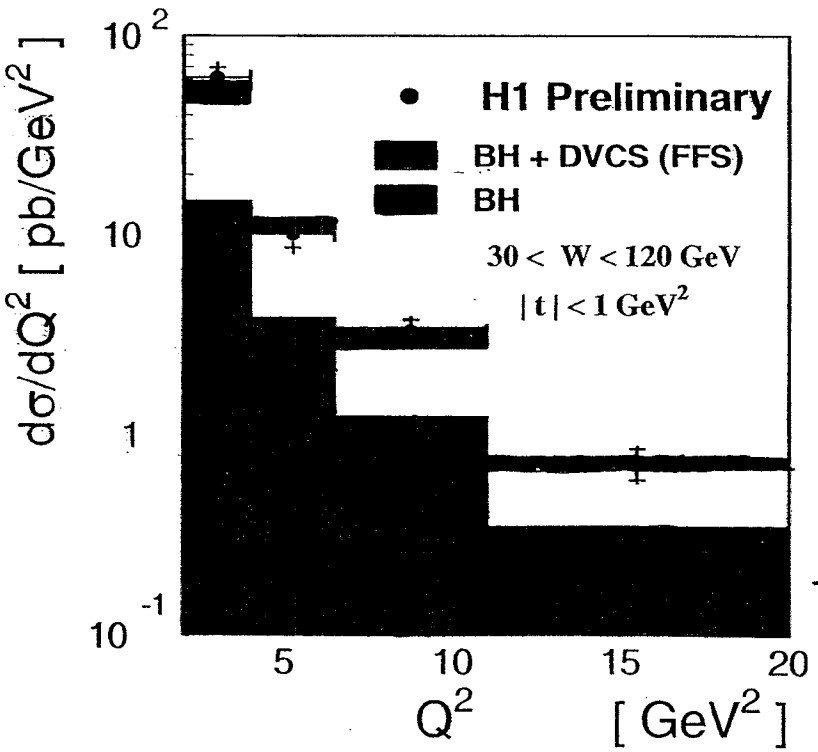

Source: R. Stamen DIS2000 Transparencies

Azimuthal Asymmetries

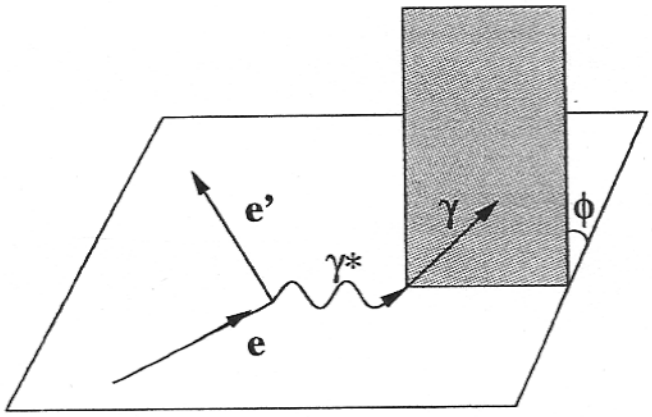

Isolate the BH-DVCS interference term ...

- Lepton Beam Charge

$$d\sigma_{e+} - d\sigma_{e-} \sim \mathrm{Re}\left[M^{1,1}\right]\cos(\phi) + \mathrm{Re}\left[M^{0,1}\right]\cos(2\phi) + \mathrm{Re}\left[M^{-1,1}\right]\cos(3\phi)$$

- Lepton Beam Helicity

$$d\sigma_{\leftarrow} - d\sigma_{\rightarrow} \sim \mathrm{Im}\left[M^{1,1}\right]\sin(\phi) + \mathrm{Im}\left[M^{0,1}\right]\sin(2\phi)$$

where $M^{i,j}$ are helicity amplitudes which dependent linearly on the SPDs.

Single Spin Asymmetry -vs- Phi

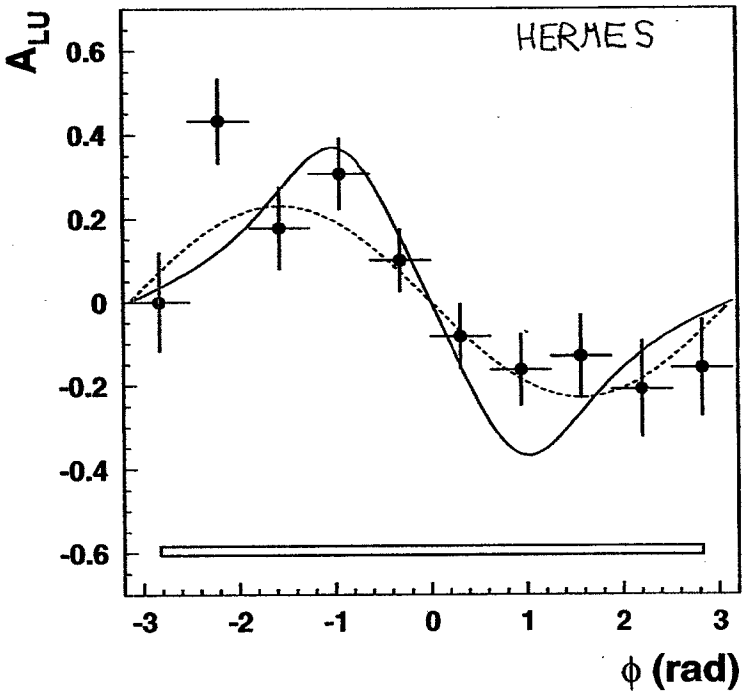

• Kivel, Polyakov, Vanderhaeghan Phys. Rev. D63 (2001) 114014

$$\mathrm{SSA} = \frac{(d\sigma^+/d\phi) - (d\sigma^-/d\phi)}{<|P_b|> (d\sigma^+/d\phi) + (d\sigma^-/d\phi)}$$

with a $0.4 < M_x < 1.4$ GeV cut was applied.

- clear $\sin(\phi)$ dependence seen in "exclusive" bin
- this dependence is not present in higher M_x bins

Single Spin Asymmetry -vs- Phi (CLAS)

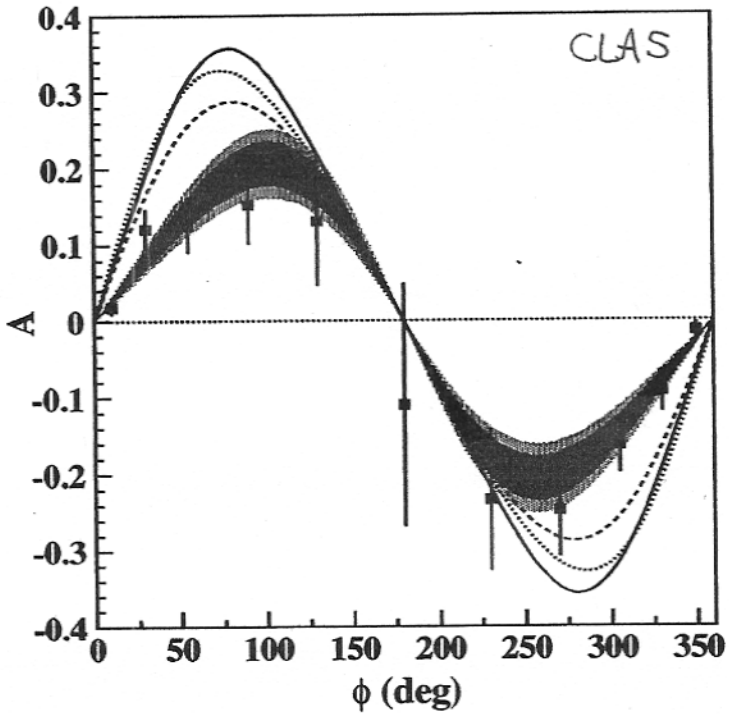

$$A = \frac{(d\sigma^+/d\phi) - (d\sigma^-/d\phi)}{<|P_b|> (d\sigma^+/d\phi) + (d\sigma^-/d\phi)}$$

π° background subtracted using $ep \to ep\pi^\circ$ data.

- clear $\sin(\phi)$ dependence seen in "exclusive" bin
- this dependence is not present in higher M_x bins

Charge Asymmetry -vs- Phi

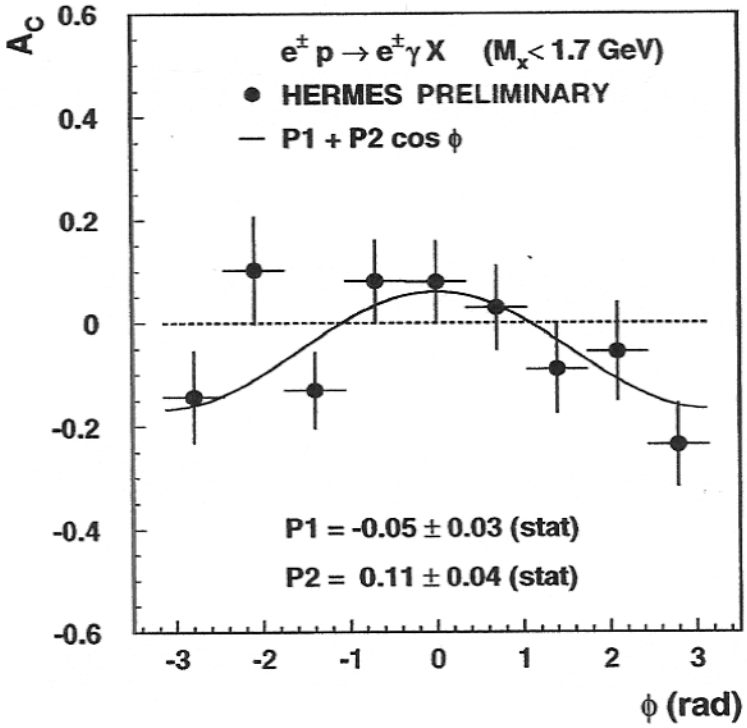

$$\mathrm{A_C}(\phi) = \frac{(d\sigma_{e^+}/d\phi) - (d\sigma_{e^-}/d\phi)}{(d\sigma_{e^+}/d\phi) + (d\sigma_{e^-}/d\phi)}$$

with a $M_x < 1.7\ \mathrm{GeV}$ cut was applied.

- clear $\cos(\phi)$ dependence seen in "exclusive" bin
- this dependence is not present in higher M_x bins

Quark-hadron duality in electron–nucleon scattering

W. Melnitchouk
Jefferson Lab, 12000 Jefferson Avenue, Newport News, VA 23606

Quark-hadron duality addresses some of the most fundamental issues in strong interaction physics, in particular the nature of the transition from perturbative to nonperturbative QCD. In this talk I summarize recent developments in quark-hadron duality in lepton–hadron scattering, and outline how duality can be studied at future high-luminosity facilities such as the electron–ion collider.

In its broadest form, quark–hadron duality postulates that physical quantities calculated in a quark-gluon basis should be identical to those evaluated in a hadronic basis. The phenomenon of duality shows up in many physical processes, such as e^+e^- annihilation into hadrons, or semi-leptonic decays of heavy mesons. One of the more intriguing examples, initially observed some 30 years ago by Bloom and Gilman [1], is in inclusive inelastic electron–nucleon scattering.

Bloom-Gilman duality refers to the observation that the inclusive F_2 structure function at low hadronic final state mass, W, generally follows a global scaling curve which describes high-W data, to which the resonance structure function averages. This behavior was more recently confirmed in high precision measurements of the F_2 structure function in the resonance region at Jefferson Lab [2]. The similarity between the averaged resonance and scaling structure functions implies that the lowest moment of F_2 is approximately independent of Q^2 [3]. Furthermore, the data [2] indicate that duality works remarkably well for each of the low-lying resonances, including the elastic, to rather low values of Q^2 (~ 0.5 GeV^2).

An important consequence of duality is that the strict distinction between the resonance and deep-inelastic regions becomes entirely artificial. This is illustrated by the observation that at $Q^2 = 1$ GeV^2 around 2/3 of the F_2 structure function comes from the resonance region, $W < 2$ GeV, while on the other hand the resonances and the deep-inelastic continuum conspire to produce only about a 10% correction to the lowest moment of F_2 at the same Q^2 [4]. Even though each resonance is built up from a multitude of twists, when combined the resonances interfere in such a way that they resemble the leading twist component. This interplay of resonances and scaling has recently been studied in the context of quark models, where it was explicitly shown that under certain conditions a sum over the squares of transition form factors yields a scaling function at high Q^2 [5].

If, in addition to its global realization, quark-hadron duality is also valid locally, one can use measured structure functions in the resonance region at large x to directly extract electromagnetic transition form factors. For the case of elastic scattering, local duality enables one to relate the elastic form factors with the deep-inelastic structure function at $x \sim 1$. Empirical electromagnetic form factors at large Q^2 can then be used to predict the $x \to 1$ behavior of deep-inelastic structure functions, or vice versa [1,3,6,7]. Analyses based on recent structure function data [2] find surprisingly good agreement between the measured elastic magnetic form factor and that extracted from the inclusive data on the basis of duality [6,7].

A largely unexplored domain of duality with potentially broad applications is the production of mesons (M) in semi-inclusive electron scattering, $eN \to e'MX$. At high energy the scattering and production mechanisms factorize, with the cross section at leading order in QCD given by a simple product of the structure function and a quark $\to$ meson fragmentation function. In terms of hadronic variables the same process can be described through the excitation of nucleon resonances, N^*, and their subsequent decays into mesons and lower lying resonances, $\widetilde{N}^*$. The hadronic description is rather elaborate, however, as the production of a fast outgoing meson in the current fragmentation region at high energy requires non-trivial cancellations of the angular distributions from various decay channels [5]. Heuristically, the duality between the quark and hadron descriptions of semi-inclusive meson production can be written as:

$$\left| \sum_{N^*, \widetilde{N}^*} F_{\gamma^* N \to N^*}(Q^2, W^2)\ \mathcal{D}_{N^* \to \widetilde{N}^* M}(W^2, \widetilde{W}^2) \right|^2 \sim \sum_q e_q^2\ q(x)\ D_{q \to M}(z)\ ,$$

where $D_{q \to M}$ is the quark $\to$ meson fragmentation function for a given $z = E_M/\nu$, $F_{\gamma^* N \to N^*}$ is the $\gamma^* N \to N^*$ transition form factor, which depends on the mass of the virtual photon and the excited nucleon ($W = M_{N^*}$), and $\mathcal{D}_{N^* \to \widetilde{N}^* M}$ is a function representing the decay $N^* \to \widetilde{N}^* M$, where $\widetilde{W}$ is the invariant mass of the final state $\widetilde{N}^*$.

The virtue of semi-inclusive production lies in its ability to identify individual quark species in the nucleon by tagging specific mesons in the final state, enabling both the flavor and spin of quarks and antiquarks to be systematically determined. To what extent factorization applies at lower energy is an open question, and the signatures of duality in the resonance region of semi-inclusive scattering are under active investigation. Confirmation of duality in inclusive hadron production would clearly open the way to an enormously rich semi-inclusive program in the pre-asymptotic regime, allowing unprecedented spin and flavor decomposition of quark distributions.

[1] E.D. Bloom and F.J. Gilman, Phys. Rev. Lett. **16**, 1140 (1970).
[2] I. Niculescu *et al.*, Phys. Rev. Lett. **85**, 1182, 1186 (2000).
[3] A. de Rújula, H. Georgi and H.D. Politzer, Ann. Phys. **103**, 315 (1975).
[4] X. Ji and P. Unrau, Phys. Rev. D **52**, 72 (1995).
[5] N. Isgur *et al.*, Phys. Rev. D **64**, 054005 (2001).
[6] R. Ent, C.E. Keppel and I. Niculescu, Phys. Rev. D **62**, 073008 (2000).
[7] W. Melnitchouk, Phys. Rev. Lett. **86**, 35 (2001).

Bloom-Gilman Duality

"Resonances average to a universal curve"

Inclusive F_2 structure function at low W follows global scaling curve which describes high W data, to which the resonance structure function averages

Equivalence of averaged resonance and scaling structure functions holds for each resonance region, over restricted regions in W
$\longrightarrow$ resonance – scaling duality exists *locally*

Recent JLab data confirm earlier observations:
$\longrightarrow$ duality works remarkably well to rather low Q^2 ($\sim$ 0.5 GeV^2)

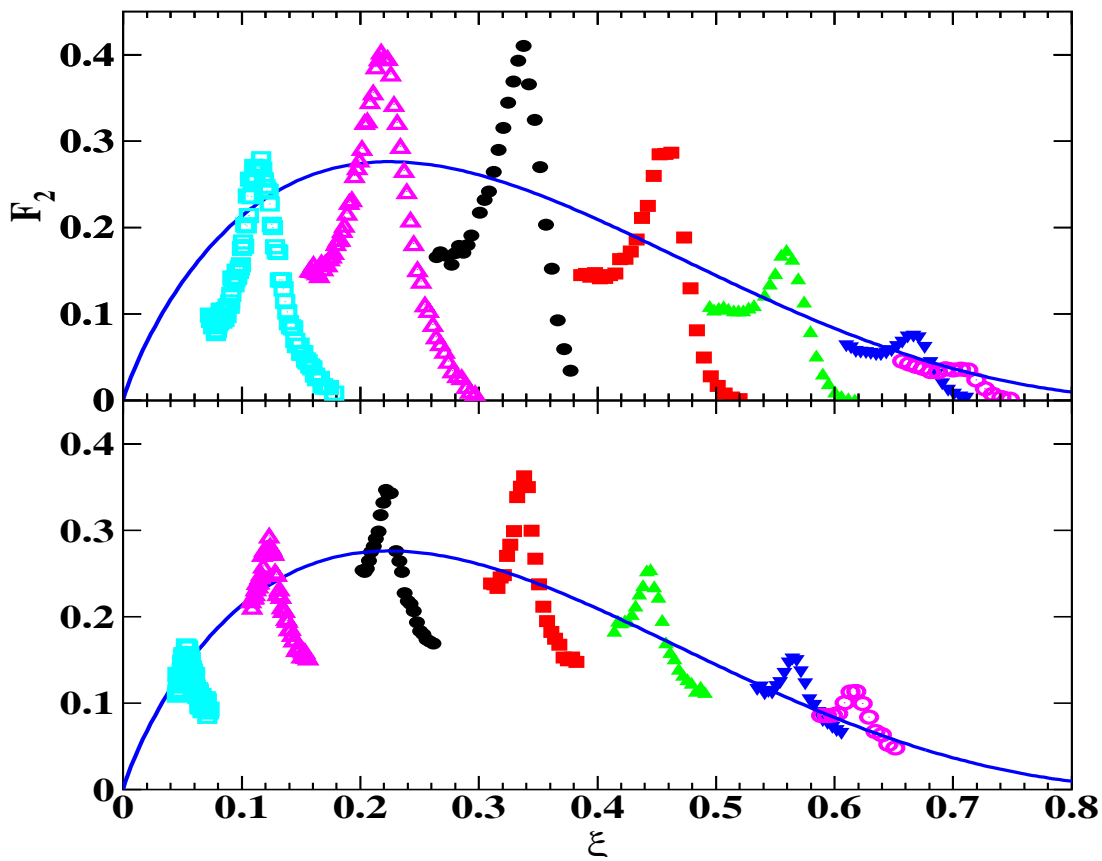

Proton F_2 structure function vs. Nachtmann ξ, in the first (upper panel) and second (lower panel) resonance regions, for Q^2 between 0.07 GeV^2 (smallest ξ) and 3 GeV^2 (largest ξ). Solid line = global scaling curve (from all resonance data)

C.S. Armstrong et al., Phys. Rev. D 63 (2001) 094008

Resonances & Global DIS Analyses

Bloom-Gilman duality $\Rightarrow$ distinction between "resonance" and "DIS" regions is artificial

Standard procedure in global DIS analyses: omit from data base entire resonance region, $W < 2$ GeV

E.g. at $Q^2 = 1$ GeV^2 about 70% of F_2 comes from $W < 2$ GeV

However, because of duality, resonances and DIS continuum conspire to produce $\sim$ 10% higher twist ($1/Q^2$) contribution!

Resonances are an integral part of the scaling structure functions !

Duality in Semi-inclusive Scattering

- Factorization of interaction and production vertices $\longrightarrow$

$$\frac{d^3\sigma}{dx dz dQ^2} \sim \sum_q e_q^2 \; q(x, Q^2) \; D_q(z, Q^2)$$

- Duality for fragmentation functions?

  $\longrightarrow$ *How do resonances build up semi-inclusive scaling curve?*

- Flavor and spin separation

- Need sufficiently large range of Q^2 and W

  $\longrightarrow$ possible with EIC!

Duality for fragmentation functions

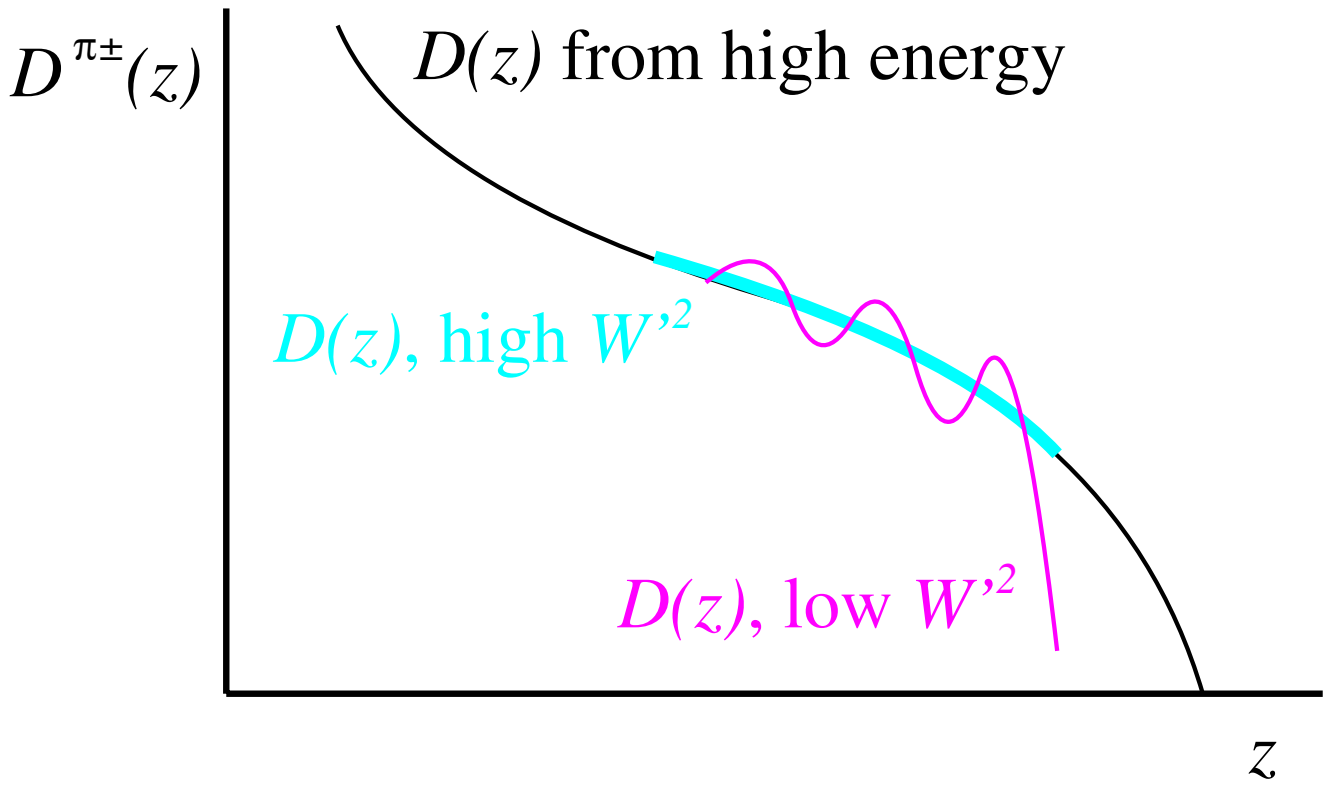

Future Transversity Measurements

M. Grosse Perdekamp[a]

[a]RIKEN BNL Research Center, Brookhaven National Laboratory, Upton, NY 11973, USA

1. Introduction

The experimental study of transversity distributions at leading twist requires observables which are the product of two objects with odd chirality. This was first discussed by Ralston and Soper [1] for Drell Yan scattering of two transversely polarized hadrons: The transverse double spin asymmetry, A_{TT}, is proportional to $\delta q \delta \bar{q}$ with even chirality.

Transverse single spin asymmetries A_T (e.g. unpolarized leptons on transversely polarized nucleon targets) in *semi-inclusive* DIS and *pp* scattering may offer an alternative way to observe helicity flip contributions at leading twist. This possibility relies on the presence of quark fragmentation functions (FF) which are sensitive to the quark polarization in the final state and possess the necessary negative chirality.

The current interest in transversity distributions results from a recent HERMES result on azimuthal single spin asymmetries [2] and a preliminary SMC result [3], which may suggest that Collins's function $H_1^\perp$ and the transversity distribution function δq in fact are different from 0; see reference [4] for a detailed discussion.

2. Future Transversity Measurements

2.1. Drell Yan

Originally the transverse double spin asymmetry, A_{TT}, in Drell Yan was viewed as a good candidate for a measurement of the transversity distribution functions at RHIC, $A_{TT} \sim \delta q \delta \bar{q}$. Unfortunately, a recent analysis by Martin et al. [5] – using PHENIX acceptances and the projected luminosities for pp-running at RHIC, $320\,\mathrm{pb}^{-1}$/year at 200 GeV – estimates A_{TT} to be about 1% with statistical errors comparable to the asymmetry itself for a projected measurement at RHIC. However, future luminosity upgrades at RHIC possibly can reach integrated luminosities of up to $\int_{year} Ldt = 8\,\mathrm{fb}^{-1}$ at 200 GeV, resulting in sufficiently large Drell Yan data samples for a transversity analysis.

2.2. Semi Inclusive Deep Inelastic Scattering

At HERMES the observable is Collins' single spin asymmetry for charged pion production in deep inelastic electron proton scattering. In a partonic picture of the nucleon the transverse single spin asymmetry A_T is related to the transversity distributions as follows:

$$A_T(x,z) \sim \frac{\sum_q e_q^2 \delta q(x) H_1^{\perp q}(z)}{\sum_q e_q^2 q(x) D_1^q(z)} \tag{1}$$

where $H_1^{\perp q}$ is the Collins function for a quark of flavor q and D_1^q is the regular spin independent fragmentation function. Korotkov, Nowak and Oganessyan have proposed an analysis procedure for the HERMES transverse asymmetries that – under the assumption of u-quark dominance, $\delta d = 0$ – results in the extraction of the shape for $\delta u(x)$ and the ratio $H_1^\perp / D_1^u$ [6]. As a normalization condition to fix the absolute size of $\delta u(x)$ and the fragmentation function ratio it is further assumed that $\delta u(x_0 = 0.25) = \Delta u(x_0)$ at some soft scale, $Q_0^2 \approx 0.4$ GeV. Alternatively, it may be worthwhile to investigate if the ratio $H_1^\perp / D_1^u$ can be determined from fragmentation function measurements in e^+e^- annihilation using LEP and b-factory data, see section (3).

A similar measurement will be attempted by the COMPASS collaboration at CERN. The higher beam energy, 100 – 200 GeV compared to 27.5 GeV may allow, for the first time, the

exploitation of interference fragmentation processes. However, truly decisive experiments to measure transversity distributions and their first moments, the tensor charge, appear to be two future high luminosity electron proton scattering experiments: At DESY a fixed target experiment has been proposed for one arm of a possible future e^+e^- linear accelerator collider at DESY: TESLA-N; it is estimated that the first moment of δu can be measured to about one percent and for δd to 6% [7]. At BNL the prospects of a future electron ion collider (EIC) with luminosities reaching $4\,\mathrm{fb}^{-1}$/year have been studied. [8]: A measurement with the statistical precision of the HERMES measurement but at lower x can be achieved in one day of running or $20\,\mathrm{pb}^{-1}$; see Fig. (1).

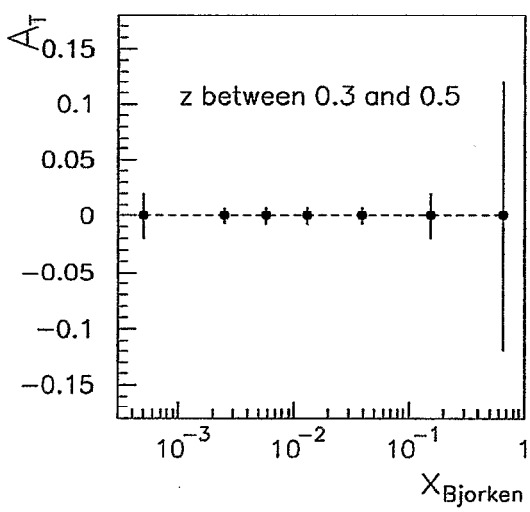

Figure 1. Projected sensitivities for the single spin asymmetries in single inclusive pion production at the EIC for $\int_{day} Ldt = 20\,\mathrm{pb}^{-1}$ and $0.3 < z = E_\pi/E_\gamma < 0.5$.

2.3. Single Spin Asymmetries in Polarized Proton Scattering

In addition to the double spin asymmetry measurements in Drell Yan the following single spin asymmetry measurements have been suggested for polarized proton scattering experiments:

- Single spin asymmetries in two pion interference fragmentation.
- The measurement of azimuthal asymmetries in the production of pions around the jet-axis (Collins fragmentation function).
- Interference fragmentation and Collins fragmentation in direct photon jet events.

With the presently available luminosities and detectors the proposal of Collins et al. [9] and Jaffe et al. [10] to utilize chiral odd two pion interference fragmentation processes appears to be the most promising approach to measure transversity at RHIC. This channel also has been studied for the RAMPEX experiment at IHEP Protvino [11].

3. Collins and Interference Fragmentation Functions in e^+e^-

All future transversity measurements have in common that their success critically depends on the knowledge of the spin dependent and chiral odd fragmentation functions giving sensitivity to transverse quark spin in the final state. Atru and Collins have provided a detailed recipe how to extract interference fragmentation functions from light quark di-jet events in e^+e^- collisions [12]. Efremov , Smirnova and Tkachev have carried out first experimental studies using LEP data from DELPHI [13]. A recent discussion of the prospects of transversity measurements using future fragmentation function information from e^+e^- can be found in reference [14].

Additional studies in e^+e^- have been proposed using the high statistic data sample of the Belle experiment at the KEK b-factory [15] with the goal to measure the two relevant fragmentation functions:

- The Collins function $H_1^\perp$: The fragmentation of a transversely polarized quark into a charged pion and the azimuthal distribution of the final state pion with respect to the initial quark momentum (jet-axis).
- Interference fragmentation functions $\delta\hat{q}^{h_1,h_2}$: The fragmentation of transversely

Table 1
Present and future measurements of transversity distributions. Different processes are used to access transversity distributions: Collins fragmentation (CF), interference fragmentation (IF) and Drell Yan (DY).

Experiment	Location	Process	$\sqrt{s}$ [GeV]	year
HERMES	DESY/HERA	DIS: CF	7.5	2001
COMPASS	CERN/SPS	DIS: CF, IF(?)	14 – 20	2003
EIC-detector	BNL/EIC	DIS: CF, IF	65 – 100	2008+
TESLA-fixed target	DESY/TESLA	DIS: CF, IF	8 – 22	2010+
RAMPEX	IHEP Protvino	pp: IF	12	2001
BRAHMS,PHOBOS	BNL/RHIC	pp: IF	50 – 500	2002
PHENIX,STAR	BNL/RHIC	pp: IF, CF, DY	50 – 500	2006

polarized quarks into pairs of hadrons in a state which is the superposition of two different partial wave amplitudes; e.g. π^+, π^- pairs in the ρ, σ invariant mass region.

High luminosities at KEKB – presently the integrated luminosity is $36.4 fb^{-1}$ – and Belle's superior particle identification will allow fragmentation function measurements over a large range in $z = E_h/E_q$ and for different combinations of final state hadrons.

REFERENCES

1. Ralston J., Soper D.E., *Nucl. Phys.* **B152**, 109 (1979).
2. Airapetian A. et al., *Phys. Rev. Lett.* **84**, 4047 (2000).
3. Bravar A., *Nucl. Phys. (Proc. Suppl.)* **B79**, 520 (1999).
4. K.A. Oganessyan, N. Bianchi, E. De Sanctis, W.D. Nowak, hep-ph/00 10261.
5. Martin O. et al., Phys. Rev. **D60**, 117502 (1999). *Phys. Rev.* **D57**, 5920 (1998).
6. V.A. Korotkov, W.-D. Nowak, K.A. Oganessyan, Eur. Phy. J. C18 (2001)639.
7. TESLA-N study group, hep-ph/0011299(2000).
8. EIC White Paper submitted to the NSAC LRP meeting, Santa Fe (2001).
9. Collins J.C. , Heppelmann S.F. and Ladinsky G.A., *Nucl. Phys.* **B420**, 565 (1994); Collins J.C. and Ladinsky G.A., Preprint PSU-TH-114, hep-ph/9411444; Collins J.C., Proceedings of the RHIC Spin Workshop, October 6 - 8, 1999, p. 158.
10. Jaffe R.L., Jin X., Tang J. et al., *Phys. Rev. Lett.* f 80, 1166 (1998);
11. Yu.I. Arestov, Proc of DIS2000, World Scientific (2001)247.
12. X. Artru and J. Collins, Z. Phys. **C69**, 277(1996).
13. A.V. Efremov, O.G. Smirnova, L.G. Tkachev, Nucl. Phys. Proc. Suppl. 74, 49 (1999), A.V. Efremov, L.G. Tkachev, Acta Physics Polonica B, Vol. 29 (1998)1385.
14. D. Boer, hep-ph/0106206.
15. M. Grosse Perdekamp, J. S. Lange, A. Ogawa, Letter of Intent to Belle Collaboration, unpublished (2001).

Measuring Transversity

Matthias Grosse Perdekamp, RBRC

- Introduction
- Avenues to access transversity

$$ep^{\uparrow}, pp^{\uparrow} \rightarrow \pi^{+/-} + X \qquad \text{(Collins effect)}$$

$$ep^{\uparrow}, pp^{\uparrow} \rightarrow \pi^{+}\pi^{-} + X \qquad \text{(Interference fragmentation)}$$

$$pp^{\uparrow} \rightarrow l^{+}l^{-} + X \qquad \text{(Drell Yan)}$$

- Current and future experiments

  HERMES, COMPASS

  Polarized HERA, EIC, TESLA-N

  RHIC

- Fragmentation Functions

Avenues to Transversity

Polarized pp

RHIC/BNL

- Collins Effect :

$$A_T(pp_\perp \to \pi^\angle + X)$$

J.C. Collins, Nucl. Phys. B396, 161(1993)

- π^+, π^- Interference Fragmentation :

$$A_T\left(p_\perp p \to (\pi^+, \pi^-) + X\right)$$

J. Collins, S. Heppelmann, G. Ladinsky, Nucl.Phys. B420 (1994)565

R. Jaffe, X.Jin, J. Tang Phys. Rev. D57 (1999)5920

- Drell Yan : $A_{TT}(p_\perp p_\perp \to ll) \Leftrightarrow \delta q \cdot \delta \bar{q}$

J.Ralston and D.E. Soper, Nucl. Phys. B152, 109(1979)

- Inclusive jet production

$$5 \cdot 10^{-4} \le A_{TT} \le 3 \cdot 10^{-3}$$

W. Vogelsang and M. Stratmann, RBRC Wrkshp on Transversity (2000)

STAR

PHENIX

Polarized DIS

HERA/DESY, SPS/CERN, EIC, TESLA-N

(Approved Transversity Programs)

HERMES

COMPASS

TESLA-N

EIC

- Collins Effect :

$$A_T(lp_\perp \to e\pi^\angle + X)$$

- π^+, π^- Interference Fragmentation :

$$A_T\left(lp_\perp \to l + (\pi^+, \pi^-) + X\right)$$

Observables $\propto \delta q \cdot H$

(O $\propto$ distribution - func. $\times$ fragmentation func.)

Transversity: Global Analysis

- Measure $\delta q \cdot \delta \hat{q}_l$ RHIC, EIC, TESLA - N

  $\delta q \cdot C$ RHIC, HERMES, COMPASS, EIC, TESLA - N

  $\delta q \cdot \delta \bar{q}$ RHIC (after luminosity upgrade)

  (See Daniel Boer's talk at the Trento workshop Nucl.Phys.Proc.Suppl.105:76-79,2002)

- Measure $\delta \hat{q}_l, C$ in e^+e^- using b - factory data (Belle, Babar)

- Tensor Charge Lattice calculation (RBRC : QCDOC)

HERMES

$ep^{\uparrow} \to \pi^{+/-} + X$ (Collins effect)

V.A. Korotkov, W.-D. Nowak, K.A. Oganessyan, hep-ph/0002268

Experimental asymmetries:

$$A_T = \frac{\sum_{\uparrow-\downarrow} \frac{|p_{h\perp}|}{zM_h} \sin(\phi_s^l + \phi_h^l)}{N^{\uparrow} + N^{\downarrow}}$$

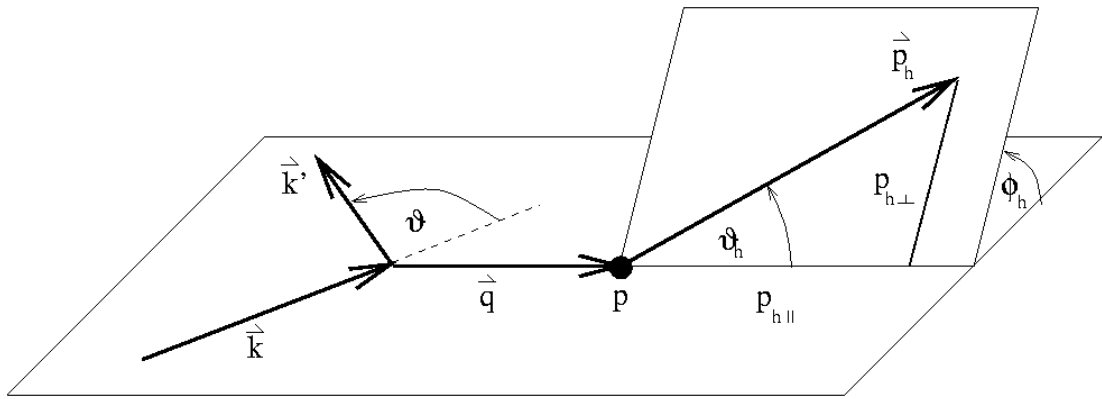

Relation to parton distributions and FF:

$$A_T(x,z) = P_T D_{nn} \frac{\sum_q e_q^2 \delta q(x) H_1^{\perp q}(z)}{\sum_q e_q^2 q(x) D_1^q(z)}$$

Factorization in x and z (?)

$$= P_T D_{nn} \frac{\delta u(x)}{u(x)} \frac{H_1^{\perp u}(z)}{D_1^u(z)}$$

u-quark dominance

Collins Effect at EIC

$$A_T^{\pi^+}(lp_\perp \to e + \pi \ + X)$$

Detector Acceptance

$-3.6 < \eta < 3.6$

Integrated Luminosity

$20\,pb^{-1}$ (less than 1 day)

Cuts: $Q^2 > 1\,\text{GeV}^2$

$x_F > 0$

$z > 0.1$

Projected errors on A in 5 z- bins

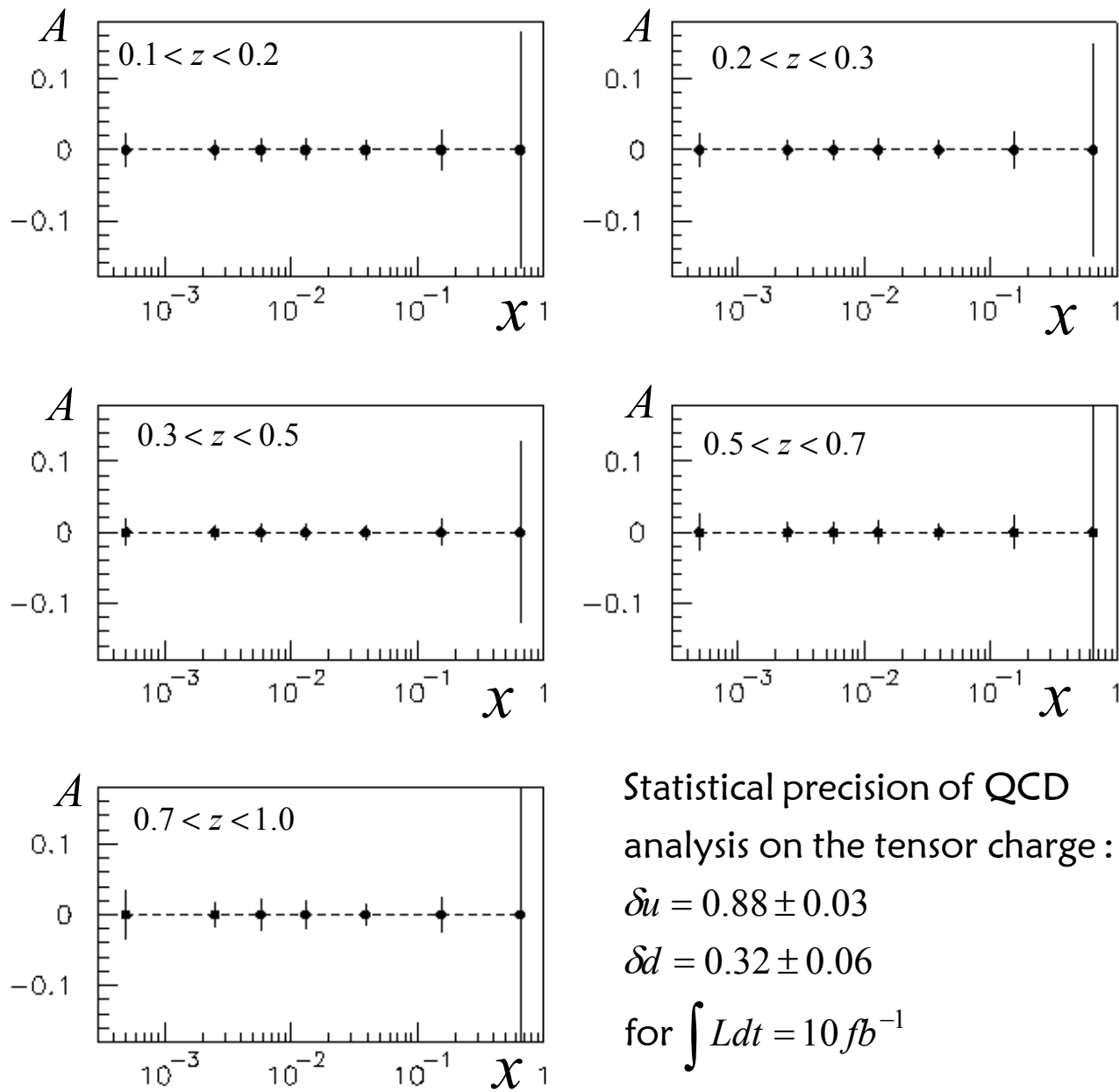

Statistical precision of QCD analysis on the tensor charge:

$\delta u = 0.88 \pm 0.03$

$\delta d = 0.32 \pm 0.06$

for $\int L dt = 10\,fb^{-1}$

FF measurements at Belle

Akio Ogawa, Soeren Lange, Matthias Grosse Perdekamp (RBRC)

Experimental Requirements e^+e^-	**Belle**
Jet production from light quarks	Off resonance data
Energy at which pQCD is applicable	$s \sim 100 GeV^2$
Moderate energy for analyzing power FF decreases as energy increases	s(Belle) < s(LEP)
Avoid complication from Z pole	s(Belle) < M_z
Requires good detector: Wide acceptance Momentum/mass resolution PID capability	Belle!

H*H and F*F can be measured (time frame: + 2years)

B factories : Belle, Babar, Cleo…

Belle

8GeV+3.5GeV
1.3/fb/week

Babar

9GeV+3.1GeV
~1/fb/week

Cleo

4.7GeV+5.6GeV
~0.35/fb/week

Peak Luminosity $6.6*10^{33}/cm^2/s$

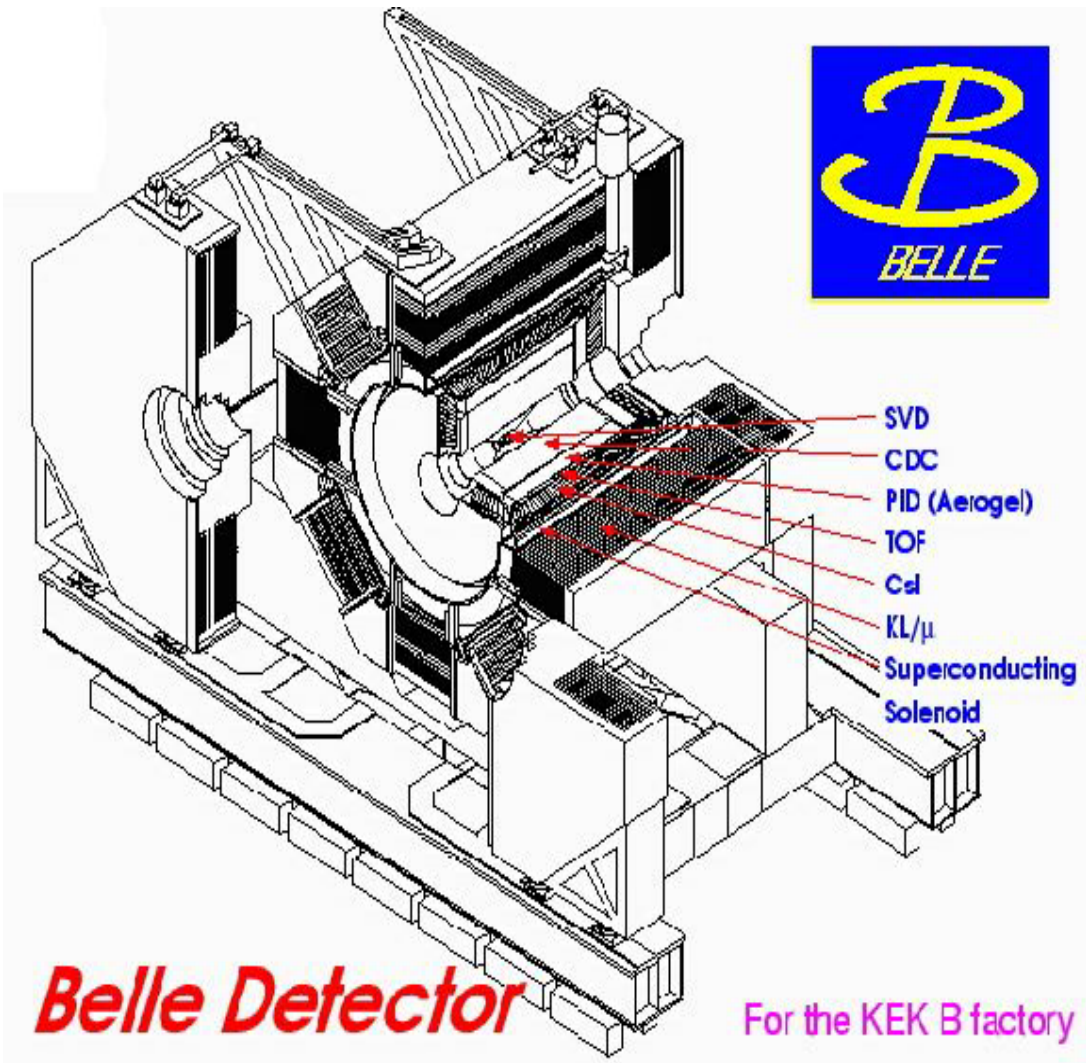

Extracting the Collins Function

$$e^+e^- \rightarrow (\pi^+)_{jet1}(\pi^-)_{jet2}X$$

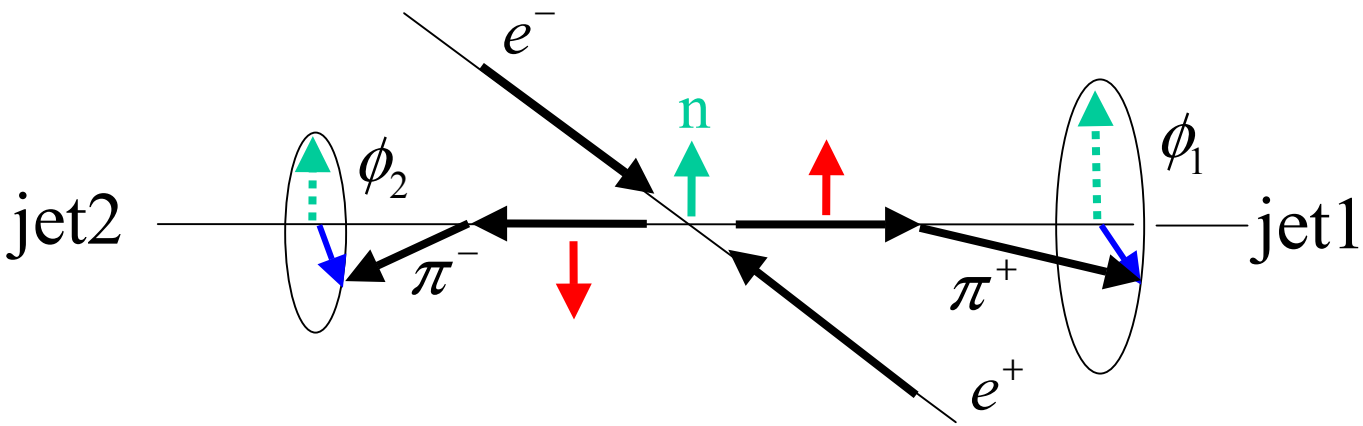

$$A \propto H(z_1)H(z_2)\cos(\phi_1 + \phi_2)$$

Extracting the Interference Frag. Func.

$$e^+e^- \rightarrow (\pi^+\pi^-)_{jet\,1}(\pi^+\pi^-)_{jet\,2}X$$

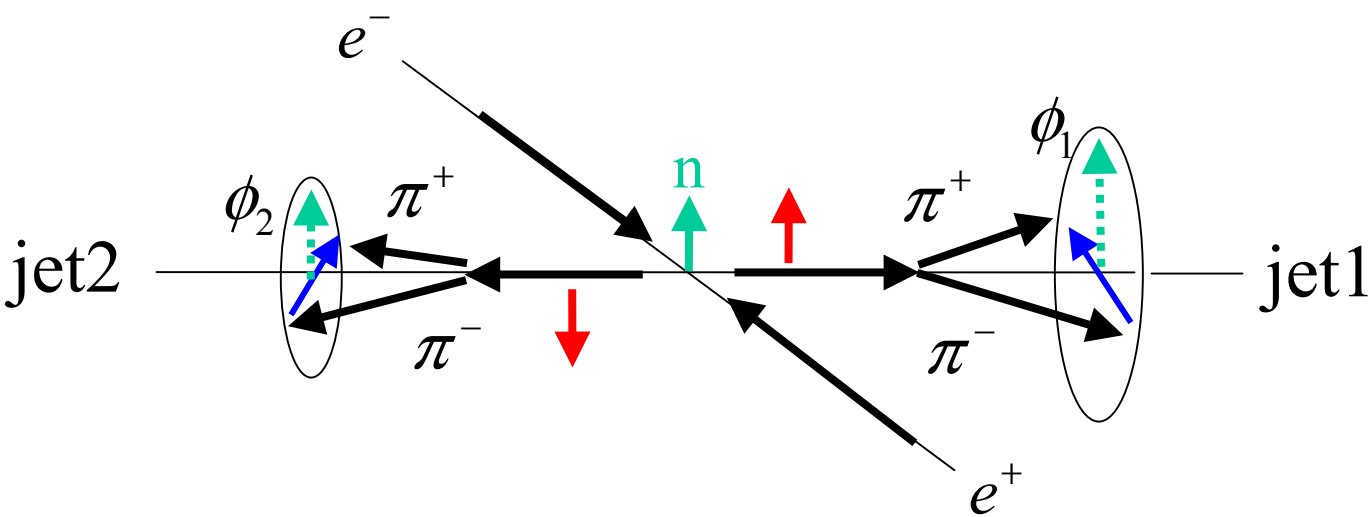

$$A \propto F(z_1,m_1)F(z_2,m_2)\cos(\phi_1+\phi_2)$$

Conclusions

- $\delta q(x)$ remain as the last unmeasured leading twist distribution functions and have attracted strong theoretical interest. Experimental methods are at hand to access transversity distributions.

- HERMES and Belle will provide first reliable information on the size of the analyzing powers in the near future.

- RHIC's transversity program comprises several channels to access transversity. A rigorous program can be carried out with existing detectors and 10 weeks of beam time.

- A future high luminosity e-p experiment appears to be needed for the precise flavor separation and determination of the tensor charge.

An initial study on measuring F_2^p at the EIC

A. Vogt

NIKHEF Theory Group
P.O. Box 41882, 1009 DB Amsterdam, The Netherlands

The deep-inelastic structure functions of the proton remain, more than 30 years after the pioneering experiments at SLAC, among the foremost observables for studying perturbative QCD, determining the proton's parton densities and measuring the strong coupling constant. An impressive amount of data has been accumulated, especially for the structure function F_2, at electron-proton (ep) and muon-proton (μp) fixed-target experiments and at the ep collider HERA at DESY. More data will be obtained, especially at high values of the scale Q^2, in the forthcoming high-luminosity runs of HERA.

Nevertheless, it is worthwhile to study the possible additional structure-function information which can be obtained by an ep run of the projected Electron-Ion Collider (EIC) at BNL. With (maximal) energies of $E_e = 10$ GeV and $E_p = 250$ GeV, the CMS energy of this machine will lie about a factor of three above that of the fixed-target μp experiments, and a factor of three below that of HERA. Thus the EIC can extend the coverage in Q^2 up (down) by one order of magnitude with respect to the former (latter) measurements while offering sizeable regions of overlap with both. Moreover, the high envisaged luminosity of the EIC, which should allow to collect a couple of inverse femtobarns during several weeks, may facilitate measurements at large values of the Bjorken variable x where HERA results will remain severely limited by statistics even after the high-luminosity runs.

For the purpose of the present initial study, it is admissible to neglect electroweak radiative corrections, proton mass effects, and the contribution of the longitudinal structure function F_L. Hence the inclusive differential cross section can be written as

$$\frac{d^2\sigma\,(ep \to eX)}{d\ln x\, d\ln Q^2} \simeq \frac{2\pi\,\alpha_{\rm em}^2}{Q^2}\,\left(1 + (1-y)^2\right)\,F_2^p(x, Q^2)$$

with $y = Q^2/(xs)$ where $s = 4\,E_e E_p$. In order to avoid regions of high background and/or low experimental resolution, the cuts $0.01 < y < 0.7$ and $E_e' > 5$ GeV^2 are imposed on y and the energy E_e' of the scattered electron. Due to the asymmetric kinematics, the minimal angle for tagging the scattered electron is not a critical parameter at the EIC.

The resulting event numbers for an integrated luminosity of 2 fb^{-1} are displayed in Fig. 1 for the inclusive cross section and in Fig. 2 for its charm-production component. The total event numbers are huge for $x < 0.3$ and $Q^2 < 300$ GeV^2. There are also well above 10^4 charm events per half-decade bin in (x, Q^2) in this region, which should facilitate measurements of $F_2^{\rm charm}$ even in view of large charm-identification losses.

In Fig. 3 we show the possible kinematic coverage and statistical accuracy of the F_2^p measurements at the EIC at $x > 0.3$, as compared to the fixed-target data of SLAC and BCDMS (note that the latter results are displayed without their correlated main systematic error, see ref. [1]). In Fig. 4 corresponding expectations for the high-luminosity results from HERA are shown for comparison. Obviously the EIC, with the beam energies and the luminosity as given above, can add quite a relevant contribution to our knowledge of F_2^p, even if a total integrated luminosity of 1 fb^{-1} is reached in the future runs of HERA

References

[1] A. Milsztain and M. Virchaux, Phys. Lett. **B274** (1992) 221

[2] M. Glück, E. Reya and A. Vogt, Eur. Phys. J. **C5** (1998) 461

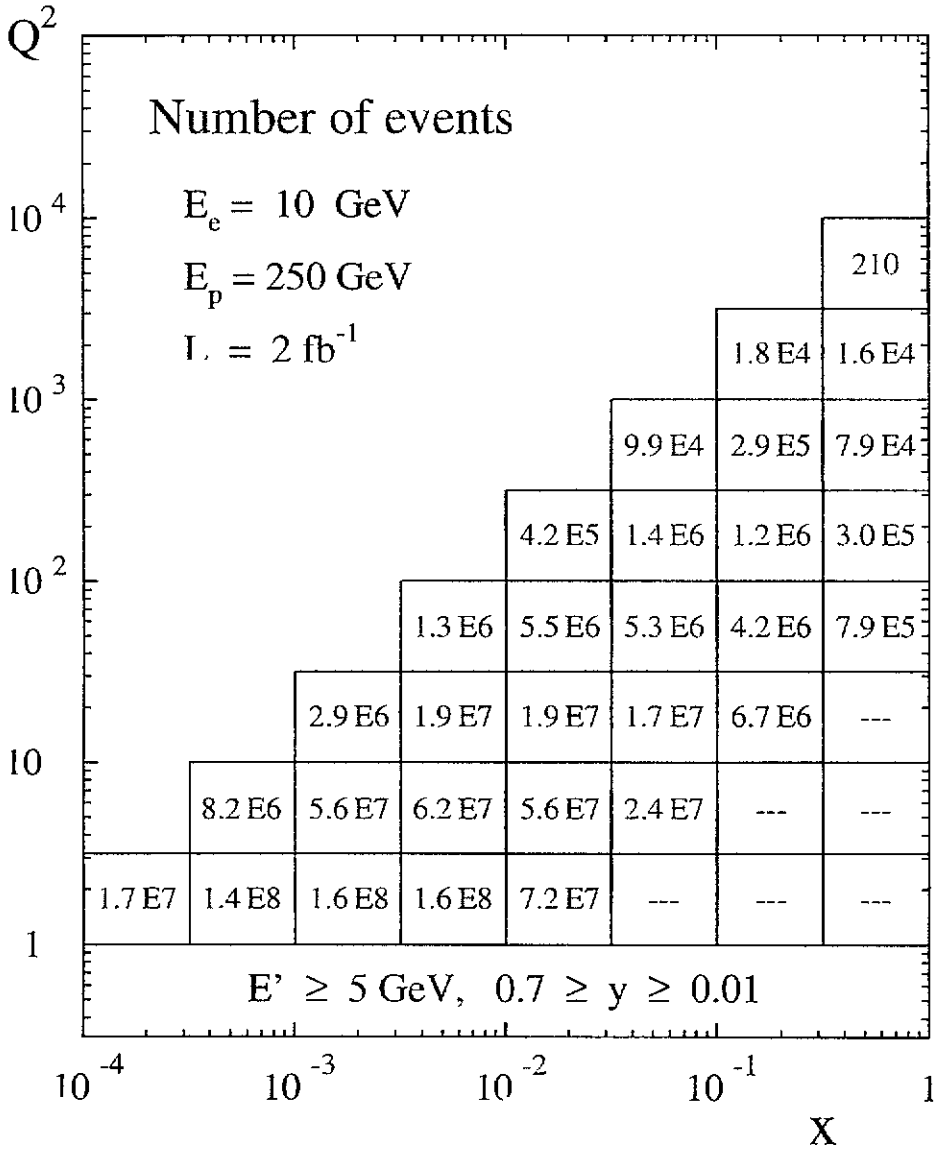

Figure 1: Estimated event numbers for inclusive electromagnetic electron-proton deep-inelastic scattering at the EIC, shown on a coarse-grained grid of two bins per decade in both x and Q^2 (given in units of GeV^2 in all figures). The results have been obtained using the GRV(98) parametrization of F_2^p [2] and neglecting the effect of the longitudinal structure function F_L.

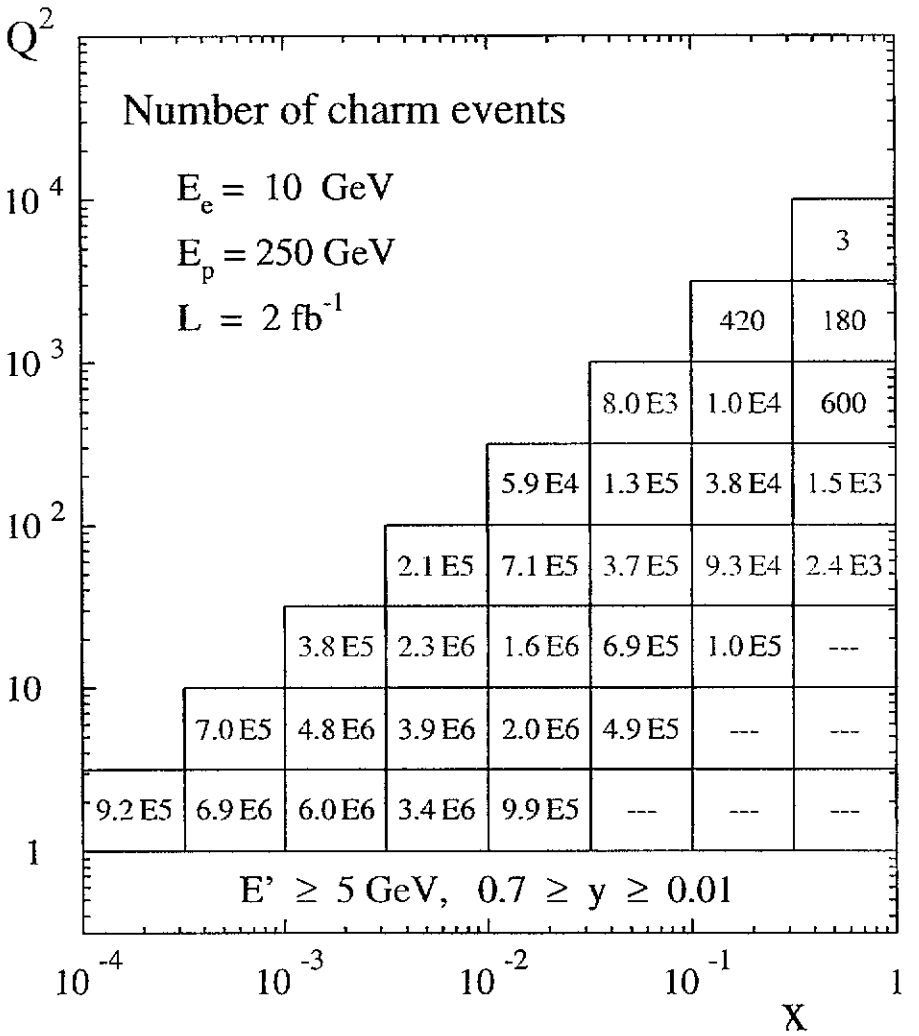

Figure 2: As Fig. 1, but counting only the charm-production events contributing to F_2^p.

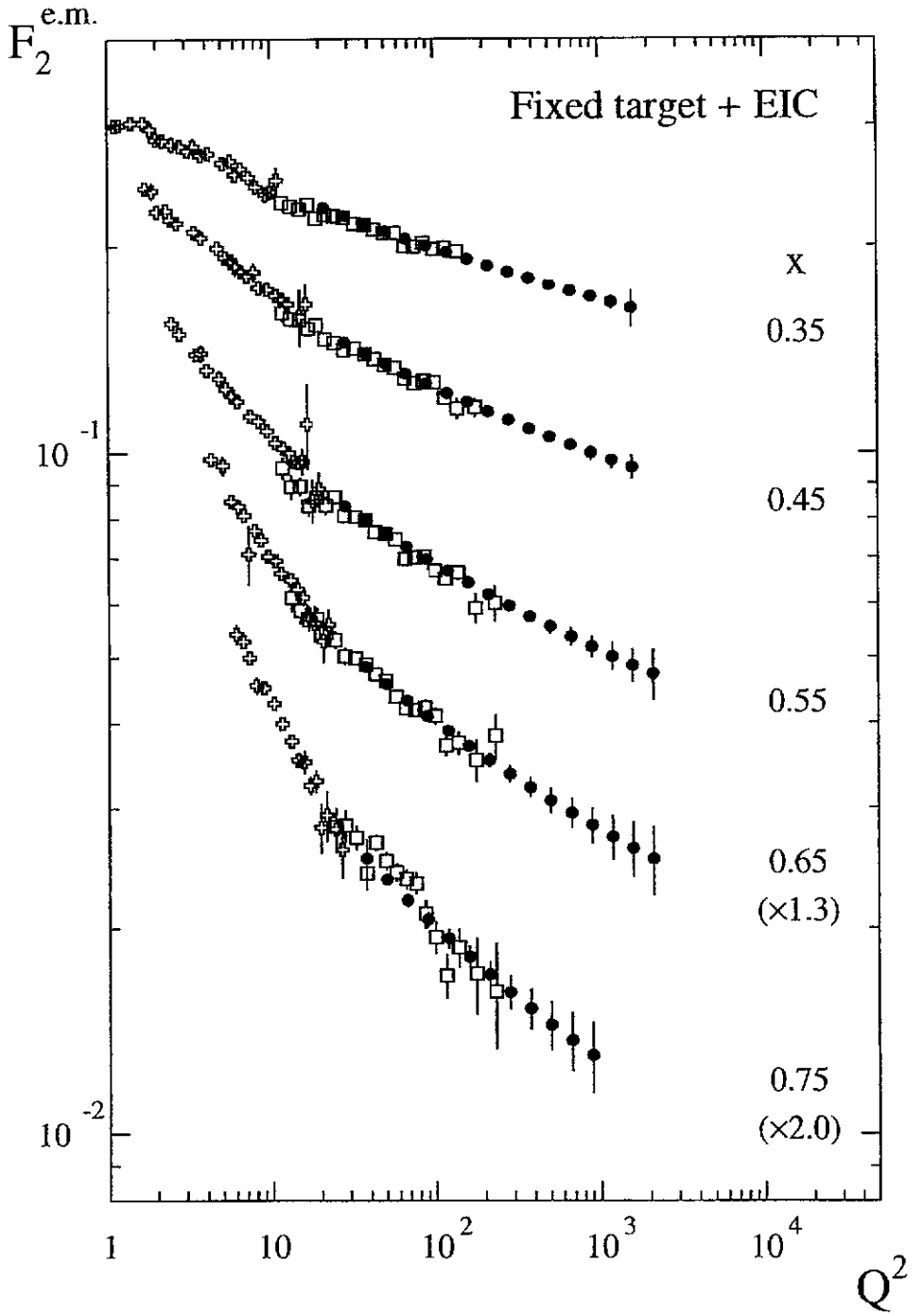

Figure 3: Kinematic coverage and statistical accuracies expected for measurements of the proton structure function $F_2^{e.m.}(x > 0.3, Q^2)$ at the EIC, for the machine parameters and cuts of Fig. 1. Also displayed (open symbols) are the fixed-target data of SLAC (left) and BCDMS (right). These data are shown as employed in the GRV(98) analysis, see footnote 3 of ref. [2].

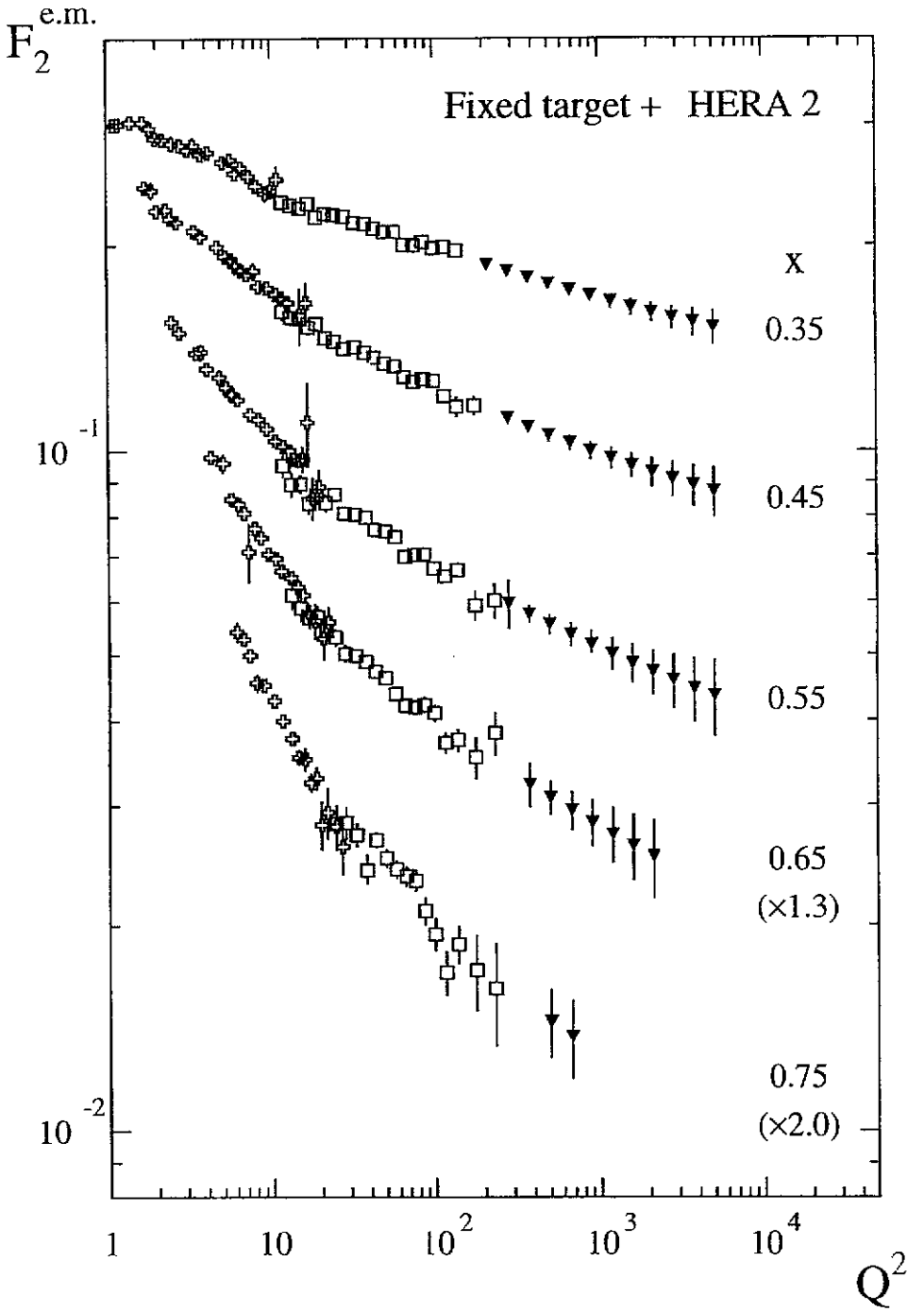

Figure 4: As Fig. 3, but for the forthcoming measurements at the *ep* collider HERA at DESY, assuming an integrated luminosity of 1 fb^{-1}. Also here the cut $0.01 < y < 0.7$ has been imposed.

S. Kretzer
(Michigan State University)
work with E. Leader, E. Christova:

Fragmentation Functions from Semi-Inclusive DIS pion Production and Implications for the Polarized Parton Densities

Abstract:
By combining recent HERMES data on semi-inclusive DIS $\pi^{\pm}$-production with the singlet fragmentation function $D_{\Sigma}^{\pi^+}$, which is well determined from e^+e^- data, we are able to extract, for the first time, the flavoured fragmentation functions $D_u^{\pi^+}$, $D_d^{\pi^+}$ and $D_s^{\pi^+}$ without making any assumptions about favoured and unfavoured transitions. Whereas $D_u^{\pi^+}$ and $D_d^{\pi^+}$ are very well determined, the accuracy of $D_s^{\pi^+}$ is limited by the uncertainty in evolving $D_{\Sigma}^{\pi^+}$ from the Z^0 pole down to the SIDIS scale of a few $(GeV)^2$. We discuss how the precision on $D_s^{\pi^+}$ could be improved. Knowledge of the $D_{q=u,d,s}^{\pi^+}$ will permit the extraction of the polarized parton densities from future polarized SIDIS asymmetry measurements. We study the precision that can be expected in such an extraction

- Light-Flavour FFs within Errors (from LO extraction)

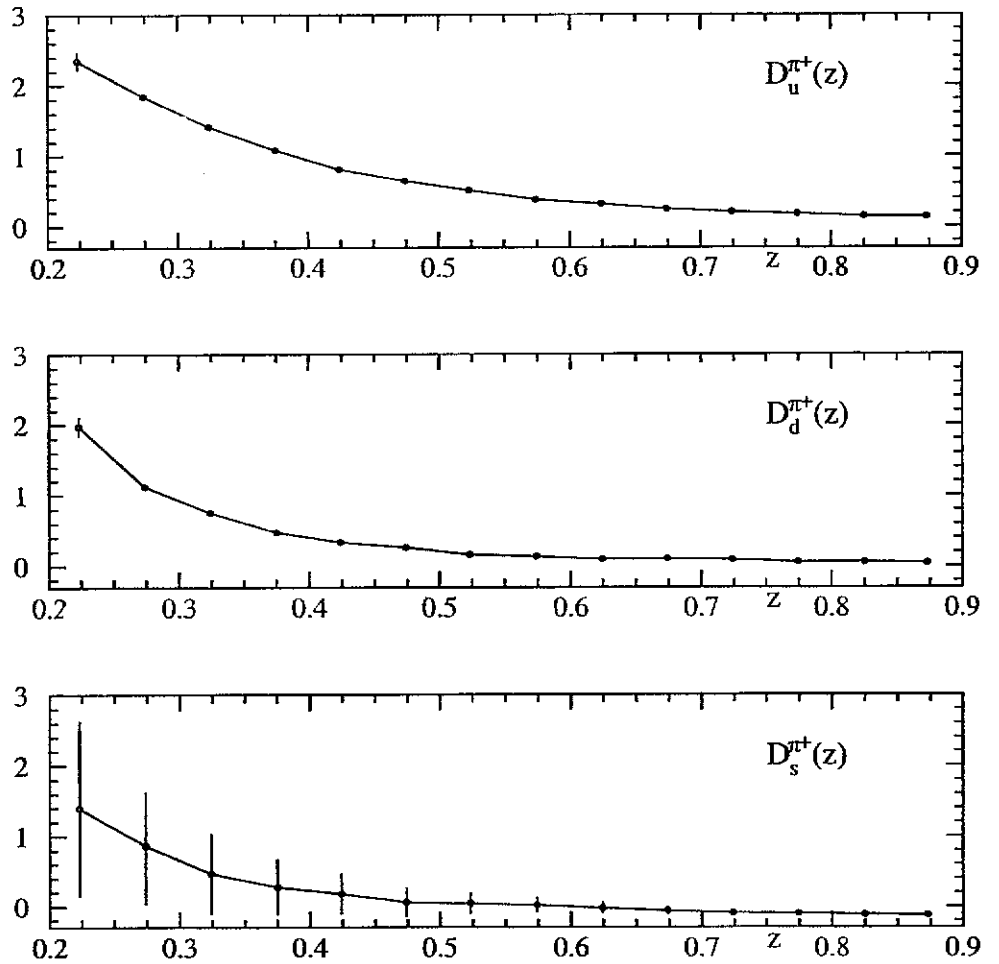

- SU(2) sector $(D_u^{\pi^+}, D_d^{\pi^+})$ well determined
- $D_s^{\pi^+}$ anything within $[0, D_d^{\pi^+}]$
- Knowledge of $D_\Sigma^{\pi^+}(\mu = \text{DIS})$ within $\sim 5\%$ would fix $D_s^{\pi^+}$ within $\sim 20 - 30\%$

- Flavour seperation of Fragmentation Functions:

Combining DIS, SIDIS and

$$
\begin{aligned}
D_u^{\pi^+} - D_d^{\pi^+} &= \frac{9\left(R_p^{\pi^+} - R_p^{\pi^-}\right)\tilde{\sigma}_p^{DIS}}{4u_V - d_V} \\
D_u^{\pi^+} + D_d^{\pi^-} &= \frac{9\left(R_p^{\pi^+} + R_p^{\pi^-}\right)\tilde{\sigma}_p^{DIS} - 4s}{4(u+\bar{u}-s)+d+\bar{d}} \\
D_s^{\pi^+} &= \frac{-9\left(R_p^{\pi^+} + R_p^{\pi^-}\right)\tilde{\sigma}_p^{DIS} + [4(u+\bar{u})+d+\bar{d}]}{4(u+\bar{u}-s)+d+\bar{d}}
\end{aligned}
$$

- Similar Equations for K, Λ

$\hookrightarrow$ Particle Identification !

$$
\begin{aligned}
\sigma_{\text{SIDIS}} &= (\Delta) f_i \otimes (\Delta)\hat{\sigma}_{ij} \otimes D_j \\
&= (\Delta) f_i \otimes \delta_{ij} \otimes D_j + \mathcal{O}(\alpha_s)
\end{aligned}
$$

- Flavoured FFs $\hookrightarrow$ <u>Flavour decomposition of Spin</u>
- EIC high scale ($Q^2 \simeq xy10^4$ GeV^2):
  - complementary to HERMES low scale ($Q^2 \simeq 1/2xy10^2$ GeV^2)
  - perturbatively clean
  - reduced evolution between SIDIS and components

EIC Detector Session

EIC Workshop

February 28-March 2, 2002

Naohito Saito

RIKEN / RBRC

Kick Off Meeting

- Lessons from HERA
  - Rear Detector and Forward Detector
  - Constraints from Machine-Detector Interface
  - Particle ID
- eA Detector Design Status
- Selections of Detector Elements
  - PID Frontier
- Relation with Other Existing Activities
  - PHENIX Silicon Upgrade
  - R&D of Accordion Calorimeter
- Discussions for Milestones towards CDR/TDR

Physics Requirements

- Physics Topics are being Discussed in Parallel Sessions … but most of final states will fall into ..
  - e, μ, γ, Jet, IDed-Hadron, b/c, and missing E_T
- We (anybody interested in Physics) need to specify
  - Energy / Momentum Range
  - Energy, Momentum, and Spatial Resolution

	eA	*ep*	*pp*	*pA*	
γ-detection	QCD	QCD	QCD, EW, BSM	QCD	EMC+γ-π&γ-Jet Separation
e-detection	DIS, EW, HQ	DIS, EW, HQ	EW, HQ, BSM	EW, HQ	EMC+Tracking+(TRD)
μ-detection	EW,HQ	EW,HQ	EW, HQ, BSM	EW, HQ	Tracking+MuID
Jet-detection	QCD	QCD	QCD, BSM	QCD	Hadron Calorimeter
Hadron PID	QCD, HQ	QCD, HQ	QCD, HQ	QCD, HQ	Cherenkov and/or TOF
b/c tagging	QCD	QCD	QCD, BSM	QCD	2nd VTX
Forward *e*-det		Photon SF			Forward Calorimeter
Missing E_T	EW	EW	EW, BSM	EW	Hermetic Calorimeter

Event Rate and Bunch Spacing

- Hi $\mathcal{L}$ option of ep → Very High Crossing Rate
  - FEE Clock, Detector Drift Time/Rise Time
- pp → Very High Event Rate
  - Hi Level-1 Rejection needed

    NB ep or eA also requires hi Level-1 rejection due to Beam Gas, Cosmics (e.g. HERA~1kHz, PHENIX Muon ~1kHz)

	ep I	ep II	eA I	eA II	HERA	pp	pA	CMS	CDF II
Luminosity (cm^{-2} s^{-1})	3.50E+32	2.45E+33			1.50E+31	5.00E+33		1.00E+34	2.00E+32
Event Rate (Hz)	207	1450			14	300M		1 G	14 M
Crossing Rate (Hz)	28M	196M			10.4 M	28M	28M	40M	7.6 M
Bunch Space (ns)	35.5	5.1			96	35.5	35.5	25	132
Average # / Cross	7.30E-06	7.30E-06			1.35E-06	11		25	1.8
Level-1 rate						30 kHz		100 kHz	50 kHz

- ep/eA options are for eRHIC, pp/pA for RHIC

Possible Combined Detector

If we could combine *eA/ep/pp/pA* ***detector...***

- **Advantage: It will become**
  a Full QCD Laboratory
  with self-assurance of Factorization Proof

- **Disadvantage: Too different event rate, bunch spacing(?), particle multiplicity, etc.**

Towards Complete Design of EIC Detector

- There should be significant iterations among
  - Physics Requirements
  - Accelerator Constraints
  - Detector Technique Practicality
- Milestones towards TDR
  - A complete TDR in 2 years possible?
    - CDF II took > 4 years from TDR to completion
  - Pre-CDR in summer-fall time scale possible?
    - Performance Goals
    - Technical Options
    - Open Issues
  - Need Dedicated Workshop for Pre-CDR after a couple of *"learning meetings"*
- One of the biggest Branching Point is
  - ep&eA Detector or ep/eA/pp/pA Detector (ref. Yale WS Proc.)

Future Meetings

- A few more "Learning" type of Meetings might be useful
  - Lessons from TEVATRON / LHC
    - Technical Options in Tracking Device
    - FEE and Trigger Systems
  - Selections of Detector Elements
  - Relation with Other Existing Activities
    - RHIC Upgrades
    - LHC
- Pre-CDR Workshop by EOY?

Recent R&D activity on a Accordion-type Calorimeter

E. Kistenev
(BNL)

Why Accordion...

- *excellent uniformity;*
- *no dead areas;*
- *excellent linearity - autocompensation for light attenuation in the fibers;*
- *best possible position resolution for a given cell size;*
- *shower shape is very sensitive to impact angle - built-in pointing;*
- *simple longitudinal segmentation - read both ends of the fibers;*
- *simple industrialization:*
  - *only one kind of scintillator tiles and only one kind of lead tiles for the whole calorimeter*

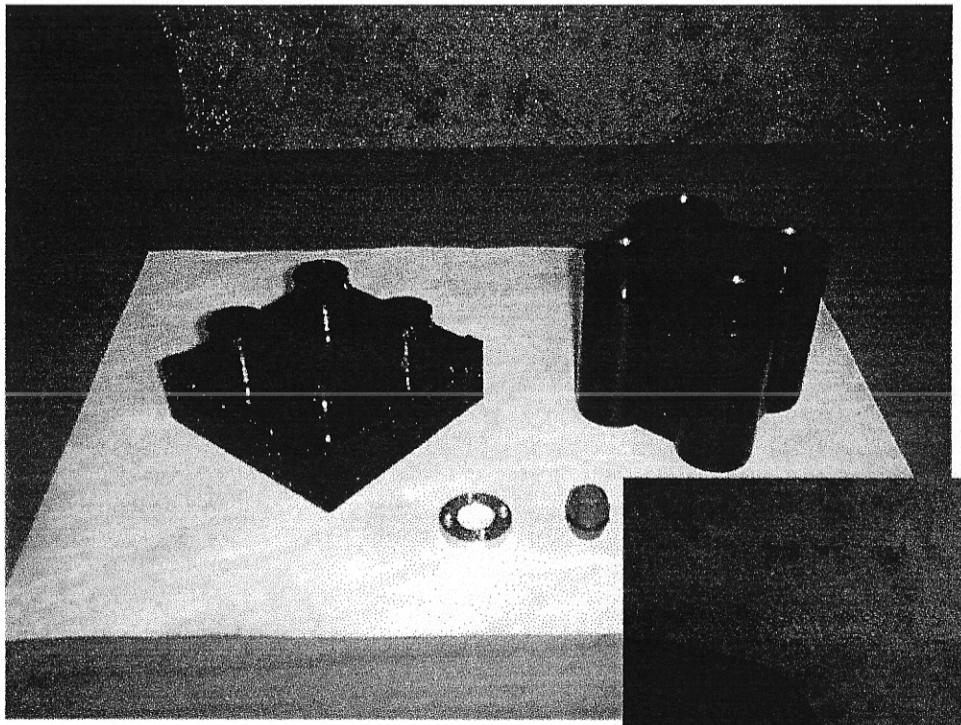

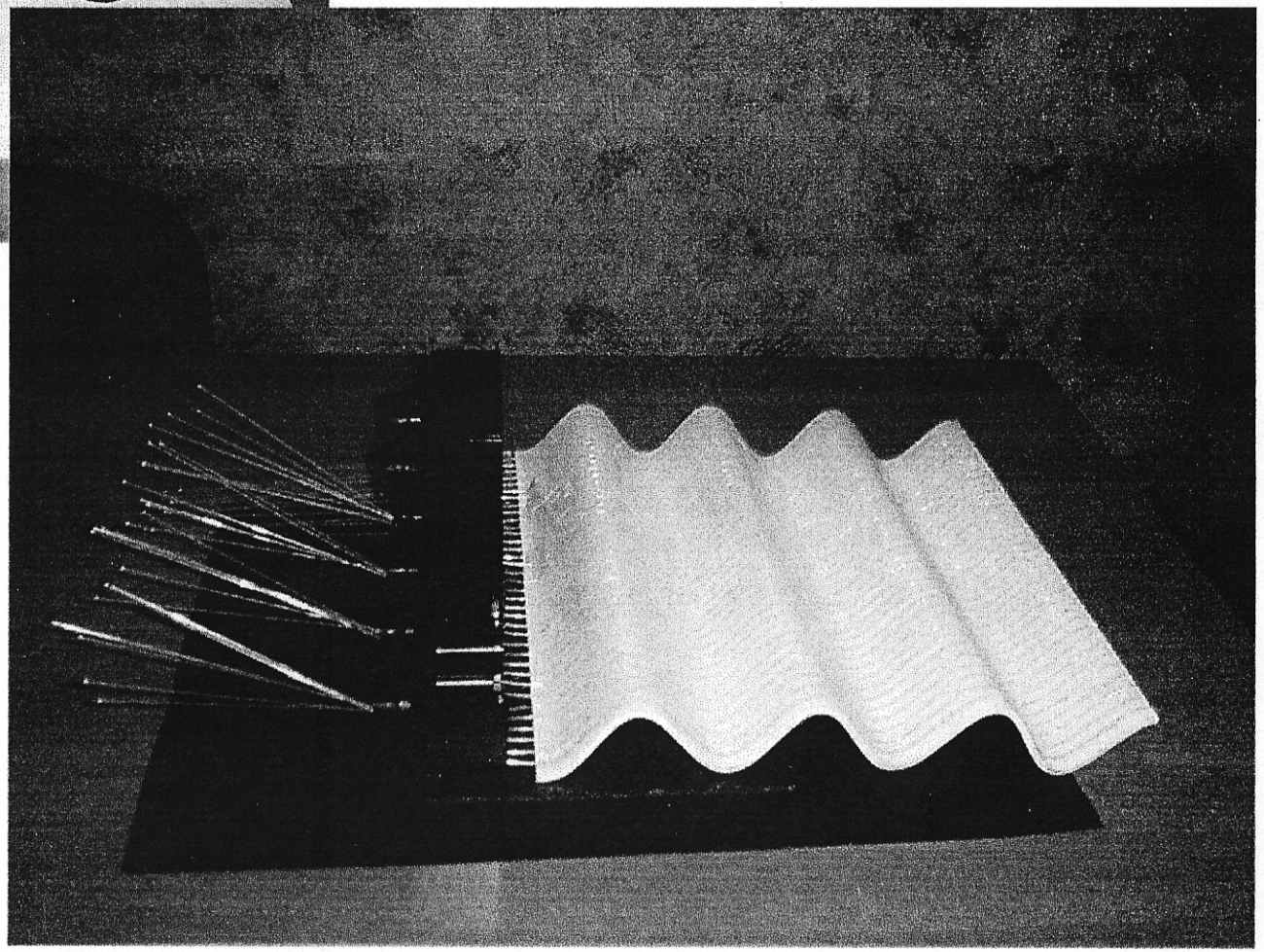

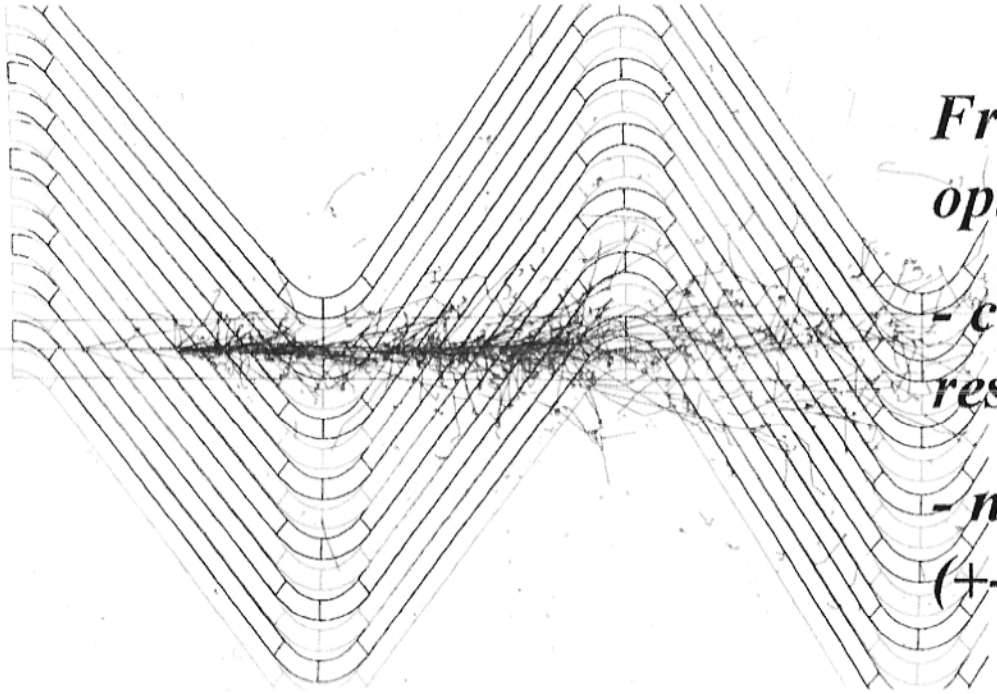

Framework for simulation and optimization is already established

- crude estimate for energy resolution ~ 17/sqrt(E)

- nonuniformity similar to ATLAS (+-4%) and very easy to correct

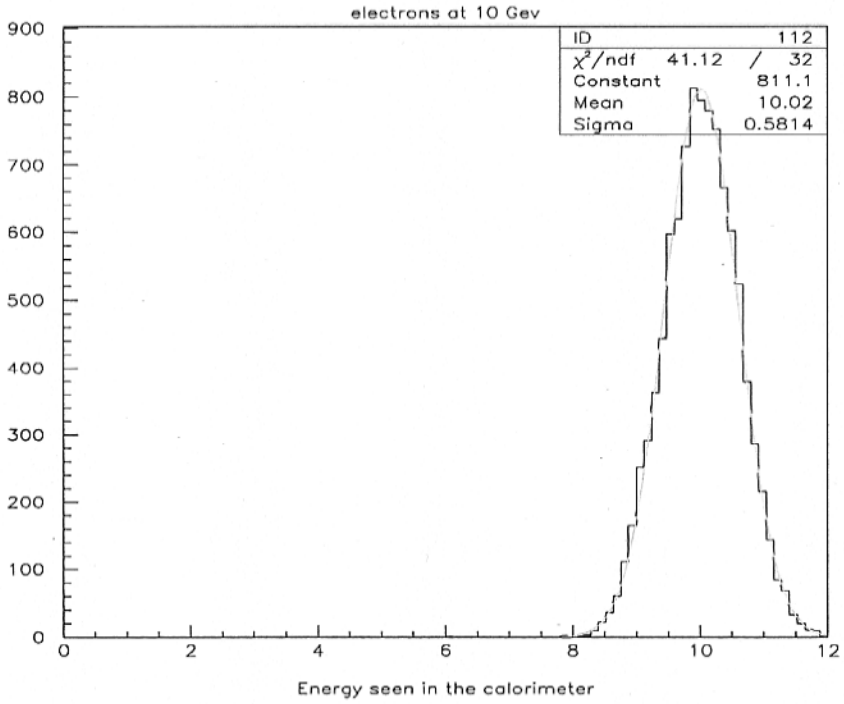

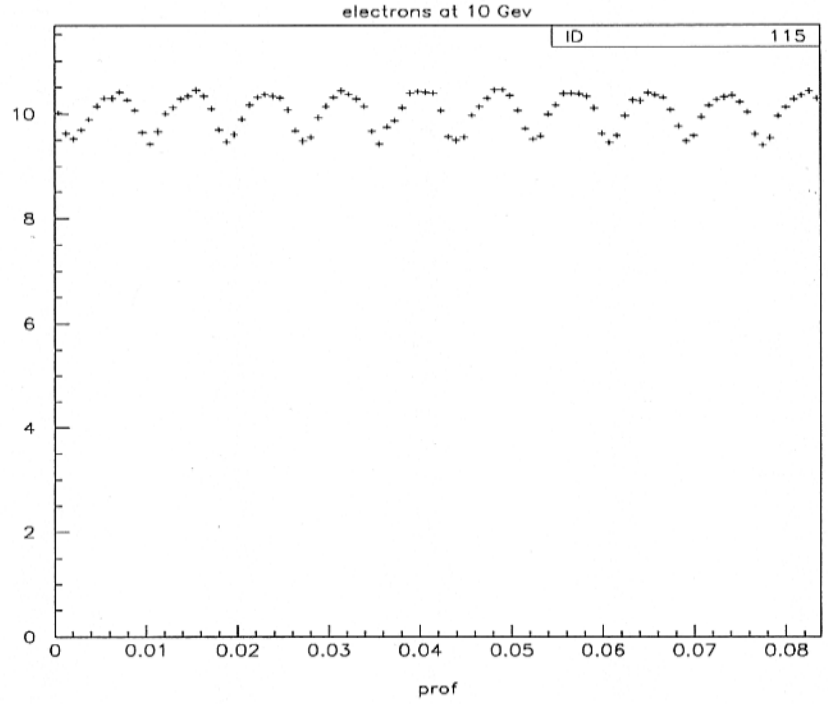

Rear Detection Systems and Luminosity Measurement at H1 and ZEUS

EIC Workshop

Brookhaven Nat Lab

01.03.2002

Uwe Schneekloth (DESY)

Outline

Overview of Detectors
Rear Calorimeters
Small Angle Detectors
Luminosity Monitors
Tagging Devices

HERA Overview

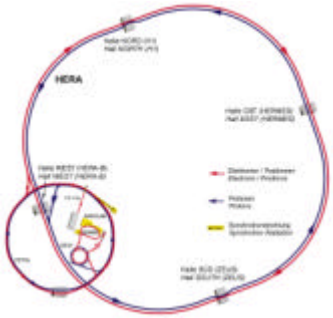

Electron (positron) - Proton Collider

Beam energies
protons 920 GeV
electrons 27.5 GeV

180 bunches
96 ns bunch spacing

180 bunches
96 ns bunch spacing

ZEUS Detector - HERA I IR

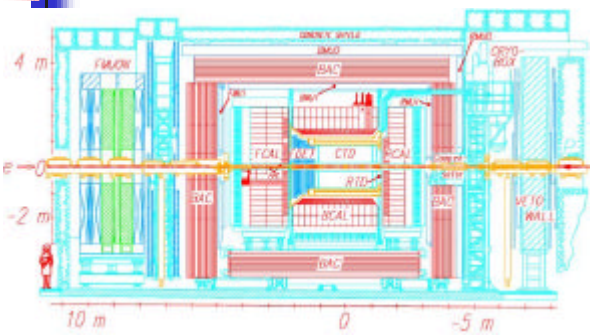

ZEUS Inner Detector

- Tracking Detectors:
  - CTD for $\theta > 25^0$
  - FTD only for $8^0 < \theta < 14^0$
  - RTD only for $158^0 < \theta < 170^0$
- CTD:
  - 72 layers
  - Stereo angle $\pm 5^0$
  - Good efficiency down to 25^0
- TRDs replaced by Straw Tube Tracker

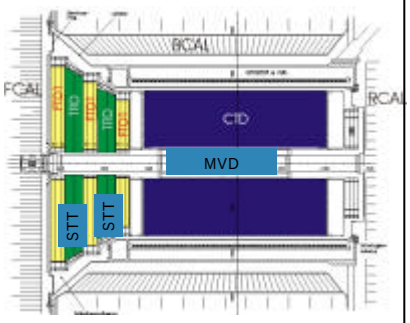

Uranium Scintillating Calorimeter

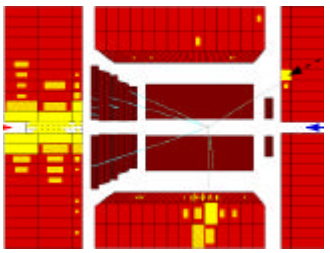

F/RCAL modules 20 cm width
Original beam pipe holes 20 x 20 cm^2

Calorimeter properties

- compensating, e/h ratio =1.0
- linear response to electrons and hadrons
- energy resolution:
  electrons
  $$s_E / E = 18\% / \sqrt{E / GeV} \otimes 2\%$$
  hadrons
  $$s_E / E = 35\% / \sqrt{E / GeV} \otimes 1\%$$
- timing resolution 1ns

Acceptance of Calorimeter

Covers 99.8% of full solid angle

Beam pipe holes:

- originally 20 x 20cm^2
- 1995 RCAL 20 x 8cm^2 + beam pipe calorimeters (low x physics)
- 1997 FPC 6.3cm diameter (diffraction)
- 2001
  - FCAL 20 x 20cm
  - RCAL 20 x 23.6cm (super-conducting HERA magnets)

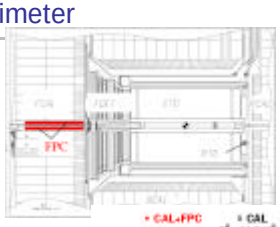

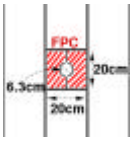

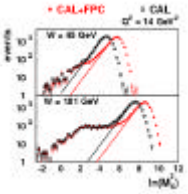

Small Angle Rear Tracking Detector

Extend kinematical region to low x, Q^2

Improve tracking (acceptance and position resolution at small angles (? > 165^0)

SRTD: finely segmented scintillator strips, PMT readout

- position resolution 0.3 cm
- aligned to 0.1 cm
- online timing < 1.5 ns

In addition:

- identify pre-showering electrons, correct for energy loss in material
- reject upstream proton beam-gas background

Rear region (not to scale)

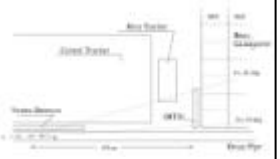

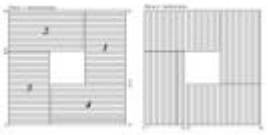

ZEUS - Beam Pipe Calorimeter

Improved detection at very low angles (1995). Very low x, Q^2 physics. Oval rear beam pipe with two thin exit windows.

- Top and bottom RCAL modules moved closer to beam (20➡8cm)
- Two small electromagnetic tungsten/scintillator calorimeters at z = -2.9m
- Measure low angle electron

- Measure QED Compton events photon and electron in coincidence
  - in-situ calibration and alignment
  - additional luminosity measurement

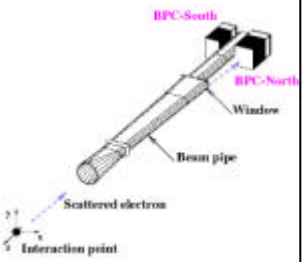

ZEUS - BPC and BPTracker

BPC Properties

- depth 24 X_0
- energy resolution 17% / sqrt E
- energy scale uncertainty ± 0.3%
- linearity < 1%
- position resolution 0.22cm / sqrt E
- timing resolution < 1 ns

BPTracker

- independent z-vertex
- reduce photoproduction backgrd
- increase position resolution

Five Si micro strip detectors
(6 x 6 x 0.03 cm^3)
100 µm strip pitch

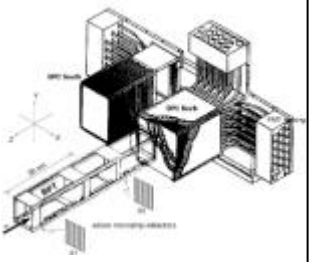

ZEUS - Event BPC/BPT

medium y, diffractive ($\eta_{max} = -0.9$)

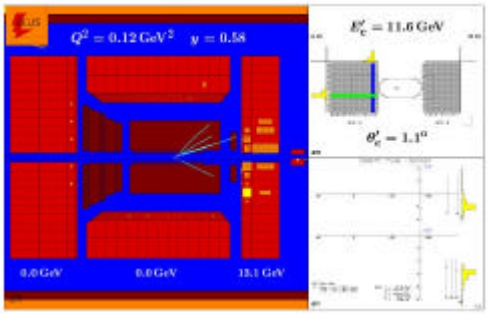

Extended Kinematical Region

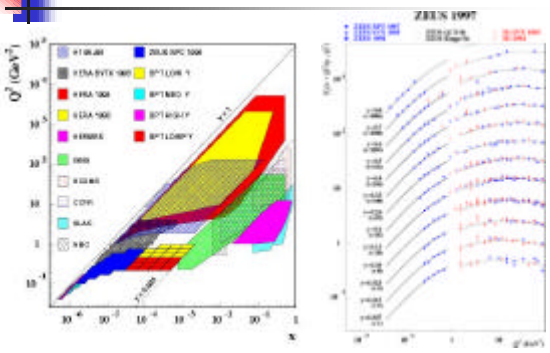

H1 Detector (HERA II IR)

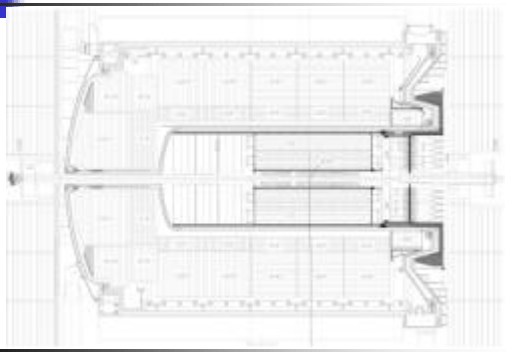

H1 - Improved Rear Detection

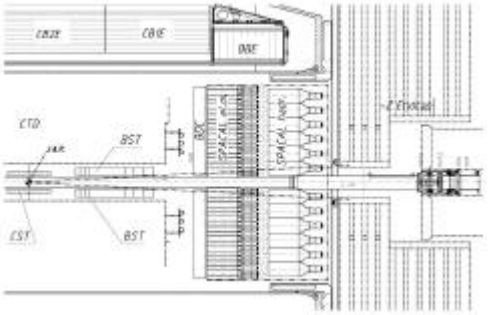

H1 - Backward Silicon Detector

Two types of Silicon detectors

r-wafers
- z-vertex determination for events with no tracks in central detector (low y, high y)
- measure ?$_e$ to determine x, y, Q^2
- need excellent position resolution 16 µm

phi-wafers
- momentum measurement
- e/p ratio: calibrate SPACAL
- subtract low momentum background (photoproduction)

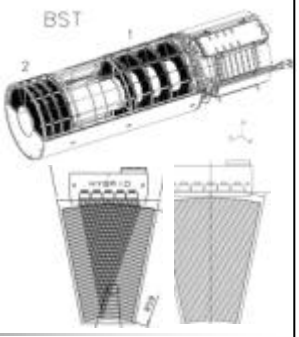

H1 - SPACAL

Electromagnetic and hadronic spaghetti type lead-scintillating fiber calorimeter

Electromagnetic calorimeter
- cell size 40.5 x 40.5 mm^2
- energy resolution $7\%/\sqrt{E(GeV)} \oplus 1\%$
- angular resolution < 2 mrad
- timing resolution , 1 ns
- angular coverage 152^0 < ? < 178^0
- low energy threshold

SPACAL module

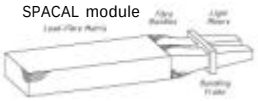

Cross section view

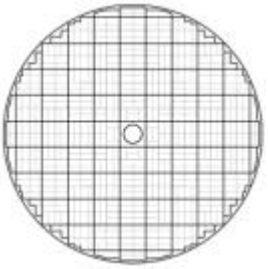

H1 - SPACAL Installation

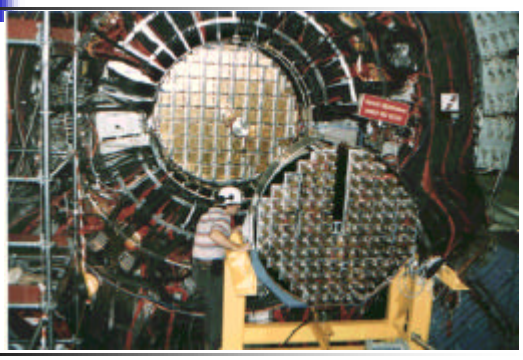

H1 - Very Low Q^2 Spectrometer

Detection of very low angle electrons
0.02 < Q^2 < 1 GeV^2

Two modules (tracker, calorimeter and time-of-flight) above and below beam pipe

Calorimeter
- tungsten/scintillator sandwich calorimeter
- horizontal and vertical scint. Strips
- $s_E / E = 14.3\% / \sqrt{E(GeV)} \oplus 2.1\% \oplus 0.11 / E(GeV)$

Tracker
- 2 double layers of Silicon strip detectors

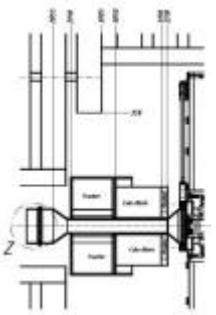

H1 - Cross Section at low Q^2

Cross section departs from F_2 at high y.
Data extends to $E_{e'}$ = 3 GeV, y=0.89

Requires to subtract large photo-production background

Assign charge (using BST) to positron candidate

Subtract statistically

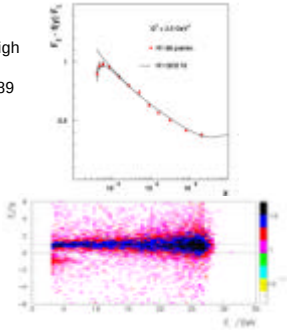

H1 - Measurement of F_L

Measurement of longitudinal structure function at low Q^2

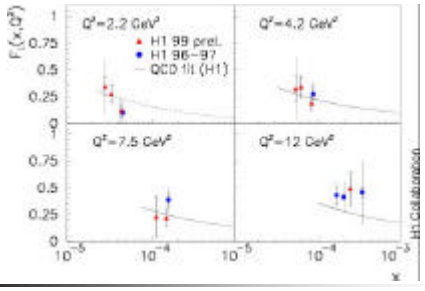

Luminosity Measurement

Method: measure rate of bremsstrahlung process $ep \rightarrow e' pg$

Originally, measure coincidence of e' and ?. $E_e = E_{e'} + E_g$
Detectors in HERA tunnel:
- Photon detector 105m from IP at 0^0 (p beam is bent upwards)
- Electron detector 35m from IP (HERA magnets act as spectrometer)

$$L = 1/s_{BH}^{obs}[R_{tot} - (I_{tot}/I_0)R_0]$$

Bethe-Heitler cross section $s_{BH}^{obs} = A_g s_{BH}^{corr}$

Main background beam gas scattering:
Subtracted using pilot bunches
- bunch structure: p 180, e 194, colliding 174

Overview of Luminosity Monitor

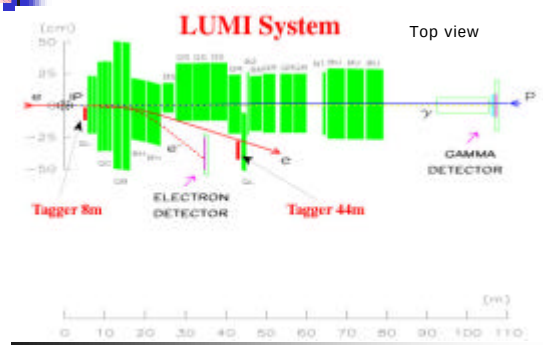

Luminosity Measurement - HERA I

Synchrotron radiation requires filter in front of calorimeter

Very good background conditions.
Good photon acceptance.
Electron acceptance more difficult
Only using photon detector for luminosity measurement

Electron detector:
- systematic checks (calibration and acceptance)
- tag photoproduction events
- estimate photoproduction events in DIS

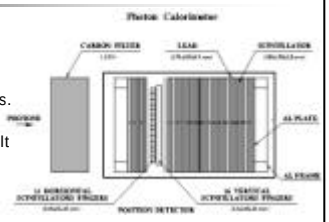

Typical systematic errors

Acceptance error	0.8%
Cross section calculation	0.5%
e gas background substr.	0.1%
Multiple event correction	0.03%
Energy scale error	0.5%
Total error	1.05%

Luminosity Monitor Upgrade-HERA II

Challenge
- Rate of bremsstrahlung photons increase by factor of 5
- Significant increase of synchrotron radiation
  - power in photon detector 400 → 1800 W
  - critical energy 35 → 150 keV
- Photon calorimeter would be damaged in a few months, expected dose O(Trad/year), need filter in front.

Upgrade
- Build radiation hard calorimeter (H1) (with increased filter thickness, ZEUS)
- Active filter (ZEUS)
  - Cerenkov detectors only sensitive to charged particles
  - correct for energy loss in filter
- Electron - Positron Pair Spectrometer (ZEUS)

H1 - Luminosity Monitor Upgrade

Requirements for new Photon Detector
- fast response: Cerenkov calorimetry
- radiation resistance: quartz fibers 200 - 400 Mrad
- good energy resolution: light yield, fine sampling
- compact: high density
- position resolution: fine granularity in x and y
- efficient synchrotron radiation filter: 2 X_0 Be in front of calorimeter

Tungsten/Quartz-Fiber Sampling Calorimeter
- 70 lozenge-shaped tungsten plates (0.7 mm thick)
- fiber angle 45^0 (Cerenkov angle of relativistic particles in quartz)
- two-dimensional strip readout
- energy resolution $s_E / E = 19\% / \sqrt{E(GeV)} \oplus 0.52\%$
- position resolution $s_x = 5mm / \sqrt{E(GeV)}$

H1 - Luminosity Monitor W/QFC

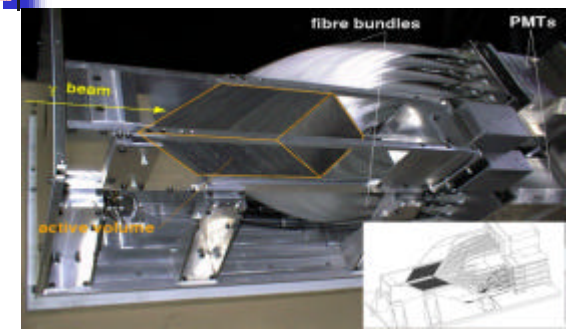

ZEUS - Overview Photon Detector

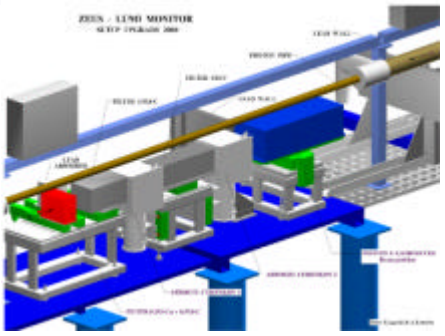

Active Filter

Huge flux of synchrotron radiation photons
- power 1.3 kW (27.5 GeV)
- energy 8 10^5 GeV/bunch cros.

Energy of SR photon larger than signal

Radiation damage of detector

Need 4 X_0 filter in front of detector

Filter deteriorates energy resolution

Build active filter

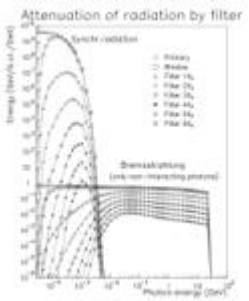

Cerenkov Detector

Only sensitive to charged particles

Synchrotron rad. signal (Compton effect need E_γ>1.6 MeV) very small.

Photons interacting in filter, correct for energy loss

Detector
- Radiator: Aerogel 5 SP (Matsushita) plates, 11x11x1cm^3
- Mirror
- Fresnel lense
- Photo-multiplier

Photon Calorimeter

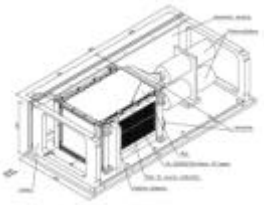

Photon calorimeter
- Pb/scintillator sandwich
- 48 layers (0.5 X_0 Pb / 2 mm scintillator)
- SCSN81TN 6 Mrad/y 5% deterioration
- energy resolution $14\% / \sqrt{E(GeV)}$

Position detector
- 14 x 16 1 cm wide scintillators
- readout Hamamatsu R5600V PMTs
- position resolution ~ 2 mm

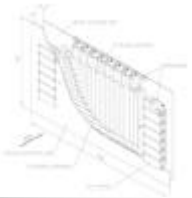

ZEUS Luminosity Pair Spectrometer

Luminosity measurement still difficult: high rate, pile-up,...

Additional complementary method

- Conversions in exit window (rate only 10%) $g \to e^+e^-$
- Dipole magnet
- 2 detectors (reuse old BPCs, acceptance 30%)

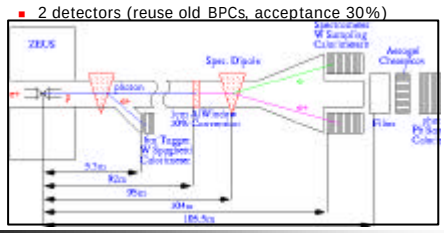

Spectrometer in HERA Tunnel

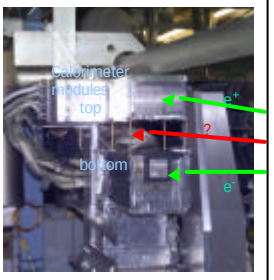

Comparison of Methods

Photon Detector

Advantages:

- simplicity
- robustness
- low cost
- long experience (HERA I)

Disadvantages:

- pile-up corrections
- maintenance of calibration
- possible radiation damage

Spectrometer

Advantages:

- no radiation damage
- no pile-up

Disadvantages:

- new technique
- small acceptance
- no experience

Redundant luminosity measurement. Calorimeter and spectrometer have very different systematic error.
Expect significant improvement of systematic error.

6m Tagger (H1 and ZEUS)

Very compact electromagnetic calorimeter
Same function as previous electron cal at 35 m.

- systematic checks (calibration and acceptance)
- tag photoproduction events
- estimate photoproduction events in DIS

New HERA IR, very limited space.
Tagger is located inside yoke gap of first normal conducting HERA magnet
Acceptance: 5 to 9 GeV
Spaghetti tungsten/fiber calorimeter
Dimensions: 85x24x100 mm^3

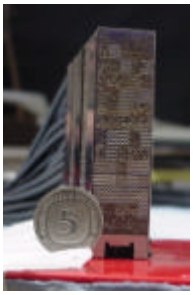

Tagging Devices

Small electromagnetic calorimeters at different locations in HERA tunnel.
HERA magnets act as spectrometer.

Taggers (HERA I IR)
position acceptance

- 44m 21 - 26 GeV
  movable vacuum chamber
- 35m 5 - 19 GeV
  luminosity electron detector
- 8m 1 - 3 GeV

Physics

- Photon-proton total cross section
- Photoproduction
- DIS: reject photoproduction backgrd
- Used for calibration

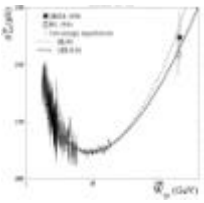

Conclusion

Extensive upgrades of rear region:

- New rear calorimeter, new backward drift chamber (H1)
- Improved acceptance and position resolution SRTD (ZEUS)
- Backward Silicon tracking (H1)
- Very small angle calorimeters with tracking (BPC, VLQ)
- Tagging devices in HERA tunnel

→ Significant improvement of kinematical region: (F_2 measurement, total cross section, F_L,...)

Upgrade of luminosity monitors

- New radiation hard photon calorimeters
- Pair spectrometer (ZEUS)
- 6m Tagger

HERA Luminosity Upgrade
Constraints on Interaction Regions

EIC Workshop

Brookhaven Nat Lab

01.03.2002

Uwe Schneekloth (DESY)

Outline

Compare original HERA interaction region and luminosity upgrade (HERA II) IR

- Layout of Interaction Regions
- Super-conducting Magnets inside Detector
- Detector Modifications
- Synchrotron Radiation
- Background Conditions
- Conclusions - Present Status

ZEUS Detector - HERA I IR

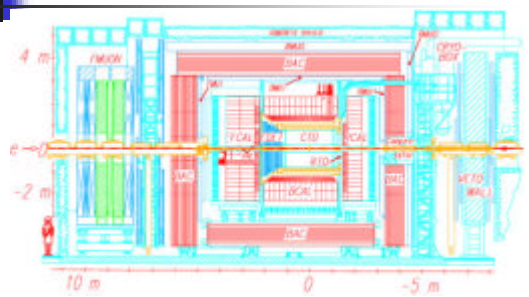

First HERA magnets (off-axis quads) at ± 5.8 m from IP
Calorimeter covers >99.8% of full solid angle
forward hole in calorimeter 6.3 cm diameter

Luminosity Upgrade - HERA II

Increase luminosity by reducing beam size at IP

- Reduce beta functions of proton and electron beams at IP
- Reduce emittance of electron beam
  (max. beam-beam tune-shift $\Delta n_y^e = 0.04$)

beta function

- Low beta quadrupole magnets as close as possible to IP
- Early beam separation
  - First magnet 1.7 m from IP (separation and focusing)
  - First proton quadrupole now at 11 m instead of 27 m from IP

Electron beam emittance

- Electron machine lattice stronger focusing
- Phase advance per cell increased from 60^0 to 72^0.

Constraints

- Try to keep good forward and backward coverage of calorimeters
- No upstream synchrotron radiation collimators anymore
- Have to remove compensating solenoids

Layout of HERA II IR

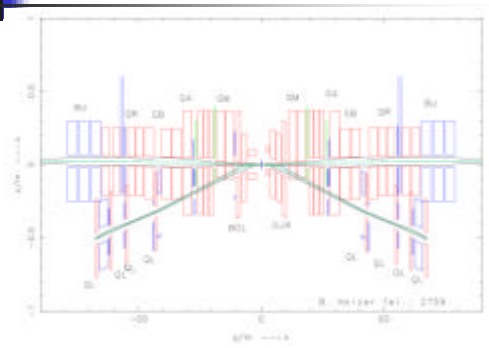

Comparison HERA I and HERA II

		HERA I Design	HERA I 2000	HERA II Design	HERA II exp. 2002
Beam energy (GeV)	p	820	920	920	920
	e	30	27.5	30	27.5
Beam emittance (nm)	p-hor/vert	5.72/5.72	4.1/4.1	5.1/5.1	4.1/4.1
	e-hor/vert	50/5	42/4	22/3.5	21/3.5
ß * function (m)	p-hor/vert	10/1	7/0.5	2.45/0.18	2.45/0.18
	e-hor/vert	2/1	1.0/0.6	0.60/0.26	0.60/0.26
Beam size (µm)	hor/vert	240/76	170/45	112/30	100/27
Aperture limit (sigma)	p-hor/vert	14/14	12/10	12/12	12/12
	e-hor/vert	>30	>15	20	20
Protons/bunch	(10^{11})	1	0.8	1	0.7
E beam current	(mA)	58	50	58	50
Beam-beam tuneshift	p-hor	.0016/.00035	.0019/.0003	.0033/.0005	.003/.0004
	e-hor	0.02	0.0161	0.0291	0.0278
Luminosity (10^{31} cm^{-2} s^{-1})		1.4	2.0	7.3	5.1

Special Magnets for new IR

Super-conducting magnets

- 1.7m from IP
- Increased beam aperture
- Higher gradients possible
- Combined function magnet: several coils inside magnet
- Good field quality
- Very limited space
- More compact than normal conducting magnets
- Inside detector fields

Final design and manufacturing BNL

Normal conducting magnets

- 6 types of magnets
- New type of septum magnet: half quad/mirror plate with triangular cutout
- High gradients (30 T/m)
- Good field quality ?B/B 10^{-4}
- Relatively large power

Final design and manufacturing Efremov Institute, St.Petersburg

Superconducting Magnets (BNL)

		GO	GC
Quadrupole	Gradient	*13 T/m*	*3.5 T/m*
	Current	*500 A*	*500 A*
	Layers	*3*	*1*
Dipole	Field	*.168 T*	*.3 T*
	Current	*500 A*	*300 A*
	Layers	*1*	*2*
SkewQuad	Gradient	*1.24 T/m*	*.54 T/m*
	Current	*150 A*	*37 A*
	Layers	*Half length*	*1*
SkewDipole	Field	*.0876 T*	*.04 T*
	Current	*150 A*	*37A*
	Layers	*Half length*	*1*
Sextupole	Field	*4 T/m²*	*3 T/m²*
	Current	*20 A*	*20A*
	Layers	*1*	*1*

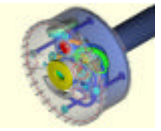

ZEUS Detector - HERA II IR

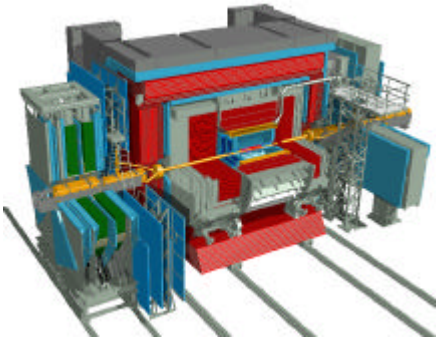

GO Magnet installed in ZEUS

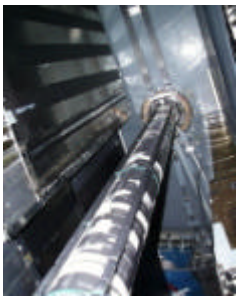

Detector Modifications

Removed detector components

- Forward Plug Calorimeter
- Increased forward and rear beam pipe holes of calorimeter
- Very low angle detectors (BPC, VLQ)
- (Forward Proton Spectrometer (ZEUS))
- Compensating solenoid

Detector upgrades

- New central beam pipe (elliptical 115x42/60 mm^2 ZEUS/H1)
- Micro Silicon vertex detector
- Improved forward tracking
- Track trigger
- Luminosity monitors

- Improved magnetic shielding of calorimeter PMTs

Impact on Detector Performance

Super-conducting HERA magnets inside detector (dead material)

Tracking detectors:

- hit multiplicity 20% increase (NC DIS $Q^2 > 10$ GeV^2)
- number tracks: small increase

Forward Calorimeter:

- 10 GeV additional energy (DIS $Q^2 > 10$ GeV^2)
- 4 GeV additional energy (DIS $Q^2 > 1000$ GeV^2)
- Diffractive events difficult

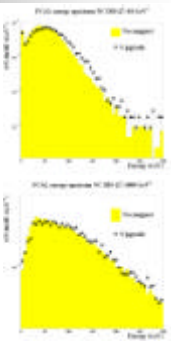

Impact on Detector Performance

Super-conducting HERA magnets inside detector (dead material)

Forward Calorimeter:

- Slight increase in number of jets in forward direction
- Significantly less than with normal conducting magnets

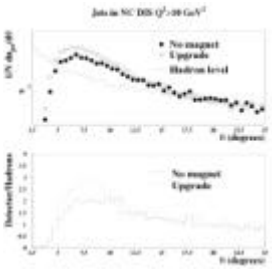

Effect of ZEUS F/RCAL on Beam

Iron support structure has strong influence on GO/GG field (max 18%). Beam orbit correction required when moving F/RCAL.

Effect studied on magnet test stand

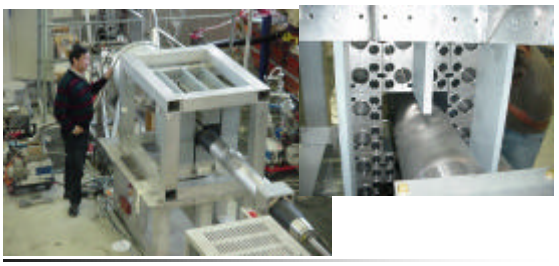

Synchrotron Radiation - HERA I

Total power 6 kW (original design 18.6 kW at 35 GeV)
Critical energy 34 keV (original design 70 keV at 35 GeV)

- Detector shielded by 3 movable upstream collimators.
- Two fixed collimators near IP against back-scattering.
- Background conditions very low.

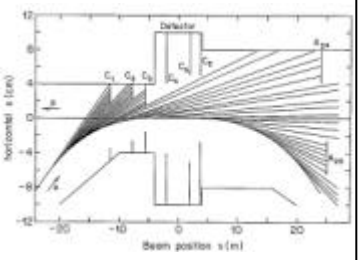

Synchrotron Radiation - HERA II

Total power 18kW (26kW at 30GeV)

Critical energy up to 115 keV (150 at 30 GeV)

"No" upstream collimators

Radiation fan must pass through IR

Main background source: back-scattering from absorbers 11 to 27 m right of IP

Small central beam pipe

Top view of interaction region

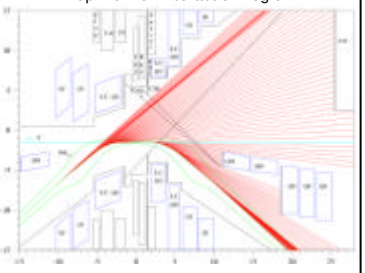

Details: talk by D. Pitzl

Layout of Interaction Region

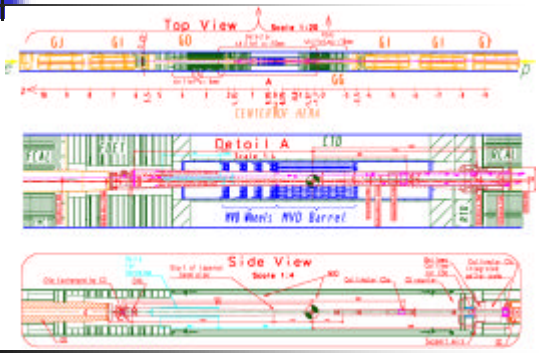

Electron Beam Gas Background

Upstream electron beam gas scattering results in off-momentum electrons deflected into detector by separation magnets

HERA I IP:

- several upstream collimator (out- and inside jaws), last collimator after final magnet

HERA II IP:

- final magnets much closer to IP, no collimator after final magnet anymore

Simulation showed background rate of 60 kHz, about 100 krad/y (radiation damage of MVD)

Solution:

- Improve upstream vacuum (distributed NEG pumps)
- Introduce chicane (bending magnets at 63 and 42 m from IP)
- Collimators at 40 and 19 m from IP

Conclusions - Present Status

HERA I IR:

- First magnets at 5.8 m from IP

HERA II IR:

- Magnets as close as possible to IP
- Super-conducting HERA magnets inside detector volume
- Small effect for $Q^2 > 10\ GeV^2$ physics
- Acceptance at small angles reduced

Status

- Installation completed July 2001
- HERA re-commissioning started in August 2001
- Achieved design specific luminosity (with low currents)
- Synchrotron radiation background too high to turn on central drift chambers
- Need additional collimators, installation February/March
- Data taking scheduled to start mid March

PROCEEDINGS

Forward Physics and Detectors at HERA

Henri Kowalski*
Columbia/BNL/DESY
E-mail: kowalski@nevis.columbia.edu

ABSTRACT: In this talk I outline the physical motivation for the precise t measurements in the diffractive processes at HERA. In addition the experimental requirements of t measurements using forward spectrometers are discussed based on experience collected by the ZEUS and H1 experiments.

HERA experiments have shown that the scattering of a small photon on the proton is different from what we know from hadron-hadron scattering. First, the total cross section exhibits a considerably stronger rise with energy than observed in hadron-hadron scattering. Secondly, the spread of the scattering system in the transverse direction which can be seen as measure of the forces keeping the scattering projectiles intact is quite different from hadron-hadron scattering. Since HERA allows the size of the photon to vary, it is possible to interpolate between short and large distances; whereas in the small size region the novel features emerge, in the large size region HERA establishes consistency with the basic features of hadron-hadron scattering.

Comparisons with QCD calculations show that the small size region can be described successfully within the framework of perturbation theory. These calculations of elastic high energy scattering at short distances can be formulated as a *radiation problem*: the incoming photon creates a quark-antiquark pair which radiates gluons and further quark-antiquark pairs. The transition from the scattering of a small size photon on a proton to hadron-hadron scattering can then be viewed as the *transition of QCD radiation from small to large transverse sizes.* Thus at HERA we can not only test our understanding of QCD at short distances but also explore the transition into the confinement region. A careful study of QCD radiation at small and large distances presents a new approach to the QCD confinement problem.

The measurement of the energy and position of the forward going proton allows to determine the value of the t parameter in the diffractive processes. The slope $B(s)$ of the exponential fall-off of the observed t distribution of the diffractive cross section determines the size of the interaction region: $R^2_{int} = 2B(s)$. In one of the transparecies we show the

*Speaker.

slope B, at a fixed energy, as a function of the effective Q^2 scale, Q^2_{eff}, for various vector meson production processes.

The slope B (and the size of the interaction region) shrinks with increasing virtuality Q^2_{eff}. In the photoproduction region, $Q^2_{eff} = 0$, the observed B values of ρ and ω are of the order 10 GeV^{-2}, and they are similar to the values observed in proton-proton scattering at high energies (with B of the order $12 - 14$ GeV^{-2}). At higher Q^2_{eff}, the B slopes at HERA become considerably smaller, $B \approx 4 - 5$ GeV^{-2}: this is, approximately, half of the B value observed in proton-proton scattering at low energies, i.e. it corresponds to the "interaction size of a single proton". This suggests that the transverse extension of the scattering system has the form shown in one of the transparencies: the interaction region is determined by the size of the proton, whereas the photon and its quark-antiquark pair (denoted by the black point) have radii much smaller than the proton. Its perturbative radiation cloud (small circles around the black dot) determines the growth of the cross section with energy, and its size is smaller than the proton radius. The nonperturbative continuation of the radiation cloud (not shown), presumably, contains large-size wee partons, but they seem to be "dormant", in that they have little influence on the growth of the total cross section.

Let us next see how the transverse shape of the scattering system evolves with energy. In order to obtain a geometric interpretation (in transverse direction) of J/Ψ photoproduction at HERA let us first consider the situation (until now still hypothetical) of a system which has a much smaller size than the J/Ψ system at $Q^2 = 0$. In this case perturbative QCD predicts a vanishing slope parameter α' which leads to the conclusion that the interaction radius does not increases with energy. This is illustrated in the transverse picture shown in the transparencies: the proton size does not change with energy, and large-size wee partons whose cloud might grow with energy are "not active". Evolution with energy takes place mainly inside the radiation cloud around the $q\bar{q}$ pair: with increasing energy the number of radiated gluons grows, and the density inside the cloud around the black dot increases.

This illustrates that the t measurement gives us access to a detailed picture of QCD radiation processes at various sizes distances. For futher information see the article "Diffraction at HERA and the confinement problem" by J. Bartels and H. Kowalski, Eur. Phys. J. C19 693 (2001).

Forward Physics and Detectors at HERA

Forward Physics ~ Physics contained in the t-distribution of the diffractive forward proton

Motivation

One-liner : $F_2^{D_4}$ is as fundamental as F_2

Rise of F_2 and diffractive F_2 is due to the frequent gluon emission processes, t-distribution is sensitive to the transverse momenta of the emitted gluons directly

Simultaneous measurement of the rising F_2 's and t-distributions gives a detailed insight into the matter formation process

Henri Kowalski
EIC Workshop, Brookhaven March 2002

Elastic VM Production at HERA

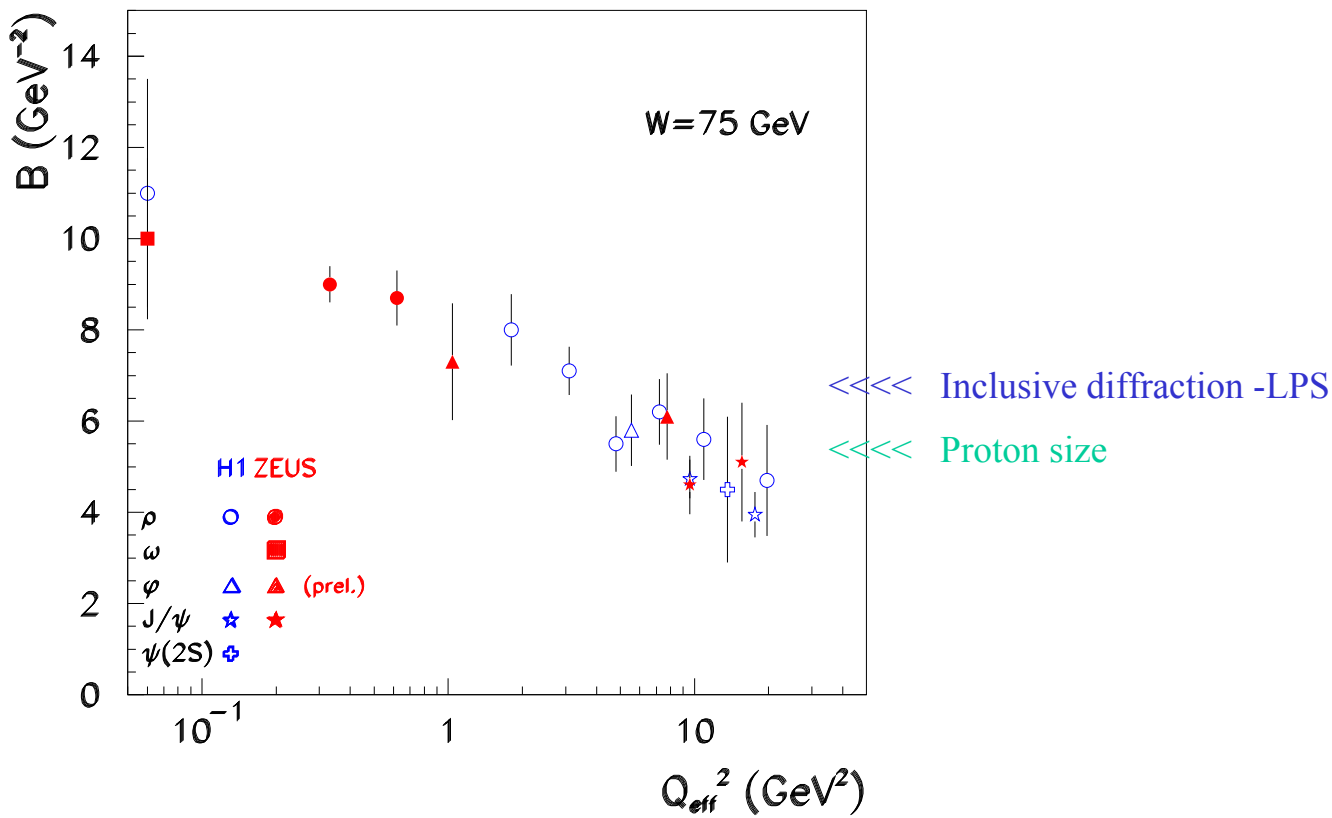

$Q_{eff}^2 = Q^2$ for ρ and ω productior

$Q_{eff}^2 = Q^2 + M_\phi^2$ for ϕ production

$Q_{eff}^2 = Q^2 + M_{J/\Psi}^2$ for J/ψ production

Transverse extension of the scattering system

a)

Proton radius >>>>

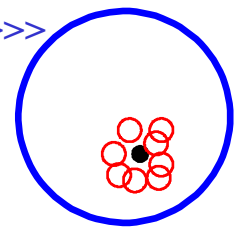

b)

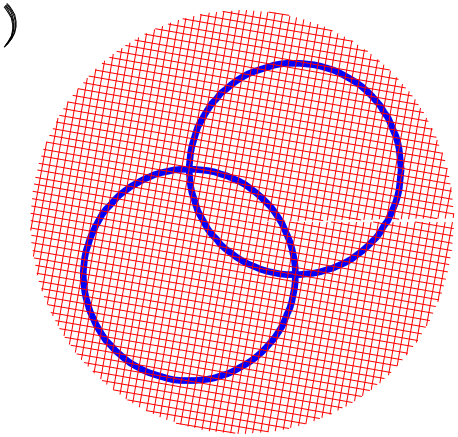

HERA	Hadron-Hadron
at high Q^2	
no growth with energy	growth with energy
perturbative description applies	Landau diffusion
transverse size of the photon cascade ~ $1/Q_0^2$	$\alpha_{IP} = 0.25$ GeV^{-2}
Q_0^2 independent on energy	
$\alpha_{IP} \sim 0$	

Leading Proton Spectrometer

Detector operation using Roman Pots

6 Ro-Pots equipped with micro-strip silicon detectors

pitch 115 micron
3 different strip orientations

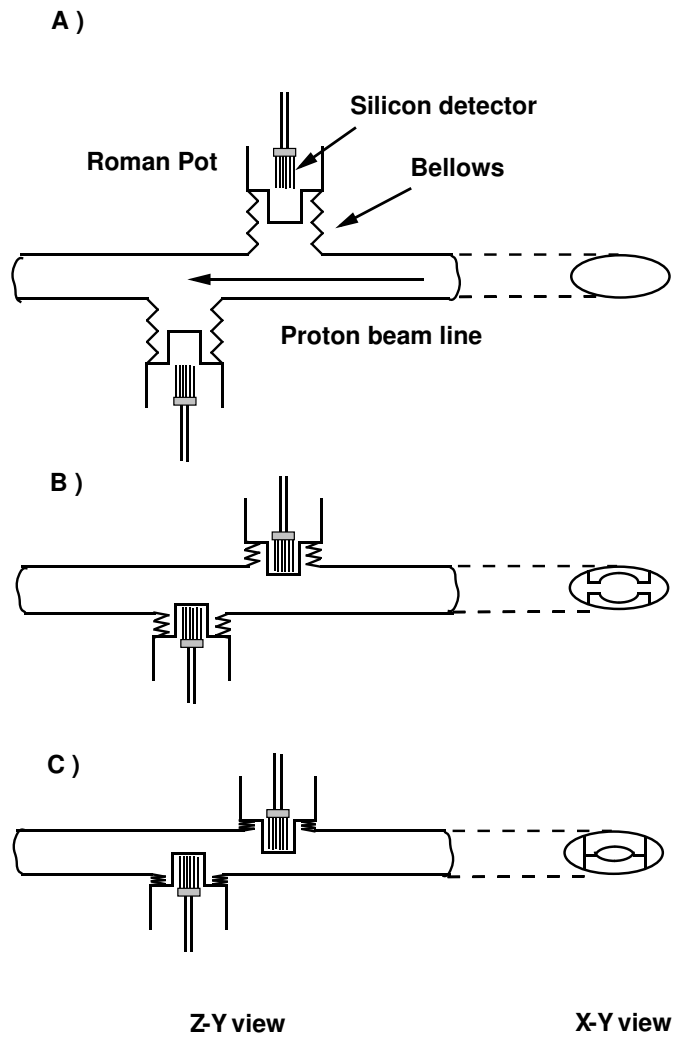

ZEUS 1994

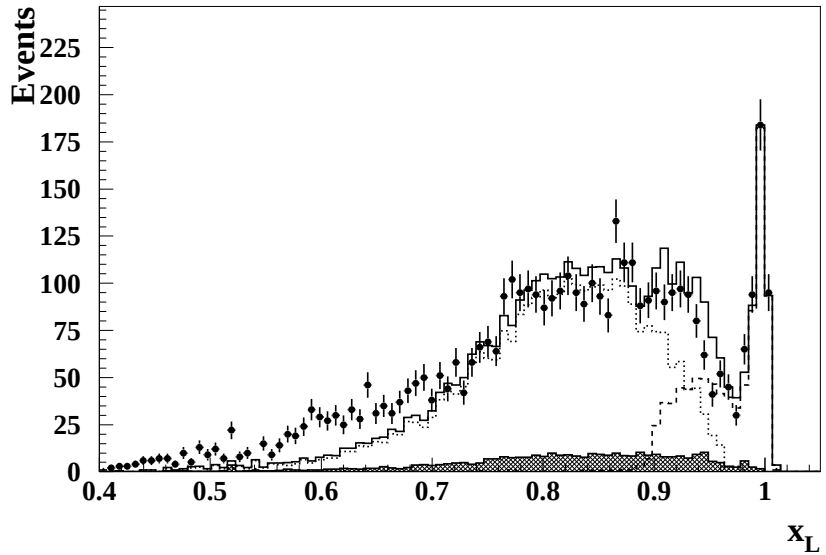

Diffractive analysis using LPS detector allows :

Clean selection of the single diffraction processes (no proton dissociation)

Measurement of ***t*** in diffractive reactions

Good reconstruction of kinematical variables when combined with the central detector

Problem - limited statistics

PARTICLE IDENTIFICATION AT HERA I

D. A. MILSTEAD
The Department of Physics, The University of Liverpool, Liverpool, L69 3BX, UK
E-mail: milstead@mail.desy.de

A review is given of particle identification techniques used by the H1 and ZEUS experiments during HERA I running.

1 Introduction

Particle identification is an essential tool to be used in investigating deep-inelastic electron-proton collisions (DIS). Measurements of the flavour structure of the hadronic final state can shed light on the partonic composition of the proton and photon and can also be used to test the environmental independence of the hadronisation process.

Both H1 and ZEUS employed a variety of techniques in identifying particles during the first phase of HERA running between 1992 and 2000. This paper describes these methods and also provides an outlook for future measurements with the upgraded experiments. Given the brevity of this article a full bibliography is provided for the interested reader.

2 Electron Identification

Both the H1 and ZEUS detectors are omnipurpose devices capable of measuring charged particle tracks and calorimeter energy depositions over a wide range of phase space. The primary method of selecting high energy electrons which are used to tag and reconstruct the deep-inelastic collision is to identify an electromagnetic cluster and associate this with a track. The H1 detector employs a liquid argon non-compensating device whilst the ZEUS detector is uranium-based and compensating. In regions of high acceptance both experiments report almost 100% efficiency in reconstructing DIS interactions[1,2] and typical electron energy resolutions of $\frac{7\%}{\sqrt{E/GeV}}$ and have been achieved[1]. In the attached slides distributions of electron energy, angle and the logarithm of inelasticity y are shown from DIS data taken by the H1 experiment. The data show a clean, well understood selection with backgrounds from, eg interactions of π^0 decay products within a hadronic jet faking electromagnetic signals being of the order of several per cent over most of the kinematic region. This background increases, however, at high values of inelasticity y and

is studied and controlled via quality variables such as the event $E - p_z$ and with QCD-based Monte Carlo programs such as Phojet.

3 π^0 and γ Measurements

In the messy hadronic environment of the aftermath of an *ep* collision the reconstruction of π^0 mesons is experimentally challenging. Below π^0 energies of approximately 8 GeV it is possible to reconstruct the π–meson with two experimentally distinct electromagnetic clusters corresponding to two decay photons from the dominant decay[3]. However, for high energies the two decay photons cannot be separated by the H1 and ZEUS calorimetry. Nevertheless, measurements of single electromagnetic clusters have been made and a low Bjorken-x π^0 production cross-section in the forward (i.e. proton) region has been published[4] owing to the fine calorimetric granularity in this region. This measurement of clean single particles reveals the QCD evolution of proton structure in a complementary way to the traditional forward jet work but which does not contain any inherent jet algorithm ambiguity bias[5].

Similarly, studies of single prompt photons also provide useful information on QCD processes and the ZEUS experiment has published several papers on this topic[6].

A challenge for these studies is to understand the hadronic background. It is thus essential to further reduce systematic uncertainties in this work that QCD modelling techniques improve.

4 V^0 Decays

Both H1 and ZEUS have measured the production rates of the K_s^0 and Λ via their weak decays into the π^+, π^- and $p\pi$, respectively[7,8]. The dipion and proton-pion mass spectra are shown in the attached slides demonstrating widths of about 8 MeV and 2 MeV, respectively. These decays are measured largely with the central drift chambers of the two experiments. These measurements revealed that the strangeness suppression factor in *ep* collisions appears to be less than 0.3, in agreement with recent e^+e^- results.

5 Particle ID through dE/dx

Both experiments have successfully calibrated their central drift chambers and use dE/dx information in their physics studies[9,10]. These have been used in heavy quark studies and measurements of the single proton production

cross-section. This latter work demonstrated an apparent proton-anti-proton asymmetry 8 units of rapidity away from the proton remnant system.

6 Particle ID through Transition Radiation

Both the H1 and ZEUS detectors operated with transition radiation (TR) systems in the forward region for HERA I. These were removed during the upgrade and replaced with drift chambers for enhanced forward track reconstruction efficiency. The TR systems were not successful largely due to the high forward particle multiplicity, much of which arose from the large flux from secondary particles produced in dead material in front of the forward chambers. Furthermore, long, well reconstructed tracks were needed and precision tracking proved difficult during HERA I operation due to the large forward multiplicities. In the attached slides, H1 results on the purity and efficiency of their TR system is shown.

7 Summary and outlook

Both the H1 and ZEUS experiments were successful in calibrating and exploiting their particle identification capabilities during HERA I. Lessons learnt include the need for high efficiency forward tracking.

Although H1 already possesses silicon tracking devices, these have now been upgraded and a further device installed for increased acceptance. The ZEUS collaboration have also now installed a silicon tracking device. These will be the cornerstone of heavy particle identification.

References

1. H1 Collaboration, Eur.Phys.J.C21:33-61,2001.
2. ZEUS Collaboration, Eur. Phys. J.C21:443-471, 2001.
3. H1 Collaboration, Eur.Phys.J.C18:293-302,2000.
4. H1 Collaboration, Phys.Lett.B462:440-452,1999.
5. H1 Collaboration, Nucl. Phys. B538:3-22,1999.
6. ZEUS Collaboration, DESY-01-043, submitted to Phys. Lett. B.
7. H1 Collaboration, Z. Phys. C76:213-221,1997.
8. ZEUS Collaboration, Z. Phys. C68:29-42, 1995.
9. H1 Collaboration Paper submitted to ICHEP 1998, Vancouver.
10. ZEUS Collaboration, Eur.Phys.J.C18:625-637, 2001.

Finding the Most Important Particle

Scattered electron defines the interaction.

- **Calorimeter+tracking triggers used**

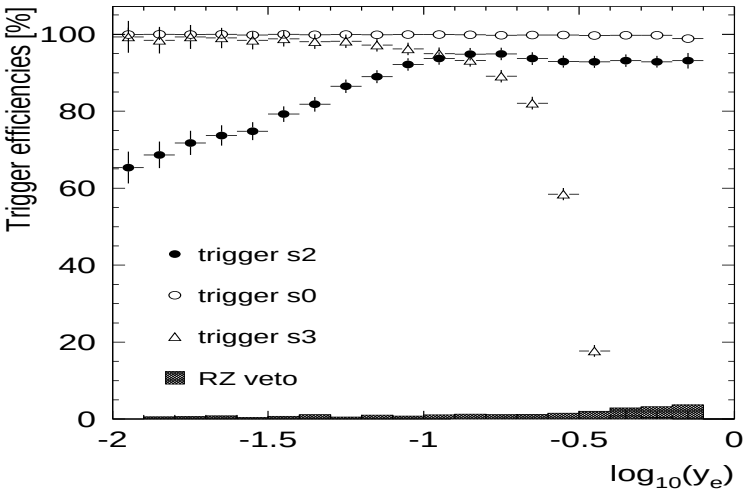

- **Well isolated cluster**

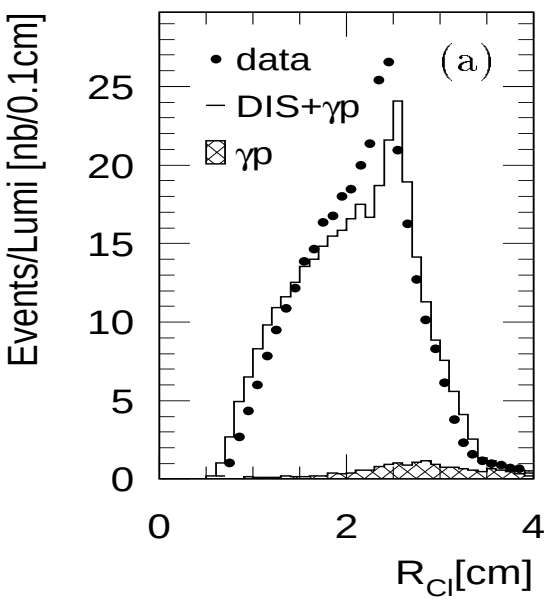

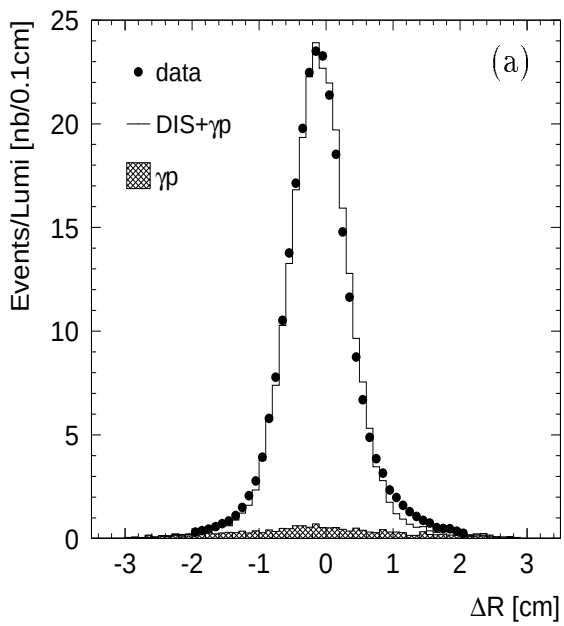

- **Resolution and background understood.**

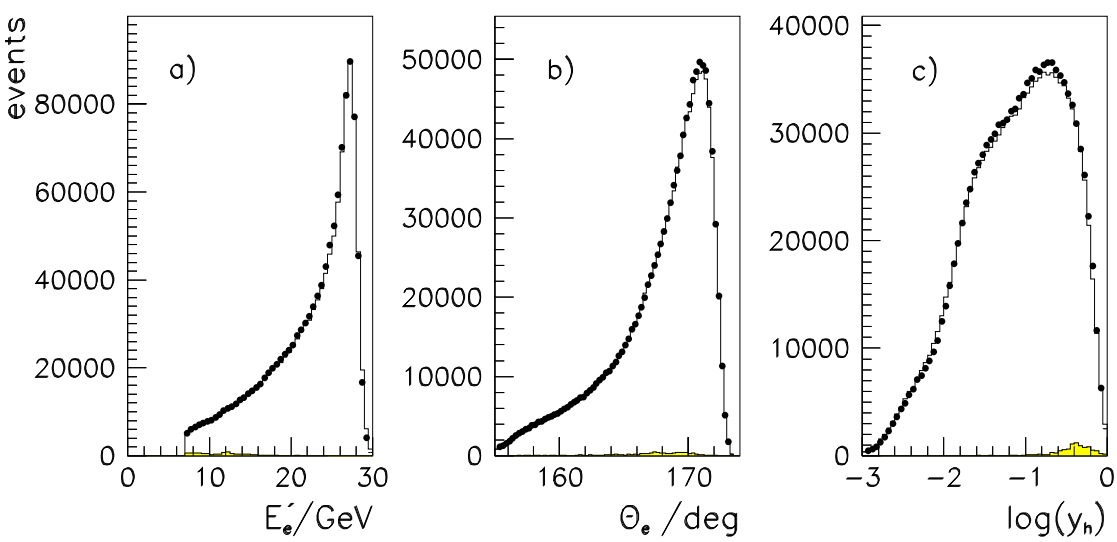

Find Strangeness through V^0s

Flavour tagging for $p_T \gtrsim 0.4$ GeV

Reconstruct $K_s^0 \to \pi^+\pi^-$ via remote vertex using jet chamber and Si.

Achieve $\sigma \approx 6 - 10$ MeV with $\approx 50\%$ acceptance.

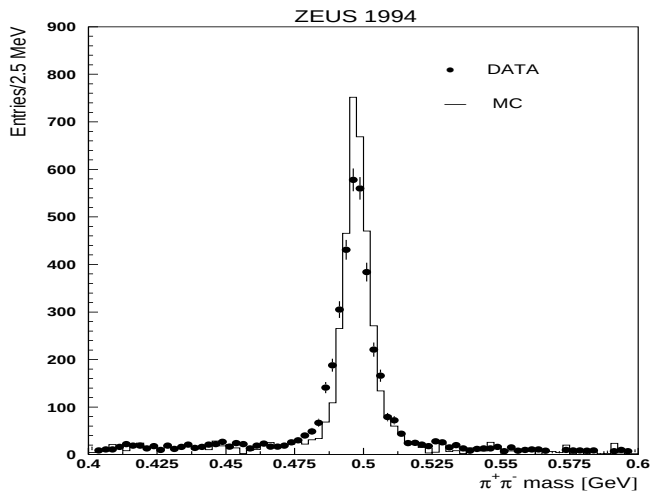

Flavour tag jets and measure strangeness suppression.

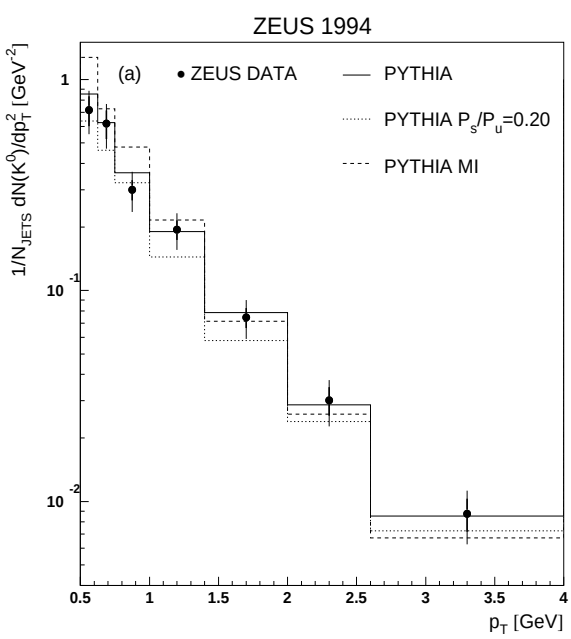

Measuring Strange Baryons

Reconstruct $\Lambda \to p\pi$ via remote vertex using jet chamber and Si.

Achieve $\sigma \approx 2 - 3$ MeV with $\approx 30\%$ acceptance.

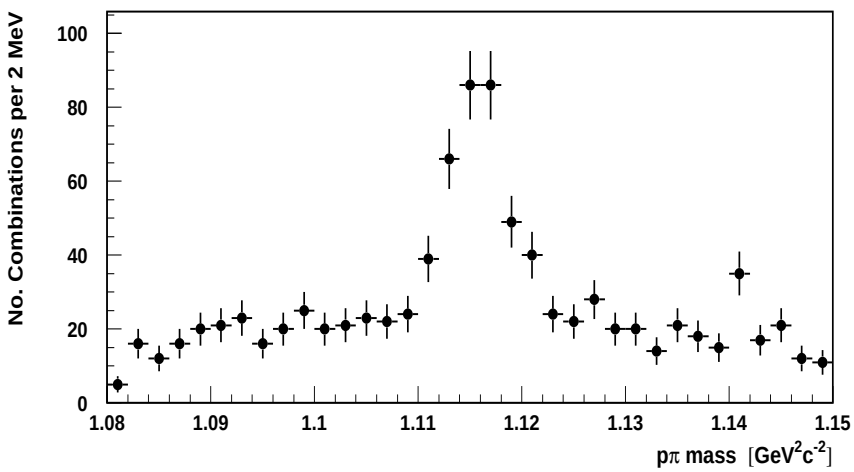

Measure baryon suppression and test pQCD

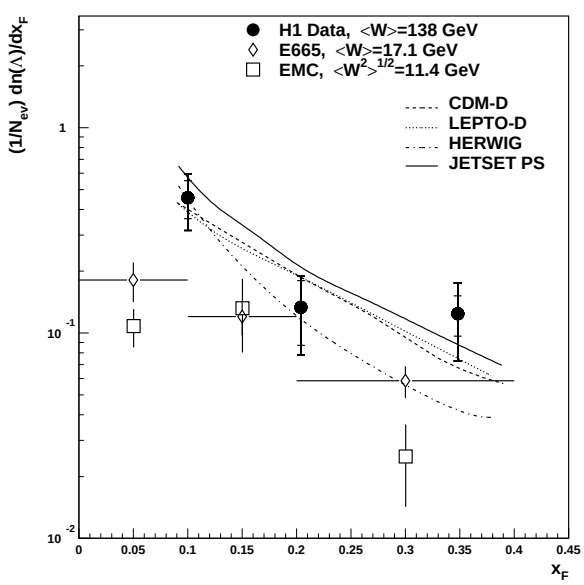

Transition Radiation at H1

Special runs with optimal gas mixtures.

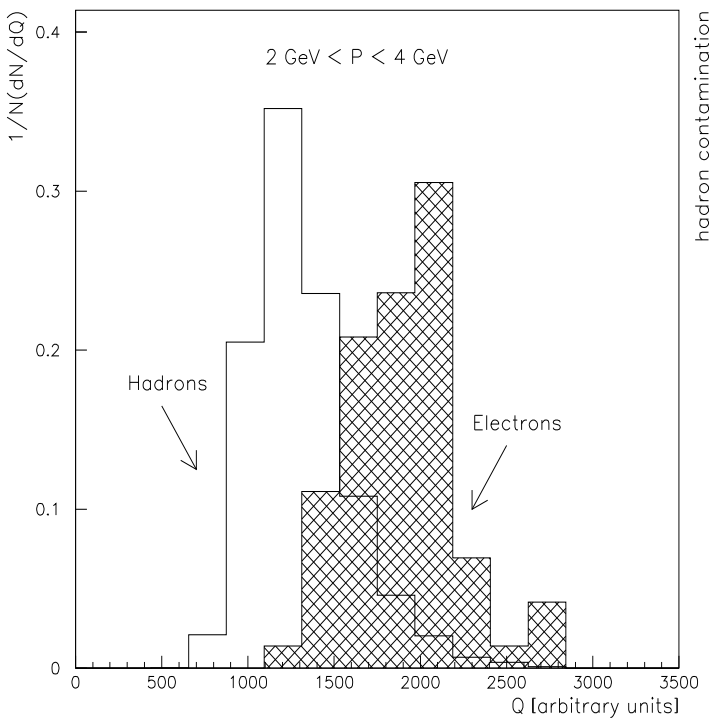

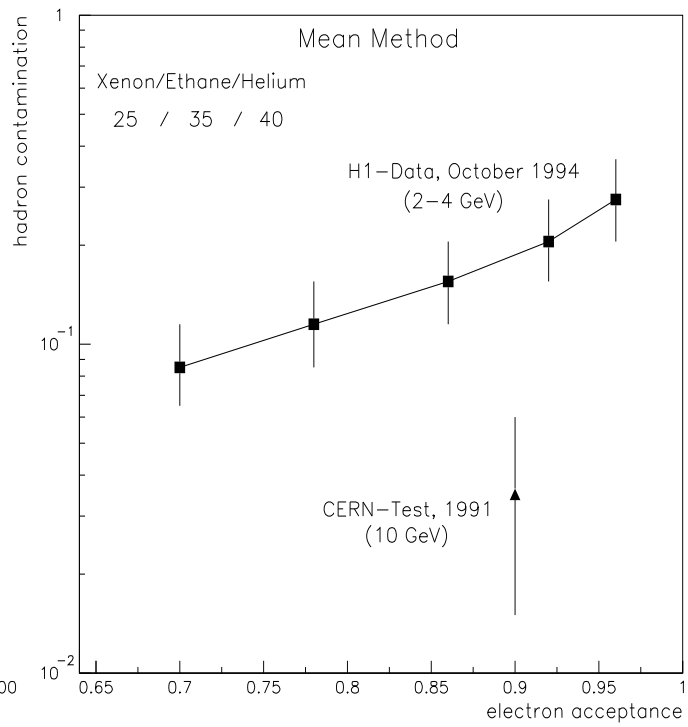

Close to test beam results.

High background, multiplicity forward region makes TR difficult.

Both H1 and ZEUS replace TR with drift chambers for high precision tracking.

Find Strangeness through V^0s

Flavour tagging for $p_T \gtrsim 0.4$ GeV

Reconstruct $K_s^0 \to \pi^+\pi^-$ via remote vertex using jet chamber and Si.

Achieve $\sigma \approx 6 - 10$ MeV with $\approx 50\%$ acceptance.

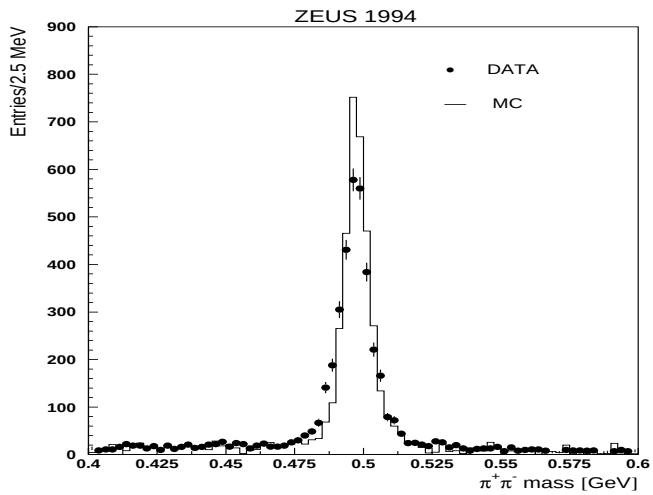

Flavour tag jets and measure strangeness suppression.

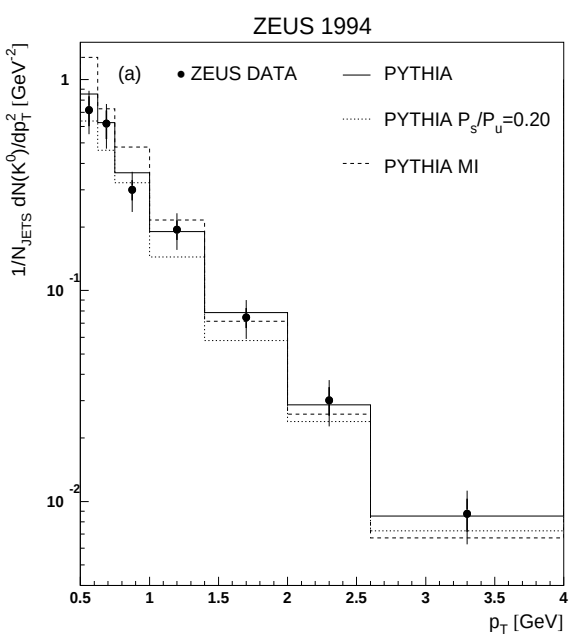

"Particle Identification at Belle"

Toru Iijima (Belle) / KEK
(iijima@bmail.kek.jp)

Talk Outline
- Introduction of Belle PID
- R&D for (present) Belle-ACC
- Present performance
- Future upgrade possibility

EIC Workshop @ BNL / Detector parallel session, March 1, 2002

Belle Detector

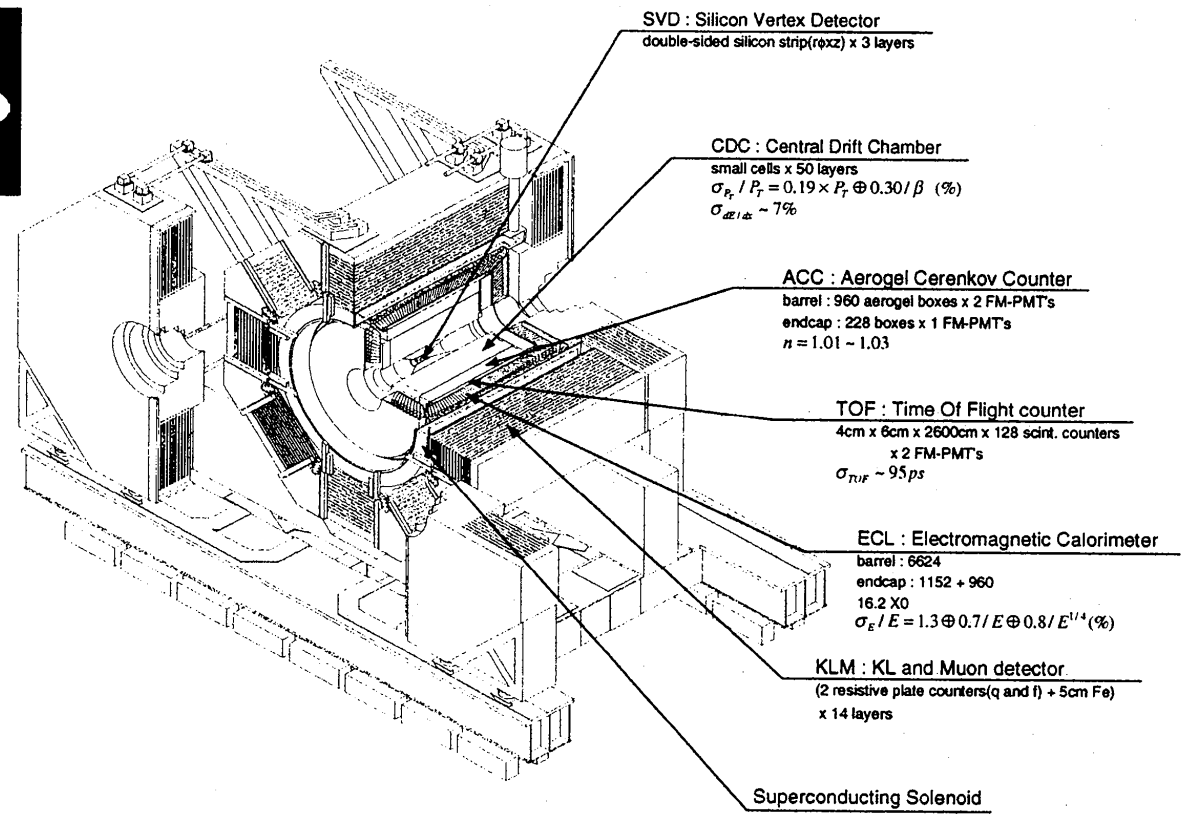

BELLE KID System

- **dE/dx** 50%He / 50% C2H6 , 50 layers
  ΔdE/dx ~5% (design)

- **TOF** BC408(4cmT × 6cmW × 255cmL),
  256 ϕ-segment
  Read-out by 2" FM-PMT at both ends
  TSC(0.5cmT) for γ background rejection
  ΔT ~ 100ps (design)

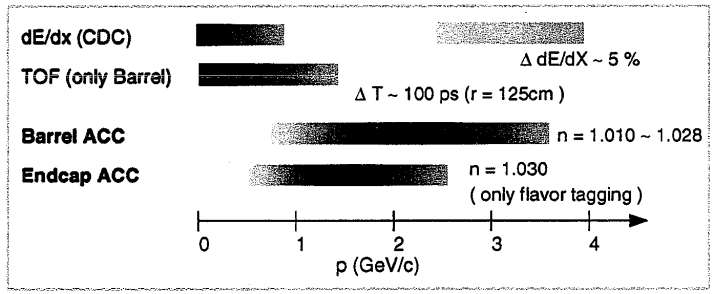

- **ACC** Barrel 960 modules in 60 ϕ-segment
  n = 1.010 ~ 1.028
  Endcap 228 modules in 5 layers
  n = 1.030
  (only for flavor tagging)
  Read-out by 2", 2.5" and 3"
  FM-PMTs

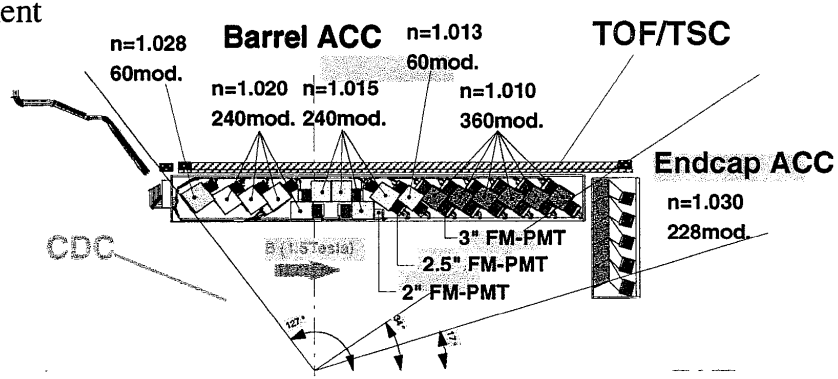

Particle ID for B-factory (cont'd)

Requirements

- **Flavor Tagging**
  $0.2 \le p(\mathrm{GeV/c}) \le 1.5$
  Rejection factor O(10^-2)

- **Two-body Decays**
  $1.5 \le p(\mathrm{GeV/c}) \le 3.8$
  Rejection factor O(10^-1)

Technology choices

- $dE/dx \propto 1/\beta^2 \left[1/2 \cdot \ln \frac{2m_e\beta^2\gamma^2 T_{max}}{I^2} - \beta^2 - \delta/2\right]$
- $TOF \propto L/\beta$
  ... effective for low momentum region

- **Cherenkov** If $\beta > 1/n \Rightarrow \cos\theta_c = 1/(\beta n)$
  [θ_c:Cerenkov angle]
  Threshold device
  Ring imaging device

Need(ed) technology development! →

BELLE : Aerogel (threshold)
BaBar : DIRC
CLEO-III: RICH with LiF+TEA

Kaon Momentum Distribution

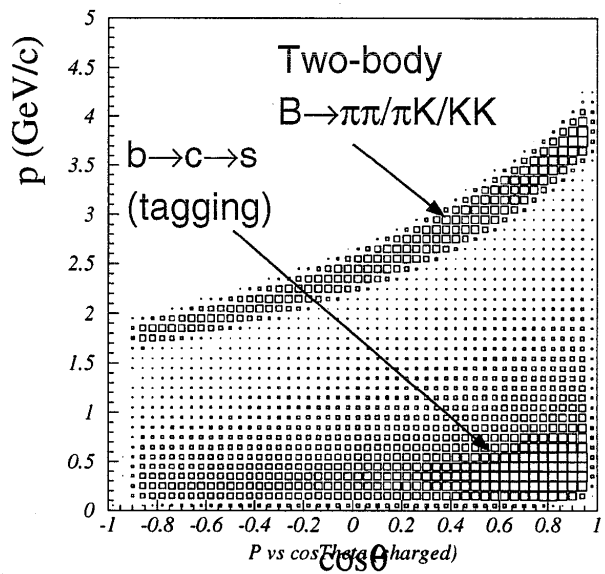

BELLE-ACC Module

- Aerogel container : Barrel ACC -- 0.2mm thick aluminum
  Endcap ACC -- 0.5mm CFRP
- Goretex reflector ⇒ diffusive reflection
- Photodetetion with one/two FM-PMT, equipped with voltage amplifier
  (Typical PMT gain ~ 10^6)

Barrel ACC Module

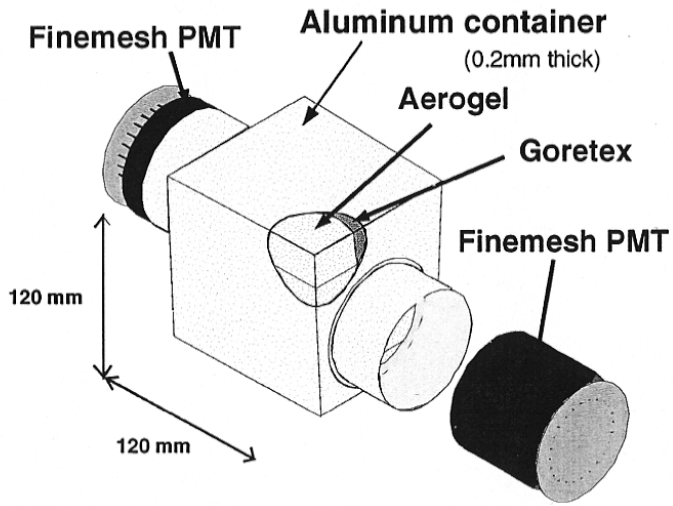

Endcap ACC Module

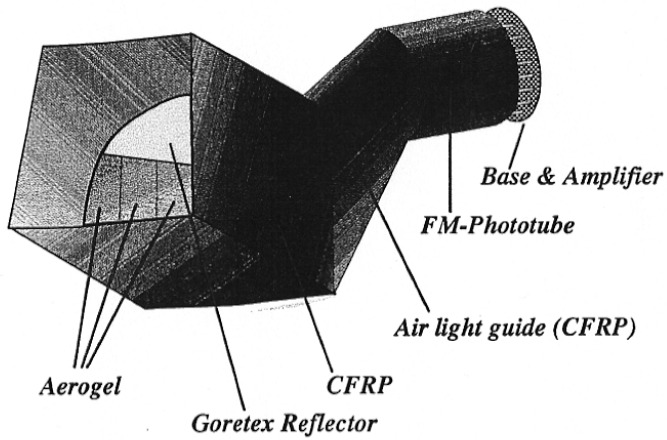

Silica Aerogel

- Silica aerogels…
  - Colloidal form of SiO2
  - R~0.1g/cm3, porosity ~95%(n=1.03)
  - N=1.006 ~ 1.06

    ⇒useful for K/p separation in GeV region

    If threshold counter, required n can be obtained only with aerogels.

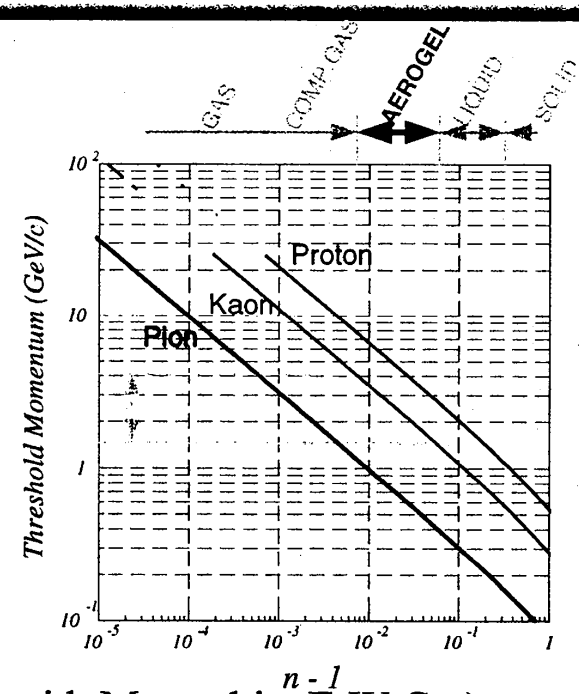

- New development for Belle-ACC
  - New production method (collaboration with Matsushita E.W.Co.)
  - High optical quality
  - Surface control →Hydrophobic
  - Radiation hardness

K/π ID Efficiency/fake

- High purity K/π track sample from D* decay chain.

$$D^{*+} \rightarrow D^0 \pi^+$$
$$\hookrightarrow K^- \pi^+$$

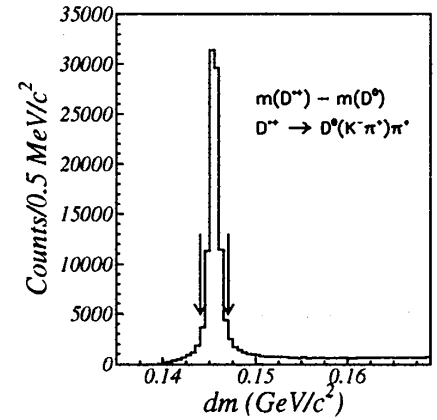

- ID method:
  K (π) probability calculated for each subdetector

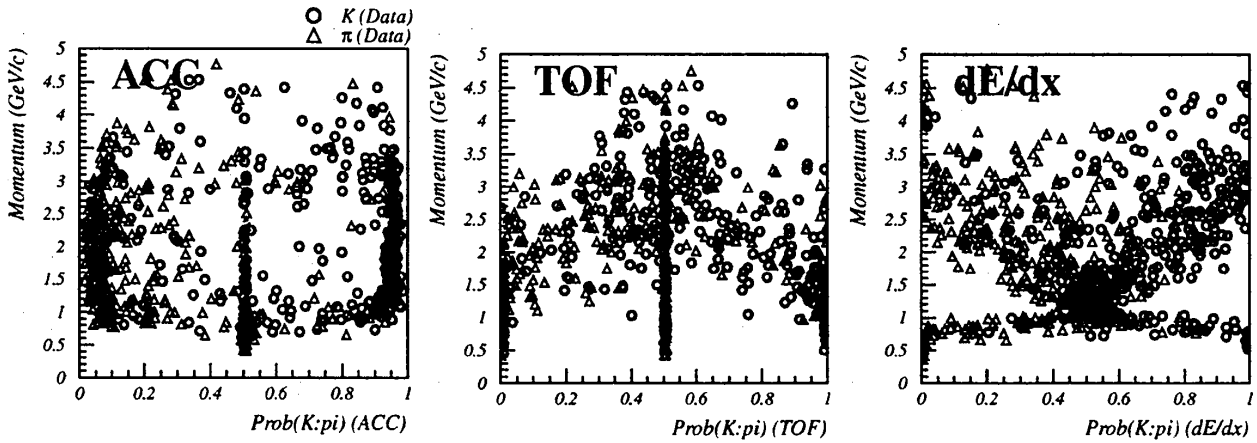

$$L_K = \mathrm{Prob}(K)/\mathrm{Prob}(K)+\mathrm{Prob}(\pi)$$

30

K/π ID Efficiency/fake (cont'd)

- Three subdetector information are combined;
  - $P_{all}(K) = P_{ACC}(K) \times P_{TOF}(K) \times P_{dE/dx}(K)$
  - $L_{all}(K) = P_{all}(K)/P_{all}(K) + P_{all}(\pi)$

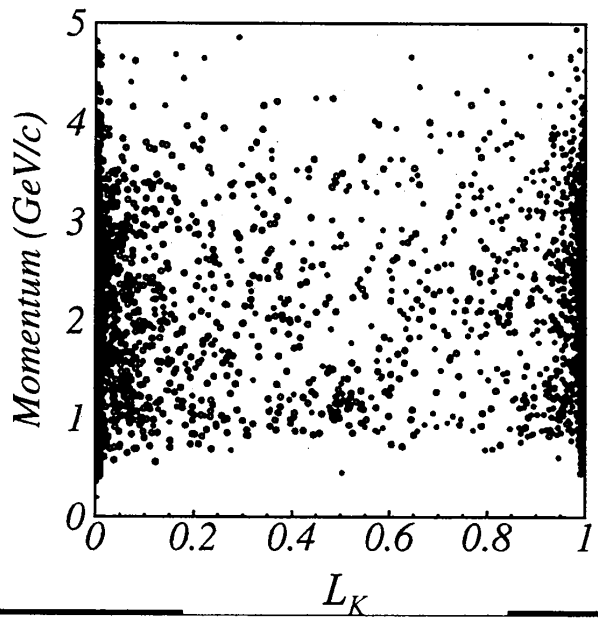

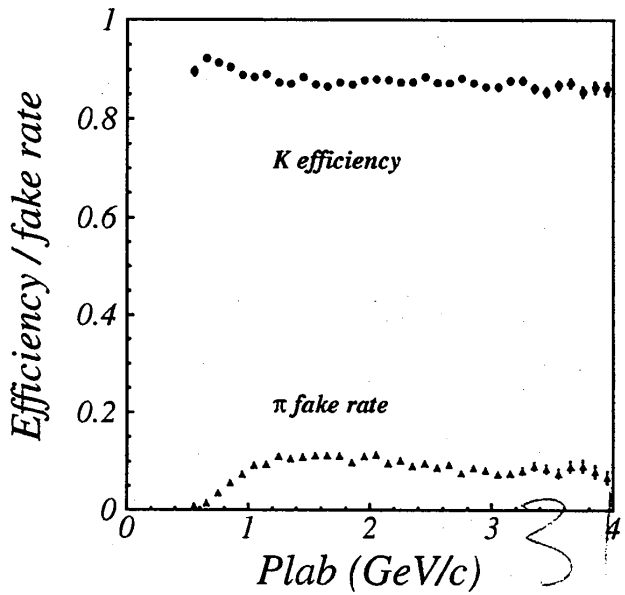

R&D Targets

- Improvement of high index aerogels
  - The present production method (know-how) is not optimized for n>1.05
  - N=1.05 sample from Novosibirsk showed 80% increase in Npe at the beam test.

⇒ *There is large potential to improve Npe* ×2

- Photodetection
  - Good effective area ratio (36% → > 70%):

⇒ *Flat pannel PMT* ×2

  - Good single photoelectron detection
    - QE
    - S/N (Peak-valley)
    - Magnetic field immunity

⇒ *Hybrid PD/APD* ×1.5

- More ideas
  - Dual-radiator option
  - Optics to increase area (light guide etc.)

Summary

- New development of aerogel Cherenkov technologies
  - Optical quality
  - Hydrophobicity
  - Photodetection in strong B field

  ⇒Successful operation @ collider experiment.
- It opened also possibility of aerogel-based RICH.

  ⇒better separation, wider momentum coverage.

  Key issues:
  - Further improvement of aerogels
  - Position sensitive photodetector

Hope we can share interest / output of R&D's.

EIC Detector Studies *

J. Chwastowski
Henryk Niewodniczański Institute of Nuclear Physics,
Cracow, Poland

1st March 2002

Abstract

The Yale '2000 Workshop detector model is presented. A short summary of the Interaction Region Group of the EIC Accelerator Workshop is given.

The Yale '2000 and present workshops extensively reviewed the physics programme for the Electron – Ion Collider (EIC). Also at Yale and during the EIC Accelerator Workshop (EICAW) possible options for the machine and the Interaction Region (IR) were discussed.

At Yale a model of a generic detector and the IR layout were proposed and discussed [1, 2]. The design criteria were:

- common detector for ep, eA, pp and pA collisions,
- reconstruction of "whole" ep and eA event,
- precise luminosity monitoring and control of radiative corrections,
- good detector quality in the fragmentation regions,
- minimal interference with the existing IR optics,
- use of the existing RHIC lattice in the spectrometer design,
- possibility of a polarized electron beam.

*Presented at EIC Workshop, 28 February – 2 March, 2002, BNL

These requirements are based on the H1 and ZEUS experiences and on the possible range of the machine parameters [3].
The electron – nucleus interaction leads to the production of jets, de-excitation gammas, "wounded" (struck by a probe) nucleons, re-scattered nucleons or heavier fragments. Figure 1 shows the pseudorapidity (η) spectrum of the

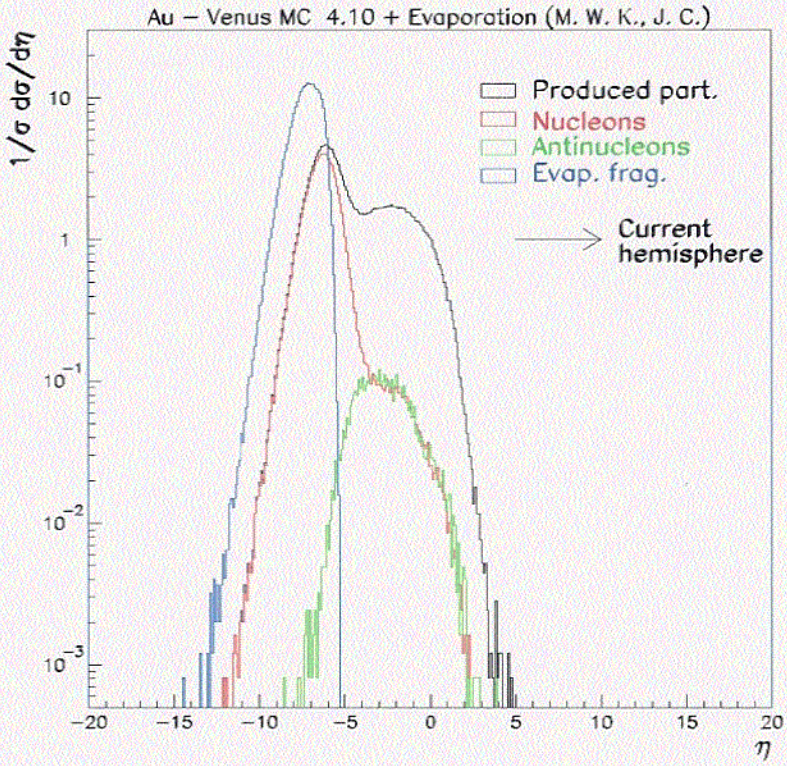

Figure 1: Finale state particle pseudorapidity distribution for e(10 GeV) – Au(100 GeV/A) collisions.

final state particles for e(10 GeV) – Au(100 GeV/A) collisions. The ZEUS and H1 detectors at HERA prior to the machine and the detectors upgrade covered roughly the range of (-5;5). Forward detectors like the Roman Pots system or the forward neutron counter were able to cover some part of the

spectrum. However, their acceptance was limited. In the electron (current) direction, the bremsstrahlung and initial state QED radiation were measured in the photon counter. The leptons scattered at small angles were detected in the electron taggers. It is obvious from Fig. 1 that to achieve a "complete" event measurement an extended "nucleus/hadron spectrometer" is necessary. The optimal choice of the nuclei species would cover uniformly the range of

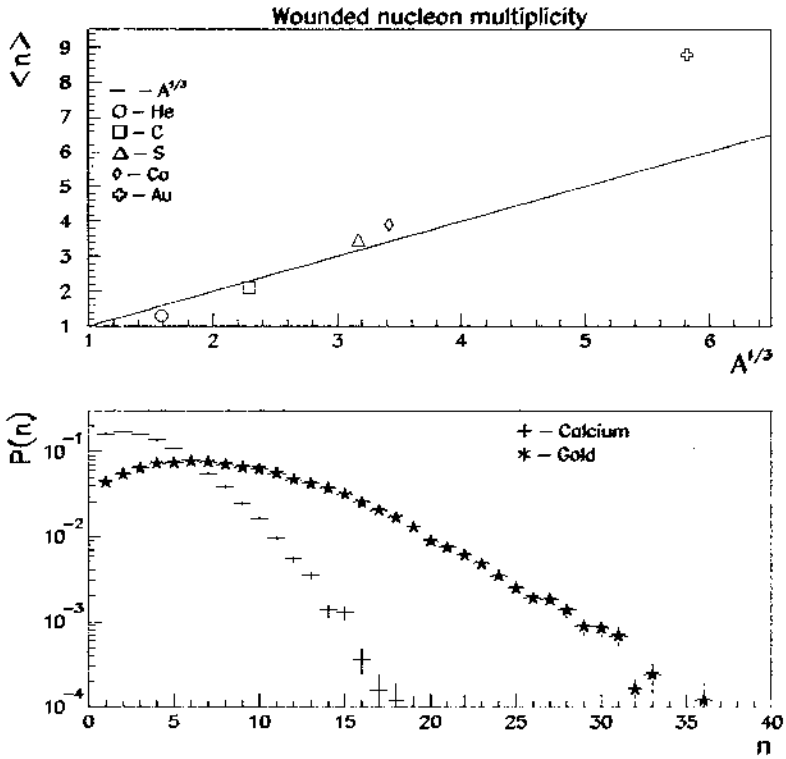

Figure 2: Wounded nucleon multiplicities.

$R \approx A^{1/3}$. Figure 2 shows the wounded nucleon average multiplicity as a function of A and compares the wounded nucleon multiplicity distributions in case of eCa and eAu interactions. The average multiplicity is approximately proportional to $A^{1/3}$. Comparison of the distributions for calcium

and gold shows that the large multiplicity tail in eCa collisions can simulate gold-like conditions.

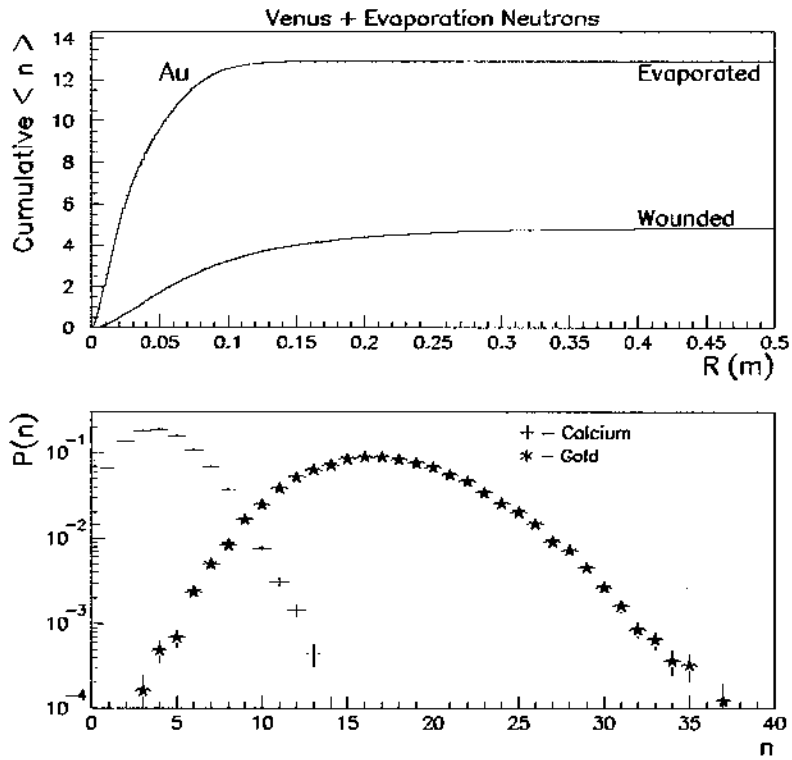

Figure 3:

In Fig. 3 the cumulative multiplicity of neutrons as a function of the distance from the beam direction is shown. The multiplicity saturates at the distance of about 15 – 20 cm. This show that the enlarged Zero Degree Calorimeter will play important role in the inelastic event tagging. The proposed model detector (reviewed in EICAW by E. Barrelet, Figs.4–6) was divided into three parts further subdivided into the detector components:

- hadron side:

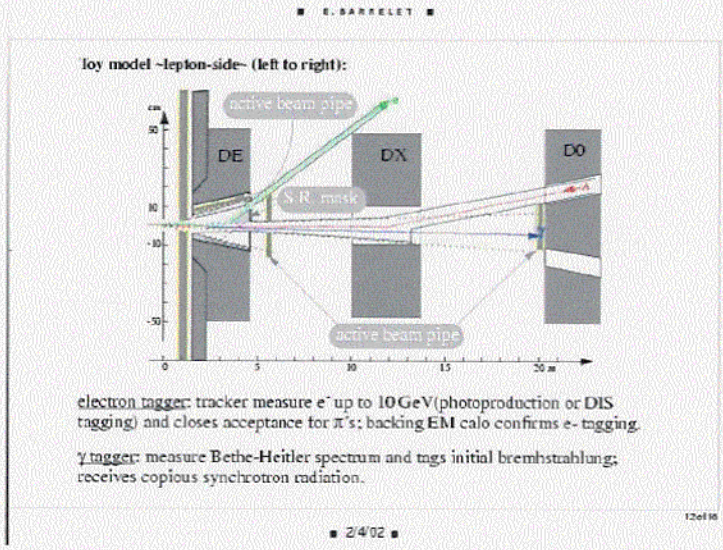

Figure 4: Yale '2000 detector and IR model. Electron side layout.

- Roman pots: diffractive scattering on beam,
- high rigidity spectrometer: EM calorimeter for nuclear $\gamma(\pi^0)$; hadron calorimeter for measuring evaporation neutrons and for p and heavier fragments identification; tracking for measuring evaporation protons and heavier fragments,
- medium rigidity spectrometer: EM calorimeter for $\gamma(\pi^0)$; hadron calorimeter to measure wounded neutrons, protons and for identification of heavier fragments; tracking system to measure $\pi^{\pm}$, protons and fragments;
- rapidity gap tagger: to close the acceptance for charged particles and to tag diffractive events;

• parton side is a compact central detector:

- the tracking chamber and the EM calorimeter inside a magnet – $\aleph/8$,
- the Spacal (H1) type end-caps,

- instrumented iron,
- μ-vertex providing small angle tracking.

- lepton side:
  - instrumented beam pipe for electron tagging
  - photon counter for the luminosity and radiative correction control, electron beam diagnostics and monitoring.

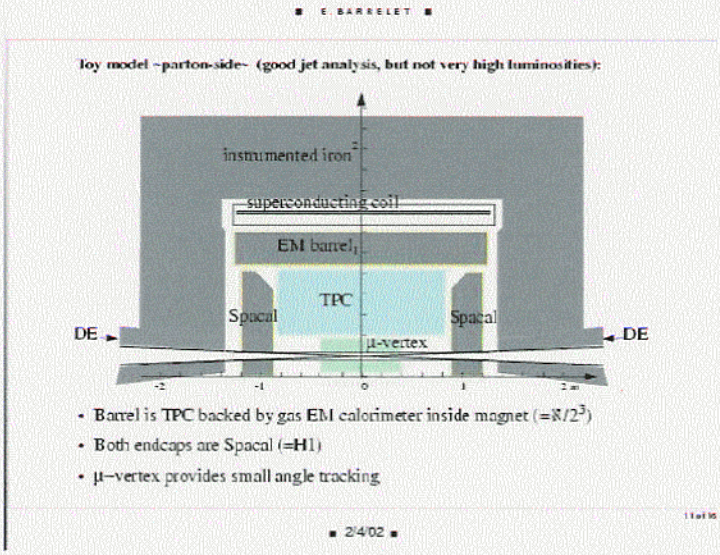

Figure 5: Yale '2000 detector and IR model. Central detector layout.

As can be seen from Figs.4–6 the electrons are early separated from the ions by the DE magnet. Magnet's parameters allow for the spin rotation and make it possible to bypass the DX magnet with the electron beam pipe. The DE magnet consists also a part of the spectrometer (medium rigidity) in the hadron direction. In the electron direction it is used to analyze the scattered electron energy. As an example a correlation between the z coordinate of the electron exit point (from the beam pipe) and its energy is shown in Fig. 7. One can observe that the position determines the electron energy. The beam angular divergence will broaden the correlation curve. The exit

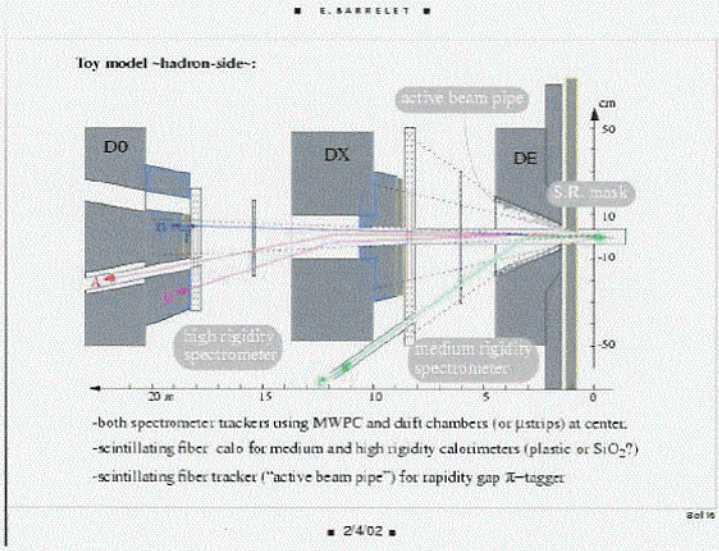

Figure 6: Yale '2000 detector and IR model. Hadron side layout.

position can be measured with help of the active beam pipe. For example with layers of the fibers. At the zero angle the gamma counter is placed. Its applications are mentioned above. In the central detector good energy measurement is achieved by the use of "good resolution" calorimeters combined with tracking. In addition, the μ-vertex will help in the interaction vertex position determination and small angle tracking. The energy distribution of the final state particles emitted with $\eta < -6$ is shown in Fig. 8. A clear energy quantisation is seen for the nuclear fragments. The fragment energy determines its composition.

The level of the synchrotron radiation with critical energy about 60 keV is a drawback of the Yale model.On the entry into the detector (hadron side), it may deteriorate the active beam pipe and the central tracking performance. On the exit (electron side), it will influence the lepton measurements leading to increased pedestals' widths. It also forces the use of the synchrotron radiation filters in front of the gamma counter.

The HERA IR region was discussed by U. Schneekloth. To achieve high luminosity the final focus magnets were introduced into the central detector. This, on one side, reduces the detector acceptance and on the other, leads to

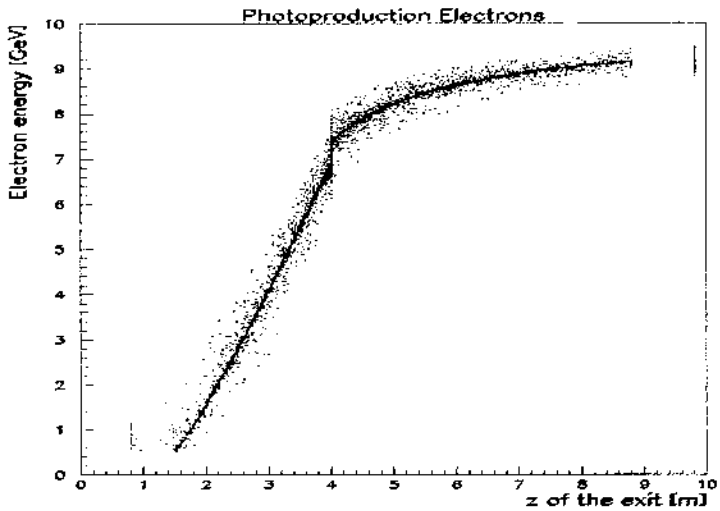

Figure 7: The scattered electron energy – position correlation.

high synchrotron radiation levels with about 10^{18} photons per second. The calculations shown by D. Pitzl show that a reduction factor of 10^{10} on the number of photons is needed. Partially, it was achieved with help of the synchrotron radiation collimators (Fig. 9).

An existing solution for the early separation of the beams was discussed by U. Wienands and is shown in Fig. 10. The price paid for the very high luminosity in PEP are the magnets which are very close to the nominal vertex and the dead area up to 20° away from the beam direction. One should note that this limitation of the detector acceptance is of less importance in case of the$\mathcal{B}$-factory. Such a solution may play a very important role in case of extreme luminosities as proposed in the Crab Crossing option (Fig. 11) for the IR.

An improved solution for the IR was shown by B. Parker (Figs. 12–13). He proposes to achieve an early separation of the beams by means of a small dipole component added to the solenoidal central field. This diminishes the synchrotron radiation influence (critical energy about 6 keV). Further, the septum magnet (in this case the Lambertson magnet, warm type) is introduced next to the central detector. The electron beam passes the field

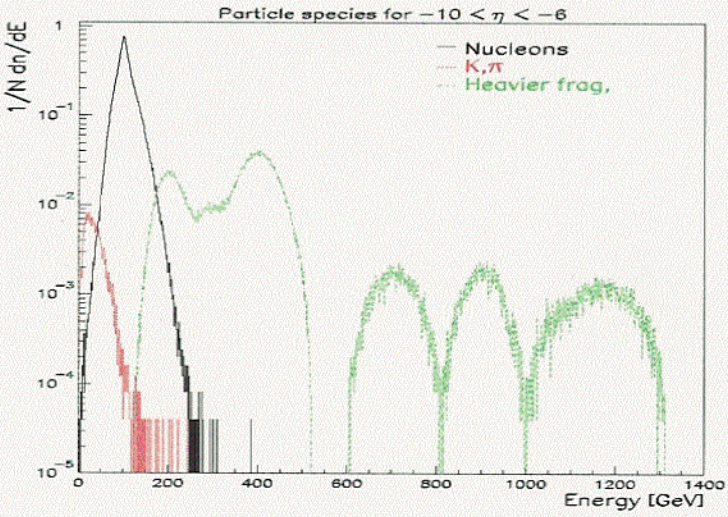

Figure 8: Energy distribution of different particle species for $-10 < \eta < -6$.

free zone while ions traverse a 1 T dipole field. This option allows for the active beam pipe and provides the spectrometer functionality. One should also note that this option offers the head-on collisions and that all three beams are present in the interaction region.

Summarizing there is no doubt that a good design of the IR and that of the detector are very closely connected. It has to emerge from the co-operation of the machine and the experimental physicists. It has to be checked whether the current designs are optimal or they should be further improved or one has to look for anew, different designs. One should note that the ratio of the lepton to the ion energies has a large impact on the detector design. So has the lepton energy tunability and possible luminosity value. Obviously one should look for the hermetic option of the detector, with the machine lattice used for the spectrometric measurements. The "complete event" option is of great value and it makes the coverage a wide range of physics processes feasible. The bremsstrahlung is a good candidate for a precise luminosity measurement both on- and off-line, and for the fast on-line lepton beam diagnostics.

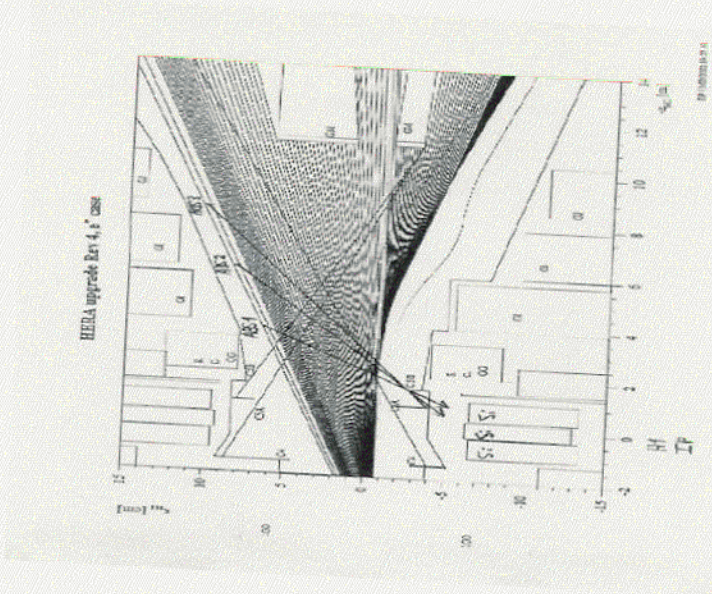

Figure 9: Synchrotron radiation in the HERA IR.

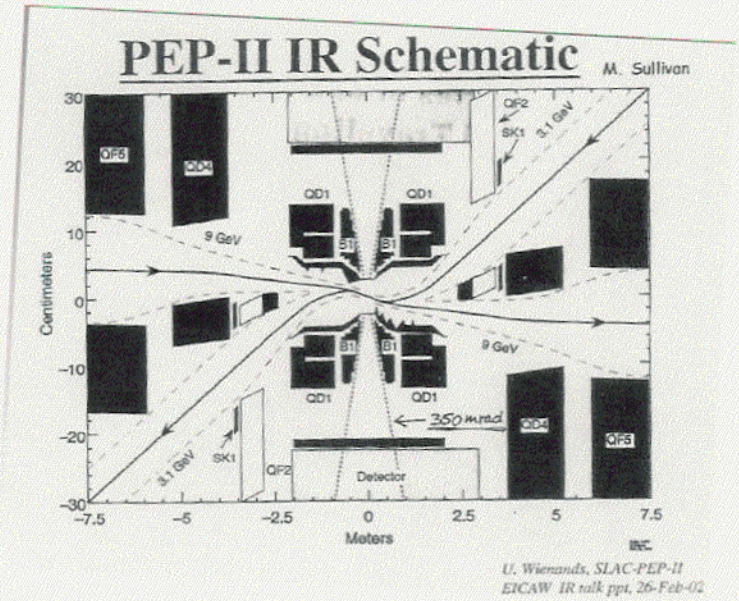

Figure 10: PEP IR.

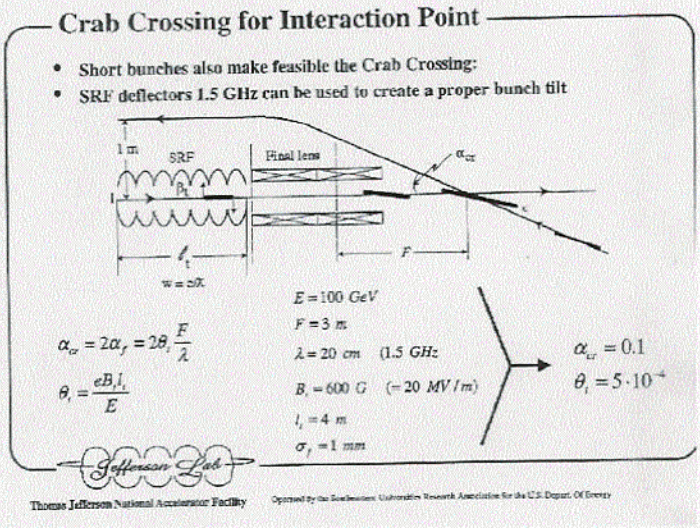

Figure 11: Crab Crossing in the IR.

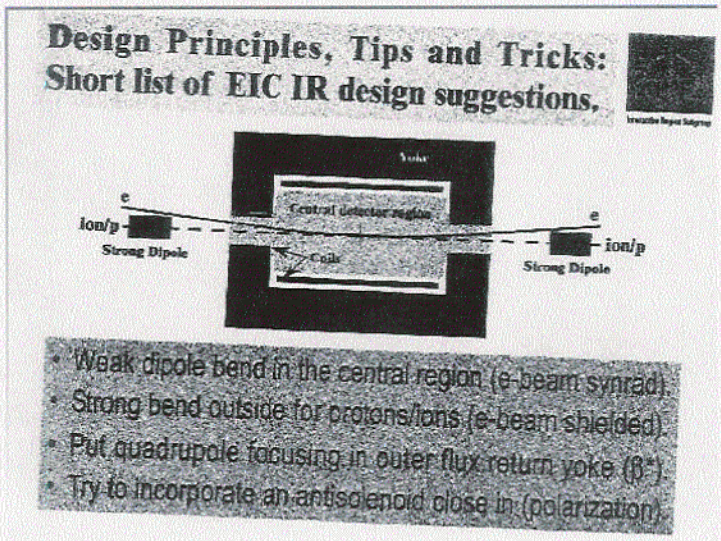

Figure 12: Early separation of beams in Parker's proposal.

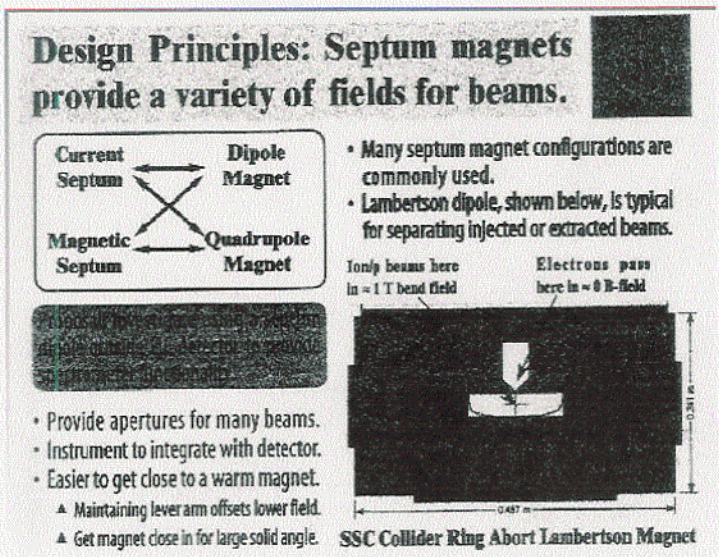

Figure 13: Lambertson magnet layout.

References

[1] M. W. Krasny, Physics of eA Collisions at RHIC and HERA, *Proc. The 2nd eRHIC Workshop*, Yale, April 6 – 8, 2000.

[2] E. Barrelet, J. Chwastowski and M. W. Krasny, Interaction Region Compromises, *Proc. The 2nd eRHIC Workshop*, Yale, April 6 – 8, 2000.

[3] I. Ben – Zvi, J. Kewisch, J. Murphy and S. Peggs, Accelerator Physics Issues in eRHIC, *Proc. The 2nd eRHIC Workshop*, Yale, April 6 – 8, 2000.

[4] Contributions to EICAW IR working group by: Etienne Barrelet, Slava Derbenev, Douglas Hasell, Jorg Kewisch, Brett Parker, Steve Peggs, Daniel Pitzl, Uwe Schneekloth, Uli Wienands.

Silicon Tracking for PHENIX Upgrade

Yuji Goto

RIKEN BNL Research Center

We, RIKEN and RBRC group, started development of a silicon tracking detector. One main interest is to build a silicon tracker system for a PHENIX upgrade. By using the detector, we will get better jet axis direction resolution, and capability to identify bottom and charmed hadrons. This extends x-coverage, increases statistics and enhances S/N ratio of the gluon polarization measurement, and, as a result, improves sensitivity of the PHENIX experiment to the gluon polarization. It is one of major goals of the RHIC/Spin project to clarify contribution of the gluon polarization to spin 1/2 of the proton.

A straw-man design of the detector system at PHENIX consists of barrel detectors and end-cap detectors. The barrel part has four layers and covers $|\eta| \leq 0.7$ and 2π azimuthal angle. The 1st (or 1st and 2nd) layer is made of silicon pixel detectors, and the 2nd to 4th (or 3rd and 4th) layers are made of silicon strip detectors. The end-cap part covers acceptance of the muon arms.

To design the detector, momentum resolution and displacement vertex resolution of the detector are required to be good enough for our physics scope. Performance with heavy-ion collisions, e.g. occupancy, is also required.

In addition to the design of the sensor chips and mechanical structure, electronics to readout signals and interface with the PHENIX DAQ system is another large element of the development. We are still at the starting point of the development, and have to overcome many critical paths.

Physics goals

- To clarify contribution of quark spin and gluon spin to the proton spin 1/2
  - gluon polarization $\Delta g(x)$
    - wider x_g coverage ➔ $\Delta g = \int_0^1 \Delta g(x)dx$
    - clean process/channel ➔ lower systematic uncertainties
    - higher statistics
  - baseline
    - pion/hadron (as an alternative of jet)
    - prompt photon
      - » central arm ϕ: $\pi/2\times2$ $|\eta|<0.35$
    - heavy flavor – single electron, J/Ψ, e-μ conincidence
      - » central arm ϕ: $\pi/2\times2$ $|\eta|<0.35$
      - » muon arm ϕ: 2π $1.2<|\eta|<2.4$
  - upgrade
    - photon + jet
    - heavy flavor – b/c-tagging

PHENIX

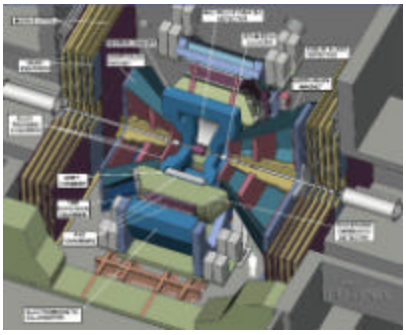

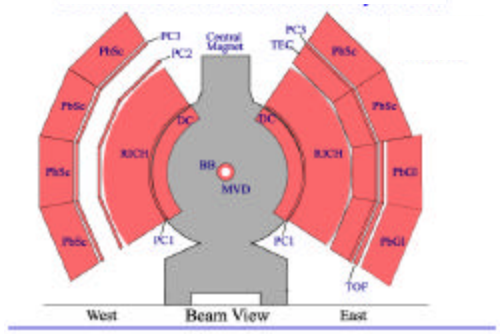

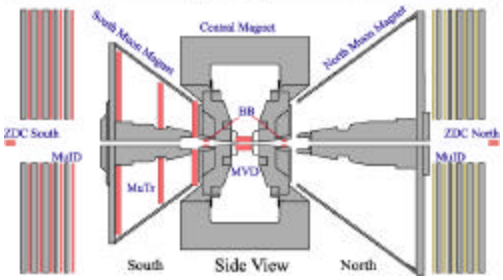

Design

- Acceptance
  - photon + jet
    - opposite side of the central arm — ϕ: $(90+\alpha)^{o}\times 2$ — $|\eta|<1$ or more
  - b/c-tagging
    - displaced vertex tag — ϕ: 360° — $|\eta|<1$ or more
    - electron tag — ϕ: $(90+\alpha)^{o}\times 2$ — $|\eta|<(0.35+\alpha)$
- Straw-man design

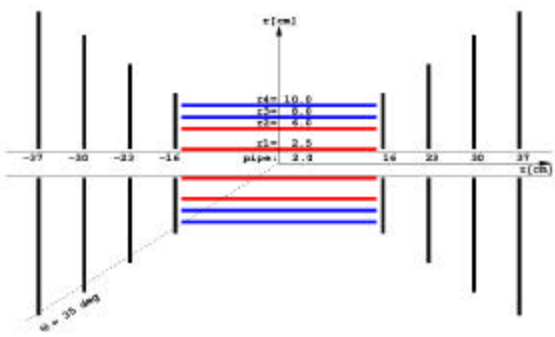

1st pixel layer
2nd-4th microstrip layer
80μm×3cm cells

Requirement for the detector

- Momentum resolution
  - need to determine jet axis
  - no need for p_T sum
- Displacement resolution
  - for b/c-tagging
- Performance in H.I. environment
  - to identify e^+e^- pair
  - occupancy
  - track association between the silicon strip detector and PC1

$B^{\pm}$ ct=496μm
B^0 ct=464μm
B_s^0 ct=315μm
$D^{\pm}$ ct=315μm
D^0 ct=123.7μm
$D_s^{\pm}$ ct=148.6μm
(τ ct=87.11μm)

Requirement for the detector

- Momentum resolution $\frac{s_p}{p} = \frac{2 \cdot s \cdot p(\mathrm{GeV}/c)}{0.3 \cdot B \cdot (dl)^2}$
  - necessary to determine jet axis
  - not for p_T sum
  - $s_p/p \sim 10\% \times p(\mathrm{GeV}/c)$
  - B = 1T with second inner coil
    - ➔ dl > 3cm
- Displacement resolution
  - for b/c-tagging $s_z = \frac{r+d}{d} s_1 \oplus \frac{r}{d} s_2 \oplus r s_q$
  - material
    - beryllium beampipe
      - ➔ 1mm/35.28cm ~ 0.3%
    - silicon
      - ➔ 1mm/9.36cm ~ 1%
  - ➔ multiple scattering

$$s_q = \frac{0.014}{p_T(\mathrm{GeV}/c)} \cdot \sqrt{X / X_0}$$

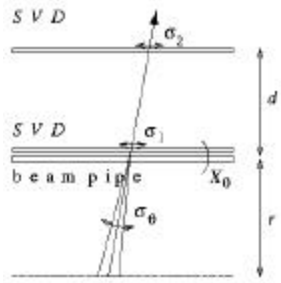

Requirement for the detector

- Displacement resolution
  - 4-layer configuration (1st & 2nd layers)
    - r=2.5cm d=3.5cm
    - multiple scattering for p_T=1GeV/c
      - s_q=0.0016 ➔ s_z~40μm
    - s_1=25μm ➔ s_z~43μm
    - s_2=25μm ➔ s_z~18μm
    - total ➔ s_z~61μm
  - 3-layer configuration (2nd & 3rd layers)
    - r_1=2cm r_2=4cm d=2cm
    - multiple scattering for p_T=1GeV/c
      - s_{q1}=0.0008 ➔ s_z~16μm
      - s_{q2}=0.0014 ➔ s_z~84μm
    - s_1=25μm ➔ s_z~100μm
    - s_2=25μm ➔ s_z~75μm
    - total ➔ s_z~154μm

Requirement for the detector

- Performance in H.I. environment
  - GEANT simulation
    - HIJING 3.15 with impact parameter < 3fm
      - no magnetic field because I don't have tracking program …
    - geometry
      - 4 layers (single-sided for simplicity)
      - 500μm thickness
      - vertex distribution σ = 10cm
  - Occupancy
    - 2nd layer r=6cm <12%
    - 4th layer r=10cm ~5%
  - Track association between the silicon strip detector and PC1
    - efficiency 86%
    - 0.4 degree in RMS
    - estimation including momentum analysis / momentum matching needs to be done

Technology options

- Microstrip (many detectors …)
  - scalable, fast (level-0/1 trigger), rad hard, reliable operation
- CCD (SLD)
  - high resolution, thin, low cost
  - rad soft, cryo system necessary
- Silicon drift (STAR, ALICE)
  - scalable
  - expensive, difficult control of environment
- Hybrid pixel (ATLAS, CMS, ALICE)
  - sensor chip and readout chip bump-bonded
  - fast (level-0/1 trigger), rad hard, low cost
  - thick
- Monolithic pixel
  - sensor and readout in one chip
  - rad hard, low cost

Readout chips

- Check points
  - rad hardness
  - pulse shaping time
  - S/N
  - DC/AC coupling
  - capacitance match
  - power consumption
  - matching with DAQ
    - trigger/readout timing
    - depth/latency of pipeline & buffer
    - data compression on chip
    - data volume
    - level-0/1 trigger
  - external electromagnetic pickup (common mode noise)

Readout chips

- Options
  - analogue multiplexor
    - VA1/VA2 (commercial – BELLE, PHOBOS)
      - shaping 0.5-2.0 μsec
      - (BELLE: high occupancy ➔ upgrade to pipeline or pixel)
  - analogue pipeline
    - SCTA (ATLAS backup)
      - rad hardness 10Mrad
      - shaping 50nsec
      - external digitization necessary – where ? how long ?
  - binary pipeline
    - SCTB
    - ABCD (ATLAS)
    - ALICE pixel chip – applicable ??
  - digitizing pipeline
    - SVX3 (CDF, PP2PP)

PHENIX DAQ

- Matching
  - level-1 in 4.3μsec
    - 106nsec×40depth-pipeline
    - backplane transfer to 5-depth buffers
  - conversion + G-link transfer to DCM in 40-80μsec
    - 25-12.5kHz
    - currently 192μsec
  - currently no level-2

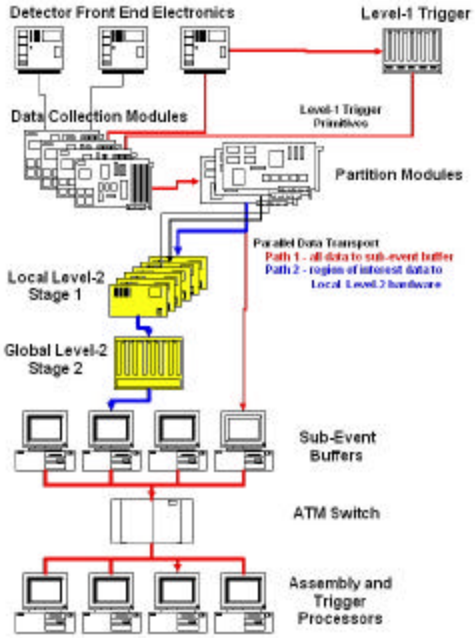

Outlook

- More and more to study …
  - realistic (GEANT) simulation
    - with magnetic field, tracking (combining barrel & endcap)
  - telescope
    - integration with readout chips (VA2), I/F, PC-DAQ, …
    - test beam in this year (before summer …)
    - test at IP12 ?
  - mechanical structure
    - to study mechanical strength, cooling, cabling, …
    - HYTEC inc. with ISU, LANL, … ?
- Schedule
  - microstrip layers in 2004
  - pixel layers in 2005 ??

Discussion: Detector Design WG

- GEANT simulation framework for EIC detector studies
- Participation in detector design studies
- Organizational issues of Detector Design WG
- Outline of Roadmap toward a CDR for EIC:
  - Physics case -> detector requirements
  - Constraints from accelerator/interaction region
  - Choice of detector technology
  - Detector simulation
  - Detector/physics studies
  - Documentation

GEANT simulation framework for the EIC detector studies

Bernd Surrow
BNL

STAR GEANT framework

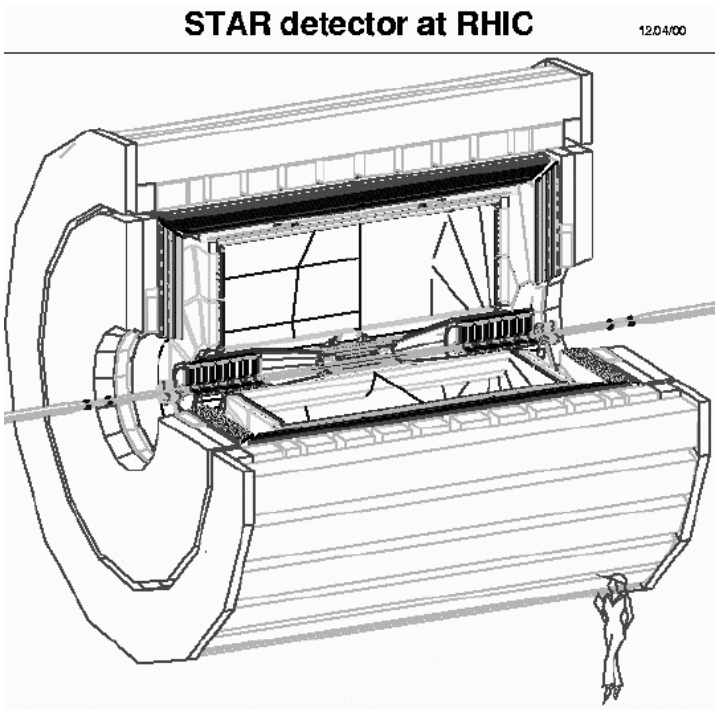

- GSTAR framework: STAR + GEANT
- GEANT version: 3.21
- The GSTAR framework allows to define the definition of
  - Geometry
  - Hits
  - Digitization

  by means of simple module files (Fortran/ASCII type statements) which are then translated into the actual Fortran GEANT user code with explicit calls to GEANT routines
- Besides avoiding repeated explicit GEANT calls, the GSTAR framework automatically handles:
  - Media numbers
  - Rotation matrix numbers etc.
- Full I/O interface can be used

➢ Thanks to Pavel Nevski!

EIC detector simulation

- Adopt existing GSTAR framework for EIC detector studies
- Provide basic detector layout for initial studies
- Provide machinery to use this code on different platforms (makefiles, steering files etc.)
- Collect various event generators for ep/eA studies
- Document and distribute software through EIC detector design WWW page
- Setup CVS repository to allow several users to work on the actual GEANT code together

EIC detector simulation

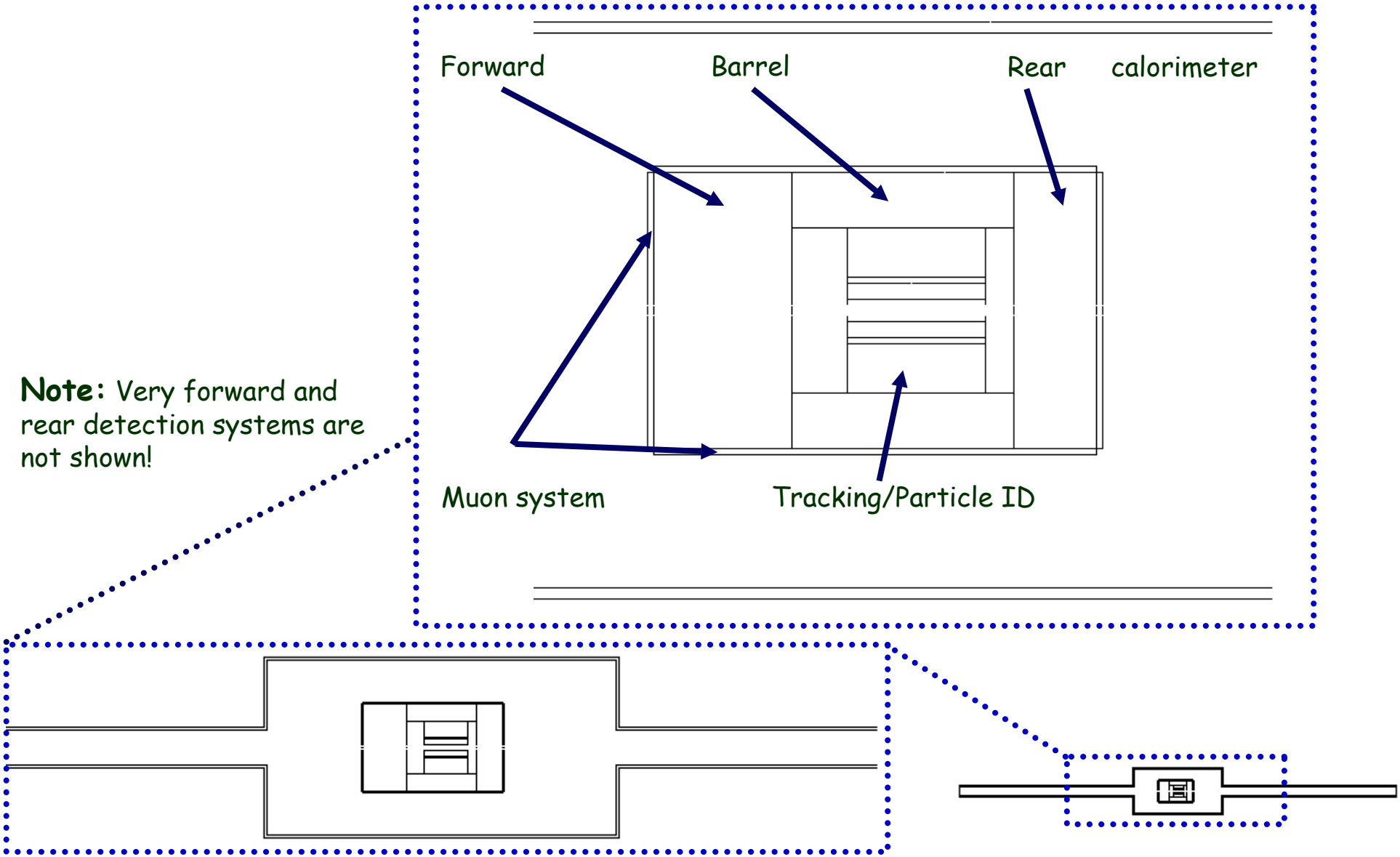

Note: Very forward and rear detection systems are not shown!

Roadmap toward a CDR for EIC

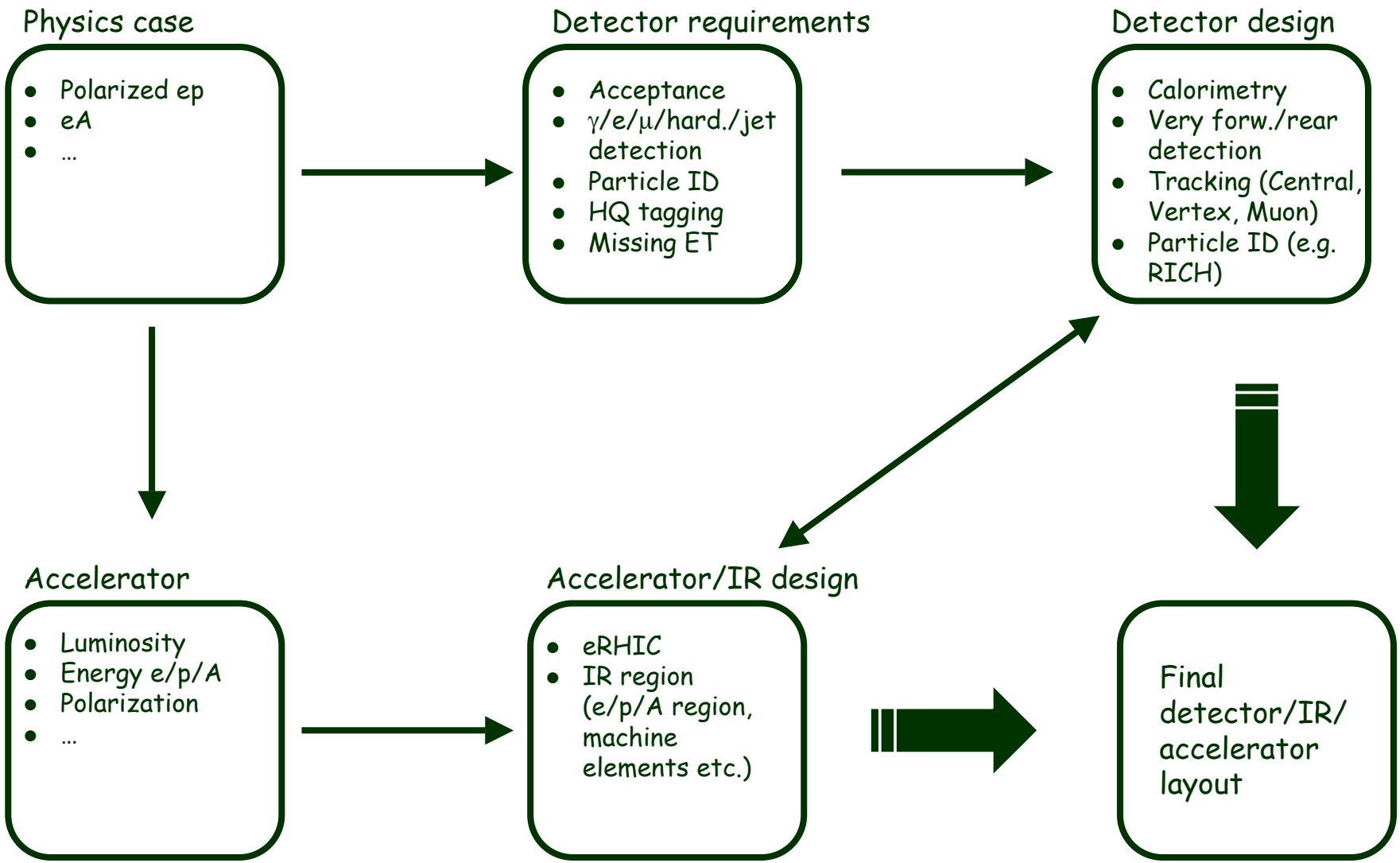

The 12 GeV Upgrade at Jefferson Lab

R. Ent

Jefferson Lab, 12000 Jefferson Avenue, Newport News, VA 23606

I INTRODUCTION

There has been a remarkable fruitful evolution of our picture of the behavior of strongly interacting matter during the almost two decades that have passed since the parameters of the Continuous Electron Beam Accelerator Facility (CEBAF) at Jefferson Lab were defined. These advances have revealed important new experimental questions best addressed by a CEBAF-class machine at higher energy. Fortunately, favorable technical developments coupled with foresight in the design of the facility make it feasible to triple (double) CEBAF's design (achieved) beam energy from 4 (6) GeV to 12 GeV, in a cost-effective manner: the Upgrade can be realized for about 15% of the cost of the initial facility. This Upgrade would enable the worldwide community to greatly expand its physics horizons.

In addition to in general improving the figure of merit and momentum transfer range of the present Jefferson Lab physics program, raising the energy of the accelerator to 12 GeV opens up two main new areas of physics:

- It allows direct exploration of the quark-gluon structure of hadrons and nuclei in the "valence quark region". It is known that inclusive electron scattering at the high momentum and energy transfers available at 12 GeV is governed by elementary interactions with quarks and, indirectly, gluons. The original CEBAF energy is not adequate to study this critical region, while with continuous 12 GeV beams one can cleanly access the entire "valence quark region" and exploit the newly discovered Generalized Parton Distributions. In addition, a 12-GeV Jefferson Lab can essentially complete the studies of the transition from hadronic to quark-gluon degrees of freedom.

- It allows crossing the threshold above which the origins of quark confinement can be investigated. Specifically, 12 GeV will enable the production of certain "exotic" mesons. Whereas in the QCD region of asymptotic freedom ample evidence for the role of gluons exist through the observation of gluon jets, direct evidence for the role of gluons in the QCD confinement region is still missing. Spectroscopy of light "exotic" mesons, with glue as essential part of their valence structure, would provide such essential evidence. In addition, with 12 GeV one crosses the threshold for charm production.

The nearly final draft of the recent NSAC long-range plan states the 12 GeV Upgrade as one of three construction recommendations: "We strongly recommend the upgrade of CEBAF at Jefferson Laboratory to 12 GeV as soon as possible. The 12 GeV upgrade of the unique CEBAF facility is critical for our continued leadership in the experimental study of hadronic matter."

Presently, the status of the 12 GeV Upgrade is that the laboratory is waiting for "CD-0", a "Statement of Mission Need", approval by DOE. Conceptual Design Reports for both accelerator upgrades and the various experimental upgrades (Halls A, B, C, and D) are anticipated by September 15, 2002.

II THE QUARK-GLUON WAVE FUNCTIONS OF THE NUCLEAR BUILDING BLOCKS

The classic program of deep inelastic scattering experiments began in the 1970's at SLAC. These measurements led to the experimental confirmation of the existence of quarks and to precision tests of the fledgling theory of QCD, eventually confirming it as the fundamental theory governing all strongly interacting (i.e. nuclear) matter. Even though such experiments have been vigorously pursued for over 30 years, it is remarkable that there has never been an experimental facility that could measure the deep inelastic cross sections in a kinematic region where the three basic ("valence") quarks of the proton and neutron dominate the wave function. This requires a high-luminosity facility, with not too high a beam energy, as the probability of finding a quark in the high Bjorken-x valence quark region is small, and becomes smaller and smaller as $x \to 1$, whereas furthermore the deep inelastic cross section decreases like Q^{-2}. In contrast, in the $x \to 1$ limit, rigorous predictions are available. The 12 GeV Upgrade will allow to map out the quark distribution functions in this "clean" valence quark region with high precision, and have a profound impact on our understanding of the structure of proton and neutron.

Where inclusive measurements probe the longitudinal momentum distribution of quarks inside the nucleon, the discovery of Generalized Parton Distributions (GPD's) and their connection to certain totally exclusive cross sections has made it possible in principle to rigorously map out the complete nucleon wave functions themselves. These GPD's, accessible through both exclusive measurements of photons and mesons, and exclusive form factor measurements, probe the full nucleon wave function at the amplitude level, and, for example, will shed light on the distribution of the transverse momentum of quarks, constrain the contribution of the quark angular momentum to the spin of the proton, and measure quark-quark correlations. Unfortunately, a lot has to be learned about the proper kinematic range over which measurements must be done to properly separate information on these GPD's from more mundane reaction mechanism effects. The general expectation exists that the 12 GeV Upgrade will allow a clean program of the investigation of GPD's through the process of Deeply-Virtual Compton Scattering, mainly empha-

sizing the region of $x > 0.1$. In addition, exploratory measurements can be done to investigate the proper kinematic range to access GPD's in deep exclusive meson electroproduction.

III DISCOVERING AND STUDYING THE EXOTIC MESONS

The phenomenon of confinement is one of the basic properties of QCD that drives all of nuclear physics, from the mass of the proton and other nuclear building blocks to the NN interaction. The naive model for confinement is that the quarks are "tied together" by gluon strings. Recent numerical simulations of QCD demonstrate that this conjecture is essentially correct. The ideal experimental test of confinement would be to study these gluon strings directly by anchoring a quark and antiquark several fermis apart and exciting the gluonic strings, causing an excitation spectrum of "exotic" mesons.

A substantial goal of the 12 GeV Upgrade is to search for such exotic mesons in the light-quark sector. Calculations indicate that the 12 GeV Upgrade provides exactly the right energy for such a search. The photon probe is considered to be optimal due to its virtual $q\bar{q}$ structure: the quarks spins are aligned, the right configuration to effectively excite the exotic mesons.

Tantalizing indications for gluonic excitations have emerged from searches with, e.g., π and K probes, but the evidence is far from solid, and the details needed for a full understanding of confinement are missing. The data in hand on the photoproduction of light mesons are sparse and essentially nonexistent.

When the spectrum and decay modes of such gluonic excitations have been mapped out experimentally, a giant step forward would have been made in our understanding of confinement.

IV EXPERIMENTAL EQUIPMENT FOR THE 12 GEV UPGRADE

Here, the upgrades and additions to the equipment in the present experimental halls, and a new experimental "Hall D", is summarized. The equipment makes efficient use of much of the existing base equipment from the original CEBAF complement.

In Hall A, both high-resolution spectrometers are retained, and are complemented by the addition of a medium-acceptance spectrometer (MAD, Medium-Acceptance Device), mainly emphasizing the study of the region of valence quark structure in Deep Inelastic Scattering.

In Hall B, the CLAS detector would be upgraded to enhance small angle detection and operation at a higher luminosity of 10^{35} cm^{-2}s^{-1}. CLAS would focus on studies

of the Generalized Parton Distributions, mainly through Deeply-Virtual Compton Scattering.

Hall C would add a new high-momentum spectrometer (SHMS, the Super-High Momentum Spectrometer), with maximum momentum close to the design beam energy. The combination of the existing High Momentum Spectrometer (HMS) and this new SHMS would be optimized for small-angle, high-momentum transfer, (deep) exclusive reactions, up to $Q^2 \approx 15$ (GeV/c)^2.

Lastly, Hall D would emphasize photoproduction of exotic mesons. This new Hall would use coherent bremstrahlung to provide 9 GeV high-intensity, polarized, real photon beams, in conjunction with a solenoid/detector system to provide nearly hermetic acceptance for both charged particles and photons.

V THE ELECTRON-LIGH ION COLLIDER (ELIC) OPTION AT JLAB

Investigations are underway for an electron-light ion collider (ELIC) capability at Jefferson Lab. The present design has substantial overlap with the previously suggested EIC and/or E-RHIC options. The main design idea is that

- The CEBAF accelarator is upgraded to have all superconducting cavities replaced by the same 7-cell cavity, 18 MV/m SRF cavities used for the 12 GeV Upgrade plans. This would give a 5 GeV (or less) electron beam energy for one turn around.
- An energy recovery linac, similar as used in the Jefferson Lab Free Electron Laser, is used for energy recovery to minimize RF power and beam dump requirements.
- To minimize the current demands from the polarized source, several electron bunches are injected in a "figure-8" circulator ring.
- The same "figure-8" storage ring is used for injection of 400 MeV light ions (H, D, ^{3}He), that will be ramped up to a maximum energy of 50 GeV.
- Flexible spin manipulations, using Siberian Snakes and Solenoids are used to align the spins at 4 independent interaction regions.
- The luminosity is optimized, to at least 10^{34} cm^{-2}s^{-1}, by a combination of this circulator ring and "crab-crossing".
- Electrons are extracted from the circulator ring before the emittance has increased too much, and steered into the energy-recovering linear accelerator.

One very attractive feature of the present design is that it can simultaneously be operated with a high-luminosity ($\approx 10^{38}$ cm^{-2}s^{-1}) fixed target program, with 25 GeV external beams. Obviously, this collider option would also be compatible with the present 12 GeV Upgrade plans.

The Future of Lepton-Nucleon Scattering

Summary of the Durham (HERA-3) Workshop 12/2001 +)

Max Klein

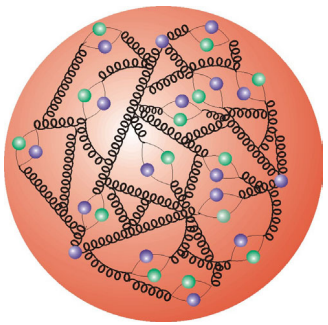

+) http://hep.ph.liv.ac.uk/~green

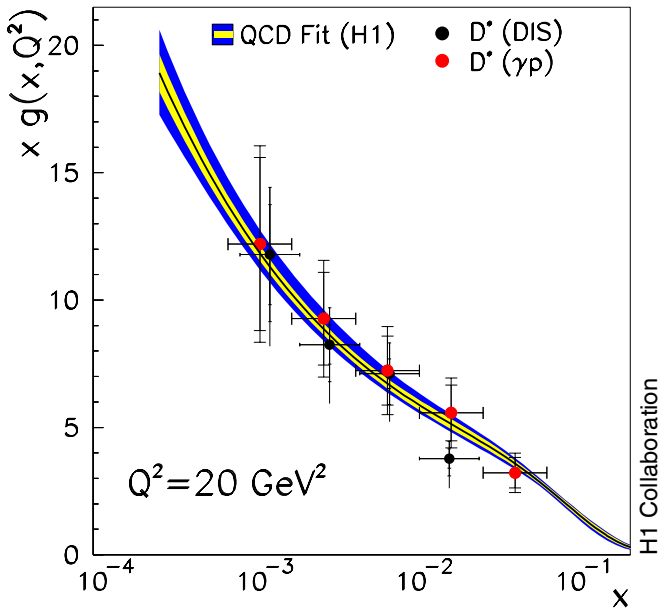

HERA2

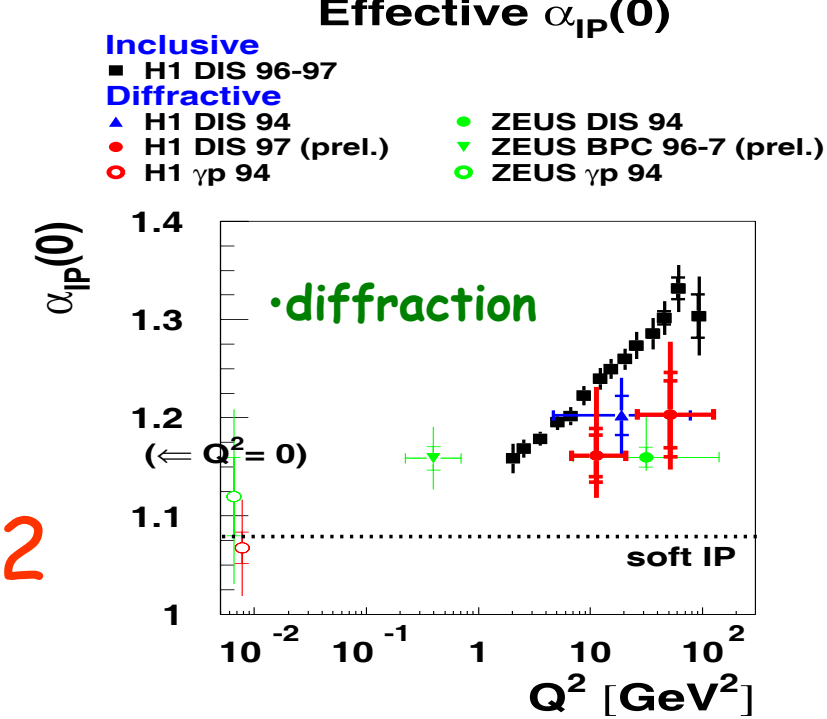

precision tests of QCD to h.o.

- gluons and quarks, u/d
- most accurate alphas
- hi Q2,x structure functions
- jets
- vector mesons
- longitudinal structure function
- charm

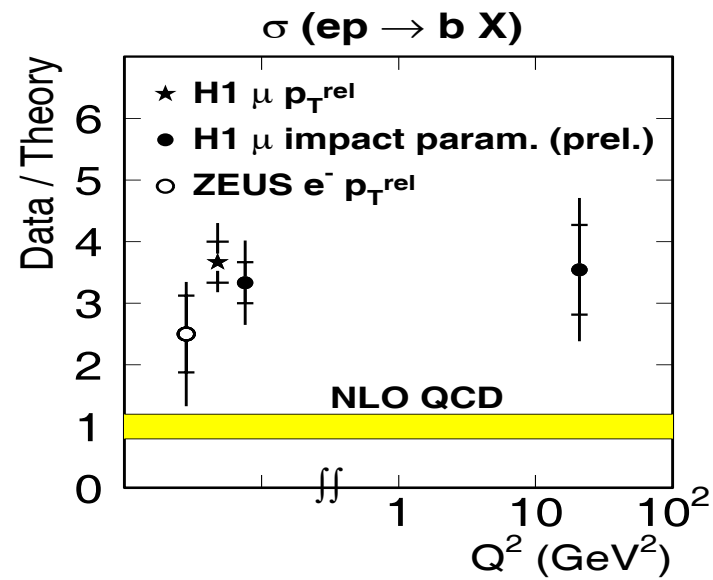

•the bottom embarrasement

HERA2

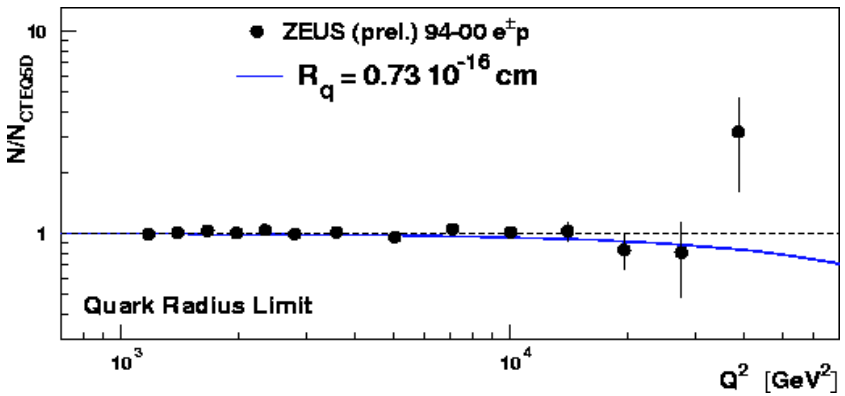

competetive searches beyond the SM

- contact interactions
- right handed charged currents
- R parity violating SUSY
- LR symmetry
- Technicolour
- different surprises

•isolated leptons

$$e^+p \to \mu^+X$$

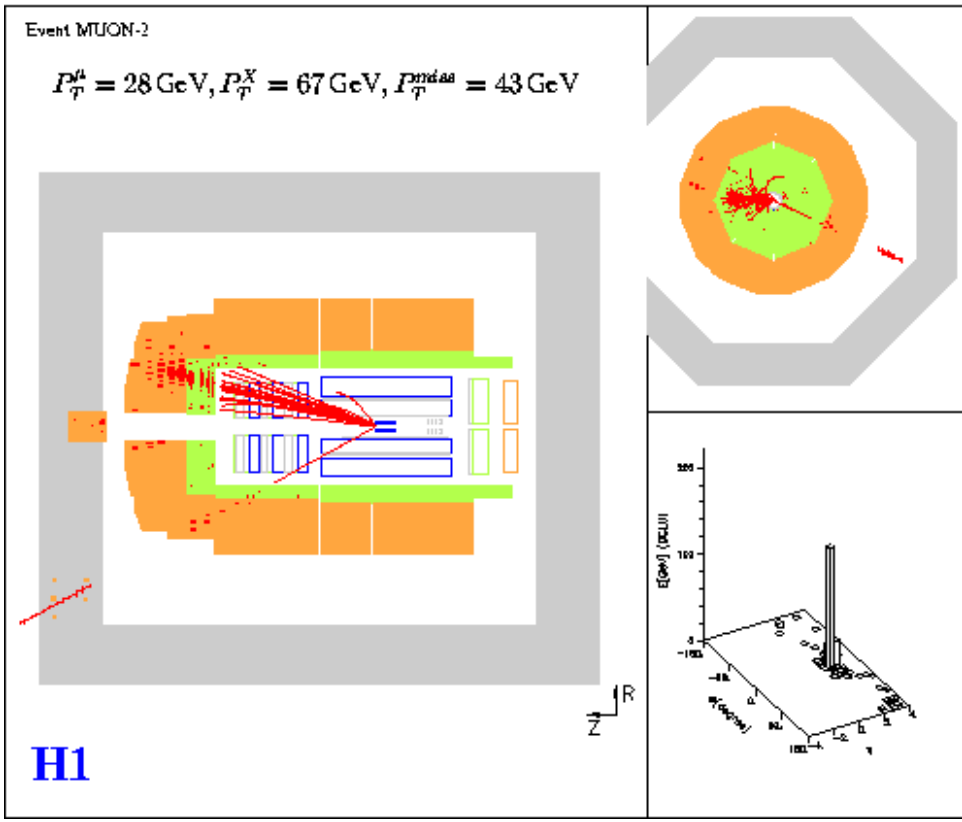

eA scattering

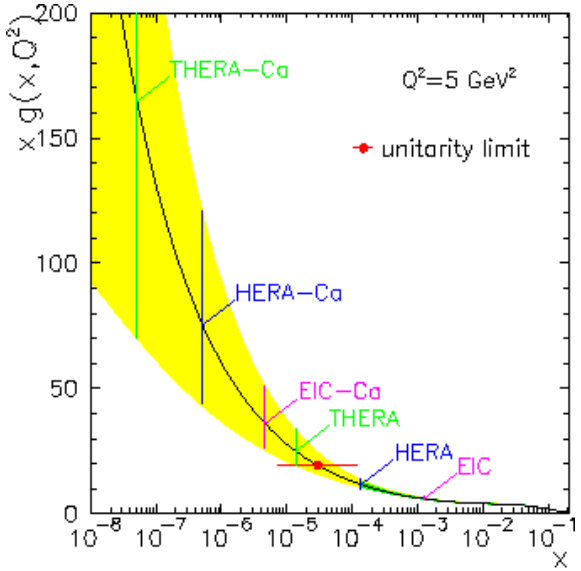

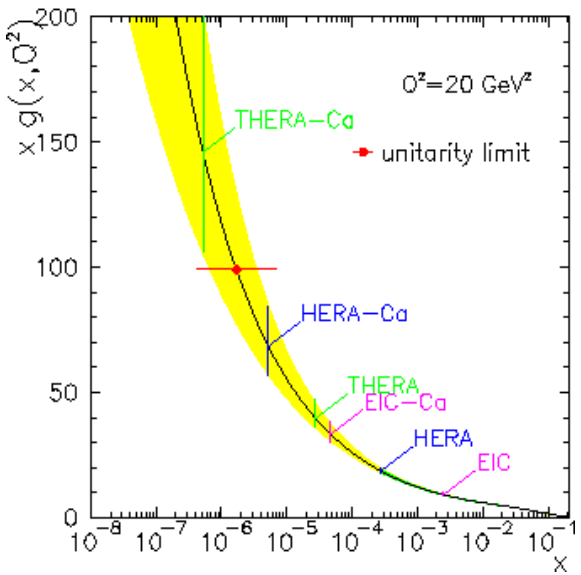

gluon density amplified with $A^{1/3}$

- low x - field strength high, large Q2 – coupling weak
  → unitarisation effects
  → new phase of matter
- deconfinement
- nuclear parton distributions
- bj → black body limit
  - $F_2 \propto Q^2 \ln(\delta / x)$
  - large diffractive cross section
  - no colour transparency
  - $\sigma(J/\psi)[A]_x$
- $d, \vec{d}, {}^{16}O, {}^{40}Ca$ with $10\,pb^{-1}/A$

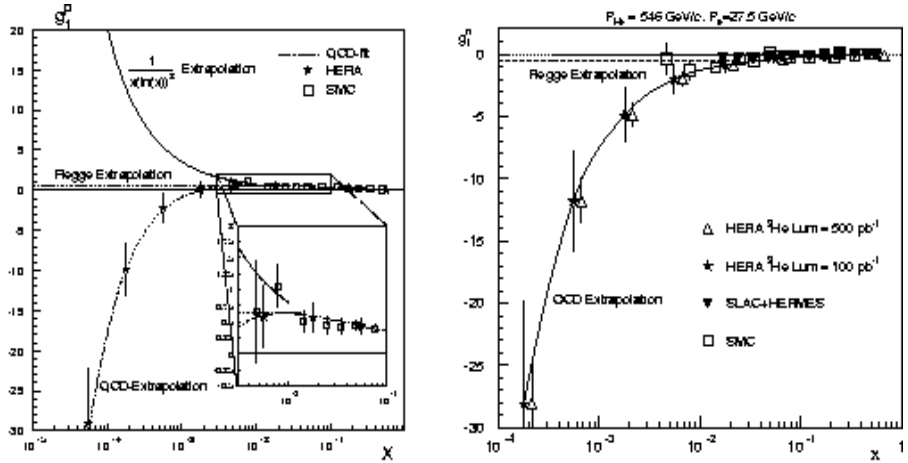

polarised eN

$$A_1 \approx 2x \cdot g_1 / F_2$$

low x – small asymmetries, high rate (H1 frontend electronics?)

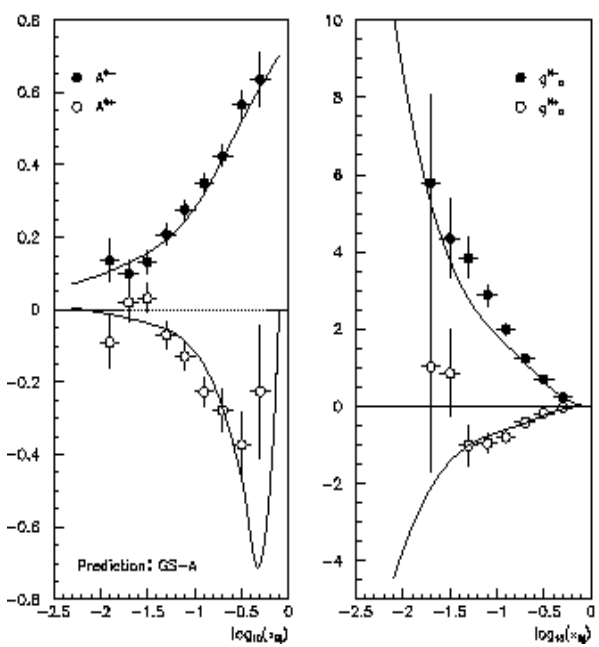

high Q2 – large asymmetries

- parton distributions
- heavy flavour
- diffraction
- charged currents
- exotics

$$A^{W\pm} \approx g_5^{W\pm} / F_1^{W\pm}$$

•Luminosity + systematic error control

HERA III

Polarized protons in HERA

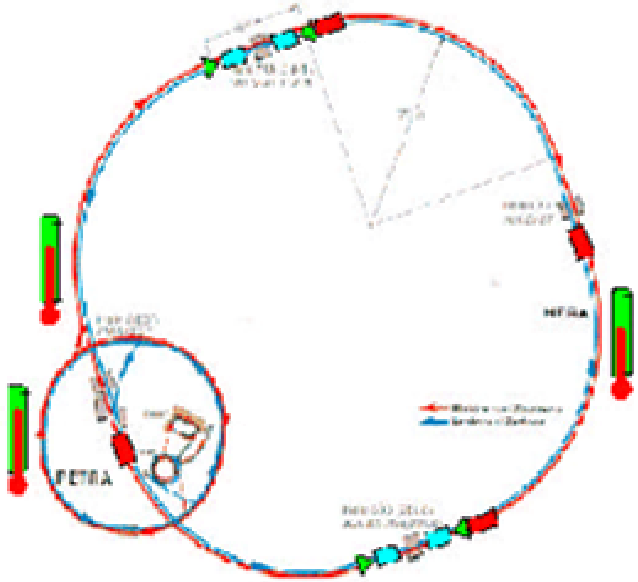

- Polarimeters
- Flattening Snakes
- Spin rotators
- At least 4 Siberian Snakes

OPPIS 20 mA, pol 80% TRIUMF → high L in reach

- Polarized protons (30MEuro)
- Polarized deuterons
- Electron precooling and cooling
- Ion acceleration (53MEuro)

$$L_A = L_p \cdot \frac{1}{A} = 7 \cdot 10^{31} \cdot \frac{1}{A}$$

- Pulse stretcher for TESLA
- Collisions with TESLA (120ME.)

$$L_{ep} = 1.6 \cdot 10^{31}$$

Georg.Hoffstaetter@DESY.de

Spin – fixed target - HERMES [+)]

- HERMES run II will give

  - first determination of δu
  - first high accurate DVCS - beam spin asymmetry
  - first measurements of DVCS – beam charge asymmetry

- HERMES run III could give

  - first data on flavour decomposition of transversity
  - exclusive reactions with (transversely) polarised target
  - →DVCS
  - →vector and pseudoscalar meson production

→ a few years running programme beyond 2006

+) D.Ryckbosch at Durham

next steps

- February 02: EIC workshop at BNL, NY
- May or June 02: HERA3 meeting at DESY
- December 02: Draft Letters of Intent
- May 03: LoI for future experimentation at HERA
  → presented to DESY Physics Research Committee
- November 03: Proposals submitted to DESY
- 2005: Proposals for the EIC
- 2007: start of HERA3 programme

current discussions focus around detectors and individuals from HERMES, ZEUS and H1

vital: close collaboration with HERA machine experts

Summary

- Lepton-nucleon scattering at HERA in this century: high precision

- HERA2 – precision QCD, electroweak physics and searches

- HERA3

  Neutron structure at low x and large Q2,x?
  Confinement and the origin of mass?
  QCD, when the coupling is small and the density high?
  Spin structure of the nucleon?

- Proposals due end of 2003, both for fixed target and collider
- may rely on existing detectors, ingenuitive upgrades (tagging, low Q2), on a luminous HERA operation and consider the EIC potential

Deep inelastic lN scattering has a future if we believe in it

DESY 01-123F vol. 4
DESY-LC-REV-2001-062
December 2001

Physics and Experimentation at a Linear Electron–Positron Collider

Volume 4: The THERA Book. Electron–Proton Scattering at $\sqrt{s} \sim 1$ TeV

TESLA

250-800 GeV e →

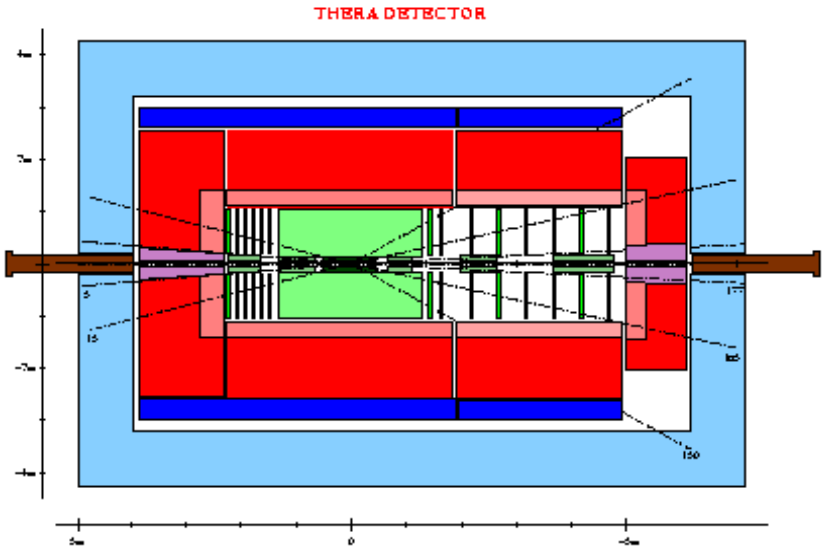

HERA

← p 350-1000 GeV

Editors: U. Katz, M. Klein, A. Levy and S. Schlenstedt

THERA

http://www.ifh.de/thera

ISSN 0418-9833

Workshops

- its time to conclude

- DESY directorate asks for proposals by end of 2003

- Physics
- Ressources
- TESLA
- synch.radiation

References

[1] http://www.desy.de/heraea/
"Physics with HERA as Electron-Nucleus Collider", Ed.s G. Ingelman and M. Strikman, May 1999;
http://www.desy.de/ heraws96
"Future Physics at HERA", Proc. Workshop, DESY 1996/97, Ed.s G. Ingelman, A. De Roeck and R. Klanner, pp 854-1092.

[2] "Prospects for Spin Physics", Proc. Workshop, Ed.s J. Blümlein and W.D. Nowak, DESY 95-200, Zeuthen 1995;
"Physics with polarized protons at HERA", Proc. Workshop, Ed.s A. De Roeck and T. Gehrmann, DESY-PROC-1998-01, Hamburg 1997;
http://www-h1.desy.de/ radel/spin99/procsent.html, "Polarized Protons at High Energies - Accelerator Challenges and Physics Opportunities", Proc. Workshop, Ed.s A. De Roeck, D. Barber and G. Rädel, DESY-PROC-1999-03 (1999), Hamburg 1999;
"The Spin Structure of the Proton and Polarized Collider Physics", S.D. Bass and A. De Roeck, Nucl. Phys. Proc. Suppl. 105 1-27 (2002);
"Transverse Spin Physics", Workshop transparencies, DESY-ZEUTHEN-01-01, 374 pp, Zeuthen 2001.

[3] http://www.phenix.bnl.gov/WWW/publish/abhay/Home_of_EIC
"The EIC White Book", R. Holt et al., BNL, March 2001.

[4] http://www-zeuthen.desy.de/thera
"THERA: Electron-Proton Scattering at $\sqrt{s} \sim 1$ TeV", TESLA TDR, DESY 2001-011, ECFA 2001-209, part VI, Appendices, pp. 99-160, Ed.s R. Klanner, U. Katz, M. Klein and A. Levy, March 2001;
"The THERA Book", Ed.s U. Katz, M. Klein, A. Levy and S. Schlenstedt, DESY-01-123, DESY-01-123-F, LC-REV-2001-062, DESY-LC-REV-2001-062, Dec 2001, 415 pp.

[5] "TESLA-N: Electron Scattering with Polarised Targets at TESLA", TESLA TDR, DESY 2001-011, ECFA 2001-209, part VI, Appendices, pp. 161-190, Ed.s R. Kaiser and W.D. Nowak.

[6] "ELFE: The Electron Laboratory for Europe", TESLA TDR, DESY 2001-011, ECFA 2001-209, part VI, Appendices, pp. 191-207, Ed.s R. Klanner, E. DeSanctis, J.-M. Laget and K. Rith.

TESLA-N Plans

V. Korotkov[1,2]
on behalf of the TESLA-N Study Group

[1] DESY Zeuthen, D-15738 Zeuthen, Germany
[2] IHEP, RU-142284 Protvino, Russia

The basic idea of TESLA-N [1] is to use one of the arms of the e^+e^- collider TESLA at DESY to realize collisions of longitudinally polarized electrons with a solid-state fixed target that may be either longitudinally or transversely polarized. The electrons for TESLA-N will be accelerated together with the positrons in the north arm of the TESLA main accelerator. This 'opposite charge option' was chosen to be able to realize a separation between the beam for the eN-experiment and the main beam by a static magnet system.

The given TESLA duty cycle of 0.5 % in conjunction with the basic machine frequency of 1.3 GHz has most severe consequences for the proposed experiment. The time structure as foreseen for the e^+e^- experiment, i.e. one bunch of 20 ps length crossing the target every 337 ns, would result in an unacceptable event rate within these 20 ps. To minimize the number of multiple events while maximizing the luminosity, it is foreseen to fill every bucket of the bunch train (one every 0.77 ns), while limiting the beam current to 20 nA. This corresponds to 20k electrons per bunch and to 6.2 million bunches per second crossing the TESLA-N target.

To reach the required high luminosity a polarized solid state target of about 1 g/cm^2 areal density will be chosen. The polarized target will consist of a ^{4}He evaporator cryostat, a 5 T Helmholtz-type magnet and a 140 GHz microwave system for permanent dynamic nuclear polarization. Presently, the target materials NH_3 ($P_T = 0.8$, f = 0.176) and ^{6}LiD ($P_T = 0.3$, f = 0.44) appear as the best choices to study electron scattering off polarized protons and deuterons, respectively.

Assuming a combined up-time of accelerator and experiment of 0.33 in conjunction with an efficiency of the experiment of 0.75, results in a maximum achievable integrated luminosity for TESLA-N of 600 fb^{-1} per effective year. All physics projections are based on an integrated luminosity of 100 fb^{-1}. This represents a conservative estimate for *one* year of data taking.

A quark of a given flavor in the nucleon is characterized by three twist-two quark distributions: the number density distribution $q(x)$, the helicity distribution $\Delta q(x)$, and the transversity distribution $\delta q(x)$, which have never been measured yet. The first moments of $\delta q(x, Q^2) - \delta\bar{q}(x, Q^2)$ are known as quark tensor charges $\delta q(Q^2)$.

The transversity distributions $\delta q(x)$ are not accessible in inclusive DIS, because they are chiral-odd and only occur in combinations with other chiral-odd objects. An observation of the Collins effect [2] offers the experimentally most direct access to $\delta q(x)$. Recent HERMES measurements [3] indicate that the polarized fragmentation function $H_1^{\perp(1)}(z)$ may be quite sizeable. Measurements

of azimuthal asymmetries [4] in the production of positive and negative pions on transversely polarized proton and deuteron targets ($A_{p,d}^{\pi^+,\pi^-}$) allow, under reasonable assumptions, the simultaneous reconstruction of the shapes of the unknown functions $\delta q(x, Q^2)$ and $H_1^{\perp(1)}(z)/D_1(z)$. The relative normalization can be fixed with a further assumption [5]. A broad range of $0.003 < x < 0.7$ can be accessed in conjunction with $1 < Q^2 < 100$ GeV^2. Projections for the accuracies of a measurement of the u- and d-quark tensor charges are ± 0.01 and ± 0.02 at the scale of 1 GeV^2, respectively.

The polarized gluon distribution function $\Delta G(x)$ in the nucleon is essentially unknown as of today. There is a variety of approaches to determine $\Delta G(x)$ from polarized eN collisions. The direct methods rely on the photon-gluon fusion subprocess measurement (see e.g. ref. [6]). Indirectly, the NLO Q^2-evolution of the structure function $g_1(x, Q^2)$ is sensitive to $\Delta G(x, Q^2)$. No NLO QCD fit to the existing data has been able to deliver a statistically convincing determination of the first moment ΔG yet. A precision measurement of $g_1(x, Q^2)$ at TESLA-N will dramatically enlarge the accuracy and the kinematic range.

The physics potential of the TESLA-N project is demonstrated with two examples showing that an accurate measurement of the x- and Q^2-dependence of both the helicity and the transversity quark distributions would be possible. Complemented by results on the polarized gluon distribution most of the components of the angular momentum structure of the nucleon will be determined with high precision. Other important possible measurements include:
- precise measurement of the longitudinal quark spin distributions $\Delta q(x)$;
- quark fragmentation functions $D_q^h(z)$;
- unpolarized gluon distribution function $G(x)$ at high x;
- specific deuteron structure functions $b_{1,2}(x)$ and $\Delta(x)$;
- the polarized structure function $g_2(x)$;
- Deeply Virtual Compton Scattering and other hard exclusive reactions.

Hence, the measurements envisaged for TESLA-N will constitute one of the most comprehensive and precise investigations of the predictive power of QCD in the polarized sector. The possibilities of using unpolarized targets and of experiments with a real photon beam turn TESLA-N into a versatile next-generation facility at the intersection of particle and nuclear physics.

References

[1] TESLA-N Study Group, M. Anselmino et al., DESY 00-160, TPR-00-20, hep-ph/0011299; TESLA Technical Design Report, DESY 2001-011, Part VI, Appendices, TESLA-N, ed.s R. Kaiser, W.-D. Nowak.

[2] J.C. Collins, *Nucl. Phys.* **B396**, 161 (1993).

[3] HERMES Coll., A. Airapetian et al., *Phys. Rev. Lett.* **80**, 4047 (2000).

[4] A.M. Kotzinian, P.J. Mulders, *Phys. Lett.* **B406**, 373 (1997).

[5] V.A. Korotkov, W.-D. Nowak, K.A. Oganessyan, *Eur.Phys. J.* **C18**, 639 (2001)

[6] HERMES Coll., A. Airapetian et al., *Phys. Rev. Lett.* **84**, 2584 (2000)

A POLARIZED FIXED-TARGET EXPERIMENT AT TESLA

Basic Idea: Use one arm of the TESLA collider for a polarized fixed target experiment in parallel to the collider experiments.

- ☐ electron arm cannot be used, because kicker magnets would not be fast enough to divert only part of the beam.
- ⇒ use positron arm for acceleration
- ⇒ static magnet system for separation from the positrons.
- ☐ the polarized beam constitutes only about 0.04% of the main current
- ⇒ additional energy consumption is negligible.

additionally needed for the experiment, besides target and spectrometer:

- ☐ polarized source and injector
- ☐ experimental hall and short tunnel
- ☐ beam dump

Civil Engineering

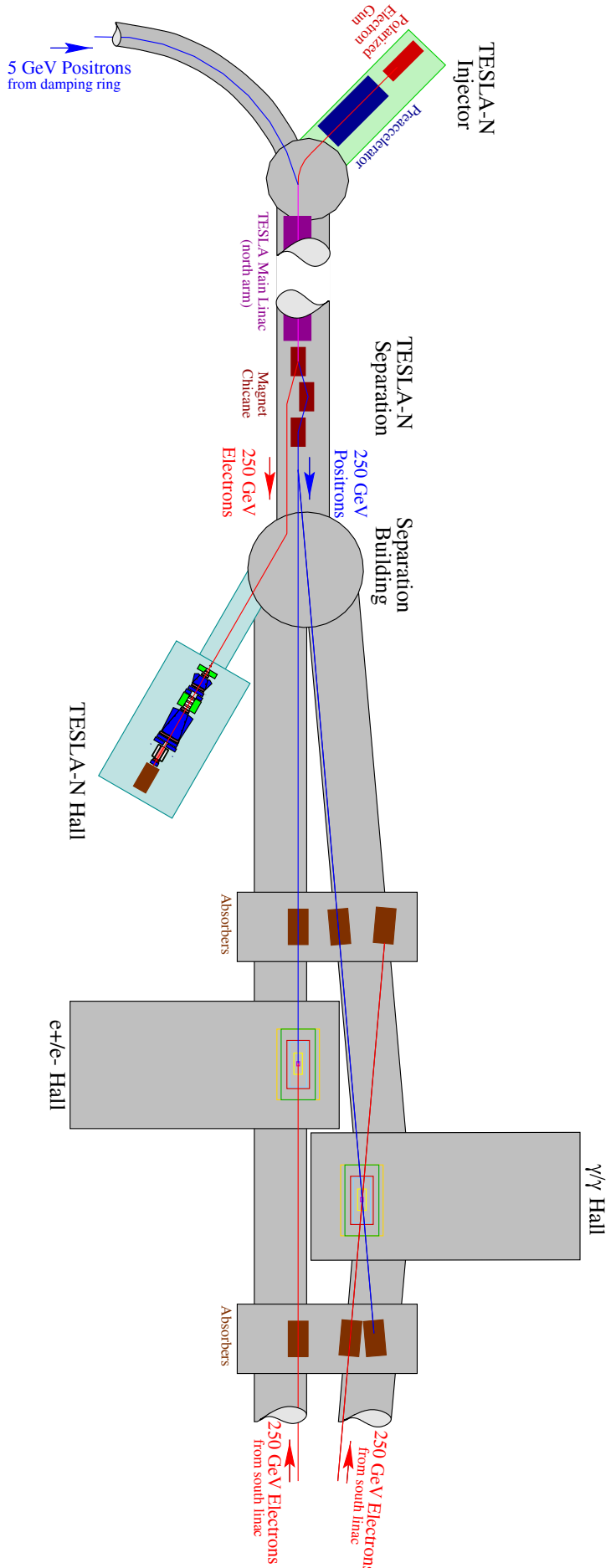

Luminosity

TESLA-N:

Luminosity L	$7.5 \cdot 10^{34}$ nucl/cm^2/s
$\int L\ dt$/s	7.5 nb^{-1}
$\int L\ dt$/e-bunch	12 mb^{-1}
$\int L\ dt$/eff. day	1.6 fb^{-1}
$\int L\ dt$/eff. year	600 fb^{-1}(upper limit)
c.m. energy	22.3 GeV

TESLA-N ansatz for efficiencies:

$$\varepsilon_{lumi} = \varepsilon_{up-time} \cdot \varepsilon_{exp} = 0.33 \cdot 0.75 = 0.25$$

conservative assumptions:

- only the time resolution of COMPASS can be reached (2 ns)
- only half of the maximum current is used to keep the multiple event fraction small

$\Rightarrow$ 100 fb^{-1} per year.

Luminosity in Comparison

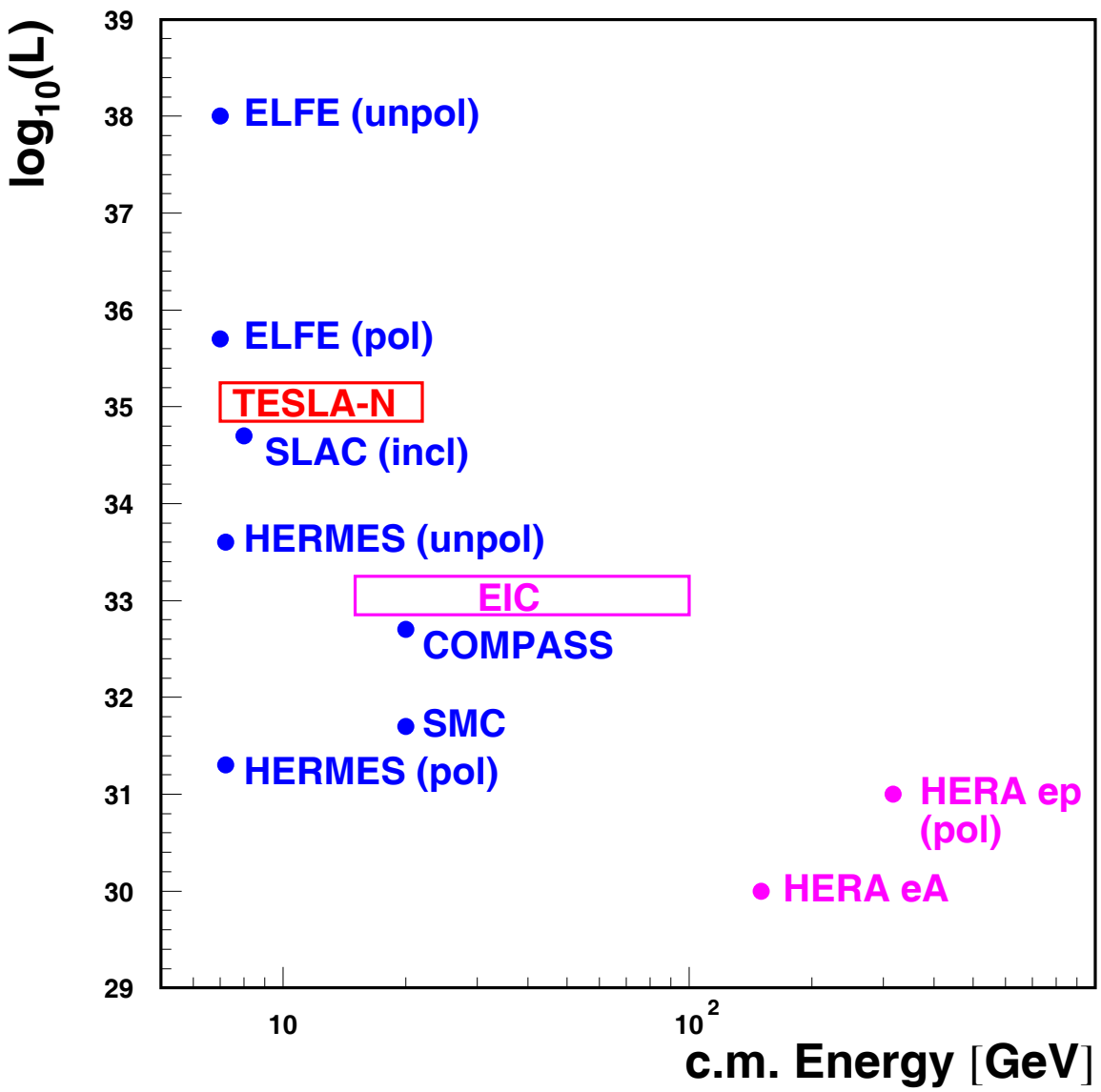

THE EFFECTIVE POLARIZED LUMINOSITY FOR A SOLID STATE FIXED TARGET EXPERIMENT IS A FACTOR OF ABOUT 25 LOWER THAN FOR POLARIZED EP-COLLIDERS.

Measurement of the Transverse Quark Spin Distributions

Measurement the asymmetries at $N_{(x,Q^2)}$ points in (x, Q^2) and at N_z points in z gives:

$4N_{(x,Q^2)} \cdot N_z$ measurements,

$4N_{(x,Q^2)}$ unknown values of $\delta q(x, Q^2)$ and

N_z unknown values of $\frac{H_1^{\perp(1)}}{D_1}(z)$

Two methods of $\delta q(x, Q_0^2)$ extraction:

- overconstrained set of coupled equations which one may resolve with a minimization procedure.
- define a parameter-dependent ansatz for every $\delta q(x, Q_0^2)$ and use the LO evolution to fit the unknown parameters and unknown values of $\frac{H_1^{\perp(1)}}{D_1}(z)$ to measured asymmetries, e.g.

$$\delta q_f(x, Q_0^2) = \eta_f x^{\alpha_f}(1-x)^{\beta_f}(1 + \gamma_f x + \rho_f \sqrt{x})$$

Projections for Transverse Spin Measurements

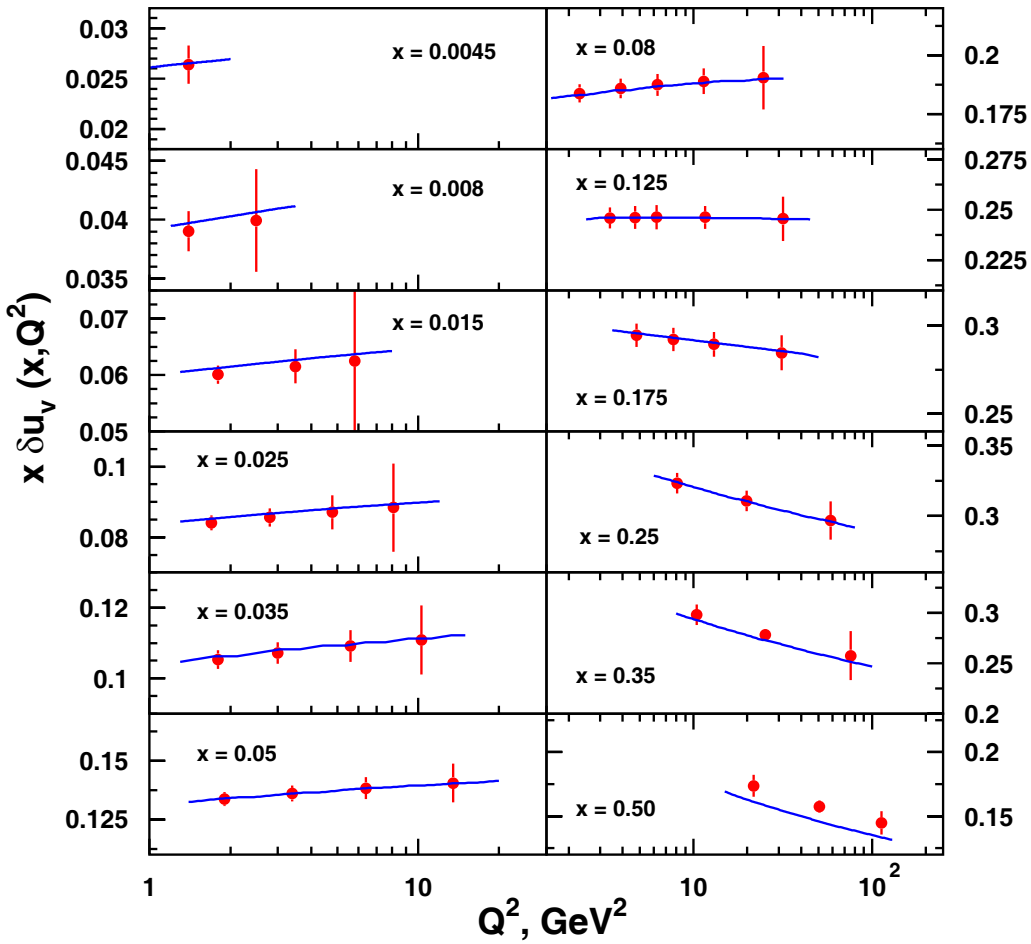

PROJECTION FOR THE VALENCE TRANSVERSE u-QUARK SPIN DISTRIBUTION BASED ON 100 fb^{-1} AND A MINIMUM DETECTOR ACCEPTANCE OF 5 mrad.

TENSOR CHARGE / TRANSVERSE SPIN OF THE NUCLEON: ('ALL-VALENCE OBJECT')

$$\delta\Sigma(Q^2) = \sum_q \int_0^1 dx(\delta q(x, Q^2) - \delta\bar{q}(x, Q^2))$$

PROJECTED ACCURACIES AT $Q^2 = 1$ GeV^2:

$$\delta u = 0.88 \pm 0.01, \; \delta d = -0.32 \pm 0.02$$

Two Meson Correlation with Transverse Spin

THE REACTION

$$ep^{\uparrow} \to e'\pi^+\pi^- X$$

OFFERS AN ALTERNATIVE POSSIBILITY TO MEASURE THE TRANSVERSE QUARK SPIN DISTRIBUTION FUNCTIONS.

THE INTERFERENCE EFFECT BETWEEN THE S- AND P-WAVES OF THE TWO-MESON SYSTEM ALLOWS THE QUARK'S POLARIZATION TO BE CARRIED THROUGH $\vec{k}_+ \times \vec{k}_- \cdot \vec{S}_\perp$ [Jaffe et al., 1998].

PROTON/DEUTERON TARGET:

$$\begin{aligned} \mathcal{A}^p &\sim (\delta u_v(x) - \tfrac{1}{4}\delta d_v(x)) \cdot \delta\hat{q}_I(z) \\ \mathcal{A}^d &\sim (\delta u_v(x) + \delta d_v(x)) \cdot \delta\hat{q}_I(z) \end{aligned}$$

THE UNKNOWN CHIRALLY ODD INTERFERENCE FRAGMENTATION FUNCTION $\delta\hat{q}_I(z)$ CAN IN PRINCIPLE BE MEASURED IN

$$e^+e^- \to (\pi^+\pi^- X)(\pi^+\pi^- X)$$

HAS BEEN CALCULATED IN A SPECTATOR MODEL

[M.Radici, R.Jakob, A.Bianconi 2001]

Projections for Two Pion Asymmetry Measurements

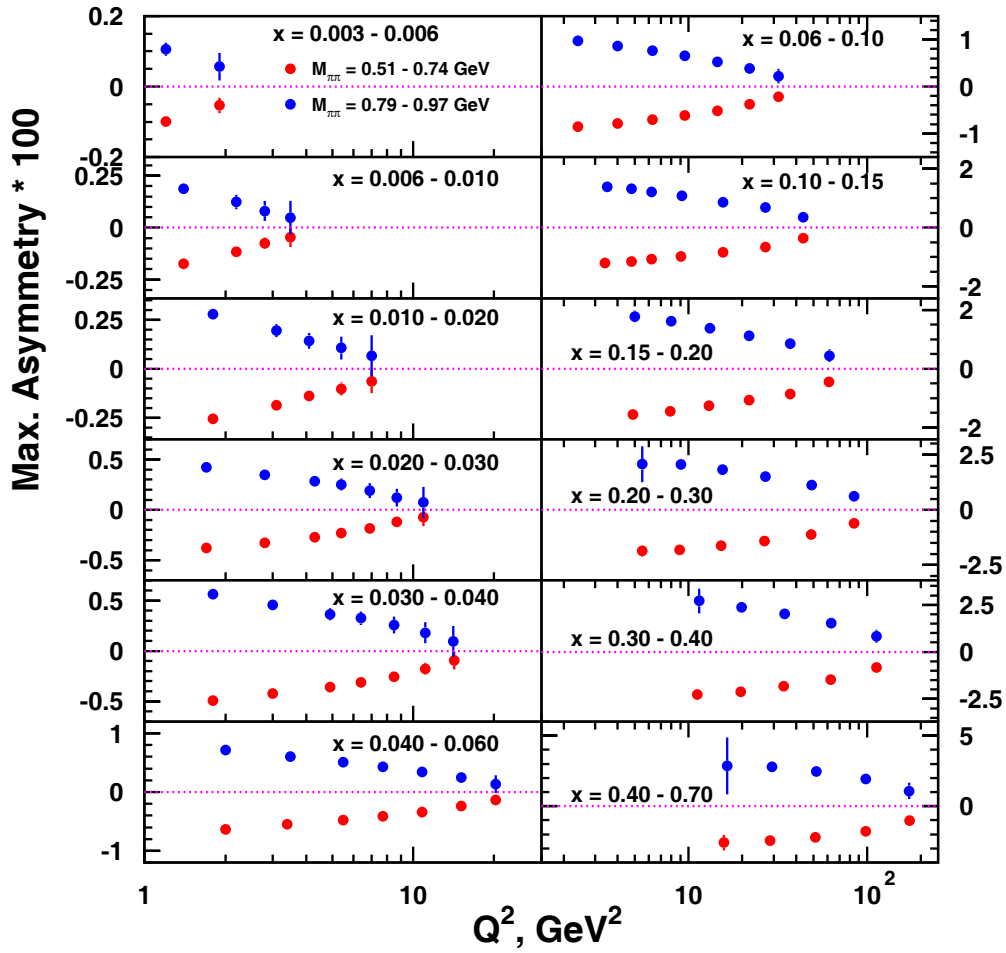

maximum asymmetry for the two-pion system as a function of x and Q^2 at TESLA-N with an integrated luminosity of 100 fb^{-1}. results are shown separately for two-pion mass regions.

Direct Measurement of $\Delta G(x)$

USE PAIRS OF $high - p_t$ HADRONS ORIGINATING FROM A LIGHT QUARK PAIR PRODUCED IN PHOTON-GLUON FUSION [COMPASS, HERMES]

$$A_{LL} \sim \frac{\Delta G(x)}{G(x)}$$

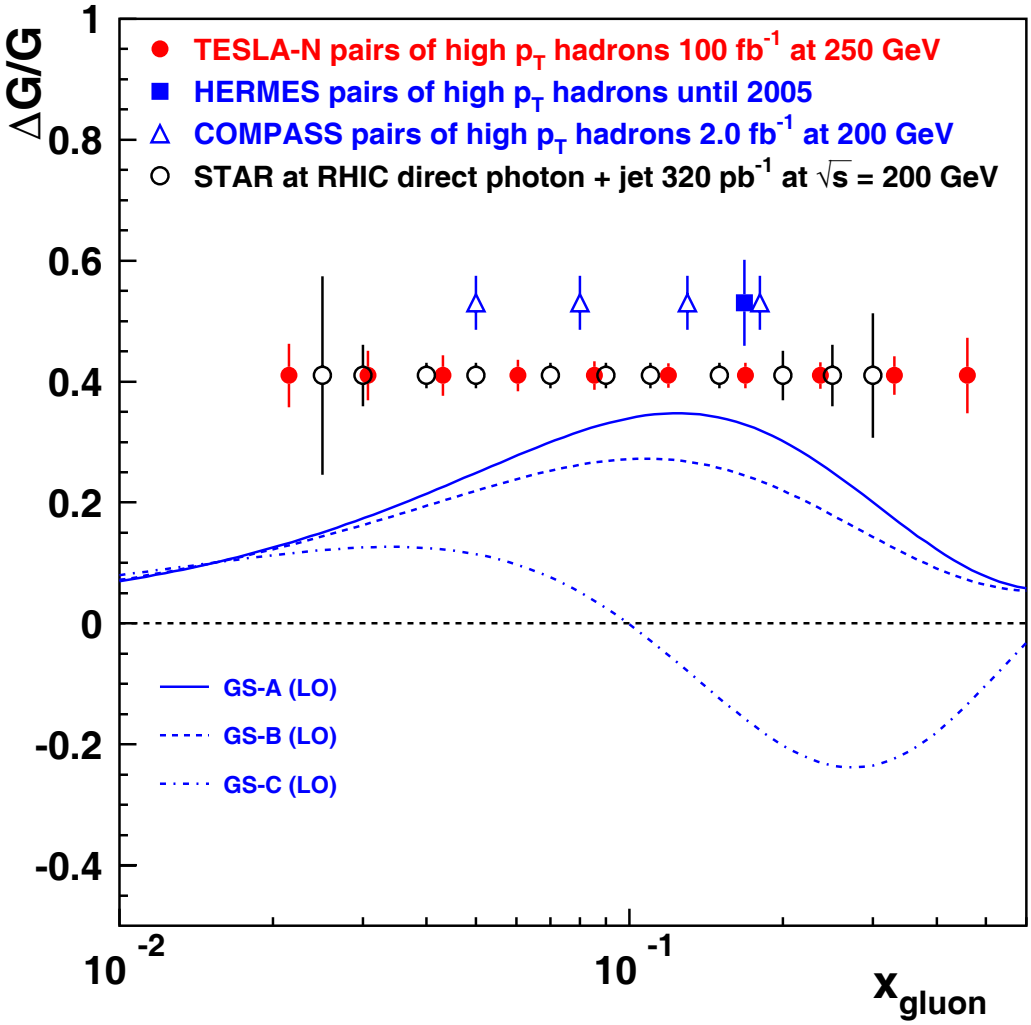

PROJECTED STATISTICAL ACCURACIES FOR DIRECT MEASUREMENTS OF $\Delta G(x)/G(x)$.

TESLA-N PROJECTIONS FOR 100 fb^{-1}.

$\Rightarrow$ BEST SENSITIVITY AT LARGE x

Inclusive Measurements/ Indirect Measurement of $\Delta G(x)$

QCD improved Quark Parton Model:

$$g_1^p = \frac{1}{2}\left(\frac{1}{n_f}\sum_{i=1}^{n_f} e_i^2\right)\left\{\delta C_{NS}\otimes\Delta q^{NS} + \delta C_S\otimes\Delta\Sigma + \delta C_G\otimes\Delta G\right\}$$

map out $g_1^p(x,Q^2)$ with high precision

$\Rightarrow$ indirect determination of $\Delta G(x)$ from QCD NLO fits to $g_1(x,Q^2)$:

	$\int dx\ \Delta G(x)$
existing data	0.43 ± 0.21
plus 100 fb^{-1} TESLA-N(p)	± 0.06
plus 100 fb^{-1} TESLA-N(d)	± 0.04

Indirect Determination of ΔG

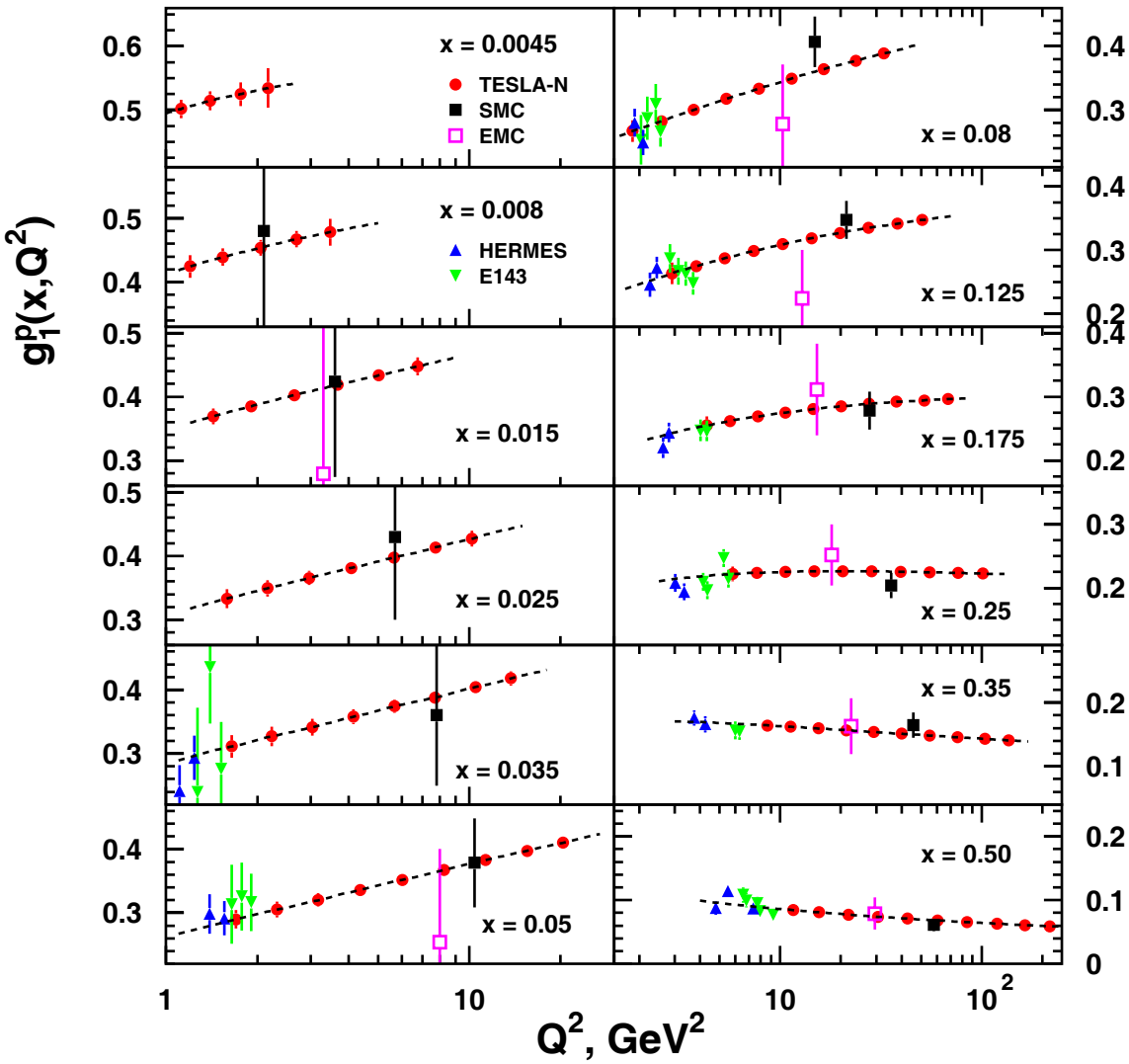

PROJECTED STATISTICAL ACCURACY FOR A MEASUREMENT OF $g_1^p(x, Q^2)$ AT TESLA-N, BASED ON A LUMINOSITY OF 100 fb^{-1} AND A MINIMUM DETECTOR ACCEPTANCE OF 5 mrad.

Further Physics Topics

- precise measurement of the longitudinal quark spin distributions
- precise measurement of $g_2(x, Q^2)$
- fragmentation functions (as input for B-factories and LHC)
- deeply virtual Compton scattering (DVCS)
- unpolarized gluon distribution function $G(x)$ at high x
- specific deuteron structure functions $b_{1,2}(x, Q^2)$ and $\Delta(x, Q^2)$
- nuclear effects in electron-nucleus scattering
- real photon scattering from nucleons and nuclei

most of these topics have not yet been studied in the context of TESLA-N.

Polarized Target

- ^{4}He evaporator cryostat guarantees temperature of 1 K for a heat load of 1 W

  ⇒ sufficient polarization only in a high magnetic field of 5 T

- target polarization must survive high radiation doses

  ⇒ deuteron material: ^{6}LiD,
  ($^6\mathrm{Li} \leftrightarrow \alpha + \mathrm{D}$)
  target dilution factor 0.44,
  target polarization 0.3

  ⇒ proton material: NH_3,
  target dilution factor 0.176,
  target polarization 0.8

- areal target density ~ 1 g/cm^2

Polarized Electron Beam

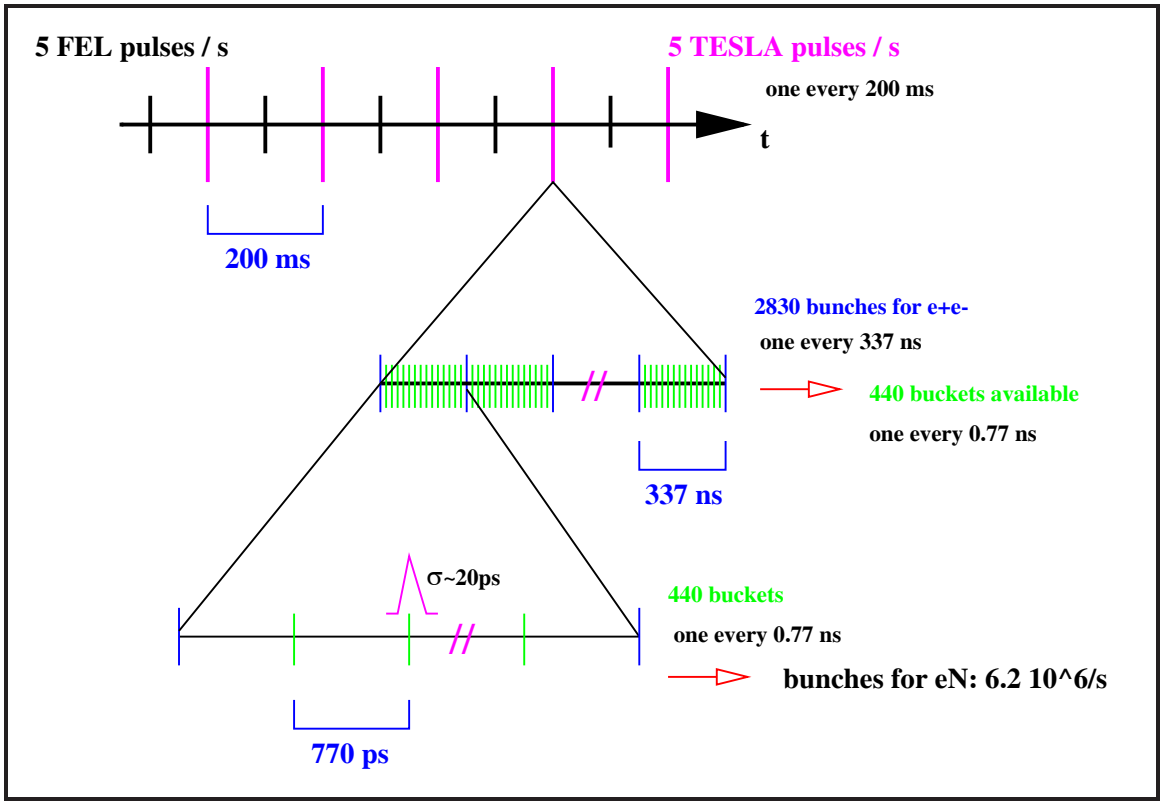

MACHINE FREQUENCY	1.3 GHz ⇒ ONE BUCKET EVERY 0.77 ns
eN-BUNCHES / S	$6.2 \cdot 10^6$
MAX. CURRENT	20 nA
# e^- / eN-BUNCH	20000

SOURCE	strained GaAs (SLAC TYPE)
ENERGY	250 - 500 GeV
POLARIZATION	$\geq$ 90 %

Polarized Electron Beam

A few improvements for eN-operation appear to be feasible:

1. A 10 Hz macropulse repetition rate could be used along the north arm. This would double all performance figures for e^-N-operation.
2. Two intermediate ejection points are technically feasible. This would allow the selection of any energy between 25 and 100 GeV in addition to the full energy of 250 GeV. This is especially important for a study of hard exclusive reactions.

Physics requirements suggest to study e^+N-interactions as well. It is technically unproblematic to install an additional (low intensity) positron source besides the separate electron source that is already required for e^-N operation. The duty cycle can not be better than 0.5% in this scenario. Presently no solution is known to obtain polarized positrons in such a configuration.

Heat Load on the Target due to the Beam

Maximum Heat Load of 1 W allowed.

Heating of the Target by

A. Energy loss processes (about 2 MeV per beam electron $\widehat{=}$ 45 mW at 20 nA)
B. Synchrotron Radiation (Total Power $\approx$ 13 W)
C. Bremsstrahlung (Total Power $\approx$ 67 W)

Energy of the photons from B and C converted to Heat in the Target by

- ☐ Photoelectric effect
- ☐ Compton Scattering
- ☐ Pair Production

energy range	Synch.rad. [mW]	Bremsstr. [mW]
$\epsilon < 10$ keV	0.02	0.003
10 keV $< \epsilon <$ 10 MeV	5.23	0.101
$\epsilon > 10$ MeV	1.65	0.063
total	6.90	0.167

$\Rightarrow$ Total Heat Load is about 50 mW much less than max. heat load of 1 W.

Detector Design Considerations

- beam energy 250 GeV

  ⇒ overall dimensions similar to COMPASS

- good momentum resolution

  ⇒ 3-stage spectrometer

  Stage 1 'Hadron Stage'
  Stage 2 'Electron Stage'
  Stage 3 'Forward Spectrometer'

- horizontal dipole fields, to direct 'sheet of flame' to the hall floor

  ⇒ two symmetric halves of the spectrometer: left and right

- semi-inclusive measurements:

  ⇒ PID as in HERMES:
  RICH, TRD, ECAL
  for Stage 1 and Stage 2,
  Stage 3 only with ECAL

Schematic Spectrometer Design

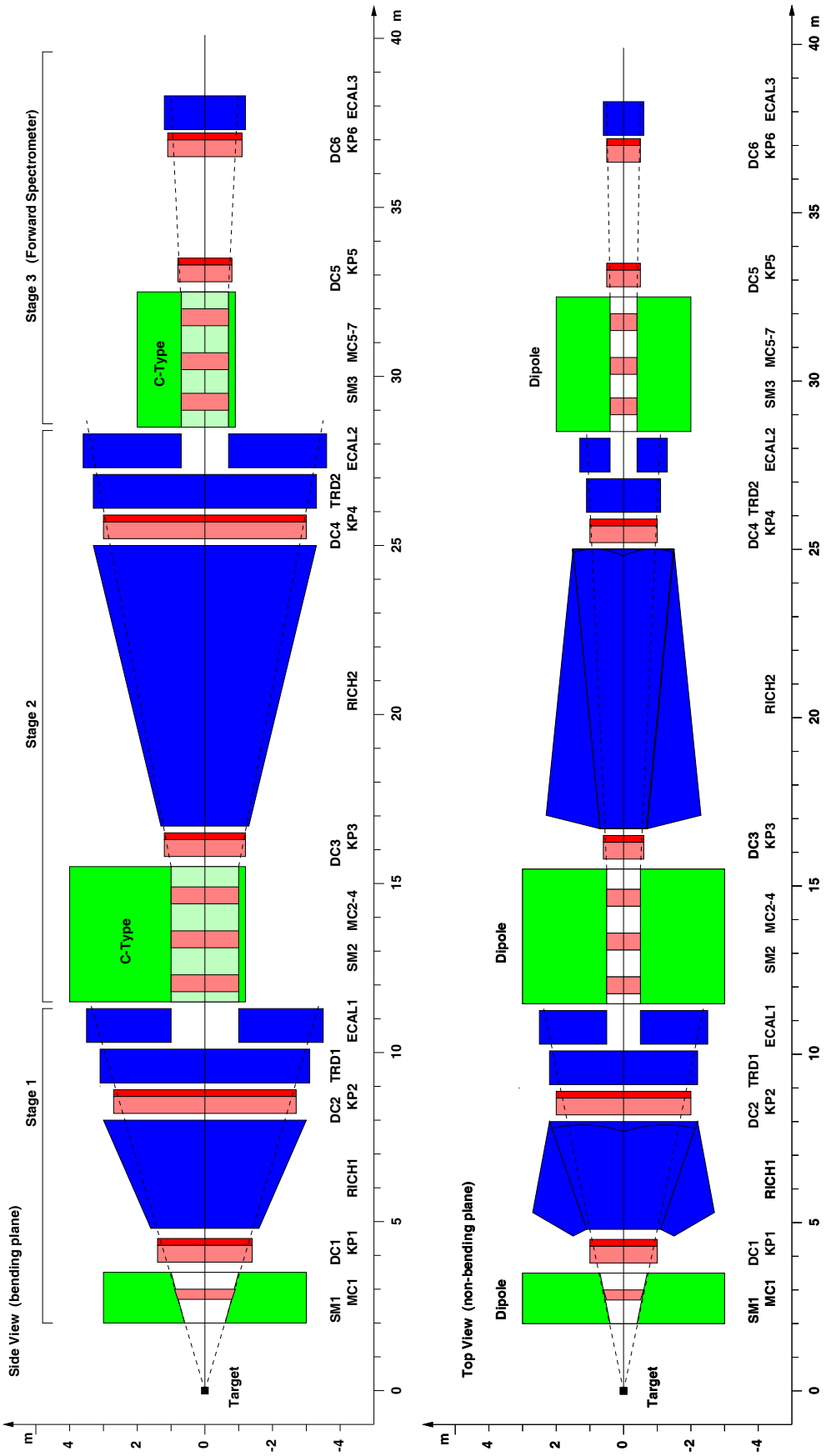

Electron Ion Collider Workshop Richard Milner Plans and Discussion

Electron Ion Collider

- Excellent physics case
  - Scientific interest from across strong interaction physics
- Feasible accelerator options
- Enthusiastic, strong support
  - e-scattering
  - h-scattering
  - A-A
  - International
  - New groups
- R&D over next several years strongly endorsed by nuclear physics long range plan

"to realize within 10 year"

Electron Ion Collider

Draft

- *RHIC/EIC R&D*

  We strongly recommend a vigorous R&D program to pursue the next generation of accelerator and detector developments needed to elucidate the QCD structure of matter.

- Two initiatives of primary interest are:
  - A luminosity upgrade at RHIC to study rare probes of the quark gluon plasma,
  - A high luminosity electron-ion collider to characterize matter at high parton density and measure new spin-dependent features of nucleon structure.

Santa Fe, March 2001

Electron Ion Collider

- Goal: to produce a conceptual design of an Electron Ion Collider within three years.
- Requires:
  - Strong physics case
  - Single, optimized machine design
  - Detailed design for research equipment, detectors, polarimeters, etc.

Time to focus effort in machine design

Electron Ion Collider

- Use RHIC for ion beam
  - Provides polarized proton, ion beams over large energy range
  - Science of eRHIC has very strong overlap with science of RHIC
  - Reduces cost and greatly improves chances of EIC realization
- Choose 10 GeV external e-ring to RHIC
  - Range of options for linac
    - 2 GeV + self-polarization $
    - 10 GeV linac + polarized e source $$
    - 10 GeV energy recovery linac $$$
  - Keep Number of IRs open
    - Develop “Parker” scenario
    - Assess # after some iteration between physics and machine communities

Conclusion: eRHIC Update

- Collisions only at one interaction region (IP12 ?)
- e-ring outside of RHIC tunnel with ¼ of RHIC circumference
- e-ring built to support polarization build-up or circulator ring for full energy (energy recovering) linac
- Existing RHIC IPs fully negotiable for electron-ion collisions

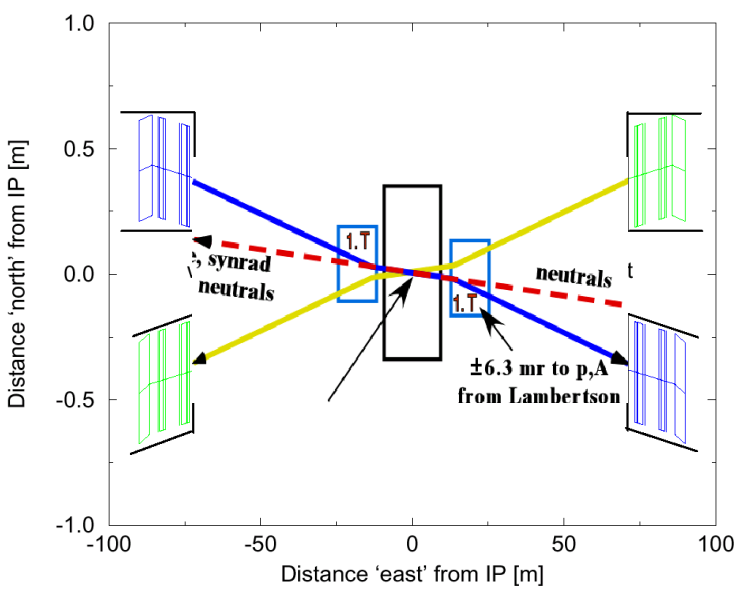

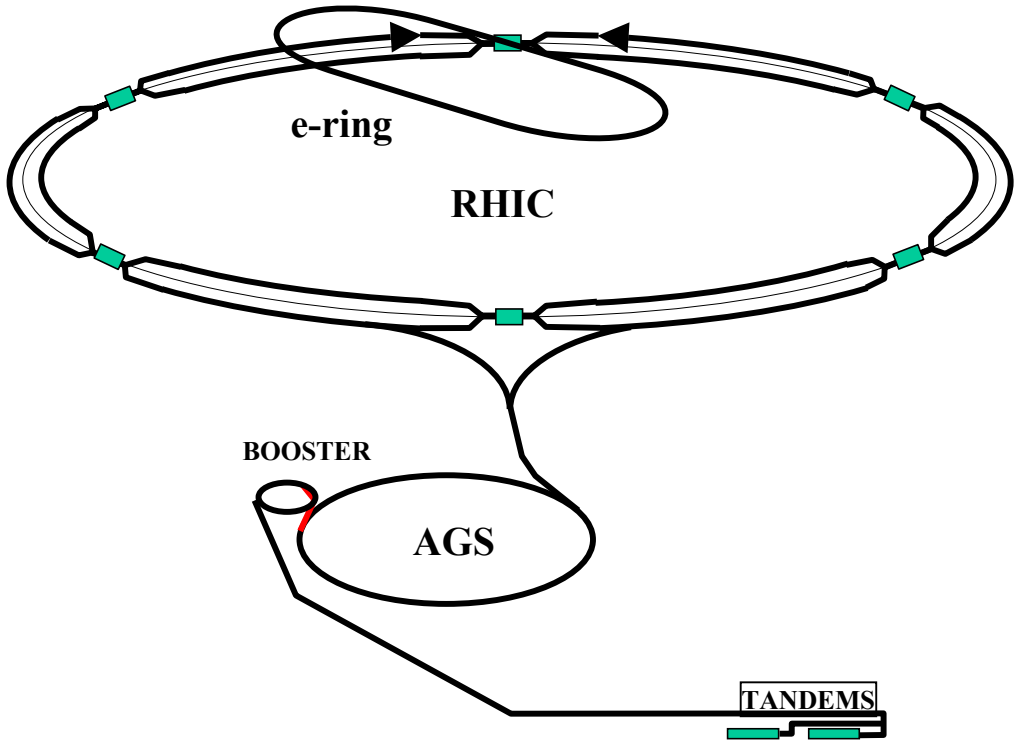

eRHIC IR with “weak – strong” bends (B. Parker)

- “Three beam” IR
- E-beam collides head on with blue at IP
- Small vertical deflection inside detector separates electrons from circulating beams
- Ions bent by 1T field inside a Lambertson dipole
- Long drift downstream of Lambertson gives spectrometer lever arm
- Keep Lambertson short to pass synchrotron radiation.
- Small vertical kicks to Blue/Yellow beams compensate before triplets – proton spin should be OK

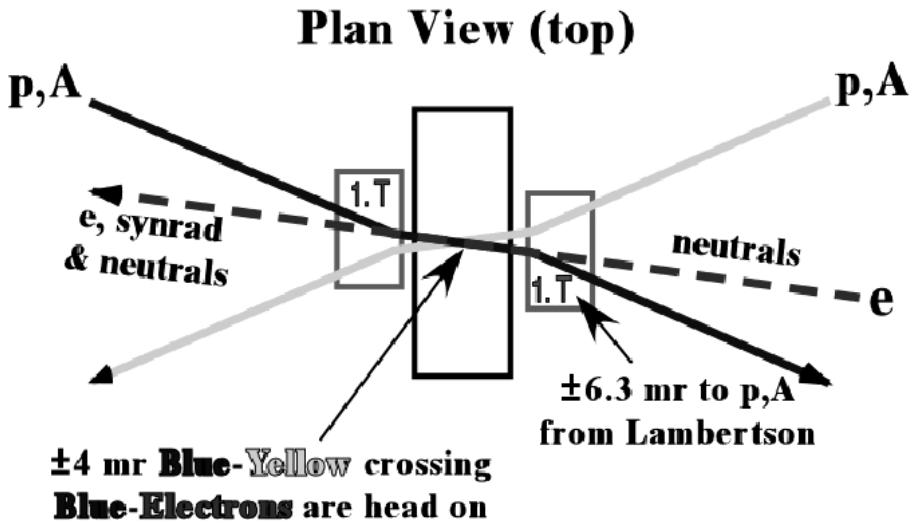

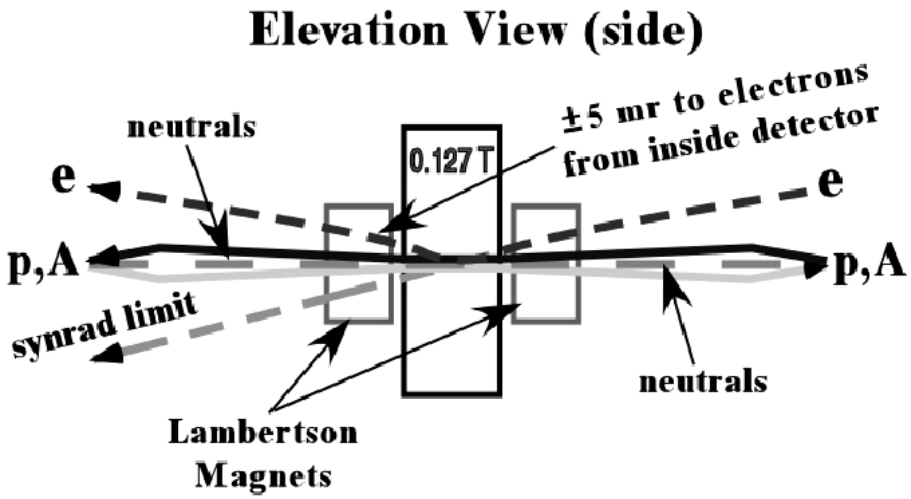

DIS Event Rates

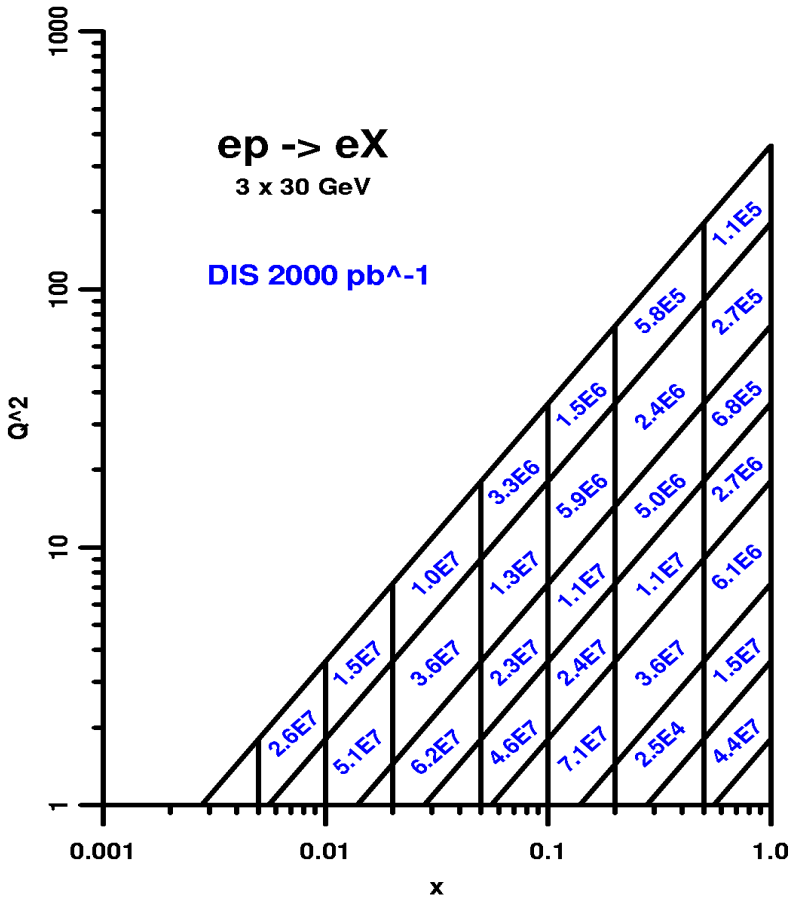

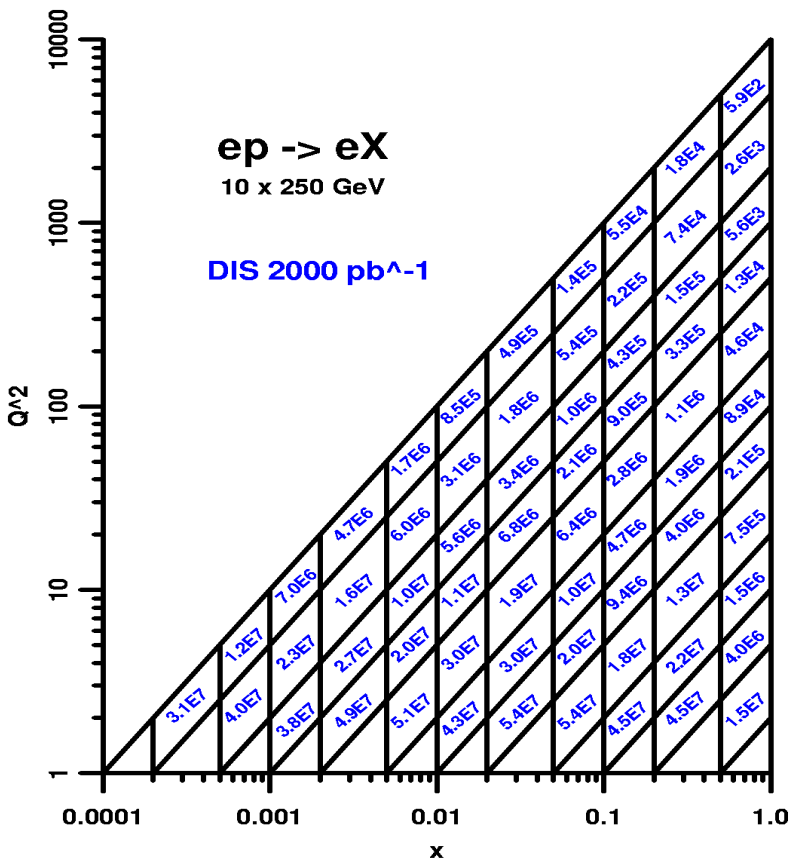

DVCS CROSS SECTION

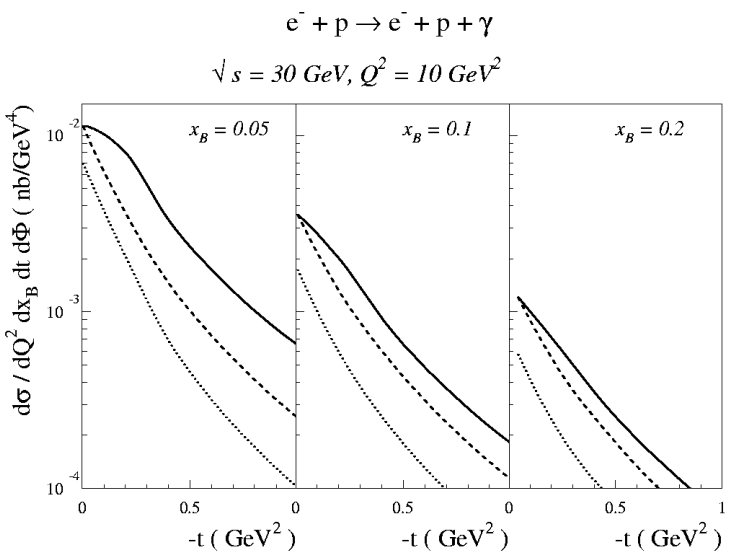

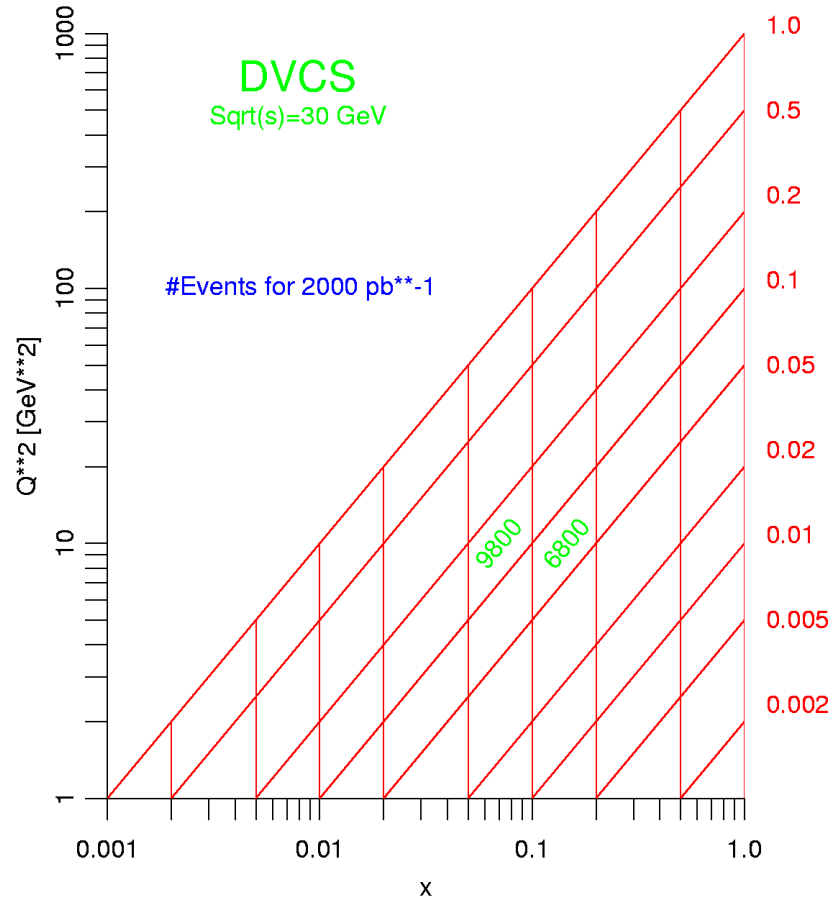

cross section at sqrt(s) = 3 (eq ~5 x 50)

event rates for previous luminosity

1% statistics

Electron Ion Collider

Steering Committee

2002-2005

- J. Cameron (IUCF)
- G. Garvey (LANL)
- R. Hold (ANL)
- V. Hughes (Yale)
- P. Jacobs (LBNL)
- R. Milner (MIT Bates)
- P. Paul (BNL)
- J.-C. Peng (Illinois)

Contact People

- A. Deshpande abhay@bnl.gov
- R. Milner milner@mitlns.mit.edu
- R. Venugopalan raju@bnl.gov

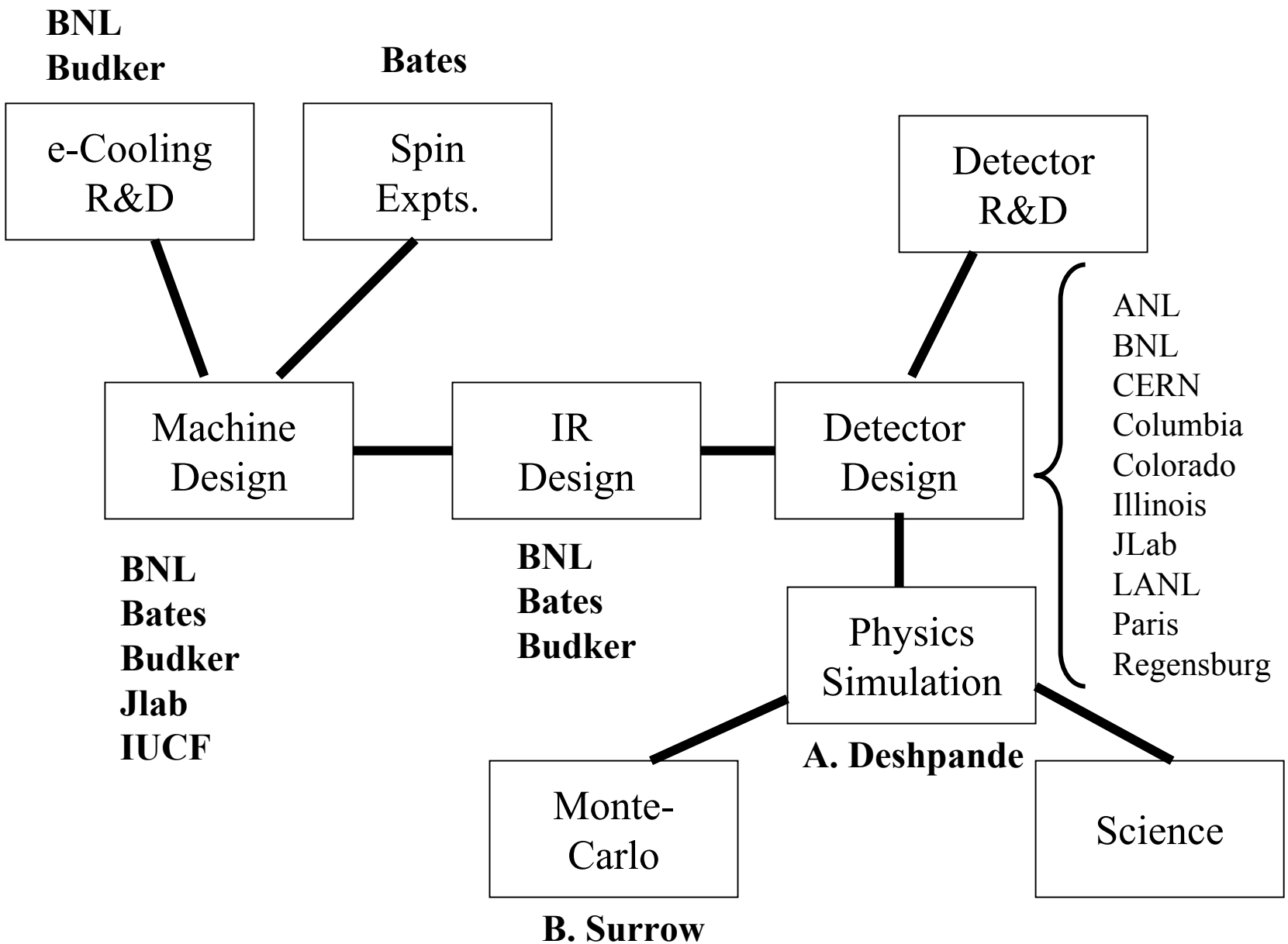
BNL
Budker
Bates
e-Cooling R&D
Spin Expts.
Detector R&D
ANL
BNL
CERN
Columbia
Colorado
Illinois
JLab
LANL
Paris
Regensburg
Machine Design
IR Design
Detector Design
BNL
Bates
Budker
Jlab
IUCF
BNL
Bates
Budker
Physics Simulation
A. Deshpande
Monte-Carlo
B. Surrow
Science

Electron Ion Collider

Physics Simulations

- Inclusive: F_2, F_L, g^p_1, g^n_1 $G_A(x)$
- Semi-Inclusive: Δq_f
- Tagged structure function: F^n_2 / F^p_2, g^n_1, high x
- Charm production: $\Delta G(x, Q^2)$
- Target fragmentation
- Deeply exclusive processes: DVCS
- Search for Saturation
- Transversity: $\delta q(x,Q^2)$
- Diffraction

Electron Ion Collider

Let's Roll!

- In partnership with funding agencies move forward
  - Detailed plan for R&D
- Establish Working Groups
  - Machine
  - IR
  - Detector
- Regular Meetings
- Next EIC Workshop in 1 year.

QCD and the OTHER FUNDAMENTAL INTERACTIONS

Vernon W. Hughes
Yale University

1. Test of QCD

Our Workshop has covered very thoroughly the specific and important topics to which the Electron Ion Collider at BNL can contribute, as well as the interesting accelerator physics involved. There follow a few remarks about Quantum Chromodynamics and the other fundamental interactions included in the standard model of particle physics.

Tests of the validity of QCD include principally:

(1) Its success in predicting and comprehending the spectrum of hadrons based on colored quarks with mass and colored massless gluons which mediate the forces between quarks.

(2) The theory of QCD involves only a single constant, the strong coupling constant α_s. This constant is determined from a number of different processes and the values of α_s obtained agree at the 1% level (Fig. 1).[1]

This agreement provides a test of perturbative QCD. It also proves the validity of the remarkable fundamental Bjorken sum rule [2], which relates nucleon spin structure functions g_1 (x) determined from DIES to the parameters of nucleon beta decay, to an accuracy of 10%.

1.1 Nucleon spin structure functions

One topic to which EIC will contribute greatly is the nucleon spin structure functions g_1^p and g_1^n. The extensive information on $F_2^p(x,Q^2)$ from unpolarized DIS done with fixed targets and also at HERA is shown in Fig. 2. [3]. The relatively sparce data on g_1^p and g_1^n are shown in Fig. 3. [4]. The extended kinematic range and the luminosity for EIC compared to other facilities for DIS are shown in Fig. 4. With EIC much more extensive data will be obtained.

The very interesting and important behavior of $g_1^p(x)$ at low x will be determined by these data. The more accurate values for the first moments of $g_1^p(x)$ and $g_1^n(x)$ will allow a more sensitive test of the Bjorken sum rule to be made, perhaps by a factor of three. The error associated with the value of α_s determined from spin dependent structure functions should be reduced by at least a factor of two.

2. Test of QED

The validity of QED has been confirmed with dramatically high precision. The g-value of the electron is perhaps the most significant quantity for the comparison of experiment and theory. The experimental value [5] for the anomalous g-value of the electron is given in Fig. 5 with its error of 3.4 *ppb*. The theoretical value has been calculated as a perturbation theory expansion in the fine structure constant α through the order α^4. [6]

Comparison of theory and experiment requires a value of α obtained from some other experiment. The various precise determinations of α^{-1} are shown in Fig. 6, including that from the assumption that QED is valid so that a_e (expt) = a_e (theor). [7]. The different α^{-1} values are in reasonable agreement, but clearly a more precise value of α from another experiment is needed.

3. QCD Results Needed for Tests of QED and the Standard Model

3.1 Lamb shift in hydrogen

The present status of the most precise determinations of the Lamb shift in hydrogen is given in Fig. 7. The contributions of proton structure to the 1s and 2s levels in hydrogen are significant and the uncertainty of 3% in our knowledge of the root mean square radius of the proton, r_p obtained from elastic e-p scattering, limits the determination of the QED Lamb shift (with r_p, = 0).

Proton structure arises from QCD, but theory is unable at present to calculate r_p. A most promising approach is to measure by laser spectroscopy the 2s – 2p energy level separation in muonic hydrogen, μ^-p (Fig. 8). For this atom because of its small size proton structure has a relatively large effect as compared to H. The pure QED 2s – 2p separation in μ^-p has been accurately evaluated. Hence a measurement of the 2s – 2p energy separation to 30 *ppm*, which an ongoing experiment at Paul Scherrer Institute in Switzerland [8] expects to achieve, should determine r_p to ~ 0.1%. This would determine the QED Lamb shift in H at least a factor of 10 better than its present value.

3.2 The anomalous magnetic moment of the muon

Comparison of experiment and theory for $a_\mu = (g_\mu - 2)/2$ provides an unusually sensitive test of the standard model and a search for "new" physics. The principal uncertainty in the theory comes from inadequate knowledge of the contribution of virtual hadrons to the photon propagator. QCD theory cannot evaluate this term from first principles and it is determined at present primarily from experimental data on $e^+e^- \rightarrow$ hadrons and on τ^- decay, $\tau^- \rightarrow \pi^- \pi^0 \nu_\tau$. [9]

Since the published [10] experimental error is 1.3 *ppm*, and is expected to be reduced, the theoretical error of 0.6 *ppm* should be improved (Fig. 9).

4. Time Variation of the Fundamental Constants

Great interest in and study of this topic have been active over many years. Recently observation of a variation of α with time has been reported. It is based on the measurement of the fine structure $[0(\alpha^z R_y]$ relative to the basic term $[0(R_y)]$ for many atoms as a function of red shift or fractional look-back time (Fig. 10). Their quoted result is $\frac{\Delta\alpha}{\alpha} = (-0.72 \pm 0.18)\times 10^{-5}$ over the red shift range $0 < z < 3.5$[11].

There seems to be no quoted limit on the variation of α_s with time. The only available evidence appears to come from natural fission reactors, which operated about two billion years ago at Oklo. These data have been analyzed to give a limit on $\dot{\alpha}$, but the analysis

relates this bound to a possible shift of thermal neutron-capture resonances, which involve the strong interaction. [12]

Direct measurement of a process at large look-back time has not been achieved.

Precision measurements in atomic spectroscopy [13,14] have achieved an accuracy and stability at the level of 10^{-15}. The ultra cold sapphire crystal oscillator has achieved a stability of 10^{-16} and is used for the atom interrogation. The atomic spectral lines which provide high precision include the hydrogen maser which operates at the frequency of the hfs interval in hydrogen, cold atom microwave fountain clocks of ^{133}Cs and ^{87}Rb involving their hfs intervals, and the 1s-2s optical transition in hydrogen. These intervals involve the fundamental constants: R_ω, α, mass ratios m/M_{nuc} and nuclear magnetic moments. The time variation of the various constants or combinations of the constants can be studied, not only the electromagnetic constant α, but also constants involving nuclear masses and magnetic moments, which relate to the strong interactions and hence to α_s. The result $|\alpha/\alpha| \leq 3.7x10^{-14}\ yr^{-1}$ has already been reported.

A recent theoretical paper discusses the time variation of the fundamental constants within the framework of the standard model and of grand unification.

This research has been supported in part by the U.S. Department of Energy.

References

[1] The Particle Data Group; C. Caso et al., Eur. Phys. J. C3, 1 (1998)
[2] J.D. Bjorken, Phys. Rev. 148,1467 (1966).
[3] H. Abramowicz and A.C. Caldwell, Rev. Mod. Phys. **71**, 1275 (1999).
[4] E.W. Hughes and R. Voss, Annu. Rev. Nucl. Sci. 49,303 (1999); SMC, B. Adeva et al., Phys. Rev. D58, 1120021 (1998).
[5] R.S. Van Dyck, P.J. Schwinberg, and H.G. Dehmelt, Phys. Rev. Lett. 59,26 (1987); R.S. Van Dyck, Jr. in Quantum Electodynamics ed. T. Kinoshita (World Scientific, Singapore, (1990) p. 322.
[6] T. Kinoshita in Quantum Electrodynamics ed. T. Kinoshita (World Scientific, Singapore, 1990) p.218.; P.J. Mohr and B.N. Taylor, Rev. Mod. Phys. 72, 351 (2000).
[7] T. Kinoshita, Rep. Prog. Phys. 59, 1459 (1996).
[8] F. Kottmann et al., "Laser Spectroscopy of the Lamb Shift in Muonic Hydrogen", Proposal for an experiment at PSI (1998).
[9] M. Davier and A.Höcker, Phys. Lett. B435, 427 (1998).
[10] g-2 Collaboration, H.N. Brown, et al., Phys. Rev. Lett. 86, 2227 (2001).
[11] J.K. Webb, et al., Phys. Rev. Lett. **87**, 091303-1 (2001).
[12] T. Damour and F. Dyson, Nucl. Phys. **B480**, 37 (1998).
[13] C. Salomon et al, in Atomic Physics 19, ed. E. Arimondo et al, (AIP Proceedings, vol. 551, New York, 2001) p. 23.
[14] R. Holzwarth, et al, ibid, p. 58.
[15] X. Calmet and H. Fritzch, hep-ph/0204258.

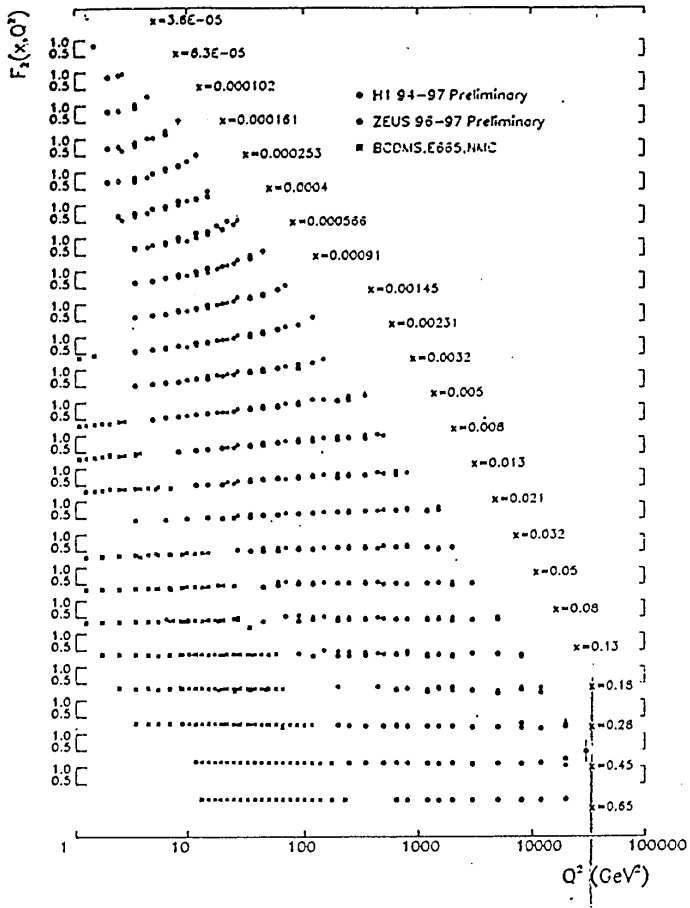

F_2 is plotted vs. Q^2 for fixed x values for the preliminary 1994-1997 HERA data, and compared to results from fixed-target experiments. F_2 shows strong scaling violations, particularly at small x.

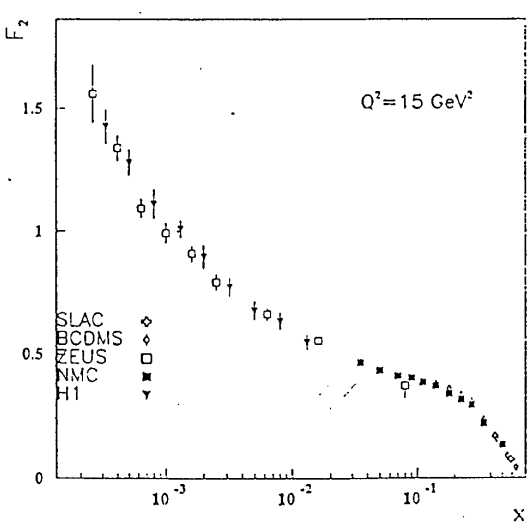

Comparison of the fixed-target and HERA data at Q^2=15 Gev^2. The data span 3.5 orders of magnitude in x and match in a smooth way.

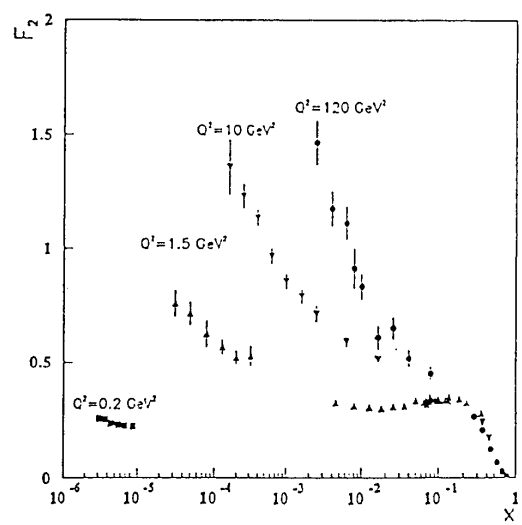

The F_2 data from HERA and from fixed-target experiments are plotted vs. x for different values of Q^2. The rise of F_2 toward smaller x depends strongly on Q^2.

Figure 2. Unpolarized Proton Structure Functions

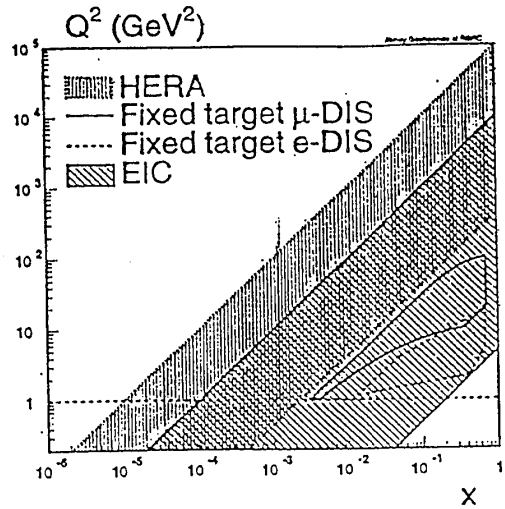

The x-Q2 range of the proposed electron-ion collider in comparison with the previously explored kinematic region by fixed target experiments and that covered by the HERA collider at DESY.

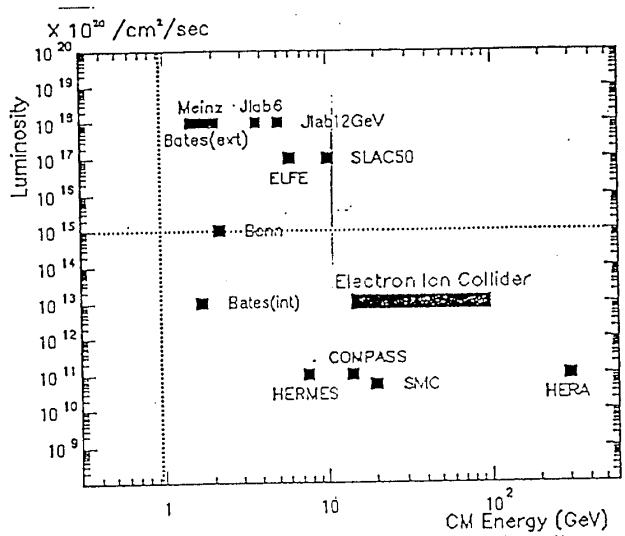

The Center of Mass energy vs. Luminosity of various existing facilities in comparison with that proposed for the electron-ion collider.

Table: Center of Mass Energies and Luminosities for Various Collisions

Facility	Particles and Energies(GeV)	$\sqrt{s}(GeV)$	L $(cm^{-2}sec^{-1})$
RHIC	$p(250) \times p(250)$	500	2×10^{32}
HERA	$e(30) \times p(900)$	300	7×10^{31}
HERA(A)	$e(30) \times A(450)$	200	$(7 \times 10^{31})/A$
eRHIC	$e(10) \times p(250)$	100	1.5×10^{33}
eRHIC(Au)	$e(10) \times$ Au(100)	60	5×10^{30}
FNAL	$\mu(600) \times p(1)$	35	$\sim 10^{31}$
EPIC	$e(3) \times p(50)$	25	$> 10^{33}$
SMC	$\mu(200) \times p(1)$	20	$\sim 10^{32}$
SLAC	$e(50) \times p(1)$	10	1.3×10^{33}
HERMES	$e(30) \times p(1)$	7	$\sim 10^{31}$

Figure 4. Kinematic Range and Luminosity

$$\vec{\mu} = g\frac{e\hbar}{2mc}\vec{S} \qquad g = \frac{\dfrac{\text{magnetic moment}}{e\hbar/2mc}}{\dfrac{\text{angular momentum}}{\hbar}}$$

For a Dirac electron $g = \frac{1}{1/2} = 2$

For a real electron $g = 2(1+a)$; a is the anomalous g-value: $a = \frac{g-2}{2}$

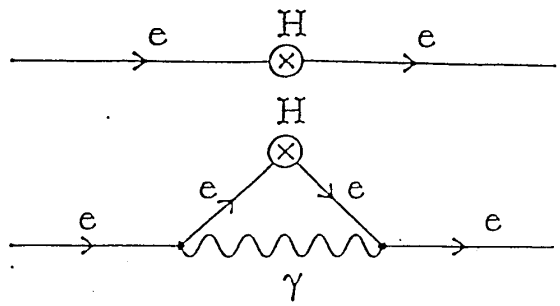

$g = 2$

$a = \frac{\alpha}{2\pi} \simeq 10^{-3}$

Experiment

$$a_e(\text{expt}) = 1\,159\,652\,188(4)\cdot 10^{-12}\ (3.4\,\text{ppb})$$

Theory

$$a_e(\text{QED}: e,\gamma) = 0.5\left(\frac{\alpha}{\pi}\right) - 0.328\,478\,965\left(\frac{\alpha}{\pi}\right)^2 + 1.181\,241\,456\left(\frac{\alpha}{\pi}\right)^3 - 1.509\,8(384)\left(\frac{\alpha}{\pi}\right)^4$$

$$a_e(\text{QED}: \mu,\tau) + a_e(\text{had}) + a_e(\text{weak}) = 4.393(27)\cdot 10^{-12}$$

Electron g-2 is a very pure QED problem involving only e^-, e^+, γ

Figure 5. g-Value of Electron

Hydrogen 1s-2s transition (optical spectroscopy)
Th. Udem et al., Phys. Rev. Lett. 79, 2646 (1997).

f(1s-2s) = 2 466 061 413 187.34(84) kHz (3.4×10^{-13})

L(1s) = 8 172.876(29) MHz (3.5 ppm)

Hydrogen 2s-2p transition (microwave spectroscopy)
F. Pipkin in Quantum Electrodynamics, ed. T. Kinoshita (1990).

L(2s) = 1 057.845(9) MHz (9 ppm)

Contributions to the hydrogen 1s Lamb shift

Contribution	Frequency (MHz)	Error (MHz)
$\alpha(Z\alpha)^4 m$ one-loop	8,114.768	
$\alpha(Z\alpha)^5 m$ one-loop binding	56.950	
$\alpha(Z\alpha)^6 m$ one-loop binding	-3.193	
$\alpha^2(Z\alpha)^4 m$ two-loop	1.017	
$\alpha^2(Z\alpha)^5 m$ two-loop binding	-0.296	0.007
$\alpha^2(Z\alpha)^6 m \ln(Z\alpha)^n$ two-loop binding	-0.028	
$(Z\alpha)^5 m^2/M$ recoil	2.402	
$\alpha(Z\alpha)^5 m^2/M$ radiative recoil	-0.014	
$(Z\alpha)^6 m^2/M$ recoil	-0.007	
uncalculated higher order QED	0.000	0.015
proton size (r_p = 0.862(12) fm)	1.164	0.032
1S Lamb Shift	**8,172.762**	**0.036**
(for r_p = 0.805(11) fm:	8,172.613	0.032)

Figure 7. Lamb Shift in Hydrogen

New Directions in QCD And the Electron Ion Collider

S. Brodsky
SLAC

BNL –EIC Workshop

March 2, 2002

Unexpected Role of Final State Interactions in DIS

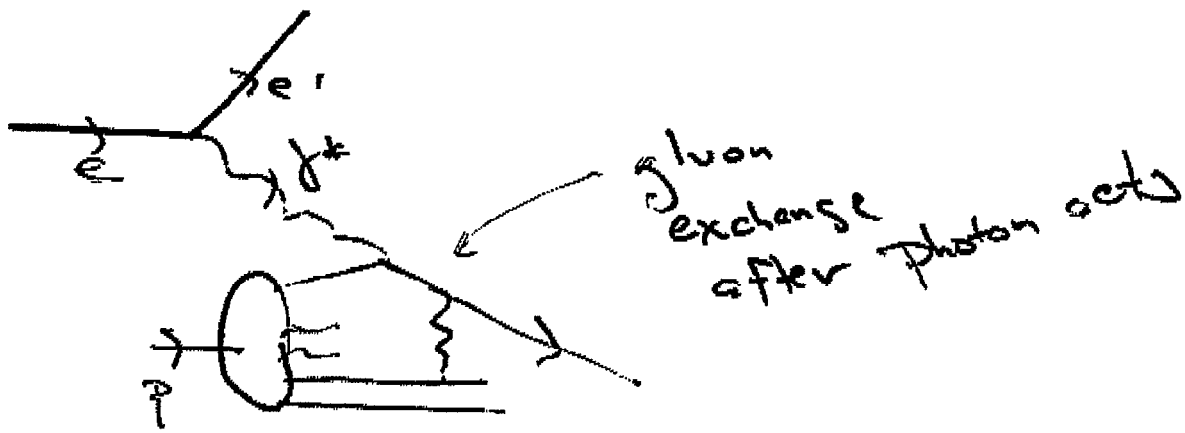

- Single-Spin Asymmetries
- Diffraction
- Shadowing
- Energy Loss
- p_T Broadening

Recent Applications of ψ_{LC}

Diffractive processes

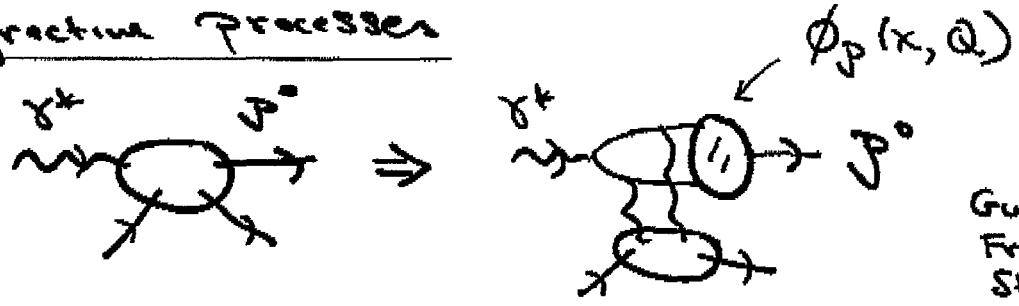

Gunion
Frankfurt
Strikman
Mueller
SJB
Collins

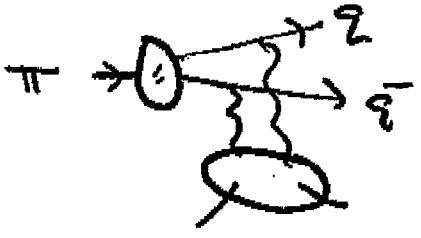

$$\frac{\partial^2 \psi_{q\bar{q}}(x, \vec{k}_\perp)}{\partial k_\perp^2}$$

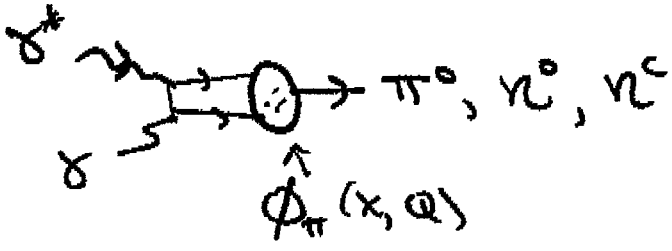

Lepage, SJB

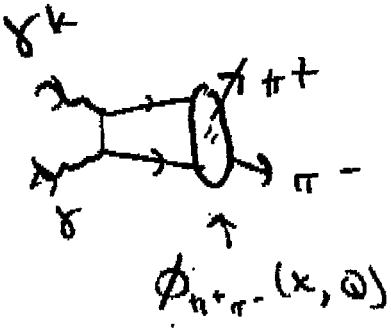

Diehl, et al

Deeply virtual Compton scatt

Einhorn
Burkardt
QCD $(1+1)_{N_c \to \infty}$

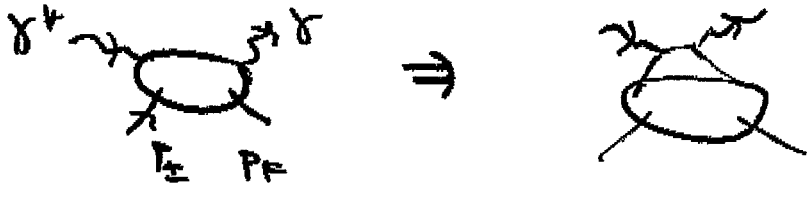

X. Ji
A. Radyushkin
Close, Gunion, SJB

Huang * Non-forward parton distributions and ψ_{LC}
Schmidt * Sum rules, * Fit cons.
Ma * Relations to EM, Gravity sum rules
SJB * Tests on quantum fluctuations of electron

$\{ \psi^{LC}_{n/H} (x_i, \vec{k}_{\perp i}, \lambda_i) \}$

repn. of hadron in terms of q, g

* Frame-independent
* $P^+, \vec{P}_\perp, J_z$ conserved for each ψ_n
* Trivial vacuum $\langle \xi \rangle = 0$
* Exact $F(t)$, OPE, $B(0) \equiv 0$
  repn.
  Vanishing gravitomagnetic moment
* $\bar{q}(x) \neq q(x)$, $\bar{u}(x) \neq \bar{d}(x)$
* $\langle \chi_Q \rangle_H \sim \frac{\Lambda^2}{m_Q^2}$ from $\langle H | G^3(0) | H \rangle$

* ψ_n predictable from PQCD at large m_n^2
  $x \to 1$, $k_\perp^2 \to \infty$, heavy see
  $x \to 0$ Lodder relns.
* Helicity retention, counting rules
* Hidden color
* Color transparency at small $b_\perp$

Diffraction leads to nuclear shadowing:

Gribov, Glauber
Pumplin, SJB

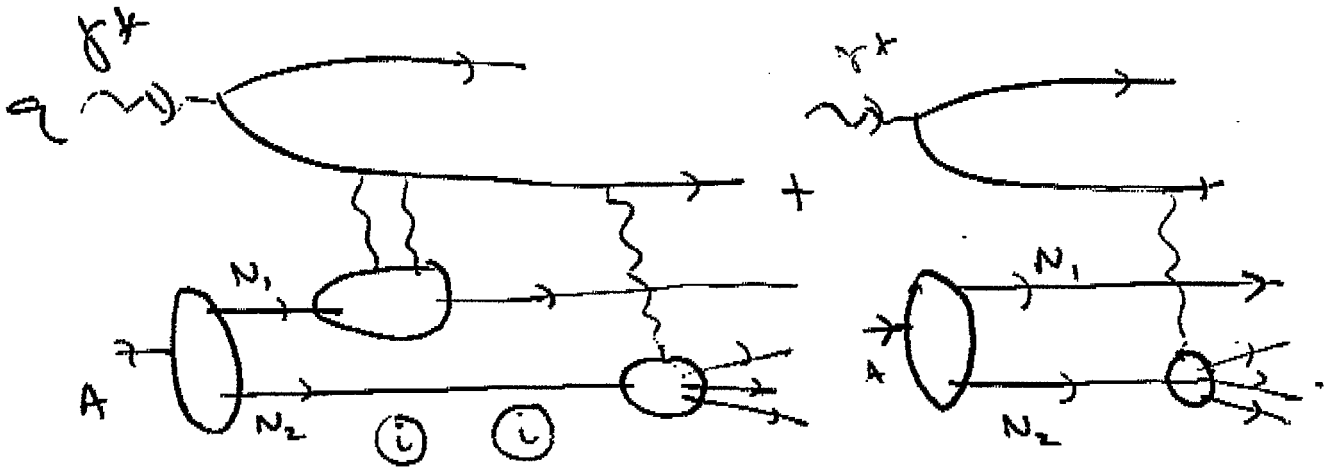

* Destructive interference leads to shadowing at low
Frankfurt, Strikman
* Shadowing of quark, gluon distributions
* Reggeon exchange leads to antishadowing
Lu, SJB

Explicit Calculation by BHMPS

Hoyer, Marchal, Peigne, Sannino
hep-ph/0104291

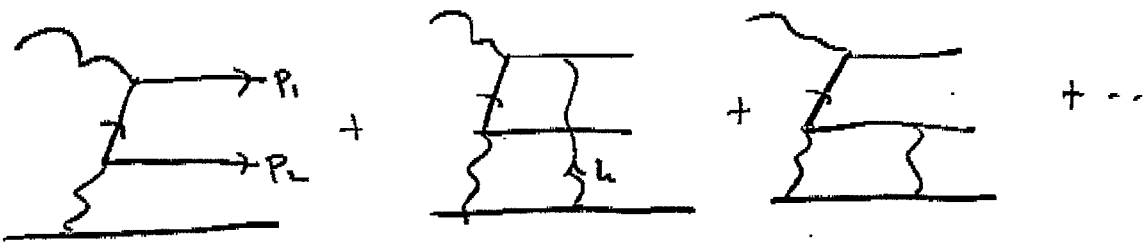

* Non-zero, leading twist FSI effect
* Gauge-independent! Feynman, LCG $\left\{ \begin{matrix} ML \\ PV \\ k \end{matrix} \right.$ prescr.

* Lesson for LCG: $g^{\mu\nu} - \dfrac{n^\mu k^\nu + k^\mu n^\nu}{n \cdot k}$

$n \cdot k = k^+$. At pole $k^+ = O(\frac{1}{v})$!

Eikonal Factor $\left(1 - e^{-i g^2 W}\right)$: $W = \frac{1}{2\pi} \log \dfrac{|\vec{R}_\perp + \vec{r}_\perp|}{R_\perp}$

not unitary

$$|m|^2 = \left| \frac{\sin g^2 W/2}{g^2 W/2} A_{Born} \right|^2$$

Consider

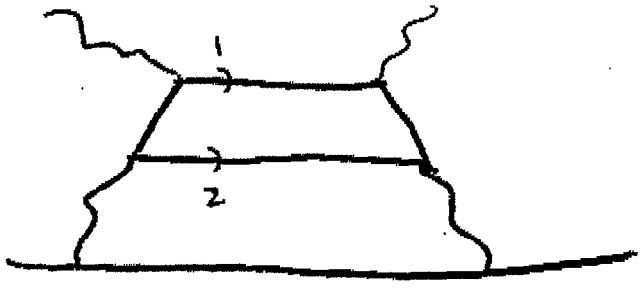

$q^+ \leq 0$

In Feynman gauge, must keep

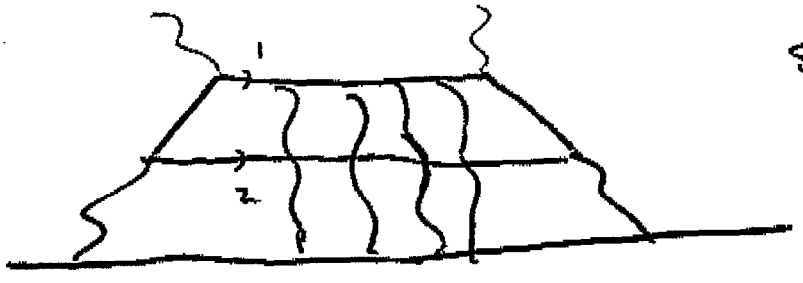

Shadowing effect from on-shell states

$$|\mathcal{M}|^2 \Rightarrow \left| \frac{\sin[g^2 W(r_\perp, R_\perp)/2]}{g^2 W(r_\perp, R_\perp)/2} \, \mathcal{M}_0 \right|^2$$

$$W(r_\perp, R_\perp) = \int d^2k_\perp \frac{1 - e^{+i r_\perp \cdot \vec{k}_\perp}}{k_\perp^2} e^{i \vec{R}_\perp \cdot \vec{k}_\perp}$$

$$= \frac{1}{2\pi} \log\left(\frac{|\vec{R}_\perp + \vec{r}_\perp|}{|R_\perp|} \right)$$

Conclusions

Shadowing of DIS cross section due to

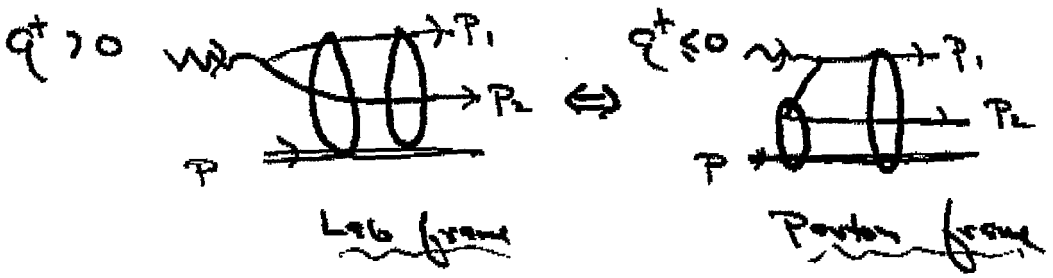

Interference of Diff. channels — Involve FSI of aligned jet!

* Shadowing from rescattering of aligned (current) quark in the target within the coherence length

$$\boxed{l_{Inf} = \frac{2\nu}{Q^2} = \frac{1}{Mx_B}}$$

∴ Structure functions not totally specified by l.c. wavefunctions!

$$F_2(x_B, Q^2) \neq \sum_n \int |\Psi_n(x_i, k_{\perp i})|^2 \times \delta(x_i - x_B)$$

Also DVCS

* Need generalized P.O.E. - $P\exp\left[ig\int_{-\infty}^{\infty} d\omega_\mu A^\mu(\omega)\right]$

* Factorization theorems, sum rules which follow from OPE unchanged.

D. S. Hwang
I. Schmidt
SJB
hep-ph/0201296

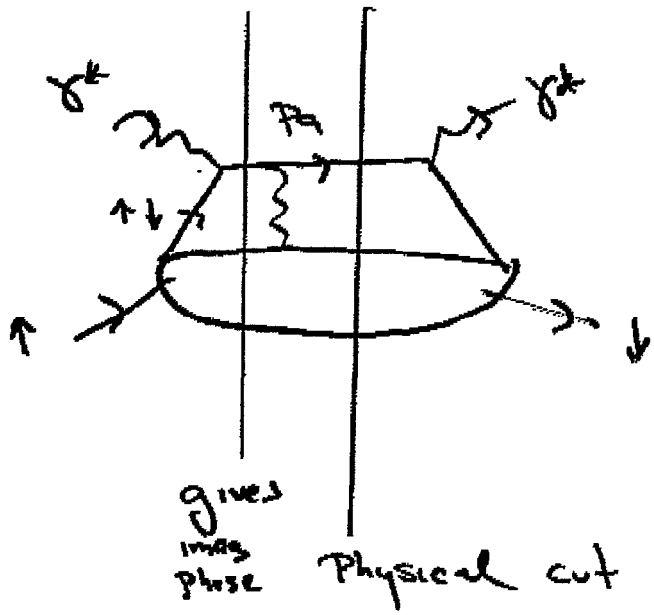

$p_q = q + r$

rescattering phase
$e^{i(\chi_1 - \chi_2)}$
infrared finite

$\Delta L_z = 1$

$$i \vec{S}_p \cdot \vec{q} \times \vec{p}_q = i S_p \cdot \vec{q} \times \vec{r}$$

$$A_n = P_y \sim O\left[\frac{\alpha_s(r_\perp^2)\, x_{Bj}\, M\, \vec{r}_\perp \ln \vec{r}_\perp^{\,2}}{r_\perp^2}\right]$$

Bjorken scaling

Same matrix elements as $F_2(0) = Q_p$

$$P_y = \frac{e_1 e_2}{8\pi} \frac{2(\Delta M + m) r'}{[(\Delta M + m)^2 + r_\perp^2]}$$

$$\left[r_\perp^2 + \Delta(1-\Delta)\left(-M^2 + \frac{m^2}{\Delta} + \frac{\lambda^2}{1-\Delta}\right)\right]$$

$$\times \frac{1}{r_\perp^2} \ln \frac{r_\perp^2 + \Delta(1-\Delta)\left(-M^2 + \frac{m^2}{\Delta} + \frac{\lambda^2}{1-\Delta}\right)}{\Delta(1-\Delta)\left(-M^2 + \frac{m^2}{\Delta} + \frac{\lambda^2}{1-\Delta}\right)}$$

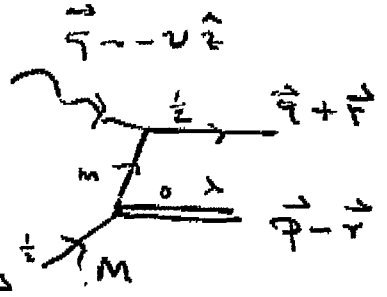

$$\vec{S}_p = \pm \hat{y}$$

$$M \, \vec{S}_p \cdot \vec{q} \times \vec{r}$$

$$\epsilon^{\mu abc} p_\mu S_a q_b r_c$$

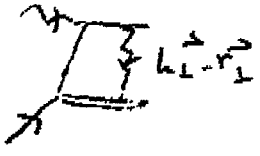

$$\frac{e_1 e_2}{4\pi} \to C_F \alpha_s(\mu^2)$$

$$\mu^2 = e^{-5/3} (\vec{k}_\perp - \vec{r}_\perp)^2$$

→ Final State Interaction Processes

<u>Single-Spin Asymmetry</u>

with respect to the jet production plane

$$\boxed{\vec{S}_p \cdot \vec{q} \times \vec{P}_{Jet}}$$

Find jet direction using thrust, etc.

Quark Fragmentation leads to

$$\boxed{\vec{S}_p \cdot \vec{q} \times \vec{P}_\pi}$$

* New QCD mechanism
* Bjorken scaling
* Reflects $\Delta L_z \neq 0$ Matrix elements.
* Similar to $F_2(0)$

Initial + Final State Interactions

* Perturbatively calculable at large $\vec{r}_\perp, \vec{q}_\perp$

* New measure $\sim \alpha_s(r_\perp^2)$

* Produce $\vec{S} \cdot \vec{P}_1 \times \vec{P}_2$. SSA with scatt + prod. planes

* Application to Drell-Yan : $\vec{S}_p \cdot \vec{P}_\pi \times \vec{q}$

$e^+e^- \to \Lambda X$

$pp \to \Lambda X$

* Bjorken scaling : $\frac{M r_\perp}{r_\perp^2}$ not $\frac{M r_\perp}{Q^2}$

Resolved Photon Wavefunction

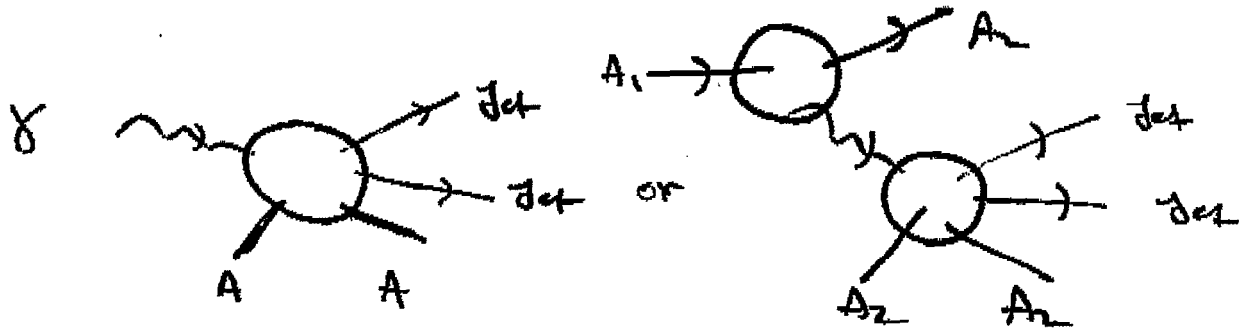

HERA RHIC, LHC, UPC

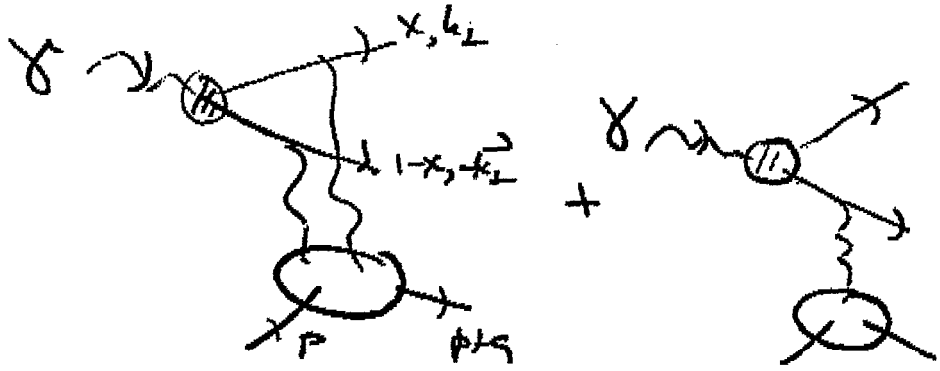

$$\mathcal{M} \sim \frac{\partial^2}{\partial k_\perp^2} \Psi_{q\bar{q}/\gamma}(x, \vec{k}_\perp) \qquad \frac{\partial}{\partial k_\perp} \Psi_{q\bar{q}}(x, k_\perp)$$

$$\mathcal{M}_\gamma \sim A F(q_\perp^2) \qquad \mathcal{M}_A \sim Z\alpha F(q_\perp^2)$$

$$\frac{d\sigma}{dk_\perp^2} \sim \frac{1}{k_\perp^6} \qquad \frac{d\sigma}{dk_\perp^2} \sim \frac{1}{k_\perp^4}$$

"Self-Resolving" e-p Interactions

HERA, ERHIC

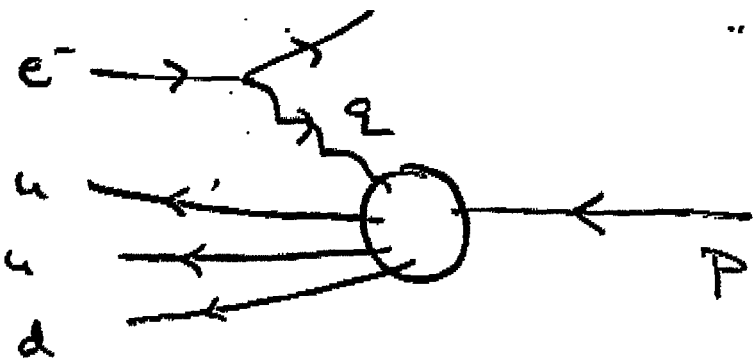

"Coulomb" dissociation of proton

Diehl
Hoyer
Peigne
SJB

Observe 3 jets $\langle q_\perp^2 \rangle \ll \langle k_\perp^2 \rangle$

at large $\vec{k}_{\perp i}$ low $q_\perp^2$

$$\frac{dN}{d\ln q_\perp^2\, dx_1\, dx_2\, d^2k_{\perp 1}\, d^2k_{\perp 2}} \sim \left| \sum_i e_i \frac{\partial \psi(\vec{k}_\perp, x)}{\partial \vec{k}_{\perp i}}\Big|_{3q/p} \right|^2$$

$$\frac{d\sigma}{d\ln q_\perp^2\, dx_1\, dx_2}\left(\vec{k}_{\perp i}^2 > \vec{k}_{\perp min}^2\right) \sim \frac{\alpha f_N^2\, g(x_i)}{(k_{\perp min}^2)^4}$$

$$[f_N] = [M^2]$$

Measure proton distribution ampl.

$\phi(x_i)$

Measure Odderon - Pomeron Interference

J. Rathsman
C. Merino, SJB

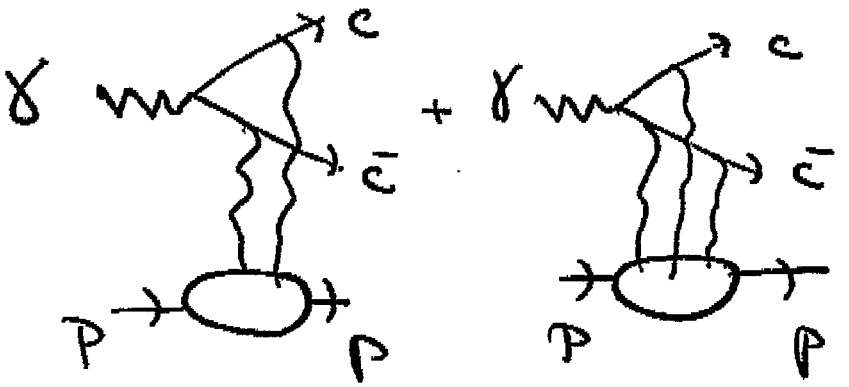

$\gamma p \to c\bar{c}p$
diffractive
(rap-gap)

$C = +$
Pomeron

$C = -$
Odderon

HERA
FNAL
SLAC
Compass
MUSES

Interference gives $c \leftrightarrow \bar{c}$ asymmetry:

$$A = \frac{\frac{d\sigma}{dt\,dm^2\,dz_c} - \frac{d\sigma}{dt\,dm^2\,dz_{\bar{c}}}}{\frac{d\sigma}{dt\,dm^2\,dz_c} + \frac{d\sigma}{dt\,dm^2\,dz_{\bar{c}}}}$$

$$\propto \sin\left[\pi\left(\frac{\alpha_O - \alpha_P}{2}\right)\right] s^{\alpha_O - \alpha_P}$$

$$\cdot \frac{2z_c - 1}{z_c^2 + (1-z_c)^2}$$

Self-Resolving Nuclear Interactions

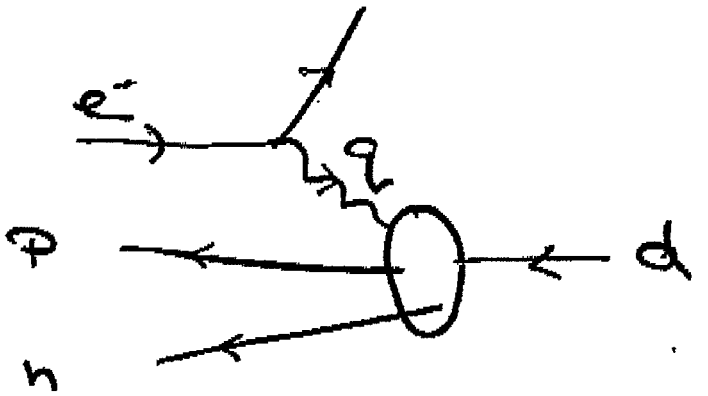

Hoyer
Peigne
SJB

$q_\perp^2 << \langle k_\perp^2 \rangle$

— photon acts first

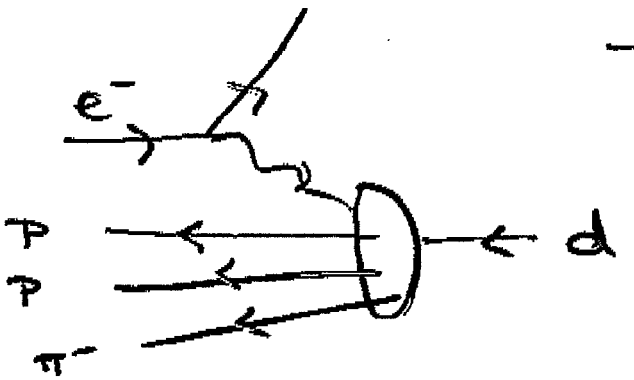

measure all Fock components of nucleus!

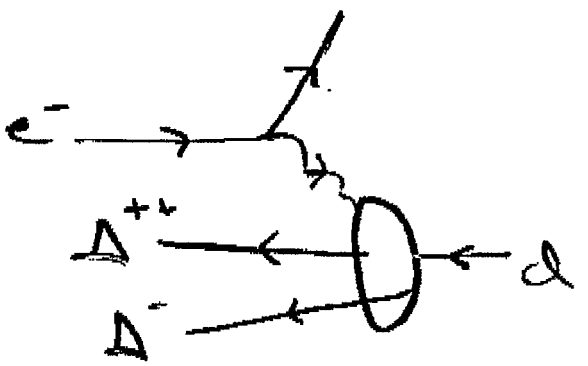

$$x = \frac{k^+}{P^+} = \frac{k^0 + k^z}{P^0 + P^z}$$

measures $\sum_i e_i \frac{\partial}{\partial k_{\perp i}} \psi_d(x_i, k_{\perp i}, \lambda_i)$

Check Hermes effect
Miller, Kerman, SJB

S. Gordon + SJB

Color - Octet Intrinsic Charm

QED:

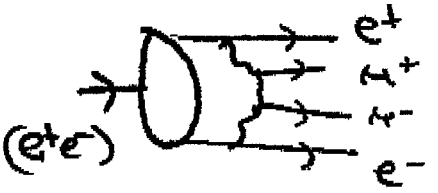

$$P_{prob} \sim \left(\frac{\mu_{Bohr}}{m_{\mu^+\mu^-}}\right)^4 \times \alpha^4$$

QCD

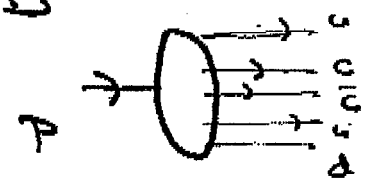

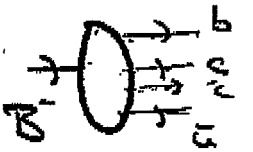

Only suppressed by $\frac{1}{m_{c\bar{c}}^2}$ if color octet

Franz et al:

$\langle x_{c\bar{c}} \rangle_H \Rightarrow$

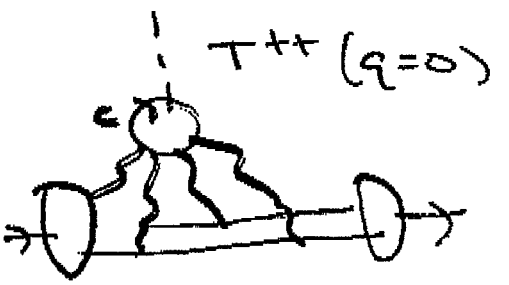

$$T^{++} \Rightarrow \frac{G^{+\nu} G^{+\mu} G_{\mu\nu}}{m_c^2} \leftarrow (A_\mu, A_\nu)$$

$$\therefore P_{prob} \sim \alpha_s^4 \frac{\mu_{Bohr}^2}{m_{Q\bar{Q}}^2}$$ for color octet

$\frac{1}{m_r} = \frac{1}{m_1} + \frac{1}{m_2}$: $\mu_{Bohr}^B \sim 2\,\mu_{Bohr}^\pi$ More IC in B!

Resolve Intrinsic Charm

Hoyer, Sokoloff
Peterson, SJB

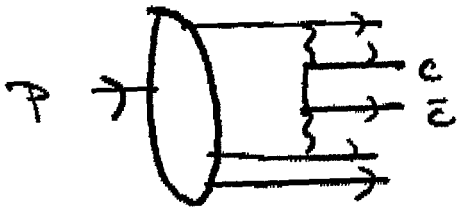

$x_c \sim \frac{m_{\perp c}}{\sum_i m_{\perp i}}$ large x_c

* Observe at $x_{Bj} \sim 0.4$ in DIS — Harris, Vogt, Smith

* Diffractively dissociate (Coulomb, Pomeron)

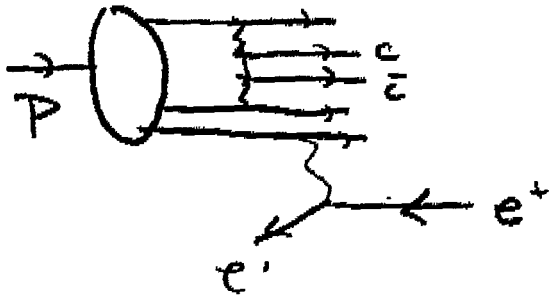

Observe Λ_c at large x_F
Observe J/ψ " "
proton frag region

$c(x) \neq c'(x)$?

* Why important:

Franz et al

- $P_{q\bar{q}} \sim \frac{1}{m_Q^2}$ non-Abelian only
- $B(J/\psi \to \rho\pi, \psi' \to \rho\pi)$ puzzle — Karliner, SJB
- Erode CKM Hierarchy in B-decays — Gardner, JT

Consequences of Intrinsic Charm

* $J/\psi \to p\pi$, $\psi' \not\to p\pi$

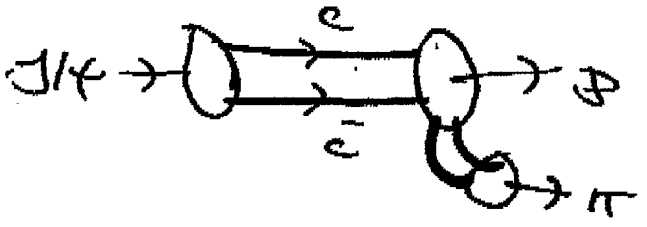

Karliner SJB

* $\Upsilon \to J/\psi\, X$ Spectrum How

* $\pi p \to D^{\pm} X$, $\Sigma p \to \Lambda_c X$

Hoyer et al

Consequences for B-decays

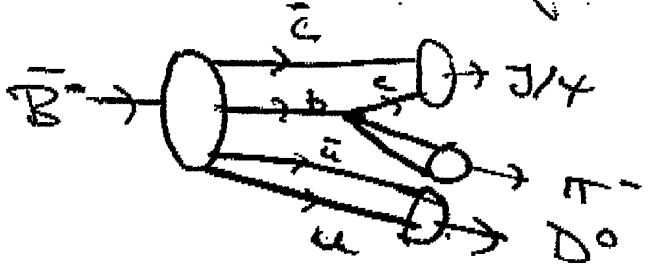

How

CLEO, Belle

bump at low $P_{J/\psi}$

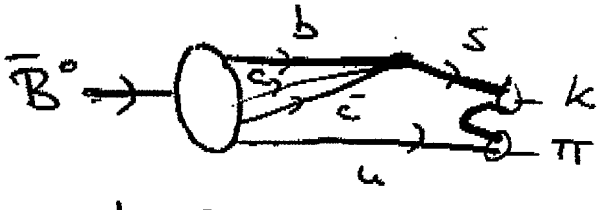

Leading CKM

Evasion of CKM !

Gardner SJB

Conclusions :

⇒ Unexpected Role of FSI, ISI

* Leading Twist Diffraction, Color Dipole Physics
* Single - Spin Asymmetries - Bjorken Scaling!
* Nuclear Shadowing - Fundamental Understanding in QCD!
* Many new tests, effects

New Questions:

* How is mom. sum rule maintained in the face of shadowing
* What is the mechanism for antishadowing Reggeons?
* How does DHG account for shadowing?

$$\int_{\nu_R}^{\infty} \frac{dN}{d\nu} \left[\sigma^{p}_{\gamma A} - \sigma^{A}_{\gamma A} \right] = \alpha' \kappa_A^2$$

Back face not seen for large A?

Participants
Electron Ion Collider Workshop

Last Name		Institution	Email
Aidala	Christine	BNL	caidala@bnl.gov
Akiba	Yasuyuki	KEK	akiba@bnl.gov
Alarcon	Ricardo	Arizona State University	ralarcon@asu.edu
Anselmino	Mauro	Torino University	anselmino@to.infn.it
Back	Birger	Argonne National Laboratory	Back@anl.gov
Baker	Mark	Brookhaven National Laboratory	Mark.Baker@bnl.gov
Balitsky	Ian	ODU/Jlab	balitsky@jlab.org
Barber	Desmond	DESY	mpybar@mail.desy.de
Barnes	Peter	Los Alamos National Lab	pdbarnes@lanl.gov
Bass	Steven	ECT*	steven.bass@cern.ch
Belitsky	Andrei	University of Maryland	belitsky@physics.umd.edu
Bond	Peter	BNL	bond@bnl.gov
Booth	Edward	Boston University	botho1@aol.com
BOTTO	Tancredi	MIT/Bates	tancredi@mitlns.mit.edu
Brodsky	Stanley	SLAC	sjbth@slac.stanford.edu
Brooks	Will	Jefferson Lab	brooksw@jlab.org
Bruell	Antje	MIT	abr@mitlns.mit.edu
Bueltmann	Stephen	BNL	bueltmann@bnl.gov
Bunce	Gerry	BNL/RBRC	bunce@bnl.gov
Caldwell	Allen	Columbia University	caldwell@nevis.columbia.edu
Cameron	John	IUCF	cameron@iucf.indiana.edu
Chwastowski	Janusz	Institue of Nuclear Physics	janusz@mail.desy.de
Cole	Brian	Columbia University	cole@nevis.columbia.edu
Dainton	John	University of Liverpool	jbd@hep.ph.liv.ac.uk
De Roeck	Albert	CERN Geneva	deroeck@mail.cern.ch
Derbenev	Yaroslav	Thomas Jefferson National Accelerator Facility	derbenev@jlab.org
Derkach	Vadim	Institute of Radiophysics and Electronics of the National Academy of sciences of Ukraine	derkach@ire.kharkov.ua
Deshpande	Abhay	RIKEN-BNL Research Center	abhay@bnl.gov
Dutta	Dipangkar	MIT	ddutta@mit.edu
Ent	Rolf	Jefferson Lab	ent@jlab.org
Farkhondeh	Manouchehr	MIT-Bates	manouch@mit.edu
Fox	Brendan	Riken BNL Research Center	bfox@bnl.gov
Franklin	Wilbur	M.I.T.- Bates	wafrankl@mit.edu
Freund	Andreas	University of Regensburg	andreas.freund@physik.uni-regensburg.de
Fries	Rainer	Duke University	rjfries@phy.duke.edu
Gao	Haiyan	Massachusetts Institute of Technology	haiyan@mit.edu
Garvey	Gerald	Los Alamos National Labortory	garvey@lanl.gov
Goto	Yuji	RIKEN BNL Research Center	goto@bnl.gov
Greenshaw	Timothy	Liverpool University	green@hep.ph.liv.ac.uk
Grosse Perdekamp	Matthias	RBRC	matthias@bnl.gov
Guryn	Wlodek	BNL	guryn@bnl.gov
Guzey	Vadim	CSSM, Adelaide U.	vguzey@physics.adelaide.edu.au

Participants
Electron Ion Collider Workshop

Haggerty	John	Brookhaven National Laboratory	haggerty@bnl.gov
Hasell	Douglas	M.I.T.	hasell@mit.edu
Holt	Roy	Argonne National Laboratory	holt@anl.gov
Huang	Huan	UCLA	huang@physics.ucla.edu
Hughes	Vernon	Yale University	vernon.hughes@yale.edu
Igo	George	Dept of Physics & Astronomy, UCLA	igo@physics.ucla.edu
Iijima	Toru	KEK	iijima@bmail.kek.jp
Jacobs	Peter	LBNL	pmjacobs@lbl.gov
Jaffe	Robert	Massachusetts Institute of Technology	jaffe@mit.edu
Jalilian-Marian	Jamal	BNL	jamal@bnl.gov
Johnson	Brant	Brookhaven National Laboratory	brant@bnl.gov
Kageya	Tsuneo	BNL/LEGS/Virginia Polytec Institute and State Univ.	kageya@bnl.gov
Keppel	Cynthia	Jefferson Lab / Hampton University	keppel@jlab.org
Kharzeev	Dmitri	BNL	kharzeev@bnl.gov
Kinney	Edward	University of Colorado	Edward.Kinney@colorado.edu
Kiryluk	Joanna	UCLA	joanna@physics.ucla.edu
Klein	Max	DESY-Zeuthen	klein@ifh.de
Kodaira	Jiro	Hiroshima Univ.	jkodaira@hiroshima-u.ac.jp
Korotkov	Vladislav	DESY Zeuthen	korotkov@ifh.de
Kovchegov	Yuri	University of Washington	yuri@phys.washington.edu
Kowalski	Henri	Columbia/BNL/DESY	kowalski@nevis.columbia.edu
Krasny	Mieczyslaw	CERN	krasny@mail.cern.ch
Krause	Shannon	MIT Bates Linear Accelerator Center	krause@mit.edu
Kruglov	Sergei	Petersburg Nuclear Physics Institute	briscoe@gwu.edu
Lajoie	John	Iowa State University	lajoie@iastate.edu
Levchenko	Boris	Institute of Nuclear Physics, Moscow State University	levtchen@mail.desy.de
Lichtenstadt	Jechiel	Tel Aviv University	jech@lepton.tau.ac.il
Liuti	Simonetta	University of Virginia	sl4y@virginia.edu
Londergan	John	Indiana University	tlonderg@indiana.edu
Lorenzon	Wolfgang	University of Michigan	lorenzon@umich.edu
Ludlam	Thomas	Brookhaven National Lab	ludlam@bnl.gov
Mallot	Gerhard	CERN	Gerhard.Mallot@cern.ch
Matthews	June	Massachusetts Institute of Technology	matthews@lns.mit.edu
Mclerran	Larry	BNL	mclerran@bnl.gov
Meissner	Falk	Lawrence Berkeley National Laboratory	FMeissner@lbl.gov
Melnitchouk	Wally	Jefferson Lab	wmelnitc@jlab.org
Meziani	Zein-Eddine	Temple University	meziani@temple.edu
Miller	Andy	TRIUMF	miller@triumf.ca
Milner	Richard	MIT-Bates	milner@mitlns.mit.edu
Milstead	David	University of Liverpool	milstead@mail.desy.de
Moss	Joel	Los Alamos National Laboratory	jmm@lanl.gov
Nadolsky	Pavel	Southern Methodist University	nadolsky@mail.physics.smu.edu

Participants
Electron Ion Collider Workshop

Ogilvie	Craig	Iowa State University	cogilvie@iastate.edu
Okorokov	Vitaly	Moscow State Engineering Physics Institute	vitaly.okorokov@bnl.gov
Ozaki	Satoshi	Brookhaven National Laboratory	ozaki@bnl.gov
Pak	Robert	Brookhaven National Laboratory	Robert.Pak@bnl.gov
Paul	Peter	Brookhaven National Laboratory	ppaul@bnl.gov
Peng	Jen-Chieh	University of Illinois	jcpeng@uiuc.edu
Pitzl	Daniel	DESY	pitzl@mail.desy.de
Qiu	Jianwei	Iowa State University	jwq@iastate.edu
Ritter	Hans Georg	LBNL	HGRitter@lbl.gov
Saito	Naohito	RIKEN/RBRC	saito@bnl.gov
Sandacz	Andrzej	SINS, Warsaw	sandacz@fuw.edu.pl
Schlein	Peter	UCLA	schlein@ucla.edu
Schneekloth	Uwe	DESY	uwe.schneekloth@desy.de
Schweda	Kai	LBNL	KOSchweda@lbl.gov
Shatunov	Yuri	Budker Institute of Nuclear _Physics	shatunov@inp.nsk.su
Sichtermann	Ernst	Yale University	Ernst.Sichtermann@yale.edu
Stoesslein	Uta	University of Colorado/Boulder	uta.stoesslein@desy.de
Stratmann	Marco	Univ. of Regensburg	marco.stratmann@physik.uni-regensburg.de
Strikman	Mark	Penn State University	strikman@phys.psu.edu
Surrow	Bernd	BNL	bernd.surrow@bnl.gov
Thomas	Anthony	CSSM, Adelaide University	athomas@physics.adelaide.edu.au
Thomas	Jim	Lawrence Berkeley National Laboratory	jhthomas@lbl.gov
Tschalaer	Christoph	MIT/Bates	chris@bates.mit.edu
Tuchin	Kirill	Institute for Nuclear Theory	tuchin@phys.washington.edu
van der Laan	Jan	MIT-Bates	janvdl@mit.edu
Venugopalan	Raju	BNL	raju@bnl.gov
Vogelsang	Werner	RBRC and BNL	wvogelsang@bnl.gov
Wang	Fuhua	MIT-Bates	fwang@rocko.mit.edu
Weigert	Heribert	University of Regensburg	heribert.weigert@physik.uni-regensburg.de
Weiss	Christian	Regensburg University	christian.weiss@physik.uni-regensburg.de
White	Sebastian	BNL	white1@bnl.gov
Woody	Craig	BNL	woody@bnl.gov
Xu	Nu	LBNL	NXu@lbl.gov
Zelenski	Anatoli	BNL	zelenski@bnl.gov
Zhalov	Michael	Petersburg Nuclear Physics Institute	zhalov@mail.pnpi.spb.ru
Zolfaghari	Abbi	MIT Bates Linear Accelerator Center	abbi@mit.edu
Zwart	Townsend	MIT Bates	zwart@bates.mit.edu